Vasilios K. Thomaidis

Cutaneous Flaps in Head and Neck Reconstruction

From Anatomy to Surgery

Springer

Cutaneous Flaps in Head and Neck Reconstruction

Vasilios K. Thomaidis

Cutaneous Flaps in Head and Neck Reconstruction

From Anatomy to Surgery

Springer

Vasilios K. Thomaidis, MD, DDS, PhD
Department of Anatomy
Medical School
Democritus University of Thrace
Alexandroupolis
Evros
Greece

With illustrations from Dr. Manos Mazinis, DDS, PhD, Medical Illustrator

ISBN 978-3-642-41253-0 ISBN 978-3-642-41254-7 (eBook)
DOI 10.1007/978-3-642-41254-7
Springer Heidelberg New York Dordrecht London

Library of Congress Control Number: 2014936600

Printed on acid-free paper

Springer is part of Springer Science+Business Media (www.springer.com)

This book is dedicated to the memory of my father Kyriakos Thomaidis
To my mother Zoi Thomaidou
I owe them what I am

To my wife Athanasia and my daughter Zoi-Maria

Foreword 1

When Dr. Vasilios Thomaidis informed me of his venture to prepare a publication regarding the anatomy of head and neck with an application to flap surgery, I was intrigued to see how he would illuminate the anatomy of the head and neck using his experience as a surgeon. Such an approach is not typical in classic textbooks of anatomy. I regarded this effort to be challenging.

The anatomical presentation takes place in a layered manner, providing systematic steps at understanding the topographical anatomy of the various layers of tissues in the head and neck area. Furthermore, various controversial issues concerning relative anatomical structures are reviewed; in all such cases, Dr. Thomaidis states his own attitude, both as an anatomist and as a surgeon. In my opinion, this is what modern anatomy is.

It is my personal belief that Dr. Thomaidis accomplished his initial aim with the wise use of remarkable anatomic drawings, which are unique because they display anatomical structures that are usually overlooked by classic anatomical textbooks but are extremely important in flap surgery.

Being a Professor of anatomy for more than 35 years, I acknowledge another function of this book, beyond its obvious benefit to surgeons. Medical students will treasure the exceptional quality of the drawings, in which they will find a clear depiction of the various complicated layers of the head and neck and the muscular, vascular and neural structures found within them. This book is valuable as a supplementary tool in the study of anatomy and surgery since it enables the illustration for students annotating important anatomical structures and their relationships as well as clarifying elusive points and modern controversial issues, addressed in a way that is not always possible in the classroom.

Thespis Dimitriou, MD, PhD
Professor of Anatomy
Alexandroupolis, Greece

Foreword 2

It is my great pleasure to write a preface for this anatomical and surgical atlas for flaps in head and neck reconstruction published by Dr. Vasilios Thomaidis.

Dr. Thomaidis' attitude to recognize the need of a tie between head-neck anatomy and flap surgery is valuable. His dual background as maxillofacial surgeon and anatomist gives him the capacity to extract from his anatomy lab experience that provides a unique insight to the structures of all regions and to correlate them with surgical techniques. As a practicing surgeon, he presents the anatomic concepts of the region, paying special attention to sidelined anatomic structures that are necessary in practice. His work reflects why a practicing surgeon needs a detailed knowledge of anatomy. A thorough understanding of surface anatomy in a layered manner is depicted and simplified by beautifully composed anatomical drawings.

For those who study head and neck surgery, this book is a valuable resource, since it is a step-by-step approach to performing flap procedures as it also acts as a surgical atlas. The numerous colored illustrations of cases depict the vast majority of local and regional cutaneous flaps that are used in head and neck reconstruction, and step-by-step instructions in flap design and harvesting techniques are a valuable asset to the book.

To the practicing surgeons: the significance of being aware of the anatomical structures in the area in which we work is imperative and is a crucial part in the success of our work. This textbook distills the anatomical knowledge of each area, simplifying preoperative assessment and making planning much easier. In addition, the text juxtaposes old techniques with new ones, giving the reader the information needed to take the appropriate steps for success.

Nikolaos Lazaridis, MD, DDS, PhD
Professor of Maxillofacial Surgery
Thessaloniki, Greece

Preface

It is said, "fear in surgery is fear of anatomy." Unfortunately there is a chasm between the anatomy learned in the traditional way and what we see during surgery. The aim of this work is to offer the means to resolve this in a comprehensive way, by bridging relative anatomy straight to the surgical use of cutaneous flaps in head and neck reconstruction, which is not normally found in a single text. Cutaneous local and regional flaps still remain a basic tool in the armamentarium of surgeons coming from different specialties that work in the head and neck area. These flaps are used even for very large defects, despite the ever-growing utilization of free flaps, due to the fact that they are time consuming, not cost effective, they do not require special microsurgical training, and represent the first choice of novice surgeons. My experience taught me that thorough knowledge of anatomy enables navigation between tissues and spaces with safety and ease, preserving important anatomical structures, and minimizes operational stress.

This book is organized in chapters according to the anatomic areas, which represent the various donor sites from which flaps are derived and used in head and neck defects. These donor sites are present separately in each chapter of the book and include: scalp, temple, posterior neck, forehead, nose, cheek, lips, chin, auricle, anterior neck, and deltopectoral region. In each chapter, firstly, I portray the superficial anatomy of each region in a layered manner, and how nerves and vessels travel through these layers. Secondly, the widely used local and regional cutaneous flaps that are derived from each donor site are demonstrated in the reconstruction of various surgical defects. Thus, I incorporate classic and modern anatomic issues and my personal experience as an anatomist and surgeon, to accomplish the above.

Special attention should be paid to the iconography of this work. I wanted to supplement the text with many illustrations so as to clearly define the areas described with as much detail as possible, without overcomplicating the anatomical aspects. Thus, this work serves as a reference to fashion a better understanding. The anatomic part is thus followed by drawings, designed and based not only on classic depictions but also on the experience of everyday surgical practice. Step-by-step photos of cases that I completed, presenting the procedure to be followed in flap surgery on the other hand, accompany the surgical part.

My hope is that this book serves as a guide and tool for new surgeons to increase their confidence in flap surgery, and to resolve possible anatomical discrepancies for seasoned surgeons.

Alexandroupoli, Greece — Vasilios K. Thomaidis, MD, DDS, PhD

Acknowledgments

Although many people have indirectly contributed to the creation of this atlas, I would like to thank those who played key roles in its preparation. First of all, I would like to thank Professor Thespis Demetriou, Director of Anatomy of the School of Medicine in Democritus University of Thrace, who encouraged me to take up to this venture and helped me clear many ambiguous points in the anatomic description of the head and neck area.

I would like to thank Dr. Konstantinos Seretis, Plastic Surgeon, and Dr. Konstantinos Dimakis, General Surgeon, who, during their residency, assisted me in many of the operations included in this book. The cases presented were operated in the University Hospital of Alexandroupolis, the Medical Center of Thrace, and the General Clinic "Kyanous Stavros": I would like to thank the anesthesiologists and staff for their loyal teamwork. I wish to thank my colleague Dr. Ioannis Tsamis, for our cooperation. Additional thanks to Dr. Theodosis Birbilis, Assoc. Professor of Neurosurgery, Dr. Konstantinos Ioannakis, Assoc. Professor of Ophthalmology, Dr. Anastasios Bounovas, Assoc. Professor of Surgery, and Dr. Antonios Karpouzis Assoc., Professor of Dermatology, for their long-time partnership and referral of patients, many of whom have been included in this book. I shall not forget to thank my assistant nurses Ms. Sotiria Karafylidou and Ms. Alexandra Alexandrou.

I would also like to thank Dr. Aliki Fiska, Pathologist and Asst. Professor of Anatomy, for clarifying anatomic issues with regards to their microstructure. I also wish to thank Niki Papavramidou, Asst. Professor in the Anatomy Laboratory, for her unfailing optimism and continuous support during this long period of preparation of this manuscript. I also thank Maria Iakovaki, Giorgos Koukouzelas, and Athanasios Paraskevas, staff of the Anatomy Laboratory who tolerated my endless hours of work in the lab and provided me with everything necessary for the completion of this atlas.

I gratefully acknowledge the invaluable assistance of Dr. Michael Anthony Manoussos B.A., Majoring in Neuroscience, and senior at the Medical School of Democritus University of Thrace, for his unyielding aid in the preparation of this book.

Special thanks and eternal gratefulness are owed to Dr. Manos Mazinis, gifted medical artist and friend, for his tolerance, enduring my continuous corrections and objections and for spending innumerable hours creating the astonishing drawings included in this atlas.

This project would have no end without the support from my wife, Athanasia, and my daughter, Zoe. I was unavailable for long periods of time, during evenings, weekends, and vacation to work on the manuscript. I am grateful to them for granting me the time and space I needed to complete this work.

Finally, the creation of this book would not have been possible without the kind support of Dr. Inga von Behrens and Desk Editor Rosmarie C. Unger from Springer for their continual aid in bringing this book together. I owe an enormous thank you to all my patients, who trusted me in a difficult period of their life and for whom I always do the best I could.

Contents

General Considerations

1

The skin is the outer covering of the entire external surface of the human body. It is regarded as the largest organ of the body with a complicated structure that performs a great number of functions. It acts as a protective barrier preventing the internal environment against infection, trauma, ultraviolet radiation, and heat. In addition, it plays an important role in thermoregulation, stores water and fat, prevents and controls fluid loss, and constitutes the largest sensory organ.

1.1 Skin Anatomy

The skin exhibits a surface area that in the adult ranges from 1.6 to 2.0 m^2 with the surface area of head and neck in the adult occupying approximately the 9 %. Its thickness varies among gender, age, and anatomic location. Male skin is thicker than female skin in all anatomic regions. The skin becomes thinner in elderly individuals through changes that occur during the aging process. The thickest skin is found on the palms of the hands and soles of the feet and the thinnest on the eyelids. This depends primarily in the varying thickness of the dermis and in a lesser degree in the varying thickness of the epidermis.

Throughout the anatomic regions, the characteristics of skin vary significantly not only in thickness but also in color and in texture. All these characteristics constitute factors that have to be scrutinized when choosing the ideal donor site of a flap.

The skin consists of two interrelated layers, the epidermis and dermis, which along with the underlying subcutaneous fatty layer cover the entire body (Fig. 1.1).

1.1.1 Epidermis

The epidermis is the outermost thin layer of the skin. Its mean thickness is 0.1 mm but varies greatly, depending upon the type of skin, age, gender, and location. At the palms of the hands and the soles, it is 1.6 mm thick, while it can become very thin like in the eyelids where it is 0.04 mm. The epidermis is a stratified squamous epithelium consisting of five distinct layers. These layers from top to the bottom are the stratum corneum, the stratum lucidum, the stratum granulosum, the stratum spinosum, and the stratum basale. The epidermis contains primarily keratinocytes in progressive stages of differentiation. Starting from the cells of the stratum basale (basal cells), new keratinocytes are formed (squamous cells), through continuous mitosis, maturate, and move up, changing shape and composition. They replace the old ones that are dead and discarded. This process is called keratinization. Specialized epidermal cells as melanocytes, Merkel cells, and Langerhans cells are also contained in the epidermis. The epidermis contains no blood vessels, and its deepest layers are nourished by diffusion from the underlying dermis.

1.1.2 Dermis

The dermis consists of connective tissue and is tightly connected to the overlying epidermis through the basal membrane. It is much thicker than the epidermis (15–40 times) and also shows a variable thickness in different locations (e.g., 0.3 mm on the eyelid). The structural components of the dermis are primarily collagen and also elastic and reticular fibers. It is divided into a superficial region called the papillary and a deep region called the reticular dermis.

The upper papillary dermis contains a thin random arrangement of collagen fibers. The deeper reticular dermis is thicker and is made of coarse collagen fibers that are arranged parallel to the surface of the skin. The dermis contains capillaries at the papillary dermis and larger blood vessels at the reticular dermis, lymphatic vessels, hair follicles with the erector pili muscle attached to each follicle, sebaceous and sweat glands, nerve endings, and sensory

V.K. Thomaidis, *Cutaneous Flaps in Head and Neck Reconstruction*,
DOI 10.1007/978-3-642-41254-7_1, © Springer-Verlag Berlin Heidelberg 2014

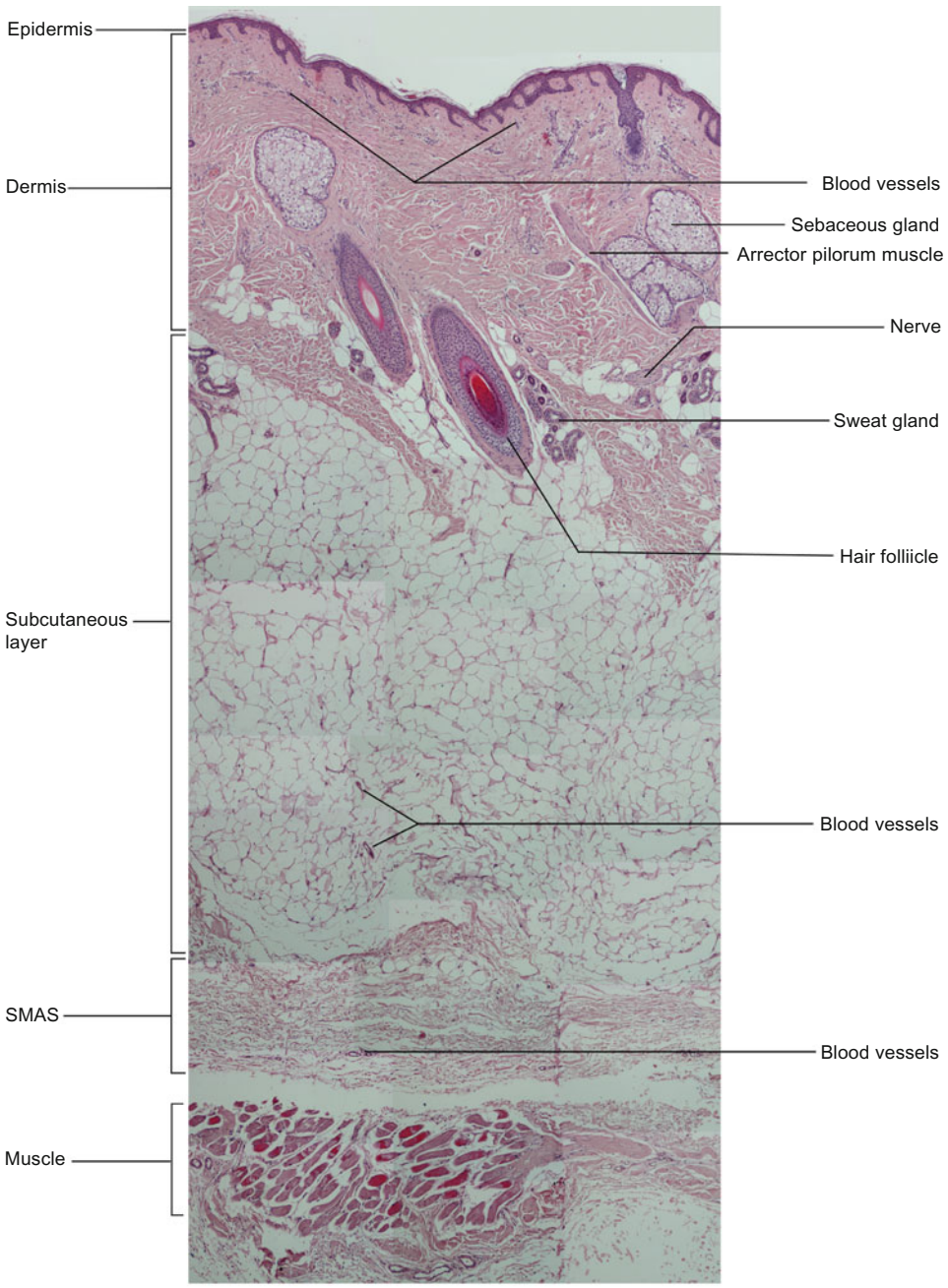

Fig. 1.1 Histologic cross section of the skin (cheek area) (hematoxylin-eosin, original magnification ×10) (With kind permission from Dr. Aliki Fiska)

receptors. Sebaceous glands are encountered over the entire body but in large concentration in the face and the scalp. Sweat glands are absent at the lip vermillion.

Hair follicles change their orientation across different ethnic groups. It is important to know the organization of hair follicles when performing incisions into the skin so as to avoid the onset of alopecia. In Caucasians, the follicles are oriented at an angle with regard to the skin surface. In Africans the follicles are more horizontal and thus run parallel to the sin surface, whereas in Asians the follicles are vertical with regard to the skin.

1.1.3 Subcutaneous Layer

The subcutaneous layer (subcutis, hypodermis, panniculus adiposus), also called subcutaneous fat layer, lies below the dermis. It consists of fat (almost the half of the body fat) and connective tissue and contains larger blood vessels, lymph vessels, and nerves. This layer attaches the skin to the underlying muscles and bones, houses the large vessels and nerves that supply the skin, and plays an important role in regulating body temperature. Its thickness varies considerably from individual to individual and among the different facial areas at the

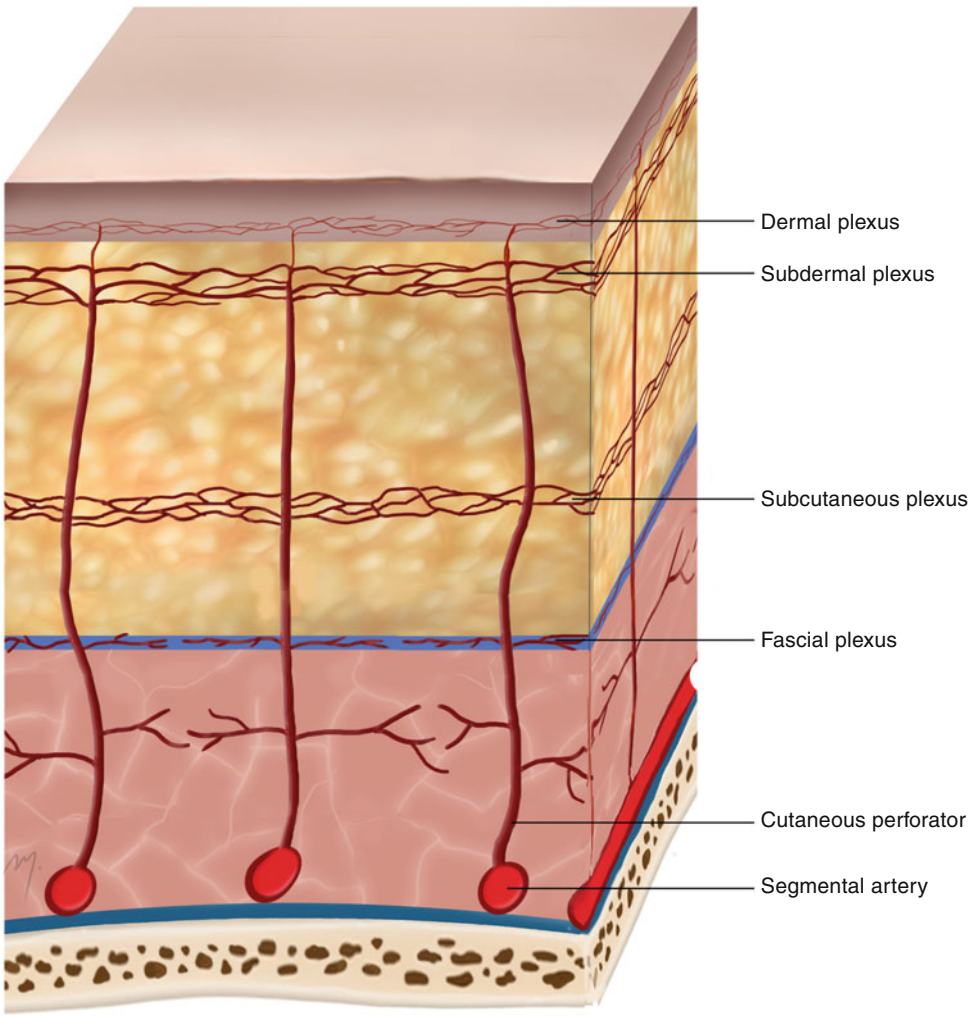

Fig. 1.2 The cutaneous circulation

same individual. It is thick at the cheeks and the neck but very thin or almost absent at the lips and the eyelids. The subcutaneous fat is divided into lobules by the fibrous septa, and in specific locations, it is sequestered in particular compartments forming the superficial fat pads (e.g., malar, submental).

1.1.4 Cutaneous Circulation

Knowing the skins' vascularization (Fig. 1.2) is crucial in the success of all flap designs due to the fact that flap survival is directly associated with adequate blood supply. The cutaneous vessels run from the underlying named vessels to the cutaneous surface as either septocutaneous or musculocutaneous arteries. The septocutaneous arteries (septocutaneous or fasciocutaneous perforators) arise directly from the underlying vessels and ascend through fascia or septa of muscles to the skin. The musculocutaneous arteries (musculocutaneous perforators) pass through the overlying muscle, and after giving small branches within the muscle mass, continue vertically to the skin. Named cutaneous vessels are direct vessels that run on top of muscles and parallel to the skin sending perpendicular branches to it. The portion of skin along with the underlying deep tissues that are supplied by a single segmental vessel, corresponding to a composite anatomic vascular territory, gave rise to the concept of angiosome that was first defined and introduced by Taylor and Palmer (1987).

Running toward the skin, the cutaneous vessels supply branches to each of the tissue layers they run through that anastomose each other forming extensive horizontal plexuses arranged in different levels in a complex network of blood vessels. The fascial plexus is formed at the level of the fascia, the subcutaneous plexus within the subcutaneous fat, and the subdermal plexus at the junction between the dermis and the subcutaneous fat. Within the dermis two plexuses are

formed: the deep dermal plexus and the superficial dermal plexus just beneath the epidermis (subepidermal plexus, subpapillary plexus).

1.1.5 Relaxed Skin Tension Lines (RSTLs)

Any incision at the face that is placed within or parallel to certain skin tension lines offers the best cosmetic result and the narrowest scar line. These skin tension lines run horizontally in the midfacial zone changing to a vertical direction laterally. These lines generally run parallel to the dermal collagen bundles but perpendicular to the underlying muscle fibers.

The relaxed skin tension lines (RSTLs) (Fig. 1.3) are those skin tension lines that follow the furrows formed when the skin is relaxed, and as they are not visible, they are generated by the act of pinching the skin and observing the furrows and ridges that are formed (Borges and Alexander 1962). The lines of maximal extensibility (LMEs) represent the directions in which the skin can be advanced with the greatest ease and run perpendicular to the RSTLs.

The historically used Langer's lines were first described by Karl Langer, Ritter von Edenberg (1819–1887) an Austrian anatomist who at 1861 observed the lines produced by driving round pins into cadaveric skin (Langer 1861). As they represent the skin tension lines in rigor mortis, they do not always correspond with the RSTL lines (Borges 1984).

In contrast to the RSTLs, the wrinkle lines (rhytids) are visible features of the skin that correspond in most cases with RSTLs (and on occasion, with the exception of the glabella and temple). As skin ages it becomes more lax and supple, and wrinkles become more numerous and obvious, in contrary to the smooth and with almost obscure wrinkles in young skin, enhancing the places to camouflage an incision. A flap must be orientated so as its incision lines lie into the skin tension lines.

The skin of the face has been divided into units with similar skin color, texture, and thickness, the facial aesthetic units (Gonzalez-Ulloa et al. 1954, Gonzalez-Ulloa 1956). These facial aesthetic units correspond in a way also to the anatomic facial regions and as a general rule when possible flaps must be donated from the same aesthetic unit where the defect is located. Moreover when the planned incisions are placed at the boundaries of a subunit, the scars are camouflaged in a favorable way. The facial aesthetic units have been further subdivided into subunits introducing the "subunit principle" as approach in the reconstruction of face (Sherris and Larrabee 2010).

Fig. 1.3 Relaxed skin tension lines (RSTLs) of the head and neck

1.2 Types of Flaps

The flaps are classified in various ways. Firstly they are distinguished by the site of their origin and secondly by the distance of the donor site from the recipient site as local, regional, and distant flaps. According to their composition and the tissue type, they are classified as cutaneous, fasciocutaneous, musculocutaneous, osteomusculocutaneous, muscle, and bone flaps.

The most common classification of skin flaps is related to their blood supply and the method of tissue movement.

1.2.1 Flap Types According to Blood Supply

According to the way that blood vessels enter into the flap at its base, the flaps are distinguished in axial pattern and random pattern flaps.

Fig. 1.4 Axial pattern flap

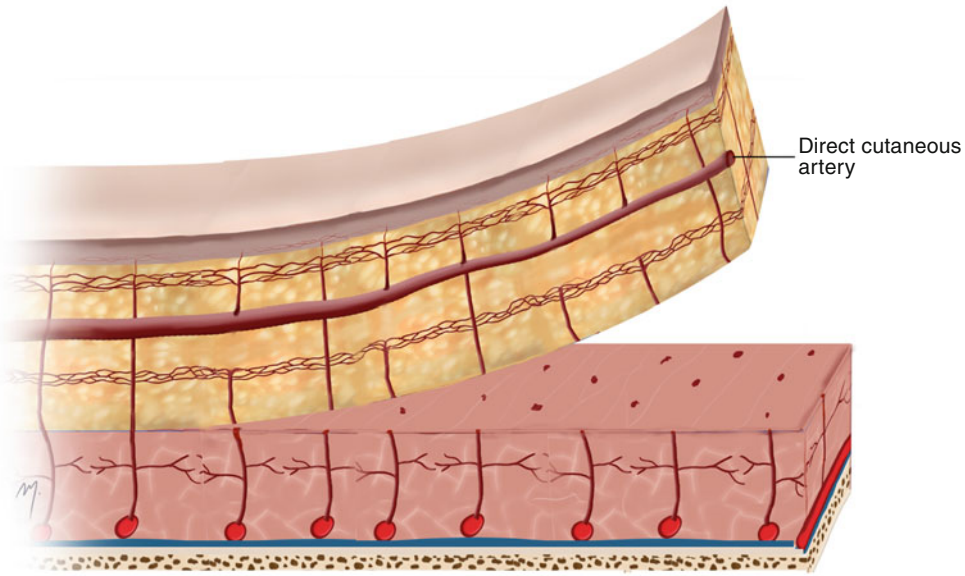

1.2.1.1 Axial Pattern Flaps

The axial pattern flaps (Fig. 1.4) are supplied by a named direct cutaneous (septocutaneous) artery and vein that is incorporated to the flap running along its long axis. This allows a large and long area to be freed from the underlying tissues with safety in a length at least equal to the length of the vessels, without obeying to the length to width ratio limitations of the random pattern flaps.

1.2.1.2 Random Pattern Flaps

The random pattern flaps (Fig. 1.5) are not based on named vessels but depend on the vascular supply of the subcutaneous and subdermal plexus fused from perforators at the base of the flap. Random pattern flaps of the face traditionally have been designed with a length to width ratio that must not exceed 3:1 to insure its survival. However, it is more likely that the survival of a flap does not depend solely on its length but the perfusion pressure and the intravascular resistance of their vascular constituents play a more significant role.

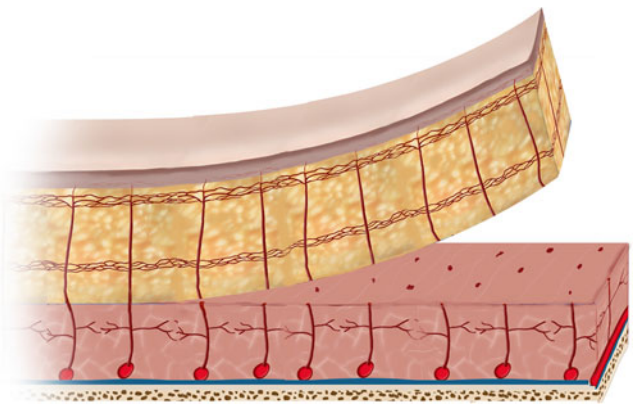

Fig. 1.5 Random pattern flap

1.2.2 Flap Types According to the Method of Transfer

According to the method of transfer, the flaps are distinguished in the following general types.

1.2.2.1 Pedicle Flaps

The tissue to be transferred remains attached to the donor site through a pedicle, as a bridge of tissue, which ensures its vascular supply and depending on the flap movement and flap design they are subdivided into:

Advancement Flaps

The flap moves directly forward and is positioned into the defect.

Transposition Flaps

The flap moves laterally in relation to a pivot point and is positioned into an adjacent defect.

Rotation Flaps

The flap rotates around a pivot point and is positioned into an adjacent defect.

Many flaps combine more than one elements of transfer in their design. In these cases the predominant movement is used to describe the flap.

1.2.2.2 Free Flaps

The tissue to be transferred is fully detached, along with its vascular pedicle as an isolated artery and vein from the donor site, and is transferred to the recipient site where its blood supply is gained by rejoining the artery and the vein through microvascular anastomosis to a new vessel adjacent to the recipient site.

1.2.3 Specific Types of Pedicle Skin Flaps

1.2.3.1 Rotation Flaps

The defect is triangulated and the flap is classically a semicircle that rotates in an arc to reach the defect (Fig. 1.6). The rotation flap has a wide base where its pivot point is located. The defect must be triangulated into a narrow isosceles triangle of 30°.

In areas with enhanced tissue laxity (e.g., cheek, neck), the rotation flap can be designed as an arc with a length three to four times the width of the defect or even more depending on the laxity of the donor site (Fig. 1.7). A dog-ear that is most of times formed at the base of the flap is adjusted by the excision of a small Burow's triangle.

A specific type of rotation flap with a unique geometry, very effective for use at the highly inelastic scalp, has been designed by Worthen (1990) (Fig. 1.8). This converts the defect to an isosceles triangle with its apex no more than 30°. From one of the triangle sides, a projection line 1,5 times its length is outlined. This line plus the triangle side is the diameter of the semicircular flap that rotates to close the defect.

1.2.3.2 Advancement Flaps

The advancement flap, the most simple in design, is moved directly along a linear axis to the recipient size (Fig. 1.9a). Classically it has a length to width ratio of 2:1–3:1. Two Burow's triangles are excised at each lateral site of the flap base preventing standing cone formation.

Two advancement flaps facing opposite one another can share a larger defect in form of bilateral advancement flap (Fig. 1.9b)

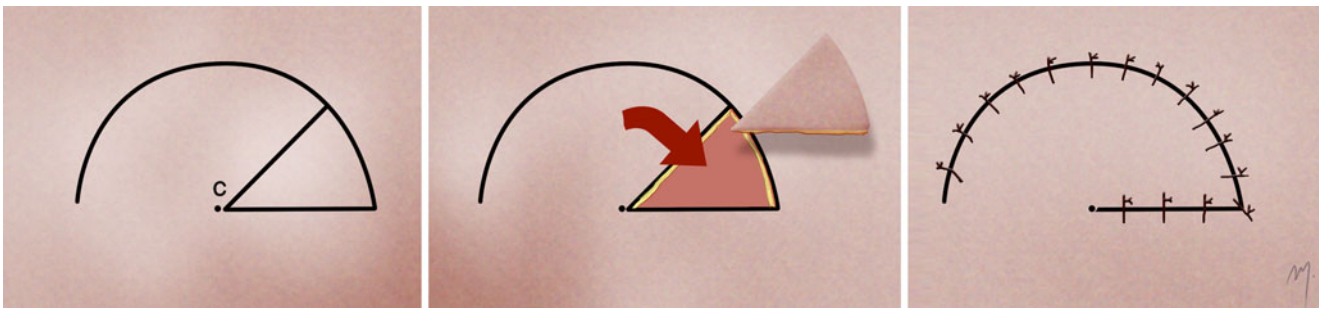

Fig. 1.6 Rotation flap designed as a semicircle

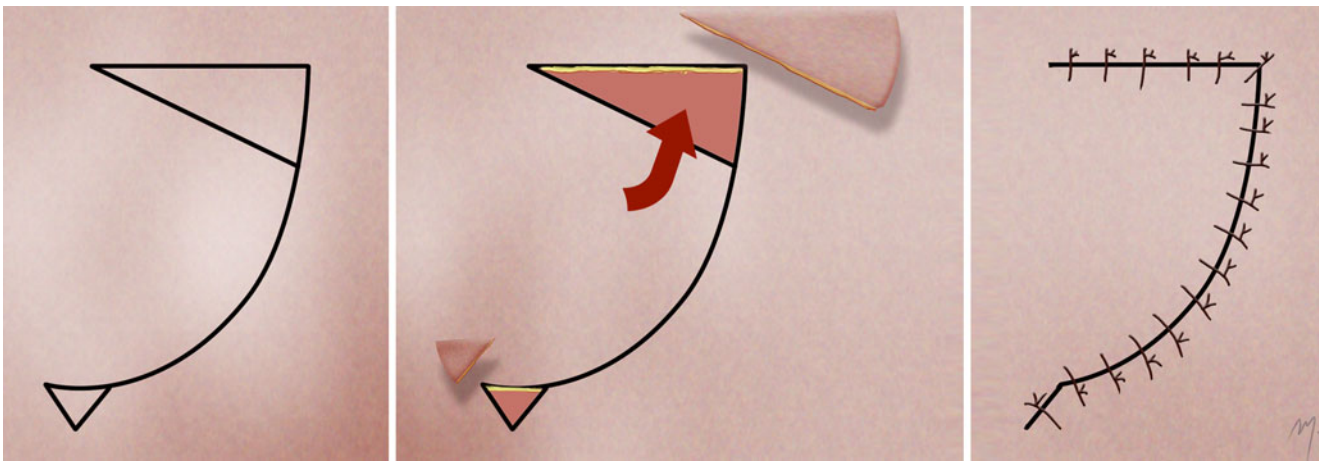

Fig. 1.7 Rotation flap designed as an arc

1.2.3.3 Island Pedicle Flap (V-Y Advancement Flap)

By this design the defect is rectangulated, and in one of its pleura, a triangular flap due to a V-shaped incision is designed (Fig. 1.10). The flap is elevated as an island, fully detached from its surrounding tissues, that is based only to its underlying subcutaneous tissue (island subcutaneous pedicle flap). It is advanced to the recipient site forming a Y-shaped suture line.

The island pedicle flap can be used as double when a larger area has to be reconstructed (Fig. 1.11).

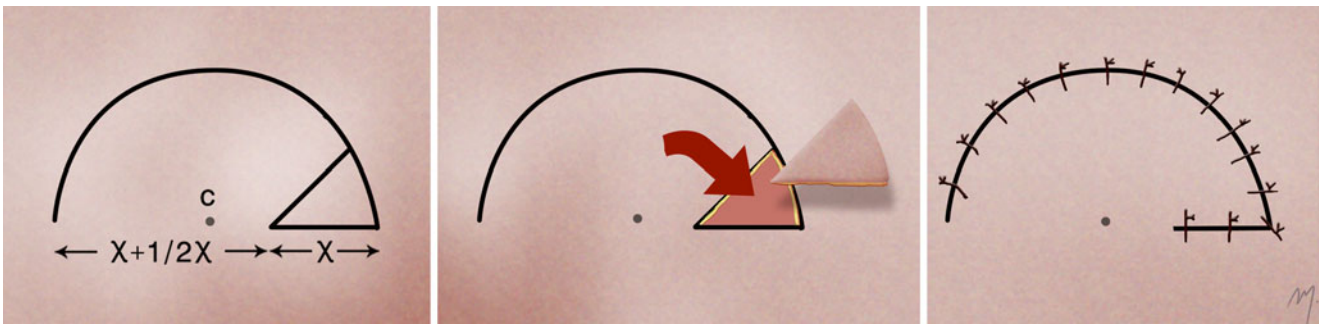

Fig. 1.8 Worthen rotation flap

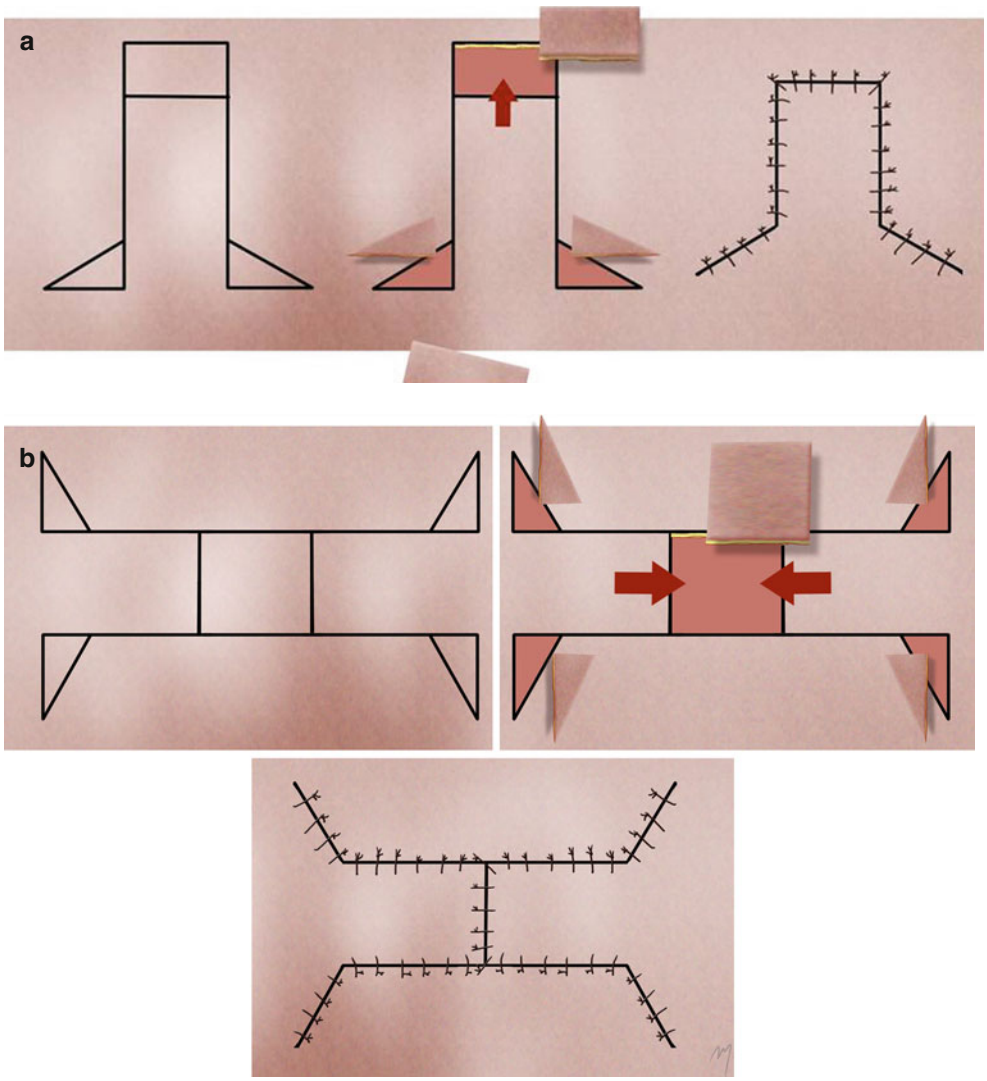

Fig. 1.9 (**a**) Advancement flap (**b**) bilateral advancement flap

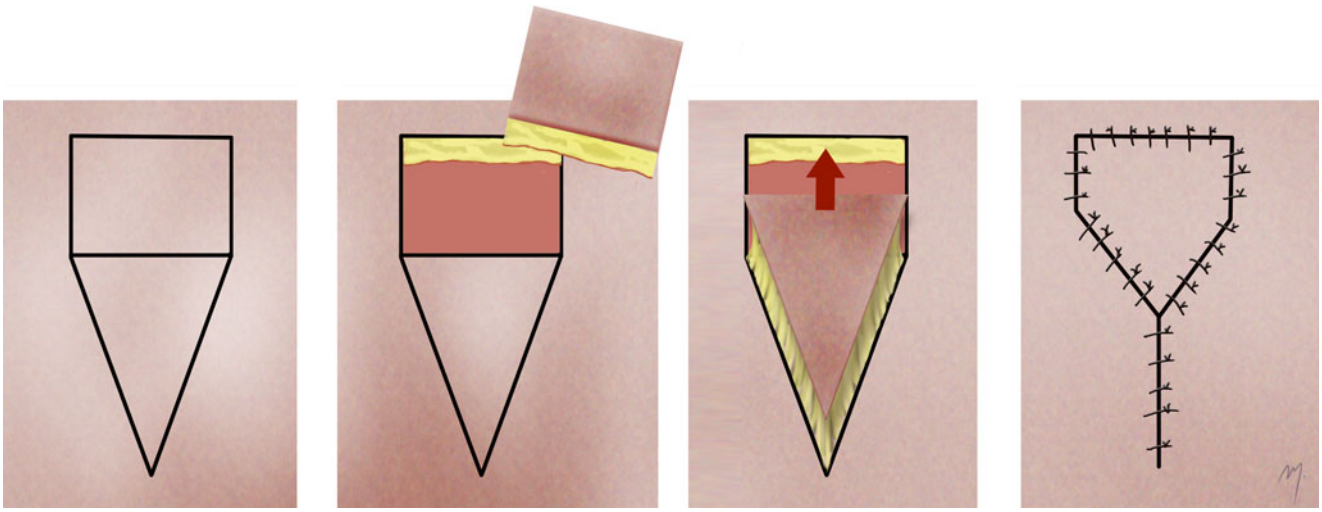

Fig. 1.10 Island pedicle flap

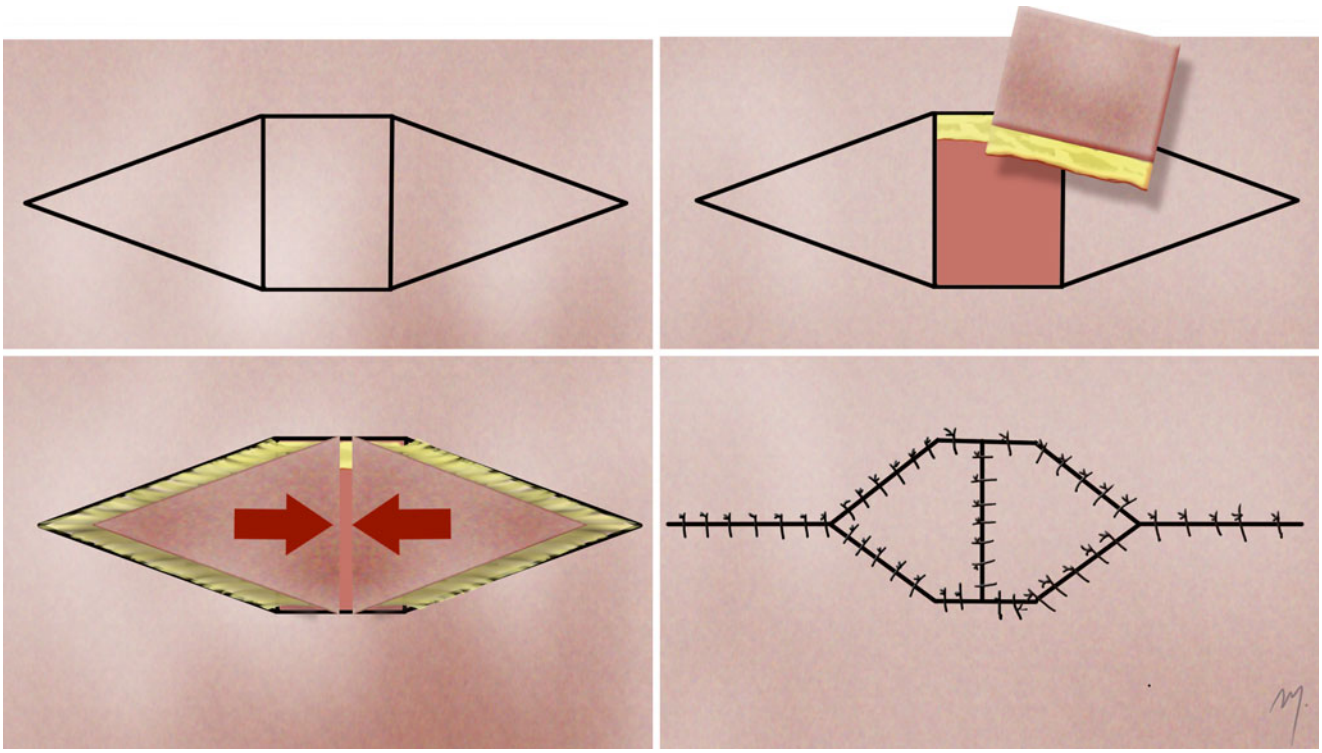

Fig. 1.11 Double island pedicle flap

1.2.3.4 Transposition Flap

The transposition flap is used to close an adjacent defect by moving laterally from its donor site, leaving thus a secondary defect, which must be closed. Depending on the surrounding tissue elasticity, the donor site defect may be closed primarily or may be closed by grafting (Fig. 1.12).

Interpolated flap is a transposition flap where the donor site not adjacent to the defect but intervening normal tissue separates the donor from the recipient site. The flap then passes over or underneath the intervening skin to reach the defect but still connected to the donor site via its vascular pedicle. In a second stage, after revascularization has formed, the pedicle is divided. Typical examples of widely used interpolated flaps in the head and neck reconstruction are the paramedian forehead flap and the deltopectoral flap.

1.2.3.5 Rhomboid Flap (Limberg Flap)

The rhomboid flap is a transposition flap with a strict geometrical design introduced by Limberg in 1946 (Fig. 1.13). The lesion is excised as a rhomboid with internal angles of 60° and 120°. The first side of the rhomboid flap is designed by drawing a line from the outer point of the 120° angle that

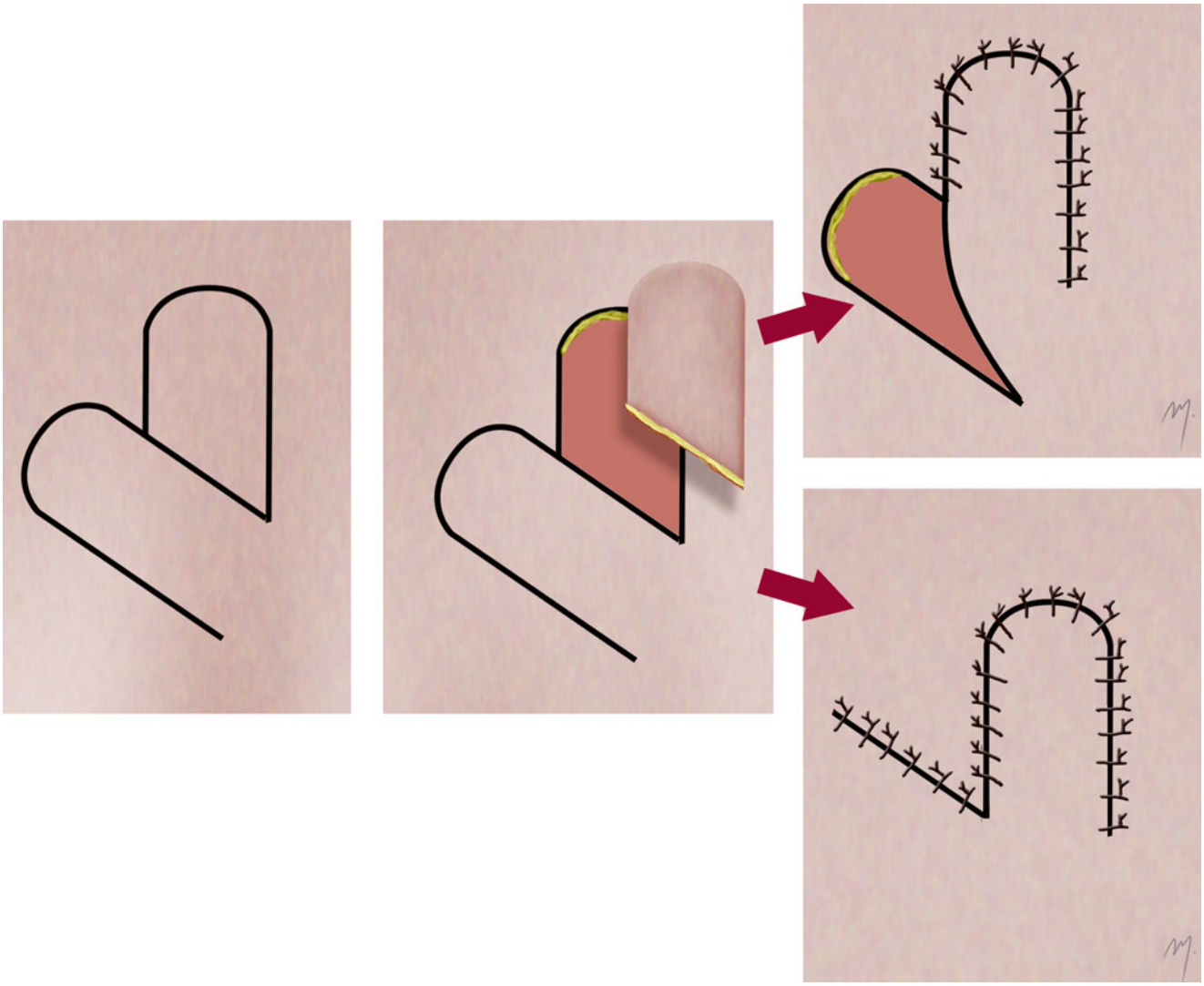

Fig. 1.12 Transposition flap

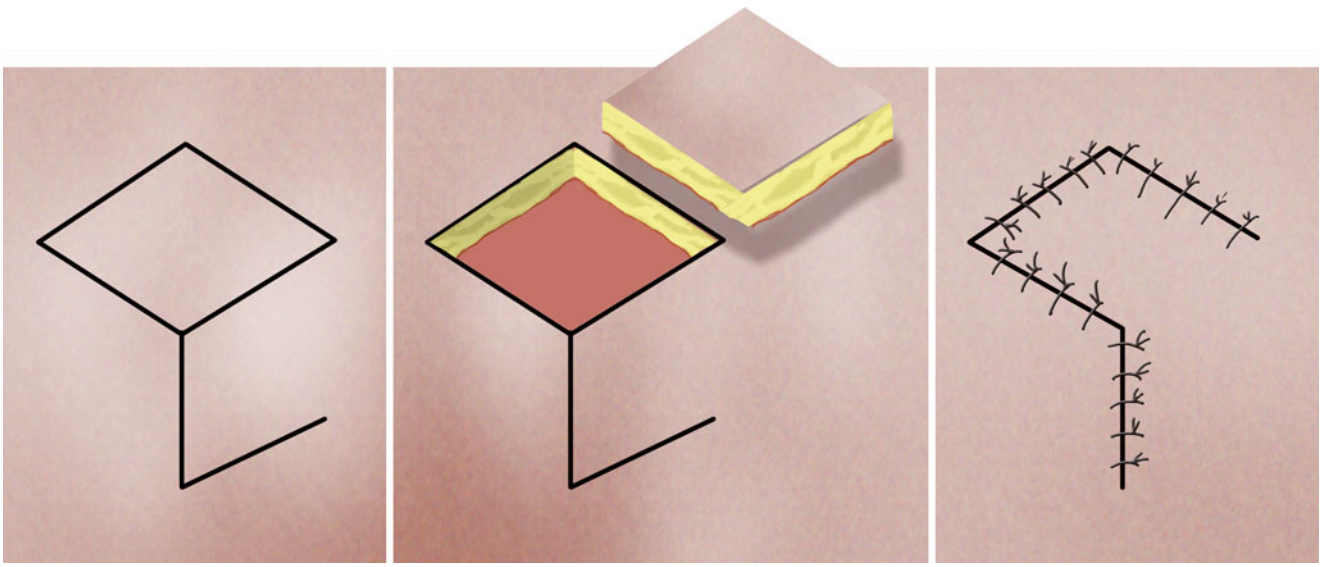

Fig. 1.13 Rhomboid flap

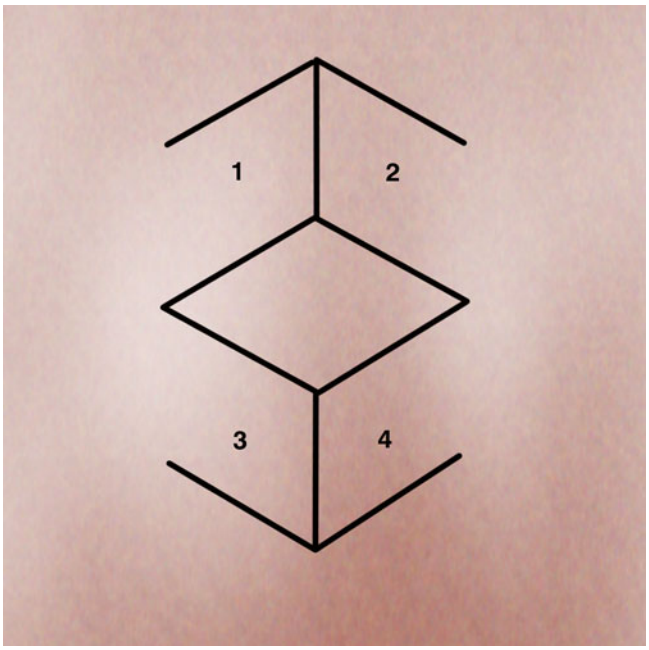

Fig. 1.14 Four potentially rhomboid flaps can be produced

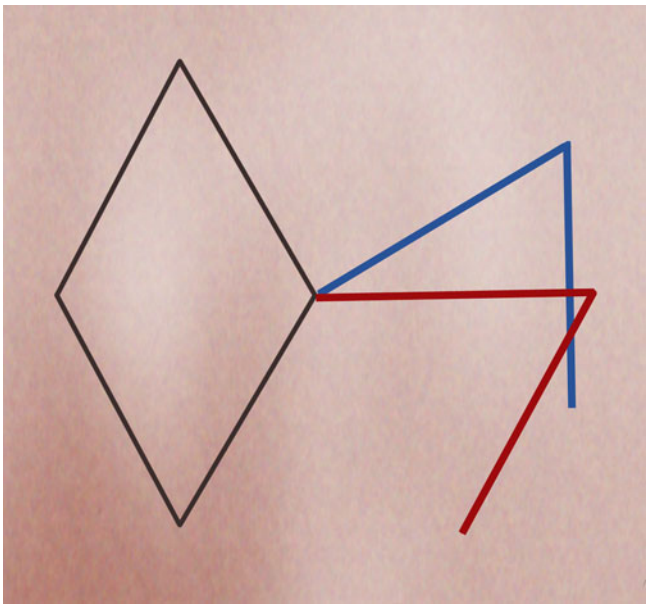

Fig. 1.15 Dufourmentel flap (*blue line*). Classic design of the rhomboid flap (*red line*)

Fig. 1.16 Bilobed flap

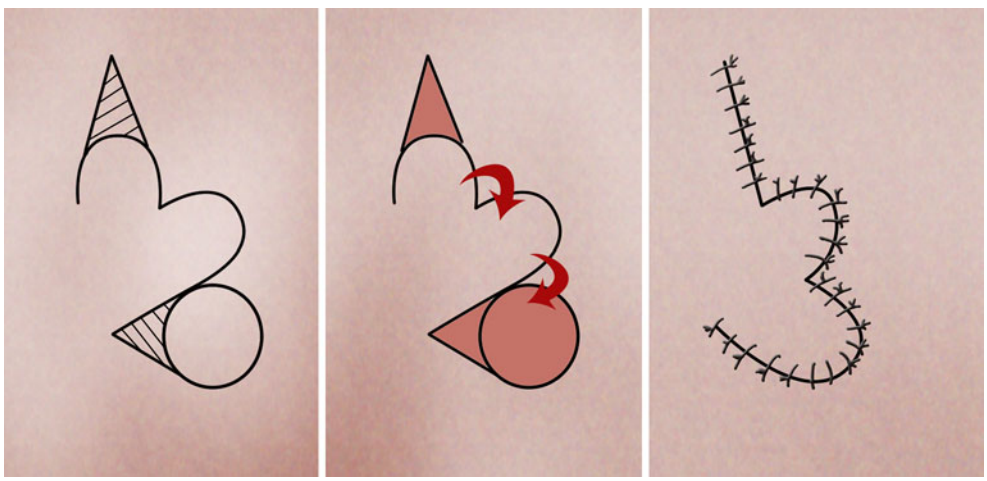

bisects the angle, and its length is equal to the rhomboid side. The second side of the flap is drawn from the outer point of the first side parallel and equal to the side of the rhomboid. An angle of 60° is thus produced at the apex of the rhomboid flap.

For each rhomboid defect, four possible rhomboid flaps can be designed (Fig. 1.14). Selection of the most appropriate one depends on location of the defect, the skin thickness of the donor site, and the orientation of the relaxed skin tension lines.

1.2.3.6 Dufourmentel Flap

Doufourmentel (1962) modified the classic Limberg rhomboid flap design changing the flap angles so as not to correspond to the 60–120° dimensions and widening the base of the flap (Fig. 1.15). This modification is suitable in a wider variety of defects, and closure of the donor site defect is much easier accomplished.

1.2.3.7 Bilobed Flap

The bilobed flap (Fig. 1.16) is a double transposition flap that was first described by Esser (1918) for nasal reconstruction.

The lesion is excised in a circular manner, and the bilobed flap is designed as two transposition flaps with a common pedicle. The first lobe of the flap is designed lying in an axis of 45–90° to the axis of the primary defect and at the same or slightly smaller size. This lobe will rotate to the primary defect creating a secondary one. The second-

ary defect will be closed with a second limb that is situated to an axis of 45–90° to the axis of the first limb and about half of its size. Thus, the total angle of transposition of the bilobed flap ranges from 90° to 180° (with a prevailing trend of 90°–100°). A Burow's triangle is outlined to be excised, at the point of rotation to the base of the flap. The excision of this triangle prevents the formation of the standing cone. A second smaller Burow's triangle is also excised at the distal part of the second limb, preventing a same dog-ear.

References

Borges AF (1984) Relaxed skin tension lines (RSTL) versus other skin lines. Plast Reconstr Surg 73(1):144–150

Borges AF, Alexander JE (1962) Relaxed skin tension lines, Z-plasties on scars, and fusiform excision of lesions. Br J Plast Surg 15:242–254

Dufourmentel C (1962) Le fermenture des pertes de substance cutance limitées le lambeau de rotation en L pour losange dit 'LLL'. Ann Chir Plast 7:60–66

Esser JFS (1918) Gestielite lokale Nasenplastik mit zweizipfligem Lappen, Deckung des sekundaren Defektes vom ersten Zipfel durch den zweiten. Deutsche Zeitschr Chir 143:385–390

Gonzalez-Ulloa M (1956) Restoration of the face covering by means of selected skin in regional aesthetic units. Br J Plast Surg 9(3):212–215

Gonzalez-Ulloa M, Castillo A, Stevens E, Alvarez Fuente SG, Leonelli F, Ubaldo F (1954) Preliminary study of the total restoration of the facial skin. Plast Reconstr Surg 13(3):151–161

Langer K (1861) Zur Anatomie und Physiologie der Haut. I. Uber die Spaltbarkeit der Cutis. SB Akad Wiss Wien 44:19–46

Limberg A (1946) Mathematical principles of local plastic procedures on the surface of the human body. Medgis, Leningrad

Sherris DA, Larrabee WF Jr (2010) Principles of facial reconstruction. A subunit approach to cutaneous repair, 2nd edn. Thieme Medical Publishers Inc, New York

Taylor GI, Palmer JH (1987) The vascular territories (angiosomes) of the body: experimental study and clinical applications. Br J Plast Surg 40(2):113–141

Worthen EF (1990) Transposition and rotation scalp flaps and rotation forehead flap. In: Grabb's encyclopedia of flaps, vol 1, Head and neck. Little Brown and Company, Boston

Scalp and Temple

2

The scalp is defined as the hair-bearing part of the soft tissues that cover the cranial vault. The scalp is bounded anteriorly by the anterior hairline, posteriorly by the superior nuchal lines, and laterally by the posterior part of the zygomatic arches. The frontal process of the zygomatic bone and the zygomatic process of the frontal bone delimit the temporal region anteriorly. Superiorly and posteriorly, the region is bordered by the superior temporal line and inferiorly by the zygomatic arch.

The hair-bearing scalp extends to the parietal and the occipital regions, but laterally, at the temporal region, it stretches in a variable area that depends on the position of the temporal hairline (Fig. 2.1).

2.1 Layered Anatomy of the Scalp

The scalp consists of five distinct layers. These are the same layers, with the same arrangement, that cover the forehead and continue superiorly covering the cranial vault until reaching the back of the head (Fig. 2.2). The layers of the scalp are consisted of the skin, the subcutaneous connective tissue, the occipitofrontalis muscle and the epicranial aponeurosis, the loose areolar connective tissue, and the pericranium (Fig. 2.3). The known mnemonic device SCALP is a useful tool to remember these layers:

S: Skin
C: Connective (subcutaneous) tissue
A: Aponeurosis and muscles
L: Loose areolar tissue
P: Pericranium

The first three layers are firmly attached to each other constituting a surgically single unit.

2.1.1 Skin

The scalp skin, being its first layer, is one of the thickest dermises of the body. It is thicker in the occipital area, with a thickness of 8 mm, and thinner in the vertex, where it is 3 mm (Matloub and Molnar 1996). Its thickness decreases during the aging process, by the presence of baldness, and it is thinner in females. It is firmly bound to the underlying subcutaneous connective tissue layer and difficult to separate

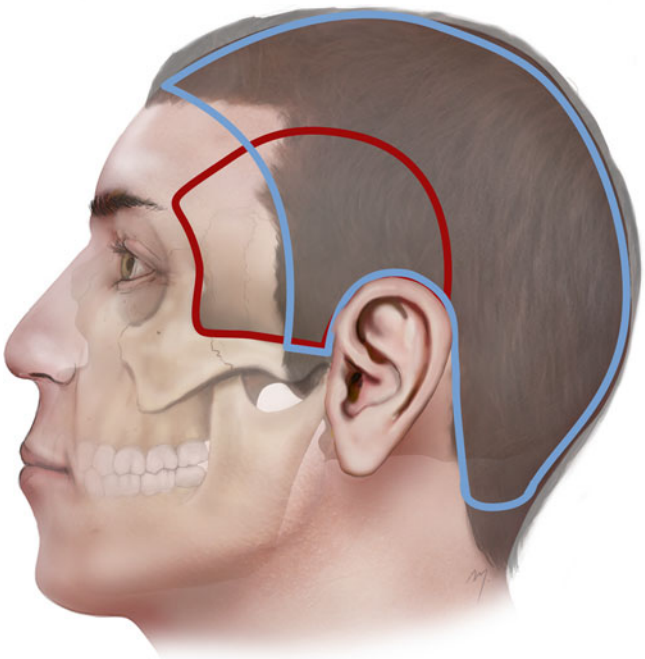

Fig. 2.1 Boundaries and overlap of the scalp to the temporal region

V.K. Thomaidis, *Cutaneous Flaps in Head and Neck Reconstruction*,
DOI 10.1007/978-3-642-41254-7_2, © Springer-Verlag Berlin Heidelberg 2014

Fig. 2.2 The same five-layered soft tissue covering of the forehead continues up to the cranial vault constituting the scalp

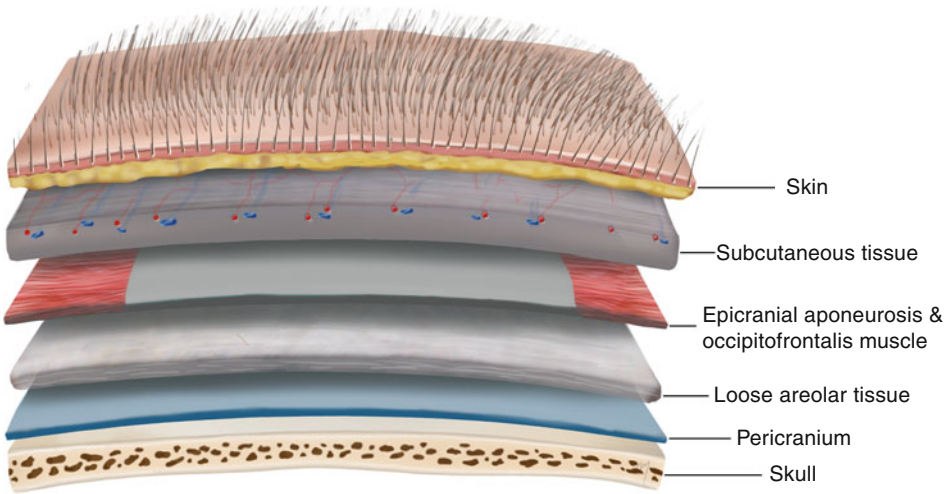

Fig. 2.3 The five layers of the SCALP

from it. It contains, beneath the dermis, the hair follicles and numerous sebaceous and sweat glands.

The relaxed skin tension lines at the scalp are oriented in a coronal direction, parallel to the ones of the forehead; at the frontal scalp, they run from front to back; at the mid-scalp, they run in a sagittal direction and turn into a horizontal direction; and at the posterior scalp, they run at a slightly oblique direction (Fig. 2.4).

2.1.2 Connective Subcutaneous Tissue

The second layer is the subcutaneous connective tissue (Fig. 2.3). It is a fibrofatty, firm, dense, and vascular layer that connects the skin to the underlying epicranial aponeurosis. It is a layer with an average thickness of 4–7 mm even though a natural thickness of 20 mm has been observed (Hayman et al. 2003).

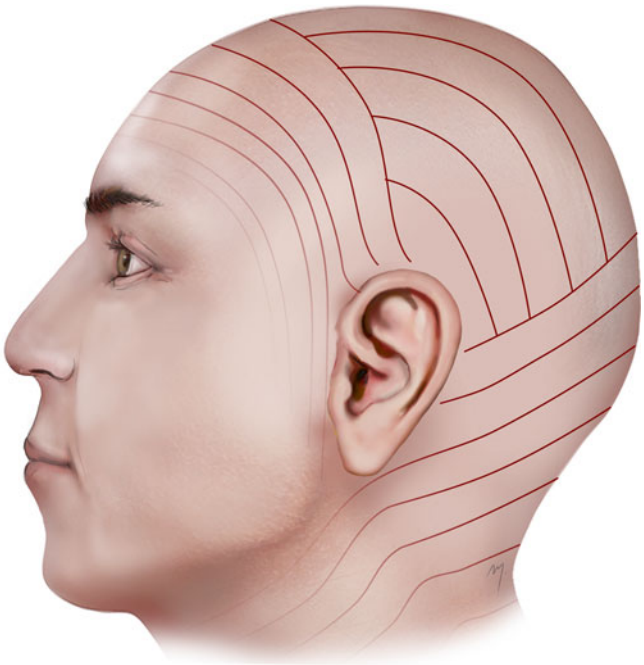

Fig. 2.4 Relaxed skin tension lines (RSTLs) at the scalp

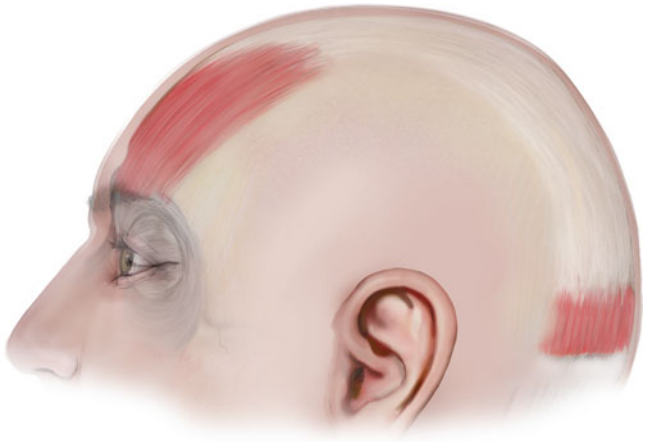

Fig. 2.5 The musculoaponeurotic layer of the scalp: frontalis muscle-galea aponeurotica-occipitalis muscle

Multiple fibrous septa divide this layer into small compartments. The large vessels that run over the surface of the underlying musculoaponeurotic layer just beneath this layer give branches within this layer that form a rich subcutaneous vascular plexus. These vessels are attached to the fibrous septa, which diminishes their ability to contract when they are cut. This leads to the profuse bleeding encountered in scalp incisions or in scalp trauma. Nerves and lymphatic vessels are situated also in this layer.

2.1.3 Aponeurosis and Muscles

The musculoaponeurotic layer, third layer, of the scalp consists of the aponeurosis, correctly termed as the epicranial aponeurosis, the occipitalis muscles, and the upper portion of the frontalis muscles (Fig. 2.5). The frontalis muscle and the occipital muscle are the anterior and posterior bellies of the two occipitofrontalis muscles that together with their intermediate connection, epicranial aponeurosis, cover, as a broad musculofibrous layer, the dome of the skull from the highest nuchal lines to the eyebrows.

2.1.3.1 Epicranial Aponeurosis

The epicranial aponeurosis (also termed galea or galea aponeurotica) is a thin, inelastic, broad tendinous sheet of connective tissue that lies over the dome of the skull, joining both the paired frontalis and occipitalis muscles. Its thickness ranges from 1 to 2 mm. In actuality, the galea, as mentioned, corresponds to the aponeurotic compartment of the occipitofrontalis muscle, which posteriorly encompasses the occipital bellies and in the forehead the frontal bellies. Laterally, in the temporal region, it fuses with the temporoparietal fascia.

The dense and tendinous nature of the galea makes the scalp flaps rigid and stiff, sometimes making it difficult to achieve adequate flap mobility so as to close a defect with ease and without tension. This is more obvious in the vertex of the scalp where the galea is much more resistant in distension. Therefore, strict geometry of flap design in the scalp is mandatory.

A useful tip to release some of the galea's tension is the "galeal scoring" (Fig. 2.6). With this technique, galeal incisions are made every 0.5–1 cm, in a depth that preserves the underlying vessels parallel to the foremost edge of the flap (Jackson 2007). Although this "tip" was first described in 1944 by Kazanjian and Holmes brought about by their experience, later, biomechanical studies of this principle were performed. Raposio et al. (1988) found out that galeotomy can reduce the closing tension even by 40 % and gain a flap lengthening approximately 1.5 mm per galeotomy.

The galea tightly adheres to the overlying subcutaneous connective tissue layer but is loosely connected to the underlying pericranium through the layer of loose areolar connective tissue.

Among the frontal and occipitalis muscles, only the last is involved with the hair-bearing scalp. The frontal muscle as far as it occupies the frontal region is examined in detail in the Chap. 3.

2.1.3.2 Occipitalis Muscle

The paired occipitalis muscles (Fig. 2.7) are thin and quadrilateral in shape originating by the tendinous fibers from the

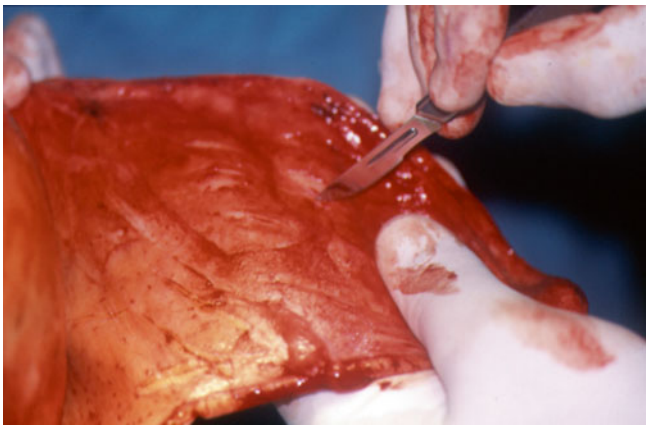

Fig. 2.6 Galeal scoring

Fig. 2.7 Occipitalis muscles

lateral two-thirds of the superior nuchal line and from the mastoid part of the temporal bone. They travel a short course after which its fibers insert into the galea. A space, which leaves between the two occipital muscles, is filled by a posterior extension of the epicranial aponeurosis. Branches of the posterior auricular and occipital arteries supply each occipitalis muscle. They are innervated by the posterior auricular branch of the facial nerve. The occipital muscles act to move the scalp backward.

2.1.4 Loose Areolar Tissue

The loose areolar tissue layer of the scalp is actually a subgaleal space that connects the musculoaponeurotic layer with the pericranium (Fig. 2.8). Its thickness ranges from 1 to 3 mm (Tremolada et al. 1994). The loose areolar tissue layer continues in the forehead and extends laterally to the temporal area, beneath the temporoparietal fascia and over the temporalis fascia. From a lateral aspect, the loose areolar tissue layer is attached in a line starting from the frontal process of the zygoma, continuing laterally along the superior aspect of the zygomatic arch, above the external auditory meatus, and over the mastoid process and superior to the attachments of the sternocleidomastoid and trapezius muscles. Posteriorly it terminates along the superior nuchal line by fusing with the periosteum (Tolhurst et al. 1991). Due to this loose layer, the galea and the tightly overlying superficial structures can freely move over the periosteum of the skull bone.

In terms of microstructure, this layer is composed of multiple and of various thickness fibrous laminae that run parallel and are loosely adherent to one another (Tremolada et al. 1994). The loose areolar tissue layer is often referred to as an avascular space although in reality it is a clearly vascularized layer. Tiny branches that are derived from the overlying

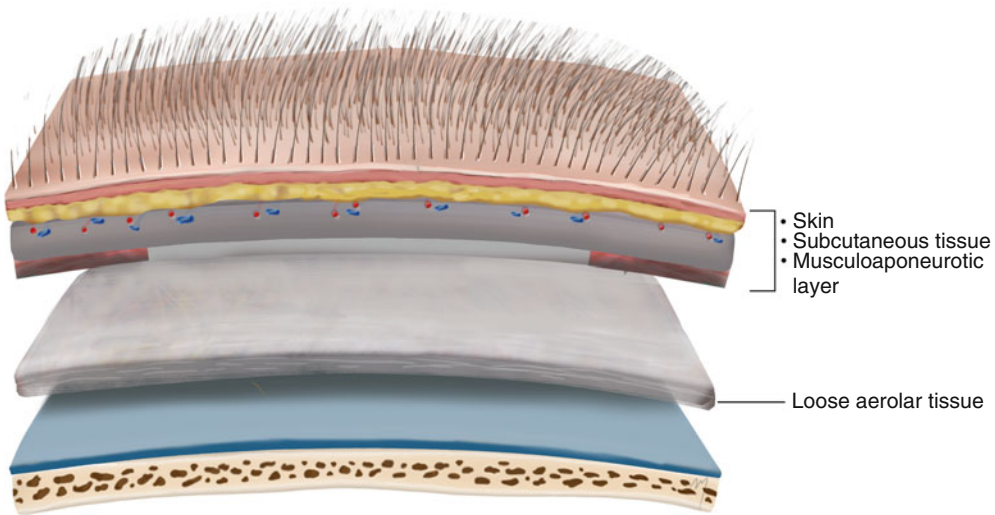

Fig. 2.8 Loose areolar tissue layer. The above the loose areolar tissue three layers are firmly attached to each other constituting a surgically single unit

blood vessels can be seen running through it. Some of these branches descend deep to the pericranium and the outer table of the skull (Cutting et al. 1984; McCarthy and Zide 1984; Casanova et al. 1986).

This subgaleal layer is of great importance in scalp surgery. Being very loose, it can be easily dissected, creating the surgical dissection plane when raising scalp flaps. Injection of a vasoconstrictive (e.g., epinephrine) solution transforms it practical to an avascular dissection plane.

2.1.5 Pericranium

The pericranium lies just beneath the loose areolar layer and is the skull's periosteum (Fig. 2.3). It is a dense layer of connective tissue that is adherent to the outer surface of the skull bones and as it runs forward over the supraorbital zone becomes even more adherent. Beyond the superior temporal line, it divides and encompasses the temporalis muscle becoming confluent with the temporalis fascia. Although the pericranium varies in thickness among the different locations, in general it is slightly thinner than the galea. It becomes continuous with the endosteum (the periosteum of the inner surface of the skull) at the interosseous suture lines of the skull bones. Even though it is often stated that the periosteum is difficult to remove at the suture lines, in practice, there is no added difficulty regarding its elevation in this area.

The pericranium receives its blood supply mainly from branches of the overlying major scalp vessels that run through the loose areolar tissue and reach the pericranium. Intracranial vessels that come from the underlying skull bones, as bone perforators, contribute also in the vascularization of the pericranium.

2.2 Layered Anatomy of the Temporal Region

The temporal region even directly related to the scalp, however, is different than the rest of it, having its unique anatomic, microstructural, and mechanical characteristics in the layered structure. In the temporal region, the scalp layers differentiate, become more complex, and increase in number. In general the difference of the five-layered scalp is summarized in the presence of the temporoparietal fascia instead of corresponding to the galea and the presence of temporalis muscle with its muscle fascia, lying between the periosteum and loose areolar tissue layer (Fig. 2.9).

The presence of an "extension" of the galea (the temporoparietal fascia) in the temporal musculoaponeurotic layer that is not so thick, stiff, and rigid leads to increased elasticity and tissue availability at the temple. The complicated course and layered position of the frontal branch of the facial nerve is another important point to be kept in mind during planning and rising of a flap when a part or the whole of it is derived from the temporal area.

Much confusion has surrounded the anatomy both in the description and nomenclature of the layers at the temporal region. In many descriptions of the 5-layered scalp, there is no differentiation between the structures of the temporoparietal region, resulting in the notion that the same layers are observed throughout. In addition further confusion is brought about concerning the various terms in the nomenclature of the structures, which vary among writers, and the absence of standardized terminology in classic anatomic textbooks. The terminology that follows is close to the precise anatomic identification of each structure but also includes a common ground across different surgical specialties.

2.2.1 Skin and Subcutaneous Tissue

The skin and subcutaneous tissue, the first two scalp layers, remain the same also in the temporal region, firmly attached the one to the other, with the same microscopic anatomic features.

2.2.2 Temporoparietal Fascia, Temporoparietalis Muscle, and Extrinsic Auricular Muscles

The musculoaponeurotic layer (3rd scalp layer) is represented in the temporal area by the temporoparietal fascia along with the extrinsic auricular and temporoparietalis muscles, encompassed by that fascia.

2.2.2.1 Temporoparietal Fascia

The temporoparietal fascia lies just beneath the subcutaneous layer. It extends like a fan from the periauricular area toward and above the superior temporal line where it fuses with the galea (Fig. 2.10). Inferiorly it passes over the zygomatic arch and becomes continuous with the superficial musculoaponeurotic layer (SMAS) of the face (Fig. 2.9).

The superficial temporal artery is related to the temporoparietal fascia. Coming from the preauricular region, it runs within the temporoparietal fascia and continues with its branches gradually transitioning more superficial over its surface. The frontal branches of the motor facial nerve run deep to the temporoparietal fascia, while the auriculotemporal sensory nerve runs above the temporoparietal fascia.

The temporoparietal fascia is thin (approximately 2–3 mm) but wide enough (approximately 15 × 15 cm) to be harvested as a thin, pliable, and broad flap. On the other hand, it is less dense compared to the galea, which makes skin flaps derived from the temple less stiff and rigid. The temporopa-

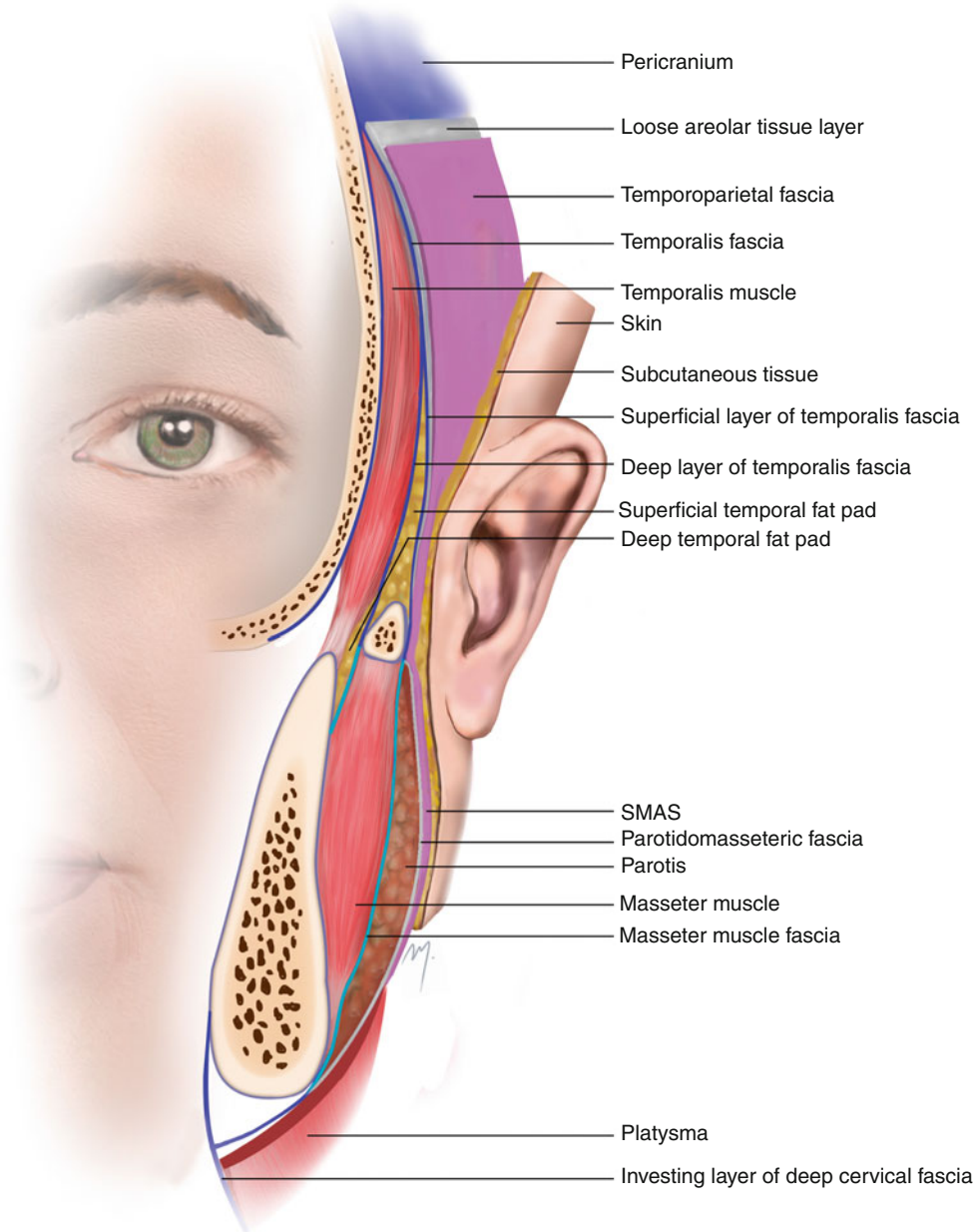

Fig. 2.9 Fascial anatomy of temporal region and lateral face

rietal fascia is responsible for the particular mobility that the scalp shows at the temporal area and in some extent at the parietal area.

2.2.2.2 Temporoparietalis Muscle and Extrinsic Auricular Muscles

The temporoparietalis muscle, often underdeveloped, belongs in the epicranial muscle group and actually is a muscle sheet, which lies between the frontal part of the occipitofrontalis and the anterior and superior auricular muscles (Fig. 2.10).

The three extrinsic auricular muscles, the auricularis anterior, auricularis superior, and auricularis posterior, are very thin muscles (fan of muscle fibers) that connect the auricle to the scalp and the skull. The auricularis anterior and auricularis superior arise from the galea, and the auricularis posterior arises from the mastoid part of the temporal bone.

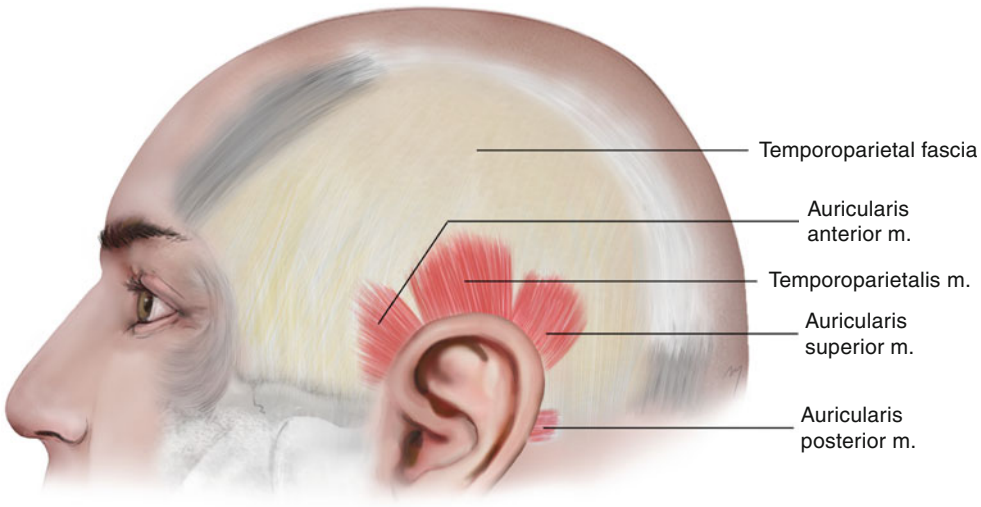

Fig. 2.10 The temporoparietal fascia, the temporoparietalis muscle, and the extrinsic auricular muscles

The muscles receive their blood supply from the posterior auricular artery and are innervated by the frontal and posterior auricular branches of the facial nerve.

2.2.3 Loose Areolar Tissue

The loose areolar tissue layer of the scalp continues at the temporal region between the overlying temporoparietal fascia and the underlying temporalis fascia (Fig. 2.9). Tiny branches coming from the superficial temporal artery are found within the loose areolar tissue layer defining it just like at the scalp as a clearly vascularized space.

The micro-architecture of the loose areolar tissue layer is quite similar to that of the rest of the scalp and is consisted of multiple fibrous laminae (Accioli de Vasconcellos et al. 2003). This layer is the conventional dissection plane for the scalp and temple, in skin flap surgery. Thus, large skin flaps that involve the scalp and the temple (and even the forehead) can be raised at the same level.

2.2.4 Temporalis Fascia

The next layer beneath the loose areolar tissue is the temporalis fascia (temporal fascia, deep temporal fascia). The temporalis fascia is the fascia that immediately lies over and covers the temporalis muscle (Fig. 2.11). It is a white, thick, dense, and strong connective tissue layer that is attached to the superior temporal line. Above the superior temporal line, it fuses with the pericranium.

As the temporalis fascia runs inferiorly, 2 cm above the zygomatic arch, a point that corresponds to the level of the superior orbital margin, it splits in two layers, the thick superficial layer (superficial lamina, superficial leaflet) of

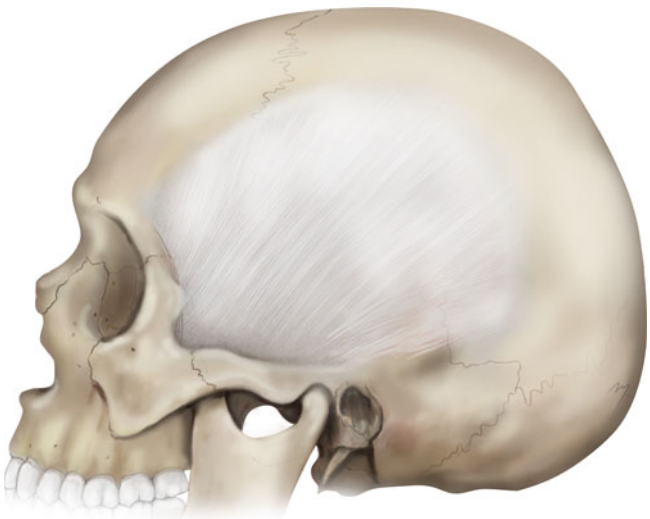

Fig. 2.11 Temporalis fascia

temporalis fascia and the thinner deep layer (deep lamina, deep leaflet) of temporalis fascia (Fig. 2.9).

The superficial layer of the temporalis fascia attaches to the lateral border of the zygomatic arch. It lies directly over the periosteum and is continuous with the fascia of the masseter muscle. The deep layer of the temporalis fascia attaches to the medial border of the arch and blends with the deep layer of the masseter muscle fascia.

2.2.4.1 Superficial Temporal Fat Pad

Between the superficial and deep layers of the temporalis fascia, a small amount of fat is encompassed: the superficial temporal fat pad (Fig. 2.9). This fat pad has been referred to as being part of the buccal fat pad (Tideman et al. 1986). In his detailed work, Stuzin et al. (1989, 1990) revealed that the superficial temporal fat pad is a distinct entity to the buccal

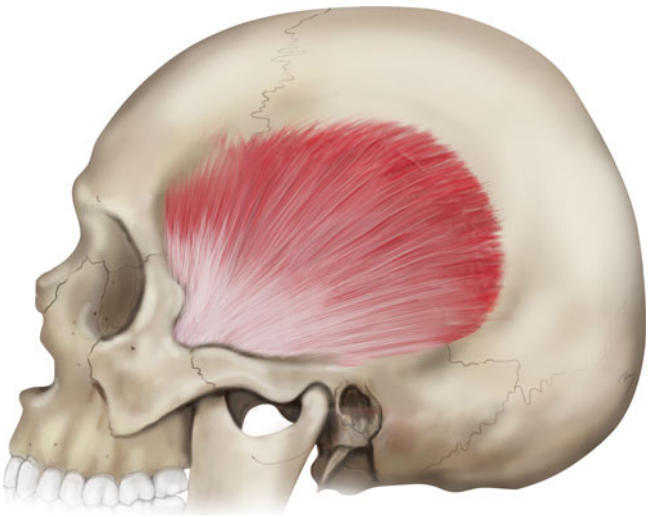

Fig. 2.12 Temporalis muscle

fat pad that has no continuation with it, such as the masticatory space, differs in appearance, and has a different vascularization as it is supplied by the middle temporal artery. The middle temporal artery, the zygomaticoorbital artery, and the zygomaticotemporal nerve are running within the superficial temporal fat pad.

2.2.4.2 Deep Temporal Fat Pad

Another thin fat pad, the deep temporal fat pad, exists at a deeper plane, between the temporalis fascia and the outer surface of the temporalis muscle (Fig. 2.9). It covers the inferior portion of the temporalis muscle, starting at a level 2–4 cm above the arch; continues beneath the arch, also covering the muscle tendon; and becomes continuous with the buccal fat pad (Stuzin et al. 1989).

The deep temporal fat pad, being the extension of the buccal fat pad superiorly, also plays a role in the function of mastication; it also allows the temporalis muscle and its tendon to move and glide easily under the zygomatic arch (Dubin et al. 1989; Stuzin et al. 1990; Tolhurst et al. 1991).

2.2.5 Temporalis Muscle

Under the temporalis fascia, the temporalis muscle is found (Figs. 2.9 and 2.12). The temporalis muscle is a fan-shaped muscle that belongs to the masticatory muscle group and fills the entire temporal fossa. Its fibers arise from the whole vicinity of the temporal fossa up to the inferior temporal line and the deep surface of its fascia (temporalis fascia). Anteriorly they are oriented in a vertical manner and become more oblique when getting posteriorly. Coming from the periphery, the fibers converge and form the temporalis muscle tendon. The tendon passes between the zygomatic arch and the side of the skull and attaches firmly to the coronoid process of the mandible and to the anterior border of the mandibular ramus as far as the third molar.

The temporal muscle is supplied by the deep temporal branches of the maxillary artery and is innervated by the deep temporal branches of the mandibular nerve. The temporalis closes the mouth by elevating the mandible.

2.2.6 Pericranium

The scalp pericranium extends laterally at the temporal area. At the superior temporal line, it fuses with the temporalis fascia and continues below the temporalis muscle covering the bones of the temporal fossa (Fig. 2.9). It is vascularized mainly from perforating branches of the superficial and deep temporal arteries with contribution from intracranial vessels that perforate and supply the underlying calvarial bone.

2.3 Superficial Anatomy of Posterior Neck

In the design of a scalp flap, the skin from the posterior neck might sometimes need to be incorporated. Usually this is raised and transferred to the recipient site together with a scalp flap that is derived from the occipital region.

The anatomy of the posterior neck that concerns the elevation of a cutaneous flap encompasses the skin and the subcutaneous tissue, the fasciae, and the muscles encountered in the superficial level.

2.3.1 Skin and Subcutaneous Tissue

The skin and subcutaneous tissue layer of the posterior cervical region is thicker than the corresponding layer of the anterior neck but thinner than that of the back of the torso. The presence of hair, as an extension from the hair-bearing occipital scalp to the nuchal region, depends on gender and race and also varies from one individual to the other. The relaxed skin tension lines are almost horizontally oriented like the ones of the posterior scalp (Fig. 2.13).

2.3.2 Deep Cervical Fascia

Just beneath the skin and subcutaneous tissue, the investing layer and the prevertebral layer of the deep cervical fascia are encountered (Fig. 2.14). The investing layer of the deep cervical fascia appears at the nape of the neck as a thin fascia that running from its bone attachments envelopes first the trapezius and then the sternocleidomastoid muscle in each side, as it passes anteriorly to encircle the whole neck (see Chap. 8). Superiorly, along the superior nuchal line, it fuses with the periosteum of the occipital bone. The prevertebral layer of the deep

Fig. 2.13 Relaxed skin tension lines (RSTLs) at the posterior neck and posterior scalp

cervical fascia lies beneath the previous one and is encountered at the gap between the sternocleidomastoid and trapezius muscles covering the splenius capitis and the semispinalis capitis muscles. The investing and the prevertebral layers of the deep cervical fascia and the tendinous origin of the upper muscle fibers of the trapezius all fuse together at the midline.

2.3.3 Superficial Muscles

The surface muscles that are encountered at the nape of the neck just under the skin and the deep cervical fascia are the trapezius, the splenius capitis, and the semispinalis capitis (Fig. 2.15). These muscles are arranged in three layers, each of them being under the other.

2.3.3.1 Trapezius Muscle

The trapezius muscle is an extended muscle of the upper limb that extends over the nape of the neck and the upper thorax. Its shape is triangular, with the upper angle corresponding to the external occipital protuberance, the lower angle to the spinous process of the twelfth thoracic vertebra, and the lateral angle to the acromion. The paired triangular muscles form a wide trapezium, from which the name is derived.

The muscle is subdivided in an upper, a middle, and a lower part according not only to the topography but also to the different muscle fibers' direction. The upper muscle part is the part of interest in the nape of the neck.

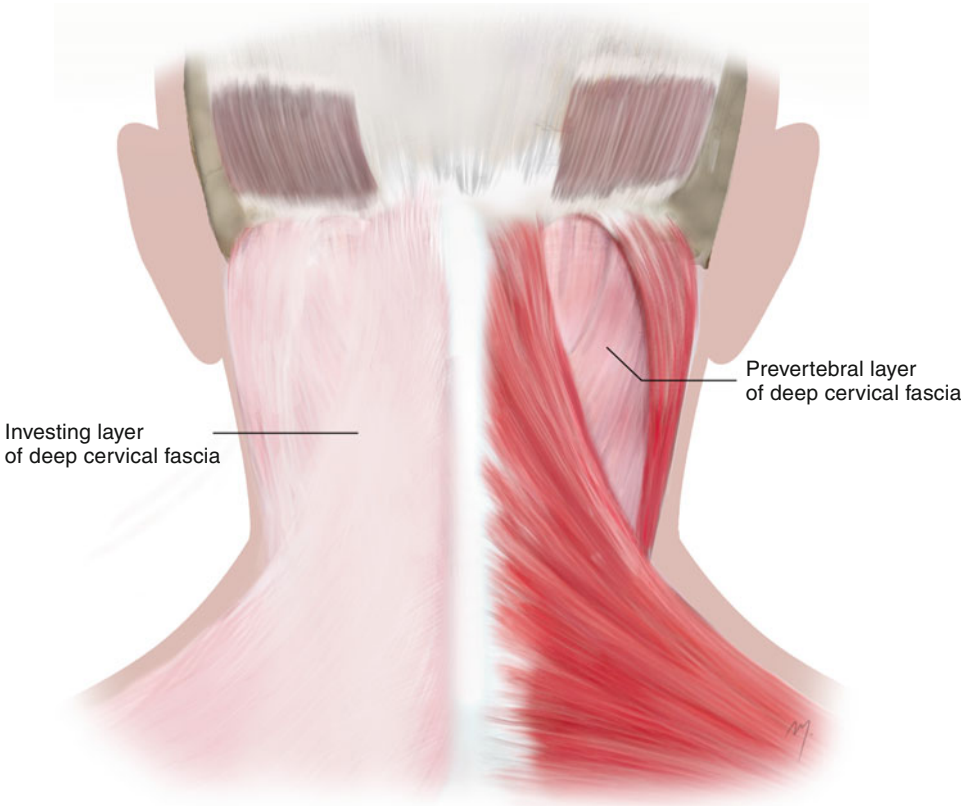

Fig. 2.14 The layers of the deep cervical fascia at the posterior neck. The investing layer lies superficial and encircles the whole neck (*left side*). When the investing layer is removed (*right side*), the deeper prevertebral layer is encountered at the gap between the sternocleidomastoid and the trapezius muscles

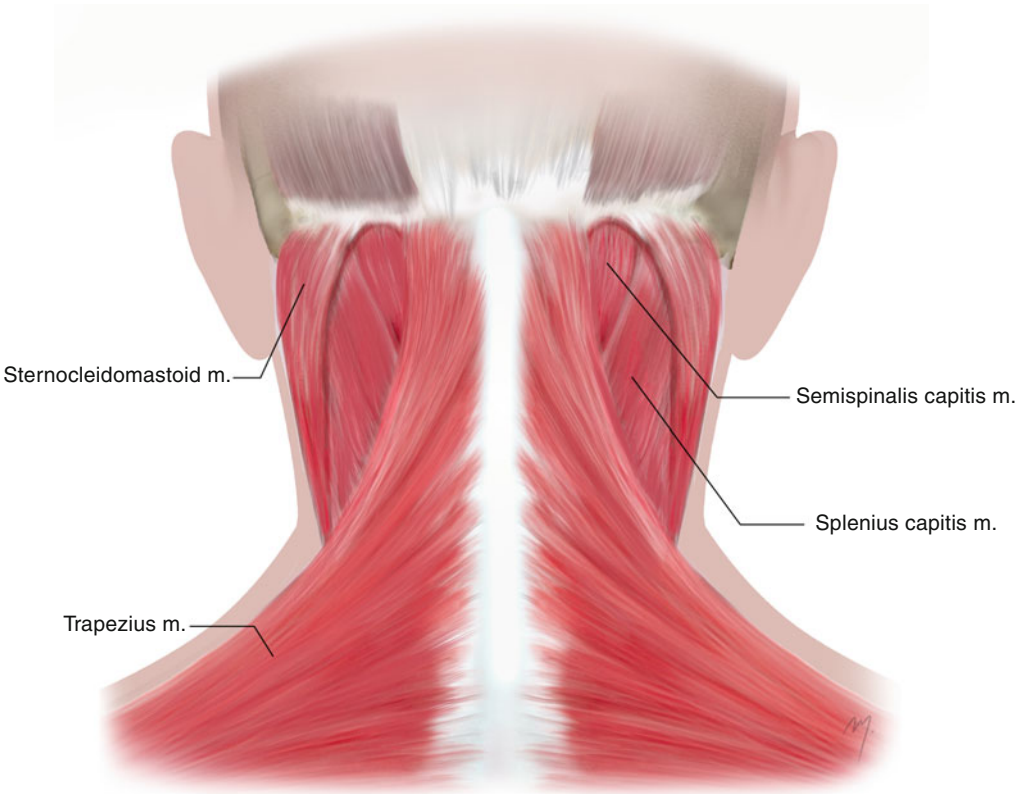

Fig. 2.15 Superficial muscles of the posterior neck

2.3.3.1.1 Upper Part of the Trapezius Muscle

The muscle fibers of the upper part arise from the medial third of the superior nuchal line, the external occipital protuberance, and the nuchal ligament. The attachment of this part is by an adherent to the skin, thin aponeurotic fibrous lamina, which is also continuous with the aponeurosis at the insertion of the sternocleidomastoid muscle. The occipital artery and the greater occipital nerve pierce this fibrous lamina. The muscle fibers of the upper part of the trapezius muscle descend to meet the horizontally running fibers of the middle muscle part and the ascending lower fibers as they all converge laterally to the shoulder. The fibers of the upper part of the trapezius are attached to the posterior border of the lateral third of the clavicle and the scapula. This part of the trapezius muscle is vascularized by the transverse muscular branch of the occipital artery (contributed by branches of the ascending superficial cervical artery) and is innervated by branches of the accessory nerve. The upper part of the trapezius elevates the scapula, and with the scapula steady, it bends the head backward and laterally.

2.3.3.2 Splenius Capitis Muscle

Splenius capitis lies deep to the trapezius muscle and its upper part beneath the sternocleidomastoid muscle. It fills the gap between the sternocleidomastoid and trapezius, forming the upper part of the floor of the posterior triangle of the neck. It completely covers the longissimus capitis and almost all of the semispinalis capitis, except a small triangle of its upper part, just suboccipital.

The muscle fibers of the splenius capitis arise from the lower half of the nuchal ligament and the spinous processes of the 7th cervical and 1st, 2nd, 3rd, and 4th thoracic vertebrae. The fibers run upward and laterally under the trapezius and the sternocleidomastoid. They insert to the mastoid process and just below the lateral third of the superior nuchal line. The descending branches of the occipital artery supply the upper portion of the splenius capitis muscle. The lateral branches of the dorsal rami of the middle cervical spinal nerves innervate the muscle. The splenius capitis acts as synergist with the contralateral sternocleidomastoid. When it acts bilaterally, it draws the head backward and extends the neck.

2.3.3.3 Semispinalis Capitis Muscle

The semispinalis capitis lies under the splenius capitis muscle and belongs to the transversospinalis muscle system of the deep muscles of the back. It arises by the tendons from the articular processes of the lower (4th, 5th, 6th) cervical vertebrae and from the transverse processes of the last cervical (7th) and the half of the thoracic vertebrae (1st–6th). The muscle fibers run upward and insert to the middle part of the area between the superior and inferior nuchal lines. A small

triangular area in the upper part of the muscle, between the trapezius and the splenius capitis, lies under the skin. This triangular part constitutes the floor of the apex of the posterior triangle of the neck. The descending branches of the occipital artery supply the upper part of the muscle. The semispinalis capitis is innervated by the dorsal rami of the cervical and thoracic spinal nerves. The semispinalis capitis extends the head turning the face slightly to the contralateral site. When acting bilaterally, they extend the head and the neck.

2.4 Vascular Anatomy

2.4.1 Arterial Anatomy of the Scalp and Temple

The vascular system of the scalp mainly consists of the superficial temporal, posterior auricular, and occipital arteries that are branched from the external carotid artery. The internal carotid system that provides the majority of blood supply to the forehead (through the supraorbital and supratrochlear arteries) supplies the anterior part of the scalp by the terminal parts of these vessels. Bone perforators of the meningeal arteries provide a small contribution to the scalp blood supply.

The major scalp arteries run within and on the surface of the musculoaponeurotic layer. They give branches directly to the above subcutaneous layer that form the subcutaneous vascular plexus and branches to the deeper loose areolar tissue layer.

2.4.1.1 Terminal Parts of the Supraorbital Artery and Supratrochlear Artery

The terminal part of the superficial branch of the supratrochlear artery as it ascends turns slightly toward the midline, where it reaches the frontal portion of the scalp, traveling in the subcutaneous level. Some of the sub-branches of the superficial branch of the supraorbital artery, as they travel lateral to the supratrochlear artery in a same plane, may sometimes reach and contribute to the vascular supply of the frontal scalp. However, both arteries perfuse significantly the vascular plexus of the frontal scalp and must be taken into account during scalp flap design (Fig. 2.16).

2.4.1.2 Superficial Temporal Artery at the Scalp

The course of the superficial temporal artery at the scalp is the part of its course over the zygomatic arch (Fig. 2.17). As the artery comes from the preauricular region, it is found passing over the posterior root of the zygomatic process. The artery runs within the temporoparietal fascia, and as it continues branching, it becomes more superficial and runs

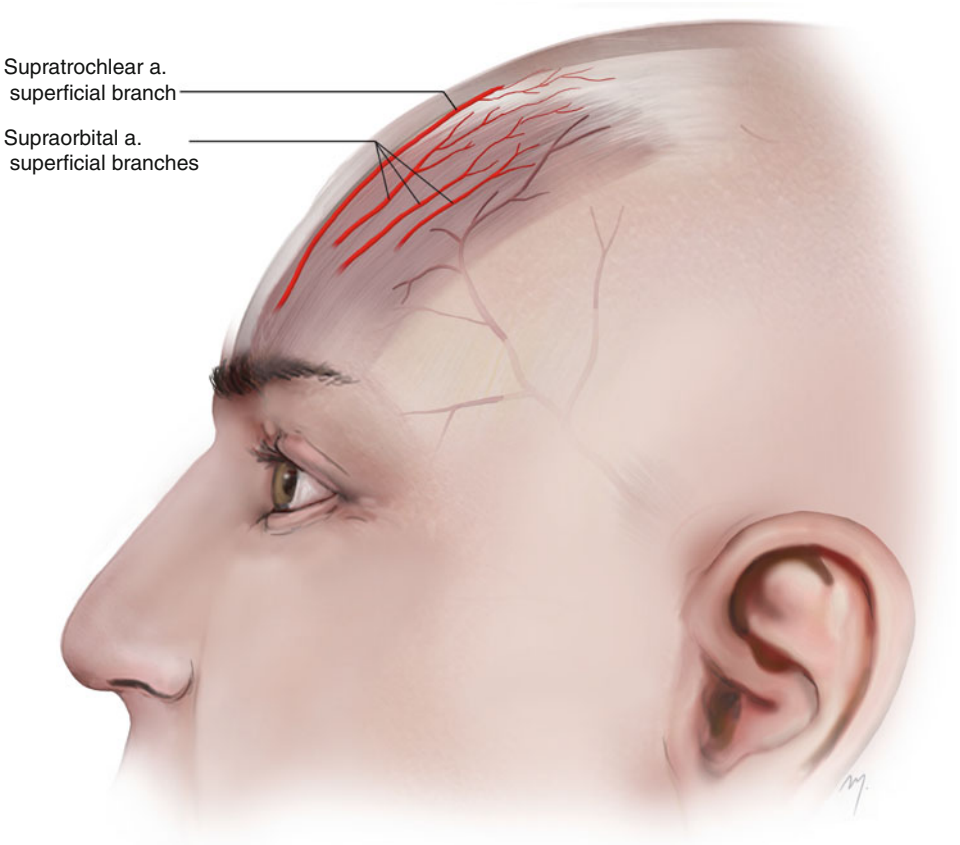

Fig. 2.16 The terminal parts of the supraorbital and supratrochlear arteries contribute to the vascular supply of the most anterior part of the scalp

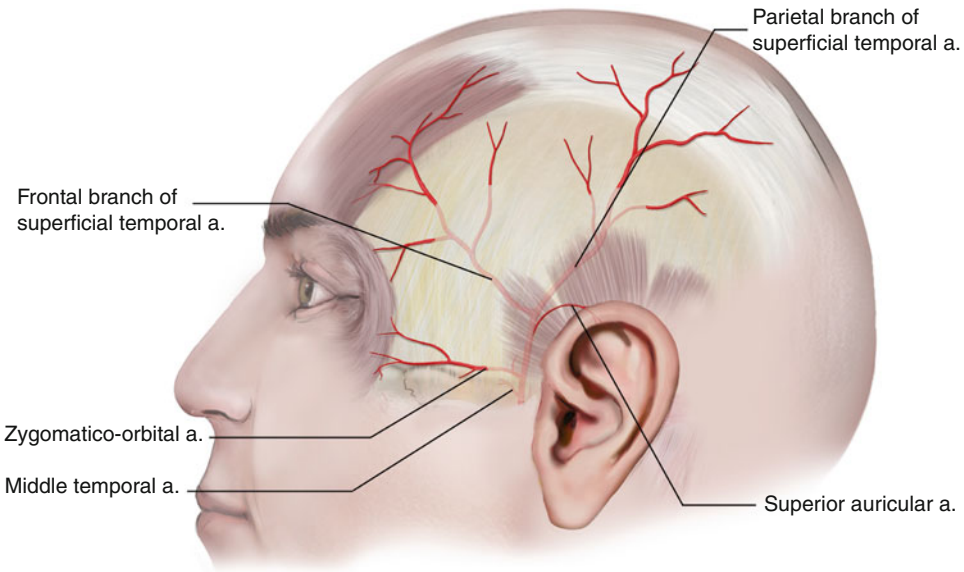

Fig. 2.17 The superficial temporal artery at the temple and its branches

over the surface of the fascia. It runs upward giving off some branches and finally bifurcates into the frontal (anterior) and parietal (posterior) final branches. The bifurcation of the superficial temporal artery into its terminal frontal and parietal branches occurs above the zygomatic arch in the majority of the individuals (60–88 %). Bifurcation at the level of the arch has been reported to range between 4 and 26 %, whereas bifurcation below the arch ranges between 8 and 11 % of individuals (Stock et al. 1980; Marano et al. 1985; Abul-Hassan et al. 1986; Czerwinski 1992; Nakajima et al. 1995; Chen et al. 1999; Pinar and Govsa 2006; Tayfur et al. 2010). Rarely, in approximately 3.7 % of cases, the artery does not bifurcate and courses only as a frontal branch, and the parietal branch is absent (Pinar and Govsa 2006).

When the bifurcation of the superficial temporal artery occurs above the zygomatic arch, it happens at a point within 2–4 cm above the arch. At the branching point, the diameter of the artery is approximately 1.8–2.7 mm (Stock et al. 1980; Marano et al. 1985; Abul-Hassan et al. 1986; Chen et al. 1999; Pinar and Govsa 2006).

2.4.1.2.1 Branches of the Superficial Temporal Artery at the Temple

The superficial temporal artery, after branching the transverse facial artery to the cheek (see Chap. 5), gives off the rest of its branches over the zygomatic arch at the temporal region (Fig. 2.17).

1. *Middle Temporal*
   The middle temporal artery arises usually at the superior border of the zygomatic arch or alternatively 1–2 cm below its upper border. It pierces the superficial layer of the temporalis fascia immediately above its attachment to the zygomatic arch, enters the superficial fat pad, and then pierces the deep layer of the temporalis fascia. It runs along the undersurface of the temporalis fascia and finally anastomoses with the deep temporal arteries (branches of the maxillary artery). The middle temporal artery supplies the superficial fat pad and contributes to the supply of the temporalis muscle.
2. *Zygomaticoorbital Artery*
   The zygomaticoorbital artery arises immediately after the middle temporal artery and runs forward to the lateral orbit, along and close to the upper border of the zygomatic arch within the superficial temporal fat pad. It anastomoses with the palpebral and lacrimal branches of the ophthalmic artery. Sometimes it arises not from the main stem of the superficial temporal artery but from its frontal branch. During its course it gives off cutaneous branches that supply the overlying skin.

   In about 20 % of the individuals, the zygomaticoorbital artery may be absent and the supply of the lateral orbital region is taken off from the transverse facial artery and by small sub-branches of the superficial temporal artery (Pinar and Govsa 2006).
3. *Superior Auricular Artery*
   The superficial temporal artery at its temporal course gives rise to the superior auricular branch a small artery that contributes to the supply of the auricle (see Chap. 7).
4. *Frontal Branch of the Superficial Temporal Artery*
   The frontal branch of the superficial temporal artery after originating from the bifurcation of the superficial temporal artery runs tortuously upward and forward giving off ascending and descending branches at the temporal area. It has been reported that the diameter of the frontal branch of the superficial temporal artery measured at the level of bifurcation has a mean range between 1.6 and 2.1 mm (Stock et al. 1980; Lang 1995; Chen et al. 1999; Pinar and Govsa 2006; Edizer et al. 2009; Tayfur et al. 2010).

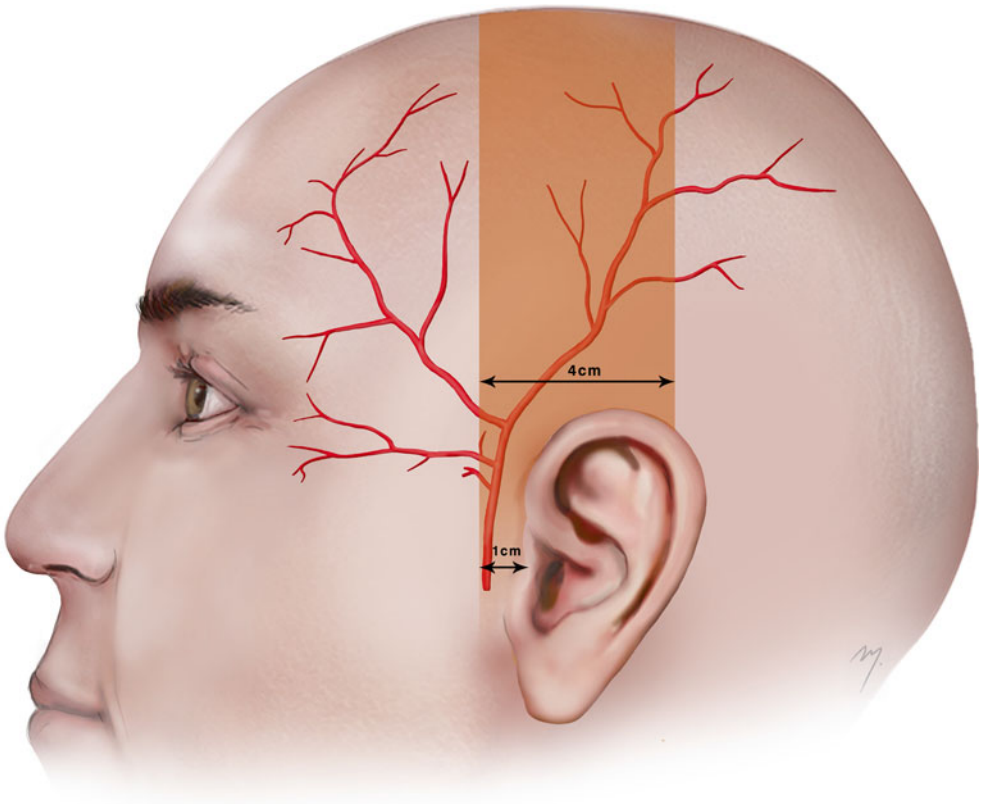

Fig. 2.18 The parietal branch in continuity with the superficial temporal artery runs within a vertical zone that starts 1 cm in front of the tragus and extends for 4 cm posteriorly

Its length is approximately 11 cm (Tayfur et al. 2010). Reaching the forehead it usually gives off a transverse branch, as the main continuation ascends superomedially. It travels superficial to the frontalis muscle becoming shallow up to the subdermal level as it approaches the midline.

The frontal branch of the superficial temporal artery supplies all the layers of the frontal scalp and constitutes the main vascular supply for the temporal subunits of the forehead. The artery is easily palpable in the temple and can be easily mapped in cases where it needs to be incorporated into the flap.

5. *Parietal Branch of the Superficial Temporal Artery*
The parietal branch of the superficial temporal artery after originating from the bifurcation of the superficial temporal artery runs on the side of the head curving slightly upward and backward. At the starting point, its diameter ranges between 1.6 and 1.8 mm (Stock et al. 1980; Lang 1995; Chen et al. 1999; Pinar and Govsa 2006; Tayfur et al. 2010). It lies initially within the temporoparietal fascia becoming more superficial and finally runs on the external surface of the galea. At a level 10–14 cm above the zygomatic arch, it becomes even more superficial and runs through the subcutaneous tissue layer (Tremolada et al. 1994).

Although the exact course of the temporal artery branches must be determined by Doppler examination, what follows is a useful landmark in regards to the position of the parietal branch that is quite accurate. The course of the parietal branch in continuity with the superficial temporal artery is presented within a vertical zone that starts 1 cm in front of the tragus and widens posteriorly for 4 cm (Fig. 2.18). Within this zone, the superficial temporal artery ascends almost vertically in front of the auricle, and after its bifurcation, the parietal branch continues curving up to the vertex. This constitutes a useful landmark in flap design when the parietal branch in continuity with the superficial temporal artery is to be caught in a scalp flap.

2.4.1.3 Posterior Auricular Artery

The posterior auricular artery is a small branch that arises from the posterior aspect of the external carotid artery above the digastric and stylohyoid muscles. It goes up between the parotid gland and the styloid process to the groove between the auricle and mastoid process. It gives off small neck branches (see Chap. 8) and at the level of the external auditory meatus pierces the deep fascia and divides into an auricular and occipital branch (Fig. 2.19).

2.4.1.3.1 Auricular Branch

The auricular branch ascends under the posterior auricular muscle. It gives off small branches that supply the skin of the posterior aspect of the ear and branches that pierce the

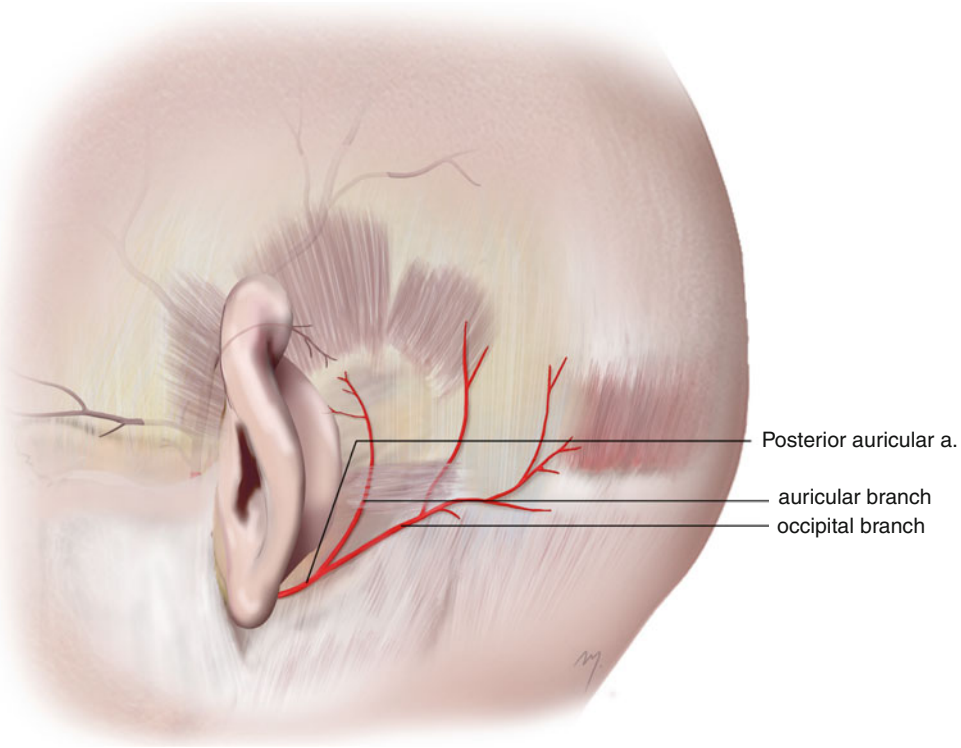

Fig. 2.19 Posterior auricular artery and its auricular and occipital branches

cartilage reaching the skin over the external surface of the ear (see Chap. 7). It anastomoses with the superior auricular artery, a branch of the superficial temporal artery.

2.4.1.3.2 Occipital Branch

The occipital branch runs laterally, across the mastoid process, over the insertion of the sternocleidomastoid muscle terminating over the occipitalis muscle. It supplies the posterolateral scalp.

2.4.1.4 Occipital Artery

The occipital artery arises from the posterior aspect of the external carotid artery about 2 cm from its origin and opposite to the origin of the facial artery. Its diameter is about 3 mm in its origin. At first it runs up- and backward, lying deep to the posterior belly of the digastric muscle. It crosses from the front the internal carotid artery, the internal jugular vein, the vagus, the hypoglossal, and the accessory nerves. Running in the occipital groove of the temporal bone and passing the medial aspect of the mastoid process, it reaches the occipital area. Here, it lies deep to the attachments of the sternocleidomastoid, splenius capitis, and longissimus capitis muscles.

In its final part, as it passes medially, it lies on to the semispinalis capitis muscle. It turns upward and 3.5–4.0 cm from the midline; the artery emerges through the attachments of the trapezius and sternocleidomastoid muscle (Fig. 2.20). After piercing the deep cervical fascia between the trapezius and sternocleidomastoid muscles, it ascends tortuously at the occipital area and divides into its terminal occipital branches.

2.4.1.4.1 Branches

The occipital artery during its long course gives off a great number of branches: meningeal branches that enter the skull through the jugular foramen; a small mastoid branch that supplies the mastoid antrum; the stylomastoid artery, which enters the stylomastoid foramen and supplies the facial nerve; and the tympanic cavity and the mastoid antrum, muscular branches that supply the digastric, stylohyoid, longissimus capitis, trapezoid, and splenius muscles.

The occipital artery gives off branches that through cutaneous or musculocutaneous perforators supply also the skin: The lower and the upper sternocleidomastoid branches supply the upper part of the sternocleidomastoid muscle and the overlying neck skin (see Chap. 8). The descending branch, the transverse muscular branch for the trapezius muscle, and the cutaneous cervical branches contribute to the supply of the skin of the nape of the neck.

The occipital artery, just after emerging from the cranial attachments of the trapezius and sternocleidomastoid muscle, appears at the posterior scalp. It ascends tortuously over the occipitalis muscle and the galea within the dense subcutaneous tissue of the scalp and divides very quickly in its terminal occipital branches. The terminal occipital branches distribute to the posterior scalp running tortuously as high as the vertex constituting the major arterial system of the posterior scalp. Many of the terminal branches run in company with branches of the greater occipital nerve often having a straight anatomic intersection, or they can be intertwined in a helical form. The final part of the occipital artery and its terminal occipital branches supply the posterior scalp and the pericranium.

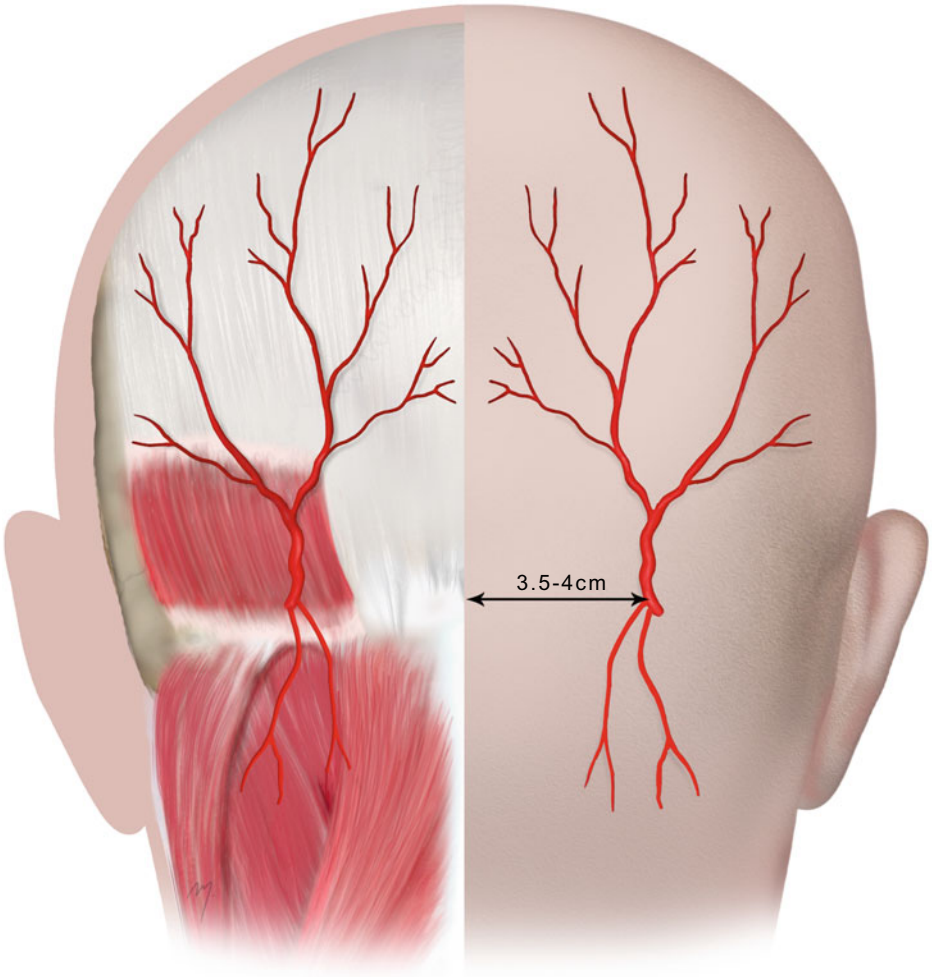

Fig. 2.20 Occipital artery. Distribution of the occipital branches to the posterior scalp and the distance of emerging point from midline

2.4.2 Vascularization of the Skin of the Posterior Neck

A major, direct cutaneous arterial vessel that supplies the posterior cervical skin does not exist. Musculocutaneous perforators are branched from the deep arteries and pierce the posterior neck muscles reaching the overlying skin. Minimum exception to this is the few direct small cutaneous branches coming from the occipital artery. The most important perforators come from branches of the occipital artery and the superficial cervical arteries (Fig. 2.21).

2.4.2.1 Branches of the Occipital Artery That Contribute to the Vascularization of the Skin of the Posterior Neck

1. The upper sternocleidomastoid branches give rise to perforators that are distributed to the skin of the upper lateral part of the nuchal region.
2. The transverse trapezius branch that arises at the level of the mastoid process reaches the upper portion of the trapezius in its deep surface. It then pierces the muscle giving off multiple small perforating vessels to the overlying skin (Standring 2008).
3. The descending branch arises from the occipital artery before it reaches semispinalis capitis. It descends and very quickly divides into a superficial and a deep ramus. The deep ramus descends below the semispinalis capitis and above the semispinalis cervicis and anastomoses with the deep cervical artery (costocervical trunk) and the vertebral artery. The superficial ramus descends above the semispinalis capitis and below the splenius capitis and anastomoses with the superficial cervical artery. Perforating vessels of these superficial rami supply the skin of the middle 3rd of the nape.
4. The cutaneous cervical branches are direct cutaneous branches, as an exception of the vascularization pattern of the skin of posterior neck. Immediately after the occipital artery emerges from the attachments of the trapezius and the sternocleidomastoid muscle, few small branches descend in the neighboring area of the upper part of the nape of the neck running into the subcutaneous tissue and supplying the skin.

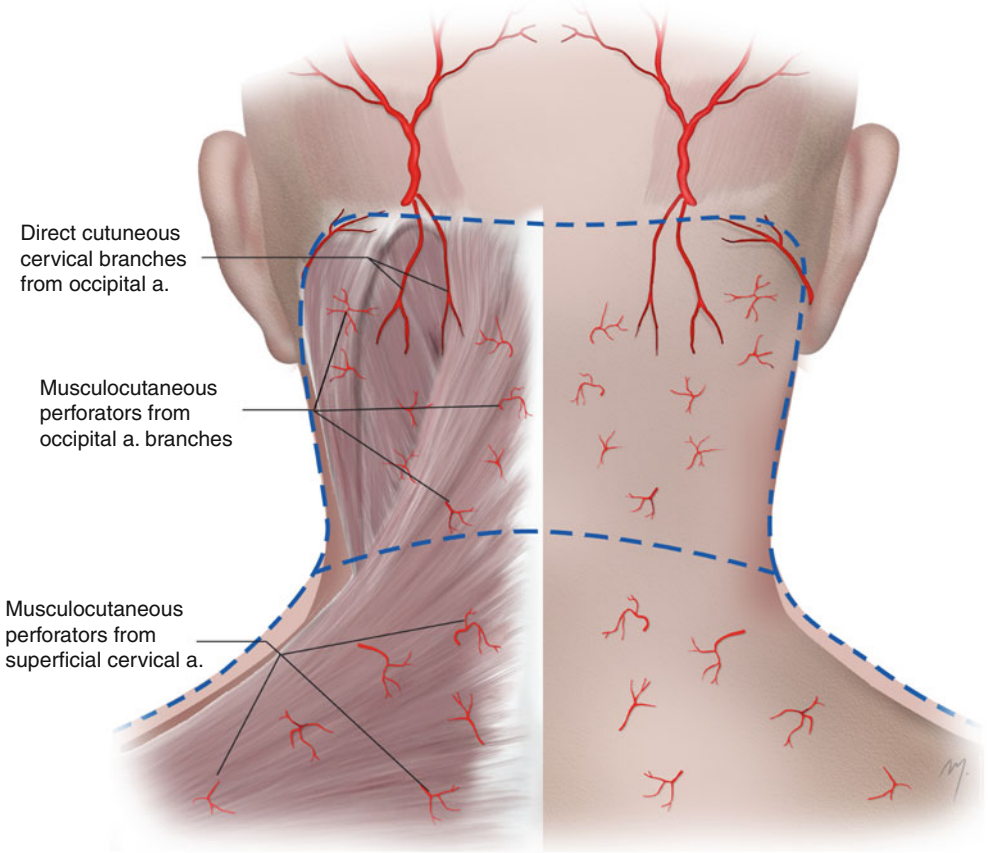

Fig. 2.21 The upper part of the skin of the nape of the neck is supplied by direct cutaneous and musculocutaneous perforators coming from branches of the occipital artery and the lower part by musculocutaneous perforators from the superficial cervical artery

2.4.2.2 Superficial Cervical Artery Musculocutaneous Branches to the Posterior Neck

The superficial cervical artery arises as an independent vessel from the thyrocervical trunk in 70 % of the cases or from a common arterial trunk, the transverse cervical artery, in the remainder along with the dorsal scapular artery, and is branched at the anterior border of the levator scapulae muscle (see Chap. 8).

Ascending beneath the anterior margin of the trapezius muscle, it gives off branches to the middle and lateral parts of the muscle (Haas et al. 2004). Musculocutaneous perforators from these branches supply the lower third of the skin of the nape of the neck. It anastomoses with the superficial ramus of the descending branch of the occipital artery.

2.4.3 Venous Drainage

The veins of the scalp (Fig. 2.22) accompany the arteries in a variable distance away from them that can be found as much as 3 cm. They form a rich anastomotic network and are also connected to the diploic veins. Small veins converge, forming gradually larger venous trunks that are the supratrochlear and supraorbital veins, the superficial temporal vein, the posterior auricular vein, and the occipital vein.

2.4.3.1 Supratrochlear and Supraorbital Veins

The supratrochlear and supraorbital veins drain the anterior scalp region and are examined in Chap. 3.

2.4.3.2 Superficial Temporal Vein

Converged veins from the lateral scalp form the frontal and parietal veins. Above the zygomatic arch, the frontal and parietal veins join together and form the superficial temporal vein. These veins run parallel to the corresponding arteries lying approximately 3 cm posterior and slightly more superficial to them, lying over the temporoparietal fascia. The superficial temporal vein descends in front of the auricle and receives the middle temporal and the transverse facial veins. It enters the parotis and unites with the maxillary vein forming the retromandibular vein.

2.4.3.3 Posterior Auricular Vein

The posterior auricular vein is formed by the venous network that drains the posterolateral region of the scalp. It descends behind the auricle and below (or some time in) the parotid gland joins the posterior division of the retromandibular vein. By the junction of the posterior auricular and the posterior division of the retromandibular veins is formed the external jugular vein.

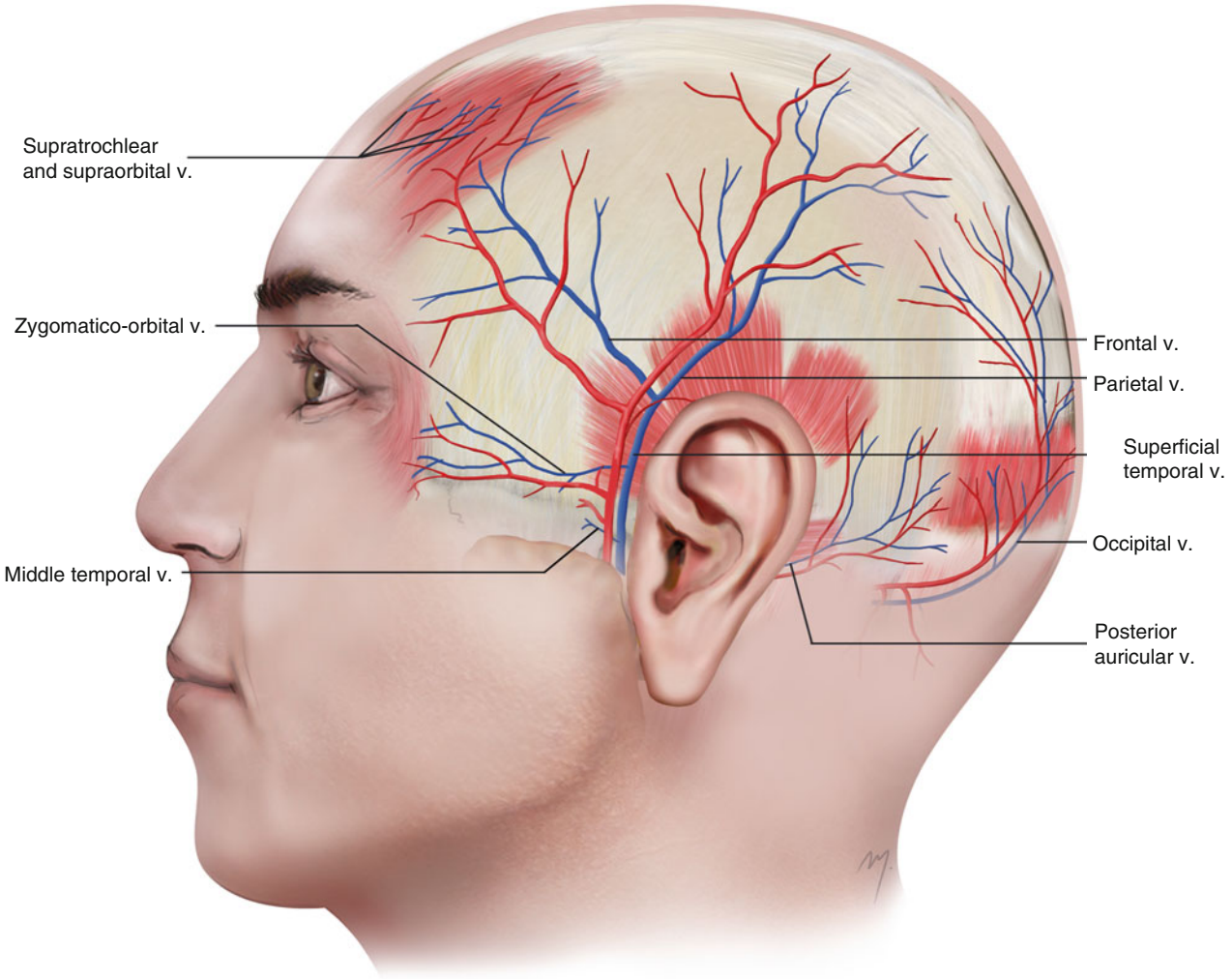

Fig. 2.22 Veins of the scalp

2.4.3.4 Occipital Vein

The small veins of the posterior scalp converge gradually and form both occipital veins. Each occipital vein descends accompanying its corresponding artery, pierces the cranial attachments of the trapezius and sternocleidomastoid muscles, and joins the deep cervical and vertebral veins. In some cases the occipital artery ends in the internal jugular vein and in other joins the posterior auricular vein and drains into the external jugular vein (Standring 2008).

2.4.4 Nerves

2.4.4.1 Sensory Nerves

Eight nerve branches of either the trigeminal or the cervical nerves supply sensory innervation of the scalp and temple (Figs. 2.23 and 2.24). The supraorbital and the supratrochlear nerves are branches of the ophthalmic division of the trigeminal nerve (V1). The zygomaticotemporal nerve is a branch of the maxillary division of the trigeminal nerve (V2), and the auriculotemporal nerve is a branch of the mandibular division of the trigeminal nerve (V3). The greater auricular and the lesser occipital nerve are branches of the cervical plexus. The greater occipital nerve is a branch of the posterior (dorsal) ramus of the second cervical nerve (C2), and the third occipital nerve, a branch of the third cervical (C3) dorsal ramus.

2.4.4.1.1 Branches of the Trigeminal Nerve

1. *Supratrochlear and Supraorbital Nerve*
   According to their length, the terminal branches of the supratrochlear nerve may reach the midportion of the anterior scalp providing sensory supply. In the similar way, the superficial (medial) branches of the supraorbital nerve provide sensation to the frontal scalp in various ranges. The deep branch (or branches) of the supraorbital nerve (see Chap. 3) ascends at the forehead in the loose areolar tissue beneath the frontalis muscle. At the level of

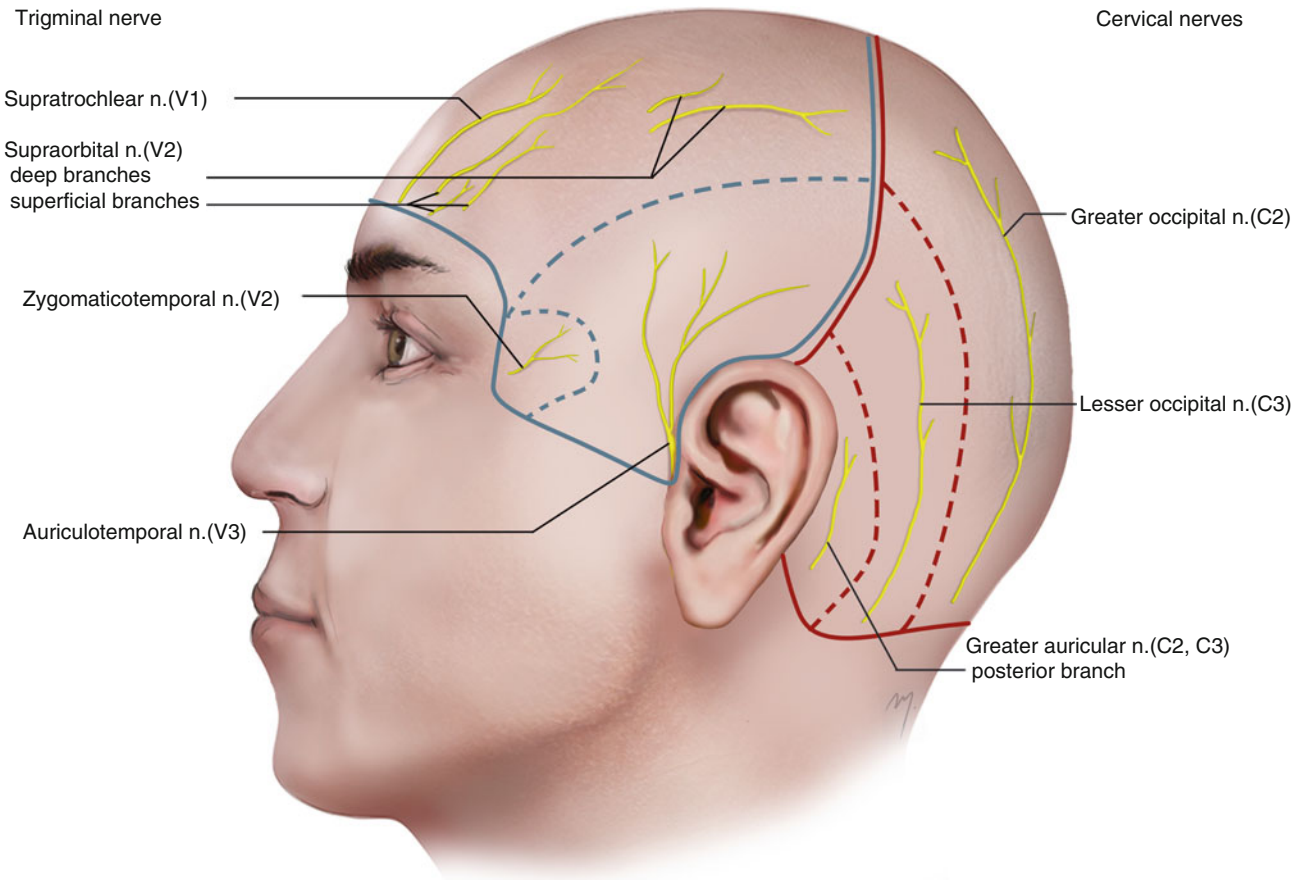

Fig. 2.23 Sensory innervation of the scalp and temple (lateral view). Blue line encompasses the area supplied by branches of the trigeminal nerve and red line the area supplied by branches of the cervical nerves

the hairline it pierces the galea becoming superficial and travels backwards (with variable length), where it divides to its terminal rami (see Chap. 3). The terminal rami supply scalp sensation to the frontoparietal region occasionally reaching the vertex of the skull.

2. *Zygomaticotemporal Nerve*

The zygomaticotemporal nerve is one of the two branches of the zygomatic nerve that arises from the maxillary nerve, the intermediate division of the trigeminal nerve. The maxillary nerve in its course in the pterygopalatine fossa gives off the zygomatic nerve along with the posterior superior alveolar nerve and the two gangleonic branches to the pterygopalatine ganglion. The zygomatic nerve enters into the orbit through the inferior orbital fissure. It runs forward along the lateral orbital wall and divides into zygomaticotemporal and zygomaticofacial nerves.

The zygomaticotemporal nerve after arising from the zygomatic nerve runs along the inferolateral angle of the orbit. It sends an anastomotic branch to the lacrimal nerve and enters the zygomaticotemporal canal of the zygomatic bone. Through this canal it exits the orbit from the zygomaticotemporal foramen and enters the anterior part of the temporal fossa. It runs upward lying between the undersurface of the temporalis muscle and the periosteum. At a point approximately 10 mm posterior and 10 mm inferior to the frontozygomatic suture and 20 mm above the zygomatic arch, it pierces the temporalis fascia (Hwang et al. 2004; Jeong et al. 2010). As it becomes subcutaneous, it innervates the scalp over a small area of the anterior part of the temple.

3. *Auriculotemporal Nerve*

The auriculotemporal nerve after its preauricular course at the cheek (see Chap. 5) passes over the posterior root of the zygomatic arch and at the temple gives off its final temporal branches. In its temporal course, the nerve is situated above the temporoparietal fascia. It runs parallel to the superficial temporal artery being in 80 % superficial or posterior to it (Jeong et al. 2010). It communicates with the zygomaticotemporal and facial nerves. The superficial temporal branches of the auriculotemporal nerve supply the skin over the tragus, the anterior portion of the ear, and the anterior temporal region.

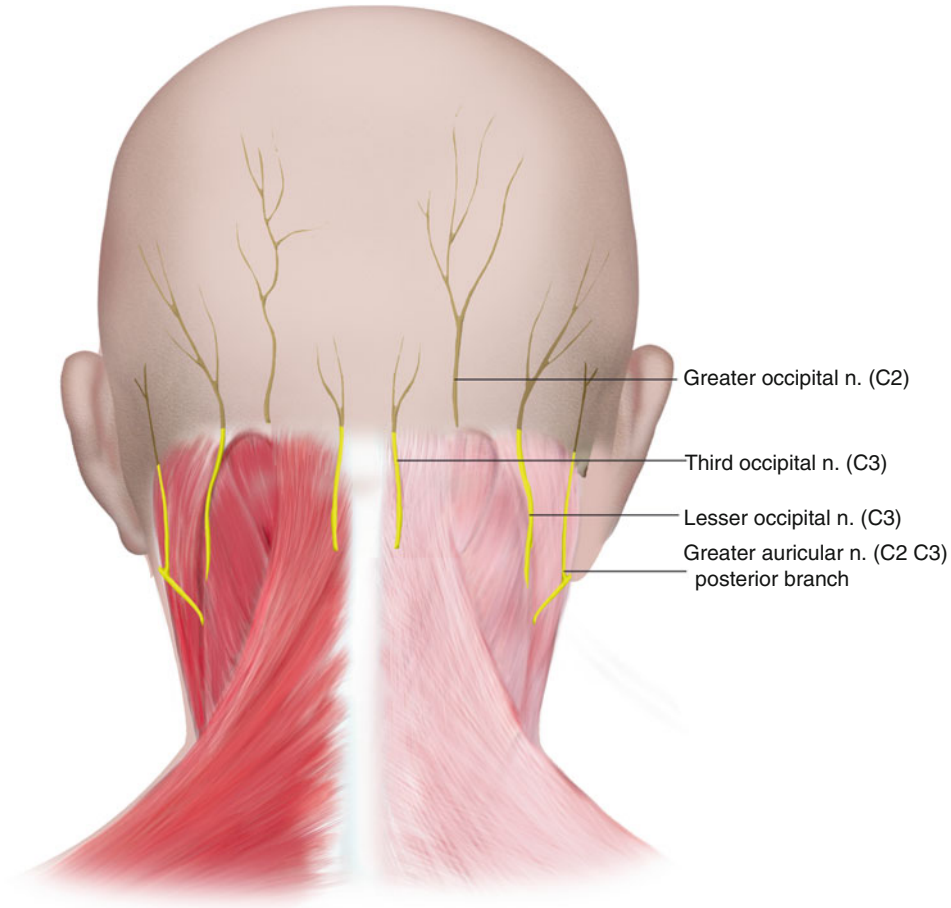

Fig. 2.24 Branches of the sensory cervical nerves to the scalp and the points where they become superficial piercing the deep cervical fascia

2.4.4.1.2 Branches of the Cervical Nerves to the Scalp

1. *Greater Auricular Nerve: Posterior Branch*
   The posterior branch of the greater auricular nerve (see Chap. 8) is branched at the level of the lower pole of the parotid gland and ascends over the upper third of the sternocleidomastoid muscle. It reaches the mastoid and the postauricular region passing in a distance of up to 1.5 cm behind the ear lobule (Izquierdo et al. 1991).

   The posterior branch supplies the skin that overlies the mastoid process and the lower part of the posterior auricle. One of its filaments pierces the auricle reaching its lateral surface and innervates the concha and the lobule, while other filaments anastomose with the lesser occipital nerve, the auricular branch of the vagus, and the posterior auricular branch of the facial nerve (Standring 2008).
2. *Lesser Occipital Nerve*
   The lesser occipital nerve is a cutaneous branch of the cervical plexus that emerges at the neck and travels along the posterior margin of the sternocleidomastoid muscle to the occiput (see Chap. 8). Near the cranium it pierces the deep fascia and enters the subcutaneous layer supplying the occipital part of the scalp. The nerve lies over the occiput 2.5 cm lateral to the occipital artery and 7 cm lateral to the external occipital protuberance (Tubbs et al. 2007; Kemp et al. 2011).
3. *Greater Occipital Nerve*
   The greater occipital nerve is the continuation of the medial branch of the second cervical (C2) dorsal ramus. The nerve runs initially over the inferior oblique capitis and thereafter over rectus capitis posterior major muscles, under the cover of the semispinalis capitis muscle. As it ascends to become superficial, it traverses the semispinalis capitis muscle, and it enters into the trapezius muscle. It then pierces the aponeurosis of the trapezius approximately 35 mm from the midline and 9 mm below the occiput and emerges into the occipital scalp (Natsis et al. 2006; Janis et al. 2010a, b).

   After reaching the occipital scalp, it runs upward within the subcutaneous areolar tissue, in company with the final branches of the occipital artery as far as the coronal suture, supplying the skin of the median occipital and parietal regions of the scalp. In about half of the individuals, an anatomic intersection between the greater occipital nerve and the occipital artery is present, mostly in helical form that could act as an additional trigger point for migraines

(Janis et al. 2010a, b). The grater occipital nerve anastomoses with the third occipital and the lesser occipital nerves and innervates the most of the posterior scalp.

4. *Third Occipital Nerve*
   The third occipital nerve is the superficial medial branch of the third cervical (C3) dorsal ramus. It emerges onto the middle area of the posterior cervical region by piercing semispinalis capitis, splenius capitis, and trapezius muscles. It becomes cutaneous, runs upward (sometimes exciding for a short distance the superior nuchal line), and innervates a small area in the middle zone of the most posterior scalp. The third occipital nerve becomes subcutaneous 5 cm inferior to the inion and lies 3 mm lateral to it (Tubbs et al. 2011). It communicates with the cutaneous branches of the greater and lesser occipital nerves.

2.4.4.2 Motor Nerves

Two branches of the facial nerve, the most important frontal branch and the posterior auricular branch, are involved in the motor supply of the musculoaponeurotic layer of the scalp.

1. *Frontal Branch of the Facial Nerve (Frontal Nerve)*
   The frontal branch of the facial nerve innervates the frontal bellies of the occipitofrontalis muscle and the anterior and superior auricularis muscles. Its exact course and the depth where it runs are of great importance so as to avoid damage and preserve it when planning a flap that involves the forehead and temple area of the scalp.

   The frontal branch also referred as temporal branch arises from the temporofacial division of the facial nerve and exits from the upper border of the parotid gland (Fig. 2.25a). The course of the frontal branch of the facial nerve follows a relatively curved course from the parotid upward and forward to the lateral brow. It crosses the zygomatic arch in its mid-third where it may divide into sub-branches. The frontal nerve appears as single branch in 16 %–28 % of individuals. It divides into two rami in 32 %–52 %, three rami in 16 %–24 % and four rami in 4 %–8 % (Woltmann et al. 2000; Zani et al. 2003). These sub-branches can be distinguished as anterior, posterior, and middle rami.

   The posterior ramus innervates the anterior auricular and temporoparietal muscles and is of no significant functional or surgical importance.

   The frontal branch (either single or subdivided in the anterior and the middle rami) continues over the zygomatic arch and passes lateral to the lateral canthus in a variable distance that ranges from 1 to 2.5 cm (Pitanguy and Ramos 1966; Stuzin et al. 1989; Schmidt et al. 2001). It reaches the lateral border of the frontalis muscle and proceeds to its undersurface.

   The anterior and middle rami frequently have anastomotic connections between them and innervate (except the frontalis muscle) the upper and lateral portion of the orbicularis muscle by terminal branches that run in a same manner to its undersurface and the upper portion of the procerus muscle. In about 60 % of the individuals, a tiny ramus runs medially to innervate the transverse head of the corrugator muscle (Tzafetta and Terzis 2010). During its course, the frontal branch (either single or ramified) is situated always in front of the frontal artery. Only the tiny posterior ramus crosses the frontal or the superficial temporal artery as it runs toward the auricular muscles.

   The frontal branch leaving the upper border of the parotid gland travels deep to the parotidomasseteric fascia, toward the zygomatic arch. Crossing the superficial surface of the zygomatic arch (Fig. 2.25b), the temporal nerve is situated within the temporoparietal fascia, and across the temporal region, it travels along the undersurface of the temporoparietal fascia (Fig. 2.25c)

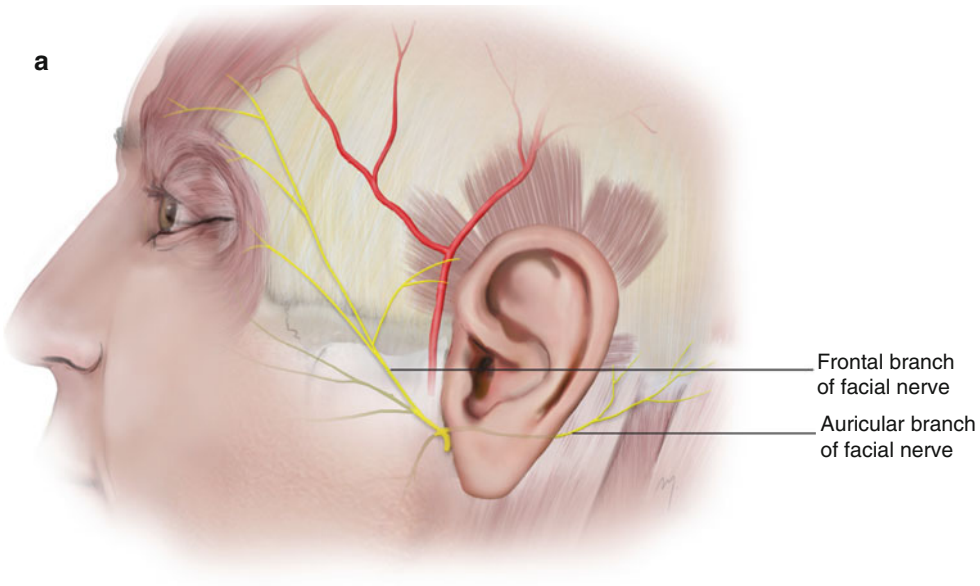

Fig. 2.25 (**a**) Frontal and posterior auricular branches of the facial nerve, (**b**) the frontal nerve at the zygomatic arch, (**c**) the frontal nerve above the zygomatic arch

Fig. 2.25 (continued)

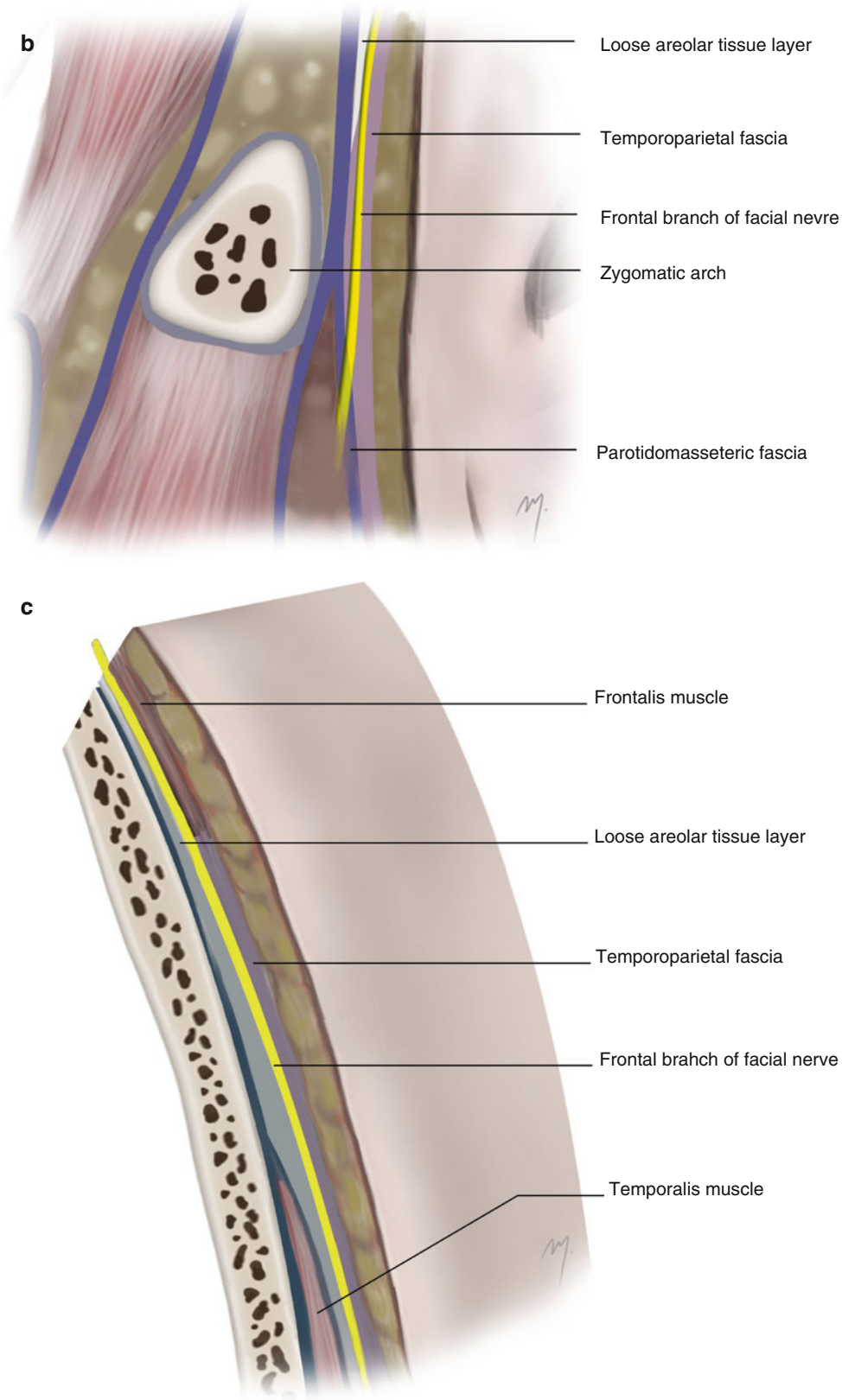

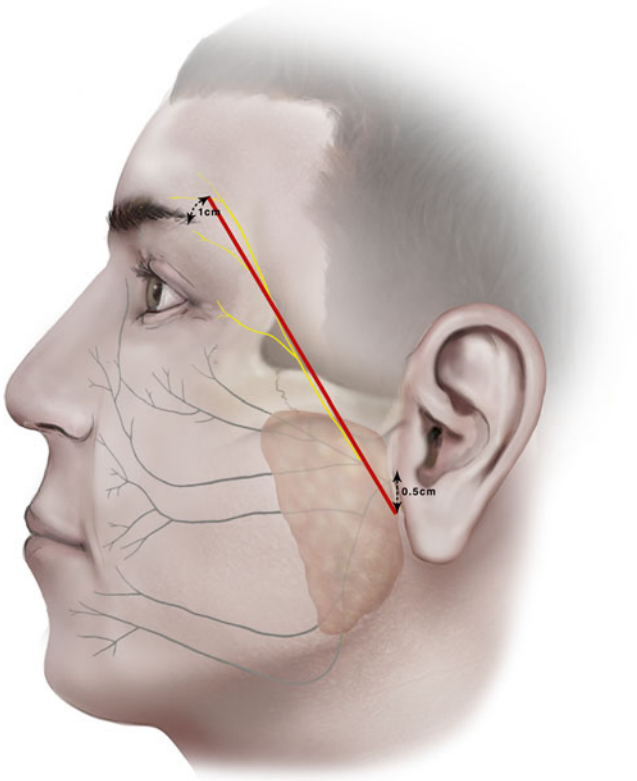

Fig. 2.26 The trajectory of the frontal nerve ("Pitanguy line")

(Stuzin et al. 1989). There are reports stating that the frontal nerve crosses the zygomatic arch in a deeper plane, just over the zygomatic arch periosteum (Owsley and Agarwal 2008; Trussler et al. 2010). Regardless of the precise level where the nerve is positioned, the fusion of planes at this level risks inadvertent nerve injury. At the lateral border of the frontalis, the frontal nerve passes under the muscle and runs under its undersurface.

The trajectory of the frontal nerve corresponds to a line named "Pitanguy line" that starts from a point 0.5 cm below the tragus and runs to a point 1 cm above the lateral edge of the eyebrow (Pitanguy and Ramos 1966) (Fig. 2.26).

2. *Posterior Auricular Nerve*
The posterior auricular (Fig. 2.25a) nerve arises from the facial nerve immediately after it emerges from the skull base at the stylomastoid foramen. It runs upward between the acoustic meatus and the mastoid process. It then runs backward along the superior nuchal line and inserts into the occipitalis muscle. As it proceeds, it gives off communicating branches to the great auricular and the lesser occipital nerves and a branch to the auricularis posterior muscle.

2.5 Flaps Derived from the Scalp and Temple

2.5.1 Flap Design Concerning Vascular Anatomy

The blood supply to the scalp is provided in a centripetal manner. The vessels, either trunks of the internal or the external carotid, reach the scalp from the periphery and run centrally as they branch. Multiple homo and heterolateral anastomoses occur forming a very extensive anastomotic network (Fig. 2.27a, b). The frontal branch of the superficial temporal artery anastomoses with the corresponding vessel of the opposite side, with its posterior parietal branch and also with the ipsilateral supraorbital and supratrochlear arteries. The parietal branch of the superficial temporal artery anastomoses with the frontal branch, the posterior auricular and the occipital arteries, and at the midline with the corresponding artery of the opposite side. The occipital branch of the posterior auricular artery anastomoses with branches of the occipital artery. Through the anastomotic rami the occipital artery anastomoses with the contralateral, the posterior auricular, and the superficial temporal arteries. This network is especially rich at a central circle with a diameter of 10 cm that corresponds to the vertex, where at the midline it exhibits one anastomosis every 5–7 mm (Marty et al. 1986). This robust vascular network of the scalp and temple allows for the design of versatile, random, or axial pattern flaps that survive even if they cross the midline.

2.5.2 Danger Zone of the Frontal Nerve

The temporal branch of the facial nerve is at great risk during dissection and flap elevation that are performed in the temporal and lateral forehead areas. Its exact course that is charted by means of landmarks in every area must be kept in mind so as to avoid injury.

The frontal nerve with its rami can be predicted to be running within a curved zone that starts from the mid-third of the zygomatic arch and ends 2.5 cm above the lateral aspect of the superior orbital rim (Fig. 2.28). Within this zone the frontal nerve is at great risk during surgical procedures. Keeping in mind the anatomy of the fascial layers in relation to the frontal nerve, the possibility of nerve injury is reduced.

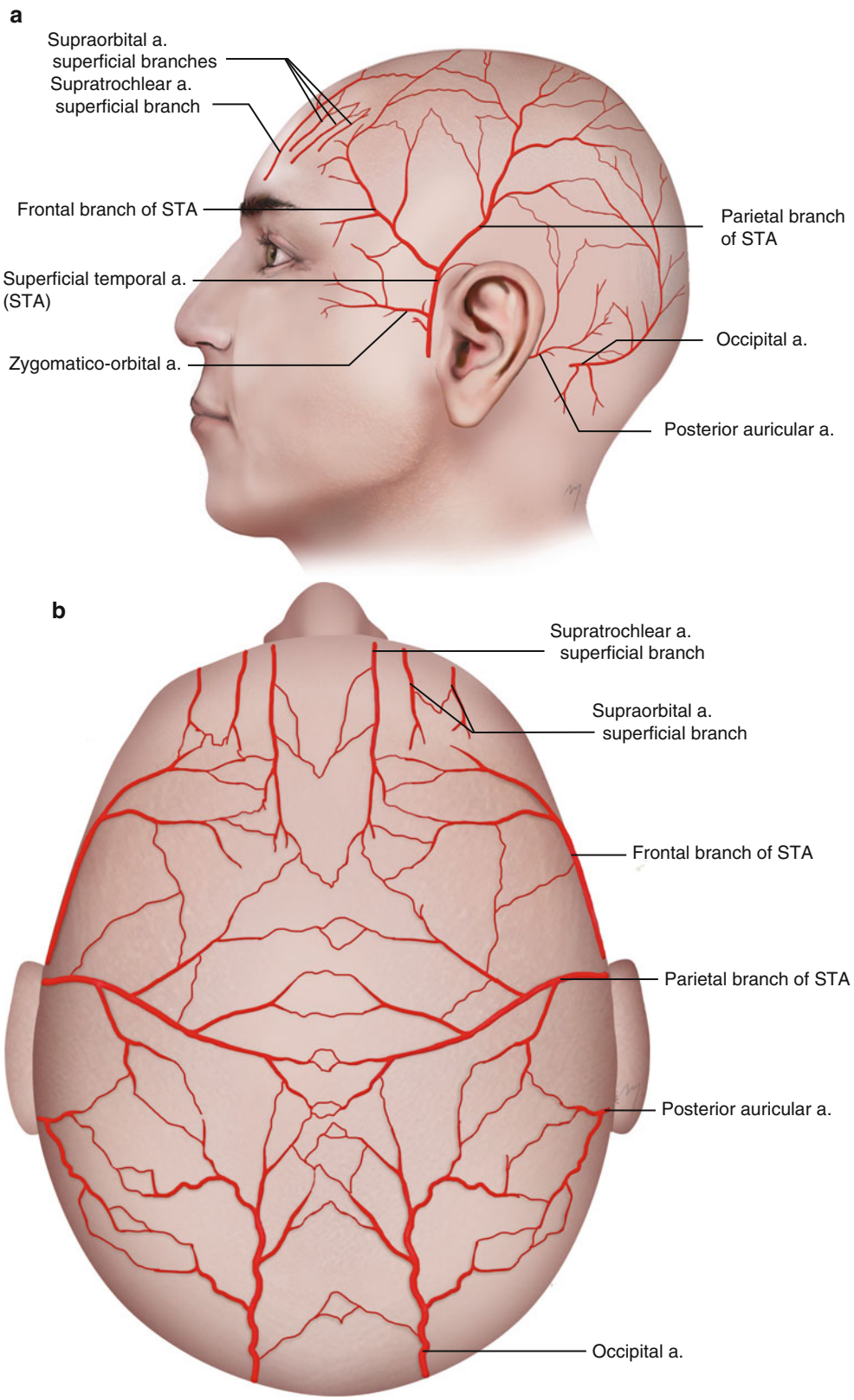

Fig. 2.27 Anastomotic network of the scalp arteries. (**a**) Lateral view. (**b**) Upper view

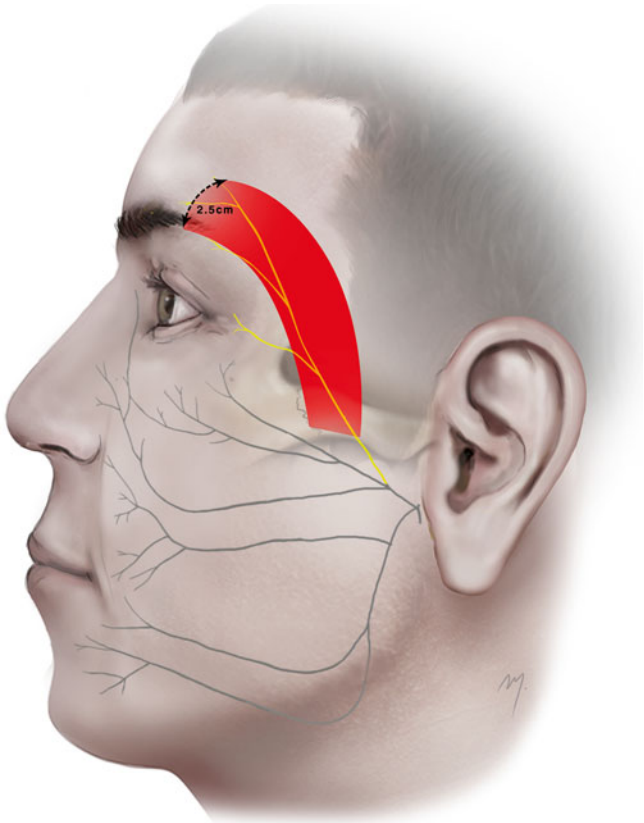

Fig. 2.28 Zone at risk of the frontal nerve

2.5.3 Flap Elevation Concerning Anatomic Planes

As opposed to other areas of the head and neck, flap elevation in the subcutaneous level at this region comes not in question due to the special anatomic features that have been already mentioned. Dissection in the loose areolar tissue (subgaleal plane) is the dissection plane in raising scalp flaps.

2.5.3.1 Subgaleal Plane (Loose Areolar Tissue Plane)

The subgaleal plane is the plane of the loose areolar tissue, which at the scalp is delimited between the musculoaponeurotic layer and the pericranium and at the temple continues between the temporoparietal fascia and the temporalis fascia.

Even though the layered architecture at the temple is not a strict continuation of the scalp, it is very easy to raise a scalp flap that includes a part from the temple in a same continuous level. Dissecting in the subgaleal plane raises the skin, subcutaneous tissue, musculoaponeurotic layer, and temporoparietal fascia as a single unit.

The nature of the loose areolar tissue layer allows a safe and rapid dissection that can be performed bluntly or sharply with scalpel, scissors, or even with the finger (Fig. 2.29a–c). Although numerous small blood vessels run through this plane, injection of a vasoconstrictive solution creates a relatively avascular dissection plane, with minimal bleeding.

By a more delicate dissection of the areolar tissue, a precise level either superficial or deep can be chosen. In the superficial level, dissection is performed at the scalp along the undersurface of the musculoaponeurotic layer and at the temporal region along the undersurface of the temporoparietal fascia. In the deep level, dissection is performed on top of the pericranium at the scalp and at the temporal region on top of the temporalis fascia.

2.5.3.2 Subperiosteal Plane

Elevation at the subperiosteal plane is very rarely needed in skin flaps of the scalp. An example of elevation at that plane is the case where a flap is extended at the supraorbital area where the subgaleal plane must transition to a subperiosteal plane so as to catch the supraorbital and supratrochlear neurovascular bundles (and their deep arterial branches), a maneuver performed mostly in forehead flaps.

Elevation at the subperiosteal plane is easily performed with periosteal elevators (Fig. 2.30). If the periosteum is detached also from its upper surface, it then constitutes a pericranial flap that can be advanced or rotated (Fig. 2.31). A pericranial flap can provide coverage to the bone devoid of pericranium or transferred to other areas acting as a bed to skin grafts, or it can be used in a variety of craniofacial procedures (e.g., sinus obliteration, dural reconstruction).

2.5.4 Worthen Rotation Flap

The design of a rotation flap at the scalp differs from other areas of the head and neck due to the stiffness and rigidity of that unit. Lack of elasticity needs strict geometry in design. A rotation flap, as designed by Worthen (1990), is very effective in reconstructing both medium and large scalp defects. Applying the geometrical principles as set by Worthen, the flap always reaches the defect easily, without the formation of a dog-ear or the need of a back-cut in its distal end as this happens in scalp rotation flaps designed in a conventional way.

2.5.4.1 Geometry of Worthen Rotation Flap

As already mentioned (see Chap. 1), the defect is converted to an isosceles triangle with its apex no more than 30°. From one of the triangle sides a projection line 1.5 times its length

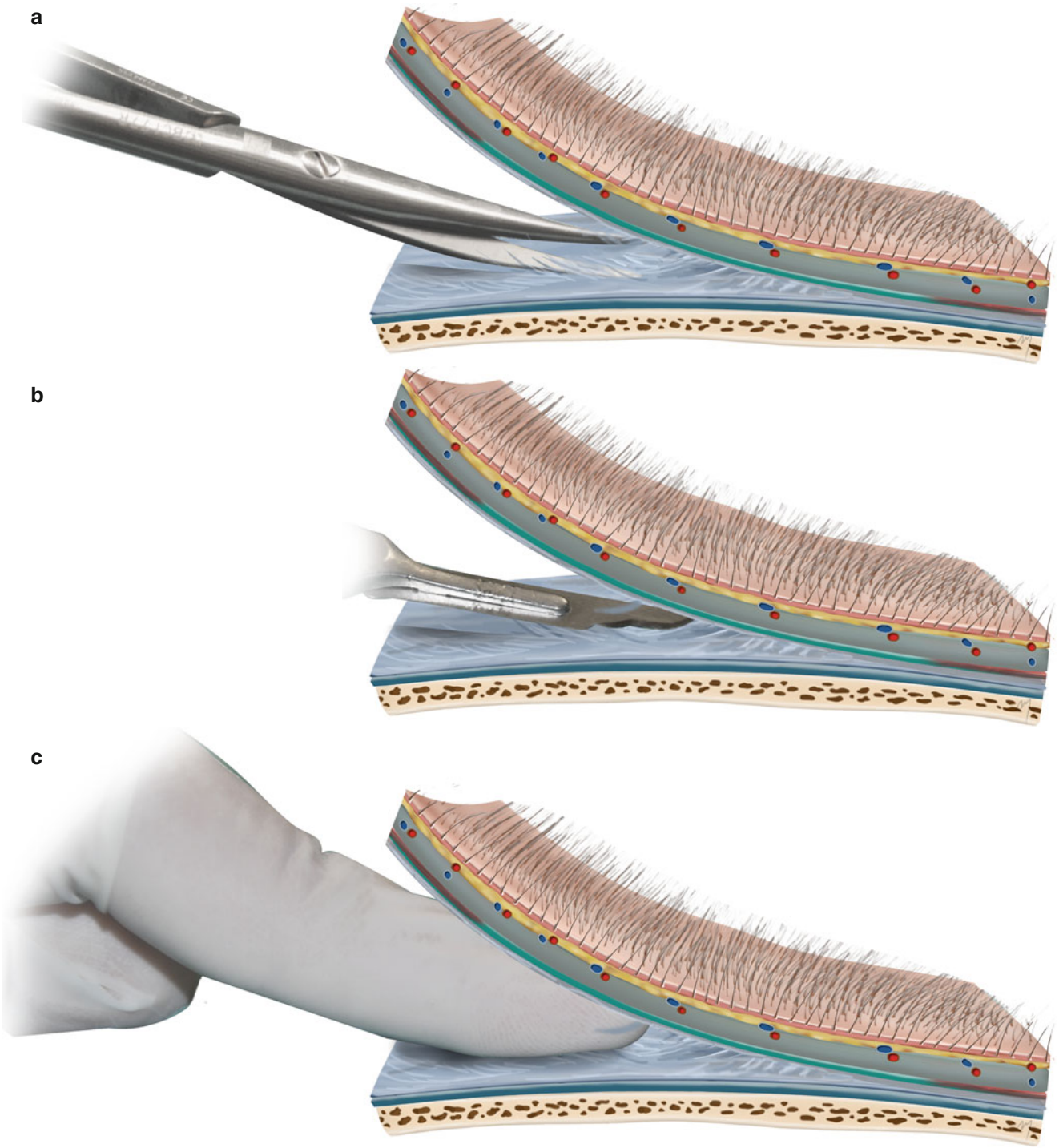

Fig. 2.29 (**a**–**c**) Dissection at the subgaleal plane can be performed quickly in various ways

is outlined. This line added to the triangle side is the diameter of the semicircular flap; thus, the arc is outlined. The above are presented in a lesion of the vertex in Fig. 2.32a. The lesion is excised and the flap raised in the subgaleal plane (Fig. 2.32b, c). The flap was rotated to the recipient site (Fig. 2.32d). The primary defect is distributed at the periphery as secondary defect, which by slight advancement of the adjacent scalp is closed without tension (Fig. 2.32e).

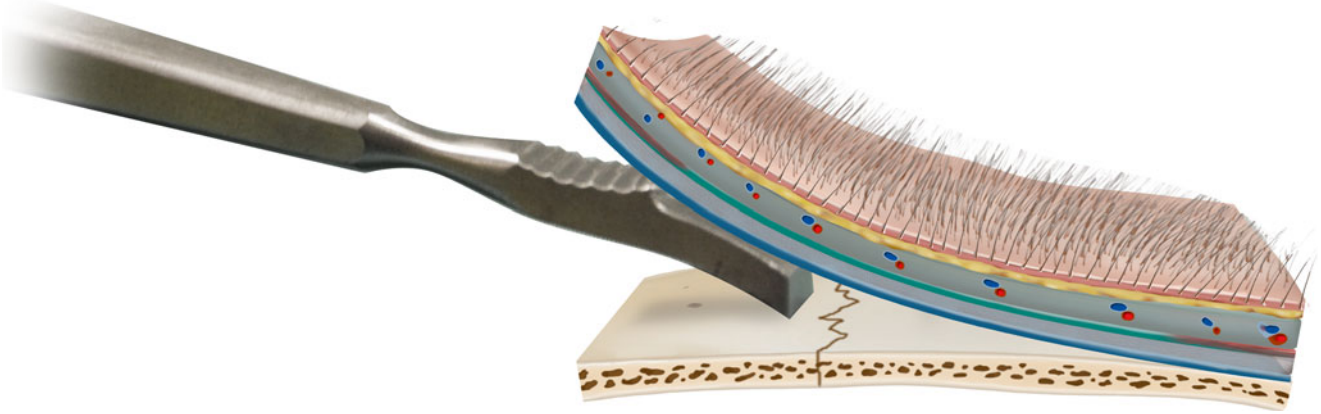

Fig. 2.30 Subperiosteal elevation is achieved by sharp square periosteal elevators

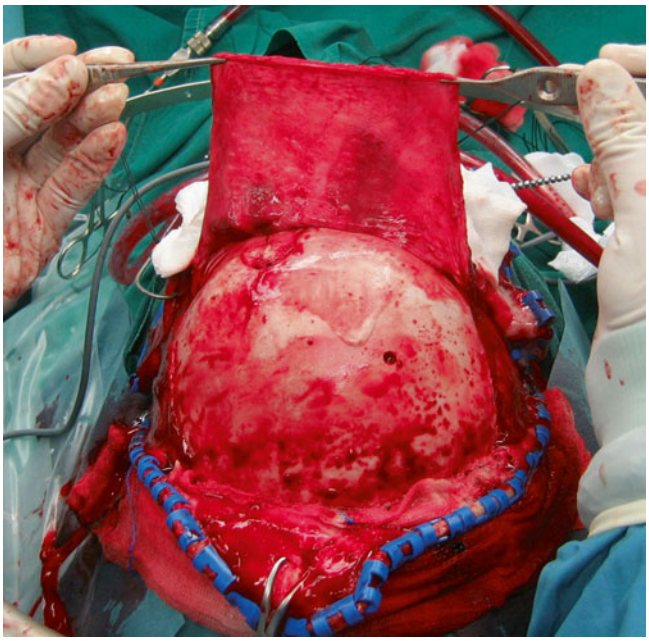

Fig. 2.31 Frontal pericranial flap

2.5.4.2 Orientation of Worthen Rotation Flap

The long axis of the lesion usually determines the orientation of the isosceles triangle that will surround the lesion thereby setting the base of the flap. There are always two options in setting the base (Fig. 2.33). In small and moderate defects, there is no need to put the base in the periphery (contrary to blood flow that comes from the periphery), as the flap will always survive. However, in large flaps at least a main vessel must always be caught (Fig. 2.34a–c).

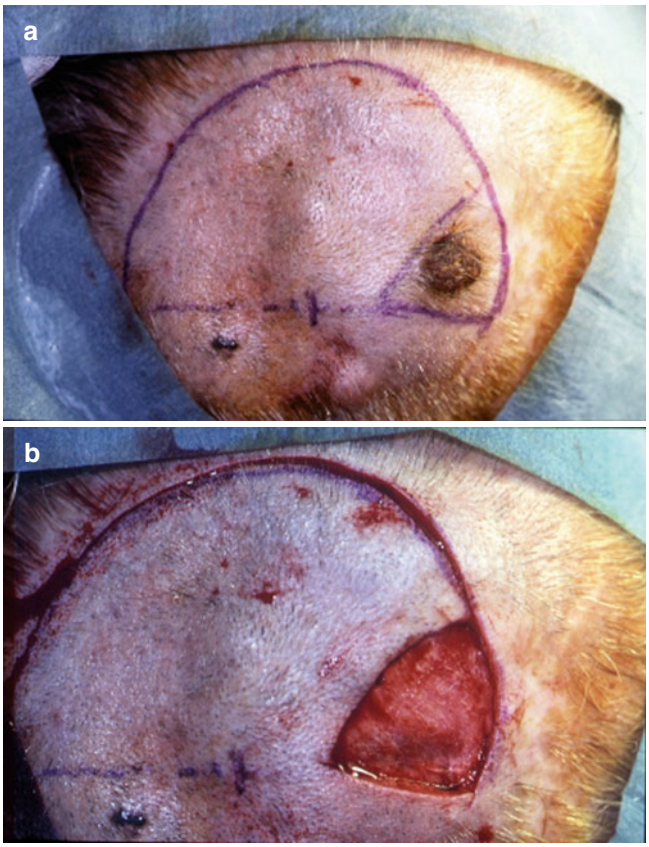

Fig. 2.32 Worthen rotation flap. (**a**) Geometry of the flap applied to a lesion at the vertex. (**b**) Lesion excised. (**c**) Rotation flap fully mobilized. (**d**) Flap rotated to the defect. The primary defect is distributed at the periphery as secondary defect. (**e**) Slight advancement of the adjacent scalp closes the secondary defect without tension

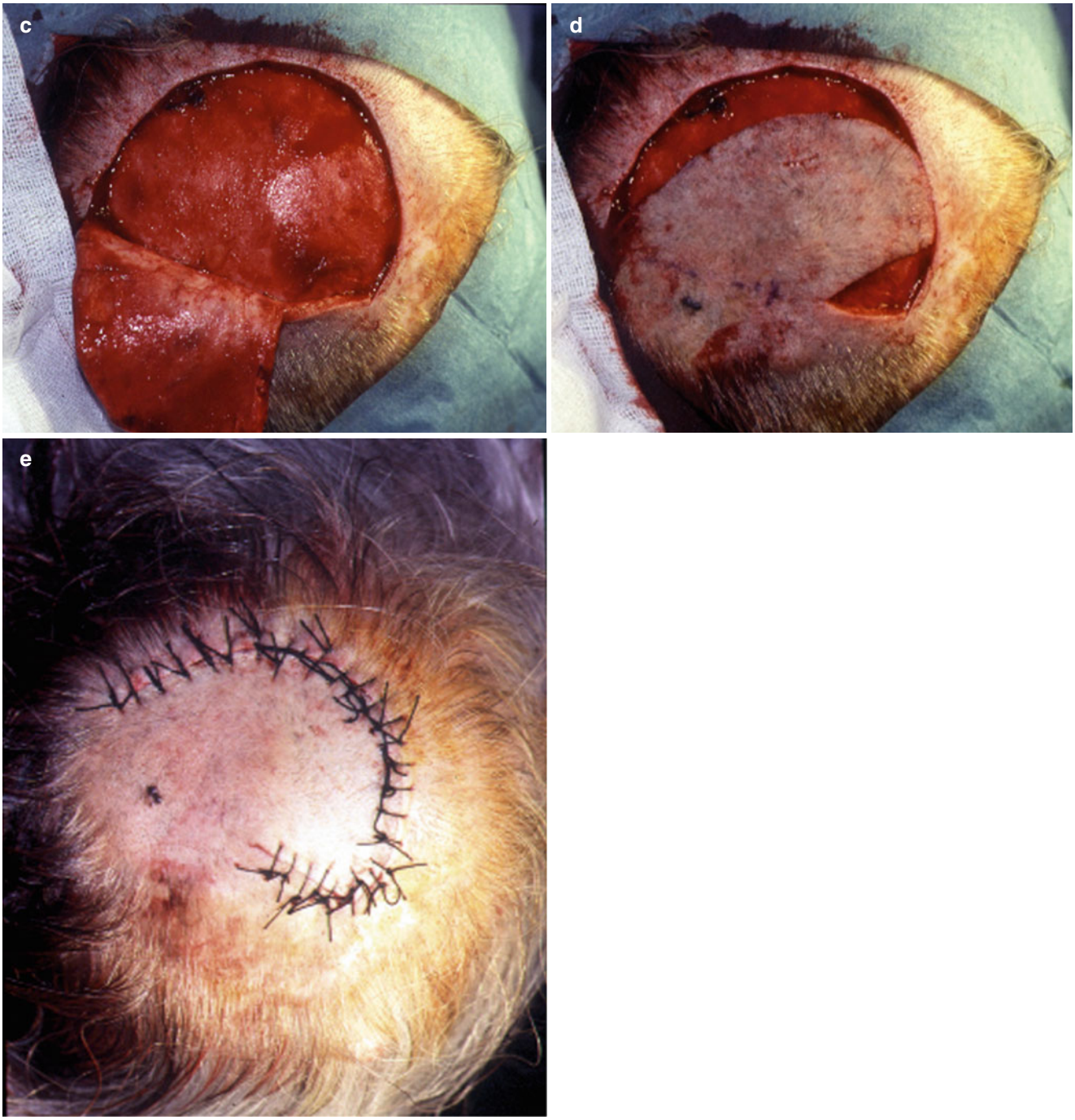

Fig. 2.32 (continued)

2.5.5 Anterolateral Rotation Scalp Flap

A large rotation flap in the case presented was used to close a defect produced by the excision of a tumor located at the temporal region (Fig. 2.35a, b).

The flap was designed according to the geometry of the Worthen flap (Fig. 2.35c, d). The flap was designed so as to transfer frontal and not the posterior scalp (as it would be more appropriate) because of the presence of a pressure ulcer in the occipital region. Thus, a slight distortion of the

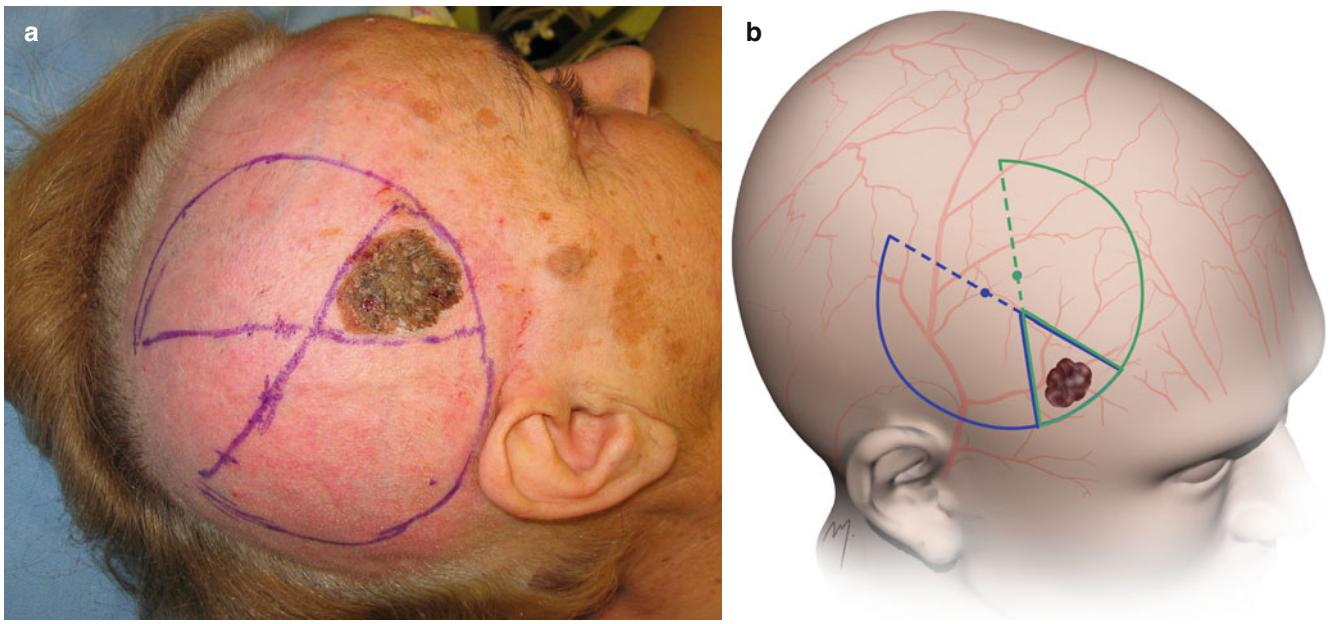

Fig. 2.33 (**a**, **b**) Two options of setting the base of a rotation scalp flap

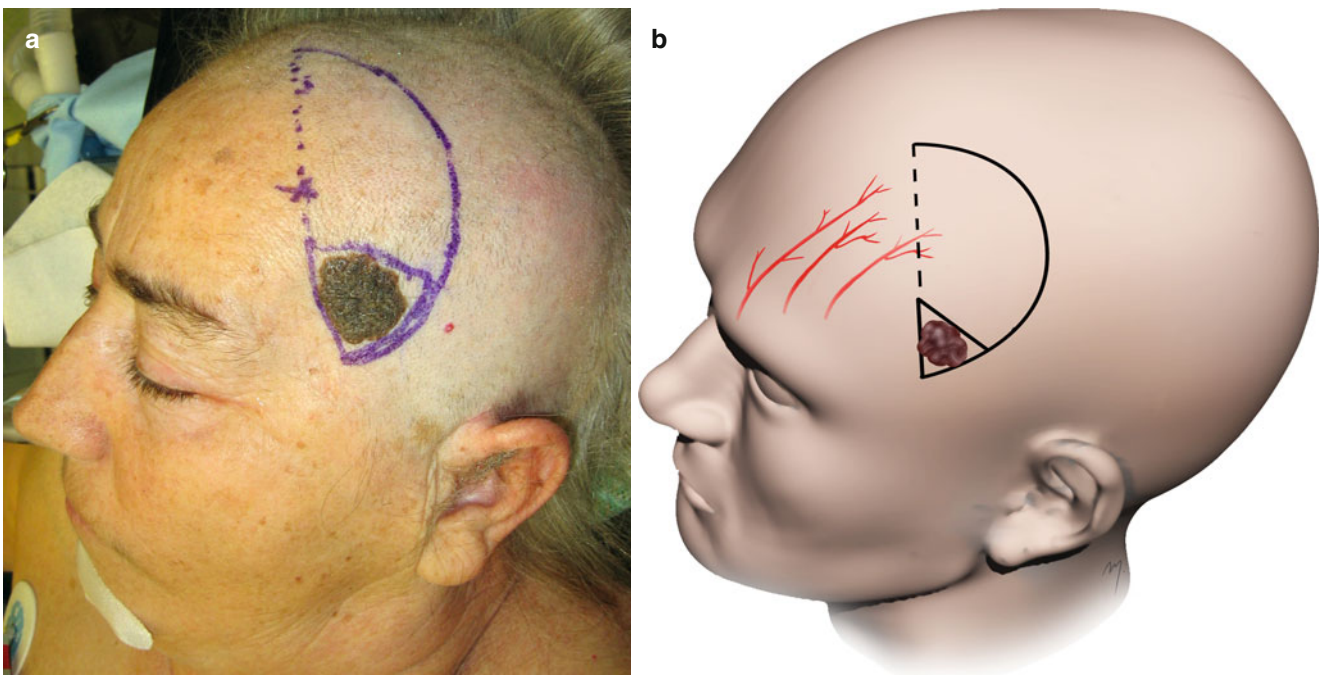

Fig. 2.34 (**a**–**c**) In this case the base was oriented in a position that the flap is perfused directly from the supraorbital and supratrochlear arteries and scars are totally hidden within the hair

Fig. 2.34 (continued)

temporal hairline is expected. Despite its size, the flap is very robust as it is supplied richly both by occipital arteries and by contralateral to the defect posterior branch of the superficial temporal artery (Fig. 2.35e). The lesion was excised and a large rotation flap was raised at the subgaleal level (Fig. 2.35f–h). The flap was easily rotated filling the defect without any tension (Fig. 2.35i, j). Postoperative appearance showed a satisfactory closure of the surgical defect without any sign of necrosis (Fig. 2.35k).

2.5.6 Anteroposterior Rotation Scalp Flap

Large defects of the forehead and frontal scalp can be reconstructed by a scalp rotation flap placed in an anterior-posterior direction. In case depicted in Fig. 2.36a, b, a large squamous cell carcinoma is situated in the mid-forehead subunit, fixed in the underlying periosteum.

The resection is outlined and a large scalp rotation flap is planned to reconstruct the defect (Fig. 2.36c, d). The aim in this case was to carry non-hair-bearing tissue from the

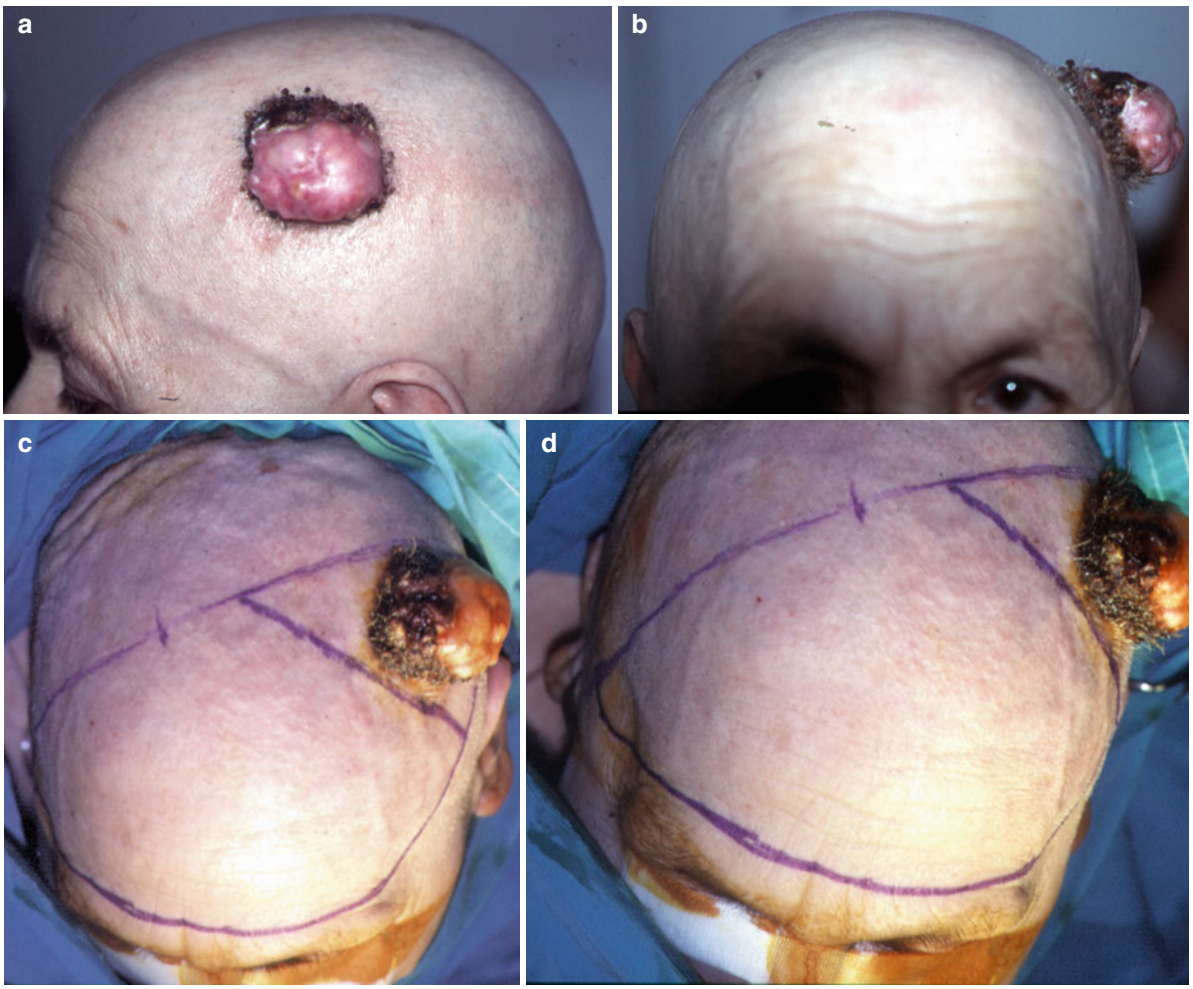

Fig. 2.35 (**a**, **b**) A large tumor located at the temporal region. (**c**, **d**) An anterolateral rotation flap outlined. (**e**) Flap is perfused mainly by both occipital arteries and by the contralateral to the defect posterior branch of the superficial temporal artery. (**f**) The defect after tumor removal. (**g**, **h**) Flap raised. (**i**, **j**) Immediate postoperative view. (**k**) Appearance at suture removal

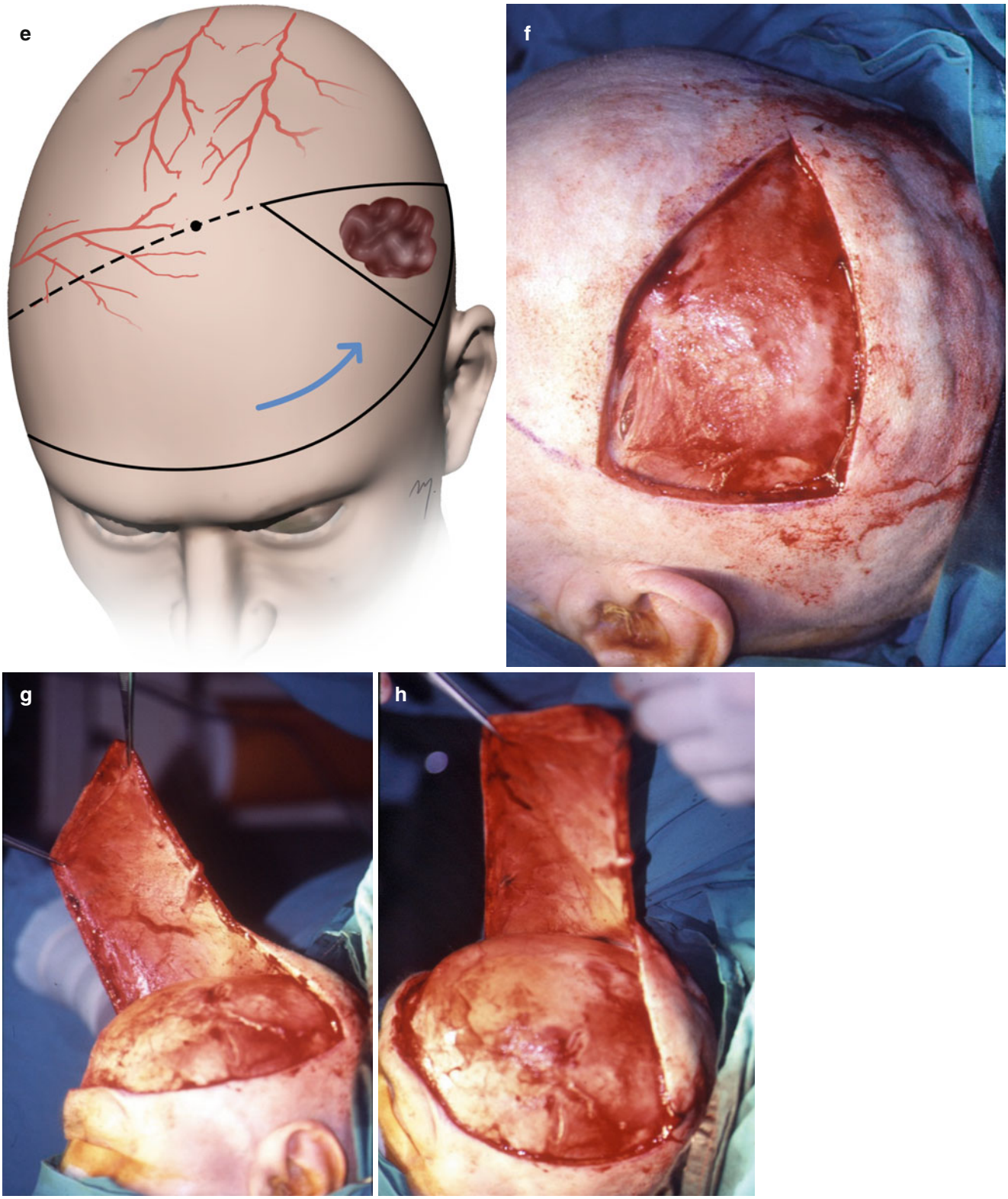

Fig. 2.35 (continued)

Fig. 2.35 (continued)

neighboring temple to the forehead. When remaining within the basic design rules of the scalp rotation flap as mentioned above, the flap is based beyond the midline and includes more than the half portion of the total scalp. Actually in this flap, the scalp is the "carrier" of the non-hair-bearing temporal skin that will be placed to the missing skin of the mid-forehead. Due to their anastomotic net, the contralateral scalp vessels feed the flap (Fig. 2.36e). The survival of this large flap that is based beyond the midline and fed by the contralateral vessels is a great paradigm of the robust vascularity of the scalp.

The lesion was removed en bloc with the underlying frontal bone (Fig. 2.36f). The dura was exposed and appeared to be clear of tumor. Tumor-free margins were revealed by frozen section biopsies. The excised pericranium around the resection leaves a zone of bare bone.

The flap was raised in the subgaleal plane (Fig. 2.36g). Good closure has been achieved in the whole periphery, without the formation of any dog-ear or standing cone. Rotation was adequate with no need of a back-cut (Fig. 2.36h). Likewise the recipient site was closed without tension or any distortion (Fig. 2.36i).

Complete resurface of the forehead with hairless skin is achieved. There is no distortion of the hairline (Fig. 2.36j, k).

2.5.7 Bilateral Rotation Scalp Flap

The patient presented in this case (Fig. 2.37a, b) had a mixed-type recurrent basal cell carcinoma after surgery and radiotherapy. The lesion was located at the lateral side of the front of the scalp.

The outlined area of the proposed excision is designed as a triangle with its base being anterior within a frown line. Excision includes the primary ulcer and the surrounding scar tissue. From the base of the triangle, two opposite horizontal incisions up to the temple are outlined within the same frown line as the base of the triangle (Fig. 2.37c, d). Both rotation flaps catch the superficial temporal arteries and also receive generous blood supply from the anterior part of the scalp arterial network (Fig. 2.37e).

Excision was completed in clear margins, revealed by frozen section biopsies. The depth of excision is to the level of

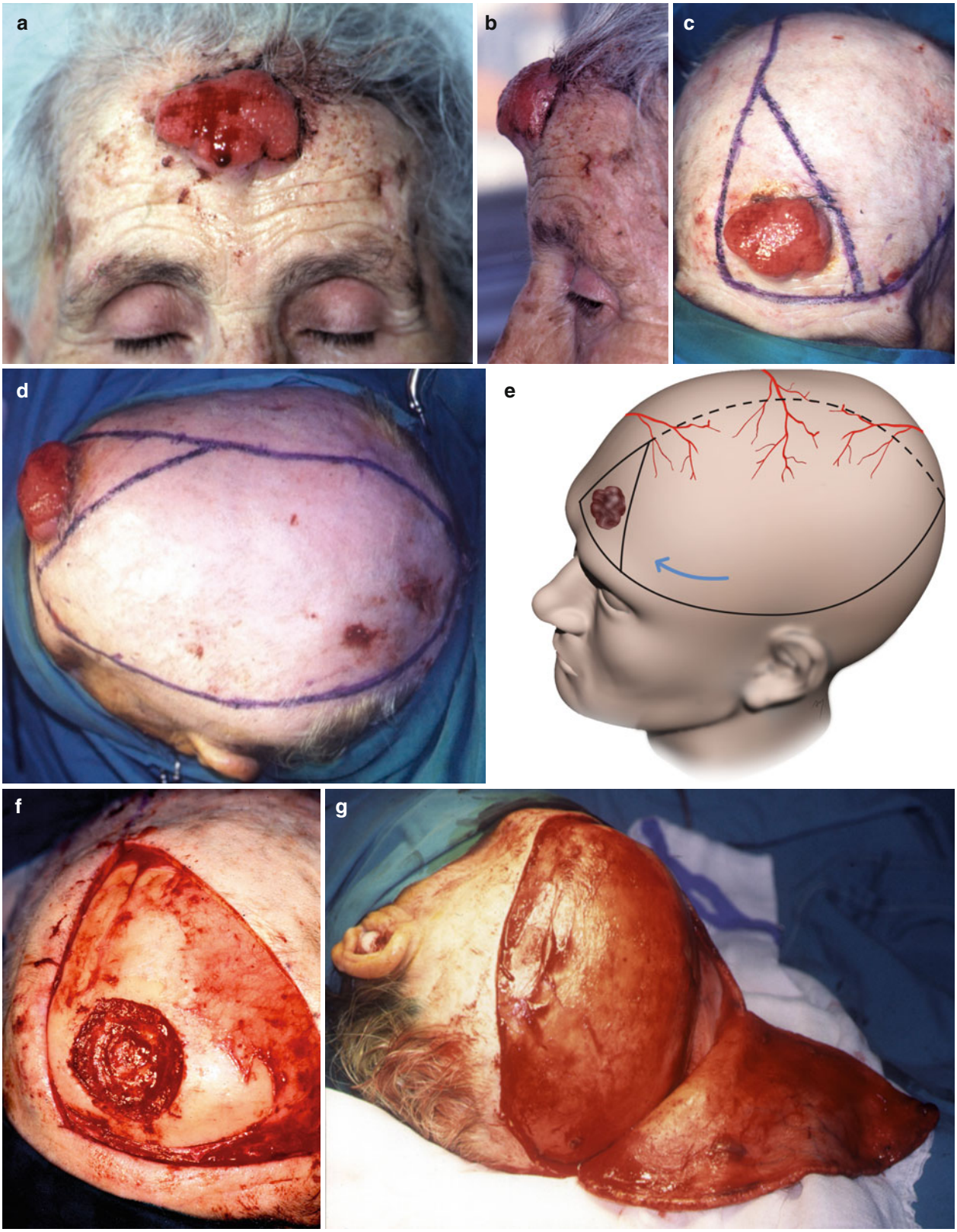

Fig. 2.36 (**a**, **b**) A squamous cell carcinoma located at the forehead. (**c**, **d**) Outline of the surgical excision and of the rotation scalp flap. (**e**) The flap is perfused by the contralateral vessels. (**f**) Excision completed. Excised pericranium around the resection leaves a zone of bare bone. (**g**) Flap raised. In its posterior part, muscle fibers of the occipital muscle are seen. In the temporal region, the upper part of the temporalis fascia is exposed. Vessels are visible, as they run through the galea. (**h**) Final closure. (**i**) Flap sutured at the recipient site without tension or any distortion. (**j**, **k**) Result at 1 year

Fig. 2.36 (continued)

the subgaleal plane, except the area of the main ulcer, where pericranium was included to the resection. At that region the skull bone is bare of pericranium (Fig. 2.37f).

The flaps were raised in the subgaleal plane (Fig. 2.37g). The superficial branches of the supraorbital and supratrochlear nerves are cut, resulting in temporary (9–12 months) denervation of the area of the frontal scalp above the horizontal line. The two flaps are then rotated medially and close the defect. The horizontal scar is camouflaged within the frown of the forehead and the vertical one within the scalp (Fig. 2.37h). The postoperative result at 6 months shows satisfactory closure of the defect (Fig. 2.37i, j).

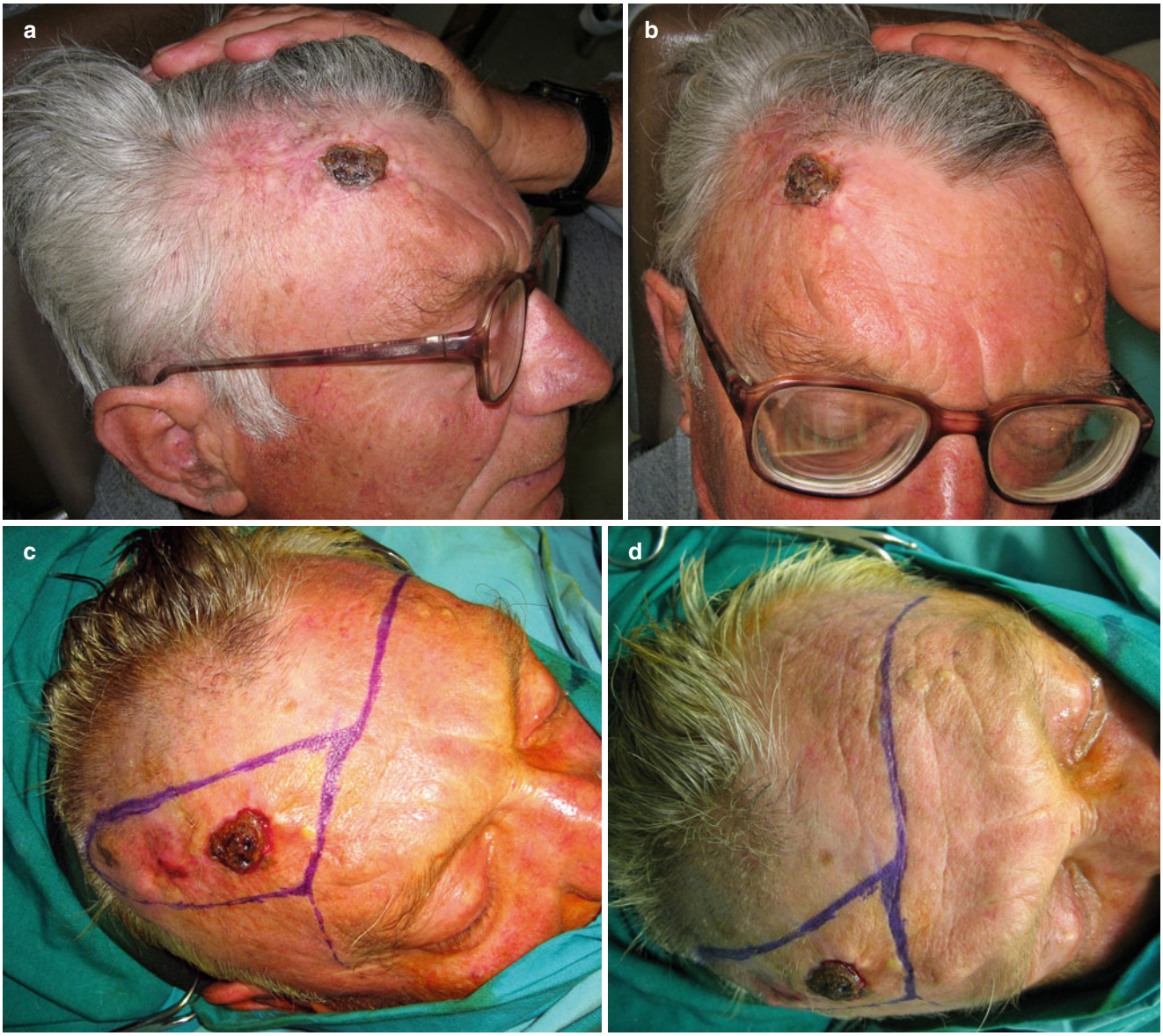

Fig. 2.37 (**a**) Recurrent basal cell carcinoma of the frontal scalp. (**b**) Frontal view. (**c**) Proposed excision and flaps outlined. (**d**) Horizontal incision extends up to the temple. (**e**) Both rotation flaps are well vascularized by the posterior part of the scalp arterial network, and both superficial temporal arteries. (**f**) Excision includes a part of pericranium, leaving bare bone. (**g**) Flap raised at the subgaleal plane just above the pericranium. (**h**) Flaps rotated and sutured in position. (**i**, **j**) Postoperative appearance at 6 months

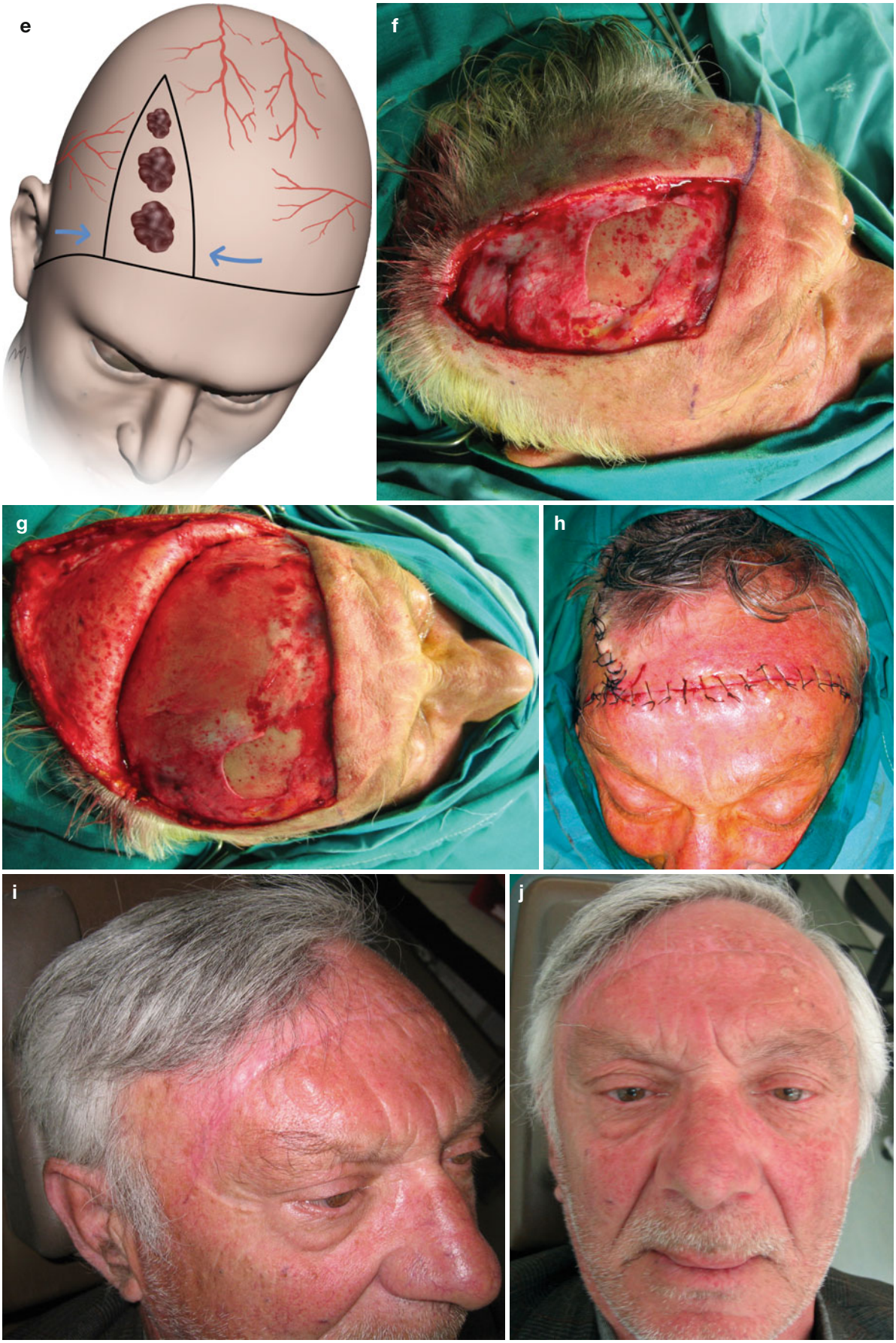

Fig. 2.37 (continued)

2.5.8 Posterior Neck Rotation Flaps

The posterior neck can be a donor site of rotation flaps that transfer skin to adjacent defects of the nape or the occipital region. This was used in a basal cell carcinoma at the posterior neck that was excised and reconstructed by a posterior neck rotation flap (Fig. 2.38a, b). The skin of the posterior neck exhibits a greater elasticity than the scalp. This allows the flap to be designed not according to the strict geometry of the Worthen rotation flap but in a conventional way.

The flap is of random pattern based on the vascular network formed by the perforators that supply the skin of the posterior neck (Fig. 2.38c). After the lesion was excised as a triangle, the flap was raised below the investing layer of the deep cervical fascia (Fig. 2.38d, e). It was rotated to the defect and sutured in place leading to a satisfactory result (Fig. 2.38f–h).

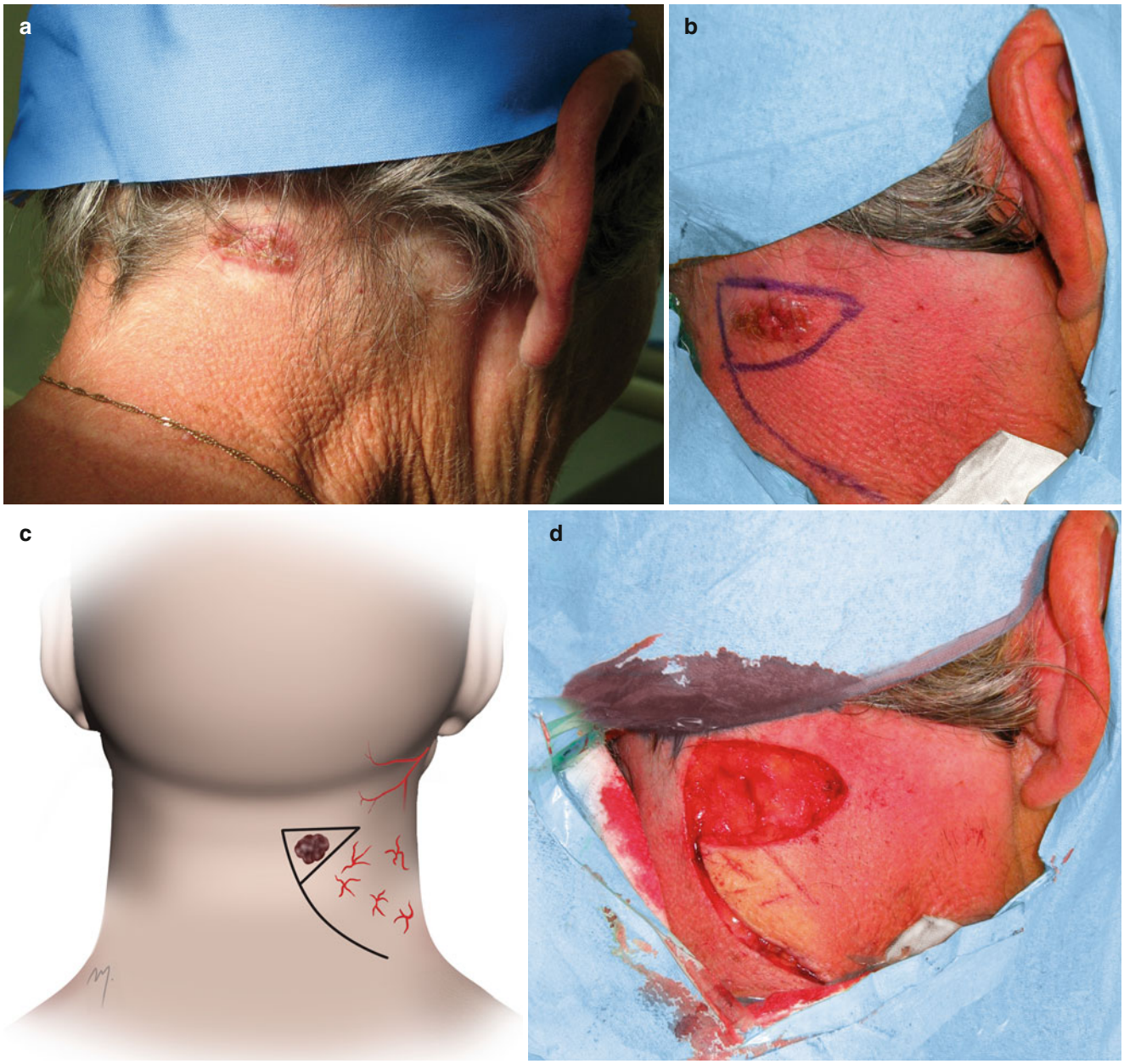

Fig. 2.38 (**a**–**h**) A posterior neck defect reconstructed by a nearby rotation flap

Fig. 2.38 (continued)

2.5.8.1 Posterior Neck Rotation Flap Reconstructing a Postauricular Defect

A similar as the above flap can be used to reconstruct a defect of the postauricular area (Fig. 2.39a). The flap is supplied by the musculocutaneous perforators of the posterior auricular artery and of the upper sternocleidomastoid arteries (branches of the occipital artery) (Fig. 2.39b). The flap is raised beneath the investing layer of the deep cervical fascia so as to enhance its vascularity (Fig. 2.39c). Rotation to the defect is done with ease and minimal tension after the excision of a small Burow's triangle at the base (Fig. 2.39d).

2.5.8.2 Posterior Neck Rotation Flap Reconstructing an Occipital Defect

In the case presented, a basal cell carcinoma is located at the occipital area (Fig. 2.40a). A large posterior neck rotation flap is planned for the resurfacing of the defect (Fig. 2.40b).

The flap is mainly of random pattern. In the lower part of its base, it is fed mainly by the occipital branch of the posterior auricular artery and in the superior part of the base from posterior branches of the parietal branch of the superficial temporal artery (Fig. 2.40c).

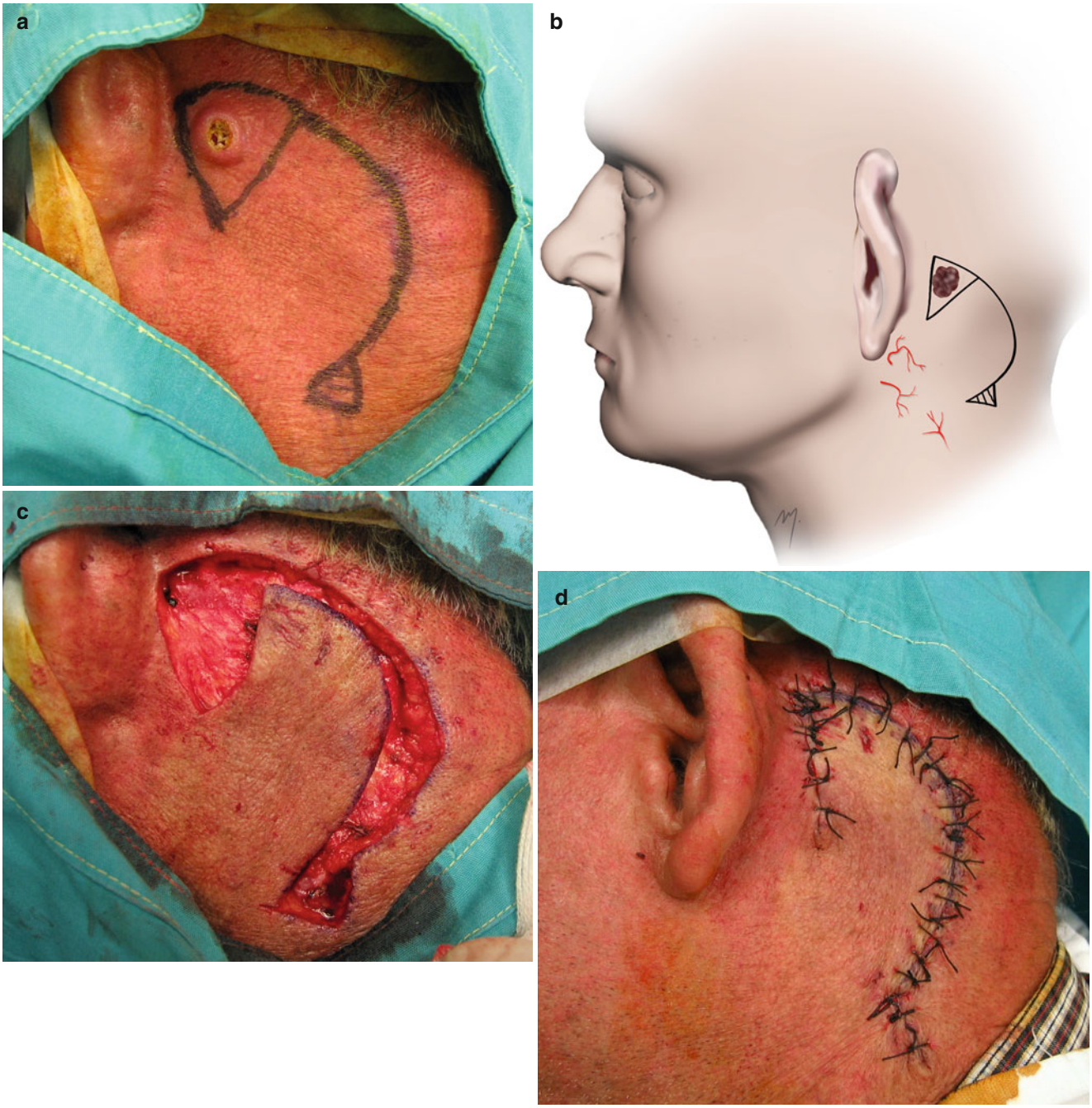

Fig. 2.39 (**a**–**d**) A rotation flap from the posterior neck is used to reconstruct a postauricular defect

The flap is then elevated including the fascia of the trapezius, splenius capitis, and the fascia of the upper part of the sternocleidomastoid muscles (Fig. 2.40d). Once the superior nuchal line is reached, further dissection is carried out with ease, in the loose areolar tissue plane of the occipital part of the scalp. At the lateral dissection, when reaching the emerging point of the final part of occipital artery, if the needed rotation is not intercepted, the artery could remain intact (or slightly mobilized). But usually the needed rotation is not gained, as in this case, and the final part of the artery has to be ligated and cut as it emerges from the cranial attachments of trapezius and sternocleidomastoid muscles.

The flap is rotated into its position covering the defect (Fig. 2.40e). Galea scoring can be performed to the occipital part of the flap to gain some more length and ensure suturing without tension.

The flap is sutured in place (Fig. 2.40f). A standing cone that is formed most of the time always disappears after a few weeks.

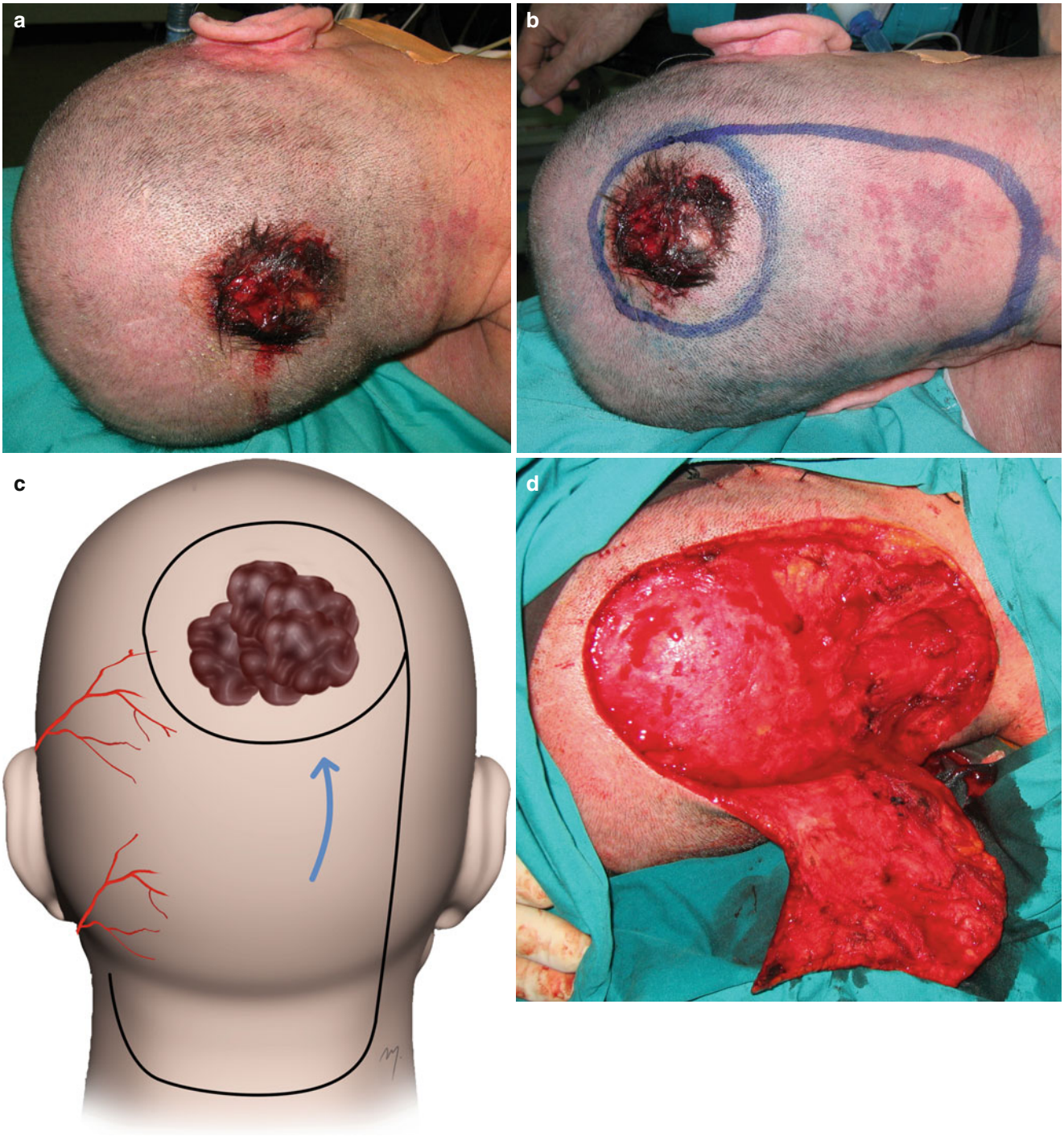

Fig. 2.40 (**a**) A large basal cell carcinoma at the occipital area. (**b**) Posterior neck rotation flap outlined. (**c**) The flap receives blood supply from the occipital branch of the posterior auricular artery and from the posterior branches of the parietal branch of the superficial temporal artery. (**d**) The flap completely elevated. The occipital vessels are dissected so as to gain the needed rotation. (**e**) The flap rotated to its position. (**f**) Suturing in place

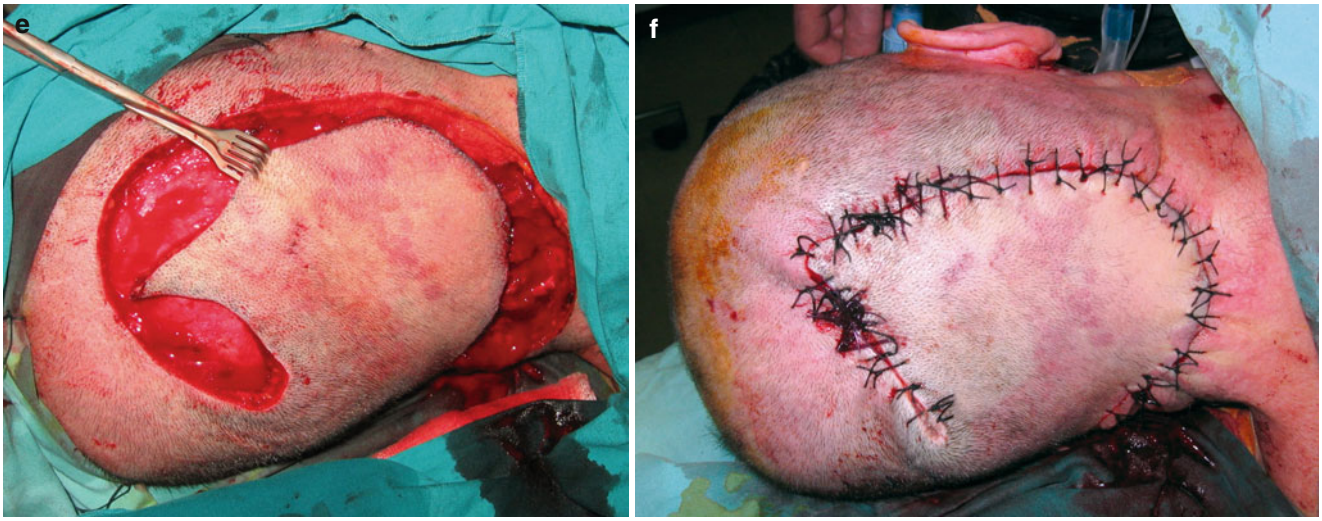

Fig. 2.40 (continued)

2.5.9 Parieto-Occipital Transposition Scalp Flap Anteriorly Based

The patient presented had a large recurrent sebaceous carcinoma formerly treated by neurosurgery (Fig. 2.41a–c). A through and through resection of the involved skull bone and acrylic cranioplasty was performed in the first operation.

A wide resection in a circular manner and reconstruction of the defect with a parieto-occipital transposition scalp flap anteriorly based was planned (Fig. 2.41d, e). The flap was outlined with its base anteriorly. The flap is axial in its anterior half, based on the frontal branch of the superficial temporal artery and the forehead vessels. Its posterior half is of random pattern receiving blood supply through the vascular network of the scalp (Fig. 2.41f).

Resection including the tumor within the surrounding tissue was performed (Fig. 2.41g). The acrylic placed in the former cranioplasty was removed and the affected bone was resected in full thickness (Fig. 2.41h). The dura was exposed but intact.

Dissection was carried out in the subgaleal plane and almost the entire of the rest of the scalp was raised as a long and large flap (Fig. 2.41i, j). As the flap is raised in the subgaleal plane, care is taken to the underlying pericranium so that it remains intact to provide a vascular bed of the subsequent skin grafting. Galeal relaxing incisions (galeal scoring) were made allowing greater stretching of the scalp flap.

The flap was rotated and covered the defect (Fig. 2.41k, l). The transposition of scalp flaps always produces a standing cone. Minor trimming is required because it resolves after a few weeks. The secondary donor site defect that is produced still has its periosteum intact and can be covered with a skin graft (Fig. 2.41m).

Postoperative appearance of the patient at 1 month shows satisfactory survival of the flap and closure of the surgical defect (Fig. 2.41n, o).

2.5.10 Parieto-Occipital Transposition Scalp Flap Medially Based

The patient shown in Fig. 2.42a was presented with a recurrent Merkel cell carcinoma that was treated previously by surgery (with no clear surgical margins) and postsurgical radiation therapy.

The local control of this aggressive neuroendocrine tumor consisted of a wide resection of the primary lesion (Fig. 2.42b). The defect was planned to be covered with a parieto-occipital transposition scalp flap anteriorly based (Fig. 2.42c).

The flap is supplied from the contralateral vascular system of the scalp through the profuse anastomotic network (Fig. 2.42d).

In a nearly same design, this flap can be extended in its distal end to the nape of the neck (Friedman et al. 1986) or to the posterior surface of the auricle and the neighboring mastoid region (Galvao 1981; Dias and Chhajlani 1977), thus carrying hair-bearing skin to the face, when used as a two-stage pedicle flap. The anteriorly based parieto-occipital transposition scalp flap must not be confused also with the nearby positioned posterior scalping flap. The posterior scalping flap is an anteriorly, based on the ipsilateral vessels, flap, with its axis vertically oriented and extended to the nape of the neck (Arena 1977; Genden et al. 2000; Mandell et al. 2000).

Surgical removal of the primary tumor required en bloc resection of the soft tissues, part of the zygomatic complex, and the lateral orbital wall and orbital exenteration

Fig. 2.41 (**a**–**c**) A large sebaceous carcinoma located at the vertex. (**d**) Area of excision outlined. (**e**) Anteriorly based parieto-occipital transposition flap is outlined. (**f**) The flap is axially in its anterior half and of random pattern in its posterior half. (**g**) Excision in clear margins. (**h**) Through and through skull bone resection. (**i**) Flap raised in the subgaleal plane. (**j**) A long anteriorly based flap is raised. Periosteum is excised around the lesion but remains intact in the flap donor site. (**k**) Key sutures holding the flap in position. (**l**) The transposition of the flap produced a secondary donor site defect. (**m**) Secondary donor site defect is covered with skin graft. (**n**, **o**) The patient at 1 month postoperative

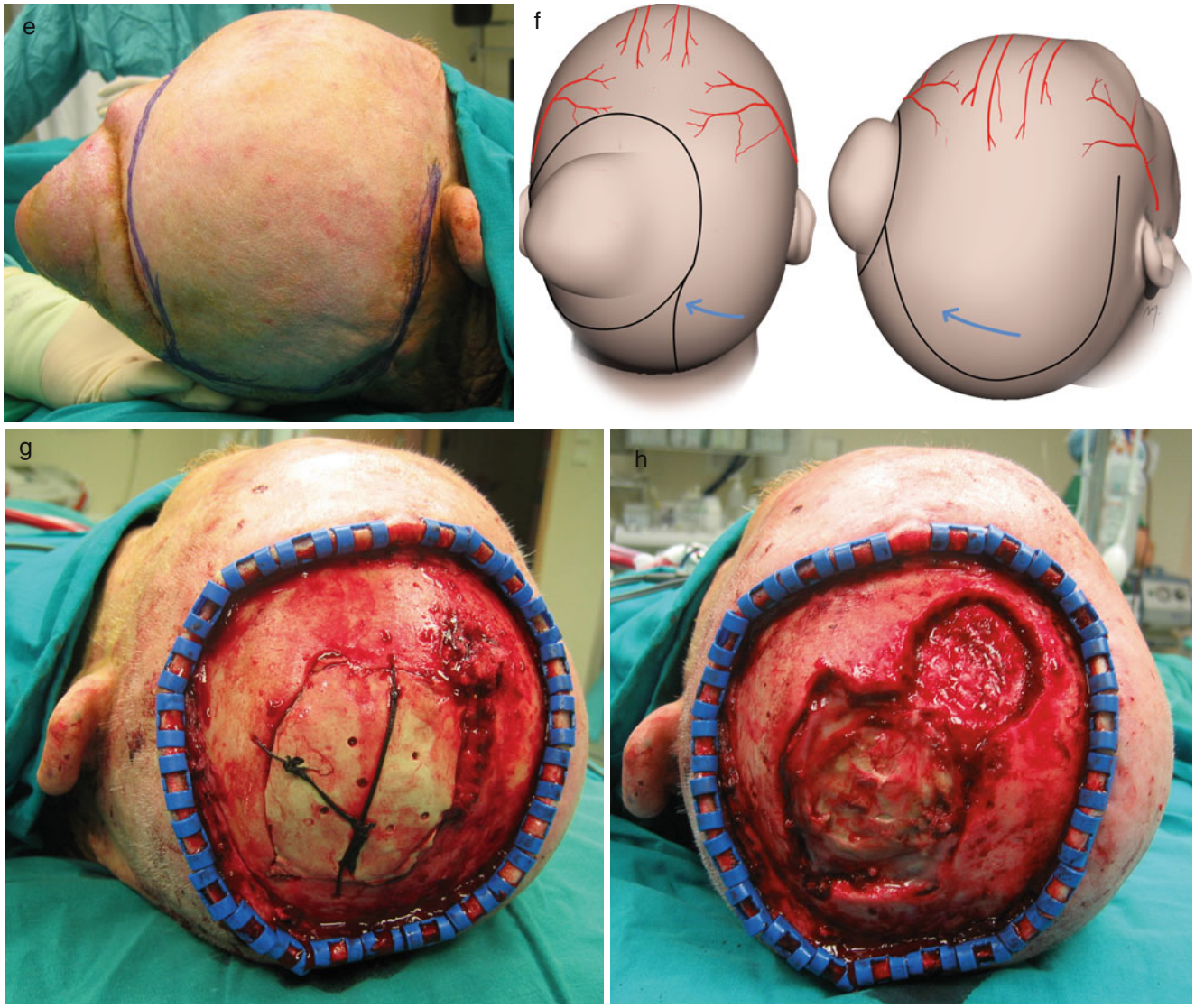

Fig. 2.41 (continued)

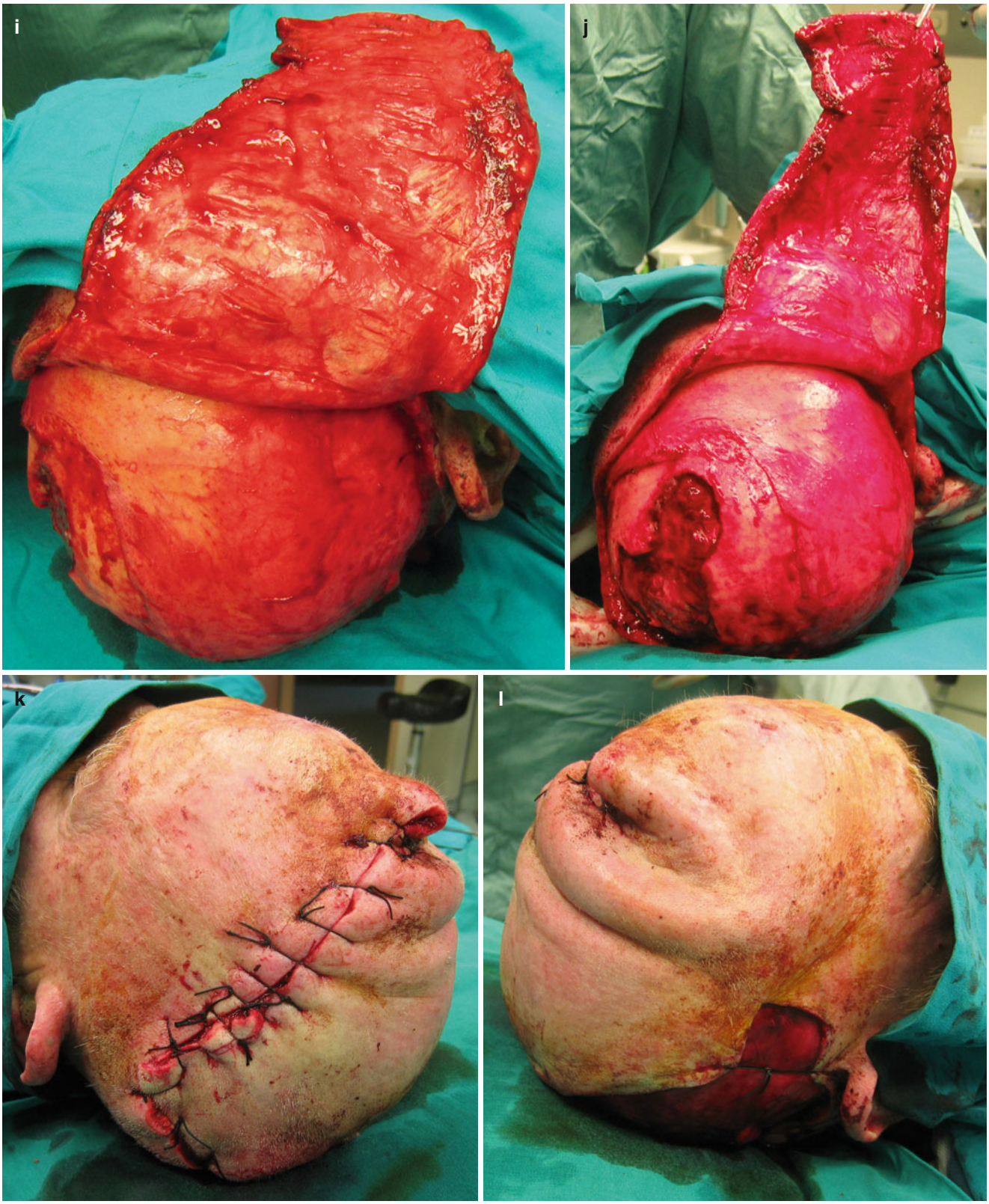

Fig. 2.41 (continued)

Fig. 2.41 (continued)

with complete removal of the periorbita (Fig. 2.42e, f). The periosteum overlying the frontal bone was excised with the specimen.

The parieto-occipital flap was dissected in the subgaleal plane (Fig. 2.42g, h) and raised up to its base. The posterior auricular artery has to be divided during the flap preparation.

A temporalis muscle flap is used to cover the bare of periosteum and orbital cavity and supply the vascular bed for a split-thickness skin graft (Fig. 2.42i).

The parieto-occipital flap is transpositioned to the recipient site, leaving a secondary defect to its donor site that is covered by a skin graft (Fig. 2.42j, k).

Even this large flap was placed in a compromised vascular area due to the previous radiation; it is so robust that the only ischemic complication was the minor superficial epidermolysis in its medial border (Fig. 2.42l). Nevertheless, epidermolysis resolved and healing completed with local wound care. Final rehabilitation can be obtained by an orbital prosthesis.

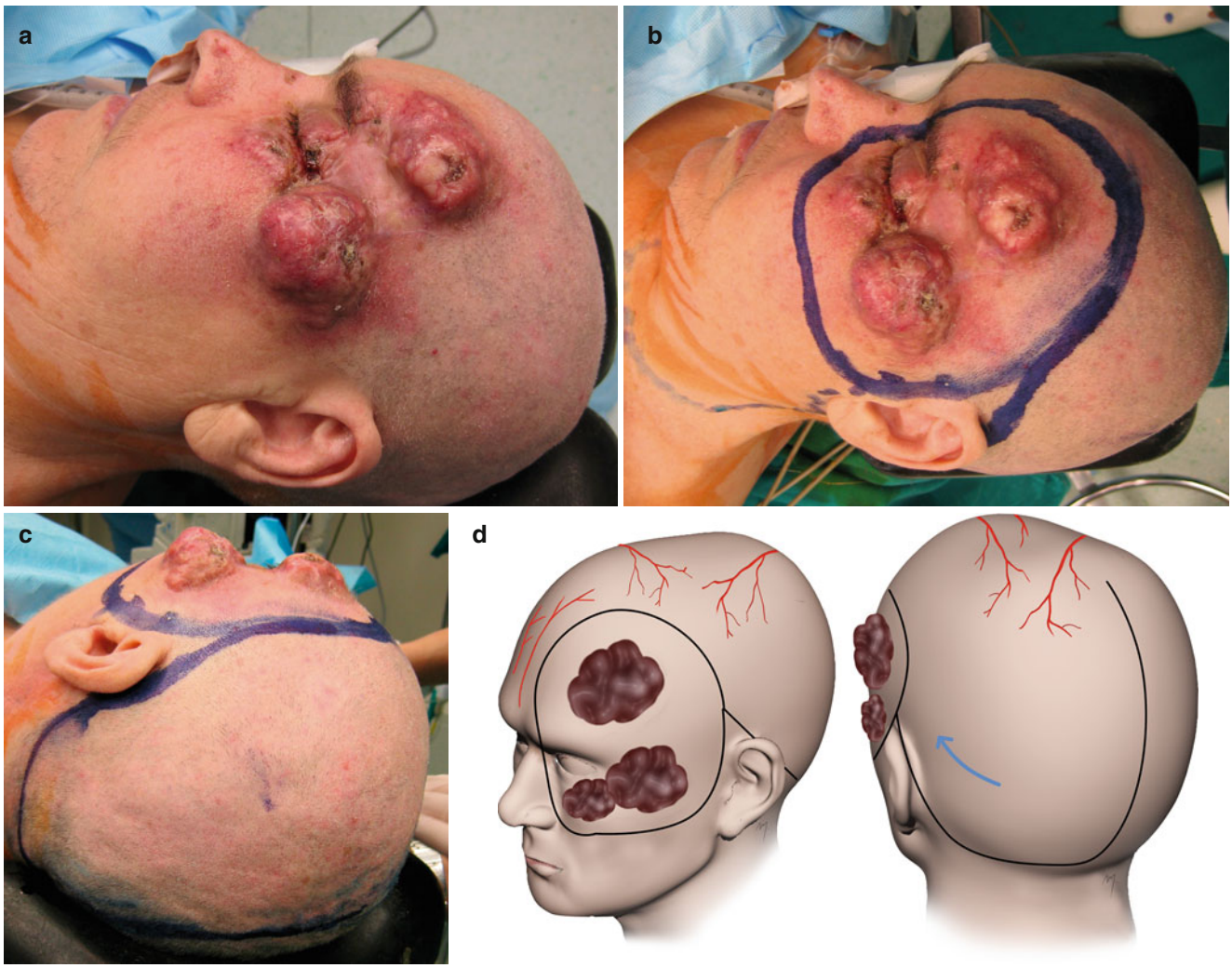

Fig. 2.42 (**a**) A recurrent Merkel cell carcinoma in multifocal appearance. (**b**) Wide local resection line is outlined. (**c**) A medially based parieto-occipital transposition flap is outlined. (**d**) The flap receives its blood supply from anastomotic network that is perfused mainly from the contralateral scalp arteries. (**e**, **f**) Resection of the tumor completed. (**g**) Periphery of the flap incised. (**h**) The flap raised. (**i**) A temporalis muscle flap is used to obliterate the orbit. (**j**) The parieto-occipital flap provides coverage to the defect. (**k**) Donor site is covered by skin graft. (**l**) Result at 1 month postoperative. Epidermolysis in the medial border of the flap resolves with local wound care

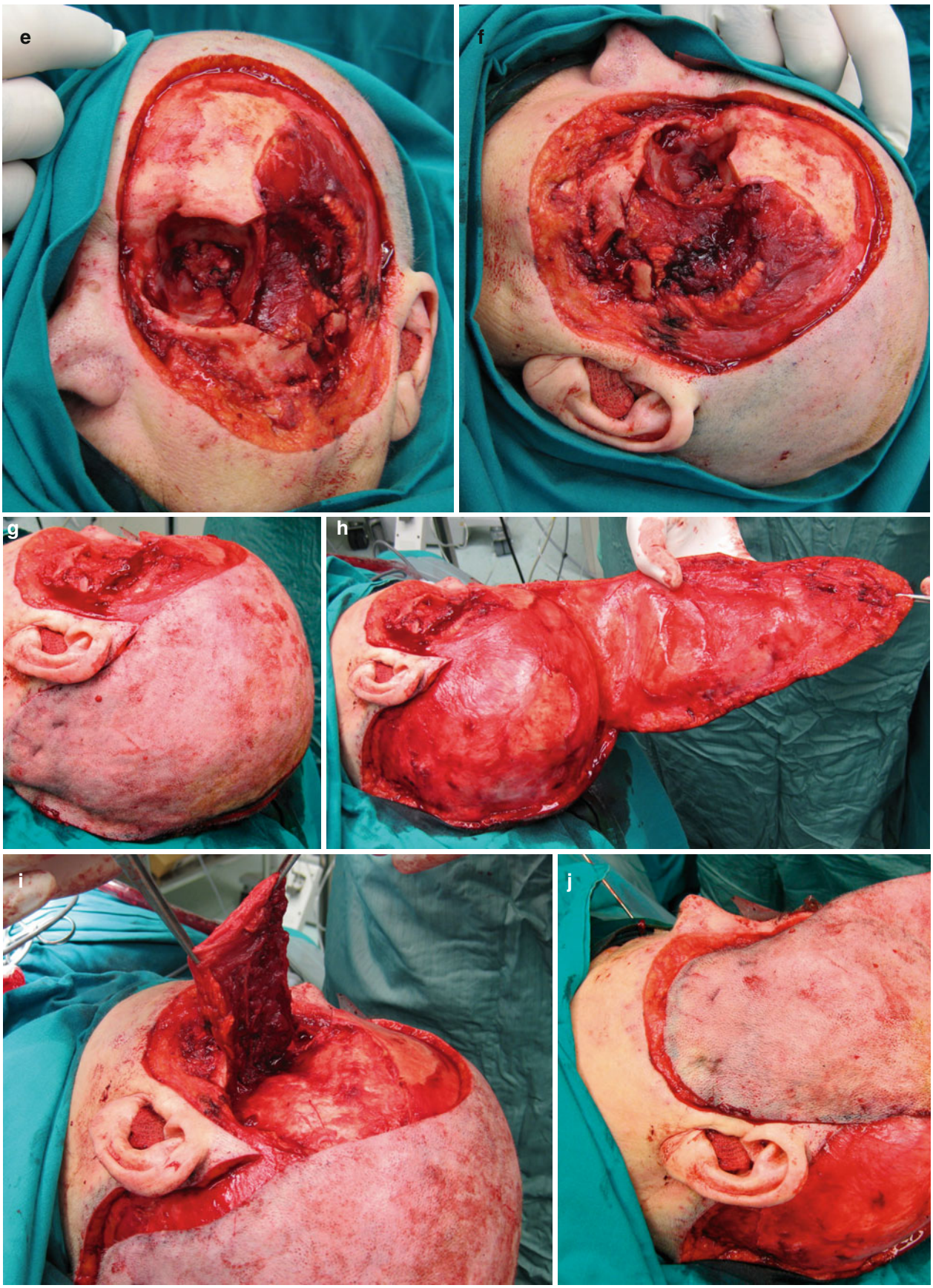

Fig. 2.42 (continued)

Fig. 2.42 (continued)

2.5.11 Multiple Scalp Flaps (Orticochea Flap)

Orticochea originally described this flap, known also as "banana peel flap," initially in 1967 as a four-flap scalp reconstruction and some years later (1971) as a three-flap modification. The Orticochea flap is an option for closing very large anterior or posterior scalp defects, with the use of local flaps.

In the case presented (Fig. 2.43a, b), a giant recurrent sebaceous gland carcinoma was located in the occipital region. The lesion was initially operated and irradiated with failure to control the tumor. A wide resection in a circular manner and reconstruction of the defect with a multiple scalp flaps, according to slight modification of the original Orticochea principles, was planned. Three large scalp flaps were outlined. Flap I (Fig. 2.43c) was based on the left superficial temporal and left posterior auricular vascular system, and flap II (Fig. 2.43d) was based on the same vessels to the right.

Flaps I and II are ended to the midline in an (supplementary = 180°) angle (Fig. 2.43e).

A third rotation flap (III) was outlined in the lower occipital area and the nape of the neck (Fig. 2.43f). This flap is based superiorly on the ipsilateral occipital branch of the posterior auricular artery and in a lesser degree of its auricular branch. The inferior part of the base receives blood from perforators of the sternocleidomastoid branches of the occipital artery.

The schematic representation of the Orticochea flap and its vascularization is shown in Fig. 2.43g.

The lesion was excised in a very wide area including almost the half of the hair-bearing scalp and the outer table of the cranial bone (Fig. 2.43h).

Flaps I, II, and III were raised in the subcutaneous level with great care to preserve the feeding vessels. Flaps I and II catch the superficial temporal arteries (Fig. 2.43i, j).

As dissection of flap III was carried on, the occipital arteries were divided and ligated at the point where they emerges from the cranial attachments of trapezius and sternocleidomastoid muscles, to gain sufficient mobilization of the flap. Lateral dissection was carried out carefully to maintain the branches of the posterior auricular artery, and the skin was not widely detached from the sternocleidomastoid muscle so as to remain as much as possible perforators of the sternocleidomastoid branches of the occipital artery to the inferior flap base (Fig. 2.43k). Finally the frontal part of the scalp was raised and the entire skull was denudated (Fig. 2.43l, m).

At the start of the reconstruction, first flap I and flap II were rotated, slid back, and juxtaposed, covering the upper portion of the defect. The lower portion of the defect was covered by flap III (Fig. 2.43n). This maneuver distributed

the initial large defect in two secondary much smaller defects. One in the nape of the neck and another one, coronal shaped, in the mid-scalp. The defect of the nape was closed primarily with ease, by mobilization and advancement of the neck skin.

The coronal-shaped defect of the mid-forehead was reduced in width by stretching back the forehead flap due to galeotomies. The forehead was stretched back as much as not bring the frontal hairline very high that would lead to a very wide and bald forehead. The remained defect was covered with a skin graft (Fig. 2.43o). One month after surgery, the flaps healed very well (Fig. 2.43p–s).

The final postoperative appearance of the patient approximately 2 years following surgery is shown in Fig. 2.43t–v. The patient refused any secondary correction of the skin-grafted bald area, as she camouflaged it by hairdressers' styling.

Fig. 2.43 (**a**) A sebaceous gland carcinoma of the occipital region. (**b**) Side view. (**c**) Flap I based on the left superficial temporal and left posterior auricular vessels. (**d**) Flap II based mainly on the right superficial temporal and right posterior auricular vessels. (**e**) Top view of flaps I and II. (**f**) Rotation flap III at the nape of the neck. (**g**) Schematic representation of the Orticochea flap and its vascularization. (**h**) Resection completed. (**i**) Flap I and III raised. (**j**) Flap II raised. (**k**) Flap III raised. (**l**, **m**) The entire skull has been uncovered in a "banana peel" manner. (**n**) Flaps I, II, and III, held in position with key sutures, cover the initial defect. The secondary defect of the nape can be closed primarily. (**o**) A skin graft was used to cover the mid-scalp defect. (**p–s**) One-month postoperative the flaps have already healed very well. (**t–v**) 2 years postoperative. Normal appearance of the forehead and position of hairline

Fig. 2.43 (continued)

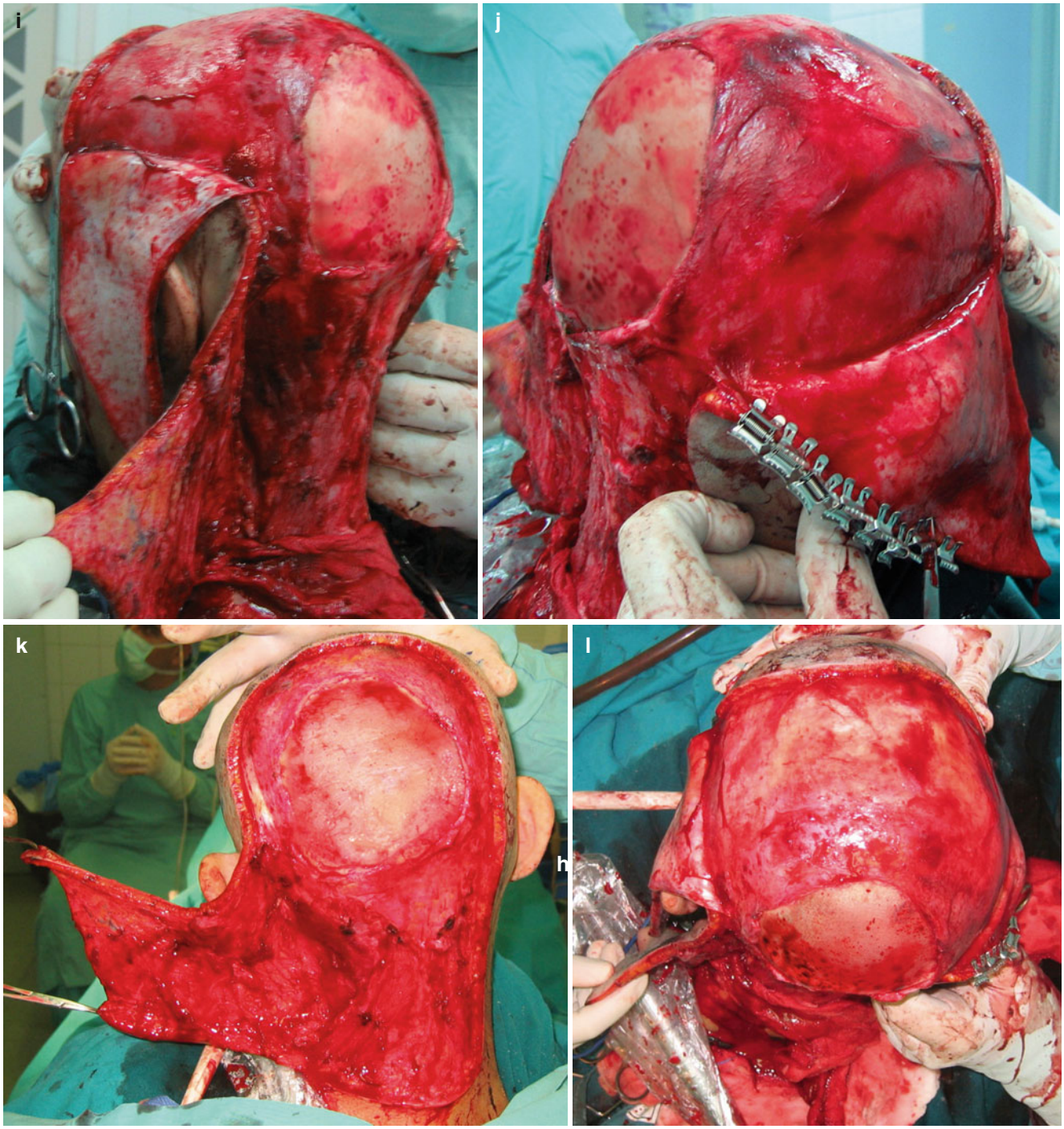

Fig. 2.43 (continued)

Fig. 2.43 (continued)

Fig. 2.43 (continued)

Fig. 2.43 (continued)

2.5.12 Rhomboid Flap

The tissue availability of the temporal area allows the design of transposition flaps with primary closure, like the rhomboid presented, with much ease than at the scalp.

Special care must also be given when working at the frontal part of the temple in the course of the frontal branch of the facial nerve which determines the selected flap option of the rhomboid defect (Fig. 2.44a, b). The lesion was excised and the flap was raised at a level just above the temporoparietal fascia. The frontal vein was encountered running over the outer surface of the temporoparietal fascia (Fig. 2.44c, b). This level ensures absolutely the integrity of the facial nerve as it runs at the undersurface of the fascia. The rhomboid flap was transferred to the defect and sutured without tension (Fig. 2.44e, f).

2.5.13 Triple Rhomboid Flap

The variations of the Limberg flap, as double or triple rhomboid flaps that were proposed by Lister and Gibson (1972) and Jervis et al. (1974), produce a multiplicity of scars, which could be a major aesthetic problem in visible areas of the face. But when these flaps are used in the scalp, the undesirable scars can be camouflaged within the hair.

The triple rhomboid flap in medium-sized scalp defects could act as an alternative, especially in the vertex, that avoids the design of a larger and wider rotation flap. By using a triple rhomboid flap, the defect closure and the tension load of the stiff and inelastic scalp is distributed in three rhomboid flaps. A Jadassohn nevus located at the vertex of the scalp is shown in Fig. 2.45a. Excision in healthy tissue and a triple rhomboid flap is outlined (Fig. 2.45b). The excision is designed in a hexagon form with equal sides. In each of the alternative corner of the hexagon, a rhomboid flap is placed. The length of each side of the rhomboid flaps is equal to the radius of the defect.

The flaps are of random pattern based at the rich arterial anastomotic network of the vertex, which secures its survival.

After the lesion was excised, the rhomboid flaps raised and pivoted in the same direction and sutured (Fig. 2.45c–e).

The postoperative result at 1 and 3 months is satisfactory (Fig. 2.45f, g). At 9 months, growth of the hair has completed and the scars are totally hidden (Fig. 2.45h).

2.5.14 Temporoparietal Fascial Flap

W.J. Brown first used the transfer of the temporoparietal fascia as a flap in 1898 for the reconstruction of an auricle defect after a horse bite. In the same year, G.H. Monks (1898) used

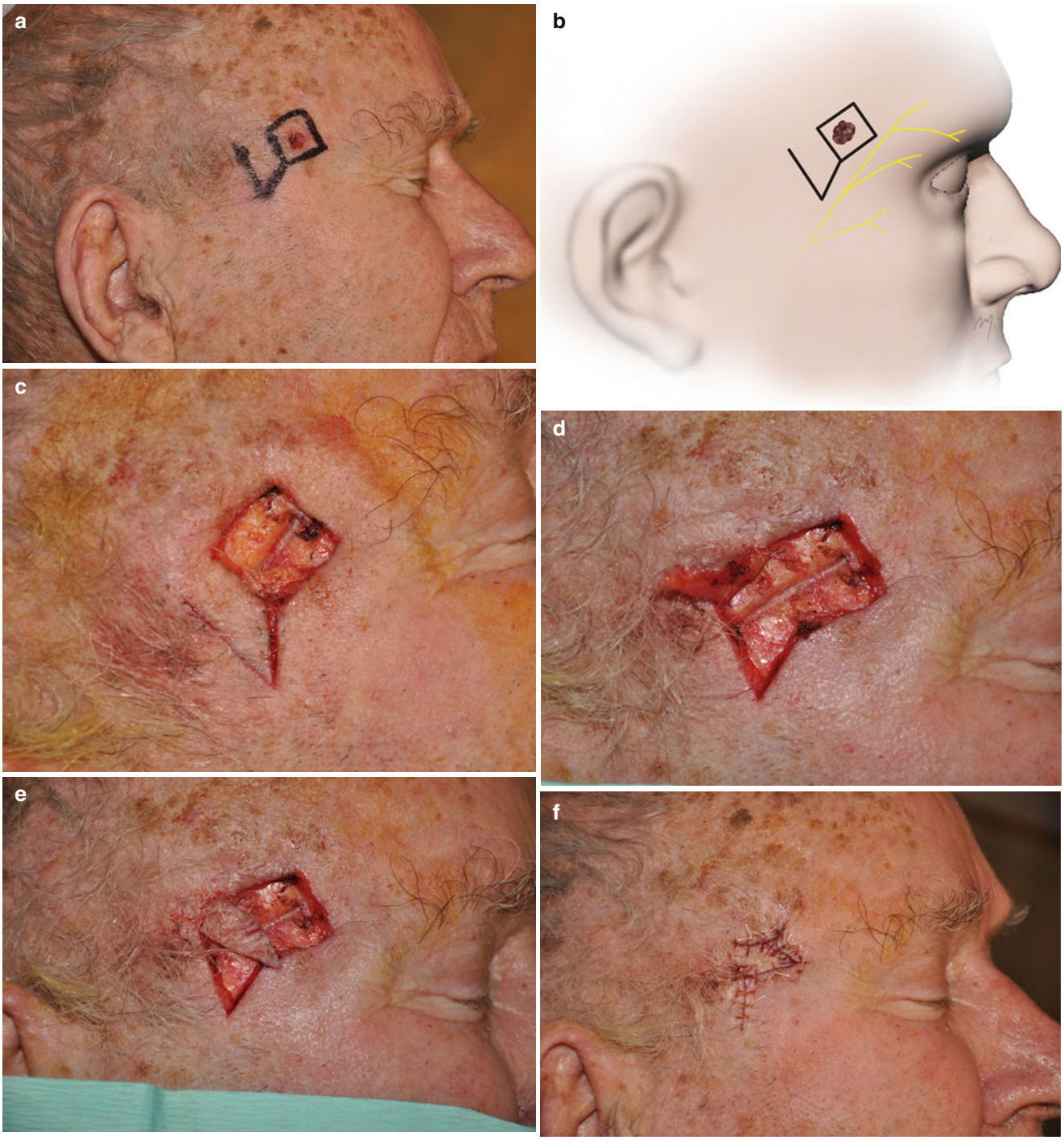

Fig. 2.44 (**a**) A basal cell carcinoma located at the anterior temple. (**b**) The lesion and the selected flap lie lateral to the expected course of the frontal nerve. (**c**, **d**) The frontal vein is seen running over the outer surface of the temporoparietal fascia. This level always ensures the integrity of the facial nerve as it runs at the undersurface of the fascia. (**e**, **f**) The flap is fully mobilized and transferred to the defect without tension

Fig. 2.45 (**a**–**h**) A triple rhomboid flap is used to reconstruct a defect at the vertex of the scalp

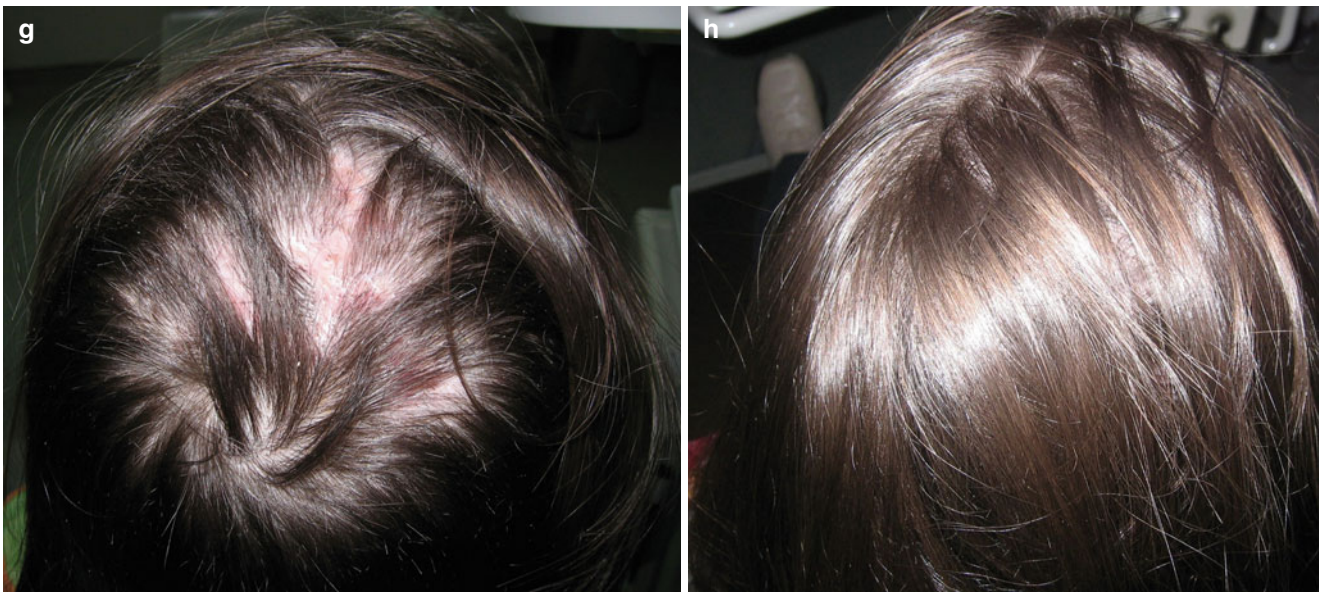

Fig. 2.45 (continued)

it for the restoration of lower eyelid. This precursor idea was not subject to common application until it was rediscovered very late for head and neck reconstruction by Brent during the 1980s (Brent and Byrd 1983; Brent et al. 1985). Since then, the temporoparietal fascial flap as a thin and pliable flap with an axial blood supply (Fig. 2.46) has been a useful tissue transfer technique, either pedicled or free, for the repair of a variety of head and neck defects but still remains underused especially in intraoral reconstruction. This flap represents an "étude" to the temporal anatomy.

The patient presented had an extensive verrucous carcinoma of the buccal mucosa extending to the labial commissure (Fig. 2.47a). The temple is chosen as the donor site by means of a pedicle temporoparietal fascial flap, to resurface the buccal defect (Fig. 2.47b). The exact position and course of the superficial temporal artery and its frontal and parietal branches are determined by a Doppler amplifier (Fig. 2.47c, d).

The skin incisions are outlined in a Y-shaped manner, starting from the root of the helix to the superior temporal line (Fig. 2.47e). Care is taken so that the incision lines are positioned next and parallel to the vessels. The preauricular incision can be extended up to the ear lobule. By this, three skin flaps an anterior, a posterior, and an upper will be raised to expose the temporoparietal fascia.

The trajectory of the temporal branch of the facial nerve is also outlined, according to the "Pitanguy line" (Fig. 2.47f). This represents the anterior area that limits the dissection of the flap. Dissection nearby and beyond this line could harm the nerve and is not necessary.

Resection of the verrucous carcinoma is performed leaving a wide (Fig. 2.47g) but not deep defect (Fig. 2.47g, h). Marginal and deep frozen section biopsies reveal the clear margins. No bulky tissue is needed for reconstruction; the thin and pliable temporoparietal fascia is the ideal solution for this certain defect. The skin flaps are raised by carrying the dissection in the subcutaneous layer, immediately deep to the hair follicles (Fig. 2.47i). When working at that level, there is no surgical plane and meticulous dissection is carried out sharply by a scalpel, taking care to leave subcutaneous fat on the dermis, thus preventing postoperative alopecia.

Gradually the outer aspect of the temporoparietal fascia is exposed.

Great care is taken to avoid vessel damage. Usually this regards veins that lie in a superficial level, at the outer aspect of the tempoparietal fascia. Here, the artery is expected to be almost entirely within the facia. The upper and the posterior skin flaps are raised until the superior temporal line.

The required part of the temporoparietal fascia that will be used as pedicle flap is outlined (Fig. 2.47j). The flap must include the parietal branches of the superficial temporal vessels. Usually the vein is visible, as it lies superficial. The artery, which lies deeper, is not seen but is easily palpated.

Incisions of the temporoparietal fascia are made through its whole thickness up to the temporalis muscular fascia (Fig. 2.47k). The frontal branches of the superficial temporal vessels are identified at the anterior edge of the flap and are divided.

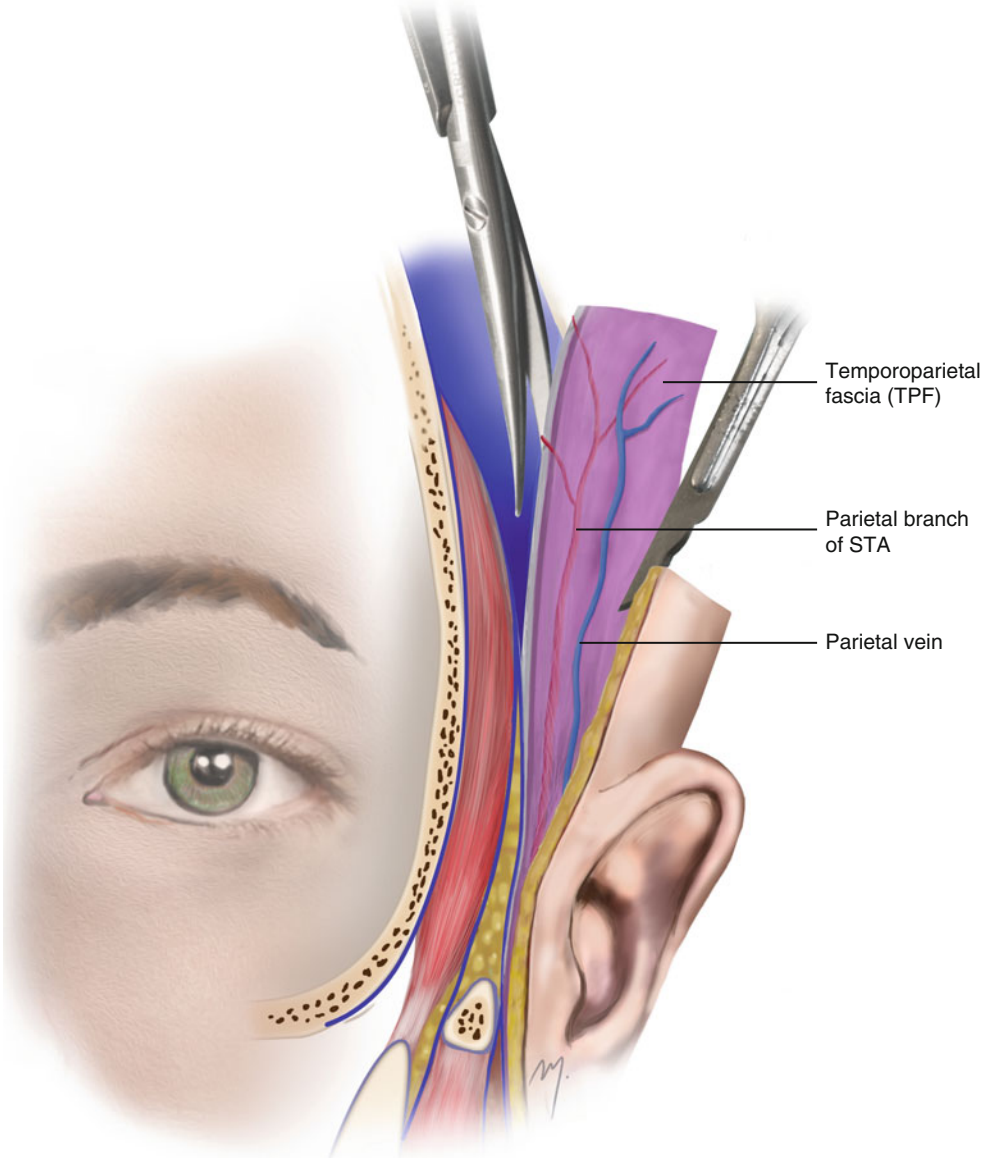

Fig. 2.46 The temporoparietal fascial flap

The flap is then raised with ease dissecting to the loose areolar tissue plane, proceeding from superior to inferior (Fig. 2.47l). When the root of the helix is reached, delicate manipulation is required so as not to damage the arterial pedicle. Once the pedicle has been distinguished, the base can be narrowed up to 2 cm to allow for ample rotation and insertion of the flap into the mouth.

The flap length is controlled, so that it reaches the defect without tension and to avoid the strangulation of the feeding vessels in its base (Fig. 2.47m, n). A skin graft is used to cover the part of the flap that when transferred intraorally will resurface the buccal defect (Fig. 2.47o). The length of the skin-grafted flap is controlled again (Fig. 2.47p), and a tunnel to the oral cavity passing deep to the zygomatic arch is created. The flap is then passed through the tunnel to the buccal defect (Fig. 2.47q). The tunnel must be sufficiently wide, so that the feeding artery and vein are not compressed (Fig. 2.47r). The flap after passing through the tunnel to the buccal defect is sewn in place (Fig. 2.47s). The skin flaps are returned and sutured (Fig. 2.47t). The flap healed well, resurfacing successfully the entire buccal defect and allowing in a normal mouth opening (Fig. 2.47u). Hair gradually grew in the donor site, completely hiding the scars (Fig. 2.47v, w). When the anatomy of the area is strictly followed, no facial nerve damage occurs (Fig. 2.47x).


a


b


c
8MHz


d


e

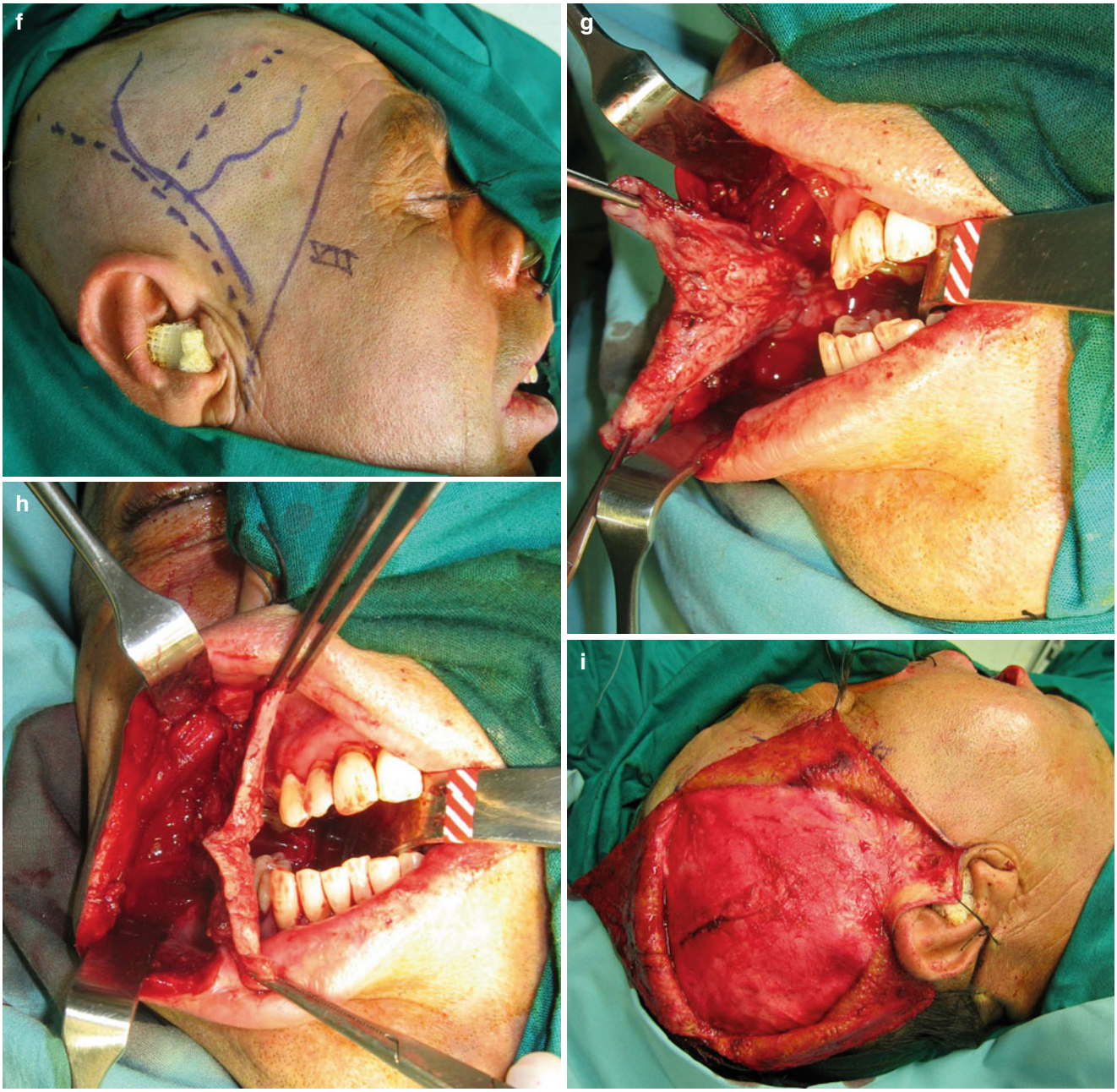

Fig. 2.47 (continued)

Fig. 2.47 (**a**) Intraoral verrucous carcinoma. (**b**) Temporoparietal fascia will be used for reconstruction and the temple is shaved. (**c**, **d**) Preoperatively, STA and its branches were marked by using Doppler US. (**e**) Skin incisions are outlined in a Y-shaped fashion. (**f**) The trajectory of the frontal branch of the facial nerve is outlined by using the "Pitanguy line." (**g**) Wide excision of the lesion. (**h**) Excisional plane. (**i**) Undermining of the skin flaps is carried out at the subcutaneous tissue level. The parietal branch of the superficial temporal vein is seen at the outer surface of the temporoparietal fascia. (**j**) The portion of the temporoparietal fascia that will be used as a flap is outlined. The parietal branch of the superficial temporal vein is included to the flap. (**k**) Temporoparietal fascia incised. (**l**) The temporoparietal fascia is raised exposing the temporalis fascia. (**m**) Flap length control. (**n**) Flap base is sufficiently released. (**o**) Skin graft to the "mucosal aspect" of the flap. (**p**) Recontrol of the skin-grafted flap. (**q**) The flap is tunneled and transferred intraorally. (**r**) Flap enters the tunnel deep to zygomatic arch. The base is rotated with discretion without being compressed or forming a sharp angulation. (**s**) The skin-grafted temporoparietal fascial flap reconstructed the buccal defect. (**t**) Donor site closed. (**u**) The buccal defect fully reconstructed. Normal mouth opening width. (**v**) Two months postoperative. (**w**) Six months postoperative. (**x**) The frontal branch of the facial nerve is intact (From: Thomaidis et al. (2006), with permission)

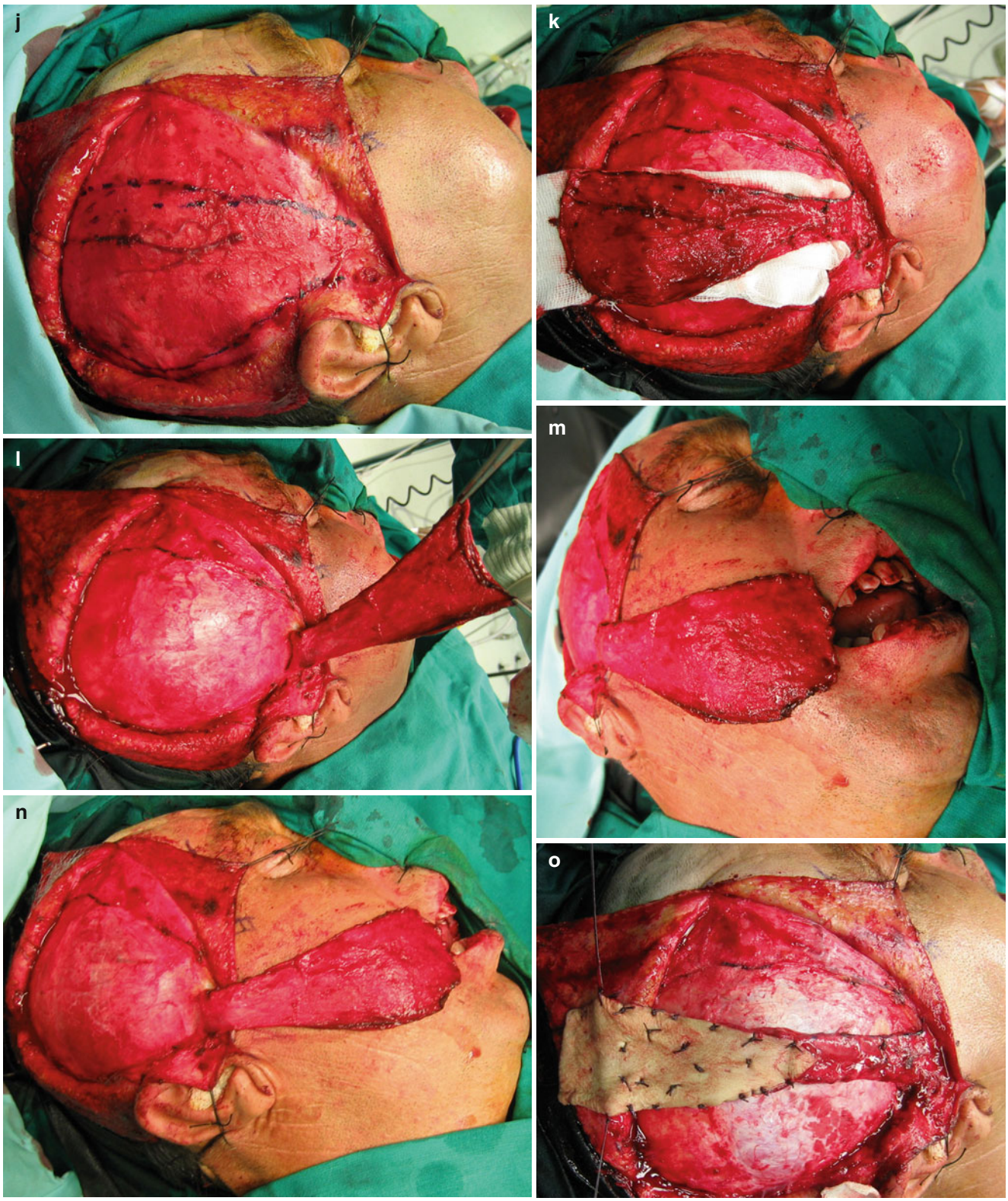

Fig. 2.47 (continued)

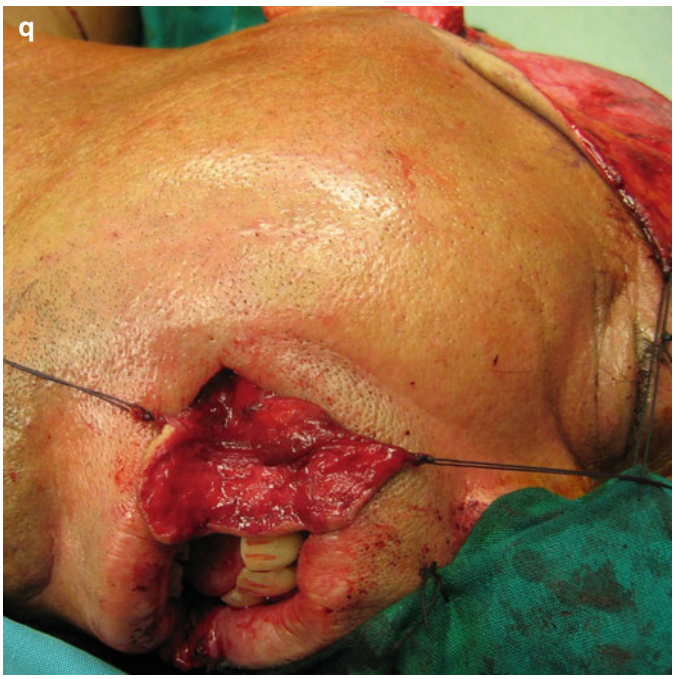

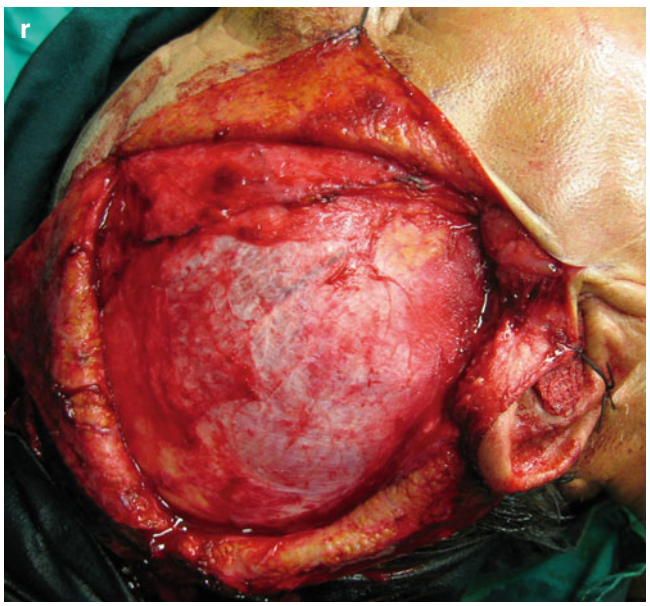

Fig. 2.47 (continued)

Fig. 2.47 (continued)

References

Abul-Hassan HS, Ascher GD, Acland RD (1986) Surgical anatomy and blood supply of the fascial layers of the temporal region. Plast Reconstr Surg 77(1):17–28

Accioli de Vasconcellos JJ, Britto JA, Henin D, Vacher C (2003) The fascial planes of the temple and face: an en-bloc anatomical study and a plea for consistency. Br J Plast Surg 56(7):623–629

Arena S (1977) The posterior scalping flap. Laryngoscope 87(1):98–104

Brent B, Byrd HS (1983) Secondary ear reconstruction with cartilage grafts covered by axial, random, and free flaps of temporoparietal fascia. Plast Reconstr Surg 72(2):141–152

Brent B, Upton J, Acland RD (1985) Experience with the temporoparietal fascial free flap. Plast Reconstr Surg 76(2):177–188

Brown WJ (1898) Extraordinary case of a horse bite: the external ear completely bitten off and successfully replaced. Lancet 1:1533

Casanova R, Cavalcante D, Grotting JC, Vasconez LO, Psillakis JM (1986) Anatomic basis for vascularized outer-table calvarial bone flaps. Plast Reconstr Surg 78(3):300–308

Chen TH, Chen CH, Shyu JF, Wu CW, Lui WY, Liu JC (1999) Distribution of the superficial temporal artery in the Chinese adult. Plast Reconstr Surg 104(5):1276–1279

Cutting CB, McCarthy JG, Berenstein A (1984) Blood supply of the upper craniofacial skeleton: the search for composite calvarial bone flaps. Plast Reconstr Surg 74(5):603–610

Czerwinski F (1992) Variability in the course of the superficial temporal artery in man. Folia Morphol 51(1):49–54

Dias AD, Chhajlani P (1977) The post-and retro-auricular scalping flap (the PARAS flap). Br J Plast Surg 40(4):360–366

Dubin B, Jackson IT, Halim A, Triplett WW, Ferreira M (1989) Anatomy of the buccal fat pad and its clinical significance. Plast Reconstr Surg 83(2):257–264

Edizer M, Beden U, Icten N (2009) Morphological parameters of the periorbital arterial arcades and potential clinical significance based on anatomical identification. J Craniofac Surg 20(1):209–214

Friedman M, Grybauskas V, Skolnik E, Katz A, Chilis T, Toriumi DM (1986) Parietal occipital nape of neck flap. A myocutaneous flap for selected head and neck reconstruction. Arch Otolaryngol Head Neck Surg 112(3):309–315

Galvao MS (1981) A postauricular flap based on the contralateral superficial temporal vessels. Plast Reconstr Surg 68(6):891–897

Genden ME, Mandell D, Urken LM (2000) The combination of posterior scalping flap and gracilis free flap for mid-face reconstruction. Oper Tech Otolaryngol Head Neck Surg 11(2):72–75

Haas F, Weiglein A, Schwarzl F, Scharnagl E (2004) The lower trapezius musculocutaneous flap from pedicled to free flap: anatomical basis and clinical applications based on the dorsal scapular artery. Plast Reconstr Surg 113(6):1580–1590

Hayman LA, Shukla V, Ly C, Taber KH (2003) Clinical and imaging anatomy of the scalp. J Comput Assist Tomogr 27(3):454–459

Hwang K, Suh MS, Lee SI, Chung IH (2004) Zygomaticotemporal nerve passage in the orbit and temporal area. J Craniofac Surg 15(2):209–214

Izquierdo R, Parry SW, Boydell CL, Almand J (1991) The great auricular nerve revisited: pertinent anatomy for SMAS-platysma rhytidectomy. Ann Plast Surg 27(1):44–48

Jackson JT (2007) Local flaps in head and neck reconstruction, 2nd edn. Quality Medical Pub, St Louis

Janis JE, Hatef DA, Ducic I, Reece EM, Hamawy AH, Becker S, Guyuron B (2010a) The anatomy of the greater occipital nerve: part II. Compression point topography. Plast Reconstr Surg 126(5):1563–1572

Janis JE, Hatef DA, Reece EM, McCluskey PD, Schaub TA, Guyuron B (2010b) Neurovascular compression of the greater occipital nerve: implications for migraine headaches. Plast Reconstr Surg 126(6):1996–2001

Jeong SM, Park KJ, Kang SH, Shin HW, Kim H, Lee HK, Chung YG (2010) Anatomical consideration of the anterior and lateral cutaneous nerves in the scalp. J Korean Med Sci 25(4): 517–522

Jervis W, Salyer KE, Busquets MA, Atkins RW (1974) Further applications of the Limberg and Dufourmentel flaps. Plast Reconstr Surg 54(3):335–340

Kazanjian VH, Holmes EM (1944) Reconstruction after radical operation for osteomyelitis of the frontal bone: experience in thirty-eight cases. Surg Gynecol Obstet 79:397

Kemp WJ 3rd, Tubbs RS, Cohen-Gadol AA (2011) The innervation of the scalp: A comprehensive review including anatomy, pathology, and neurosurgical correlates Surg Neurol Int 2:178

Lang J (1995) Skull base and related structures, atlas of clinical anatomy. Schattauer Stuttgart, New York

Lister GD, Gibson T (1972) Closure of rhomboid skin defects: the flaps of Limberg and Dufourmentel. Br J Plast Surg 25(3):300–314

Mandell DL, Genden EM, Biller HF, Urken ML (2000) Posterior scalping flap revisited. Arch Otolaryngol Head Neck Surg 126(3): 303–307

Marano SR, Fischer DW, Gaines C, Sonntag VK (1985) Anatomical study of the superficial temporal artery. Neurosurgery 16(6): 786–790

Marty F, Montandon D, Gumener R, Zbrodowski A (1986) Subcutaneous tissue in the scalp: anatomical, physiological, and clinical study. Ann Plast Surg 16(5):368–376

Matloub H, Molnar J (1996) Anatomy of the scalp. In: Stough D, Haber R (eds) Hair replacement. Mosby, St. Louis

McCarthy JG, Zide BM (1984) The spectrum of calvarial bone grafting: Introduction of the vascularised calvarial bone flap. Plast Reconstr Surg 74(1):10–18

Monks GH (1898) The restoration of a lower lid by a new method. Boston Med Surg J 139:385

Nakajima H, Imanishi N, Minabe T (1995) The arterial anatomy of the temporal region and the vascular basis of various temporal flaps. Br J Plast Surg 48(7):439–450

Natsis K, Baraliakos X, Appell HJ, Tsikaras P, Gigis I, Koebke J (2006) The course of the greater occipital nerve in the suboccipital region: a proposal for setting landmarks for local anesthesia in patients with occipital neuralgia. Clin Anat 19(4):332–336

Orticochea M (1967) Four flap scalp reconstruction technique. Br J Plast Surg 20(2):159–171

Orticochea M (1971) Three flap scalp reconstruction technique. Br J Plast Surg 24(2):184–188

Owsley JQ, Agarwal CA (2008) Safely navigating around the facial nerve in three dimensions. Clin Plast Surg 35(4):469–477

Pinar YA, Govsa F (2006) Anatomy of the superficial temporal artery and its branches: its importance for surgery. Surg Radiol Anat 28(3):248–253

Pitanguy I, Ramos AS (1966) The frontal branch of the facial nerve: the importance of its variations in face lifting. Plast Reconstr Surg 38(4):352–356

Raposio E, Santi P, Nordstrom RE (1988) Effects of galeotomies on scalp flaps. Ann Plast Surg 41(1):17–21

Schmidt BL, Pogrel MA, Hakim-Faal Z (2001) The course of the temporal branch of the facial nerve in the periorbital region. J Oral Maxillofac Surg 59(2):178–184

Standring S (2008) Gray's anatomy. The anatomical basis of clinical practice, 40th edn. Churchill Livingstone-Elsevier, Edinburg

Stock AL, Collins HP, Davidson TM (1980) Anatomy of the superficial temporal artery. Head Neck Surg 2(6):466–469

Stuzin JM, Wagstrom L, Kawamoto HK, Wolfe SA (1989) Anatomy of the frontal branch of the facial nerve: the significance of the temporal fat pad. Plast Reconstr Surg 83(2):265–271

Stuzin JM, Wagstrom L, Kawamoto HK, Baker TJ, Wolfe SA (1990) The anatomy and clinical applications of the buccal fat pad. Plast Reconstr Surg 85(1):29–37

Tayfur V, Edizer M, Magden O (2010) Anatomic bases of superficial temporal artery and temporal branch of facial nerve. J Craniofac Surg 21(6):1945–1947

Thomaidis VK et al (2006) "The temporoparietal fascial flap in reconstruction of large intraoral defects (article in. Greek) Hell Arch Oral Maxillofac Surg 7(4):173–183

Tideman H, Bosanquet A, Scott J (1986) Use of the buccal fat pad as a pedicled graft. J Oral Maxillofac Surg 44(6):435–440

Tolhurst ED, Carstens HM, Greco JR, Hurwitz JD (1991) The surgical anatomy of the scalp. Plast Reconstr Surg 87(4):603–612

Tremolada C, Candiani P, Signorini M, Vigano M, Donati L (1994) The surgical anatomy of the subcutaneous fascial system of the scalp. Ann Plast Surg 32(1):8–14

Trussler AP, Stephan P, Hatef D, Schaverien M, Meade R, Barton FE (2010) The frontal branch of the facial nerve across the zygomatic arch: anatomical relevance of the high-SMAS technique. Plast Reconstr Surg 125(4):1221–1229

Tubbs RS, Salter EG, Wellons JC, Blount JP, Oakes WJ (2007) Landmarks for the identification of the cutaneous nerves of the occiput and nuchal regions. Clin Anat 20(3):235–238

Tubbs RS, Mortazavi MM, Loukas M, D'Antoni AV, Shoja MM, Chern JJ, Cohen-Gadol AA (2011) Anatomical study of the third occipital nerve and its potential role in occipital headache/neck pain following midline dissections of the craniocervical junction. J Neurosurg Spine 15(1):71–75

Tzafetta K, Terzis JK (2010) Essays on the facial nerve. Part 1 microanatomy. Plast Reconstr Surg 125(3):879–889

Woltmann M, Faveri R, Sgrott EA (2000) Anatomical distances of the facial nerve branches associated with the temporomandibular joint in adult negroes and caucasians. Braz J morphol Sci 17(2): 107–111

Worthen EF (1990) Transposition and rotation scalp flaps and rotation forehead flap. In: Grabb's encyclopedia of flaps, vol 1, Head and neck. Little Brown and Company, Boston

Zani R, Fadul R Jr, Da Rocha MA, Santos RA, Alves MC, Ferreira LM (2003) Facial nerve in rhytidoplasty: anatomic study of its trajectory in the overlying skin and the most common sites of injury. Ann Plast Surg 51(3):236–242

Forehead

3

The forehead is a prominent element that constitutes the upper face. In its midsection, it is slightly convex, flatters laterally, and becomes concave as it transitions to the temple.

The anatomic boundaries of the forehead (Fig. 3.1) are the anterior hairline superiorly and inferiorly the nasion, the glabella, and the eyebrows. The lateral ends of the eyebrows determine the lateral borders of the main forehead. The temporal area extends beyond this borderline.

The anterior hairline defines the upper limit of the forehead and is the boundary between it and the scalp, but in the presence of alopecia, it cannot be a stable landmark. In this case, the superior border is determined by the superior edge of the frontalis muscle.

The glabella is a bony structure in the smooth elevation between the superciliary arches. As forehead subunit, glabella is the smooth and hairless area between the eyebrows. However, during the aging process, transverse and vertical glabellar rhytides begin to appear.

The supraorbital rims are palpable along their whole length as a sharp prominence in the lateral two-thirds and rounded in the medial third. At the junction of the medial third and lateral two-thirds, the supraorbital notch can also be felt.

The eyebrows are two arched, hair-covered skin ridges lying over the supraorbital rims, protecting the eyes from flowing forehead sweat and sunlight. The position and contour of this minor forehead anatomic feature play a major role in the aesthetic appearance and must be taken into great account, to avoid its distortion when planning forehead flaps. Eyebrow shape and position change depending on gender. In males, the brow is more horizontal and thicker and is found in a lower position at the level of supraorbital rim. In females, the brow is more arched, thinner, and in a somewhat higher position, above the level of the supraorbital rim. Approximately 200–250 short and thick hairs (without having arrector pili muscles) are set in the eyebrows. The number of eyebrow hair remains almost stable during life, with the exception of older males where, during the aging process, growth of eyebrow hair increases. When making incisions to the eyebrow and elevating a flap in this area, it is very important to know the direction of the hair in order to cut parallel to them. In the medial eyebrow part, hair follicles are all directed superiorly; in the upper portion of the central and lateral parts of the brow, follicles are directed inferiorly; and in the lower portion, follicles are directed superiorly (Lemke and Stasior 1982). Muscle fibers insert into the dermis of the eyebrow, moving it in several directions. The eyebrow mobility is significant in creating the full range of emotional expressions of the face. The frontalis muscle acting as a brow elevator achieves these movements, while the antagonistic procerus, corrugator, orbicularis oculi, and depressor supercilii act as brow depressor muscles.

Fig. 3.1 Boundaries of the forehead

V.K. Thomaidis, *Cutaneous Flaps in Head and Neck Reconstruction*,
DOI 10.1007/978-3-642-41254-7_3, © Springer-Verlag Berlin Heidelberg 2014

3.1 Layered Anatomy of Forehead

The forehead could be considered as the hairless frontal elongation of the scalp. Being an anatomic continuity of the scalp, it consists of the same five distinct layers: the skin, connective subcutaneous tissue, galea aponeurotica, loose areolar connective tissue, and periosteum (Fig. 3.2).

3.1.1 Skin and Subcutaneous Tissue

The skin and subcutaneous tissue of the forehead (first and second layer, respectively) are very firmly attached, and therefore it is very difficult to work with it individually from a surgical perspective.

The forehead skin, rich in sebaceous and sweat glands, is one of the thickest skins of the face with an average thickness of 2.4 mm. It varies from one individual to other but also changes by age and sun exposure. The skin of the forehead decreases progressively in thickness and sebaceous gland concentration, when moving from the suprabrow area toward the anterior hairline. This occurs in the same manner in the temporal region when moving from the lateral canthus to the scalp hairline. The central forehead skin is densely adherent to the abundant underlying subcutaneous tissue forming a soft tissue layer that is relatively thick, rigid, and minimally mobile. From the medial to lateral regions, the mobility increases. In the temporal area, the connections are loose, to the underlying temporalis fascia, which results in enhanced skin mobility over this area. Thus, the lateral forehead temporal region may act as a tissue reservoir for reconstruction of more medially located defects (Vuyk 2006; Sykes 2009).

The relaxed skin tension lines (RSTLs) on the forehead run horizontally slightly curving in a vertical direction laterally. At the glabellar region, they are vertically oriented (Fig. 3.3).

The subcutaneous tissue is richly vascularized containing a homogenous layer of adipose tissue. The subcutaneous fat of the forehead attaches to the underlying galea aponeurotica by fibrous septa, which contain vessels, nerves, and lymphatics. Also numerous transverse fibrous septa from the frontalis muscle to the dermis are found within this layer in the forehead (Sykes 2009). These septa are partially responsible for the deep, horizontal forehead lines providing excellent camouflage of scars (Seline and Siegle 2005).

3.1.2 Epicranial Aponeurosis-Forehead Muscular Layer

3.1.2.1 Galea

The epicranial aponeurosis named also galea or galea aponeurotica, as mentioned in the previous chapter, is the thin tendinous sheet of connective tissue that encompasses the entire dome of the skull, joining both the paired frontalis and occipitalis muscles. The galea at the forehead joins the two

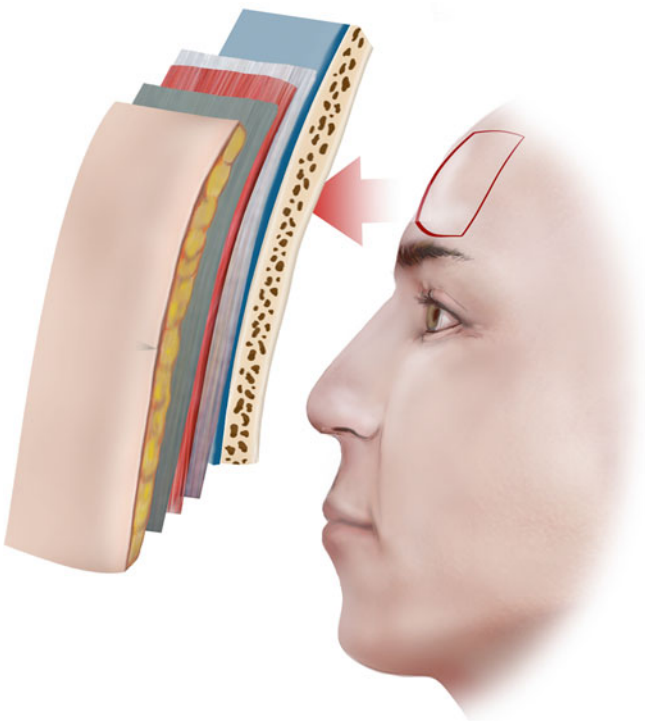

Fig. 3.2 The forehead consists of the same five layers of the scalp

Fig. 3.3 Relaxed skin tension lines (RSTLs) at the forehead

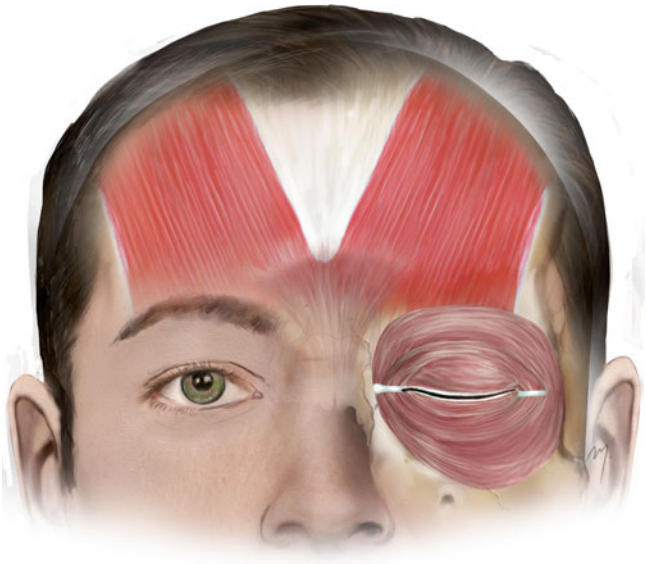

Fig. 3.4 Galea and frontalis muscle

frontalis muscles but also fills the gap between them sending a short, narrow prolongation between their two bellies (Fig. 3.4). On its course from the upper to the lower forehead, the galea splits several times in various layers, which reunite again to the supraorbital margin (Tarbet and Lemke 1997; Knize 2001, 2007; Sykes 2009). In actuality, the galea is the fibromuscular extension of the superficial musculoaponeurotic system (SMAS), which becomes continuous with the temporoparietal fascia in the temple (Mitz and Peyronie 1976). The galea is loosely connected to the underlying pericranium by the layer of loose areolar connective tissue enabling it to be mobile, thus moving and sliding freely over the pericranium.

As the galea passes into the upper forehead, it splits into two layers, the superficial galea layer and the deep galea layer which encompass the frontalis muscle.

The superficial layer of galea is thin and lies anteriorly to each frontalis muscle. It covers the surface of the frontalis muscle and continues over the surface of the orbicularis oculi muscle, as a single, filmy layer.

The deep layer of galea is thicker than the superficial and lies under the muscle. As the deep galea layer runs to the supraorbital area, it splits again and envelops a fat pocket, the retro-orbicularis oculi fat (ROOF).

3.1.2.2 Forehead Muscular Layer

The muscular layer of the forehead is composed of frontalis, procerus, corrugator supercilii, depressor supercilii, and the orbital part of the orbicularis oculi muscles. These muscles are arranged in three levels: the superficial level (frontalis, procerus, and orbicularis oculi muscles), the intermediate level (depressor supercilii muscle), and the deep level (corrugator supercilii muscle).

3.1.2.2.1 Frontalis Muscle

The paired frontalis muscles are the frontal parts of the two occipitofrontalis muscles. The frontalis muscles are thin, quadrilateral, and broader with longer fibers than the occipital part that extend from the anterior edge of the epicranial aponeurosis to the eyebrow (Fig. 3.4). The two bellies of the frontalis muscle are placed symmetrically and are vertically oriented, but they leave the mid-forehead region free of muscle fibers. The superior side of the muscle, which is its origin field, lies adjacent to the coronal suture line of the skull. The lateral side of the muscle extends slightly more cephalad than the medial side, and the lateral margin of frontalis muscle is thinner along the superior temporal line (Knize 1996a, b).

The frontalis muscle has no bony attachments and originates from the anterior edge of galea aponeurotica. Its muscle fibers extend toward the supraorbital rim where they merge with those of the adjacent muscles, entering the deep orbicularis oculi muscle surface. The medial fibers of the frontalis blend with those of the procerus muscle. Under the brow, the lateral fibers of the frontalis muscle interdigitate with the corrugator supercilii and the orbital portion of orbicularis oculi muscles.

The insertion of the frontalis muscle fibers represents more of a blend with the other muscle fibers than a direct dermal insertion.

Frontalis muscle receives its arterial supply from branches of the superficial temporal supraorbital and supratrochlear arteries and is innervated by the temporal branches of the facial nerve from its undersurface.

The frontalis muscles, with its fibers offering no true bony insertion but blending with neighboring muscles, are the primary elevators of the brow. Acting from above, they raise the eyebrows and the skin over the root of the nose (expression of surprise, fright, horror). These muscles are antagonistic to the brow depressor muscles (procerus, corrugator, orbicularis oculi, and depressor supercilii), which do have real bony insertions. Acting from below, they draw the scalp forward. Due to the multiple attachments of the vertically oriented fiber septa to the dermis of the forehead skin, they are responsible for the formation of horizontal forehead rhytides. Acting alternately with the occipital muscles, they move the entire scalp backward and forward.

3.1.2.2.2 Procerus Muscle

Procerus is a vertical, flat, thin, and pyramidal shape muscle (Fig. 3.5). Although the procerus belongs anatomically in the

Fig. 3.5 Procerus muscle

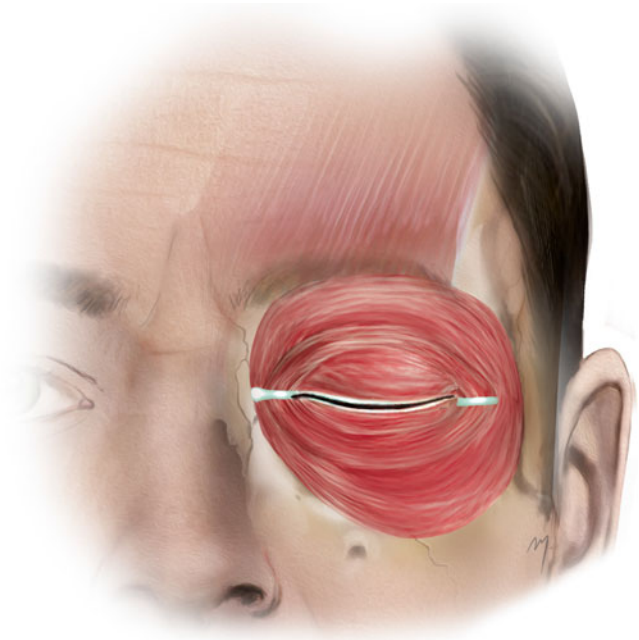

Fig. 3.6 Orbicularis muscle

group of nasal musculature, functionally it is much more a forehead muscle, involved in eyebrow movement.

It originates at the nasal bone and arises from the tendinous fibers attached to a fibrous fascia that covers the lower part of the nasal bones, the upper part of the lateral nasal cartilage, and the aponeurosis of the transverse part of nasalis (Keller and Mashkevich 2009). All these anatomic elements from where procerus originates are parts of the nasal SMAS (see Chap. 4). The muscle courses superiorly with its fibers oriented vertically, medial to the depressor supercilii muscle and the medial head of the orbicularis oculi muscle. As it courses superiorly, above the nose, the fibers of the procerus become continuous with the medial fibers of the frontalis muscle. The muscle fibers insert into the glabellar skin, in a varied width, over the lower mid-forehead and between the eyebrows.

Procerus receives its arterial supply mainly from branches of the facial artery. It is innervated by the facial nerve and more specifically the angular nerve (the buccal branch of the facial nerve, after receiving a contribution from the zygomatic branch; see Chap. 5) (Caminer et al. 2006). The frontal branch of the facial nerve contributes also to the innervation of the upper portion of the muscle.

The procerus is a brow depressor that draws down the medial angle of the eyebrow (frowning, "concentration," reduces the glare of bright sunlight) and forms horizontal glabellar furrows.

3.1.2.2.3 Orbicularis Oculi Muscle

The orbicularis oculi is a broad, elliptical, and flat muscle sheet that is regarded as a component of the superficial musculoaponeurotic system (SMAS). The muscle surrounds the circumference of the orbit sealing it (Fig. 3.6). Although it belongs in circumorbital and palpebral musculature group, it spreads into the forehead region interdigitating with the forehead muscles.

It consists of three parts, the palpebral, the lacrimal, and the orbital part. The palpebral part (divided topographically in a preseptal and a pretarsal portion), thin and pale, arises from the superficial surface of the medial canthal ligament and from the bone immediately above and below the ligament. The fibers sweep across the eyelids anteriorly to the orbital septum and interlace at the lateral commissure to form the lateral palpebral raphe. The lacrimal part lies behind the lacrimal sac, attached to the lacrimal fascia, to the upper part of the crest of the lacrimal bone, and adjacent part of the lateral surface of the lacrimal bone. The orbital part, thicker than the other two, is the part involved in the lower forehead. It lies over the supraorbital rim and interdigitates with the neighboring forehead muscle fibers.

Orbital Part of the Orbicularis Oculi Muscle

The muscle fibers of the orbital part arise from the superior edge of medial canthal ligament, the nasal component of the frontal bone, and the frontal process of the maxilla. The fibers arc superiorly and inferiorly over the orbital rim, without interruption on the lateral side, where there is no bony attachment. The upper muscle fibers extend superiorly and intermix with the frontalis and corrugator supercilii muscles. The fibers from the medial part are fixed to dermis under the medial head of the eyebrow (Knize 2000). Some of the

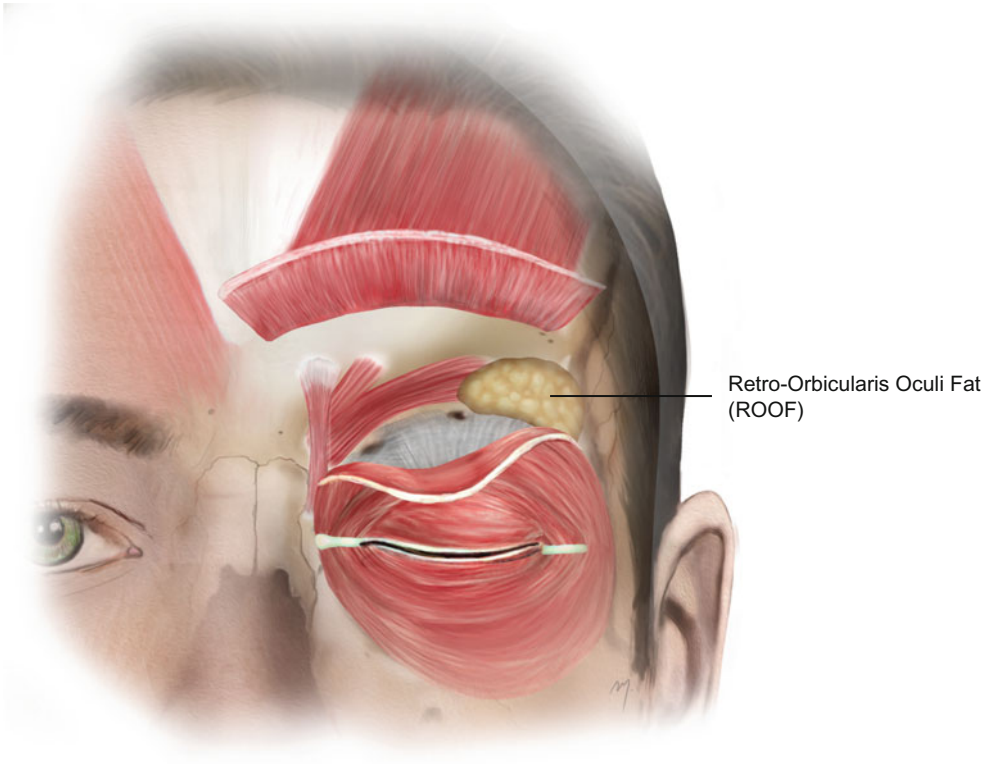

Fig. 3.7 Retro-orbicularis oculi fat (ROOF)

medial or lateral fibers of the orbital part of the orbicularis oculi may form distinct muscle bands (medial, lateral muscular bands of orbicularis oculi muscle) that are attached to the cheek skin, to the frontal muscle, or to the zygomatic arch (Park et al. 2011, 2012).

The fibers of the orbicularis, after completing their circular course, insert medially at the inferior edge of medial canthal ligament, just below their points of origin.

The orbicularis attaches only medially to the medial orbital margin and the medial canthal ligament. Elsewhere, the orbicularis is attached by retaining ligaments from the periosteum to the fascia on its undersurface (Keller and Mashkevich 2009).

The orbicularis oculi is innervated from the temporal, zygomatic, and buccal branches of the facial nerve. The nerves are horizontally oriented and gather to the undersurface of the muscle from its temporal and inferior side. The anterior and middle rami of the frontal branch run deep to the undersurface of orbicularis muscle and innervate the upper and superolateral part of orbicularis. The zygomatic branch innervates the lower and inferolateral part of the muscle. The buccal branch receives a contribution from the zygomatic branch and forms the angular nerve. The angular nerve, running cranially to the medial canthal ligament, sends rami to the undersurface of the low and medial part of orbicularis, on its way to reach the procerus and the oblique head of corrugator supercilii (Caminer et al. 2006). The innervation takes place by means of anastomotic neural plexuses formed by the involved nerves (Nemoto et al. 2001; Ouattara et al. 2004).

The orbital part of the muscle is used in forced eyelid closure. Furthermore, the medial head of this part acts by depressing the medial brow, along with the oblique head of the corrugator supercilii and the depressor supercilii (depressor muscle group for the medial eyebrow) (Knize 2000).

Just under the superolateral portion of the orbicularis muscle is situated a deep fat facial pocket, the retro-orbicularis oculi fat (ROOF).

Retro-Orbicularis Oculi Fat (ROOF)

The retro-orbicularis oculi fat (ROOF) is a transverse band of 5 mm thick fibroadipose tissue, which extends under the orbicularis muscle and the lower part of frontalis muscle enveloped by a split of the deep galea layer (Fig. 3.7). It extends above the orbital rims having a vertical height of approximately 1 cm and across the forehead for an additional 2–5 cm lateral to the supraorbital notch (foramen) (May et al. 1990; Hwang et al. 2007). It is situated superiorly to the orbital septum and the thinner, preseptal fat. In contrast with the orbital fat, which consists of fatty tissue, ROOF contains more fibrofatty tissue (May et al. 1990; Hwang et al. 2007). Through this fat pocket, run the lacrimal nerve and anastomotic veins to the supraorbital vein (Zide 2006). Within ROOF lies the lateral part of the transverse head of corrugator muscle. It plays an

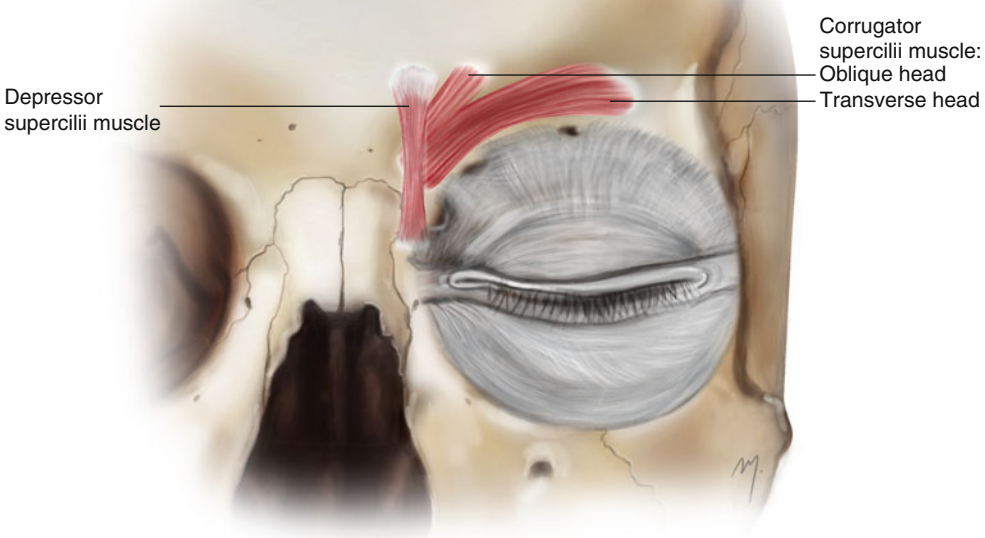

Fig. 3.8 The depressor supercilii and the corrugator muscles constituting the intermediate and the deep muscle layer of the forehead muscles, respectively

important role in eyebrow ptosis, as it slips downward during the aging process and is resected or reduced in aesthetic blepharoplasty operations. The ROOF is considered a part of the overall galea fat pad (which extends cranially for about 2–3 cm beneath the frontalis muscle and between the subdivisions of the deep galea layer) (Knize 2001; Zide 2006). These fat pads act as a brow pillow, allowing it to move freely.

3.1.2.2.4 Depressor Supercilii Muscle

There has been much confusion pertaining to the depressor supercilii muscle, because of the fact that it is difficult to discern whether or not the muscle is an extension of the medial head of the orbicularis oculi muscle or if it is a distinct muscle on its own (Lemke and Stasior 1982; Zide and Jelks 1985; Abramo 1995; Flowers 1998; Macdonald et al. 1998). Just in the late 1990s, Daniel and Landon (1997) confirmed that the depressor supercilii muscle is a distinct entity. Their findings reasserted later on, by Knize (2000, 2001) and Cook et al. (2001) who provided a description and a clear detailed schematic of the muscle.

According to these studies, the depressor supercilii lies anteriorly to the corrugator supercilii muscle and arises from the frontal process of the maxilla approximately 10 mm above the medial canthal tendon, near the edge of the bony medial orbital rim which is slightly posterior and superior to the posterior lacrimal crest, approximately 2–5 mm below the frontomaxillary suture line (Daniel and Landon 1997; Cook et al. 2001) (Fig. 3.8). After its origin, the muscle travels superiorly, toward the glabellar area, for 4–5 mm in the subcutaneous tissue. Its fibers are more vertically oriented than those of the corrugator. At its anterior side, the muscle comes in contact with the angular vessels. Cook et al. (2001) observed that the depressor supercilii appears to originate from two distinct heads in half of the cases studied. The two heads of the depressor supercilii muscle are located superiorly, while the angular vessels pass between them and merge before inserting in the dermis. The muscle fibers insert in the dermis near the medial eyebrow, at a point approximately 13–15 mm superior to the medial canthal tendon (Cook et al. 2001). The dermal insertion of depressor supercilii lies a few millimeters medial to the dermal insertion of the oblique head of the corrugator supercilii muscle (Knize 2000, 2001).

The depressor supercilii receives innervation from the angular nerve. It depresses the medial brow belonging to the depressor muscle group for the medial eyebrow.

3.1.2.2.5 Corrugator Supercilii Muscle

The corrugator supercilii muscle is comprised of two muscle bands (heads) that lie below the upper border of the superciliary arch and are located beneath the eyebrow. The corrugator muscle lies deep in the frontalis and orbicularis oculi muscles composing the deep muscular layer of the forehead (Fig. 3.8). It arises from the frontal bone at the superomedial orbital rim, slightly cranially to the trochlea. The origin has a wide base, with an average width of 10 mm being also 10 mm above the medial canthus. After arising from its origin, the muscle divides into its two heads, the small oblique head and the large transverse. The average thickness of the transverse head is 7.5 mm, while the oblique head 2 mm (Walden et al. 2005).

The small oblique head is situated underneath the depressor supercilii muscle. Its fibers run superiorly, parallel to the fibers of the depressor supercilii, across the glabellar region. After a short distance and interdigitation with neighboring muscle fibers of orbicularis and frontalis, it inserts in the dermis along the medial brow at a point approximately few mm, lateral to the insertion of the depressor supercilii muscle. A clear discrimination of the oblique head of the corrugator is not always possible, because occasionally, after its origin, its muscle fibers quickly parallel with the fibers of the larger transverse head (Janis et al. 2007).

The large transverse head passes laterally and slightly upward along the superior orbital rim and runs for about 3.5–4 cm lateral to the midline. The muscle lies beneath the orbicularis muscle, within the galea fat pad, between the layers of the deep galea plane. On the way to its dermal insertion, it becomes more superficial, piercing the frontalis and orbicularis oculi muscles (Knize 1996a, b).

The muscle fibers of the corrugator pierce and interdigitate with the fibers of the frontalis and orbicularis oculi muscles. The fibers of the transverse head usually insert into the deep surface of the middle eyebrow skin although more lateral extension has also been described (Isse and Elahi 2001). The fibers of the oblique head insert into the deep surface of the medial part of the eyebrow.

Corrugator supercilii has a dual nerve supply from both the frontal branch of the facial nerve and the angular nerve. The transverse head is innervated from the terminal branches of the frontal branch of the facial nerve. The oblique head receives its nerve supply from the angular nerve (Caminer et al. 2006). The angular nerve passes in front of the medial canthus reaching the muscle inferiorly.

The corrugator muscle is a brow depressor, which cooperates with the orbicularis oculi to draw the eyebrows medially and inferiorly (frowning, shielding the eyes in sunlight). The combined action of the two muscles produces vertical glabellar wrinkles.

This muscle is resected in forehead rejuvenation procedures and surgical treatment of migraine headaches.

3.1.3 Loose Areolar Tissue

The loose areolar tissue layer continues from the scalp to the forehead as the same subgaleal space, connecting the galea aponeurotica with the forehead pericranium. It also continues laterally at the temporal area as already examined, situated below the temporoparietal fascia and over the temporalis fascia. It receives blood from all the major forehead vessels due numerous tiny branches. The supraorbital and supratrochlear neurovascular bundles traverse this space within the supraorbital margin. Although this subgaleal space is vascular (as in the scalp) an effortless injection of a vasoconstrictive solution transforms it to an avascular dissection plane. Also here the areolar space is of great importance in forehead surgery because it can be easily dissected, creating a surgical dissection plane for large forehead flaps or allowing combined scalp-forehead flaps to be raised at the same plane.

3.1.4 Forehead Periosteum

The periosteum of the forehead is the same dense connective tissue layer over the frontal bone, which as pericranium covers the entire skull. In the frontal area, it is slightly thinner than in the other skull parts. It is loosely adherent to the outer surface of the frontal bone and lies just beneath the loose areolar layer. It becomes densely adherent to the bone over a transverse, 2.5 cm wide area, just above the orbital rims, and in a 6 mm wide band, medial to the superior temporal line (Knize 1996a, b, 2001).

Anteriorly, the periosteum becomes continuous with the periorbita (the inner lining of the orbital bones) at the orbital rims. The transition between the outer periosteum and the inner periorbita of the orbit is known as the arcus marginalis, a thickened connective tissue layer densely adherent almost to the entire orbital rim. Along the supraorbital rim at the arcus marginalis, the periosteum merges with the orbital septum (Zide and Jelks 1985).

At the forehead, Sullivan et al. (2006) described the presence of four retaining ligaments located around the orbit: an inferomedial (just medial to the supraorbital notch), a superomedial (13 mm lateral to the midline and 11 mm above the supraorbital rim), a superolateral (23 mm lateral to the midline and 10 mm above the rim), and a broad lateral one across the lateral aspect of the supraorbital rim.

3.2 Arterial Anatomy

The forehead arterial system consists of a latticework of anastomoses mainly supplied from three pairs of arteries. These arteries are the supraorbital and the supratrochlear arteries and the frontal branches of the superficial temporal arteries. Additionally, the dorsal nasal artery (although anatomically belongs to the nasal arteries) contributes to the blood supply of the mid-forehead area.

The supraorbital and the supratrochlear arteries constitute facial branches of the ophthalmic artery.

3.2.1 Ophthalmic Artery

The ophthalmic artery arises from the cerebral part of the internal carotid artery (rarely it arises from the middle meningeal artery). After entering the orbit, through the optic

canal, it gives off many small branches (posterior ciliary artery, muscular branches) and one large branch (the lacrimal artery) to the contents of the orbit.

The lacrimal artery runs forward at the junction of orbital roof and lateral wall and supplies the lacrimal gland. It is then distributed to the eyelids and conjunctiva. Terminal branches of the lacrimal artery are branched as superior and inferolateral palpebral arteries. They anastomose with the medial palpebral arteries. Within the orbit, the lacrimal artery gives also rise to the zygomatic artery, which subdivides further into the zygomaticofacial and the zygomaticotemporal arteries. In 1 %, the lacrimal artery rises from the middle meningeal artery via the superior orbital fissure, and in 2 % it arises from an abnormal ophthalmic artery.

Continuing its course, the ophthalmic artery passes over (or sometimes under) the optic nerve and gives off the supraorbital artery. It then reaches the medial orbital wall, in an anterior direction, below the superior oblique muscle, and gives off the anterior and posterior ethmoidal arteries. Anteriorly to the trochlea, the medial palpebral arteries arise, and the ophthalmic artery divides into its two terminal branches, the supratrochlear artery and the dorsal nasal artery.

The supratrochlear, supraorbital, lacrimal, medial palpebral, and dorsal nasal arteries are the branches of the ophthalmic artery that supply the face.

3.2.2 Supraorbital Artery

The supraorbital artery, after arising from the ophthalmic artery, runs anteriorly, between the orbital roof and levator palpebrae superioris and in company of the supraorbital nerve. The supraorbital artery is slightly wider than the supratrochlear artery. Its mean diameter ranges from 0.84 to 0.87 mm (Erdogmus and Govsa 2007).

It exits the orbit (Fig. 3.9), through the supraorbital notch or foramen, together with the supraorbital nerve and supraorbital vein, which lies anterior to the artery. In 13 % of cases, the supraorbital artery and the supratrochlear artery exit the orbit as a single vessel and separate immediately after exiting from the foramen (notch) (Erdogmus and Govsa 2007).

3.2.2.1 Supraorbital Notch (Foramen)

The supraorbital notch (foramen) is situated approximately 2.5–3 cm from the midline (Webster et al. 1986; Miller et al. 2000; Park et al. 2003). Bilateral notches are present more often (60–90 %) than bilateral foramina (Webster et al. 1986; Chung et al 1995; Saylam et al. 2003; Cuzalina and Holmes 2005). Rarely, one notch may be found on one side and one foramen on the other side. The foramen often represents the exit of a small supraorbital canal from where the neurovascular bundle passes from the orbit to the forehead. When a foramen is present, it is located and usually palpated up to 15 mm in relation to the supraorbital rim. In cases where palpability is questionable, an additional landmark can be used; the vertical location of the foramen is situated approximately on the midpupillary line. Great diversity and variants of these notches (foramina) exist from one individual to the other due to sex and race differences (Chung et al. 1995; Kimura 1977; Cheng et al. 2006; Agthong et al. 2005; Jeong et al. 2010; Chrcanovic et al. 2011). In cases where a supraorbital notch is present, it transforms into a "foramen" by a ligament (supraorbital ligament).

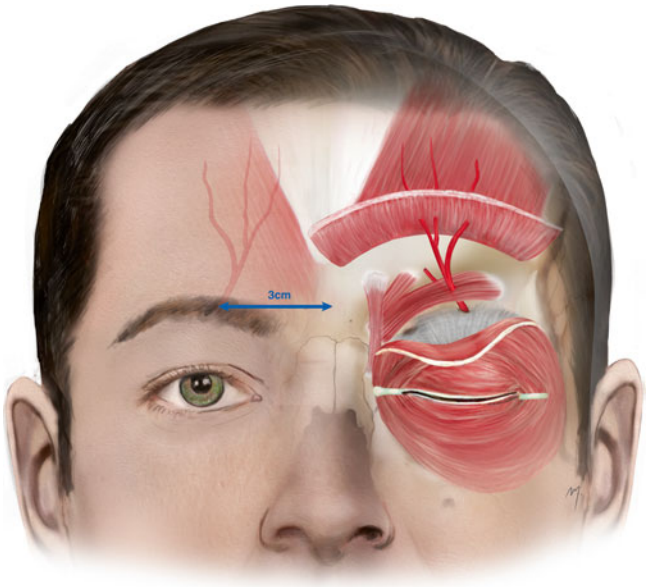

Fig. 3.9 Exit point of the supraorbital artery and the course of its superficial branch

The supraorbital artery continues running over the supraorbital rim slightly from medial to lateral and enters the corrugator muscle where it divides into a superficial branch, which supplies the superficial layers of the scalp, and a deep branch supplying the pericranium. The division of the supraorbital artery in 80–90 % of individuals happens at the level of the supraorbital rim or below. In the remainder, division occurs approximately 8.5 mm above the orbital rim (Yoshioka and Kishimoto 1991; Yoshioka and Rhoton 2005).

3.2.2.2 Superficial Branch of the Supraorbital Artery

The superficial branch of the supraorbital artery (Fig. 3.9) enters the corrugator, the orbicularis oculi, and the lowest part of the frontalis muscle, traveling for a short distance within these muscles and divides into 2–4 subbranches. In a distance approximately 2–3 cm above the supraorbital rim, they pierce the frontalis muscle and the galea, becoming more superficial, and travel within the subcutaneous tissue layer.

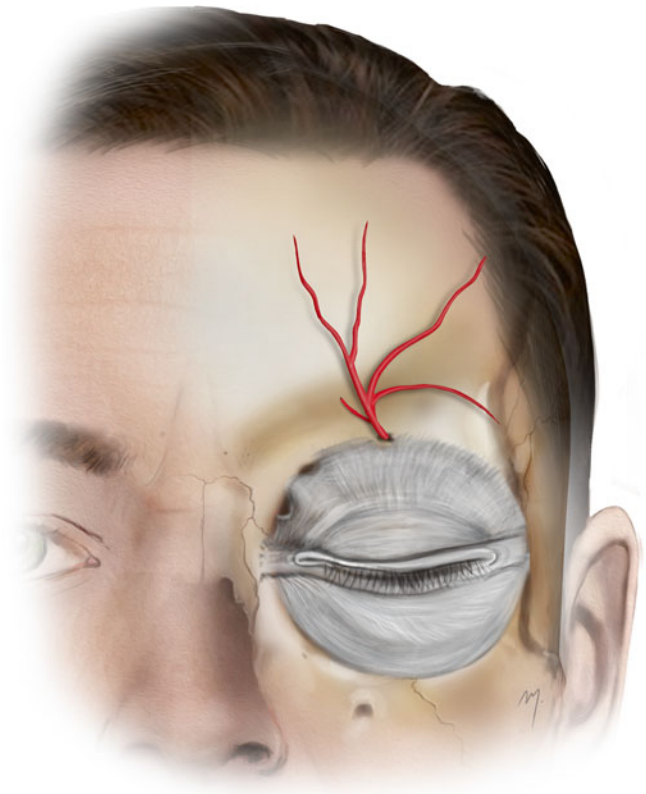

Fig. 3.10 Deep branch of the supraorbital artery

The superficial branch of the supraorbital artery does not have as long a course as the accompanying supraorbital nerve.

3.2.2.3 Deep Branch of the Supraorbital Artery

After dividing from the main trunk, the deep branch (Fig. 3.10) gives off 2–4 branches, with a mean diameter of 0.6 mm (Yoshioka and Rhoton 2005). These branches run axially as independent tiny vessels above the pericranium within the loose areolar tissue layer, for a distance of about 1.5–4 cm (Erdogmus and Govsa 2007).

Kleintjes (2007) demonstrated a detailed branching pattern of the deep supraorbital artery. According to his study, three branches usually exist: vertical branches, which run anteriorly and almost parallel; the oblique branch running anterolaterally over the periosteum, which anastomoses with the frontal branch of the superficial temporal artery; and the horizontal branch which runs laterally and above the orbital rim.

One vessel of the deep branches supplies the diploe of the frontal bone and the mucoperiosteum of the frontal sinus (Cormack and Lamberty 1994).

Both branches of the supraorbital artery supply the skin and the muscles of the upper eyelid, the forehead and scalp, the diploe and the periosteum of the frontal bone, and the mucous membrane of the frontal sinus.

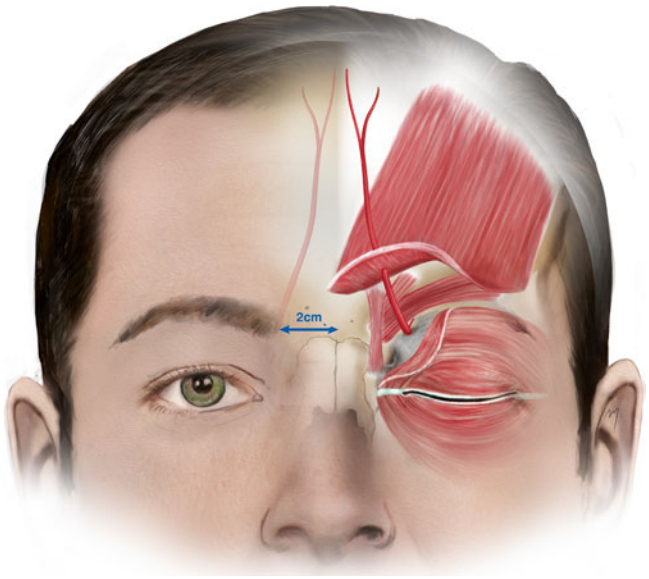

Fig. 3.11 Exit point of the supratrochlear artery and the course of its superficial branch

3.2.3 Supratrochlear Artery

The supratrochlear artery, after having divided from the ophthalmic artery, runs in the superomedial orbit to the orbital rim. It is usually the largest terminal branch measuring about 0.8 mm in diameter.

It exits the orbit (Fig. 3.11) approximately 2 cm from the midline through the supratrochlear notch, piercing the orbital septum, together with the supratrochlear nerve and vein. At this point, occasionally the artery bends sharply before getting under the muscles. In a small percentage (13 %), the supratrochlear and supraorbital arteries exit the orbit as a single vessel as mentioned above (Erdogmus and Govsa 2007).

3.2.3.1 Supratrochlear Notch

Medial to supraorbital notch/foramen lies a small notch, the supratrochlear notch, which represents the point where the supratrochlear nerve and artery exit the orbit. In about 2 %, this exit point is present not as a notch, but as foramen, known as the supratrochlear foramen. The supratrochlear notch is located approximately 2 cm lateral to the midline of the forehead and medial to the supraorbital notch/foramen.

After exiting the orbit, at the supraorbital rim, it travels over the periosteum and quickly, proximal to the corrugator muscle, divides into a deep branch and a superficial branch (Schumrick and Smith 1992; Reece et al. 2008).

3.2.3.2 Superficial Branch of the Supratrochlear Artery

The superficial branch (Fig. 3.11) initially lies over the corrugator muscle and deep to orbicularis and the lower part of

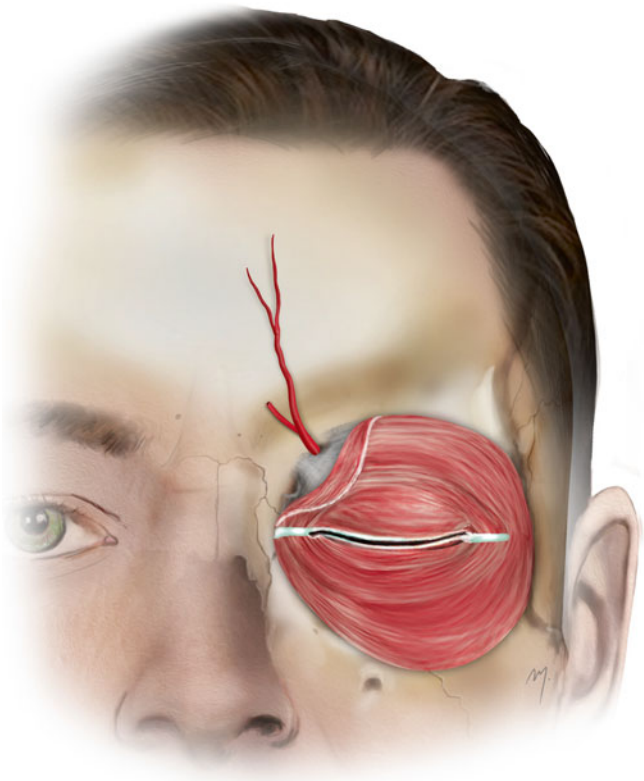

Fig. 3.12 Deep branch of the supratrochlear artery

frontalis muscle. Approximately 1.5 cm above the supraorbital rim, it pierces the muscles and becomes subcutaneous. From this point, it runs superiorly and slightly medially in the subcutaneous plane. The superficial branch travels for about 7–10 cm above the supraorbital rim. When terminating its course, axial final branches sometimes slightly extend beyond midline while starting to communicate with the contralaterals.

3.2.3.3 Deep Branch of the Supratrochlear Artery

The deep branch of the supratrochlear artery, being its periosteal branch, continues on the periosteum for at least 3–4 cm (Fig. 3.12).

The supratrochlear artery, by both of its branches, supplies the central forehead skin, the forehead muscles, and the pericranium of the central forehead.

3.2.4 Frontal Branch of the Superficial Temporal Artery (Terminal Part)

The frontal branch of the superficial temporal artery after originating from the bifurcation of the superficial temporal artery runs at the temple tortuously upward and forward.

As it enters the forehead (Fig. 3.13), it usually gives a transverse branch, as the main continuation ascends

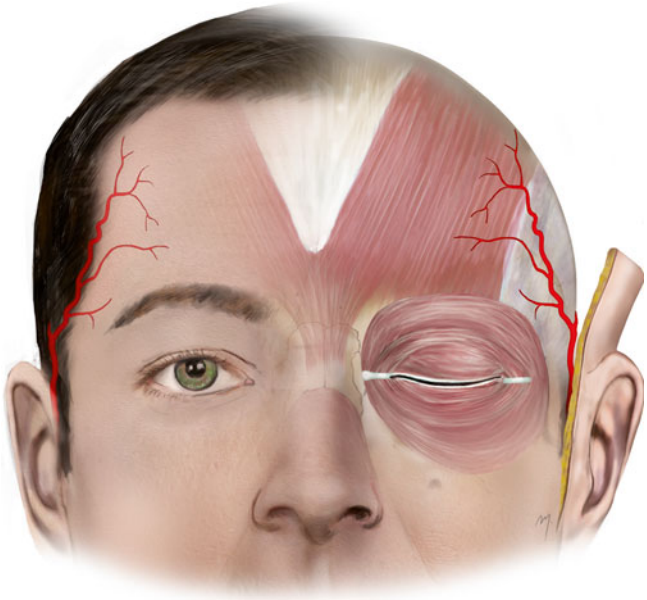

Fig. 3.13 Frontal branch of the superficial temporal artery

superomedially. Its final part reaches the forehead at the inferior or middle forehead level, at the orbital rim vertical line (Kleintjes 2007). The artery travels superficially to the frontalis muscle, becoming shallow up to the subdermal level as it approaches the midline. The frontal branch is the main vascular supply for the temporal subunits of the forehead.

3.2.5 Glabellar Branch of the Dorsal Nasal Artery

The dorsal nasal artery (see Chap. 4) contributes in the forehead vascular supply by a superior glabellar branch (Fig. 3.14). The glabellar branch arises from the dorsal nasal artery, after its exit from the orbit, and extends cephalad to the glabella or even up to the inferior central forehead. This branch supplies the skin and periosteum of glabella and anastomoses with the supratrochlear artery and its contralateral. The dorsal nasal artery also gives off, from its initial part, small deep ascending branches that supply the glabellar periosteum. The superior branch of the dorsal nasal artery anastomoses with the supratrochlear artery and its contralateral.

3.3 Venous Drainage

The venous anatomy of the forehead exhibits significant variations, and the following description regatds those being relatively more constant (Fig. 3.15).

Venous drainage of forehead starts from a rich venous plexus that extends wide from the forehead to scalp. Small

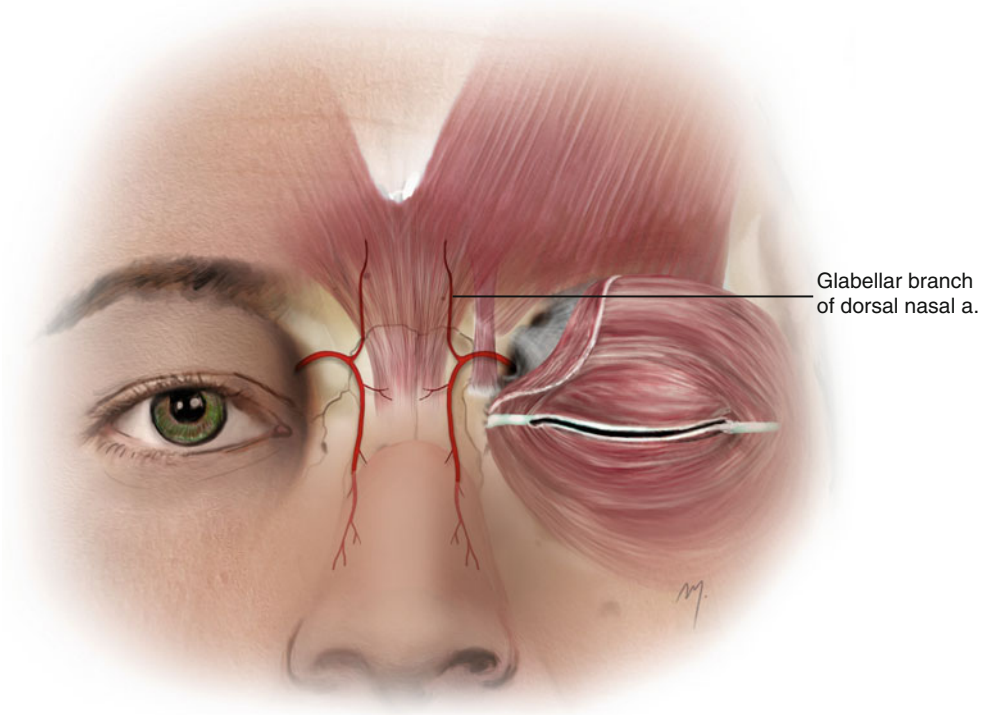

Fig. 3.14 Glabellar branch of the dorsal nasal artery

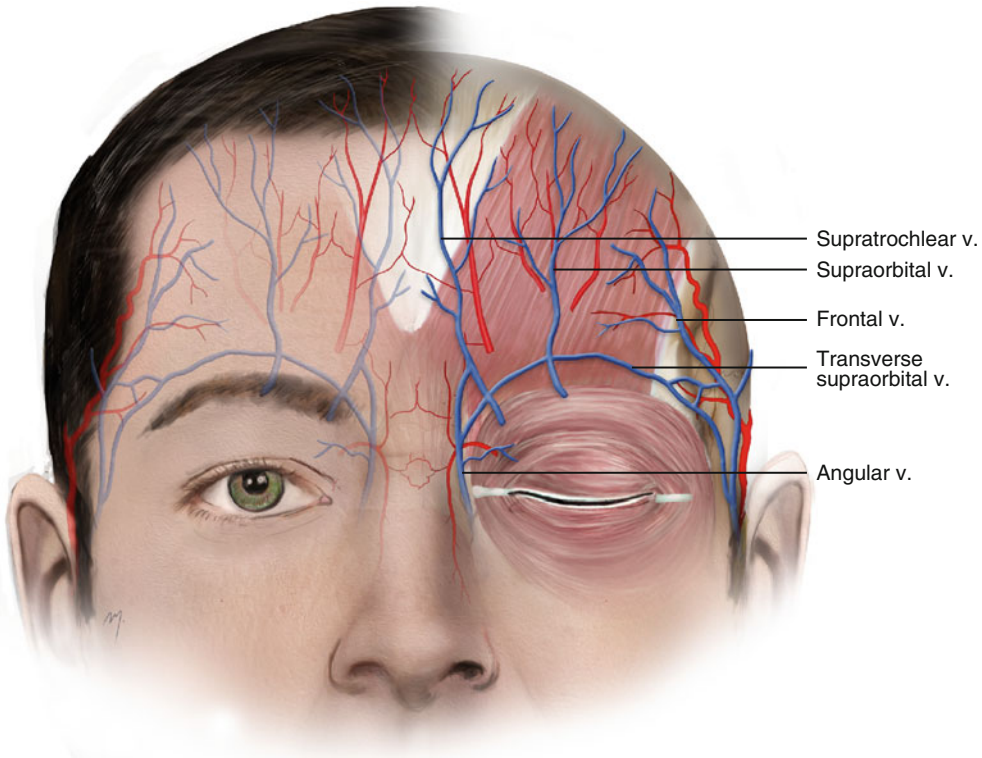

Fig. 3.15 The veins of the forehead

veins converge, forming gradually larger venous trunks. These trunks found in the middle forehead are the supratrochlear vein and the supraorbital vein, and in the lateral forehead the frontal vein.

3.3.1 Supratrochlear Vein

The supratrochlear vein starts from the venous plexus, near the forehead midline, and descends to the root of the nose,

parallel with its contralateral. Across the nose, the two supratrochlear veins are connected with the transverse nasal arch, a small vein that drains the dorsum of the nose in this area and the glabella. It then divides, and one branch penetrates the orbital septum and enters the orbit through the supratrochlear notch, while the other subdivision joins the supraorbital vein near the medial canthus to form the angular vein.

The supratrochlear vein runs a course parallel and medially to its artery, but a distance between them exists that sometimes can range up to 10 mm. This is very important when designing paramedian forehead flaps. To ensure catching both artery and vein into the flap, the width, especially in its base, should not be narrower than 1.5–2.0 cm.

3.3.2 Supraorbital Vein

The supraorbital vein starts from the forehead venous plexus and descends to the supraorbital rim accompanying the supraorbital artery. Before entering the orbit through the supraorbital notch (foramen), it divides, and one branch runs medially to join the supratrochlear vein and form the angular vein. The intraorbital branch along with the intraorbital branch of the supratrochlear vein forms the superior ophthalmic vein that runs to the cavernous sinus.

The supraorbital vein is connected to the frontal branch of the superficial temporal and the middle temporal veins, through a transverse venous trunk, the transverse supraorbital vein. This venous arch courses in about 60 %, at the level of the supraorbital rim. The remaining 40 % lies approximately 9 mm above it (Erdogmus and Govsa 2007). This limb of venous drainage of the frontal region has the best chance of being preserved, with the condition that the dissection of the galea frontalis layer from the pericranium does not extend into 10–15 mm above the supraorbital rim (Yoshioka and Rhoton 2005).

3.3.3 Frontal Vein

The frontal vein starts from the converged veins of the frontolateral venous scalp plexus. Above the zygomatic arch, it joins with the parietal vein and forms the superficial temporal vein. The frontal branch of the superficial temporal vein is also connected to the supraorbital artery through the transverse supraorbital vein.

3.4 Nerves

Sensory innervation of the forehead and anterior scalp is supplied by the supraorbital and supratrochlear nerves, which are branches of the frontal nerve.

The frontal nerve is the largest branch of the ophthalmic division (V1) of the trigeminal nerve. It enters the orbit through the superior orbital fissure above the annulus of Zinn and runs forward between the levator palpebrae superioris muscle and the periorbita. About halfway between the apex and the orbital rim, it divides into its terminal branches, the small supratrochlear and the large supraorbital nerve. The motor nerve that is encountered to the forehead is the frontal branch of the facial nerve.

3.4.1 Supraorbital Nerve

After arising from the frontal nerve, the supraorbital nerve runs forward nearly to the midline of the orbit. It exits the orbit through the supraorbital notch (foramen) (Fig. 3.16). This point is marked grossly on the orbital rim at the junction of the medial and middle thirds of the supraorbital margin and as mentioned approximately 2.5–3 cm lateral to the midline. Sometimes the supraorbital nerve can leave the orbit with several branches through separate periosteal canals (Fatah 1991). In an extensive anatomic study of 1014 orbits, Beer et al. (1998) concluded that "(1) the exit point(s) of the supraorbital nerve are not at all constant; (2) the supraorbital nerve leaves the orbital rim either undivided or in its two branches via two separate exit points; (3) the exit point(s) can be either a notch or a foramen; (4) the exit point(s) can be located along the whole orbital rim and even laterally of it; and (5) the exit point(s) can be significantly cephalad to the orbital rim." Due to these numerous variations and despite the mentioned supraorbital notch/foramen landmarks, it is very important when dissecting in this area during forehead or brow surgery to identify the notch (foramen) under vision in order to avoid nerve injury.

As the supraorbital nerve exits the orbit, it gives off small palpebral filaments to the upper eyelid and conjunctiva. Also, small branches supply the mucous membrane of the frontal sinus entering it through foramina in the floor of the supraorbital notch (foramen). After leaving the orbit, the supraorbital nerve trunk divides into a large, lateral deep branch and a smaller, medial superficial branch (Fig. 3.16). In 15 %, the supraorbital nerve leaves the orbital cavity already having those two branches (Beer et al. 1998). A variation to the above, is that the lateral deep branch exits the orbit from a separate foramen, located up to 1.5 cm, cephalad to the supraorbital notch (Erdogmus and Govsa 2007; Keller and Mashkevich 2009). Initially, these branches lie in the submuscular plane, deep to the orbicularis, frontalis, and corrugator supercilii muscles, in close approximation to the periosteum of the supraorbital ridge, in a position respectively in the middle third of the corrugator.

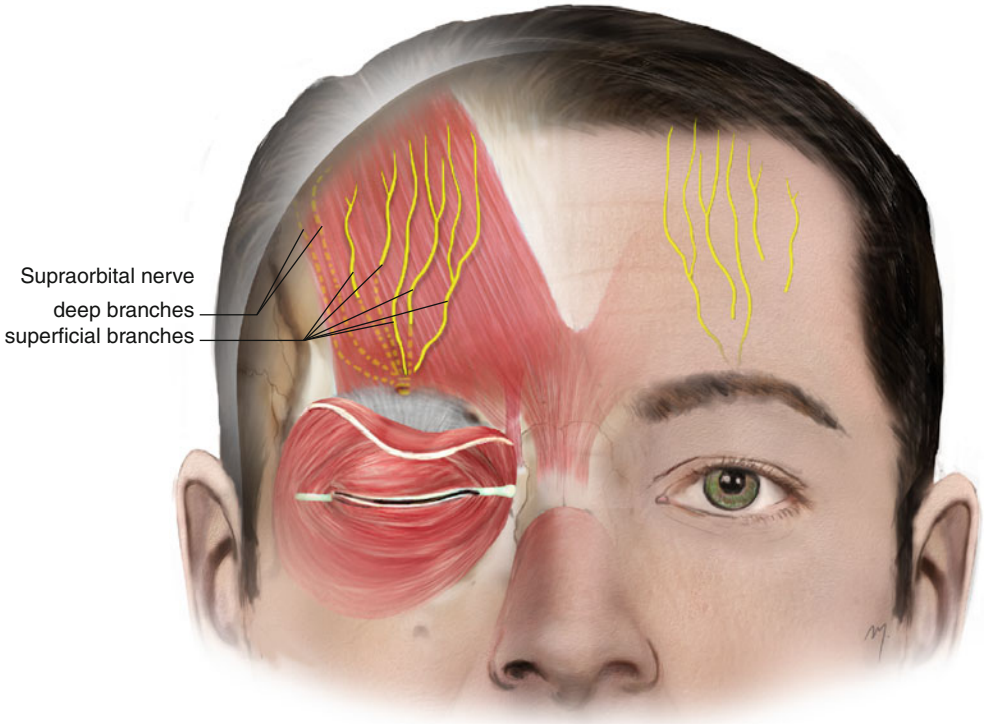

Fig. 3.16 The supraorbital nerve entering the forehead divides into its superficial and its deep branches

3.4.1.1 Superficial Branch of the Supraorbital Nerve

The superficial branch of supraorbital nerve quickly divides into multiple smaller branches. As they ascend, they pass through the corrugator supercilii and frontalis muscle, becoming more superficial. In 22 %, branching occurs more cephalad, close to the superior margin of the corrugator muscle (Janis et al. 2008). After perforating the frontalis muscle at various points from the orbital rim to the mid-forehead level, they run over its surface, along with the supratrochlear nerve branches, reaching and traveling into the subcutaneous plane. These smaller branches form a wide fan pattern, before entering the frontal scalp (Knize 1995). The length of the medial branches has been reported to be from 1.5 to 11.7 cm (Malet et al. 1997; Erdogmus and Govsa 2007; Andersen et al. 2001).

According to their length, they supply sensation to the forehead skin and to the frontal scalp in various ranges.

3.4.1.2 Deep Branch of the Supraorbital Nerve

The deep branch of the supraorbital nerve exits the orbit as one branch in 34 %, as two branches in 60 % and in the remaining 6 % of cases, as multiple branches (Knize 2001; Erdogmus and Govsa 2007). The one or two branches (being parallel each other) at first run laterally, above the periosteum and along the orbital rim or occasionally up to 1.5 cm superior to the rim. At the level of the lateral third of the eyebrow, they turn cephalad. After turning cephalad, the deep branch (single or double) runs in a superolateral direction, parallel and 0.5–1.5 cm medial to the superior temporal line (Knize 1995). It courses in the loose areolar tissue, beneath the frontalis muscle and the galea, and above the pericranium and gives off very small branches, which innervate the periosteum. In the cases where the deep branch presents two branches, one is larger than the other, and together they run without any further branching (Erdogmus and Govsa 2007). At the level of the hairline, near the coronal suture, it turns medially and pierces the galea becoming more superficial and then divides to its terminal rami (Knize 1995). The deep branch is longer than the superficial with a length ranging from 35 to 145 mm (Malet et al. 1997; Andersen et al. 2001). These branches supply scalp sensation to the frontoparietal region occasionally reaching the vertex of the skull.

The presence of a small, horizontal, additional branch of the deep branch of the supraorbital nerve has recently been described (Vestal et al. 1994; Hwang et al. 2005; Janis et al. 2008). This horizontal branch exits the supraorbital foramen (notch) as 1–2 rami. It runs upward about 10 mm and turns laterally parallel to the supraorbital rim, along the undersurface of the corrugator muscle, ending at the end of the brow. It supplies sensation in a skin area of 3 cm at the lateral mid of the eyebrow. In approximately half of individuals, this horizontal branch anastomoses with the temporal branch of the facial nerve (Hwang et al. 2005).

Both of the branches of the supraorbital nerve supply sensation to the skin of the lateral forehead, the anterior scalp, the frontoparietal scalp, the mucous membrane of the frontal sinus, and the pericranium of the forehead and anterior scalp region.

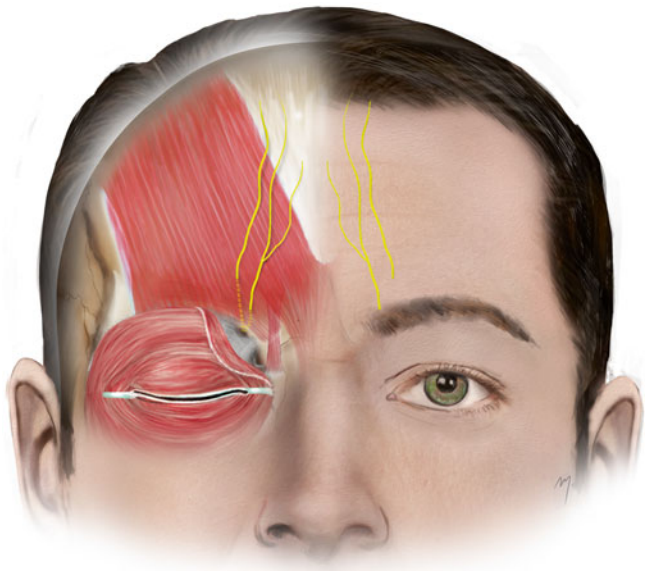

Fig. 3.17 Supratrochlear nerve

3.4.2 Supratrochlear Nerve

The supratrochlear nerve is smaller than the nearby supraorbital nerve. After dividing from the frontal nerve, it courses anteromedially in the roof of the orbit, passes above the trochlea of the oblique superior muscle, and gives off a descending filament to join the infratrochlear branch of the nasociliary nerve.

It exits the orbit at the superior orbital rim, between the trochlea and the supraorbital foramen through the supratrochlear notch (Fig. 3.17). At the supraorbital rim, it first pierces the orbital septum; then curves up on to the forehead close to the bone, in company with the supratrochlear artery; and ascends at first beneath and through the corrugator supercilii muscle. Within the corrugator muscle, the supratrochlear nerve divides into one to three branches. These branches as they run upward, these branches become more superficial, piercing the corrugator and frontalis muscle, and then enter the subcutaneous tissue of the central forehead. The terminal branches never cross the midline. The length of the supratrochlear nerve ranges between 23 and 70 mm (Andersen et al. 2001).

The supratrochlear nerve supplies cutaneous sensation to a central vertical strip of forehead and to the medial one-third of the upper eyelid skin and conjunctiva. There is an overlap of the supratrochlear nerve sensory area by the sensory area of the superficial division of the supraorbital nerve.

3.4.3 Forehead Regional Anesthesia

A great number of small to medium lesions at the forehead can be excised, and minor flap reconstruction is achieved by a forehead block. The supraorbital nerve is blocked by its exit from supraorbital foramen (notch). The foramen (notch) is palpated at the supraorbital rim, and if this is unclear, its quite possible position 2.5–3 cm lateral to the midline is marked. At this point, about 1 ml of local anesthetic solution is injected just above the bone (Fig. 3.18). Direct injection within the foramen must be avoided because it may result in nerve damage. The supratrochlear nerve is blocked by infiltrating the same amount of local anesthetic solution along the supraorbital rim, 2 cm lateral to the midline or 1 cm medial to the previous point (Fig. 3.19). By blocking both nerves, complete anesthesia of the hemiforehead is achieved.

Fig. 3.18 Supraorbital nerve block

3.4.4 Frontal Branch of the Facial Nerve

At the forehead, the frontal branch of the facial nerve is present due to its final part (Fig. 3.20). As the frontal nerve comes from the temple, it reaches the forehead 1.0–1.5 cm above the lateral extremity of the brows. Situated at the temple along the undersurface of the temporoparietal fascia as it reaches the lateral border of the frontalis muscle, it pierces

Fig. 3.19 Supratrochlear nerve block

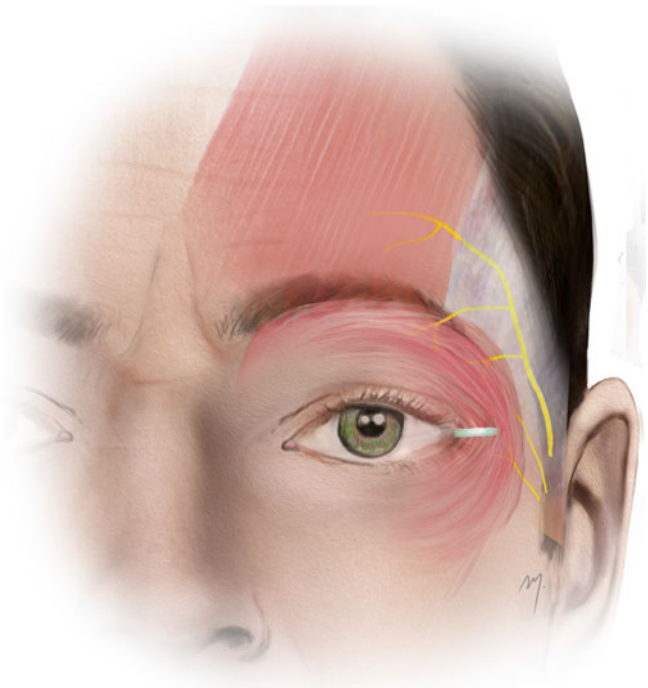

Fig. 3.20 Frontal branch of the facial nerve at the forehead

the fascia and continues to the undersurface of the frontalis muscle providing its innervation. A tiny ramus that runs medially to innervate the transverse head of the corrugator muscle has been found in 60 % of the individuals (Tzafetta and Terzis 2010).

3.5 Flaps Derived from the Forehead

The forehead constitutes a wide donor site of flap material that can be harvested in great quantity. Flaps derived from the forehead can be used in closing its own defects, but the forehead is also the ideal donor site of regional flaps in order to reconstruct medium and large nasal defects. In the past, the robust forehead flaps have been used also for cheek reconstruction, nowadays abandoned due to better reconstructive solutions.

3.5.1 Flap Design Concerning Vascular Anatomy

The supratrochlear, supraorbital, dorsal nasal, and frontal branches of the superficial temporal artery anastomose each other, forming a rich superficial (Fig. 3.21a) and deep arterial network (Fig. 3.21b), in the following way.

The supraorbital arteries anastomose with the superficial temporal arteries and the ipsilateral supratrochlear artery. The superficial branches of the supraorbital artery anastomose each other and with the frontal branch of superficial temporal artery and the superficial branches of the supratrochlear artery. The deep branches of the supraorbital artery anastomose each other and with the deep branches of the supratrochlear artery. Moreover, the deep oblique branch of the supraorbital artery, at the superior temporal line and at the junction of the inferior and middle forehead, pierces the frontalis muscle and anastomoses with the frontal branch of the superficial temporal artery (Kleintjes 2007). The supratrochlear artery, either the superficial or the deep branches, anastomoses with the supraorbital artery, the dorsal nasal artery, and its contralaterals.

The arteries that supply the forehead skin delimit clear vascular territories that the surgeon must have in mind when planning and designing cutaneous flaps (Fig. 3.21c). The deep arterial forehead network is related to the vascularity of the forehead pericranium, and a classic flap based on this rich deep network, which is used in various craniofacial procedures, is the frontal pericranial flap (Fig. 3.22). If a cutaneous flap from the forehead incorporates the underlying pericranium that will of course enhance its vascularity.

Based on the described rich cutaneous plexuses, all kinds of random pattern flaps can be designed on the forehead. The size and location of the defect, the RSTLs, and the skin laxity

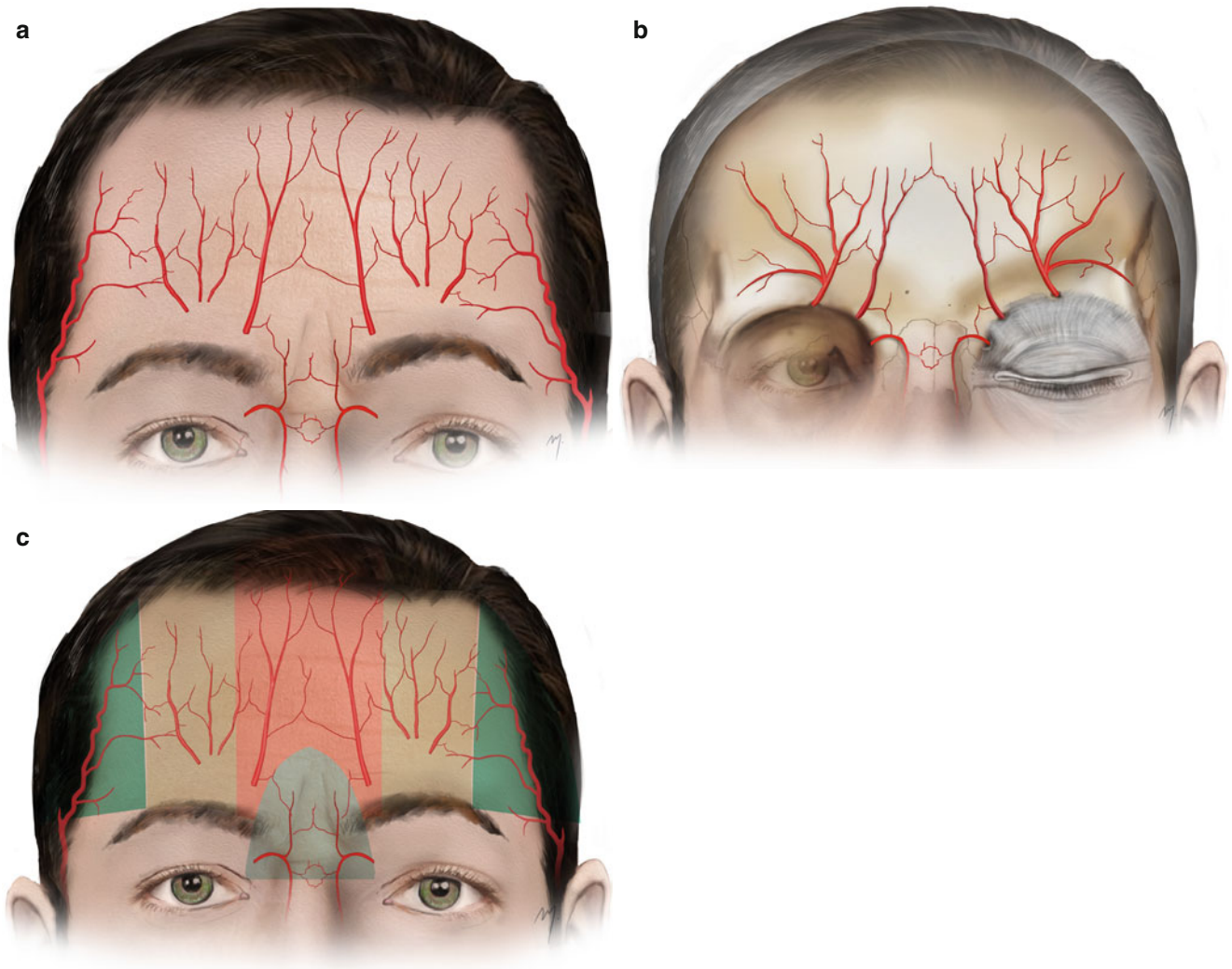

Fig. 3.21 (**a**) Superficial forehead arterial network. (**b**) Deep forehead arterial network. (**c**) Vascular territories of the arteries that supply the skin of the forehead

Fig. 3.22 The frontal pericranial flap is based on the rich deep anastomotic network of the forehead

of the forehead subunit to be reconstructed determine the choice of the best solution. All of the arteries of the forehead can provide axial supply to a great majority of flaps. On the side, the supratrochlear, the supraorbital, the dorsal nasal, and the frontal branch of the superficial temporal arteries, alone or in combination, can ensure axial flaps in various designs in order to reconstruct the forehead or nasal defects.

3.5.2 Flap Elevation Concerning Anatomic Planes

When raising a flap, the depth depends on the defect size, its location, and the type of the chosen flap. In forehead reconstruction, flaps are dissected in three different but certain anatomic planes. These are the subcutaneous plane, the loose areolar tissue plane, and the subperiosteal plane.

3.5.2.1 Subcutaneous Plane

The flap raised in this plane consists of skin and subcutaneous tissue, which preserve the subdermal vascular plexus. Small local flaps can be raised in this plane with vascular

feeding safety. Dissection is performed sharply and creates more bleeding in comparison to working in the deeper forehead planes. Thus, it might be difficult at times and requires experience, because the tissue is dissected around neurovascular branches that need to be protected. Depending on the amount of subcutaneous tissue, dissection can be carried out through a midsubcutaneous or a deep subcutaneous level plane.

When no important anatomic structures have to be protected, the deep subcutaneous plane dissection located just above to the superficial galea layer is one of the choices. It strengthens vascularity or incorporates axial vessels into the flap. In the brow, this plane must be used exclusively, so as not to disturb the hair follicles, ensuring that cutting is carried out beneath them.

Midsubcutaneous plane dissection prevents damage of superficial running sensory and motor nerve branches. It should always be performed in the lateral eyebrow area and its extension to the temple. Even though this plane slightly impairs flap vascularity, however it reduces the possibility of injury of the temporal (frontal) branch of facial nerve that runs deep to the SMAS.

3.5.2.2 Subgaleal Plane (Loose Areolar Tissue Plane)

The subgaleal plane is also referred to, as the subgaleal-submuscular plane but in fact is actually only subgaleal. Anatomically this is recognized, as the deep layer of galea covers the under surface of the muscles of the forehead. This plane is used for raising large forehead flaps (rotation or advancement flaps, Worthen flap). Carrying the dissection below the frontalis muscle and its deep galea layer to the pericranium, undermining of the flap takes place within the areolar tissue, a very loose space. By blunt dissection, even with the finger, flaps can be raised at this level with ease and at a rapid pace.

Although numerous blood vessels run within this plane, injection of a vasoconstrictive solution creates a dissection plane with minimal bleeding.

Flaps raised in this plane are thick gaining (even the large) a robust vascular supply enhancing their viability. Additionally they are bulky enough to cover deep defects, and can reconstruct the contour for a more natural appearance. Depending on design, the position of transverse incision lines may lead to superficial sensory nerve transection.

3.5.2.3 Subperiosteal Plane

Even though raising a forehead flap at the subperiosteal plane, catching the pericranium and the deep arterial network, greatly enhances vascularization, this is not always necessary. The subperiosteal plane is of course the deep dissection plane of an anteriorly based pericranial flap (see Chap. 2) but in cutaneous forehead flaps is mostly used at the supraorbital zone where a flap may transition to this deeper level. Although the pericranium of the forehead is densely adherent to the underlying frontal bone at the supraorbital zone, it can be easily detached by means of periosteal elevators.

3.5.3 Bilateral Transverse Advancement Flap (H-Plasty)

The random pattern bilateral advancement flap is an ideal choice for closing moderate defects that are located in the central subunit of the forehead. The lesion is excised in a rectangular form, and two flaps from each of the lateral and the medial sides are elevated and advanced to close the defect. Its main advantage is that the long vertical incisions are camouflaged in the RST lines.

In the case presented, a basal cell carcinoma of the central forehead (Fig. 3.23a) is planned to be excised. After control of the transverse laxity (Fig. 3.23b), bilateral transverse advancement flaps are chosen to reconstruct the defect (Fig. 3.23c, d).

The lesion was excised, and clear margins were revealed by frozen biopsies (Fig. 3.23e). The flaps were raised by dissecting in the deep subcutaneous plane, just above the galea centrally and superficial to the frontalis muscle laterally (Fig. 3.23f, g). With advancement, both flaps reach the defect, share it (Fig. 3.23h) and are sutured into place without tension (Fig. 3.23i). The postoperative result is quite satisfactory (Fig. 3.23j).

3.5.4 Double Island Pedicle Flap

This versatile flap is very suitable in other facial areas with greater skin elasticity and plenty of subcutaneous tissue. In the forehead, it can be used in selected cases for closing small defects. The ability of advancing this flap in the forehead is limited, and thus it is better to design it as double than single flap. By this way, the two flaps share the defect area, each advancing halfway.

This technique is presented in a case of a basal cell carcinoma located at the forehead (Fig. 3.24a). A rectangular-shaped excision and the triangular flaps are outlined (Fig. 3.24b, c). The line of advancement of the flap is designed parallel to the forehead skin tension lines. Each flap is designed equal to the length of the diameter of the defect in the direction of the closure, thus both flaps being double the defect length.

The subcutaneous tissue beneath the triangular flaps is their pedicle. In contrast with other facial areas (e.g., cheek), the pedicle in the forehead cannot be extended very deep so as to enhance its mobility. The flaps are of random pattern, but on occasion, depending on where they need to be placed, they can be based over an axial vessel.

Each flap is undermined down to the subcutaneous tissue into the muscle, tapering outward so as to widen its base. After gaining sufficient mobility, they are advanced and sutured to the defect in a V-Y manner (Fig. 3.24d).

3.5.5 Hatchet Flaps

Hatchet flap, described by Emmett (1977), is a variant of V-Y flap. This triangular flap is not incised circumferential

completely but keeps additionally a small skin pedicle except the subcutaneous one. The hatchet flaps in contrast to the V-Y flap are not exclusively advancement flaps, but they include also a slight rotation movement.

In the patient demonstrated, a malignant eccrine poroma is present in the lateral suprabrow area (Fig. 3.25a). Position and contour of eyebrow are the main goal of reconstruction. Even the lesion is small in size; a flap is necessary, because simple closure would lead to brow displacement.

Double hatchet flaps were chosen in this diabetic patient because the additional skin pedicle would enhance circulation and flap viability. Excision line and bilateral Hatched flaps are

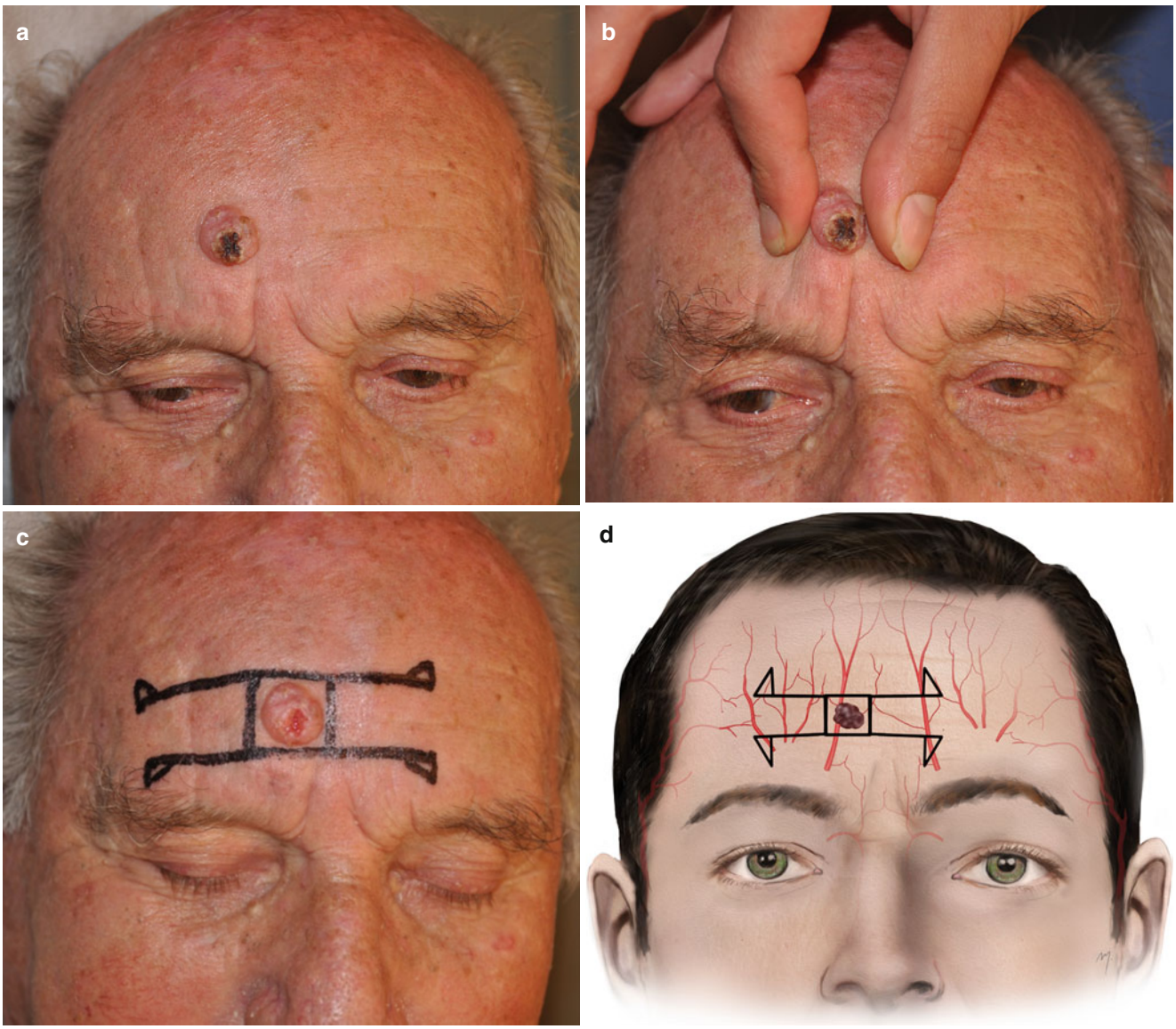

Fig. 3.23 (**a**) A cystic-type basal cell carcinoma at the central forehead. (**b**) Control of transverse skin laxity. (**c**) Outline of bilateral transverse advancement flaps. (**d**) By this flap, the supraorbital and supratrochlear arteries are transected, and the random pattern flap is perfused by branches of the frontal artery. (**e**) The lesion is excised in the plane just above the galea. (**f**) Flap is incised and Burow's triangles excised. (**g**) Flap raised at the deep subcutaneous level. The galea and the frontalis are clearly seen. (**h**) The flaps advanced. (**i**) Final closure. (**j**) Result at 4 months

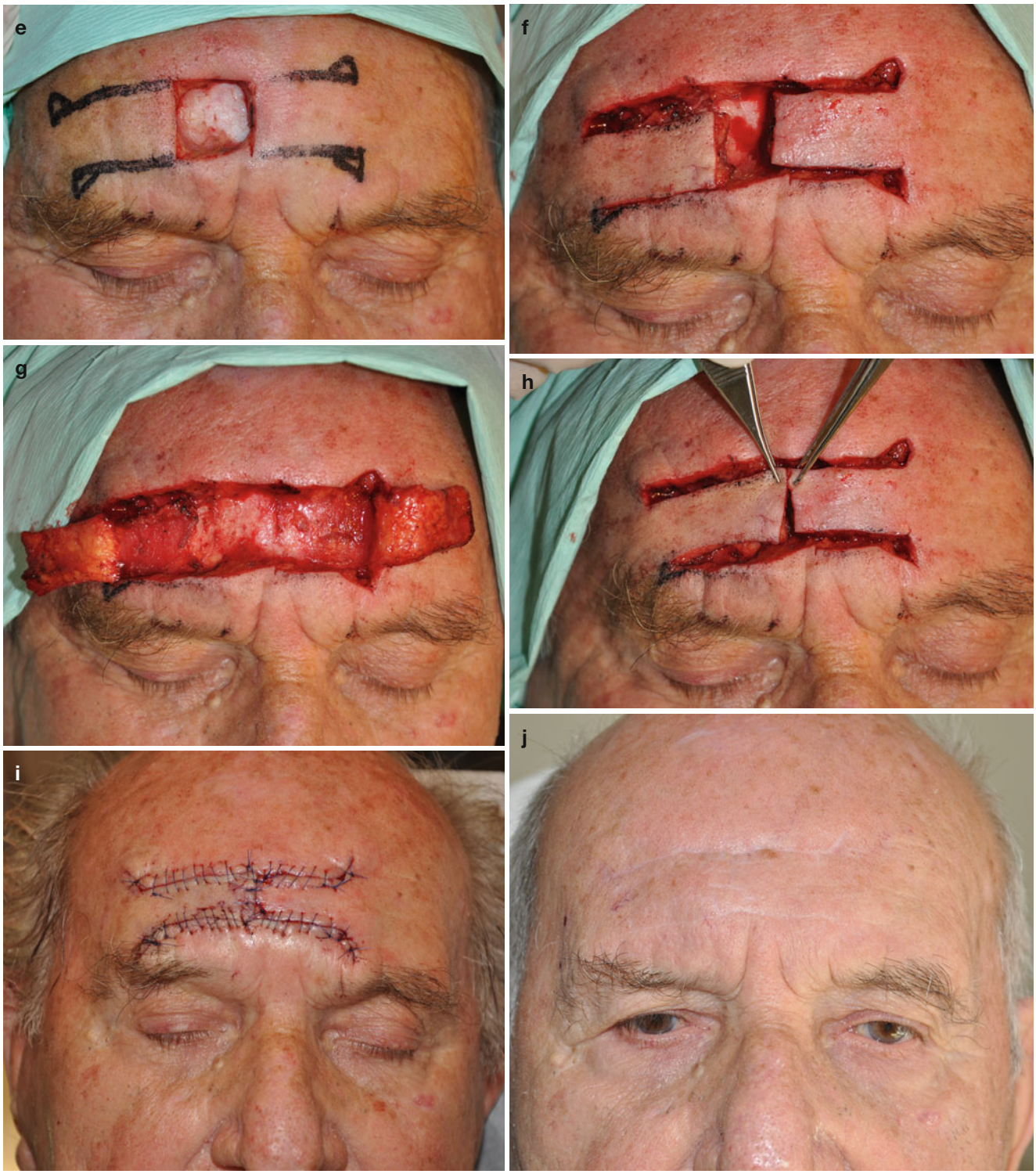

Fig. 3.23 (continued)

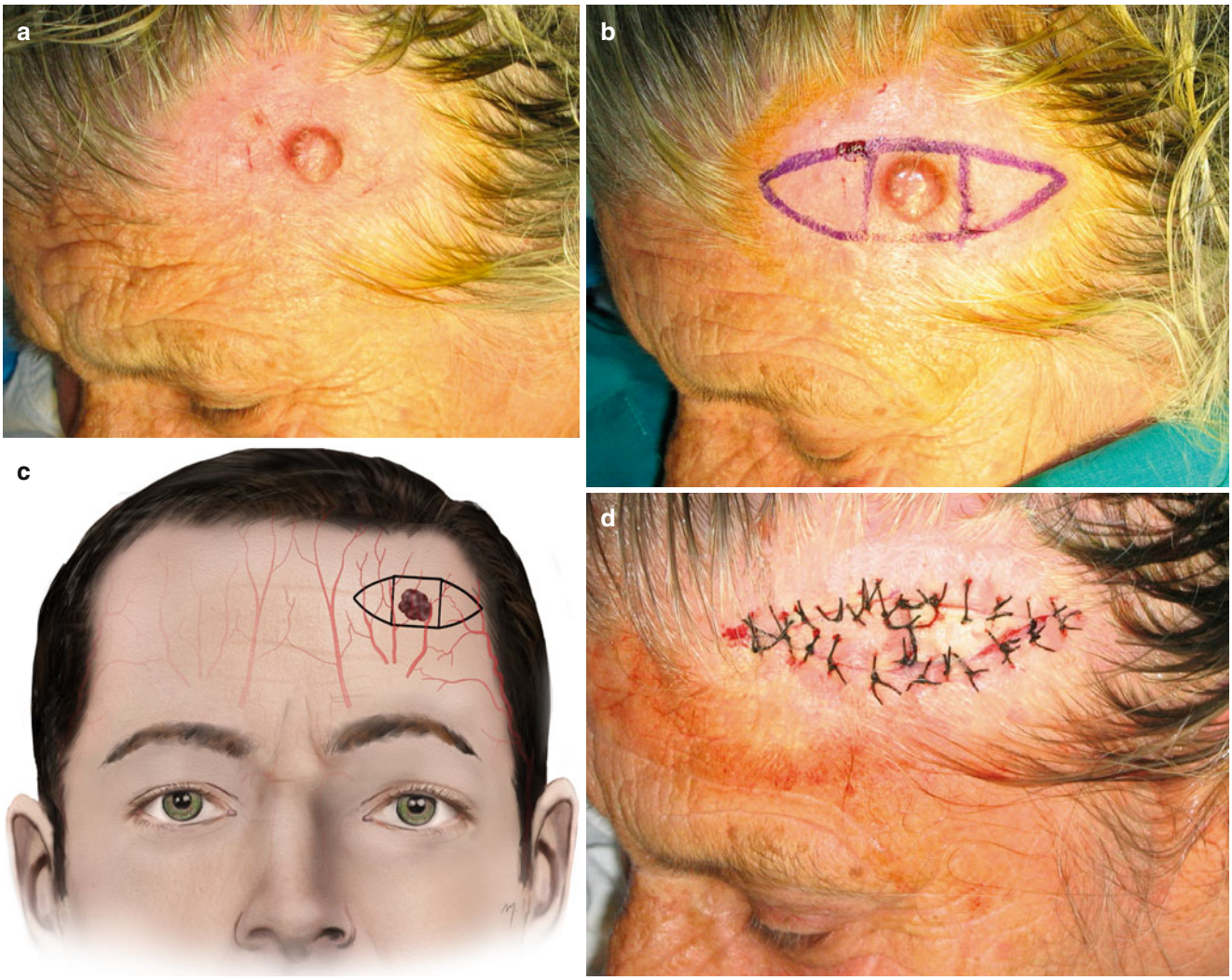

Fig. 3.24 (**a**) A cystic basal carcinoma located at the lateral forehead. (**b**) A double island pedicle flap is outlined. (**c**) The flaps are random pattern, but depending on where they need to be placed, they can be based over an axial vessel. (**d**) Flaps advanced and sutured to the defect in a V-Y manner

outlined as two triangles keeping two small skin pedicles facing each other (Fig. 3.25b, c). The lesion is excised in a circular fashion (Fig. 3.25d). Flaps are undermined to the deep subcutaneous plane, creating the subcutaneous pedicle. Dissection in this area and at this plane must be done very carefully, to protect the facial nerve. In addition, the small skin pedicle is maintained. Staying at a subcutaneous level by carefully dissecting the frontal branch of the facial nerve is protected.

After advancing the flaps, the first two sutures transfix (or nail) the apex of each flap into the middle of periphery of the round-shaped excision site (Fig. 3.25e).

Suturing continues at the bases of the triangle flaps and the rest is closed in a V-Y manner (Fig. 3.25f). The defect is closed without tension. Contour and position of the brow are not disrupted.

3.5.6 A to T Flap for Brow Defects

This advancement flap is a simple but an ideal reconstruction of small- and medium-sized defects of the eyebrow. The defect is excised in a triangular manner with its base inferiorly, and two horizontal incisions on opposite sides of the base are outlined within the brow (Fig. 3.26a, b). By this, nearby tissue is advanced to the defect in a horizontal manner, thus not disturbing the eyebrow position.

The goal of the restoration is not only to maintain brow position but also to prevent brow alopecia. This is achieved by carrying the horizontal incision parallel to the multidirectional hair follicles and undermining the flaps to the deep subcutaneous plane. The flap shifts eyebrow hair in the defect, fully restoring the brow continuity (Fig. 3.26c).

Fig. 3.25 (**a**) A malignant eccrine poroma located at the lateral brow area. (**b**) Hatched flaps are outlined. (**c**) In this case, the frontal nerve must be considered at the lateral triangle of the flap. (**d**) Lesion excised. (**e**) The flaps advanced. (**f**) Final suturing

The horizontal scar line is totally hidden within the brow. Finally, the reconstruction results in a normal brow (Fig. 3.26d).

3.5.7 A to T Flap for Suprabrow Defects

A- to T-plasty is a commodity solution for reconstructing small to medium defects of the supraorbital subunit.

The excision of this basal cell carcinoma of the case presented leads to a midsized supraorbital defect. The defect is excised in a triangular manner with its base inferiorly. The two horizontal incisions are outlined lying within a relaxed skin tension line (Fig. 3.27a, b).

The flap is raised in the midsubcutaneous plane by blunt dissection (Fig. 3.27c). This reduces the possibility of injury of the frontal branch of facial nerve that runs at the distal side of the flap. Dissecting the proximal side, there is no danger for the facial nerve, as this exists under the frontalis muscle.

The two triangular sides of the flap are advanced and cover the defect (Fig. 3.27d). The horizontal incisions are camouflaged into the RSTL, and the vertical one heals always well without a noticeable scar.

Postoperative result at 3 months achieved a good cosmetic and functional result (Fig. 3.27e, f).

3.5.8 Bilateral Forehead Rotation Flap

A large basal cell carcinoma of the upper part of midforehead is presented in this case (Fig. 3.28a). An exceptional method to reconstruct this medium-sized defect is the use of bilateral rotation flaps.

Fig. 3.26 (**a**) Outline of the flaps. (**b**) No danger of the frontal nerve exists when dissecting in the deep subcutaneous level as the nerve travels at the undersurface of the frontal muscle. (**c**) The flaps advanced and sutured in place. (**d**) Postoperative result at 6 months

The excision line and flap design outlined with the defect triangulated with its base superiorly (Fig. 3.28b). Both rotation flaps are inferiorly based so as to catch the axial feeding vessels (Fig. 3.28c). They receive their blood supply from the supraorbital arteries in their middle third, the frontal branch of superficial temporal arteries in the lateral third, and the supratrochlear arteries in the medial portion. The horizontal incision lies slightly posterior to the frontal hairline within a relaxed skin tension line.

Although the lesion does not extend into the deep tissues, excision is carried out deep to the subgaleal plane so as the two large flaps will be raised in the same loose areolar tissue anatomic plane (Fig. 3.28d). Subgaleal dissection is carried out bluntly in the subgaleal plane, within the loose areolar tissue. This provides safe and sufficient mobilization and easy rotation of the flaps to the donor site (Fig. 3.28e). By making the horizontal incision in that depth, all of the terminal branches of the superficial sensory nerves are transected,

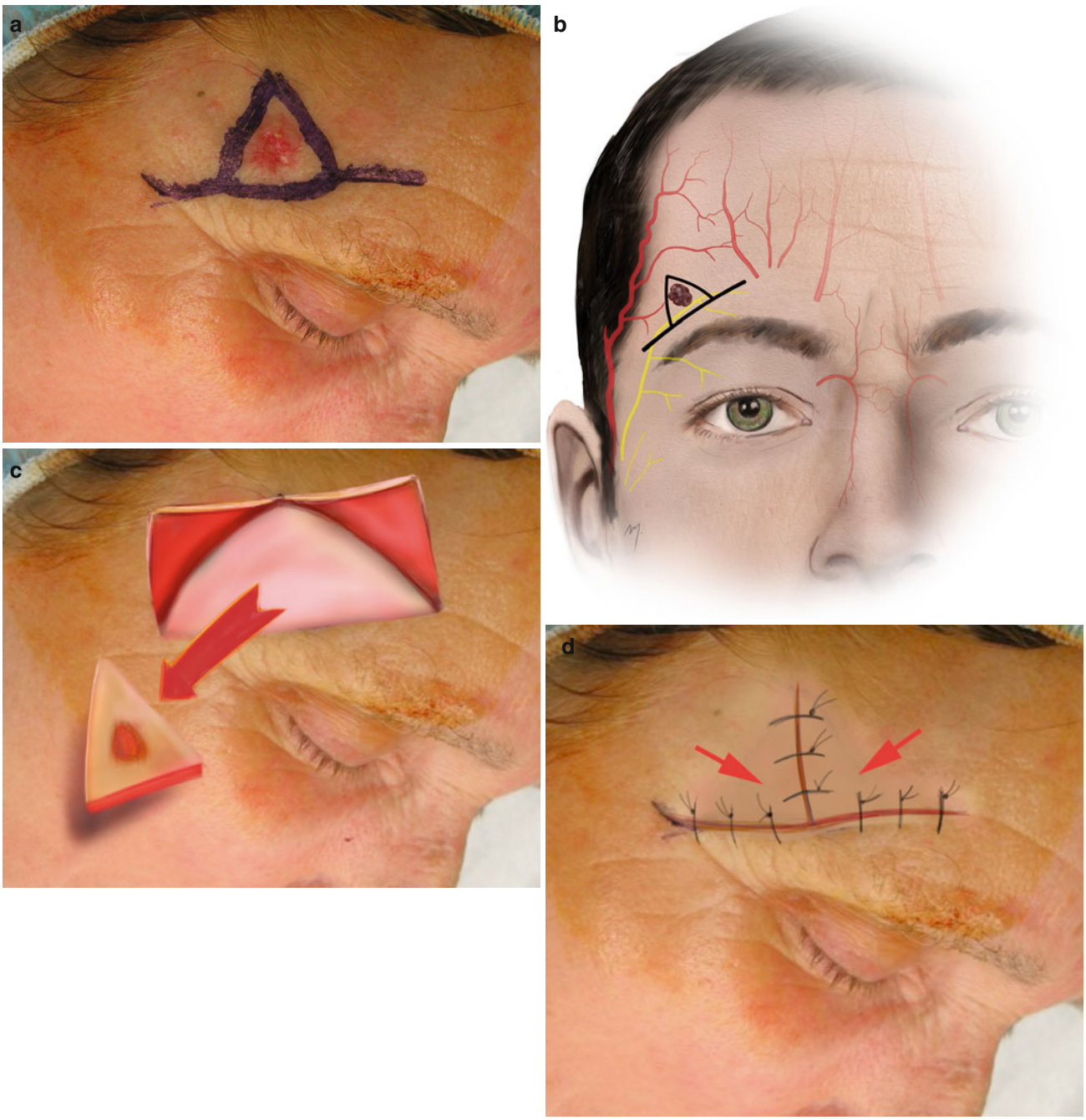

Fig. 3.27 (**a**) Outline of the flap. (**b**) In this case, the frontal nerve must be considered at the lateral limb of the flap. (**c**) Flaps raised. (**d**) Suturing in place. (**e**) Result at 3 months following surgery. (**f**) Frontal nerve is intact

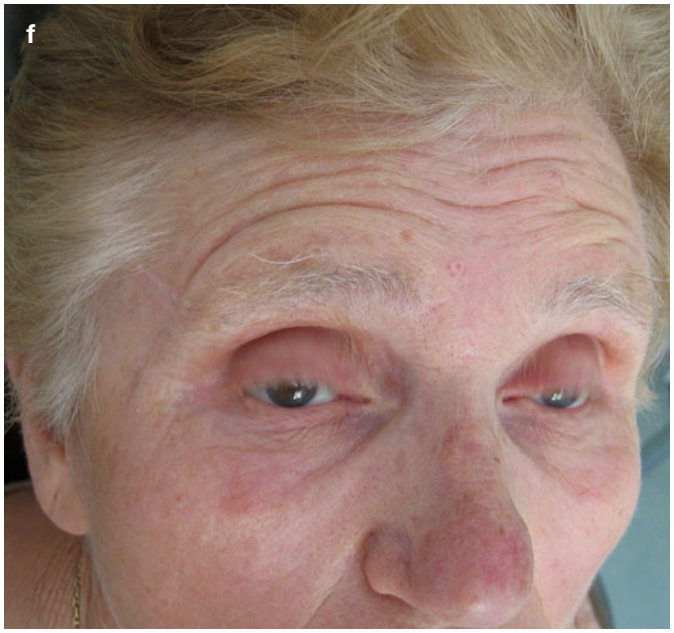

Fig. 3.27 (continued)

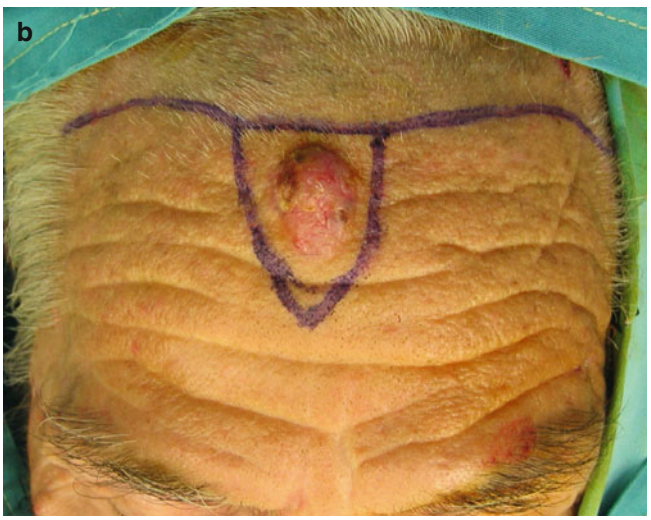

Fig. 3.28 (**a**) A basal cell carcinoma located at the upper part of the mid-forehead. (**b**) Excision line and flap design outlined. (**c**) The rotation flaps catch the axial feeding vessels but transect all of the superficial sensory nerves. (**d**) Lesion excised. (**e**) Flaps raised at the subgaleal plane. Small vessels running over the periosteum are seen. (**f**) Final suturing. (**g**) Satisfactory result after 3 months

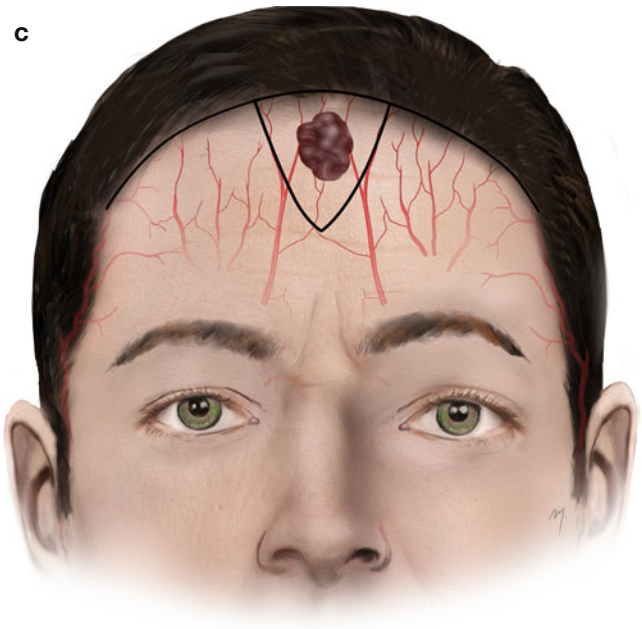

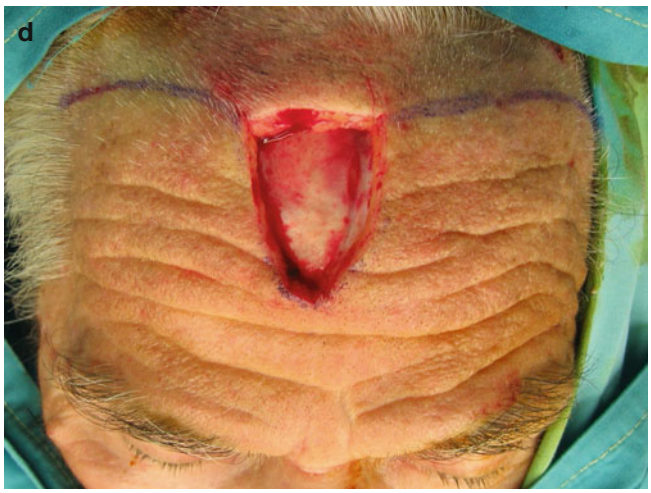

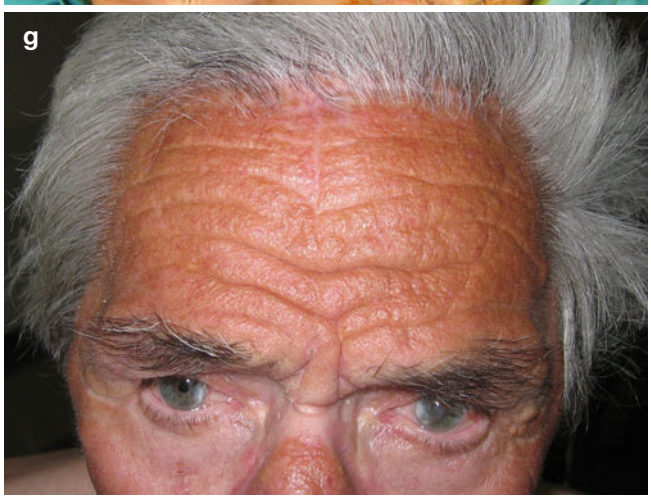

Fig. 3.28 (continued)

resulting in temporary numbness of the anterior scalp for usually 9–12 months. As dissection proceeds laterally, care must be taken to avoid the deep branches of the supraorbital nerve that run approximately 1 cm medially to the superior temporal line, preserving the sensation of the upper forehead and bregma.

The flaps are rotated to the defect and suturing is achieved without tension (Fig. 3.28f). If approximation is under tension, the incisions can be extended to the temporal hairline and the flaps undermined to a larger area of tissue reservoir in lateral forehead and temple. The postoperative result is satisfactory (Fig. 3.28g).

3.5.9 Worthen Forehead Rotation Flap

This large flap, used to reconstruct large lateral, almost hemiforehead, defects, was first described by Worthen in 1974. Resurface is gained by rotating the entire remaining healthy forehead to the recipient site. The flap is an axial flap based on the supratrochlear, supraorbital, and frontal arteries.

The following case demonstrates a recurrent forehead squamous cell carcinoma after two times surgery and radiotherapy. Scar tissue and multiple operations demand a wide excision so as to ensure clear margins and vascularized tissue.

The flap was outlined as its incision line was placed behind the frontal hairline (Fig. 3.29a,b). The flap catches ipsilateral to the defect side supratrochlear artery and the contralateral supratrochlear, supraorbital, and frontal arteries (Fig. 3.29c).

A large lateral forehead defect is created after tumor excision (Fig. 3.29d). Periosteum beneath the tumor was also excised. Clear margins were determined by frozen section biopsies.

The flap is elevated by blunt dissection in the loose areolar tissue plane carried out to the supraorbital area. At a line 2 cm above the supraorbital rims, the dissection transitions to a subperiosteal plane (Fig. 3.29e). At this point, injury prophylaxis of supratrochlear and supraorbital bundles is mandatory. The flap incorporates the frontalis, galea, and supraorbital muscles. Scoring the galea in its undersurface is a useful maneuver to gain extra flap length.

After rotation, the flap is sutured in place (Fig. 3.29f). Wide undermining of the frontal scalp is necessary to achieve closure in the periphery of the flap.

Even though this flap is very reliable, it is stiff, sometimes resulting in a moderate degree of difficulty regarding the closure of large wounds without tension, even after scoring the galea. This may lead to scar formation and brow asymmetry of the recipient side, needing secondary correction (Fig. 3.29g, h).

3.5.10 Paramedian Forehead Flap

The forehead has been acknowledged as one of the most ideal donor sites in nasal reconstruction, after the nose itself. The forehead is adjacent to the nose, and its skin is pliable enough to fold, thus allowing it to be crafted into the complicated contour of the nose. The big tissue availability of the forehead allows the flap to receive not only suitable width but also the adequate length in cases where columella and alar rims should be reconstructed. The complexion and texture of the forehead skin have a considerable resemblance to that of the nose, and the reconstruction is very satisfactory aesthetically, avoiding a "patch" impression (Coleman 1959; Millard 1966).

The axial flaps that are based in the forehead vascularity and are used in nasal reconstruction emerged during the years as improvement of the ancient Indian flap.

These basic variabilities of the flap appear in the literature with a confusing nomenclature. A clear and brief definition of them according to the feeding vessels and the flap axis follows.

The median forehead flap (Fig. 3.30a), according to the classic India design, was drawn along a straight vertical axis and extended from the glabella to the hairline. It has a wide pedicle gaining axial supply from both supratrochlear arteries. The skin paddle is oriented vertically in the mid-forehead.

The paramedian flap has a narrower pedicle, based laterally to the previous. Its base is located at the medial brow capturing one supratrochlear artery. The flap paddle can be vertically (Fig. 3.30b) or obliquely (Fig. 3.30c) oriented beyond the midline, where its distal part becomes random pattern.

The midline forehead flap (Fig. 3.30d) mixes the median and paramedian flaps. It has its pedicle like the paramedian flap, at the medial brow having its axial supply from one supratrochlear artery, and its paddle in the central forehead like the median flap.

The "gull-wing" flap (Fig. 3.30e) is a modification of the paramedian forehead flap and was first described by Gillies (1920) and refined by Millard (1974). With this design, transverse extensions are created on the standard paramedian flap. These can be used to cover extensive bilateral nasal tip, infratip, and lobule defects. The donor site can be closed primarily in a T-form. Its main vascular supply is the supratrochlear bundle based on the medial aspect of the one brow. The circulation to the distal portions of the flap is primarily random pattern.

No other flap has focused so much interest than the Indian forehead flap. The Indian flap in nasal reconstruction has been used for thousands of years, and its development and modifications reflect each time the knowledge of the anatomic vascular pattern of the forehead. In an attempt to understand the reliability and viability of this ancient flap

and to develop further modifications, surgeons rather than anatomists performed research on this topic. This is obvious in classical anatomic textbooks and illustrations where the anatomy of forehead vessels is poorly described. Knowing the history of the flap leads to a better understanding not only of the flap itself but also of forehead vascular anatomy.

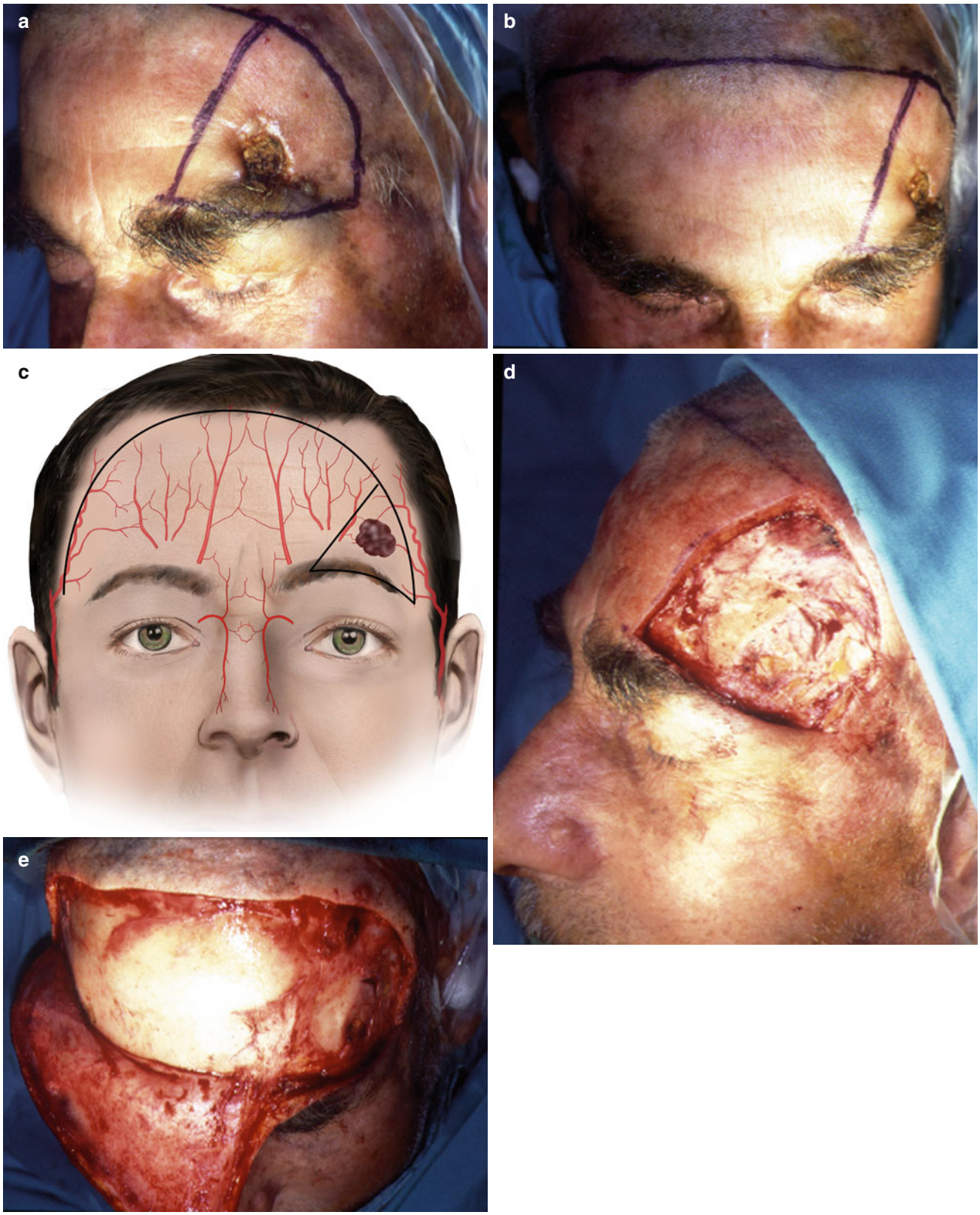

Fig. 3.29 (**a**, **b**) Excision line and flap design outlined. (**c**) The flap is based on the supratrochlear, supraorbital, and frontal arteries. (**d**) Lesion excised. (**e**) The flap is elevated at the subgaleal plane and 2 cm above the supraorbital rims proceeds to the subperiosteal plane. (**f**) Immediate postoperative view. (**g**, **h**) Result at 6 months. Scar formation and brow asymmetry, needing correction, are evident

Fig. 3.29 (continued)

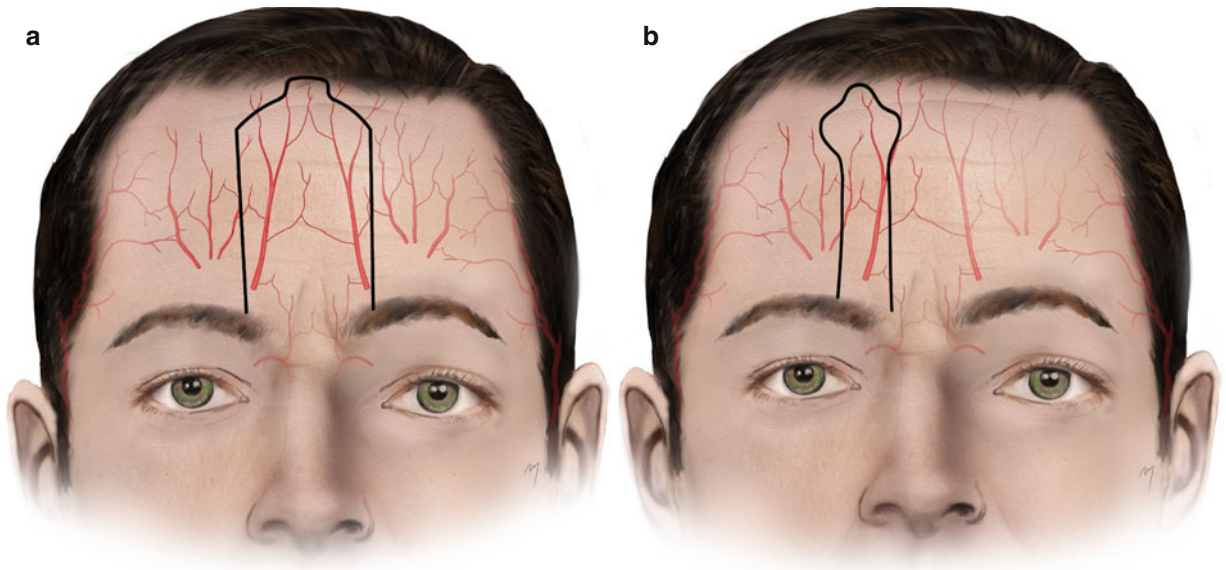

Fig. 3.30 (**a**) Median forehead flap (India flap). (**b**) Paramedian forehead flap (vertical). (**c**) Paramedian forehead flap (oblique). (**d**) Midline forehead flap. (**e**) "Gull-wing" flap

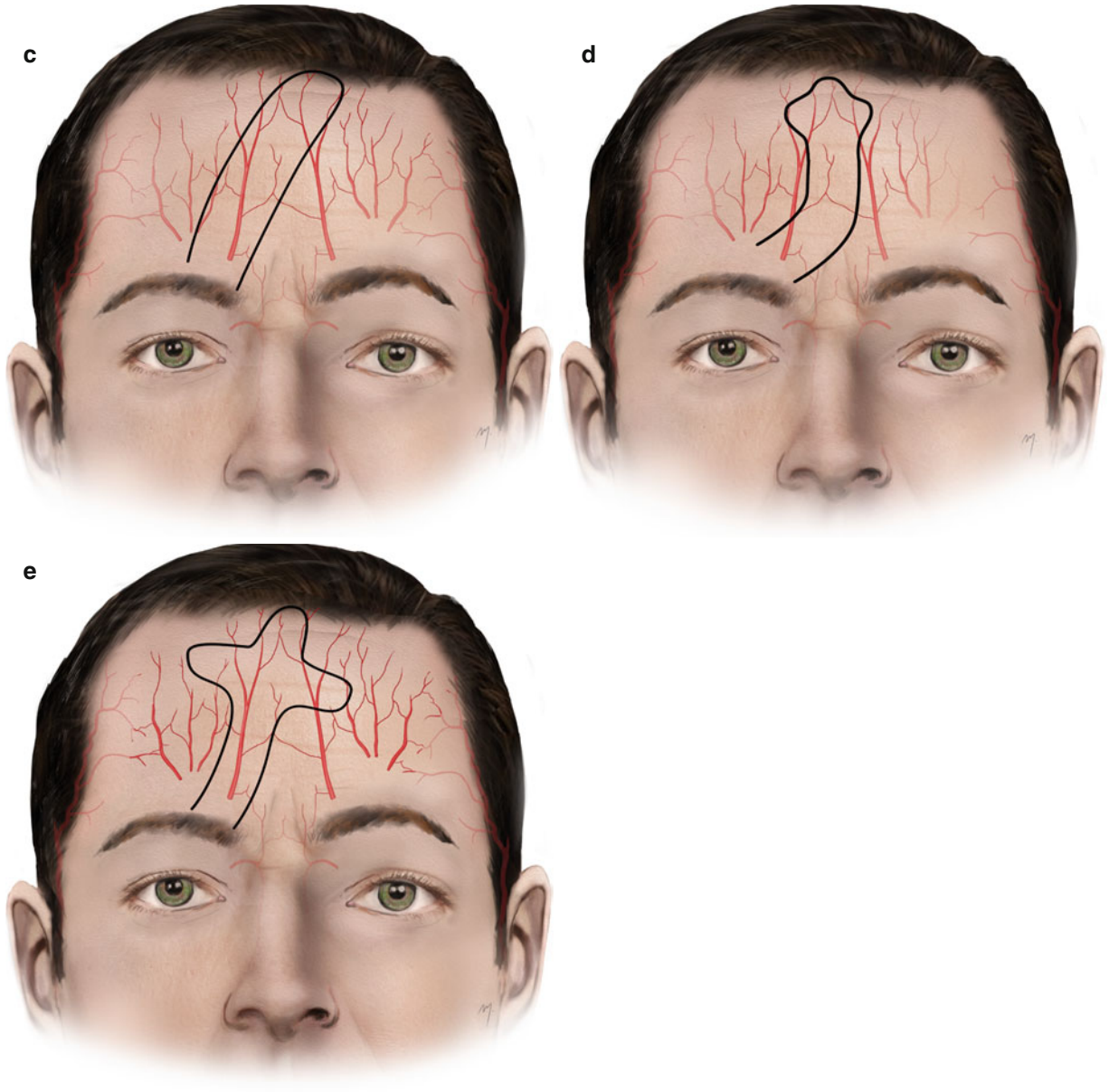

Fig. 3.30 (continued)

3.5.10.1 History of the Indian Flap

The first description of nasal reconstruction is found in India in the Sanskrit text Sushruta Samhita (600 BC), a Brahmin holy text, where nose amputation was a way of punishment. The operation of reconstruction was performed by a caste of Indian potters and bricklayers. Buddhist missionaries who practiced Ayurvedic medicine probably spread this technique to Greece during the Golden Age. After a very long period, this knowledge possibly influenced Gaspare Tagliacozzi, who developed a technique in 1597 known as the Italian flap, by using a pedicle from the inner arm for nasal reconstruction. The forehead flap technique was not performed in Western medicine for hundreds of years. An editorial published in the "Gentleman's Magazine of London" (1794), describing the reconstruction of an amputated nose with a forehead flap, inspired J.C. Carpue to perform two successful medial forehead flaps in England (1814), spreading the method through Europe (Reece et al. 2008; Whitaker et al. 2007).

In the twentieth century, during World War I, a young surgeon (who became later a legend in surgery and Sir) named Harold Delf Gillies treated war injuries and burns by using forehead flaps. These first forehead flaps, named by Gillies "up and down flaps," were based in both supraorbital arteries, having a U shape. Gillies standardized his techniques and established the discipline of "plastic surgery." In 1920,

his textbook "Plastic Surgery of the Face" was published, setting down the principles of modern plastic surgery, principles which were adopted by surgeons from every part of the world (Gillies 1920, 1935; Gillies and Millard 1957).

In 1946, Kazanjian popularized the midline forehead flap in the American literature. Kazanjian designed the forehead flap in the midline, determining that the blood supply of the flap was the supratrochlear and supraorbital arteries and closed the donor site primarily enhancing the final esthetical result (Kazanjian 1946). Since then, many surgeons based on detailed vascular anatomic studies of the forehead developed many alternative modifications to the India forehead flap.

In the decade of the 1960s, Converse and Wood-Smith (1963), in an attempt to reconstruct nasal dorsum defects, based the forehead flap in a subcutaneous pedicle, developed thus the first forehead island flap. Some years later, Millard (1966, 1967) designed a large standard paramedian forehead flap with two transverse extensions, called the "gull-wing flap." This flap can be used to cover extensive bilateral nasal tip, infratip, and lobule defects. The donor site can be closed primarily in a T-form. Its main vascular supply is the supratrochlear bundle based on the medial aspect of one brow. The circulation to the transverse distal portions of the flap is a primarily random pattern.

Converse (1969) described the scalping forehead flap. This flap, originally described by Converse in 1942, harvests a large area of lateral forehead skin, based on a wide pedicle of hair-bearing scalp. The flap is actually the improvement of classic Indian flap, constituting one of the best techniques for total and subtotal nasal reconstruction. The flap is long and supple enough to fold on itself, so that recreates the alar rims and the lobular portion of the nose (Converse 1977; Converse and McCarthy 1981; McCarthy 1990). The reliability of this flap is ensured by the rich arterial vascularization from supratrochlear and supraorbital arteries as well as by the anterior branch of the superficial temporal artery of its base.

Having already gained trust in the forehead flap and after the modifications in design that were developed, research interest became oriented in the deeper anatomic understanding of flap vascularization and as a result in total forehead vascularity.

The importance, not only of the supratrochlear artery but also of the dorsal nasal artery in the vasculature of the forehead flap, begins to become apparent both in clinical (Sawhney 1979) and in anatomic reports (Mangold et al. 1980).

Mangold et al. (1980), in latex-like injection studies and cadaveric dissections, showed that the branches of the ophthalmic artery—dorsal nasal artery, supratrochlear artery, and supraorbital artery—are the vessels that supply the forehead skin. All of them anastomose with the frontal branch of the superficial temporal artery.

Furthermore Mangold et al. proved the importance of the forehead branch of the dorsal nasal artery in supplying the central part of the forehead. These vessels along with the supratrochlear artery that lies on the paramedian line communicate with each other and are the primary nutrition vessels of the paramedian forehead flap.

In 1985, McCarthy et al. studied the median forehead flap blood supply in a cadaveric study. They injected the facial arteries of six fresh cadavers with disulfine blue dye and Microfil, after the supratrochlear and supraorbital arteries had been ligated. Nevertheless, sufficient flow into the forehead, by the anastomotic relationship between the angular artery and the dorsal nasal artery, was demonstrated. The results confirmed in a way Mangold's studies. The authors suggested that the median forehead flap could be elevated without incorporation of the supratrochlear vessels.

In an attempt to gain additional length to the paramedian flap, Burget and Menick (1985, 1986, 1989) extended the incisions for the pedicle below the orbital rim. This usually is necessary in nasal tip reconstruction, where otherwise the need for extra length would extend the flap into the hair-bearing scalp. Intraoperatively, they also noticed that the terminal branches of the supratrochlear artery lie over the superficial fascia of the frontalis muscle, immediately under the dermis. Thus, they stated that fat and frontalis muscle could be removed without danger from distal flap skin necrosis. In 1990, Menick further refines the design of paramedian flap, by making the pedicle narrower and so gaining a suppler flap.

An extensive anatomic evaluation of the arterial system of the face was performed by Whetzel and Mathes (1992). By using numerous anatomic techniques (selective ink injections, dissection and measurement of latex-hardened perforators, and radiographic examination of transverse sections of barium-injected specimens) in cadavers, they defined 11 vascular territories and the dominant arteries of the face and scalp. Regarding the vasculature of the forehead, they delimited the perforators of supratrochlear, supraorbital, and superficial temporal arteries and found among other findings that the anastomosis between the supraorbital artery and the superficial temporal artery occurred through its deep branch.

At the same time, Schumrick and Smith (1992) carried out an important cadaveric study to define the precise arterial basis for the forehead flap design, concerning the vascular topography of central forehead. By means of roentgenographic examinations of injected cadaver heads, anatomic dissections of injected cadaver heads, and Doppler examination of normal subjects, they described the course of the supratrochlear artery in detail. Moreover, they evinced the anastomosing network between the angular, supratrochlear, supraorbital, and superficial temporal arteries.

Fukuta et al. (1994) and Potparic et al. (1996), being in mainly the same research group, investigating the blood

supply of galeal flaps, demonstrated a detailed arterial branching pattern of the supratrochlear, supraorbital, and superficial temporal arteries.

As forehead vascular research progresses, branches now from the dominant arteries of the forehead begin to be used as axis of additional flaps (Capizzi et al. 1999).

Still at 2000, the exact role and contribution of the angular artery in median and paramedian flaps were not been clarified (Fan 2000; Park 2000). Relation of the anatomic location of the supratrochlear artery with regard to the glabellar frown lines, studied by cadaveric dissection and Doppler imaging, begins to serve as novel anatomic landmark for the pedicle position of paramedian forehead flap (Vural et al. 2000).

In a static and dynamic anatomic study of the vascular system of forehead, Reece et al. (2008) revealed that, despite of the forehead arterial anastomosing network, a certain supraorbital arterial plexus exists above the supraorbital rim. This plexus connects the dorsal nasal, supratrochlear, and supraorbital arteries. The superior margin of this plexus extends to a maximum of 7 mm above the supraorbital rim.

This is an important anatomic structure reclaimed in designing and raising the paramedian forehead flap with a distal cross forehead transverse limb (Rohrich's modification). According to the anatomic study of Kelly et al. (2008) an abundant vascular arcade exists within the medial canthal and paranasal region. This is comprised of the supratrochlear, supraorbital, and dorsal nasal arteries above and further down by the angular, infraorbital, and lateral nasal arteries. This anatomic feature allowed Jackson (2007) to base median forehead flaps, with a narrow pedicle, at the level of or even below the medial canthus, gaining much longer and safe forehead flaps. It seems that the forehead flap has not revealed all of its secrets during the past 2,500 years. Questions regarding the exact arterial pattern of it's pedicle remain unclarified and answers resulting from different experimental methods, differ from writer to writer.

Through this development, the paramedian design of the forehead flap becomes the most useful and popular in the reconstruction of medium and large nasal defects. The paramedian forehead flap is based in one supratrochlear and dorsal nasal artery, and its paddle can be oriented in a straight or a vertical orientation. The length of the flap needed and the position of the frontal hairline determine the vertical or oblique design of the flap. In patients who have a high hairline, the flap can be in such a length as to reach even the tip of the nose.

3.5.10.2 Vertical Paramedian Forehead Flap

3.5.10.2.1 Flap Design

The patient that is demonstrated in Fig. 3.31 presented with a basal cell carcinoma located at the tip of the nose. Resection of the lesion and reconstruction with a paramedian forehead flap was planed. Due to patient's high forehead, a vertically directed paramedian forehead flap can be designed (Fig. 3.32a). The area of excision is outlined and transferred to a template that is used to outline the exact needed forehead skin (Fig. 3.32b, c).

Fig. 3.31 A basal cell carcinoma located at the tip of the nose

The proposed flap length is controlled, and the flap must be outlined slightly longer than actually seems to be necessary (Fig. 3.32d, e). Since the flap is to be turned (almost 180°), some length is lost in rotation, but in spite of this, it must be rotated without any tension so as not to compromise its blood supply.

The base of the flap is centered over the supratrochlear artery. The origin of the artery is usually found to be 2 cm lateral to the midline (Fig. 3.32f, g). Palpation of the artery is also useful to ensure its position, but if the surgeon lacks experience and still feels uncomfortable, a Doppler amplifier can be used to find the location of the supplying vessel. A pedicle width of 1.5–2 cm is enough to incorporate the vessels and to allow easy rotation of the flap, without strangulating them (Fig. 3.32h). The width of a paramedian forehead flap, which allows primary closure of the donor site, is approximately 2.5–3 cm.

3.5.10.2.2 Flap Elevation

After the resection of the lesion, the flap is elevated. Initial incisions are made inside the marked lines through the skin, subcutaneous tissue, and muscles (frontalis, procerus, and the upper part of orbicularis muscle) leaving the corrugator intact at this stage. Elevation starts at the cephalic end of the flap in the subgaleal plane and proceeds quickly by either sharp or blunt dissection (Fig. 3.33a, b).

Proceeding to the base, 1 cm above the supraorbital rim, the periosteum is incised, and dissection transitions in the deeper subperiosteal plane (Fig. 3.33c, d). Before incising the periosteum, the corrugator muscle fibers are carefully separated by blunt dissection, so as to preserve the vascular

branches, while restricting bands of muscle are released and sectioned (Fig. 3.33e). The supratrochlear neurovascular bundle now is well protected, being above the periosteum.

3.5.10.2.3 Donor Site Closure

Donor site defects of the forehead up to 3 cm can be closed primarily. Primary closure of the donor defect usually requires extensive mobilization of the forehead. This is done at the subgaleal plane by wide blunt dissection up to the forehead borders (Fig. 3.34a, b). Primary closure is then easy and is done in two layers (Fig. 3.34c).

3.5.10.2.4 Thinning of the Flap

If the flap is too bulky to resurface the nose defect, elevation is followed by the thinning of its borders and no more than its distal 2 cm (Baker 2011). The galea, frontalis muscle, and

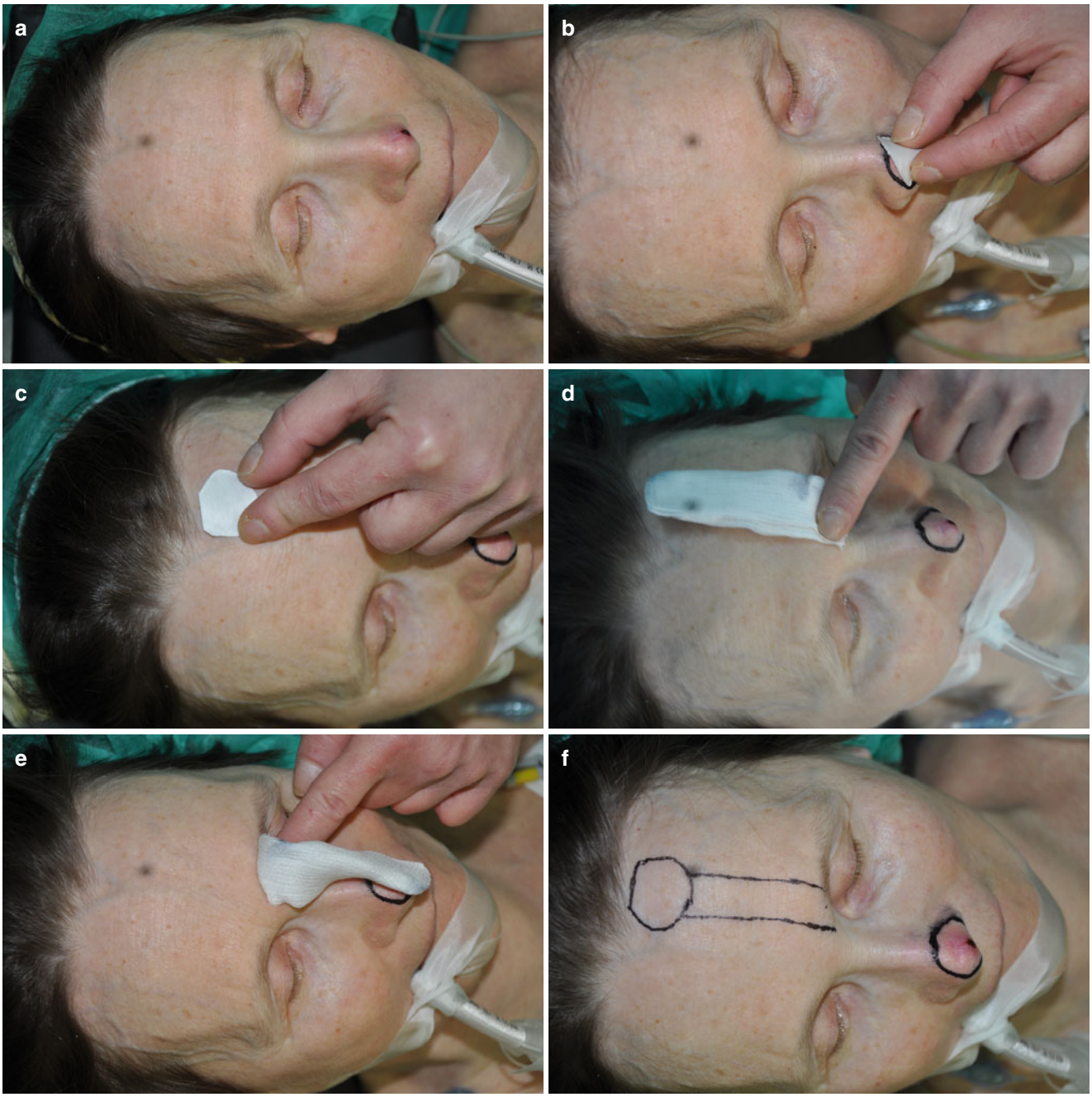

Fig. 3.32 (**a**) The patient has a high forehead allowing the flap to be directed vertically. (**b**) A template imprints the area of excision. (**c**) The template is transferred to the donor site and used to outline the exact needed skin. (**d**, **e**) Flap length controlled. The flap must be outlined slightly longer than the measured distance. (**f**) The exit point of the supratrochlear artery to the forehead is marked 2 cm lateral to the midline and the paramedian flap outlined. (**g**) Flap centered over the supratrochlear artery. (**h**) The flap base is about 1.5–2 cm wide

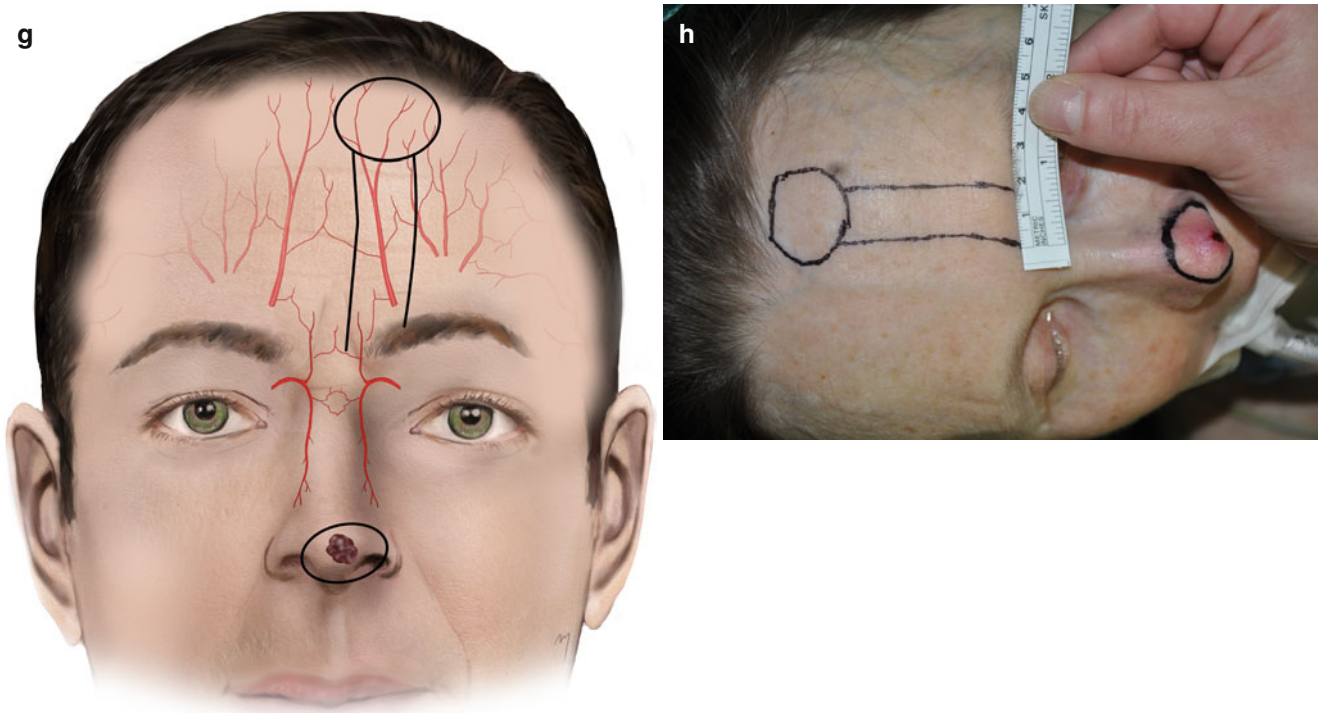

Fig. 3.32 (continued)

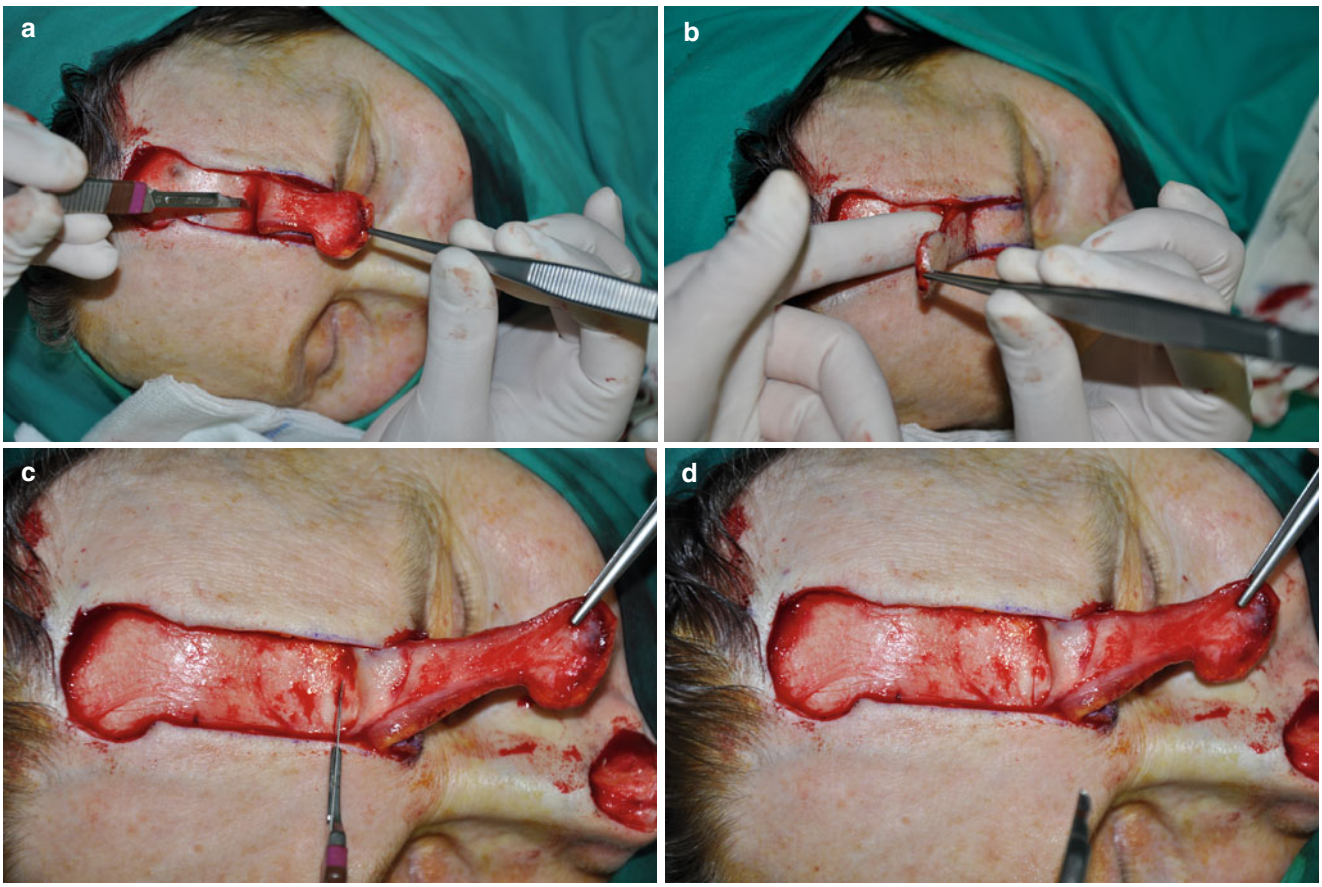

Fig. 3.33 (**a**, **b**) Elevation starts at the cephalic end in the subgaleal plane, and dissection is performed sharply or bluntly either with the finger. (**c**, **d**) 1 cm above the supraorbital rim, the periosteum is incised, and dissection deepens to the subperiosteal plane. (**e**) Corrugator muscle fibers are separated

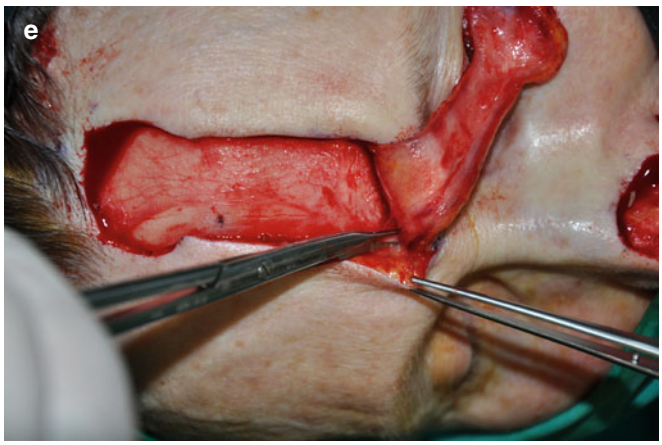

Fig. 3.33 (continued)

subcutaneous fat are removed (Fig. 3.35a). During this procedure, axial terminal branches of the arteries may be visible in the subcutaneous tissue very close to the dermis and thus can be carefully preserved (Fig. 3.35b). If the surgeon feels that the thinning imperils the safety of the flap, it is better to perform it in a later surgical correction. The flap is then sutured in place resurfacing the initial defect (Fig. 3.36a, b).

3.5.10.2.5 Pedicle Division

The skin pedicle remains for a period of 2–3 weeks (Fig. 3.37a, b) and at the second surgical stage is divided and the final reconstruction takes place.

The base of the pedicle is divided, at a level that leaves sufficient glabellar skin (Fig. 3.38a). It is inset as a Greek letter Λ, 1 cm high, just medial to the eyebrow (Fig. 3.38b). Thus, the inter-eyebrow distance and glabella wrinkle lines are restored to normal. The distal part of the flap that surrounds the superior part of the defect has a vascular efficiency that allows it to be elevated from the nasal defect for approximately 1 cm. By this, it can be thinned of fat and muscle, trimmed, and shaped to an ideal nose contour.

Even in the early postoperative period, the result is excellent (Fig. 3.39a, b).

3.5.10.3 Oblique Paramedian Forehead Flap

In the patient presented, a basal cell carcinoma of the tip was excised, and reconstruction was performed with the use of an oblique paramedian flap (Fig. 3.40a–m). The axis of the paramedian flap was determined by the relative low position of the frontal hairline. The difference in this design is that the oblique paramedian flap is of axial pattern except the portion that extends midline. In this case, the deep infiltrating tumor determined a wide and deep resection of the tip that needed bulky tissue to restore completely its contour. For this reason, no flap thinning was done, resulting in a normal postoperative appearance.

3.5.10.4 Paramedian Forehead Flaps Combined with Lining Flaps

The robust forehead flap can safely lie on a bed even if it is the undersurface of a random pattern turn-over flap that lines the nasal mucosa of a through and through defect. In certain cases, flap thickness is able to round the nose contour and shape. The flap is stiff enough to provide a stable restoration, with no need of cartilage grafting, and does not collapse, acting as a valve, in breathing function. Two examples of such cases in different nasal defect locations are presented.

3.5.10.4.1 Through and Through Nasal Tip Defect

The patient that is presented had a full-thickness nasal defect after resection of an ulcerative basal cell carcinoma located at the tip of the nose (Fig. 3.41a–g). A turn-over flap of the adjacent nasal skin adjacent to the defect was used to reline the nasal cavity. The external skin coverage was restored by a paramedian forehead flap. No cartilage grafting was used. The combination of forehead skin and lining skin provided adequate tissue bulk to round out nasal contour.

3.5.10.4.2 Full-Thickness Alar Defect

In the deep invasive recurrent basal cell carcinoma demonstrated, wide and full-thickness resection of the ala was needed to get tumor-free surgical margins (Fig. 3.42a–g). A paramedian flap based contralaterally was designed for external cover. A turn-over flap was outlined to provide the internal cover. The presence of a nevus located at the side of the nose modified the axis of the turn-over to a slightly oblique position.

The alar rim contour was reconstructed by not folding the distal part of the forehead flap but folding the turn-over flap. Folding the turn-over flap to reconstruct the alar rim, skin closer in color and texture to the area was provided, even though an additional linear scar is “endowed.” The final result of this leads to the enhanced concealment of the “new” alar rim and a more normal appearance in this aesthetically crucial nose part. The paramedian flap resurfaced the rest of the defect, and an aesthetically and functionally postoperative result was obtained.

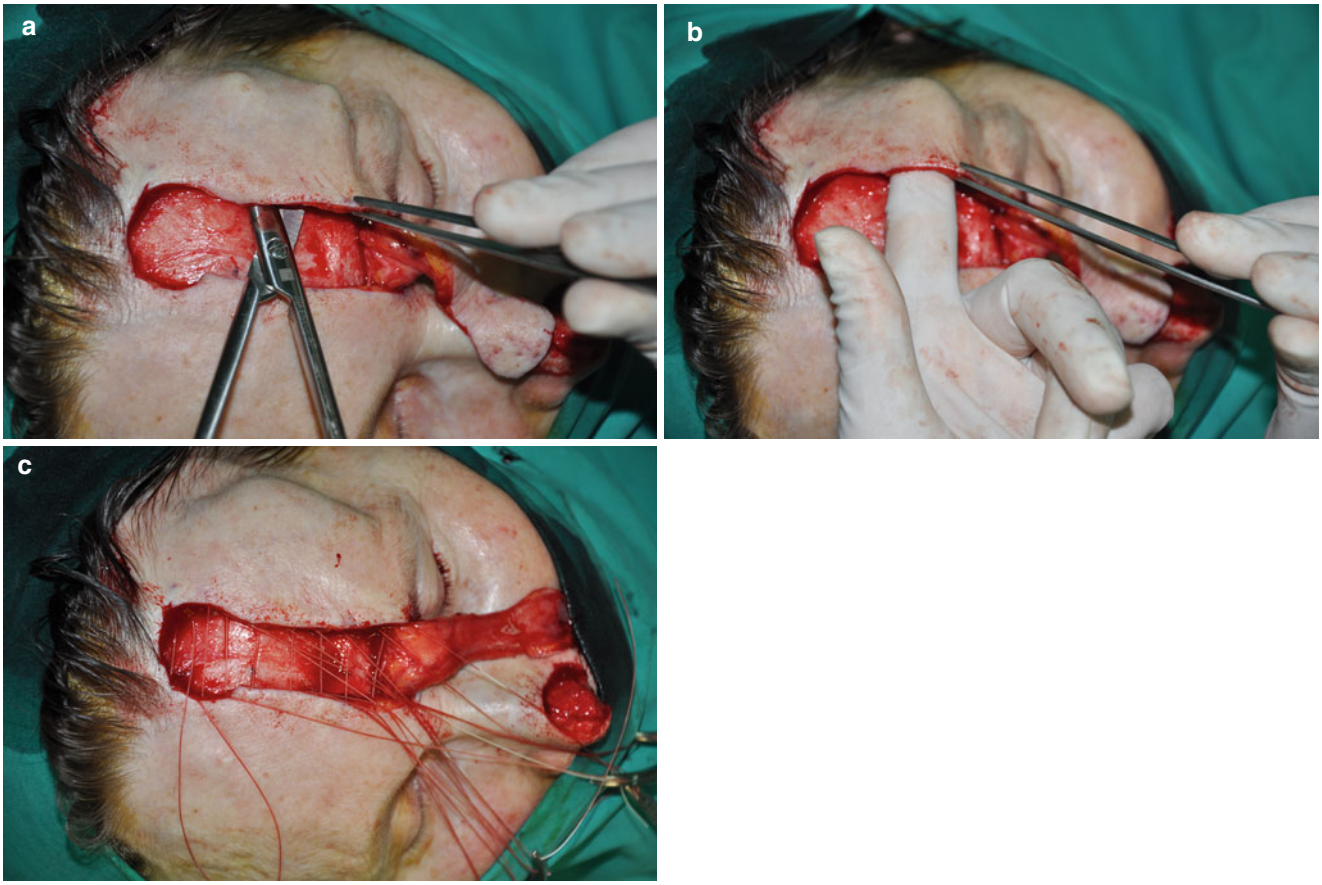

Fig. 3.34 (**a**, **b**) Wide undermining of the donor site in the subgaleal space. (**c**) Donor site is closed in two layers. Forehead muscle and galea are approximated by interrupted absorbable sutures

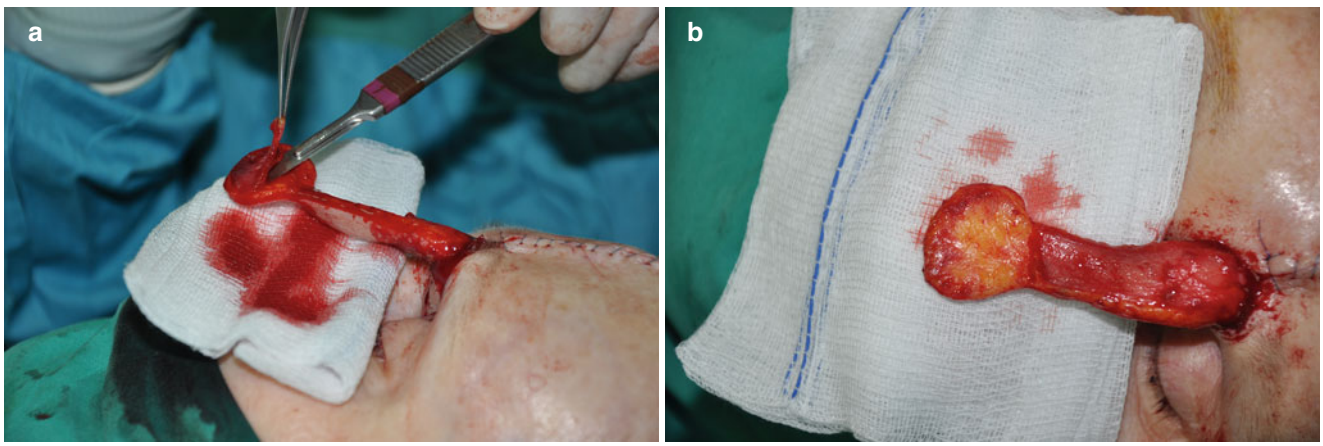

Fig. 3.35 (**a**, **b**) Thinning of the flap

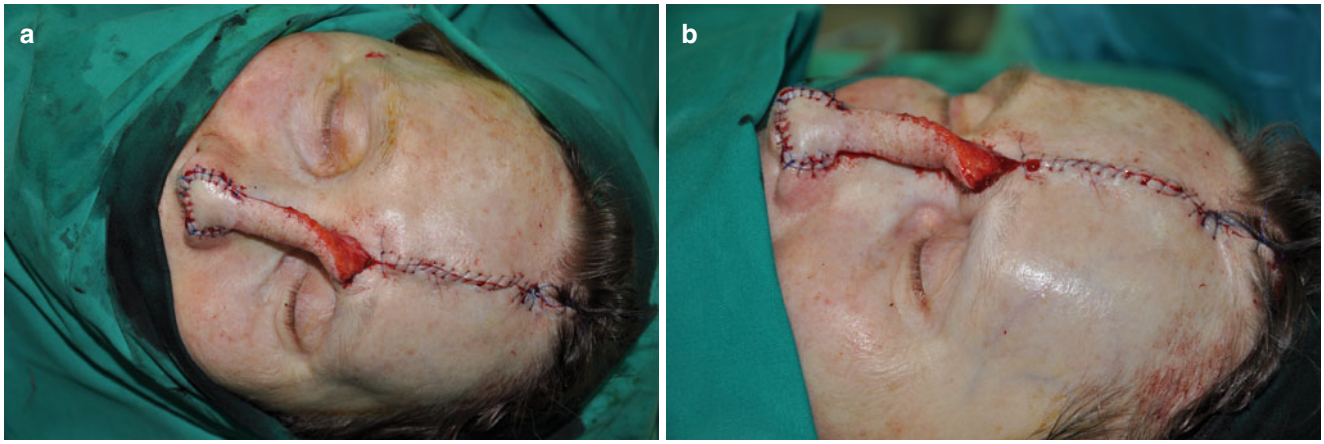

Fig. 3.36 (**a**, **b**) The forehead flap sutured in place reconstructing the nose defect

Fig. 3.37 (**a**, **b**) Skin pedicle remains for 2–3 weeks

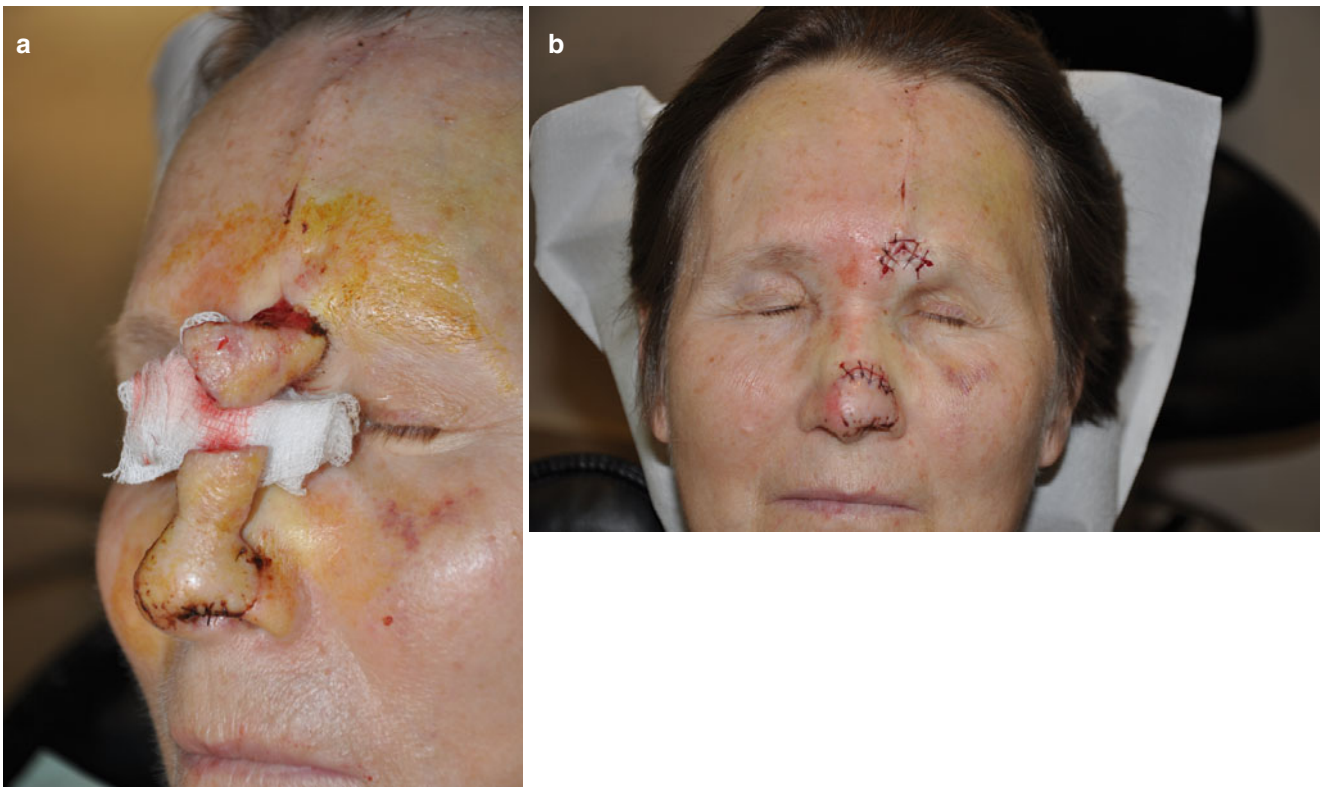

Fig. 3.38 (**a**, **b**) Pedicle divided

Fig. 3.39 (**a**, **b**) Result at 3 months

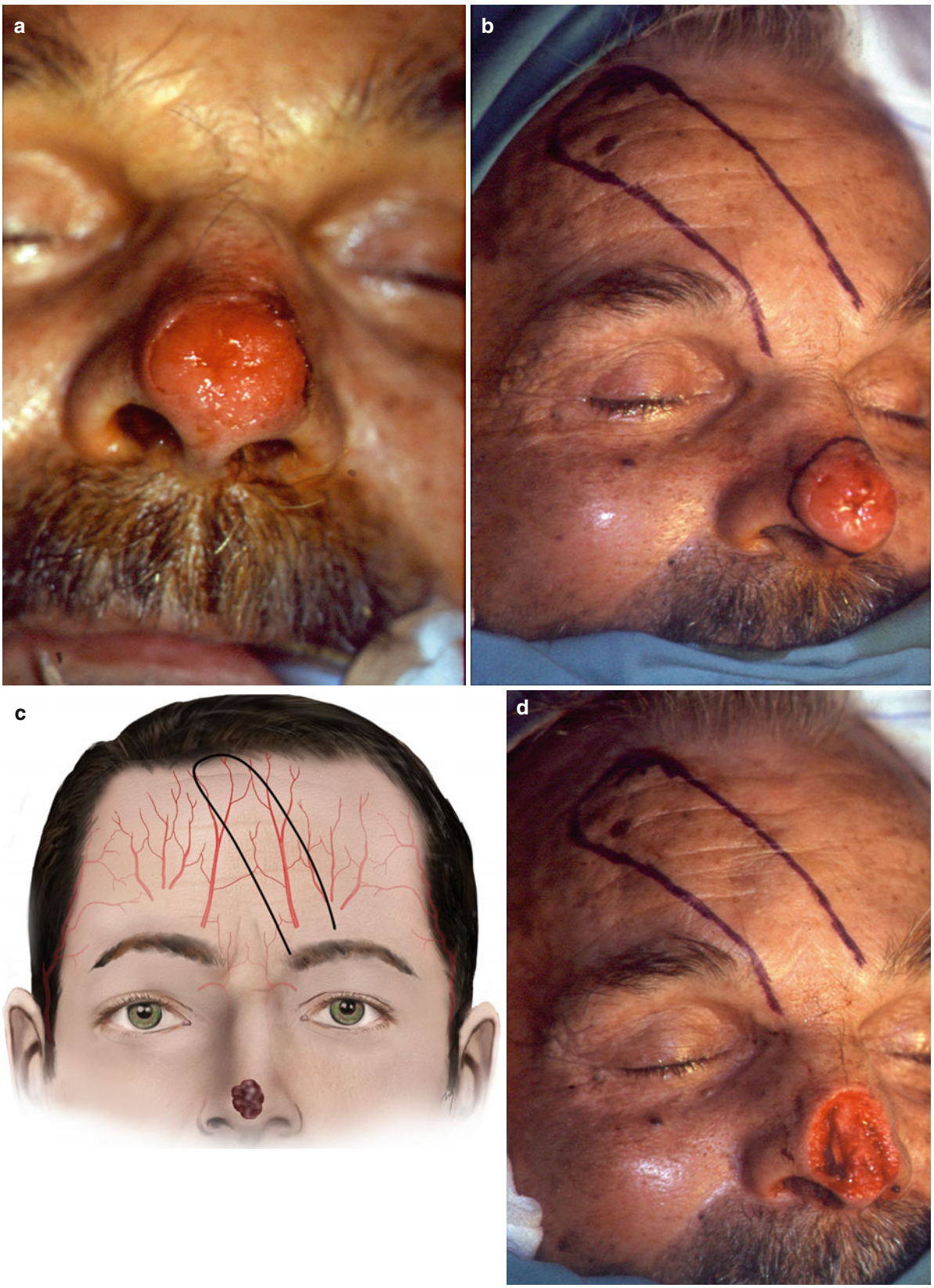

Fig. 3.40 (**a**) A deep invasive basal cell carcinoma located at the tip of the nose. (**b**) Excision line and flap are outlined. (**c**) The oblique paramedian flap is of axial pattern except the portion that extends midline. Based slightly medial, it catches also the glabellar branch of the dorsal nasal artery. (**d**) Tumor excised. (**e**) Flap periphery incised. (**f**) Flap elevated. (**g**) Final suturing. (**h**, **i**) Pedicle remained for 3 weeks. (**j**) Pedicle divided. (**k**) Result at 3 months. (**l**, **m**) No flap thinning was done. The bulky flap restored the contour of the nose tip

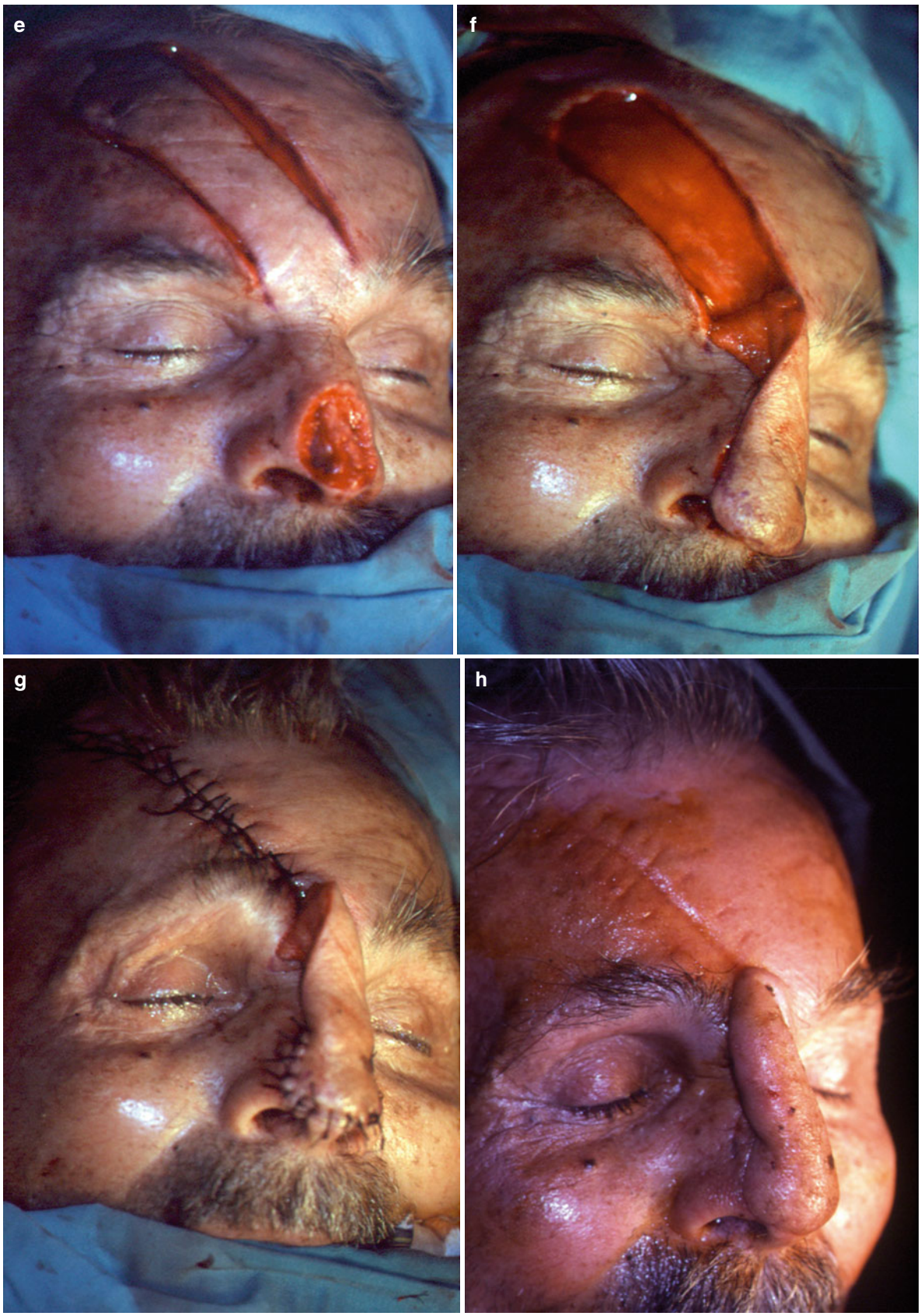

Fig. 3.40 (continued)

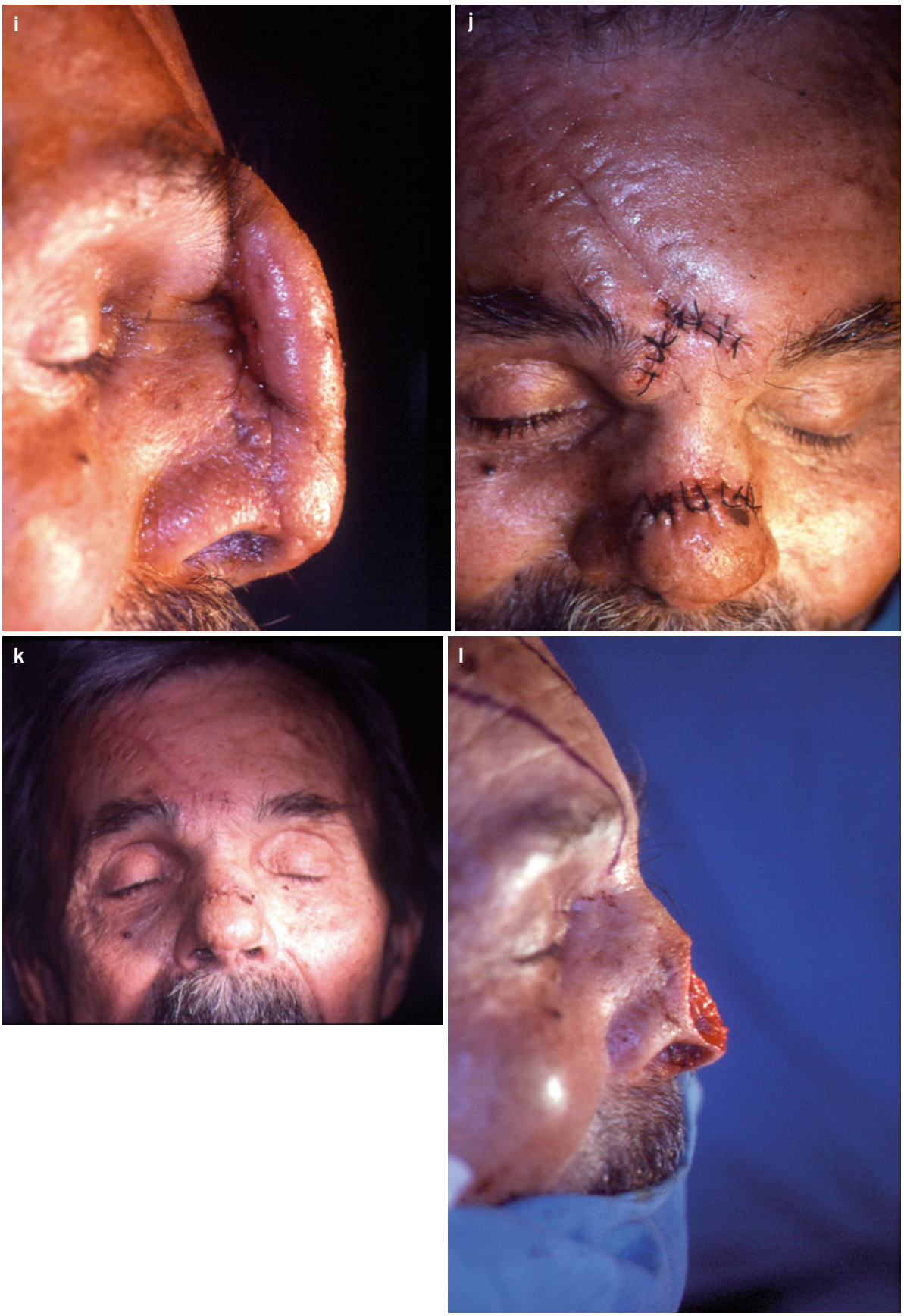

Fig. 3.40 (continued)

Fig. 3.40 (continued)

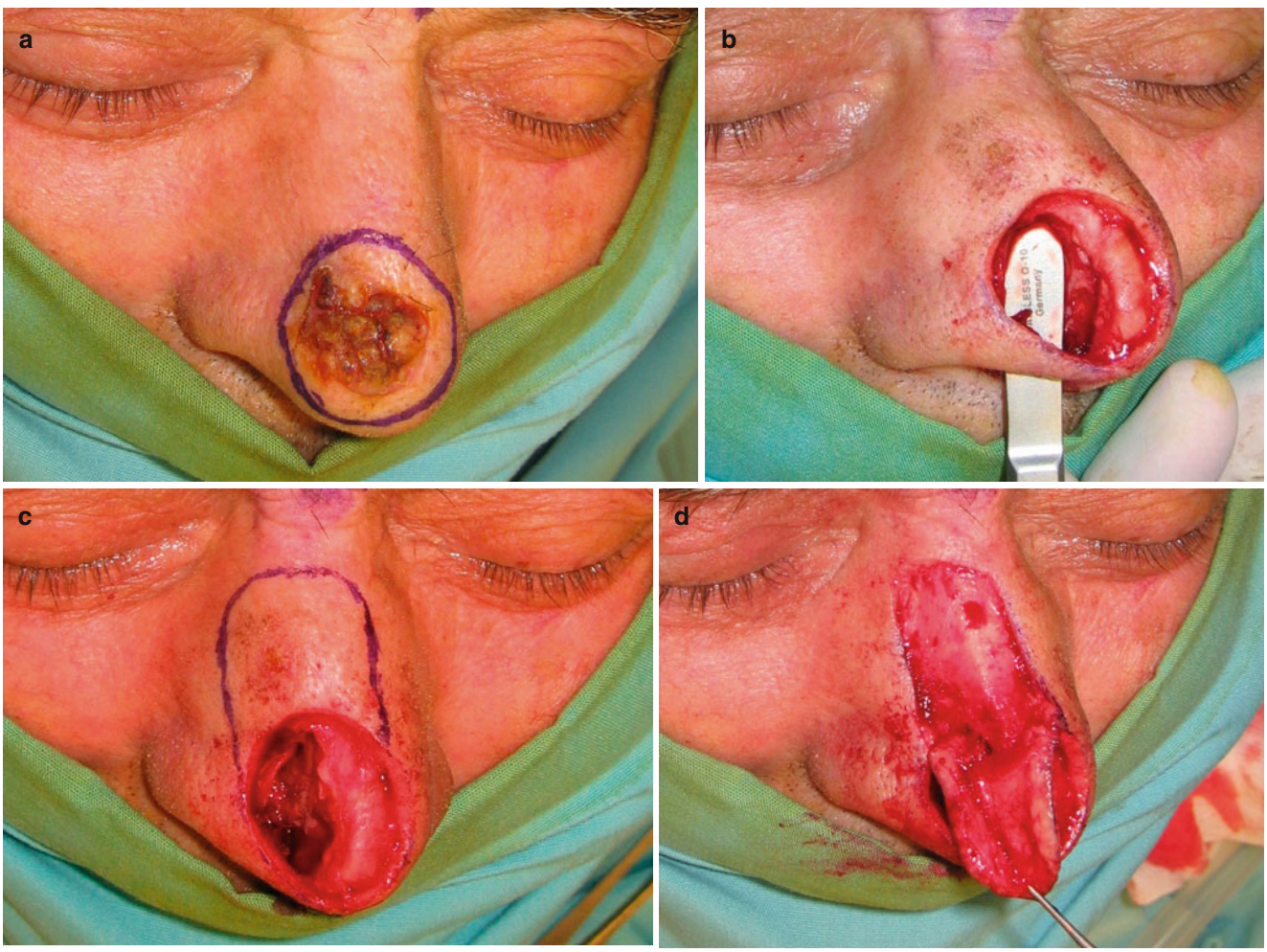

Fig. 3.41 (**a**–**g**) A through and through nasal tip defect restored with a combined paramedian forehead and turn-over flap

Fig. 3.41 (continued)

3.5.11 Paramedian Forehead Flap with a Transverse Limb (Rohrich's Modification)

Rorich modified the paramedian forehead flap by designing a long transverse limb in its distal portion so that more length could be gained (Reece et al. 2008). Although the suggestion is not to design in the forehead the general rule is not to design random flaps with length more than five times the base. Contrary to this, Rohrich`s modification at the transverse limb often exceeds the guideline without distal flap necrosis. His research group found out that a certain supraorbital arterial plexus exists above the supraorbital rim connecting the dorsal nasal, supratrochlear, and supraorbital arteries and that the supratrochlear vessels ran axially into the forehead flap continuing for a short distance across its transverse limb so preventing it from distal necrosis (Reece et al. 2008). Moreover, the deep periosteal branch of supratrochlear artery is incorporated to the flap optimizing its blood flow.

The patient of Fig. 3.43a had traumatic large nasal defect with total loss of the ala, a portion of the nasal tip, and nasal sidewall. A paramedian forehead flap with a transverse limb, according to Rorich, was planned to reconstruct the mixed skin and lining defect (Fig. 3.43b, c).

The flap initially was raised in the subgaleal plane. Attention was needed during its preparation to the base by incorporating the periosteum in its proximal 3 cm and preserving 7 mm of tissue above the supraorbital rim as a zone of safety for the base.

This ensures the capture of the deep (periosteal) branch of the supratrochlear artery and preservation of the superior orbital plexus.

The distal portion of the flap was folded on itself to provide both skin cover and lining (Fig. 3.43d). Cartilaginous grafts were used for skeletal support. The donor site was closed primarily, and a silicon tube was used to provide support in the early stages of healing of the lining, cartilage

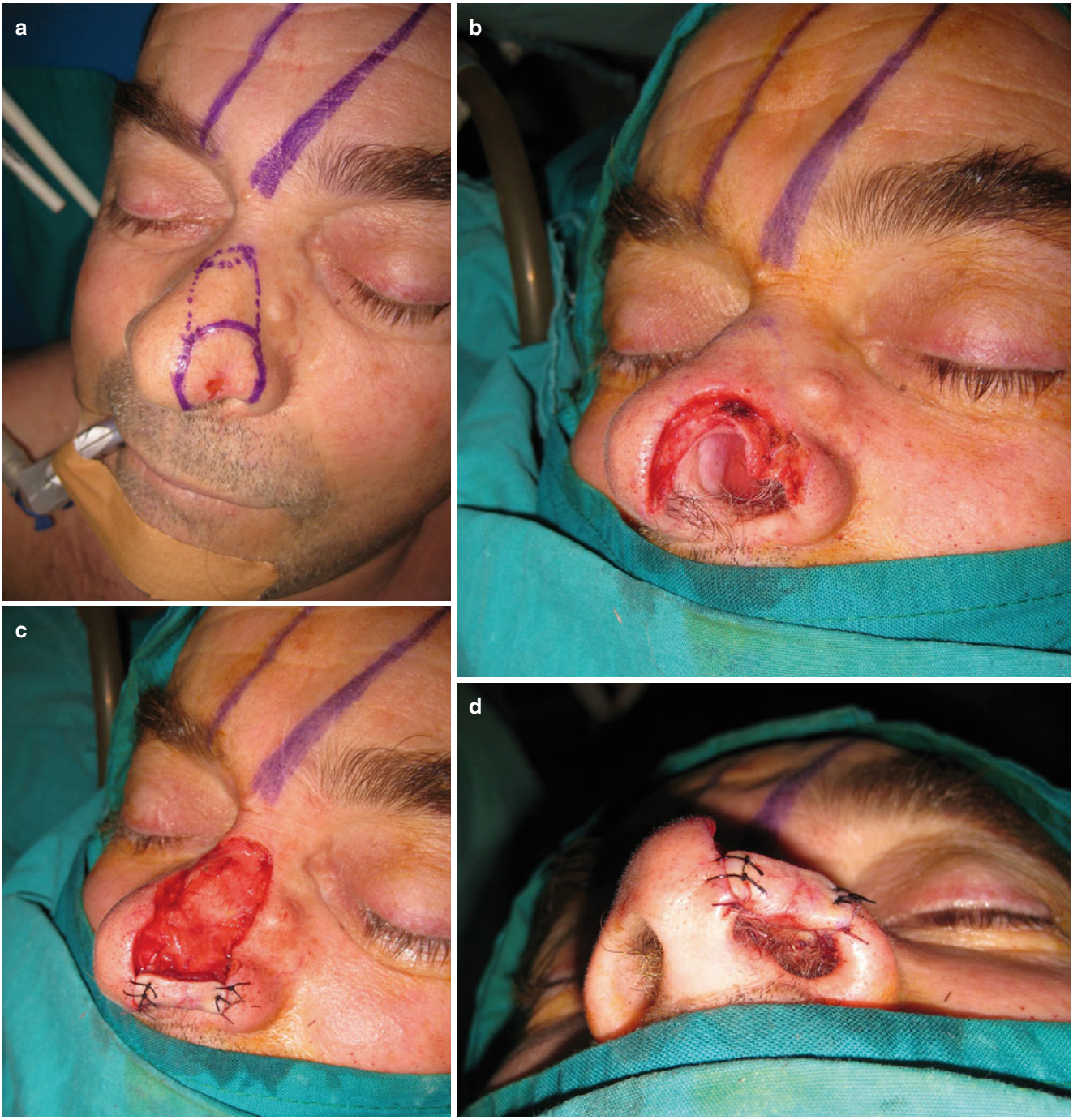

Fig. 3.42 (**a**–**g**) A full-thickness alar defect restored with a combined paramedian forehead and turn-over flap

Fig. 3.42 (continued)

graft, and forehead flap. The flap reconstructed fully the defect without any sign of necrosis (Fig. 3.43e).

3.5.12 Forked Forehead Flap

In complex nasal-medial canthus-eyelid defects, a forehead flap can be a very useful tool used to reconstruct the whole structure at once (McGregor and McGregor 1986; Jackson 2007). In these cases, a paramedian forehead flap is designed slightly wider and larger than the standard one. The distal part is incised to create a fork, and the limbs of the fork are then set into the lid defects, as the rest of the flap resurfaces the nasal and medial canthus defect.

It is of crucial importance to reconstruct the inner canthus, after the completion of the excision. In particular, the inner canthus should be placed and fixed in the correct anatomic position. Failure to do this will lead to obvious asymmetry. Lacrimal reconstruction at this stage could be postponed, since it may not be necessary because epiphora may not be a long-term problem. There is always the possibility that the tumor will recur. If recurrence does not occur, reconstruction is indicated and can be preformed in a later stage (Jackson 2007).

A forked flap was used to a patient with a basal cell carcinoma of the nasal-canthal area and involvement of the medial parts of the upper and lower eyelids (Fig. 3.44a). The forehead flap was slightly wider and larger than the standard one so as to adapt properly to the concave and the convexities of the area under reconstruction (Fig. 3.44b).

The tumor was resected and clear margins were revealed by frozen section biopsies. The medial canthus and the medial parts of the upper and lower lids were sacrificed (Fig. 3.44c). The medial conjunctival pocket was recon-

Fig. 3.43 (**a**) Traumatic loss of a big part of the nose. (**b**) Outline of the paramedian forehead flap with a transverse limb. (**c**) Schematic representation of the flap. (**d**) Flap raised in position. Its distal portion is folded providing skin cover and lining. (**e**) Result at 6 months. Scar and nostril minor revisions are planned for a second-stage surgery

Fig. 3.43 (continued)

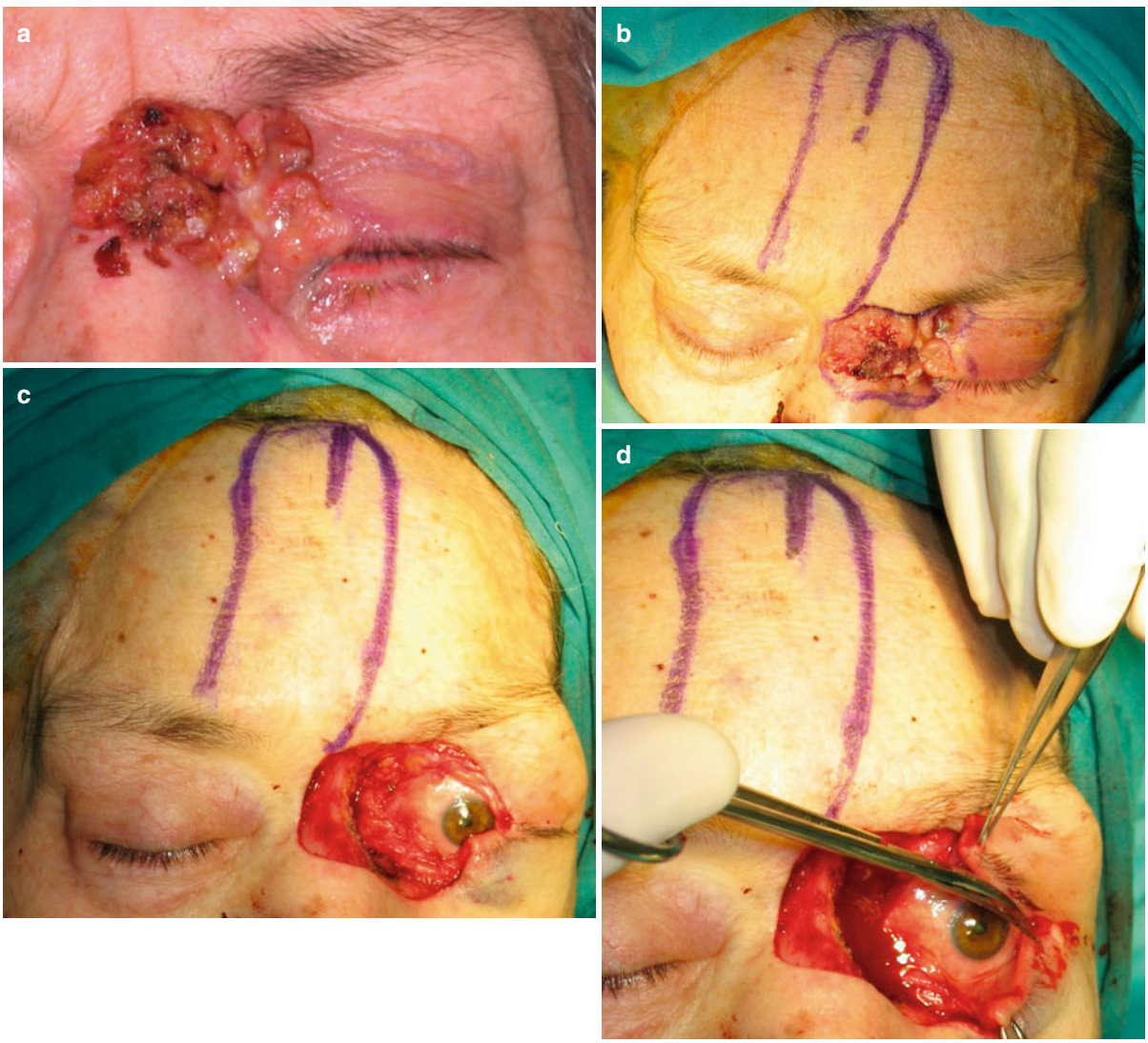

Fig. 3.44 (**a**) A lesion involving the nasal-canthal area and the two eyelids. (**b**) A long forked forehead flap outlined. (**c**) The defect after tumor resection. (**d**) Lateral canthotomy. (**e**) Flap is transposed into the defect and splits into two limbs. (**f**) Final suturing. (**g**) Result at 3 months

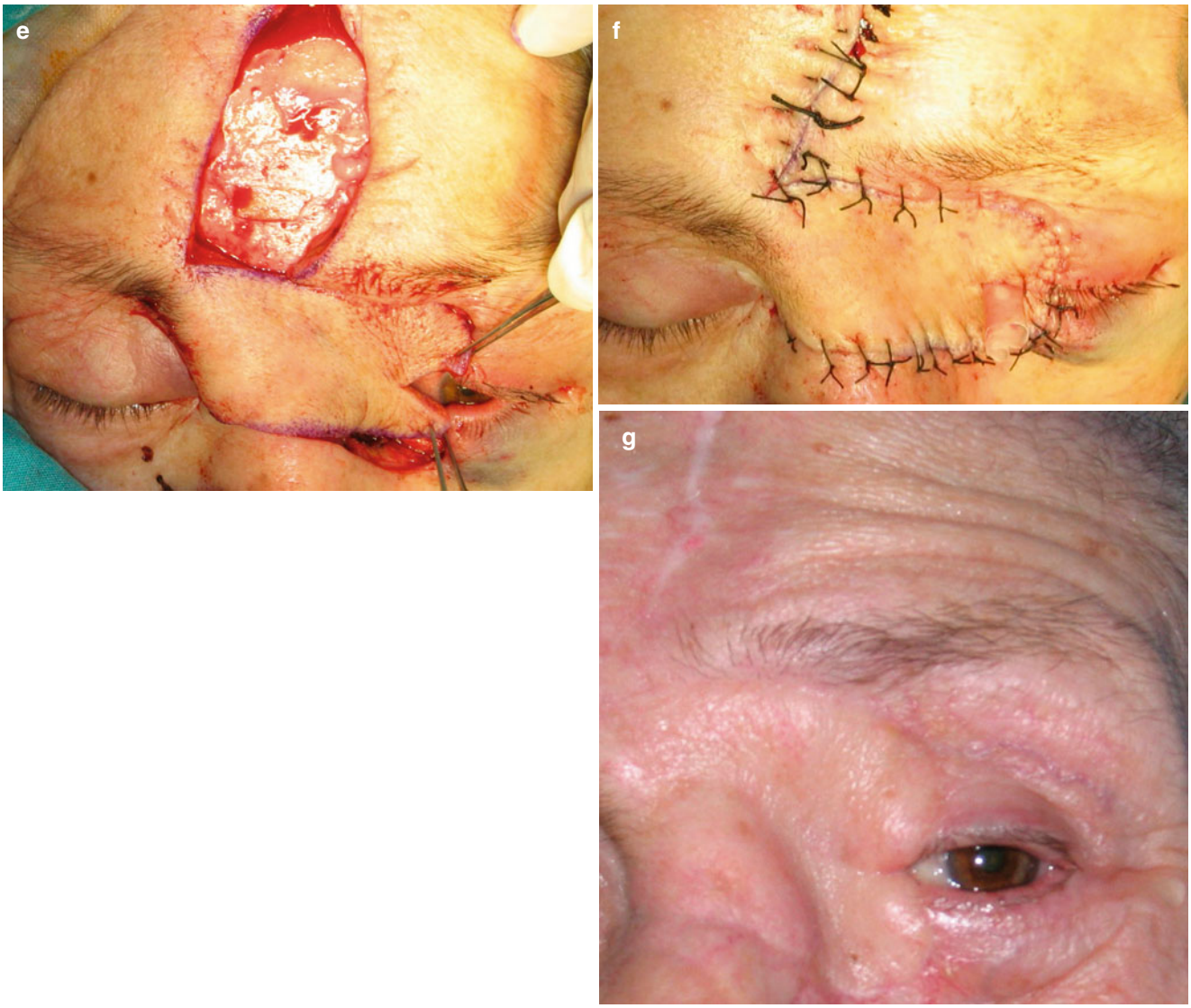

Fig. 3.44 (continued)

structed by mobilization of the conjunctiva to the limbus. At this point, the lateral canthal ligament was divided with sharp scissors to allow lid advancement (Fig. 3.44d).

After lateral canthotomy, it was easy to move the whole lids medially to reduce the defect. The flap was then transposed into the defect and split at its free end, until the correct position for the new medial canthus was obtained (Fig. 3.44e).

The flap was sutured in place covering the nose-canthal-eyelid defect, and the forehead defect was closed directly (Fig. 3.44f). The combined defect was reconstructed easily and by one flap led to a quite acceptable postoperative result (Fig. 3.44g). Revision procedures can be performed at a later stage.

3.5.13 Scalping Forehead Flap

The scalping forehead flap constitutes one of the best techniques for total and subtotal nasal reconstruction. This flap, which was originally described by Converse in 1942, is actually also an improvement of the classic Indian flap (Converse 1942, 1969, 1977; Converse and McCarthy 1981).

The flap is supple enough to fold, for the recreation of the lobular portion of the nose; it is similar in color and texture to the nasal skin and satisfies the requirements in length, in cases where creation of alar rims and columella is needed as in the presented case (Fig. 3.45a–c).

Based on defect dimensions that would occur, a scalping forehead flap was planned considering the width and length, so that the reconstruction of the columella and the alar rims would be allowed (Fig. 3.45d–g). The flap is drawn initially in form of semicircle with coronary direction which starts from the tip of the auricle. It continues in the anterior part of

Fig. 3.45 (**a**–**c**) A large basal cell carcinoma located at the tip of the nose. (**d**–**g**) Resection lines and scalping forehead flap outlined. (**h**) The flap id fused by both supratrochlear arteries and the supraorbital and the anterior branch of the superficial temporal arteries of its base. (**i**–**k**) The defect after tumor resction. (**l**, **m**) Elevation of the flap. (**n**) Flap length control. (**o**) Flap sutured at place. (**p**, **q**) Pedicle division. (**r**–**t**) Result at one year (From: Thomaidis et al. (2007), with permission)

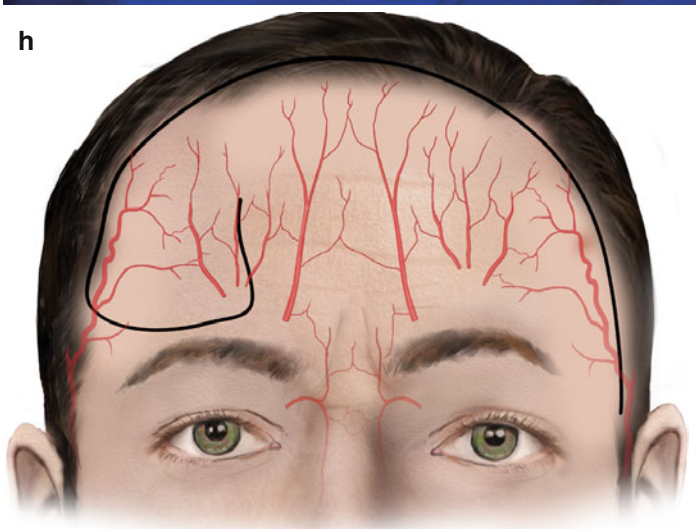

Fig. 3.45 (continued)

Fig. 3.45 (continued)

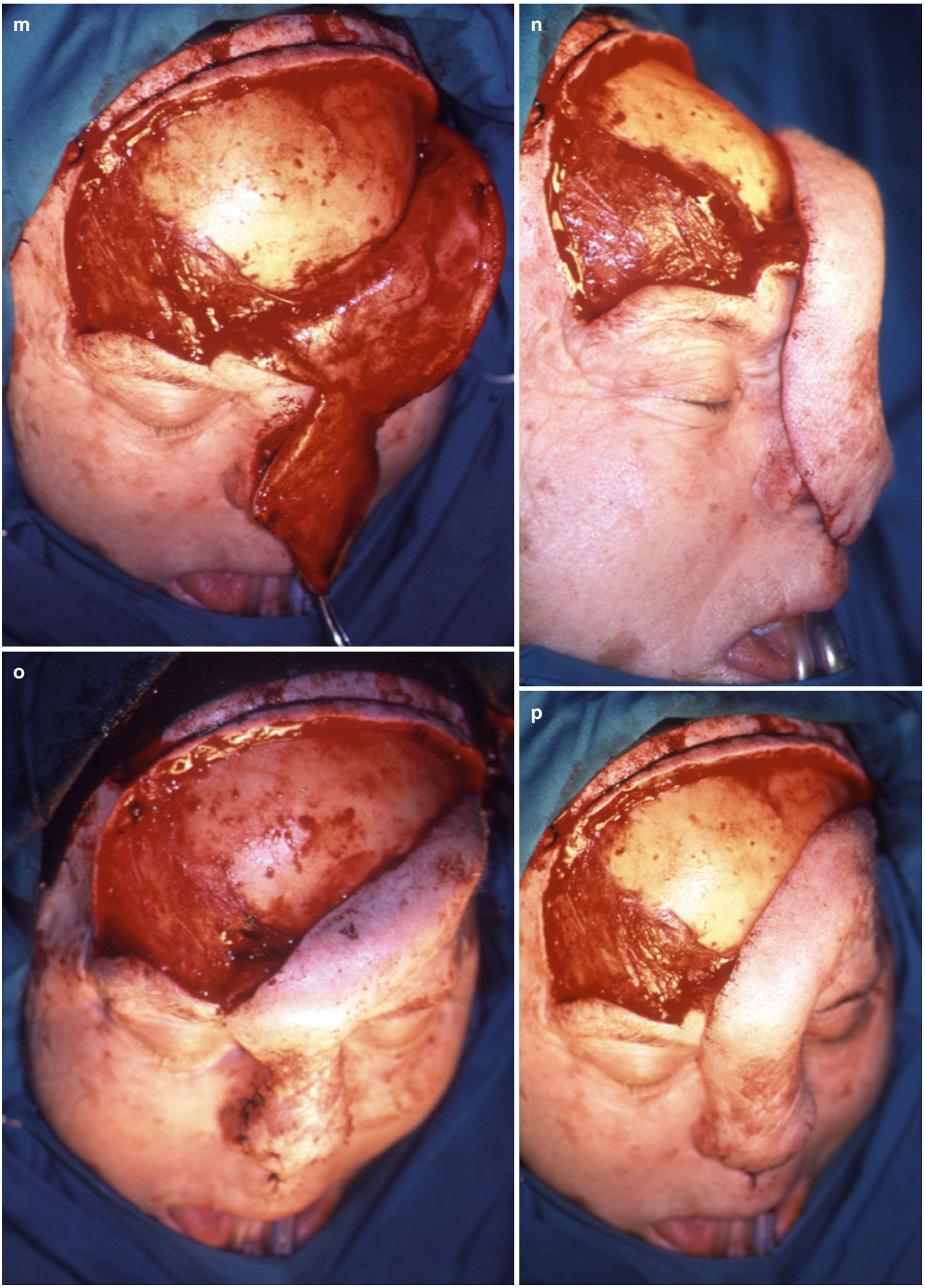

Fig. 3.45 (continued)

Fig. 3.45 (continued)

the hair-bearing skin, and it curves at the contralateral forehead, above the eyebrow and along it, while the final part is drawn with cephalic direction throughout the extent of the forehead, depending on the extent of skin that is required to cover the defect. Its reliability is ensured by rich arterial vascularization from both supratrochlear arteries and the supraorbital artery as well as by the anterior branch of the superficial temporal artery of its base (Fig. 3.45h).

A complete tumoral resection was performed, including the skin and nasal muscles, the medial crus of the greater alar cartilages, part of anterior edge of cartilaginous diaphragm, and small mucosal area into the mucocutaneous junction of nostrils, leaving intact the lateral cartilages and the lateral crus of greater alar cartilages (Fig. 3.45i–k). Clear margins were revealed by frozen section biopsies.

The flap is raised beginning from the donor portion of the forehead, superficial to the frontalis muscle, leaving the muscle in its place. It is important that this part of the frontalis muscle be not raised with the flap, as it constitutes the bed of free skin graft, in the second surgical stage, ensuring the expressive movements of the forehead in this point. Next, the coronary incision of the hair-bearing skin takes place, and the flap is elevated to the level of loose areolar tissue, between the galea and the pericranium. The elevation is continued with the dissection of the flap into the loose areolar tissue plane in the remaining part of the forehead being this time underneath the frontalis muscle (Fig. 3.45l, m). In the temporal region, elevation proceeds to the same level, and the frontal branch of the superficial temporal vessels is incorporated to the flap. In the pedicle base, in a dissection ending 3–4 cm above the supraorbital rim, the flap usually gains its necessary length, ensuring also the integrity of the supraorbital and supratrochlear vessels.

After the flap length control, the distal portion of the flap is trimmed, proportionally folded, and stitched in the recipient site, so that the alar rims, mucocutaneous junction, and columella are reconstructed (Fig. 3.45n, o).

Three weeks later, the pedicle is divided, and the transferring portion of the flap is repositioned to the forehead (Fig. 3.45p, q). The defect at the donor site is covered, in this stage, with full-thickness skin graft. The postoperative result is satisfactory (Fig. 3.45r–t).

3.5.13.1 Scalping Forehead Flap Combined with Lining Flaps

When extended parts of nasal mucosa are invaded by a skin tumor and need to be excised, folding of the scalping flap may not be adequate to provide the optimal lining reconstruction. In these cases, the scalping forehead flap can be combined with lining flaps providing most of the time a bulky reconstruction that may not need nasal support by immediate cartilage grafting.

The patient that is demonstrated in Fig. 3.46a presented with an extended lesion of the right half of the nose and is the same patient of the case presented in subchapter "forehead forked flap." She had been operated for the basal cell carcinoma of the inner canthus and eyelids, with defect restoration with the paramedian forehead flap, 4 years ago. In the meantime, she had not attended the scheduled follow-ups and seek medical help only after the recently and rapidly progressed appeared lesion. Biopsy specimen revealed this time a squamous cell carcinoma.

The surgical reconstruction was planned with defect coverage with the scalping forehead flap, as a second paramedian forehead flap from the other side would be risky due to the previous operation (Fig. 3.46b). Moreover, a scalping flap would provide enough skin transferred into the defect by a flap, which catches three supplying arteries.

A complete tumor resection was performed, including a big part of the right nasal sidewall, in full-thickness defect. Clear margins were revealed by frozen section biopsies. An ipsilateral nasolabial flap was used for lining, which was lifted on its medial subcutaneous pedicle, turned over, and sutured in the mucosal defect (Fig. 3.46c, d).

The scalping forehead flap was performed as previously described (Fig. 3.46e, f).

The aesthetic and functional results, 2 years postoperatively, were reasonably satisfactory (Fig. 3.46g).

3.5.14 Glabellar Finger Flap

This transposition flap is the first choice in reconstruction of moderate-sized, medial canthal defects. The flap is inferiorly based, is adjacent to the defect, and provides non-hair-bearing skin of same color and texture. The feeding artery of the flap is the small glabellar branch of dorsal nasal artery, and thus the flap can be regarded as an axial one.

In the patient of Fig. 3.47a, a middle-sized basal cell carcinoma was located at the medial canthal area. The flap was designed in a finger-shaped manner, inferiorly based, and a Burow's triangle was planned to be excised to allow primary closure of the donor site (Fig. 3.47b, c). After the lesion was excised, the flap was elevated by dissecting deep to the subcutaneous layer and above the nasal bone periosteum (Fig. 3.47e, f). Thinning of the flap is necessary, to provide tissue that has been adjusted to the thickness of the thin medial canthal region. Thinning can be performed, with safety up to the distal half of the flap, without compromising its feeding branch of the dorsal

Fig. 3.46 (**a**) Squamous cell carcinoma of the nose. (**b**) Scalping forehead flap outlined. (**c**, **d**) Excision completed, and a nasolabial flap is used to reconstruct the mucosal defect. (**e**, **f**) The scalping forehead flap provides external cover. (**g**) Final result (From: Thomaidis et al. (2007), with permission)

Fig. 3.46 (continued)

nasal artery. After thinning and trimming, the flap is placed to the defect and fixed by sutures (Fig. 3.47g). The excised Burow's triangle led to a donor site primary closure without a standing cone. The result after 9 months is excellent (Fig. 3.47h).

3.5.15 Vertical Mid-forehead Advancement Flap Superiorly Based

This flap, donated by the mid-forehead, was used to reconstruct the defect after excision of a basal cell carcinoma, in

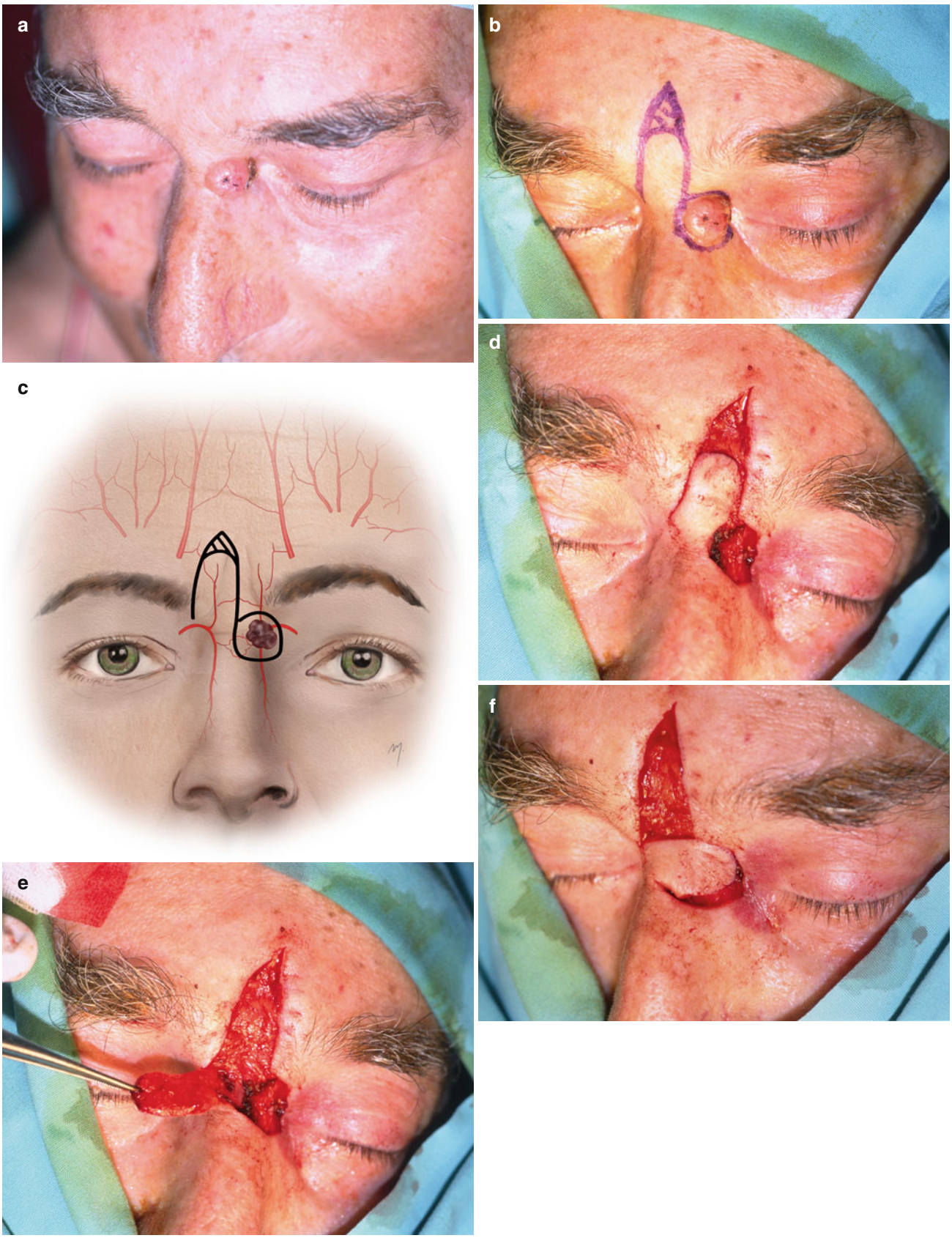

Fig. 3.47 (**a**) Cystic basal cell carcinoma at the medial canthal area. (**b**) Flap outlined. (**c**) The flap can be regarded axial based at the glabellar branch of the dorsal nasal artery. (**d**) Lesion excised. (**e**) Flap raised at the deep subcutaneous level. (**f**) Positioned into the defect. (**g**) Sutured in place. (**h**) Result 9 months after surgery

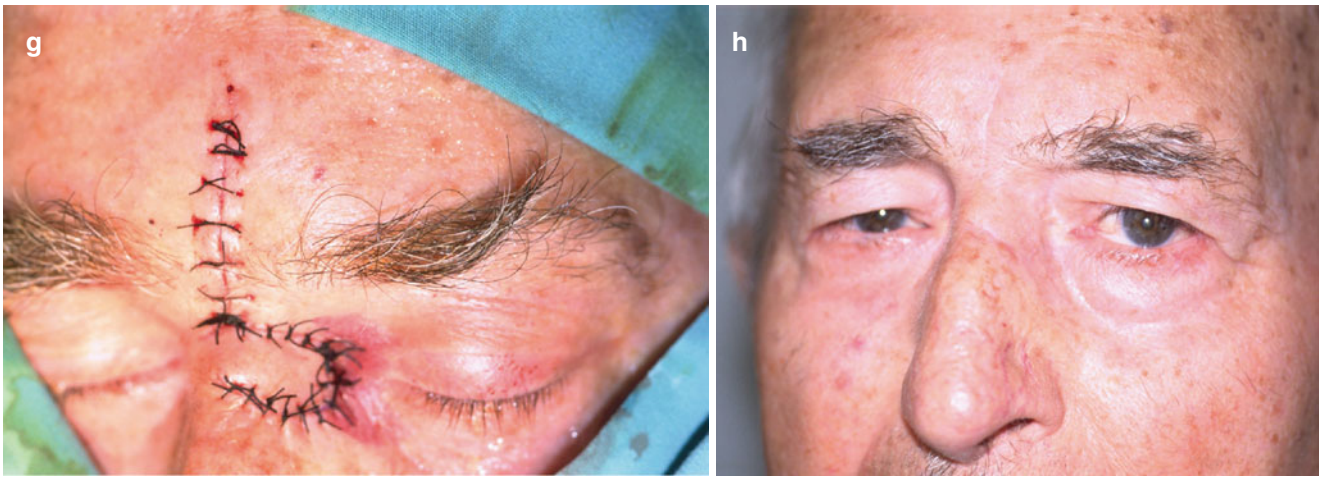

Fig. 3.47 (continued)

the root of the nose (Fig. 3.48a). The advancement flap outlined in that direction is of random pattern (Fig. 3.48b, c) and could be described as an "overmounted" Rintala flap, a flap usually used to reconstruct nasal defects (see Chap. 4). The flap is designed with an approximate 3:1 ratio of length to width. Bilateral Burow's triangles are excised to allow advancement and avoid creation of dog-ears.

The lesion is excised rectangularly, and some bleeding occurs when cutting the horizontal and ascending branches of the dorsal nasal artery (Fig. 3.48d). The flap is undermined with dissection plane down to the periosteum (Fig. 3.48e, f).

By dissecting in this plane and including a part of the procerus muscle and the galea superiorly, vascularization of this long random pattern flap is enhanced.

The flap is advanced downward and sutured in place (Fig. 3.48g). The short suture lines of Burow's triangles are hidden into the transverse forehead rhytides. The postoperative result is excellent (Fig. 3.48h, i). Slight shallow of the frontonasal angle is expected leading to a "classic ancient Greek profile" appearance (McGregor and McGregor 1986).

3.5.15.1 Vertical Mid-forehead Advancement Flap Superiorly Based in Through and Through Nasal Dorsum Defects

In cases of small- to moderate-sized but deep tumors in this area, where nasal bone and mucosa have to be excised leading to a through and through defect, the flap alone can cover the defect and survive, without any other deep (mucosal or bony) restoration (Fig. 3.49a–e). As long as the flap is anchored, it can be overlapped to an all round zone of rigid and healthy bone margin. This prevents contraction, and the rough, bare undersurface of the flap heals by epithelization from the edges of mucosal defect.

Fig. 3.48 (**a**–**i**) Reconstruction of a defect located at the root of the nose with a vertical mid-forehead advancement flap superiorly based

Fig. 3.48 (continued)

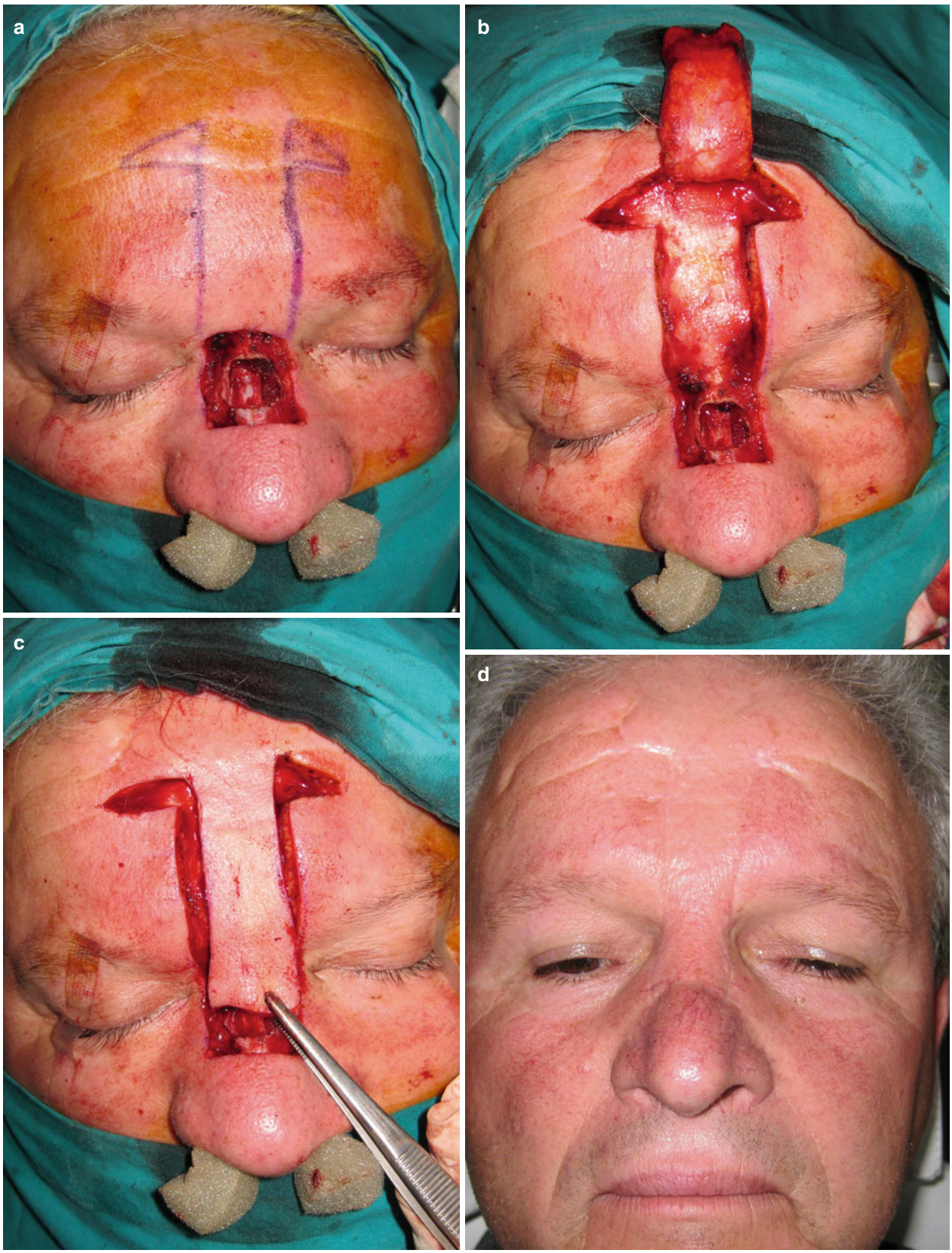

Fig. 3.49 (**a**–**e**) The superiorly based vertical mid-forehead advancement flap was used in a through and through defect of the nasal dorsum without any other mucosal or bony restoration

Fig. 3.49 (continued)

References

Abramo AC (1995) Anatomy of the forehead muscles: the basis for the videoendoscopic approach in forehead rhytidoplasty. Plast Reconstr Surg 95(7):1170–1177

Agthong S, Huanmanop T, Chentanez V (2005) Anatomical variations of the supraorbital, infraorbital, and mental foramina related to gender and side. J Oral Maxillofac Surg 63(6):800–804

Andersen NB, Bovim G, Sjstad O (2001) The frontotemporal peripheral nerves. Topographic variations of the supraorbital, supratrochlear and auriculotemporal nerves and their possible clinical significance. Surg Radiol Anat 23(2):97–104

Baker RS (2011) Interpolated paramedian forehead flaps. In: Baker SR (ed) Principles of nasal reconstruction. Springer, New York/Heidelberg/London

Beer GM, Putz R, Mager K, Schumacher M, Keil W (1998) Variations of the frontal exit of the supraorbital nerve: an anatomic study. Plast Reconstr Surg 102(2):334–341

Burget GC, Menick FJ (1985) The subunit principle in nasal reconstruction. Plast Reconstr Surg 76(2):239–247

Burget GC, Menick FJ (1986) Nasal reconstruction: seeking a fourth dimension. Plast Reconstr Surg 78(2):145–157

Burget GC, Menick FJ (1989) Nasal support and lining: the marriage of beauty and blood supply. Plast Reconstr Surg 84(2):189–202

Caminer DM, Newman MI, Boyd JB (2006) Angular nerve: new insights on innervation of the corrugator supercilii and procerus muscles. J Plast Reconstr Aesthet Surg 59(4):366–372

Capizzi PJ, Eaves FF, Kane WJ (1999) The transverse orbicularis oculi myocutaneous flap: its use as nasal lining. Plast Reconstr Surg 104(5):1419–1423

Cheng AC, Yuen HK, Lucas PW, Lam DS, So KF (2006) Characterization and localization of the supraorbital and frontal exits of the supraorbital nerve in Chinese: an anatomic study. Ophthal Plast Reconstr Surg 22(3):209–213

Chrcanovic BR, Nogueira MH, Abreu G, Custodio ALN (2011) A morphometric analysis of supraorbital and infraorbital foramina relative to surgical landmarks. Surg Radiol Anat 33(4):329–335

Chung MS, Kim HJ, Kang HS, Chung IH (1995) Locational relationship of the supraorbital notch or foramen and infraorbital and mental foramina in Koreans. Acta Anat (Basel) 154(2):162–166

Coleman CC (1959) Scalp flap reconstruction in head and neck cancer patients. Plast Reconstr Surg 24(1):45–54

Converse JM (1942) New forehead flap for nasal reconstruction. Proc R Soc Med 35:811

Converse JM (1969) Clinical applications of the scalping flap in the reconstruction of the nose. Plast Reconstr Surg 43(3):247–259

Converse JM (1977) Full-thickness loss of nasal tissue. In: Converse JM (ed) Reconstructive plastic surgery, vol 2, 2nd edn. Saunders, Philadelphia

Converse JM, McCarthy JG (1981) The scalping forehead flap revisited. Clin Plast Surg 8(3):413–434

Converse JM, Wood-Smith D (1963) Experiences with the forehead island flap with a subcutaneous pedicle. Plast Reconstr Surg 31:521–527

Cook BE Jr, Lucarelli MJ, Lemke BN (2001) Depressor supercilii muscle: anatomy, histology, and cosmetic implications. Ophthal Plast Reconstr Surg 17(6):404–411

Cormack GC, Lamberty BGH (1994) The arterial anatomy of skin flaps, 2nd edn. Churchill Livingstone, Edinburgh

Cuzalina AL, Holmes JD (2005) A simple and reliable landmark for identification of the supraorbital nerve in surgery of the forehead: an in vivo anatomical study. J Oral Maxillofac Surg 63(1):25–27

Daniel RK, Landon B (1997) Endoscopic forehead lift: anatomic basis. Aesthetic Surg J 17(2):97–104

Emmett AJ (1977) The closure of defects by using adjacent triangular flaps with subcutaneous pedicles. Plast Reconstr Surg 59(1):45–52

Erdogmus S, Govsa F (2007) Anatomy of the supraorbital region and the evaluation of it for the reconstruction of facial defects. J Craniofac Surg 18(1):104–112

Erdogmus S, Govsa F, Celic S (2007) Innervation features of the extraocular muscles. J Craniofac Surg 18(6):1439–1446

Fan J (2000) A new technique of scarless expanded forehead flap for reconstructive surgery. Plast Reconstr Surg 106(4):777–785

Fatah MF (1991) Innervation and functional reconstruction of the forehead. Br J Plast Surg 44(5):351–358

Flowers RS (1998) The open approach to forehead and brow lifting. Aesthetic Surg J 18(6):463–464

Fukuta K, Potparic Z, Sugihara T, Rachmiel A, Forte RA, Jackson IT (1994) A cadaver investigation of the blood supply of the galeal frontalis flap. Plast Reconstr Surg 94(6):794–800

Gillies HD (1920) Plastic surgery of the face. Oxford Medical Publications, London

Gillies HD (1935) Experiences with the tubed pedicle flaps. Surg Gynecol Obstet 60:291–293

Gillies HD, Millard R (1957) The principles and art of plastic surgery. Little Brown, Boston

Hwang K, Hwang JH, Cho HJ, Kim DJ, Chung IH (2005) Horizontal branch of the supraorbital nerve and temporal branch of the facial nerve. J Craniofac Surg 16(5):647–649

Hwang SH, Hwang K, Jin S, Kim DJ (2007) Location and nature of retro-orbicularis oculus fat and suborbicularis oculi fat. J Craniofac Surg 18(2):387–390

Isse NG, Elahi MM (2001) The corrugator supercilii muscle revisited. Aesthetic Surg J 21(3):209–215

Jackson JT (2007) Local flaps in head and neck reconstruction, 2nd edn. Quality Medical Pub, St Louis

Janis JE, Ghavami A, Lemmon JA, Leedy JE, Guyuron B (2007) Anatomy of the corrugator supercilii muscle: part I. Corrugator topography. Plast Reconstr Surg 120(6):1647–1653

Janis JE, Ghavami A, Lemmon JA, Leedy JE, Guyuron B (2008) The anatomy of the corrugator supercilii muscle: part II. Supraorbital nerve branching patterns. Plast Reconstr Surg 121(1):233–240

Jeong SM, Park KJ, Kang SH, Shin HW, Kim H, Lee HK, Chung YG (2010) Anatomical consideration of the anterior and lateral cutaneous nerves in the scalp. J Korean Med Sci 25(4):517–522

Kazanjian VH (1946) The repair of nasal defects with the median forehead flap: primary closure of the forehead wound. Surg Gynecol Obstet 83:37–49

Keller GS, Mashkevich G (2009) Endoscopic forehead and brow lift. Facial Plast Surg 25(4):222–233

Kelly CP, Yavuzer R, Keskin M, Bradford M, Govila L, Jackson IT (2008) Functional anastomotic relationship between the supratrochlear and facial arteries: an anatomical study. Plast Reconstr Surg 121(2):458–465

Kimura K (1977) Foramina and notches on the supraorbital margin in some racial groups. Acta Anat 52(3):203–209

Kleintjes WG (2007) Forehead anatomy: arterial variations and venous link of the midline forehead flap. J Plast Reconstr Aesthet Surg 60(6):593–606

Knize DM (1995) A study of the supraorbital nerve. Plast Reconstr Surg 96(3):564–569

Knize DM (1996a) An anatomically based study of the mechanism of eyebrow ptosis. Plast Reconstr Surg 97(7):1321–1333

Knize DM (1996b) Limited-incision forehead lift for eyebrow elevation to enhance upper blepharoplasty. Plast Reconstr Surg 97(7):1334–1342

Knize DM (2000) Muscles that act on glabellar skin: a closer look. Plast Reconstr Surg 105(1):350–361

Knize DM (2001) The forehead and temporal fossa: anatomy and technique. Lippincott Williams & Wilkins, Philadelphia

Knize DM (2007) Letter: the importance of the retaining ligamentous attachments of the forehead for selective eyebrow reshaping and forehead rejuvenation. Plast Reconstr Surg 119(3):1119–1123

Lemke BN, Stasior OG (1982) The anatomy of eyebrow ptosis. Arch Ophthalmol 100(6):981–986

Macdonald MR, Spiegel JH, Raven RB, Kabaker SS, Ms CS (1998) An anatomical approach to glabellar rhytids. Arch Otolaryngol Head Neck Surg 124(12):1315–1320

Malet T, Braun M, Fyad JP, George JL (1997) Anatomic study of the distal supraorbital nerve. Surg Radiol Anat 19(6):377–384

Mangold U, Lierse W, Pfeifer G (1980) The arteries of the forehead as the basis of nasal reconstruction with forehead flaps (in German). Acta Anat (Basel) 107(1):18–25

May JW Jr, Fearon J, Ingarelli P (1990) Retro-orbicularis oculus fat (ROOF) resection in aesthetic blepharoplasty: a 6-year study in 63 patients. Plast Reconstr Surg 86(4):682–689

McCarthy JG (1990) Scalping forehead flap. In: Grabb's encyclopedia of flaps, vol 1, Head and neck. Little Brown and Company, Boston

McCarthy JG, Lorenc ZP, Cutting C, Rachesky M (1985) The median forehead flap revisited: the blood supply. Plast Reconstr Surg 76(6):866–869

McGregor IA, McGregor FM (1986) Cancer of the face and mouth: pathology and management for surgeons. Churchill Livingstone, Edinburgh/London/Melbourne/New York

Menick FJ (1990) Aesthetic refinements in use of forehead for nasal reconstruction: the paramedian forehead flap. Clin Plast Surg 17(4):607–622

Millard DR (1966) Total reconstructive rhinoplasty and a missing link. Plast Reconstr Surg 37(3):167–183

Millard DR (1967) Hemi-rhinoplasty. Plast Reconstr Surg 40(5):440–445

Millard DR Jr (1974) Reconstructive rhinoplasty for the lower half of the nose. Plast Reconstr Surg 53(2):133–139

Miller TA, Rudkin G, Honig M, Elabi M, Adams J (2000) Lateral subcutaneous brow lift and interbrow muscle resection: clinical experience and anatomic studies. Plast Reconstr Surg 105(3):1120–1127

Mitz V, Peyronie M (1976) The superficial musculo-aponeurotic system (SMAS) in the parotid and cheek area. Plast Reconstr Surg 58(1):80–88

Nemoto Y, Sekino Y, Kaneko H (2001) Facial nerve anatomy in eyelids and periorbit. Jpn J Ophthalmol 45(5):445–452

Ouattara D, Vacher C, de Vasconcellos JJ, Kassanyou S, Gnanazan G, N'Guessan B (2004) Anatomical study of the variations in innervation of the orbicularis oculi by the facial nerve. Surg Radiol Anat 26(1):51–53

Park SS (2000) Reconstruction of nasal defects larger than 1.5 centimeters in diameter. Laryngoscope 110(8):1241–1250

Park JI, Hoagland TM, Park MS (2003) Anatomy of the corrugator supercilii muscle. Arch Facial Plast Surg 5(5):412–415

Park JT, Youn KH, Hur MS, Hu KS, Kim HJ, Kim HJ (2011) Malaris muscle, the lateral muscular band of orbicularis oculi muscle. J Craniofac Surg 22(2):659–662

Park JT, Youn KH, Lee JG, Kwak HH, Hu KS, Kim HJ (2012) Medial muscular band of the orbicularis oculi muscle. J Craniofac Surg 23(1):195–197

Potparic Z, Fukuta K, Colen LB, Jackson IT, Carraway JH (1996) Galeo-pericranial flaps in the forehead: a study of blood supply and volumes. Br J Plast Surg 49(8):519–528

Reece EM, Schaverien M, Rohrich RJ (2008) The paramedian forehead flap: a dynamic anatomical vascular study verifying safety and clinical implications. Plast Reconstr Surg 121(6):1956–1963

Sawhney CP (1979) Use of a larger midline forehead flap for rhinoplasty, with new design for donor site. Plast Reconstr Surg 63(3):395–397

Saylam C, Ozer MA, Ozerk C, Gurler T (2003) Anatomical variations of the frontal and supraorbital transcranial passages. J Craniofac Surg 14(1):10–12

Schumrick KA, Smith TL (1992) The anatomic basis for the design of forehead flaps in nasal reconstruction. Arch Otolaryngol Head Neck Surg 118(4):373–379

Seline PC, Siegle RJ (2005) Forehead reconstruction. Dermatol Clin 23(1):1–11

Sullivan PK, Salomon JA, Woo AS, Freeman MB (2006) The importance of the retaining ligamentous attachments of the forehead for selective eyebrow reshaping and forehead rejuvenation. Plast Reconstr Surg 117(1):95–104

Sykes JM (2009) Applied anatomy of the temporal region and forehead for injectable fillers. J Drugs Dermatol 8(10 Suppl):24–27

Tarbet KJ, Lemke BN (1997) Clinical anatomy of the upper face. Int Opthalmol Clin 37(3):11–28

Thomaidis VK et al (2007) The scalping forehead flap in nasal reconstruction: report of Two cases. J Oral Maxillofac Surg 65(3): 532–540

Tzafetta K, Terzis JK (2010) Essays on the facial nerve, part 1 microanatomy. Plast Reconstr Surg 125(3):879–889

Vestal KP, Rathbun ER, Seiff SR (1994) Anatomy of the terminal nerves in the upper eyelid. Ophthal Plast Reconstr Surg 10(1):1–5

Vural E, Batay F, Key JM (2000) Glabella frown lines as a reliable landmark for the supratrochlear artery. Otolaryngol Head Neck Surg 123(5):543–546

Vuyk HD (2006) Forehead, temple and scalp reconstruction. In: Vuyk HD, Lohuis PJFM (eds) Facial plastic and reconstructive surgery. Hodder Arnold Publication, London

Walden JL, Brown CC, Klapper AJ, Chia CT, Aston SJ (2005) An anatomical comparison of transpalpebral, endoscopic, and coronal approaches to demonstrate exposure and extent of brow depressor muscle resection. Plast Reconstr Surg 116(5):1479–1487

Webster RC, Gaunt JM, Hamdan US, Fuleihan NS, Giandello PR, Smith RC (1986) Supraorbital and supratrochlear notches and foramina: anatomical variations and surgical relevance. Laryngoscope 96(3):311–315

Whetzel TP, Mathes SJ (1992) Arterial anatomy of the face: an analysis of vascular territories and perforating cutaneous vessels. Plast Reconstr Surg 89(4):591–603

Whitaker IS, Karoo RO, Spyrou G, Fenton OM (2007) The birth of plastic surgery: the story of nasal reconstruction from the Edwin Smith Papyrus to the twenty-first century. Plast Reconstr Surg 120(1):327–336

Worthen EF (1974) Repair of forehead defects by rotation of local flaps. Plast Reconstr Surg 57(2):204–206

Yoshioka N, Kishimoto S (1991) Anteriorly based pericranial flap: an anatomic study of feeding arteries. Skull Base Surg 1(3): 161–164

Yoshioka N, Rhoton LA (2005) Vascular anatomy of the anteriorly based pericranial flap. Neurosurgery 57(1 Suppl):11–16

Zide BM (2006) Surgical anatomy around the orbit. The system of zones. Lippincott Williams & Wilkins, Philadelphia

Zide BM, Jelks GW (1985) Surgical anatomy of the orbit. Raven, New York

Nose

4

The nose is the most prominent of all facial features situated just at the center of the face. Its complicated contour is elsewhere convex or concave; the presence of nostrils and its functional importance in breathing makes it a unique functional organ and a predominant aesthetic unit with great impact in appearance.

In contrast to the other features of the face, the nose exhibits significant differences in general regarding its shape and size, specifically in many of its components (tip, alar lobule, columella), in skin and fibrofatty tissue thickness, among the ethnic groups (Watanabe 1994; Ofodile and Bokhari 1992; Ofodile et al. 1993; Chun et al. 2008).

4.1 Subunits-Topographic Landmarks

The nose can be subdivided into ten topographic subunits, which exhibit aesthetic importance. These subunits include the root of the nose, the dorsum, the two nasal sidewalls, the nasal tip, the philtrum, the two alar lobules, and the two soft triangles (Fig. 4.1).

Its most important topographic landmarks include the nasion, the rhinion, the nasal facial sulcus, the pronasalae, the supra-alar crease, and the alar-facial sulcus (Fig. 4.2).

The nasion (sela nasi) is the point where the forehead meets the nose. It corresponds to the nasofrontal bony junction and is marked as a depression of the nasal root.

The dorsum of the nose has two parts: a superior part defined by the nasal bones, the bony dorsum, and an inferior part defined by cartilage, the cartilaginous dorsum. The point where these parts are joined is termed the rhinion.

The nasal facial sulcus borders the sidewall and the cheek. The pronasalae is the most prominent point of the nasal tip. Just caudal to it, the infratip lobule is located.

The alar lobule shows a sidewall and a base. The supra-alar crease (alar groove, alar crease, alar sulcus) borders curvilinearly the lobule. This line continues to the alar-facial sulcus that corresponds to the borderline between cheek, upper lip, and alar base.

The soft triangle is a flat area that consists only of two skin layers—the external skin and the skin of the nasal vestibule—and corresponds at the area of the inferolateral border of the intermediate crus of the alar cartilage.

4.2 Layered Anatomy

The soft tissues of the nose are arranged in discrete components that lie over the osseocartilaginous nasal skeleton. Outermost is the nose skin with special and variable

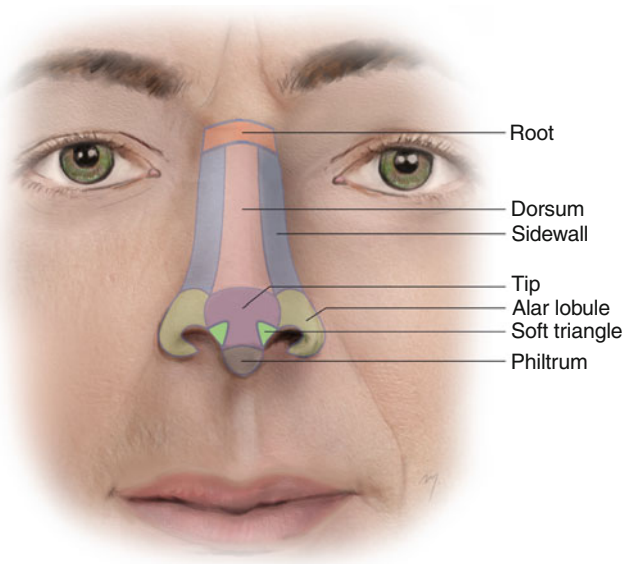

Fig. 4.1 The subunits of the nose

V.K. Thomaidis, *Cutaneous Flaps in Head and Neck Reconstruction*,
DOI 10.1007/978-3-642-41254-7_4, © Springer-Verlag Berlin Heidelberg 2014

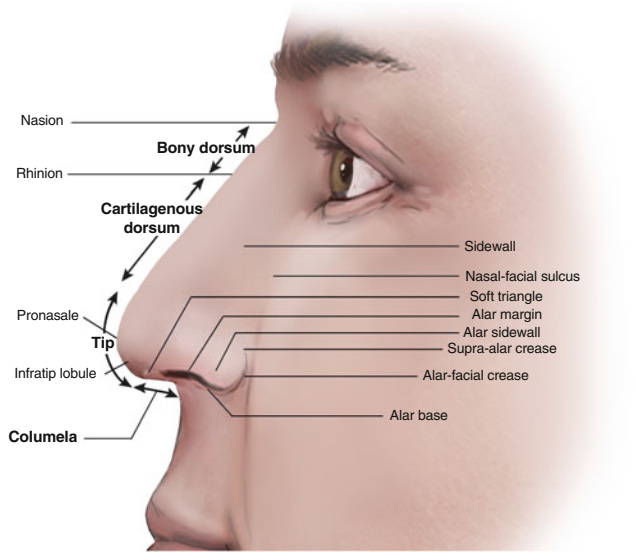

Fig. 4.2 Topographic landmarks of the nose

Fig. 4.3 Relaxed skin tension lines (RSTLs) of the nose

characteristics. Just below the skin are layered the subcutaneous tissue, the nasal superficial musculoaponeurotic system (nasal SMAS), the deep areolar (deep fatty) layer, and the periosteum-perichondrium layer (Letourneau and Daniel 1988; Oneal et al. 1996, 2000).

4.2.1 Skin

The thickness of the nasal skin varies markedly from person to person and among the nasal areas. It is in general thicker at the tip and the alae. Over the bony skeleton and lateral cartilages, the skin is thinner showing a degree of mobility. The average skin thickness is 1.2 mm at the nasofrontal groove and 0.7 mm at the rhinion (Lessard and Daniel 1985). At the nasal tip and over the alar cartilages, the skin is thick, approximately 1.7 mm, and is adherent to the underlying structures, with virtually no mobility.

The number and the activity of the sebaceous glands of nasal skin play an important role in the nasal skin characteristics and must always be preoperatively assessed. The concentration of sebaceous glands varies enormously in different patients and also in different parts of the nose in the same patient. The number and activity increase in the caudal half of the nasal skin. The same happens during the aging process; thus, older individuals reveal a "fatty" and thick nasal skin. The increased sebaceous activity leads to a thick, immobile, and highly vascular nasal skin, which is difficult to work with when used as a nasal flap.

The ease, with which the skin can be stripped from the underlying skeleton, changes at the line between the lateral and alar cartilages. Above this line the skin strips easily in contrast to the alar skin that is very adherent. The relaxed skin tension lines (RSTLs) on the nose run horizontally, while on the lobules they are directed in an oblique direction (Fig. 4.3).

4.2.2 Subcutaneous Tissue Layer

The subcutaneous tissue layer lies immediately below the skin and consists of fibrofatty tissue. Numerous fibrous intertwining septa run vertical from the underlying SMAS layer to the deep surface of dermis within the fat. The subcutaneous tissue layer is more abundant at the tip, the alar lobules, and the glabella and becomes thinner in the rest of the nose.

4.2.3 Nasal Superficial Musculoaponeurotic System (Nasal SMAS)

The nasal superficial musculoaponeurotic system (SMAS) is a continuous fibromuscular layer that encompasses and connects the nasal musculature. This layer has similar histologic characteristics with the superficial musculoaponeurotic system found in the face and functionally distributes the nasal

muscle forces affecting respiration (Letourneau and Daniel 1988). It extends from the radix to the margin of the nostrils and continues to the facial SMAS. All the major arterial, venous, and lymphatic vessels run in or above the nasal SMAS (Toriumi et al. 1996). The nasal SMAS seems to divide at the level of the nasal valve into a deep and a superficial layer (Saban et al. 2008). In the supratip area, the nasal SMAS becomes thicker (Tardy 1990). A part of the nasal SMAS that includes the nasalis muscles and the aponeurotic sheath between them has been termed as superficial nasalis aponeurotic system (SNAS) and used as a flap for nasal reconstruction (O'Hara et al. 1997; Riml et al. 2011).

4.2.3.1 Nasal Musculature

The external nose has been considered to be a static organ, and its muscles are underestimated in surgery. On the contrary, several electromyographic (Bruintjes et al. 1996; Aksoy et al. 2010) and MRI investigations (Clark et al. 1998) revealed that there is muscle activity in this region, making the nose a dynamic and movable structure that plays a role not only in respiration and phonation but also in facial expression. This is obvious in unilateral facial paralysis, where loss of muscle function on one side exhibits a remarkable static and dynamic asymmetry (Clark et al. 1998). Effort must be given when raising nasal flaps to stay in a plane beneath the muscles (sub-SMAS dissection) so as not to compromise the nasal muscles, thus obtaining a much better aesthetic and functional final result.

The muscles that cover the osteochondral skeleton of the nose belong anatomically to the nasal muscle group. This group includes procerus, nasalis, levator labii superioris alaeque nasi, dilator naris anterior, depressor septi nasi, and anomalous and compressor narium minor.

4.2.3.1.1 Procerus Muscle

The procerus muscle (Fig. 4.4) covers the upper third of the nose, as it originates at the nasal bones, the upper lateral cartilages, and the aponeurosis of the transverse part of nasalis, coursing superiorly to the forehead. This muscle is included to the nasal muscle group, but as it is related to the forehead, it is described in the Forehead chapter.

4.2.3.1.2 Nasalis Muscle

The nasalis muscle (Fig. 4.4) consists of two distinct parts, the transverse nasalis (compressor naris muscle) and the alar nasalis (dilator naris posterior muscle), which sometimes diverge from one another from a same origin.

Transverse Nasalis Muscle

The transverse nasalis muscle, flat and triangular in shape, originates from the maxilla at a point above and lateral to the incisor fossa and lateral to the origin of its alar part. In 35 % of individuals, the muscle arises as two muscle bellies from the maxilla and the upper half of the alar-facial crease (Hur et al. 2010). Its muscle fibers run upward and lateral to the dorsum of the nose. As the muscle fibers reach the bridge of the nose, they expand into a thin aponeurotic sheet that is continuous over the bridge of the nose with the aponeurosis of the opposite muscle and the aponeurosis of the procerus muscle.

This part belongs to the compressor muscles of the nasal musculature, as it compresses the nasal opening and narrows the nostrils.

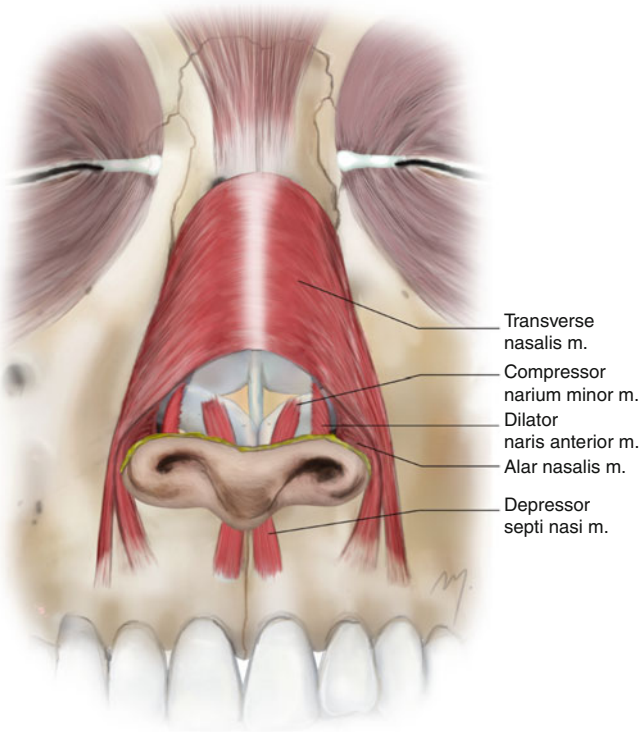

Fig. 4.4 Nasal muscles front view. The procerus, nasalis, depressor septi nasi, dilator naris anterior, and compressor narium minor muscles are seen

Alar Nasalis Muscle

The alar part of the nasalis muscle (dilator naris posterior) originates from the maxillary bone, above the lateral incisor and canine teeth, medial to the origin of the transverse nasalis, and lateral to the bony origin of the depressor septi nasi muscle. The muscle fibers run initially upward and then anteriorly in a direction parallel to the alar margin. The fibers of the muscle insert into the dermis of the skin of the posterior circumference of the alar, above the lateral crus of the alar cartilage. Some fibers also insert into the posterior part of the mobile septum. The alar

muscle draws the ala and the posterior part of the columella inferiorly and laterally widening the nares during deep inspiration.

Both parts of the nasalis muscle receive blood supply by branches from the infraorbital branch of the maxillary artery and from the facial artery. The buccal and zygomatic branches of the facial nerve innervate the transverse and alar nasalis muscles.

4.2.3.1.3 Depressor Septi Nasi Muscle

The depressor septi (Fig. 4.4) belongs to the depressor muscle group of the nasal musculature. In some individuals it may be absent or undeveloped (Standring 2008). The depressor septi nasi originates from the periosteum of the maxilla just above the central or lateral incisor teeth and the anterior nasal spine. Some fibers also arise as continuation from the upper fibers of the orbicularis oris muscle (Clark et al. 1998). Its fibers ascend, lying deep to the upper lip mucosa and passing to the columella. It inserts into the columella, the membranous septum, and the footplate segment of the medial crus of the alar cartilage.

The depressor septi nasi tenses to some extent the nasal septum and depresses the columella and the nasal tip, expanding the nares. The depressor septi nasi receives its vascular supply from the superior labial branch of the facial artery. The buccal branch and the zygomatic branch of the facial nerve innervate the muscle.

Song et al. (2002) demonstrated in cadaveric and histologic studies the presence of an antagonist to the depressor septi nasi newly found muscle and named it the levator septi nasi muscle. This paired muscle was found between the medial crura of the two alar cartilages inserting into the base of the columella and seemed to be more developed in Asian people.

4.2.3.1.4 Dilator Naris Anterior Muscle

The dilator naris anterior (apicis nasi) (Fig. 4.4) is a small fanlike muscle that originates from the upper lateral cartilage in front of the alar nasalis muscle and inserts into the caudal margin of the lateral crus and the lateral alar skin. The muscle expands the nostril during inspiration.

In an anatomic and histologic study, Hur et al. (2011) described for the first time the presence of a muscle located between the external and vestibular alar skin, with its fibers radiating around the alar lobule. They named this muscle dilator naris vestibularis muscle.

4.2.3.1.5 Compressor Narium Minor Muscle

This small inconstant muscle (Fig. 4.4) arises from the anterior part of the lower lateral cartilage and inserts into the skin near the margins of the nares. It is present in slightly more than half of the individuals and seems to play a role in decreasing slightly the nasal aperture (Letourneau and Daniel 1988; Clark et al. 1998).

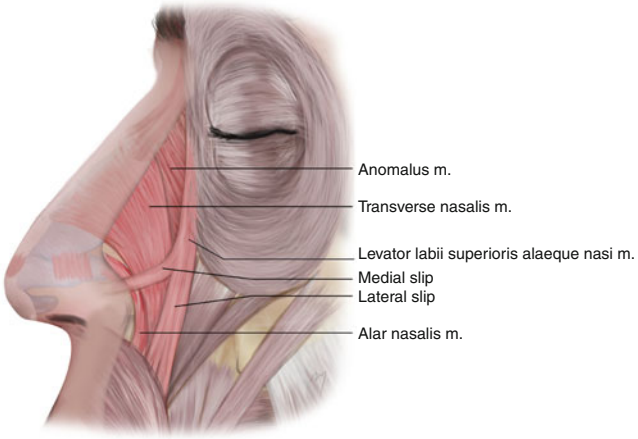

Fig. 4.5 Nasal muscles side view. The two slips of the levator labii superioris alaeque nasi muscle and the anomalous muscle are seen

4.2.3.1.6 Levator Labii Superioris Alaeque Nasi Muscle

The levator labii superioris alaeque nasi muscle (Fig. 4.5) is a triangular thin muscle and belongs to the elevator muscles of the nasal musculature. It originates from the upper part of the frontal process of the maxilla and the medial part of the orbicularis oculi. The fibers originating from the frontal process of the maxilla lie deep to the orbicularis oculi muscle. After its origin it divides into two slips: a medial slip (also called angular head) and a lateral slip. Both muscle slips run obliquely downward and laterally. The medial slip blends into the perichondrium of the lateral crus of the alar cartilage and the skin over it. The lateral slip reaches the lateral part of the upper lip and blends with fibers of the orbicularis oris and levator labii superioris muscles.

The medial slip pulls the lateral crus superiorly, thus dilating the nares while the lateral slip elevates the upper lip.

The levator labii superioris alaeque nasi muscle receives its blood supply by branches from the infraorbital branch of the maxillary artery and from the facial artery. Buccal and zygomatic branches of the facial nerve innervate the levator labii superioris alaeque nasi muscle.

Hur et al. (2010) reported the presence of a second deep muscle layer of the levator labii superioris alaeque nasi muscle that inserts between the levator anguli oris and the orbicularis oris muscles.

4.2.3.1.7 Anomalous Nasi Muscle

This anomalous nasi muscle (Fig. 4.5) is not constant in terms of its existence. If it is present, it lies at the lateral side of the nasal bones and the upper lateral cartilage, a region

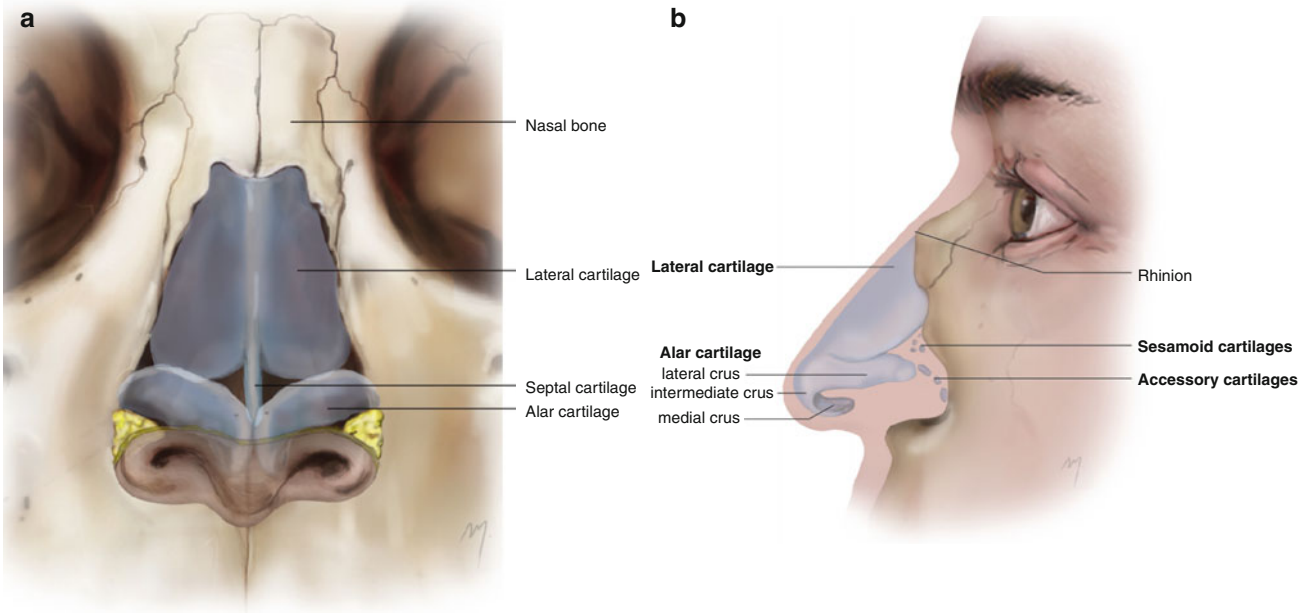

Fig. 4.6 Nasal pyramid. (**a**) Front view. (**b**) Lateral view

normally devoid of muscles. It originates from the frontal process of the maxilla and inserts into the nasal bones, the upper lateral cartilages, the procerus, and the transverse part of nasalis. Its position implicates that it is a compressor muscle and may help the nose to elongate (Clark et al. 1998).

4.2.4 Deep Areolar Layer

Beneath the nasal SMAS layer and above the periosteum-perichondrium lies the deep areolar (deep fatty) layer. It consists of loose areolar fatty tissue, and unlike the subcutaneous layer, fibrous septa are not present here. The superficial blood vessels and the nerves are found in this layer. Dissecting deep to this plane, just over the periosteum-perichondrium, the raising of a nose skin flap is easily accomplished due to the absence of any fibrous connective septa. On the other hand, the skin is raised in a relatively avascular plane as the dissection plane leaves the superficial vessels on the flap. Moreover, elevation of flaps in this plane does not disrupt the subcutaneous tissues and includes the nasal muscles in the flap leading to a better scar formation.

4.2.5 Osseocartilaginous Nasal Skeleton

The framework of the external nose consists of its bony and cartilaginous skeleton. It is invested by the nasal periosteum and perichondrium. The nasal periosteum covers the nasal bones and laterally fuses with the periosteum of the piriform process. The perichondrium covers the nasal cartilages and provides their nourishing vasculature.

4.2.5.1 Bony Skeleton of the External Nose

The paired nasal bones (Fig. 4.6) constitute the upper third of the nose (bony vault), forming the nasal bridge. Each nasal bone is small and rectangular in shape that is narrow in its superior border and wider inferiorly and shorter in its lateral border than in the medial one.

The external surface of the nasal bone is usually smooth and convex. In its lower half, vessels and nerves transverse through foramina. One of these foramina is slightly wider and transmits a small vein. Easily controlled bleeding is expected when dissecting subperiosteally in this area. Procerus and transverse nasalis muscles and their aponeuroses cover the external surface. The internal surface is rough and concave. It carries a longitudinal groove for the anterior ethmoidal nerve.

The nasal bones become thinner as they progress inferiorly. So the superior border is thick and articulates with the nasal part of the frontal bone. The inferior border is thinner and overlaps, for a variable distance, the lateral nasal cartilage. The medial border is thick superiorly and thin inferiorly and articulates with the medial border of the contralateral nasal bone. It articulates also with the nasal spine of the frontal nasal, the perpendicular plate of the ethmoid nasal and the nasal septal cartilage. The lateral border articulates with the frontal process of the maxilla.

Although the nasal bones vary in shape and size, they usually demonstrate, when both articulated, an inferior width of approximately 16 mm, a superior width of approximately 13 mm, and a height of approximately 25 mm (Lang 1989).

4.2.5.2 Cartilaginous Skeleton of the External Nose

The cartilaginous skeleton of the external nose (Fig. 4.6) consists of the paired lateral cartilages, the alar cartilages (greater alar cartilages), and several minor alar cartilages: the accessory and sesamoid cartilages. Due to their elasticity, but also due to the way that the cartilages are joined together in the different nasal parts, minimal movement in various degrees is allowed.

4.2.5.2.1 Lateral Nasal Cartilages

The paired lateral cartilages (sometimes named upper lateral cartilages) constitute the middle third of the nose (cartilaginous vault) and form its sidewalls.

The lateral nasal cartilage is triangular in shape, with its apex pointing inferiorly. The average length of the lateral cartilage has been measured to be 23 mm and its width 14 mm (Lang 1989; Potter et al. 2000).

Superiorly the lateral cartilages are underlapped and adherent, by fibrous connections, to the nasal bones, and inferolaterally, they lie underneath the piriform aperture. The nasal bone-cartilage junction in the midline corresponds to the rhinion. The nasal bone overlap to the lateral cartilage is greatest at the rhinion. It has been reported in a variable extent that ranges from 1 to 15 mm (Drumheller 1973; Galindo De Lara et al. 1977; Lang 1989; Potter et al. 2000). The degree of overlap tapers off as it passes laterally. Despite the overlapping, the perichondrium of the lateral cartilage is continuous with the periosteum of the nasal bone (Bruintjes et al. 1988). Regarding this, in the junction area, as a subosteal dissection proceeds to become subcartilage, both covering structures are raised as one.

The lateral nasal cartilages and the septal cartilage are related in various ways. In 12 %, they are completely separated by loose fibrous tissue; in 20 %, they are completely fused with hyaline cartilage along their entire length; and in the remainder fusion exists only in the upper one or the upper two-thirds (Potter et al. 2000).

4.2.5.2.2 Alar Nasal Cartilages

The alar cartilages (greater alar cartilages) are a pair of thin and flexible C-shaped cartilages that provide the structural support of the lower third of the nose. Its variable shape and size are reflected (along with the caudal septum, the minor cartilages, and the overlying soft tissues) in the variability of shape and size of the nasal lobule, columella, and alae.

The alar cartilages are subdivided into three parts: the medial part or medial crus, the intermediate part or intermediate crus, and the lateral part or lateral crus.

The medial crus is narrow and consists of two segments. It begins inferiorly at the columellar base (footplate segment) and extends into the columella (columellar segment) joining the intermediate crus in a point that represents the junction of the columella and the tip. The average length of the medial crus is 19 mm, while its width is 6 mm (Lang 1989). Both medial crura are loosely connected by fibrous tissue, one to each other and to the anteroinferior part of the septal cartilage, forming the cartilaginous support of the columella. Tight skin, with minimal presence of subcutaneous fat, covers the medial crura.

The intermediate crus is the small zone, between the medial and lateral crura, where the alar cartilage is angulated around the anterior part of the naris. This angle between the medial and the lateral crus ranges between 38° and 86° (Lang 1989). The intermediate crus is subdivided into domal and lobular segments. The medial crura are attached firmly to each other by the fibrous interdomal ligament (Janeke and Wright 1971).

The lateral crus is the largest part of the alar cartilage. It runs superolaterally up to the anterior half of the nostril rim, providing it support. The average length of the lateral crus is 23 mm, while its width is 13 mm (Lang 1989). Despite the differences of the African and the Caucasian nose, the alar cartilages have been reported, in contrast to the popular impression, to be the same size between the two ethnic groups (Ofodile and James 1977). The lateral border of the lateral crus is connected to the piriform aperture by fibrous tissue that contains the minor alar cartilages. In most cases, the upper border of the lateral crus overlaps the lower border of the lateral cartilage. The overlap distance is about 3 mm (Lang 1989).

4.2.5.2.3 Accessory and Sesamoid and Cartilages

Between the lateral border of the lateral crus and the piriform aperture, underneath the alar groove, a number of 3–4 small cartilages are found and named accessory cartilages (Fig. 4.6b). These cartilages are usually ellipsoid in shape, connected to each other by dense connective tissue, forming a fibrocartilaginous chain that connects the alar cartilage to the frontal process of the maxilla.

The sesamoid cartilages are much smaller than the accessory ones, varying in size and number, and are located in the area between the lateral border of the lateral cartilage and the piriform aperture. They are also attached to each other and to the neighboring structures by fibrous tissue. Although varied in number and size, ethnic variations of the sesamoid cartilages seem to exist among different ethnic groups (Ebrahimi et al. 2012a, b). Both accessory and sesamoid cartilages constitute the minor alar nasal cartilages.

External Lateral Triangle-Internal Nasal Valve

All these minor alar nasal cartilages are contained in a surgically important space named external lateral triangle. This triangle is limited by the lateral border of the lateral cartilage, the most lateral portion of the lateral crus, and the piriform aperture. Its inner surface is covered by nasal mucosa;

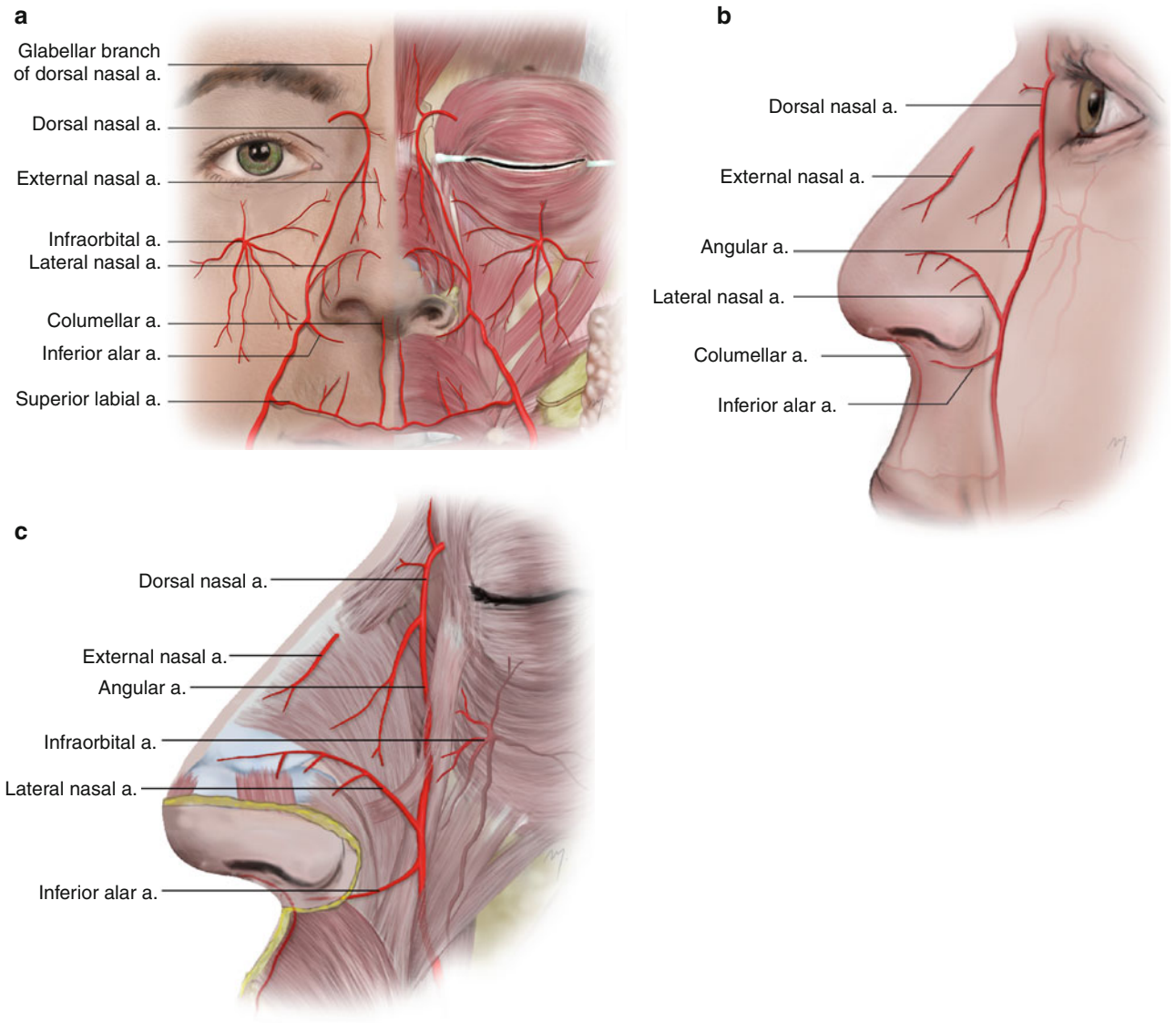

Fig. 4.7 Arterial supply to the nose. (**a**) Front view. (**b**, **c**) Lateral view

the outer surface is covered by the transverse part of the nasalis muscle; it contains the minor alar cartilages and is filled by fibrofatty tissue that contributes to the lateral aspect of the internal nasal valve (Jewett and Baker 2011). Scar formation in this area, after reconstructive surgery, may lead to nasal obstruction.

4.3 Arterial Anatomy

The external nose receives its blood supply from branches of both external and internal carotid arteries. The arteries that supply the nose from cephalad to caudal are the dorsal nasal artery, the external nasal artery, the lateral nasal artery, and the columellar artery (Fig. 4.7). These arteries anastomose each other and form a subdermal vascular plexus that becomes very reach in the tip area. Nasal branches from the infraorbital artery also contribute to the supply of the nasal sidewall.

4.3.1 Dorsal Nasal Artery

The dorsal nasal artery is one of the two terminal branches (the other one being the supratrochlear artery) of the ophthalmic artery. The mean diameter of the vessel is about 0.8 mm (Erdogmus and Govsa 2006). The dorsal nasal artery emerges from the orbit, between the trochlea and the medial palpebral ligament, penetrating the orbital septum just below the supratrochlear artery, running on to the root of the nose (Fig. 4.7). After emerging from the orbit, it gives off the glabellar branch (see Chap. 3) and the main continuation runs

inferomedially giving its terminal branches in the upper nose, along the lateral side and the dorsum, and anastomoses with the neighboring arteries.

The dorsal nasal artery supplies the upper part of the nose and the skin and periosteum of glabella. It anastomoses with the medial palpebral artery, the angular artery, the supratrochlear artery, and its contralateral.

Anastomoses with angular arteries usually occur with a thick branch and less commonly with a thin branch (Erdogmus and Govsa 2006). There has been confusion within the literature regarding the thick branch and as to whether the dorsal artery is a branch of the angular and not of the ophthalmic artery. The anastomosis with the artery of the opposite side occurs with a branch running along the dorsum of the nose.

The dorsal nasal artery can be identified usually 6–8 mm above the medial canthus.

4.3.2 External Nasal Artery

The external nasal artery is a terminal branch of the anterior ethmoidal artery. The anterior ethmoidal artery arises as a branch of the ophthalmic artery in the medial orbital wall (see Chap. 3). It passes through the anterior ethmoidal canal, in company with the anterior ethmoidal nerve, and supplies the anterior and middle ethmoidal and frontal air sinuses. Entering the cranium it gives off a meningeal branch and nasal branches to the superior aspect of the nasal cavity that supply the lateral wall and the septum. One of its terminal branches emerges between the nasal bone and the lateral cartilage, named as the external nasal artery (Fig. 4.7), and supplies the area of the overlying nasal skin and the skin of the upper part of the nasal tip.

4.3.3 Lateral Nasal Artery

The lateral nasal artery is derived from the angular artery, as it ascends along the side of the nose (Fig. 4.7). It is located 2–3 mm above the alar groove, within the subdermal plexus (Rohrich et al. 1995). Its mean diameter is approximately 1.5 mm. It passes to the side of the nose, runs medial to the tip, and continues down the columella where it anastomoses with the columellar artery forming thus an alar arcade along the cephalic margin of the lateral crura. During its course above the alar groove, it gives off branches that descend, passing over the lateral crus toward the alar rim (Toriumi et al. 1996). It supplies the skin over the nostril and the tip and is located superficial to the nasal SMAS within the subdermal fat.

A small artery, running parallel to the lateral nasal, has been described by Saban et al. (2012) and termed marginal alar artery. According to their description, the marginal alar artery usually branches from the facial artery before the lateral nasal at a more caudal point. Sometimes it arises from the lateral nasal artery itself. It runs along the caudal border of the lateral crus of the alar cartilage toward the nasal tip.

4.3.4 Inferior Alar Artery

The inferior alar artery (alar base artery, subnasal artery) originates from the facial artery (Fig. 4.7). It courses along the inferior margin of the nostril and gives off small branches that supply the inferior edge of the ala. Some other small branches descend for a short distance to the upper lip, contributing to its vascular supply (Nakajima et al. 2002). The inferior alar artery may arise from the superior labial-columellar artery usually in the cases of an undeveloped and early ending facial artery.

4.3.5 Columellar Artery

The columellar artery (Fig. 4.7) is a branch of the superior labial artery (see Chap. 6). It arises at the philtrum of the upper lip and ascends to the columella just superficial to the medial crura. It usually anastomoses with the lateral nasal artery and forms the alar arcade (Toriumi et al. 1996). The columellar artery can be present bilaterally or unilaterally and in 23 % absent (Rohrich et al. 1995). It supplies the columellar base and contributes to the vascularization of the nasal tip. Columellar arteries typically are divided by the transcolumellar incision in open rhinoplasty approach, without compromising the nasal tip blood supply so long as the nasal tip supply is mainly derived from the lateral nasal arteries with the columellar artery playing a variable contributing role (Rohrich et al. 1995, 2000).

4.4 Venous Drainage

The venous drainage of the nose starts from a subcutaneous system that extends to every region of the nose (dorsum, sidewall, tip) and is situated above the nasal SMAS. The small veins converge to the larger ones. Although the anatomy of these veins varies, essentially they generally follow the associated arteries and are named by them. Most of them drain laterally into the facial vein or the angular vein (Fig. 4.8).

The angular vein arises with the union of the supratrochlear and supraorbital veins near the inner canthus. The angular vein continues inferiorly by the side of the nose, now termed the facial vein, in a same manner as the associated facial and angular arteries. The angular-facial vein most of

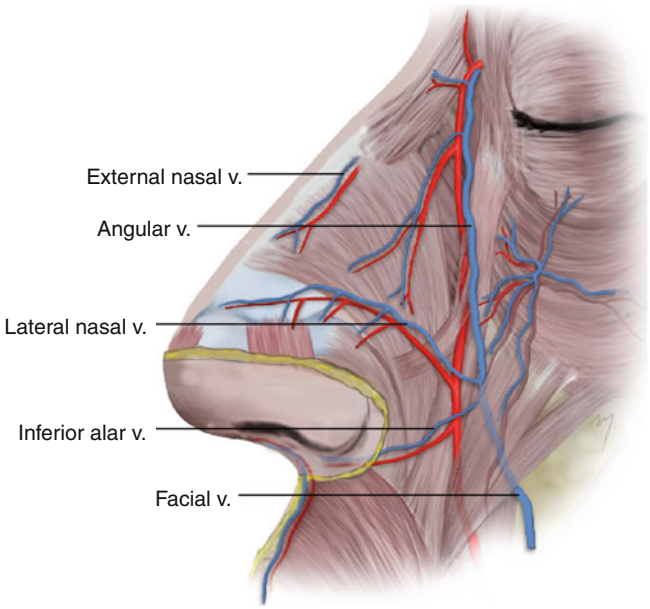

Fig. 4.8 Venous drainage of the nose

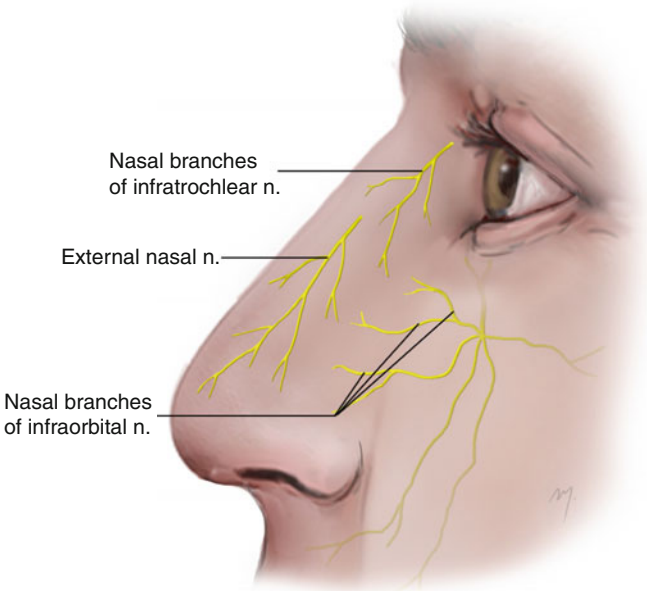

Fig. 4.9 Sensory nerves of the external nose

the time run increasingly posterior to the corresponding angular-facial artery.

4.5 Nerves

The sensory supply of the external nose is gained by branches of the infratrochlear, anterior ethmoidal, and infraorbital nerves (Fig. 4.9).

4.5.1 Nasal Branches of the Infratrochlear Nerve

The infratrochlear nerve branches from the nasociliary nerve (branch of the ophthalmic nerve which in turn is the first division of the trigeminal nerve) near the anterior ethmoidal foramen and courses along the medial orbital wall. It leaves the orbit below the trochlea and gives branches to the skin of the eyelids, the conjunctiva, lacrimal sac, and nose. Its nasal branches supply the skin of the root of the nose, the rhinion, and the upper part of the nasal sidewall.

4.5.2 External Nasal Nerve

The external nasal nerve is the terminal branch of the anterior ethmoidal nerve. The anterior ethmoidal nerve branches from the nasociliary nerve and pass through the anterior ethmoidal foramen. After its intracranial and intranasal course, it emerges to the external nose, between the nasal bone and the lateral cartilage, as external nasal nerve, in company with the external nasal vessels. It pierces the transverse part of the nasalis muscle, runs as far as the tip, and supplies the skin of the caudal half of the nose.

4.5.3 Nasal Branches of the Infraorbital Nerve

The infraorbital nerve exits the orbit and emerges onto the face through the infraorbital foramen. It gives off palpebral, superior labial, and nasal branches (see Chap. 5). The small nasal branches run inferomedially, join the external nasal nerve, and supply the skin of the lateral side of the nose and the ala. Few small branches pass to the skin of the vestibule (internal nasal rami).

4.6 Flaps Derived from the Nose

The nose as donor site can provide flaps that reconstruct defects only of the nose itself. As a general rule, primary closure cannot be achieved and a flap is needed, when the nasal defect is larger than 1 cm in the dorsum and the nasal sidewall and larger than 0.5 cm in the nasal tip. Flaps derived from the nose can close nasal skin defects up to 2.5 cm but this depends also from the individuals' nasal skin properties, mobility, and laxity. Reservoir of mobile nasal skin that can be reclaimed by local flaps is presented in the upper half of the nose, either in the dorsum or in the sidewall. Larger defects require tissue from donor sites outside of the nose.

A nasal cutaneous flap provides the skin of the same color, texture, and thickness and constitutes the ideal solution to repair a defect of the nose.

When planning a nasal reconstruction, two main facts should be taken into account: the subunit principle and the need of skeletal support of the nose. Even though these issues are not the subject and the purpose of this chapter, they should be briefly mentioned, because both of them are crucial and they may be reasons to determine the most appropriate flap in a nasal reconstruction.

4.6.1 Subunit Principle

Initially Millard (1981) adapted Gonzales-Ulloa's et al. (1954) concept of facial "regional aesthetic units" to nasal reconstruction. Burget (1985) and Burget and Menick (1985) identified the specific topographic subunits as the dorsum, tip, columella, and the paired alae, sidewalls, and soft triangles. Later on this principle adapted in Orientals as well (Yotsuvanagi et al. 2000).

According to the subunit principle, if a defect is greater than 50 % of the aesthetic nasal unit, the defect is enlarged to include the entire aesthetic unit, provided that after enlargement, it does not exceed the dimensions of the donor flap.

Although an aesthetic unit replaced as a whole generally looks better than a partially replaced one, there are objections in the need of sacrificing healthy tissue. Moreover, replacing a whole aesthetic unit may involve more extensive surgery to close the donor site than in the case of a smaller recipient site wound. Rohrich et al. (2004) in a retrospective analysis of more than 1,300 patients support that excellent results can be obtained without adhering to subunit principle.

4.6.2 Cartilage Grafting

The appropriate timing for the introduction of nasal support has been a controversial point in the course of nasal surgery. There is an argument whether one should wait until soft tissue reconstruction is complete and sound vascularity has been established before inserting skeletal support or if it is better to insert skeletal support at the time of the application of the soft tissue draping; if the soft tissue is left to heal in a contracted position, it is much more difficult to recapture its original dimensions and pliability.

Although most authors now disagree with the delayed approach to providing skeletal support of the nose, it should be taken under consideration that bulky flaps (mainly those derived from the forehead, see Chap. 3) provide adequate tissue bulk to round out nasal contours and to recreate by itself even a missing ala. Nevertheless, if contour is an issue after the flap reconstruction, cartilage can always be added later.

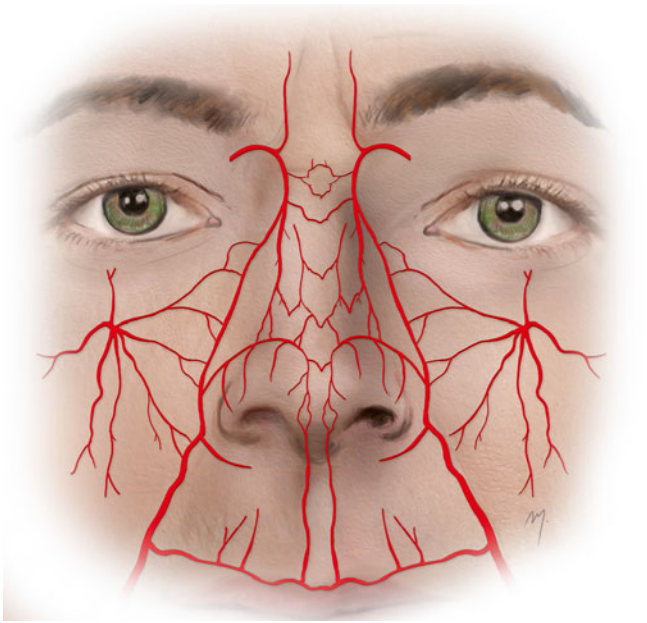

Fig. 4.10 Arterial anastomotic network of the nose

4.6.3 Flap Design Concerning Vascular Anatomy

The arteries that supply the nose anastomose each other and form a rich arterial network (Fig. 4.10). The dorsal nasal artery anastomoses with the ipsilateral angular artery and its opposite along the dorsum. The external nasal artery communicates with its opposite and with the lateral nasal artery which in turn anastomoses with the columellar artery at its final part. The nasal branches from the infraorbital artery contribute to the arterial network by anastomosing rami at the sidewall.

This superficial arterial network provided actually by the internal and the external carotid arteries is multidirectional in its flow. Saban et al. (2012) described the anastomotic network as a polygononal system formed by the intercarotid and the transfacial anastomoses over the nose. They state that this complex describes the normal blood flow to the nose with respect to the blood pressure in the internal and external carotid arteries, as well as the possibility of the change of the balance of that flow due to a change in arterial blood pressure. The result of this is the reason that nasal flaps pedicled in unconventional positions can be surprisingly robust.

4.6.4 Flap Elevation Concerning Anatomic Planes

The dissection plane of a flap raised over the nose is determined by the size and the thickness of the nasal defect to be covered, which in turn depends on the size and the depth of infiltration of the lesion. As a general rule, the ideal dissection

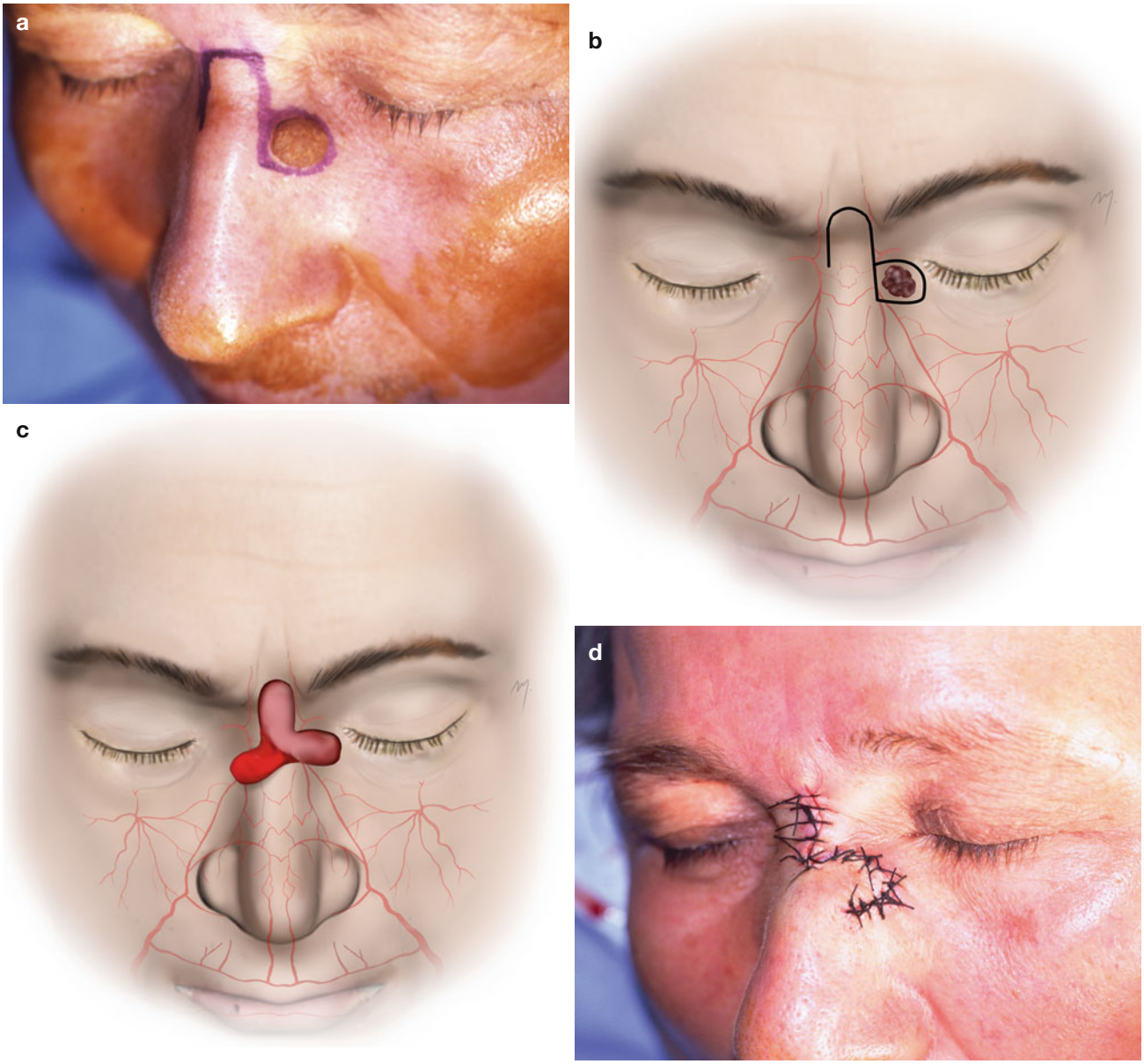

Fig. 4.11 (**a**–**d**) Finger flap

plane of a flap derived from the nose is through the deep areolar layer, so as the nasal SMAS layer is elevated with the flap and incorporated to it.

A flap is raised in the subcutaneous level only when the lesion does not invade deep structures (e.g., cystic type of basal cell carcinoma) and the area to be covered requires a small flap.

In a deep invasive tumor, where the muscles underneath have to be excised, the flap should always be raised beneath the nasal SMAS layer. Also, when a large nasal flap has to be raised, its safety enhances largely when the nasal SMAS is incorporated to the flap.

To enhance the viability of the flap in cases where blood flow reserves are reduced (smoking, diabetes, prior radiation), the dissection can be performed in the subperiosteal-subperichondrial level.

4.6.5 Finger Flap

This is a small midline transposition flap that is harvested from the dorsum of the upper third of the nose and closes small sidewall defects (Fig. 4.11a, b). The same principle can also be used in the lower two-thirds of the nose, referred to as "banner flap" (Masson and Mendelson 1977; Jackson 2007). The flap is a random pattern flap and based inferiorly. The long axis of the flap must be designed slightly longer than needed to reach and close the defect without any

distortion. Dissection is carried out in a subcutaneous plane and the flap is raised above the nasal SMAS; thus, the procerus, the transverse nasalis muscle, and their aponeurotic sheet are left in place.

The flap is transposed, trimmed, and sutured in place (Fig. 4.11c, d). An inferior standing dog-ear that might result must be trimmed carefully so as not to narrow the base. The skin laxity of the dorsum allows the direct closure of the vertical donor site defect with ease.

4.6.6 Rhomboid Flaps

The rhomboid flap is a flap of choice in small defects situated in every nasal subunit. Wherever orienting, the flap always survives due to the robust vascularity of the nose. The decision of where to place its base must not be made regarding anatomic structures of vascularity, but by the special characteristics of each subunit so as to avoid distortion of the nasal contour and shape.

4.6.6.1 Rhomboid Flap in Nasal Sidewall Reconstruction

The cystic-type basal cell carcinoma that is demonstrated (Fig. 4.12a) is at the same site and size as the one in the previous case. The defect can be alternatively reconstructed by a rhomboid flap (Fig. 4.12b, c). The lesion is excised in clear margins and the flap is raised in the subcutaneous plane (Fig. 4.12d, e). After minor trimming, the flap is sutured in place and the donor site, which after the needed undermining, is closed directly (Fig. 4.12f). A satisfactory postoperative result is achieved (Fig. 4.12g).

4.6.6.2 Rhomboid Flap in Nasal Tip Reconstruction

In small tip or supratip defects, the rhomboid flap can be used for reconstruction. The chosen rhomboid flap must be the one that transfers dorsal skin to the recipient site (Fig. 4.13a–c). Dorsal skin moves easier and distortion of the alar rim is avoided. The final result is almost excellent (Fig. 4.13d).

4.6.6.3 Rhomboid Flap in Nasal Lobule Reconstruction

A lesion located at the lobule is planned to be excised and reconstructed by a rhomboid flap (Fig. 4.14a–g). The chosen rhomboid flap is medially based. The lesion was excised in clear margins and the flap was raised in the subnasal SMAS plane. The flap was transferred to the defect, and after closure of the donor site, it was sutured in place.

Alternatively, with the same rhomboid design at the same area, the chosen rhomboid flap can be laterally based as it is demonstrated in Fig. 4.15a–e. The decision of which alternative flap will be used depends upon which site provides the more elastic skin and which donor site leads to a reconstruction with none or minimal distortion.

When the lesion is situated at the lateral part of the alar lobule, just close to the alar-facial sulcus, only one alternative in the design of the rhomboid flap exists (Fig. 4.16a, b): the rhomboid flap that is derived from the nasal sidewall and not from the nearby cheek. This constitutes the only alternative rhomboid flap that transfers skin without affecting the aesthetically important alar-facial unit (Fig. 4.14c, d).

4.6.7 Bilobed Flaps

The bilobed flap was first described for nasal reconstruction by Esser in (1918). This double transposition flap is a very useful tool for covering defects of the lower third of the nose, up to 1.5 cm, especially located in its lateral aspect. It is a brilliant paradigm of taking advantage of the lax tissue from the upper nose to close a remote side defect, where the skin elasticity is reduced, by using an intermediate and also distributing the wound closure tension. Zitelli (1989) improved its standard design, modified the angle of rotation, and resolved the problem of the standing cone at the point of rotation.

The bilobed flap can be based either medially or laterally. Lateral defects of the inferior third of the nose must be pedicled medially and defects toward the tip, lateral.

4.6.7.1 Medially Based Bilobed Flap in Lobule Reconstruction

The patient seen in Fig. 4.17 had a basal cell carcinoma located in the alar lobule.

The site of surgical excision is marked and a medially based bilobed flap is outlined (Fig. 4.17a, b). The first limb of the flap is designed lying in an axis of 45° to the axis of the primary defect and at the same or slightly smaller size. This limb will rotate to the primary defect creating a secondary one. The secondary defect will be closed with the second limb from the nearby dorsum. The second limb is situated to an axis of 45° to the axis of the first limb and about half of its size. Thus, the total angle of transposition of the bilobed flap is about 90°. A Burow's triangle is outlined to be excised, at the point of rotation to the base of the flap. The excision of this triangle prevents the formation of the standing cone. A second smaller Burow's triangle is also excised at the distal part of the second limb, preventing a same dog-ear at the root of the nose.

The lesion and the first Burow's triangle were excised, and clear margins were revealed by frozen section biopsies (Fig. 4.17c). Elevation of the flap starts from the first lobe for a distance and proceeds to the second lobe, usually in the sub-SMAS plane (Fig. 4.17d). Dissection is carried out

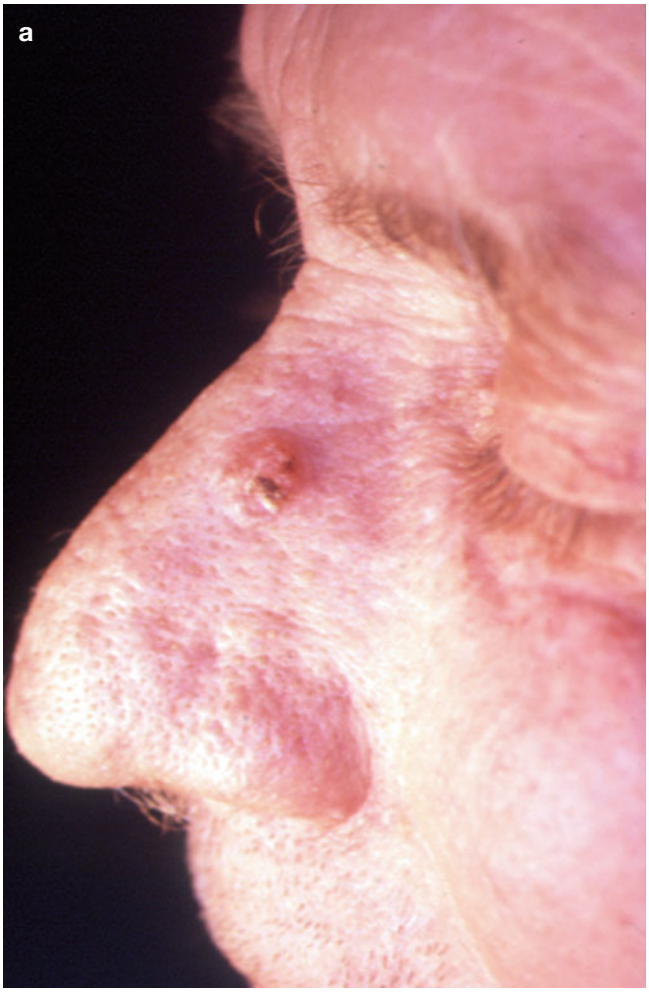

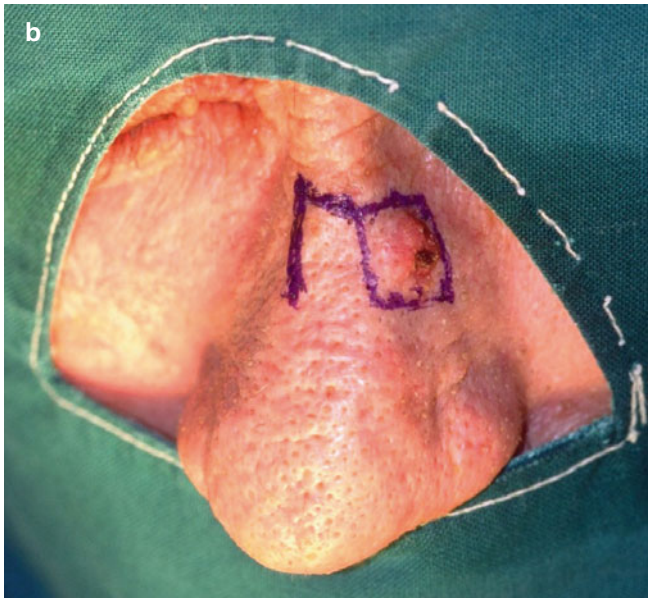

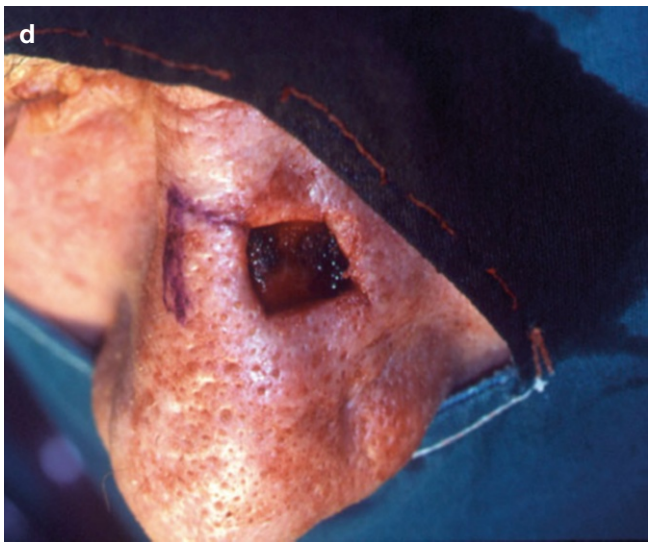

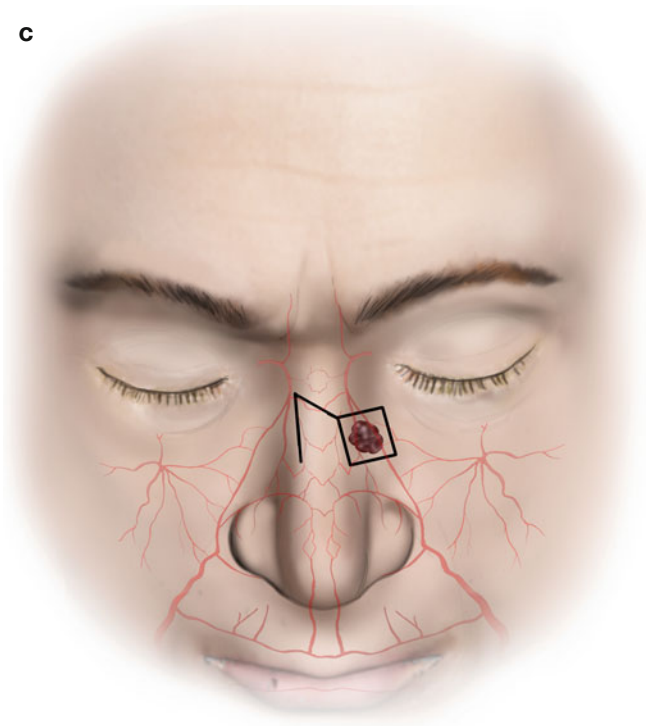

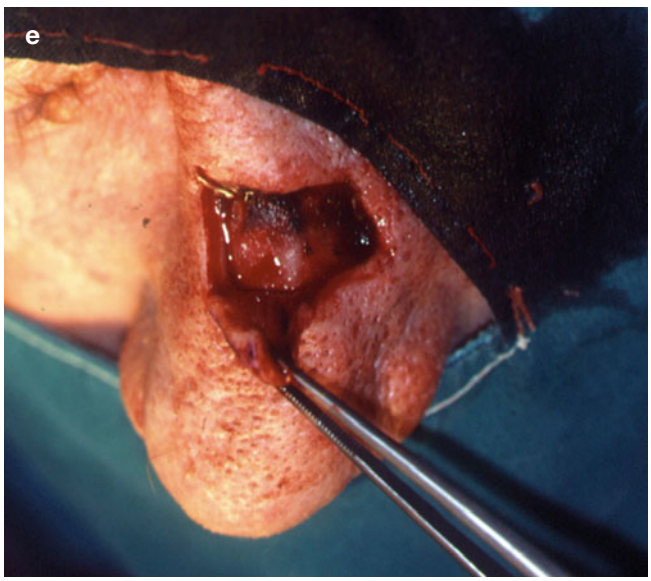

Fig. 4.12 (**a**–**g**) Rhomboid flap in nasal sidewall reconstruction

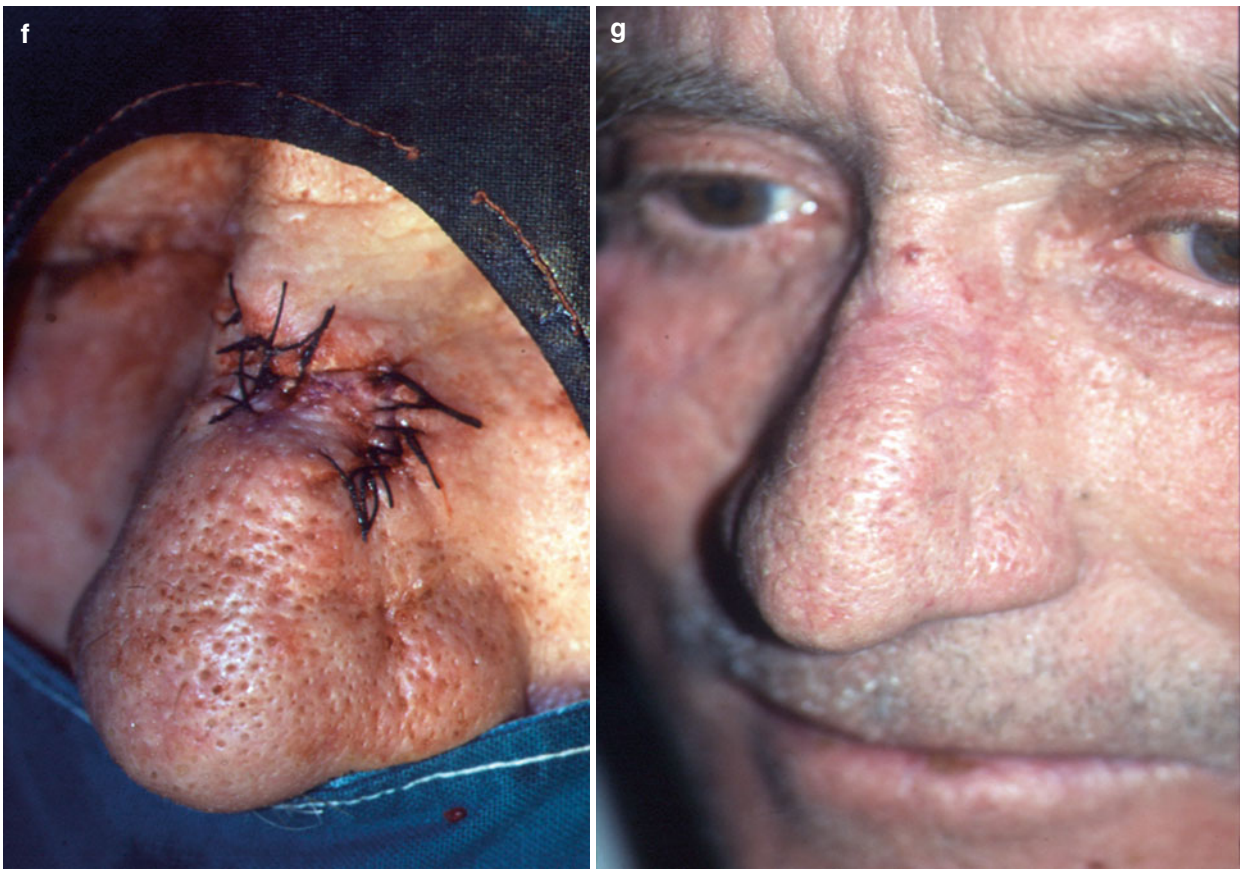

Fig. 4.12 (continued)

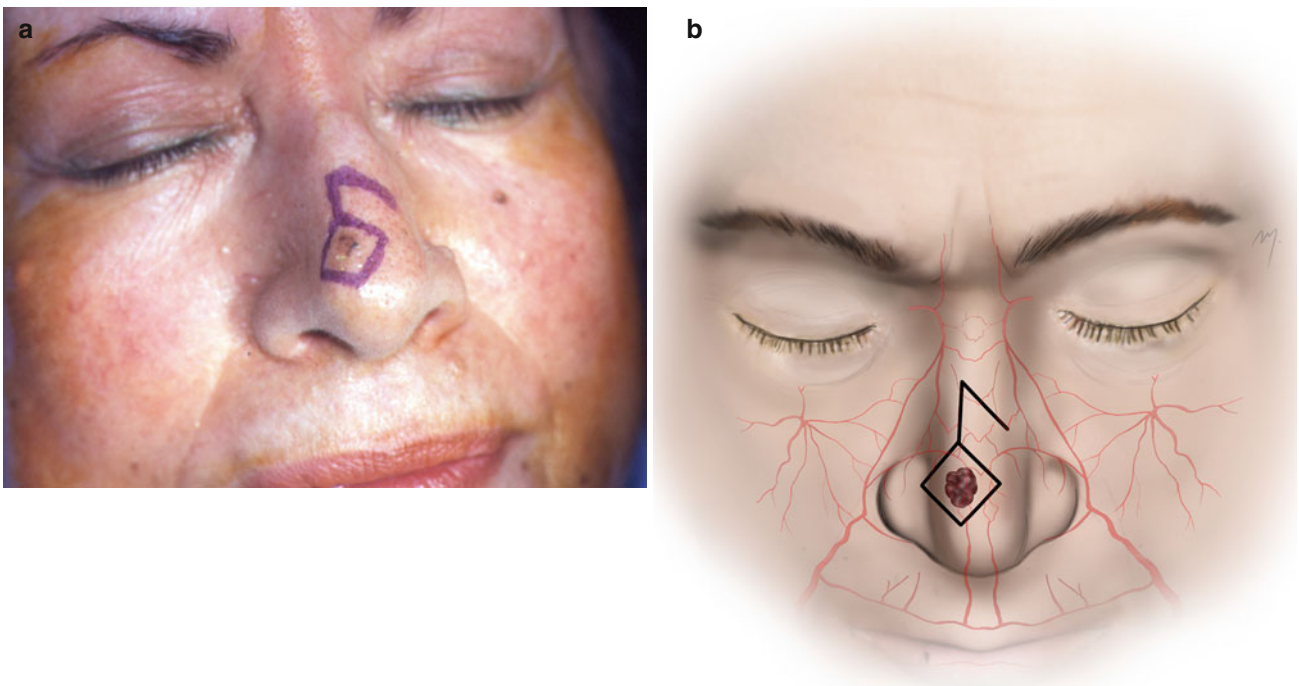

Fig. 4.13 (**a**–**d**) Rhomboid flap in nasal tip reconstruction

Fig. 4.13 (continued)

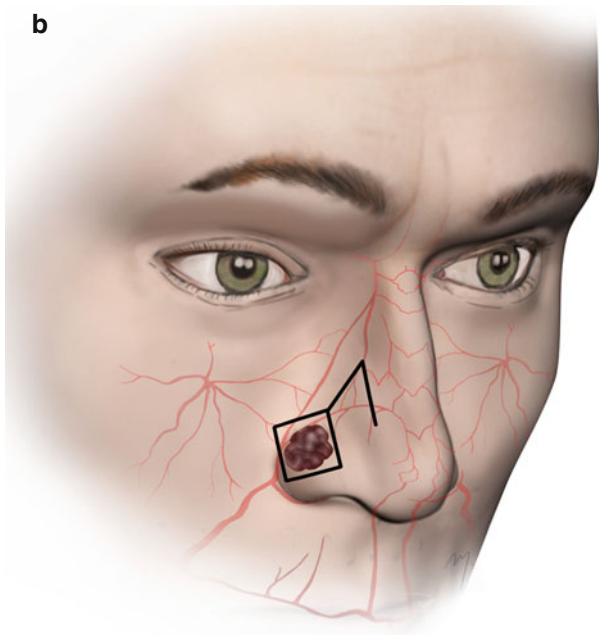

Fig. 4.14 (**a**–**g**) Rhomboid flap in lobule reconstruction. The chosen flap is medially based

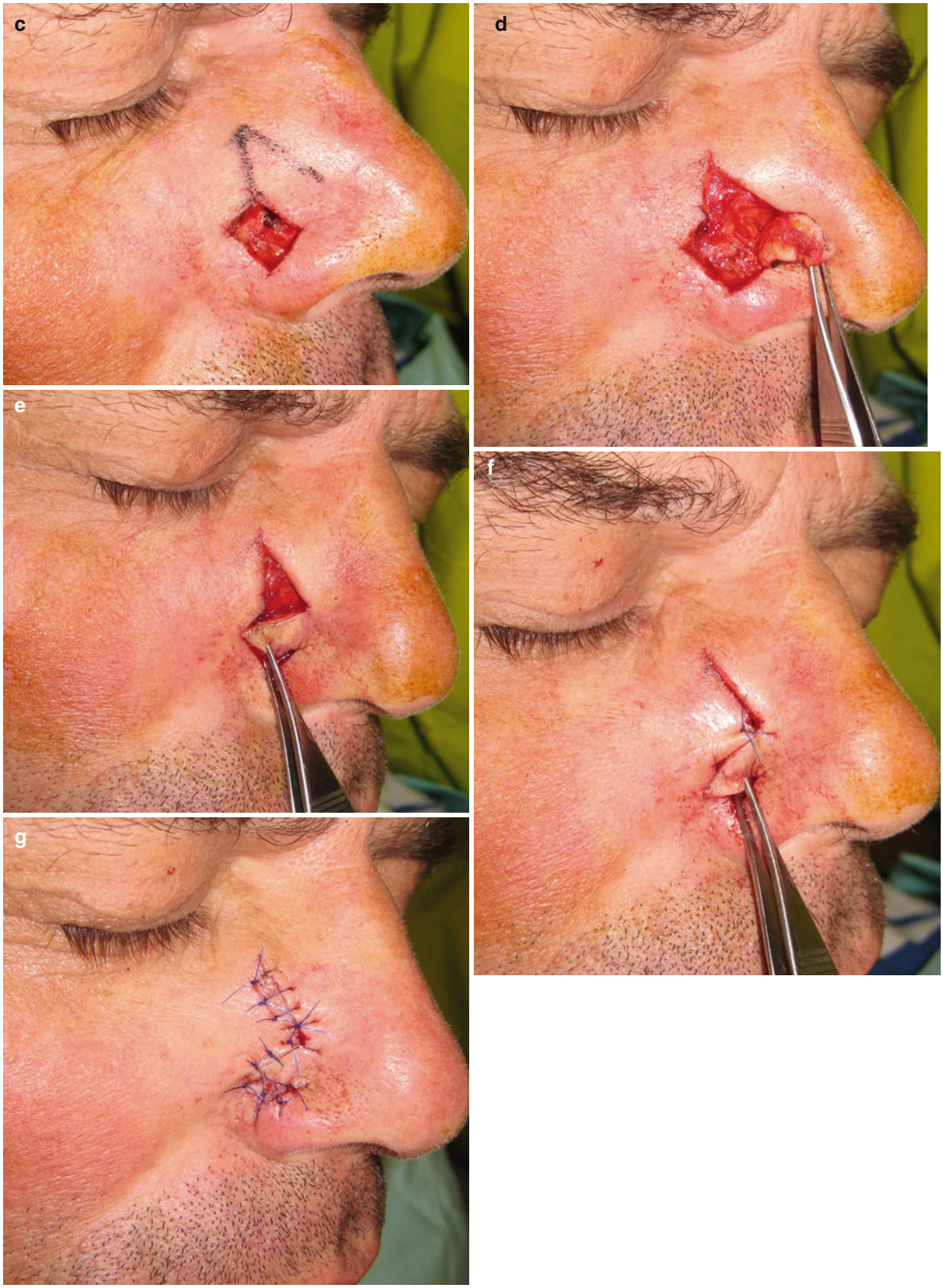

Fig. 4.14 (continued)

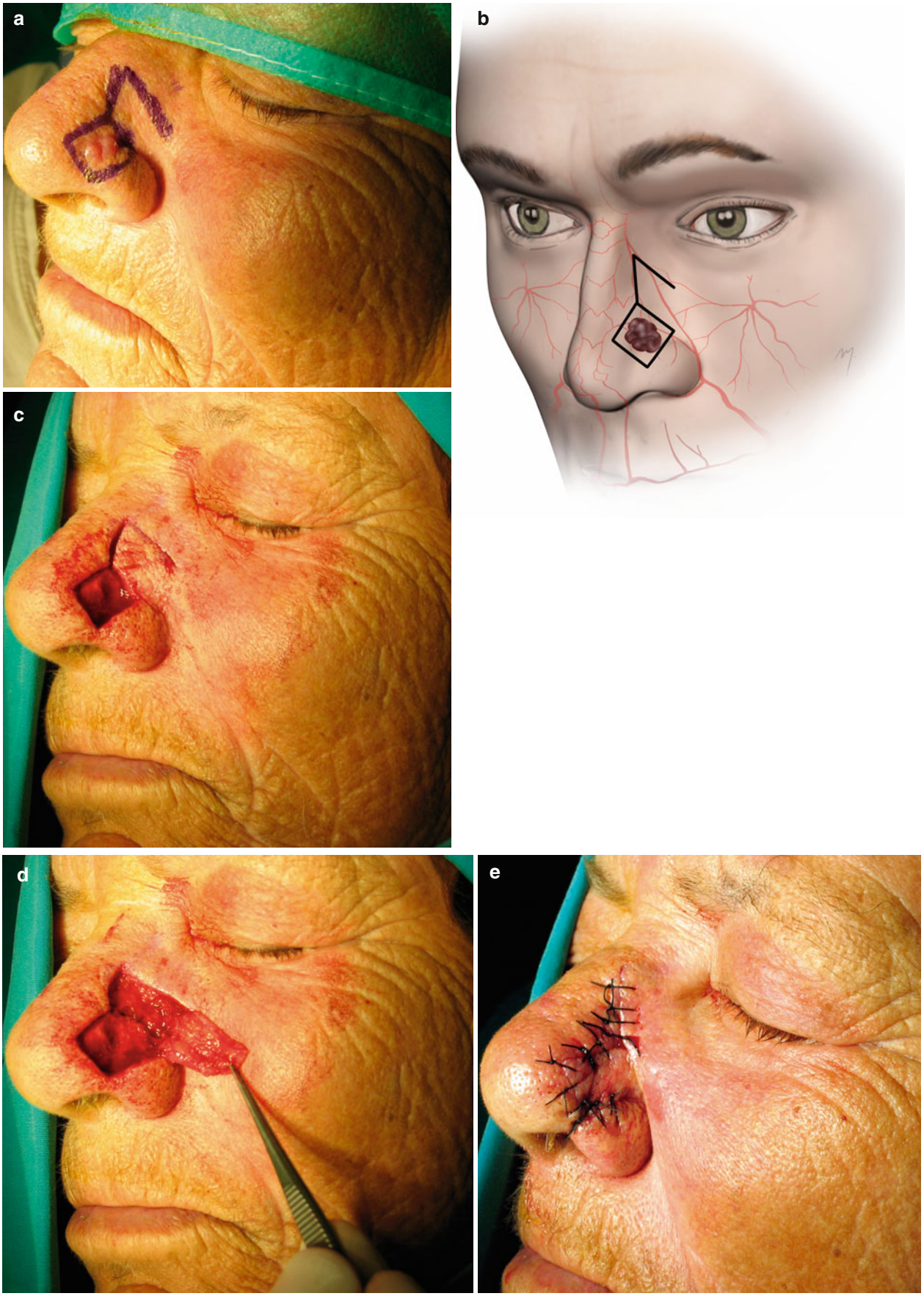

Fig. 4.15 (**a**–**e**) Rhomboid flap in lobule reconstruction. The chosen flap is laterally based

Fig. 4.16 (**a**–**d**) Rhomboid flap in the reconstruction of the lateral portion of the lobule

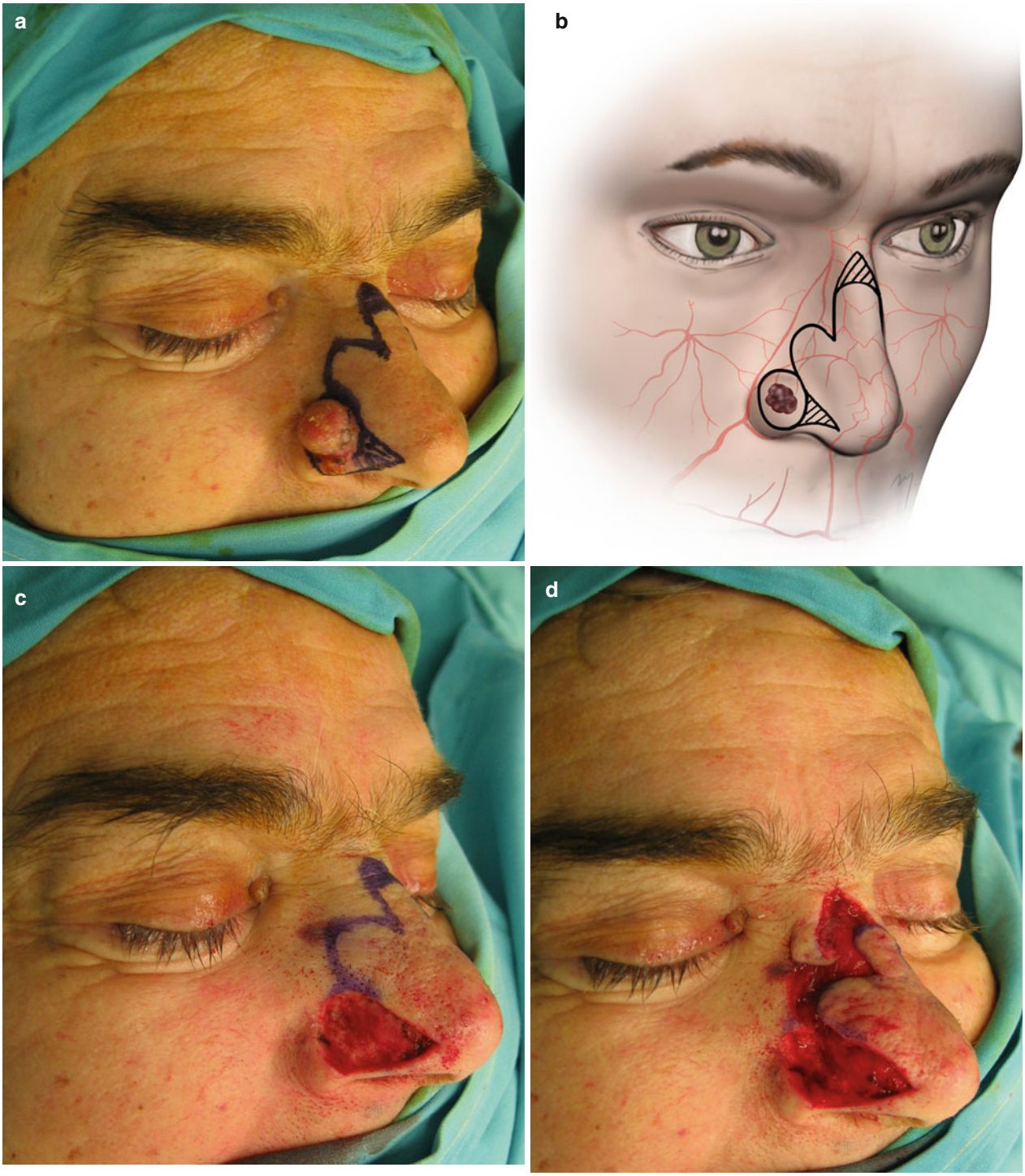

Fig. 4.17 (**a**–**g**) Medially based bilobed flap in lobule reconstruction

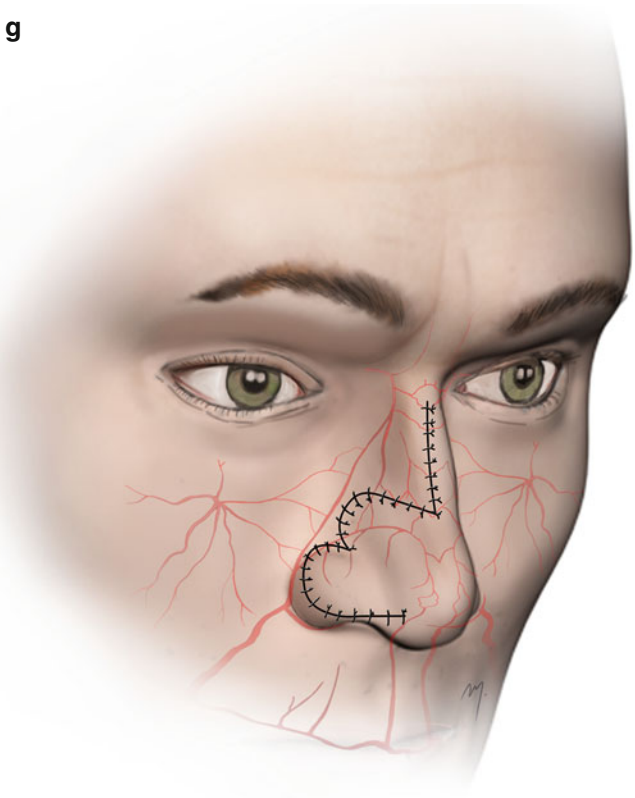

Fig. 4.17 (continued)

beyond the base of the flap to the opposite side of the nose in an extensive area (Fig. 4.17e). The wide undermining is very important so as to allow easy and without tension transposition of each lobe to its new position. The first limb of the flap is placed to the primary defect, the second limb covers its initial place, and the donor site of it is closed with ease (Fig. 4.17f, g).

4.6.7.2 Medially Based Bilobed Flap in Reconstruction of the Lateral Tip Area

The lateral tip area is the medial limit where the bilobed flap can be used with its base located medially in small defects. The patient presented had a small ulcerative basal cell carcinoma at the lateral tip area (Fig. 4.18a). A medially based bilobed flap was planned for the reconstruction of the defect,

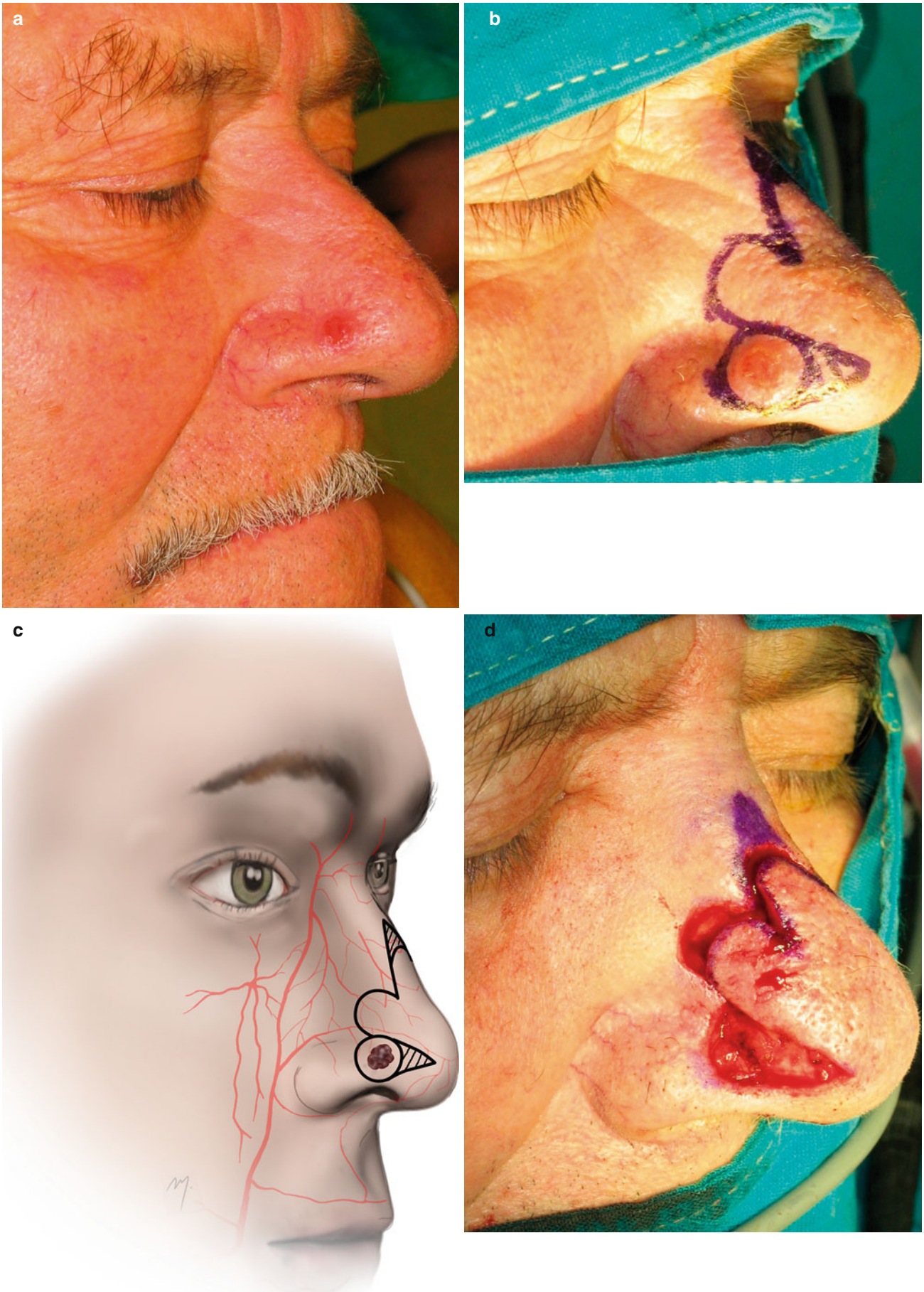

Fig. 4.18 (**a**–**g**) Medially based bilobed flap in lateral tip reconstruction

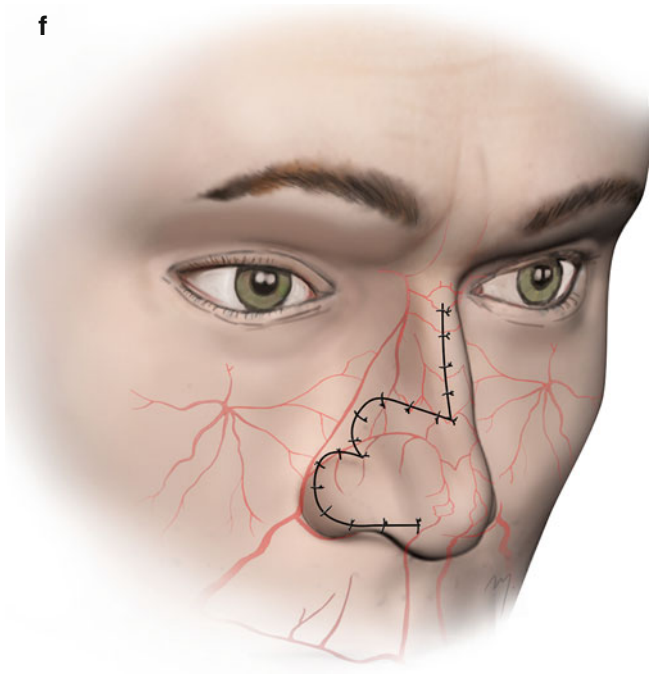

Fig. 4.18 (continued)

according to the rules mentioned above (Fig. 4.18b, c). Complete resection required excision of the lesion deep to the perichondrium of the cartilage (Fig. 4.18d). The flap was raised in the subchondral plane and undermined extensively, rotated, and sutured in place (Fig. 4.18e, f). The postoperative result at 6 months is satisfactory (Fig. 4.18g).

4.6.7.3 Laterally Based Bilobed Flap

The bilobed flap can be based laterally to restore defects located at the side of the tip. In the case presented, a basal carcinoma of the lateral aspect of the tip is planned to be excised and the defect reconstructed with a laterally based bilobed flap (Fig. 4.19a). The flap is strongly

vascularized, as it catches the lateral nasal artery to the first flap limb in its base (Fig. 4.19b). This allowed reduction of the rotation angle and narrowing its pedicle with safety, thus minimising the tension over the alar margin thereby preventing an eventual displacement. The flap was raised in the subcutaneous level and sutured in place (Fig. 4.19c–e). When the flap is planned properly, little trimming is required.

4.6.7.4 Bilobed Flap in Tip Reconstruction

The bilobed flap can be used in tip defects but in these cases must be designed in its maximum degree of rotation: almost 180°. This is demonstrated in the patient of this case. The bilobed flap is designed with the axis of the defect toward the first lobe at 90° and the axis of the first to the second lobe at the same degrees (Fig. 4.20a, b). Each of the lobes rotates 90° and the overall rotation of the flap is through 180°

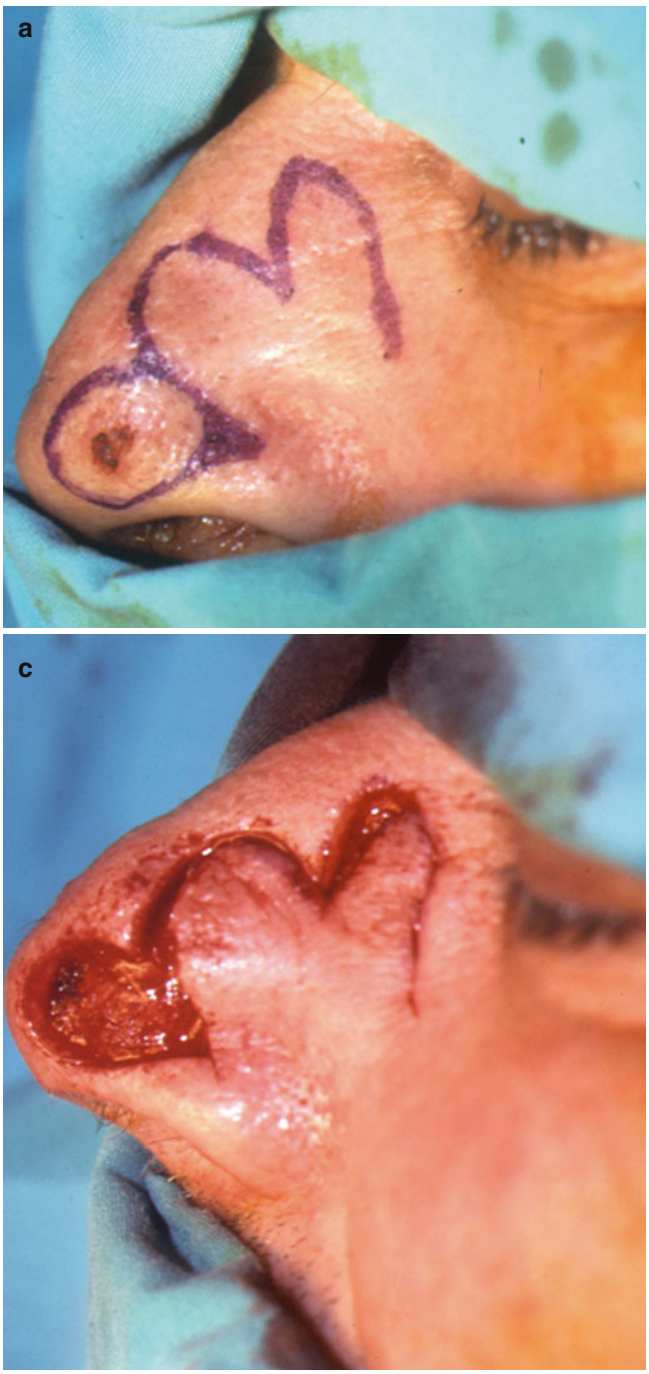

Fig. 4.19 (**a**–**e**) Laterally based bilobed flap

Fig. 4.19 (continued)

(Fig. 4.20c, d). The postoperative result despite the long arc of rotation does not cause distortion. Slight trapdoor deformity also resolves by time (Fig. 4.20e, f).

4.6.8 Dorsal Nasal Flap

The dorsal nasal flap constitutes a reliable technique for the reconstruction of medium-sized defects, up to 2.5 cm in diameter of the lower third of the nose. Originally described as a random pattern flap (Rieger 1967), it was modified into an axial pattern (Marchac 1970; Marchac and Toth 1985). The flap received minor modifications until today and also described with different names. It is actually a rotation-advancement flap that provides a sufficient amount of skin from the dorsum for the reconstruction of nasal defects.

The patient demonstrated had a basal cell carcinoma of the superolateral aspect of the tip of the nose (Fig. 4.21a).

The lesion was outlined in a circular manner and the flap was designed as follows (Fig. 4.21b). The incision line runs initially from the inferior border of the defect to the alar-facial sulcus of the same to the defect side. It then goes straight upward along the nasofacial sulcus to the glabella, constituting the vertical incision limb. In the glabella it forms an inverted V, placing the line if possible within vertical wrinkles, and ends to the contralateral to the defect inner canthal area. The contralateral now inner canthal area is the base of the flap. This elevates the whole nasal skin of the upper two-thirds. A Burow's triangle is outlined on the ipsilateral side of the pedicle, having its base at the medial border of the defect, slightly oblique and its apex pointing the inner canthus. The excision of this relatively large triangle allows the easy rotation and advancement of the flap to the defect.

A second Burow's triangle is excised from the opposite side, joining the lateral border of the defect with the vertical limb. The flap is an axial pattern flap, as at its base enters the dorsal nasal artery and its glabellar and nasal branches are distributed to the whole extent of the flap (Fig. 4.21c).

The lesion was excised up to the perichondrium of the alar cartilage (Fig. 4.21d). Even if a lesion does not infiltrate to that depth, the incision must be deepened to that level, when a dorsal nasal flap has been chosen for restoration. The Burow's triangles are excised at the same level.

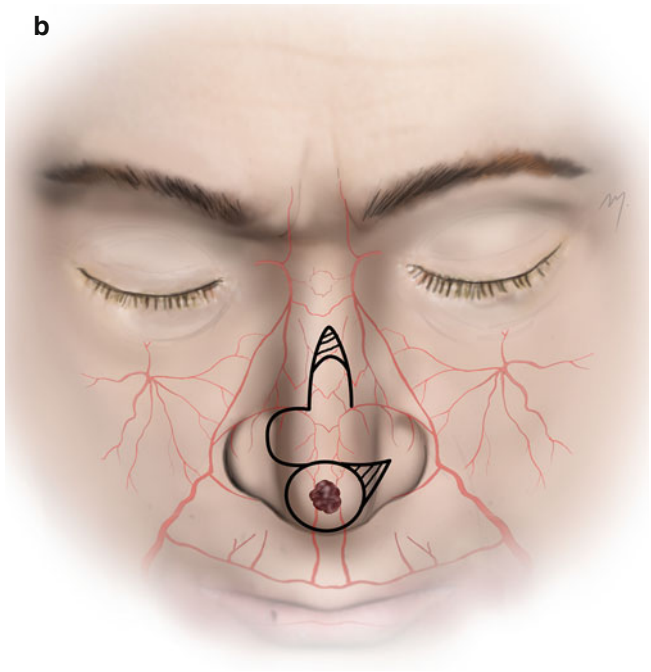

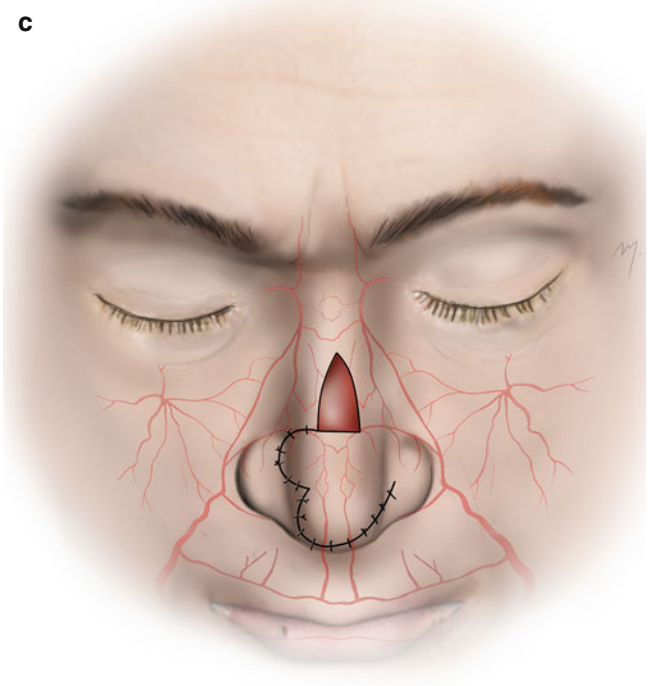

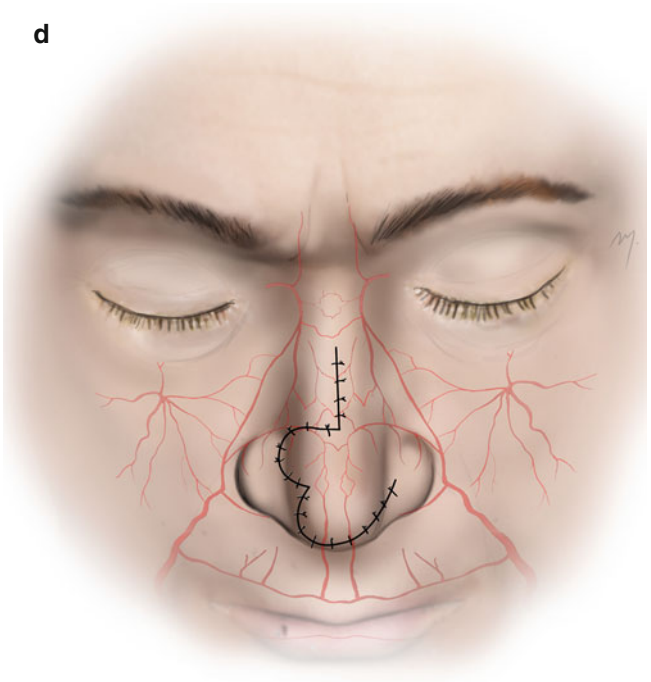

Fig. 4.20 (**a**–**f**) For the tip defects, the bilobed flap is designed in 180° rotation arc

Fig. 4.20 (continued)

Elevation of the flap starts from its distal part and is performed by dissecting below the nasal SMAS, while in the glabellar region, it is performed in the subcutaneous layer (Fig. 4.21e).

As nearly the whole flap is raised, attention is now given to its base. Dissection here must be performed bluntly with extreme care so as not to compromise the dorsal nasal artery (Fig. 4.21f). The flap is rotated and advanced and is controlled that reaches the defect without any tension that could retract the alar rim (Fig. 4.21g).

The flap was sutured in place and the glabellar defect closed in a V-Y manner (Fig. 4.21h).

4.6.8.1 Heminasal Flap

The heminasal flap is a modification of the dorsal nasal flap that uses a part and not the whole of the dorsal nasal skin, by extending the vertical limb from the lateral border of the defect straight upward over the side of the dorsum, and not along the nasofacial sulcus. Due to the fact that it diminishes the extent of the dorsal nasal skin that is raised, it is named heminasal flap.

The patient presented in Fig. 4.22a had a basal cell carcinoma of the tip of the nose. The lesion was outlined in a circular manner and the flap designed with its vertical limb incision line, running from the lateral border of the defect straight upward over the side of the dorsum to the glabella. As usual in the glabella, it forms the inverted V and ends to the contralateral to the defect inner canthal area. Only one Burow's triangle is needed to be excised in the ipsilateral side of the pedicle (Fig. 4.22b, c). The lesion was excised up to the perichondrium of the alar cartilage (Fig. 4.22d) and the Burow's triangle at the same level (Fig. 4.22e). Flap incision and elevation was performed below the nasal SMAS (Fig. 4.22f, g). Blunt dissection at the base ensures protection of the dorsal nasal artery. The distal part of the flap reaches the defect without tension (Fig. 4.22h). The flap was sutured in place and the glabellar defect closed in a V-Y manner (Fig. 4.22i). The result is always very good except a linear scar in the nasal sidewall (Fig. 4.22j).

4.6.8.2 Dorsal Nasal Flap with a Very Narrow Pedicle

There are cases where the dorsal nasal flap shifts over the defect with difficulty and not without tension, distorting the alar rim. To increase significantly the degree of flap rotation and gain a tension-free position, the base can be considerably narrowed. Due to the robust supply through an intact dorsal nasal artery, there is no risk in flap survival.

In the case demonstrated, a patient had a basal cell carcinoma of the tip of the nose (Fig. 4.23a). Excision of the lesion and reconstruction by a dorsal nasal flap were planned. The dorsal nasal flap was designed as a heminasal flap (Fig. 4.23b).

Fig. 4.21 (**a**) A basal cell carcinoma located at the tip of the nose. (**b**) Outline of the dorsal nasal flap. (**c**) The flap is an axial pattern flap based at the dorsal nasal artery. (**d**) Lesion excised. (**e**) Elevation of the flap below the nasal SMAS. (**f**) Dissection at the base is performed bluntly with extreme care. (**g**) Flap into position. (**h**) Flap sutured in place (From: Thomaidis et al. (2006), with permission)

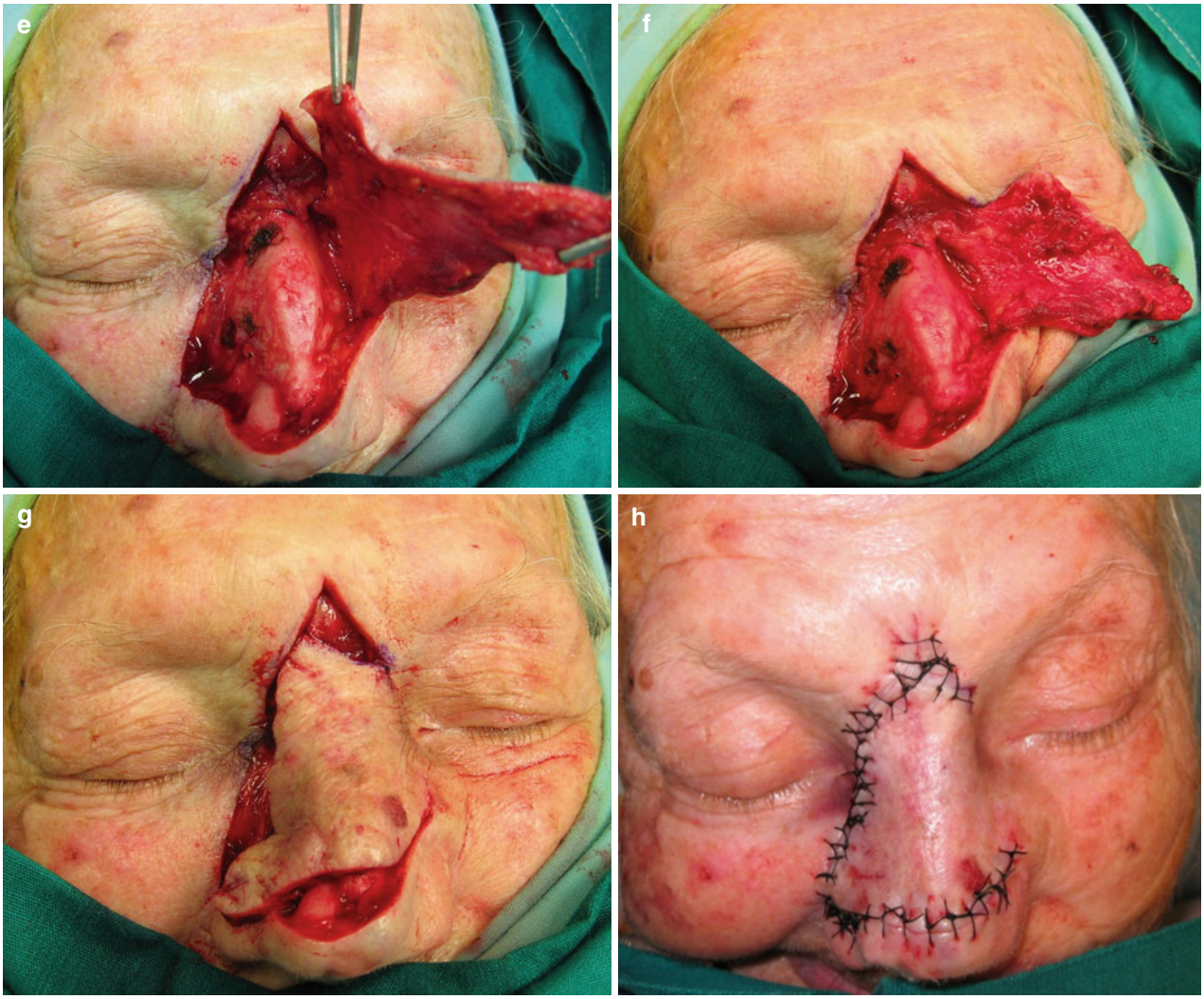

Fig. 4.21 (continued)

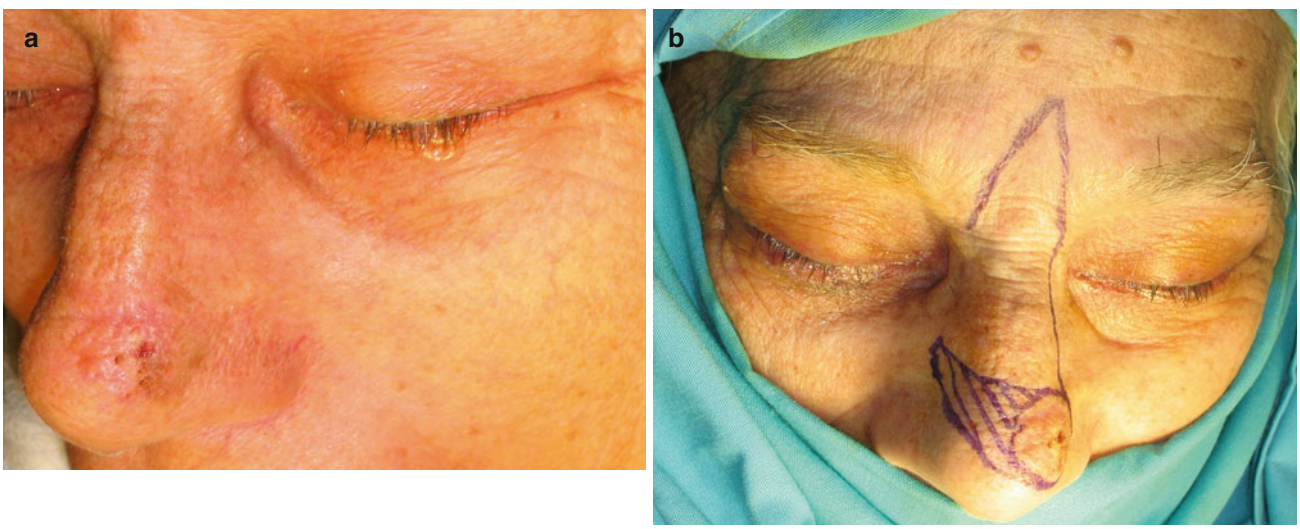

Fig. 4.22 (**a**–**j**) Heminasal flap

Fig. 4.22 (continued)

Fig. 4.22 (continued)

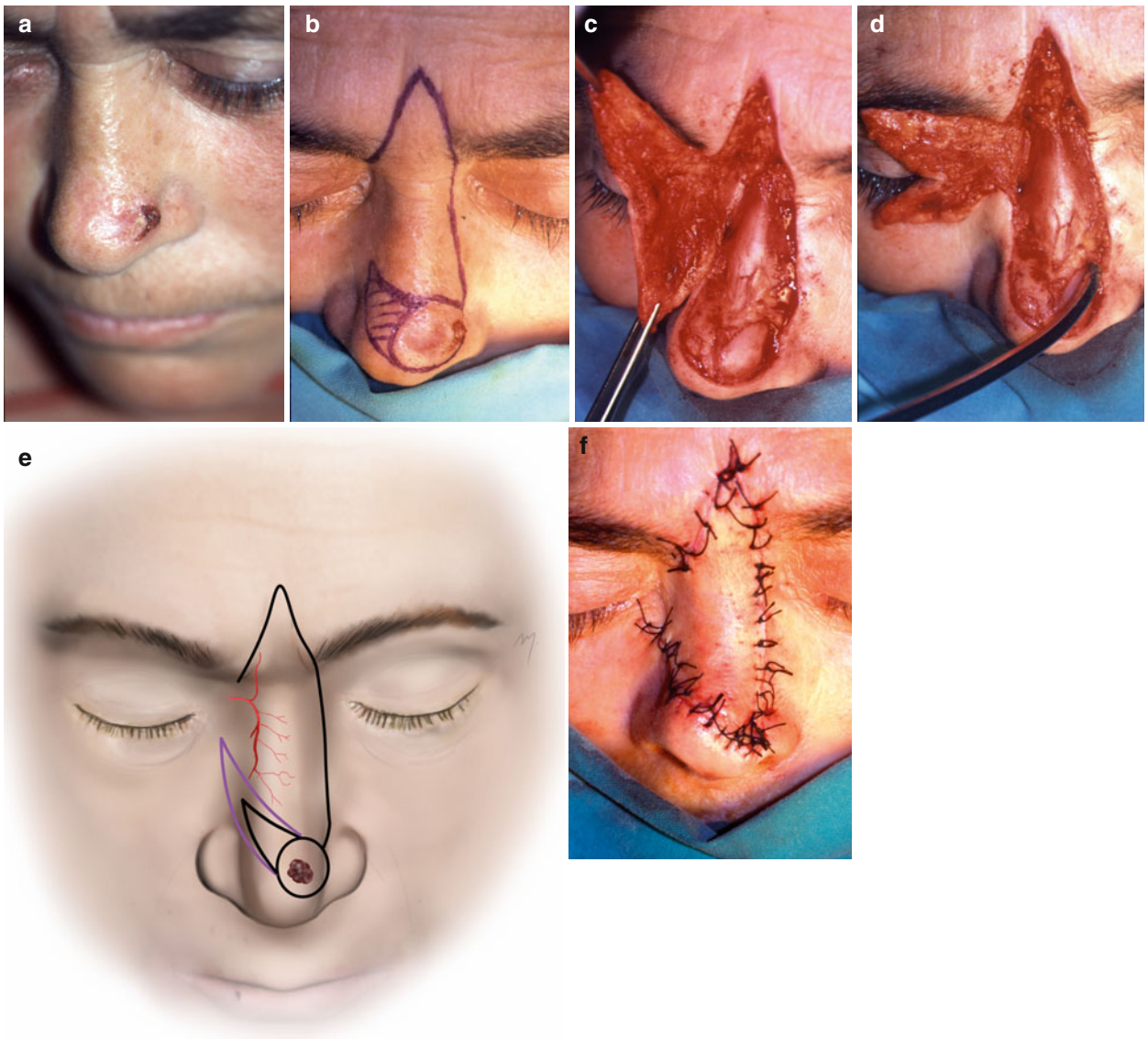

Fig. 4.23 Dorsal nasal flap with a very narrow pedicle. (**a**) A lesion located at the tip of the nose. (**b**) Dorsal nasal flap outlined. (**c**) Flap is raised. (**d**) Flap base is further narrowed. (**e**) Outline of initial design of the dorsal nasal flap. The purple outline indicates the needed final extension, which considerably narrowed the pedicle. (**f**) Flap sutured in place without any tension to the ala. (**g–i**) Postoperative result at 6 months

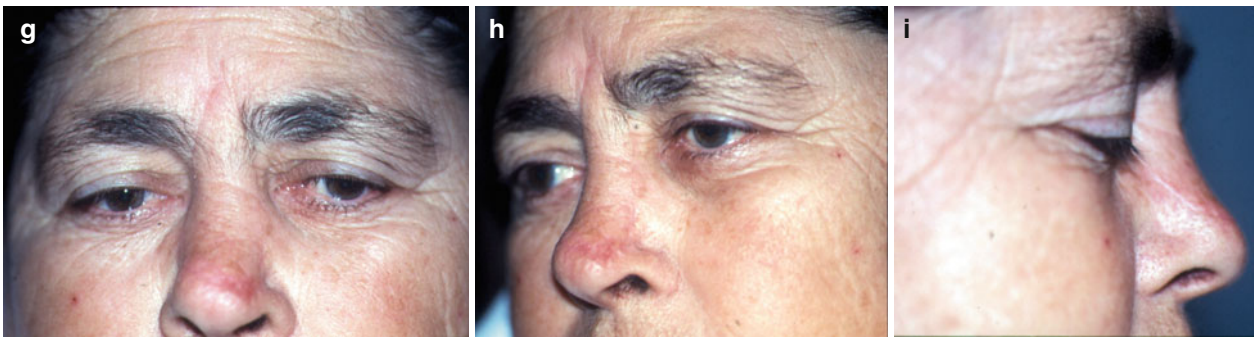

Fig. 4.23 (continued)

The flap was raised in the usual manner but placing it into the recipient side was done under tension (Fig. 4.23c). After identifying the dorsal nasal artery, the base was narrowed by extending the initial incisions (Fig. 4.23d, e). Flap rotation and advancement was increased and the flap was sutured in place without any tension (Fig. 4.23f). The flap healed without any sign of necrosis ensuring a favorable result (Fig. 4.23g–i).

4.6.9 Rintala Flap

Initially designed by Rintala and Asko-Seljavara (1969), it is a random pattern, advancement flap, located at the midline of the nose with its base on the glabella or the lower forehead, and was first referred to as "Rintala flap" by Jackson (1985). Based on the initial principles of the "Rintala flap", slight modifications of it have also been proposed (Chiu et al. 1994; Blandini et al. 1996; Ebrahimi et al. 2012a, b). The flap is a very useful tool for the reconstruction of tip or supratip defects, situated to the midline and up to 2 cm. Due to the fact that it's a random pattern flap, when designed in an approximate 3:1 ratio of length to width, it never risks distal necrosis. But this is not always possible when the defect is situated at the tip and a longer flap is needed.

In the patient presented, a Rintala flap was used to reconstruct a defect after the excision of a supratip basal cell carcinoma (Fig. 4.24a). The flap is of random pattern based at the vascular network of the glabella (Fig. 4.24b). The flap is outlined as an advancement flap with its two parallel vertical incision lines running from each of the lateral borders of the defect, along the sides of the nasal dorsum, directly upward to the glabella. Two bilateral Burow's triangles are outlined from each side of the flap base. The length of the medial side of each Burow's triangle is equal to the "height" of the defect, representing the distance of flap advancement. The lesion was excised in clear margins that were revealed by frozen section biopsies (Fig. 4.24c).

The dissection was carried out through the nasal sub-SMAS plane, starting from the distal side of the flap proceeding to its base. The Burow's triangles are excised and the flap is completely raised (Fig. 4.24d, e). The flap had been set well in place and was sutured (Fig. 4.22f). The postoperative result is satisfactory (Fig. 4.24g–i). This flap always shallows the frontonasal angle leading to a "classic ancient Greek profile" appearance (McGregor and McGregor 1986).

4.6.10 Lining Flaps

4.6.10.1 Turn-Over Flap

The nose can also provide skin for the lining of through and through nasal defects.

In the patient shown, the excision of a basal cell carcinoma required excision of cartilage and nasal mucosa leading to a through and through nasal defect (Fig. 4.25a, b). The adjacent dorsal nasal skin was used by means of a hinged turn-over flap to reline the nasal cavity (Fig. 4.25c, d). The flap was based on subcutaneous tissue and muscle, which was carefully preserved in the process of creating the hinge action of the flap. By this, the skin from the external surface of the nose moved into the mucosal defect and was reoriented to line the nasal cavity (Fig. 4.25e). (The complete nasal reconstruction is demonstrated at Sect. 3.5.10.)

4.6.10.2 Folded Turn-Over Flap

An invasive recurrent basal cell carcinoma leads to a full-thickness resection of the ala (Fig. 4.26a, b). The flap was oriented on an oblique axis to avoid the shifting of the nearby nevus into the nasal cavity (Fig. 4.26c). The turn-over flap provided the nasal lining, and it was folded in its distal end so as to reconstruct the contour of the alar rim (Fig. 4.26d). (The complete nasal reconstruction is demonstrated at Sect. 3.5.10.)

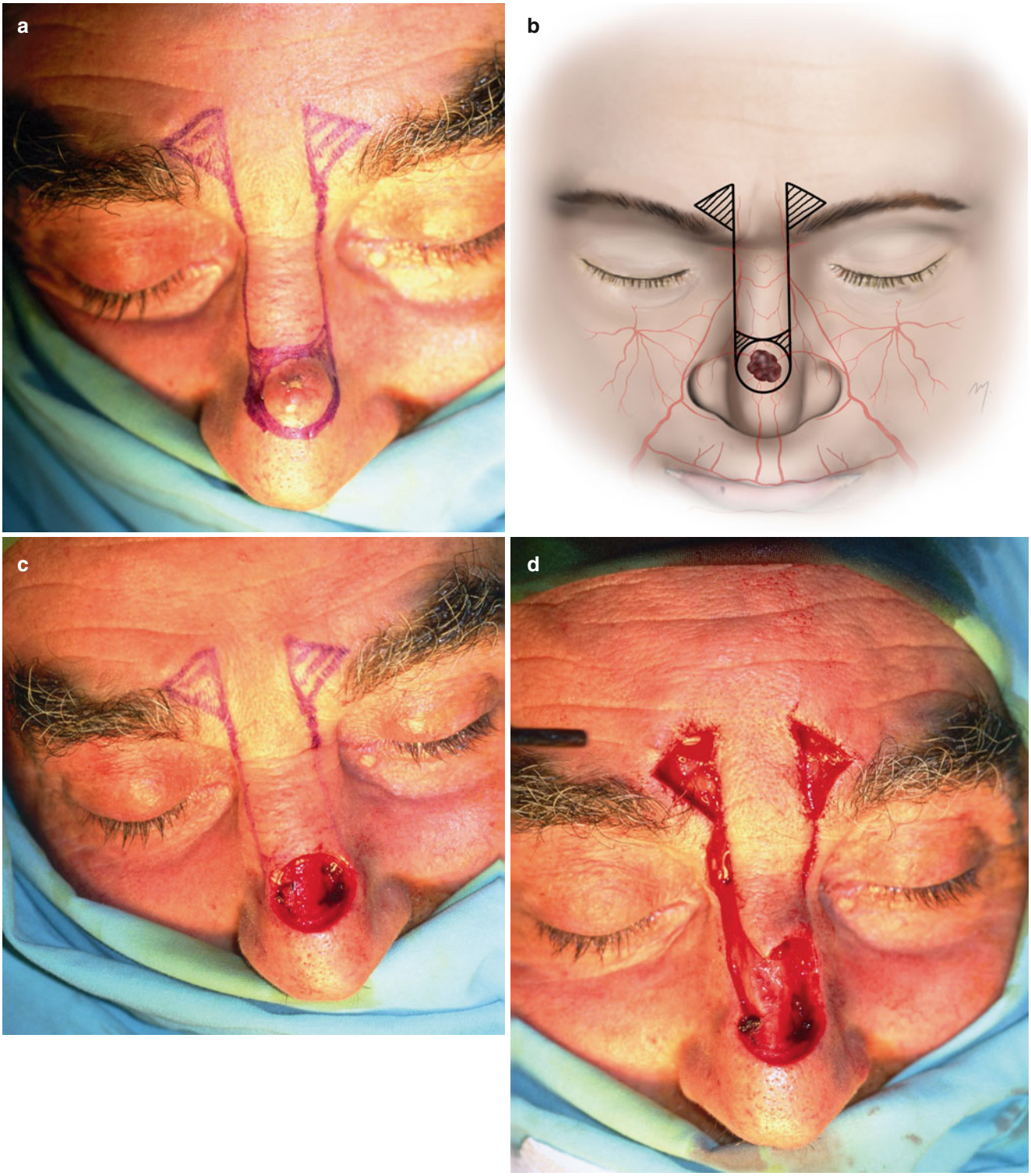

Fig. 4.24 Rintala flap. (**a**) Design of the Rintala flap. (**b**) The flap is of random pattern. (**c**) Lesion excised. (**d**) Flap elevation. (**e**) Flap fully mobilized. (**f**) Final suturing. (**g–i**) Result at 6 months

Fig. 4.24 (continued)

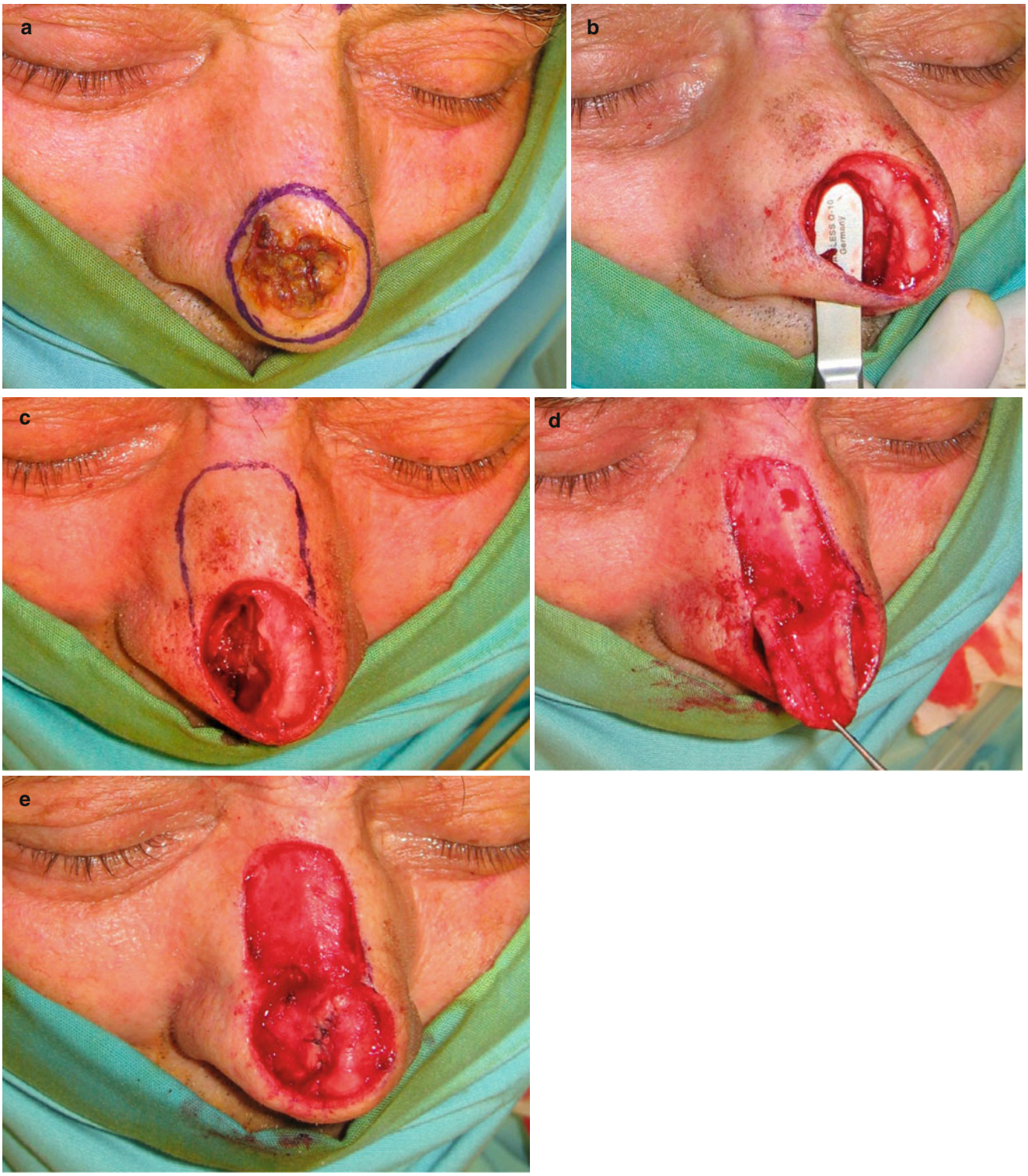

Fig. 4.25 (**a**–**e**) Hinged turn-over flap

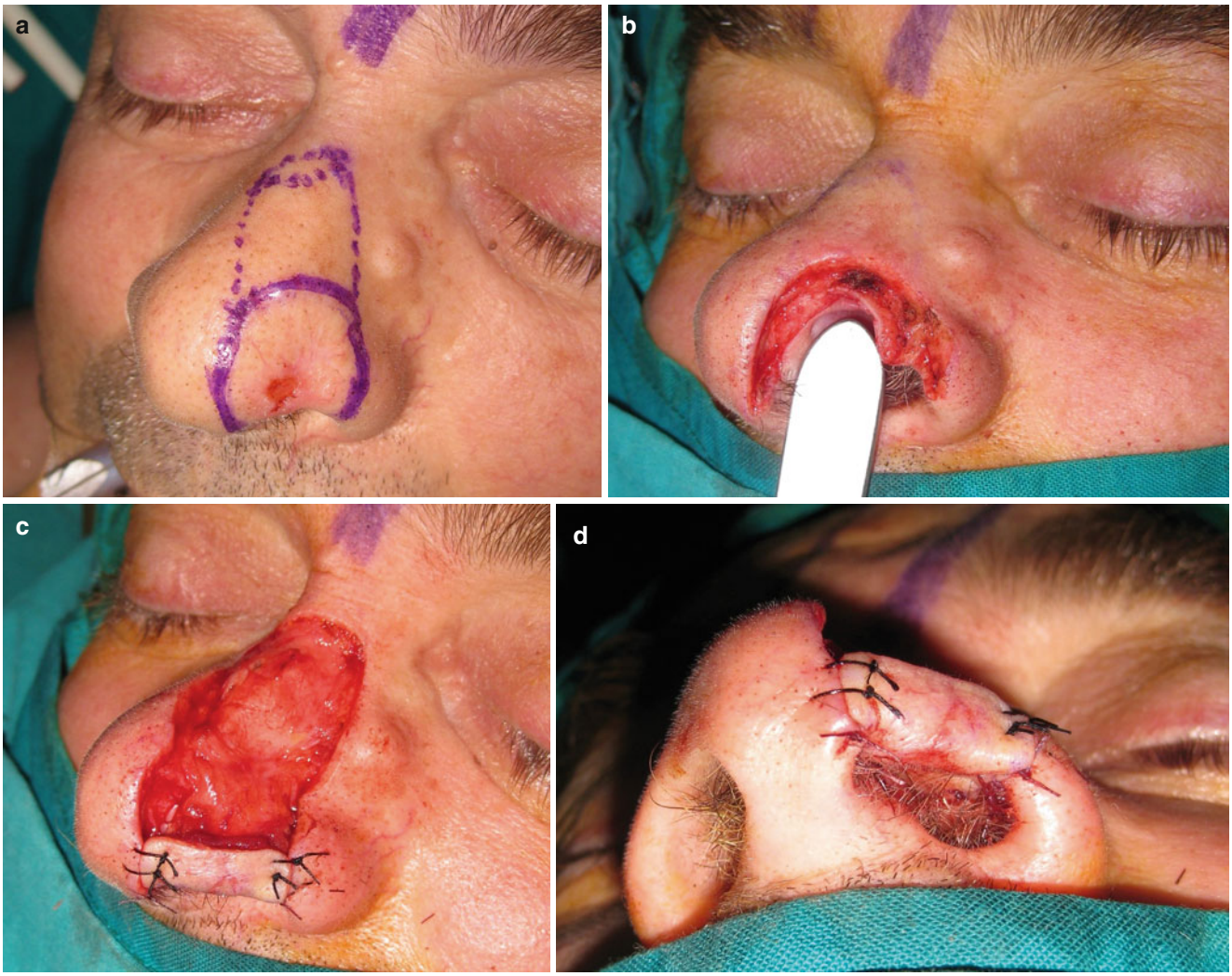

Fig. 4.26 (**a**–**d**) Folded turn-over flap

References

Aksoy F, Veyseller B, Yildirim YS, Acar H, Demirhan H, Ozturan O (2010) Role of nasal muscles in nasal valve collapse. Otolaryngol Head Neck Surg 142(3):365–369

Blandini D, Tremolada C, Beretta M, Mascetti M (1996) Use of a versatile axial dorsonasal musculocutaneous flap in repair of the nasal lobule. Plast Reconstr Surg 98(2):260–268

Bruintjes TD, van Olpen AF, Hillen B, Huizing EH (1988) A functional anatomic study of the nasal cartilages and muscles to the nasal valve area. Laryngoscope 108(7):1025–1032

Bruintjes TD, Olphen AF, Hillen B, Weijs WA (1996) Electromyography of the human nasal muscles. Eur Arch Otorhinolaryngol 253(8):464–469

Burget GC (1985) Aesthetic restoration of the nose. Clin Plast Surg 12(3):463–480

Burget GC, Menick FJ (1985) The subunit principle in nasal reconstruction. Plast Reconstr Surg 76(2):239–247

Chiu LD, Hybarger CP, Todes-Taylor N (1994) The Rintala flap revisited. Plast Reconstr Surg 94(6):801–807

Chun KW, Kang HJ, Han SK, Lee ES, Chang H, Kim SB, Kim WK (2008) Anatomy of the alar lobule in the Asian nose. J Plast Reconstr Aesthet Surg 61(4):400–407

Clark M, Greenfield B, Hunt N, Hall-Craggs M, McGrouther D (1998) Function of the nasal muscles in normal subjects assessed by dynamic MRI and EMG: its relevance to rhinoplasty surgery. Plast Reconstr Surg 101(7):1945–1955

Drumheller GW (1973) Topology of the lateral nasal cartilages: the anatomical relationship of the lateral nasal to the greater alar cartilage, lateral crus. Anat Rec 176(3):321–327

Ebrahimi A, Motamedi MHK, Nejadsarvari N (2012a) Morphologic variations of sesamoid cartilages of the nose in Iranian cadavers. Oral Surg Oral Med Oral Pathol Oral Radiol 114(2):22–25

Ebrahimi A, Nejadsarvari N, Koushki ES (2012b) Application of modified Rintala flap in nasal tip reconstruction. Am J Otolaryngol 33(6):685–688

Esser JFS (1918) Gestielite lokale Nasenplastik mit zweizipfligem Lappen, Deckung des sekundaren Defektes vom ersten Zipfel durch den zweiten. Deutsche Zeitschr Chir 143:385–390

Erdogmus S, Govsa F (2006) Arterial features of inner canthus region: confirming the safety for the flap design. J Craniofac Surg 17(5): 864–868

Galindo De Lara S, De Cuspinera GE, Cardenas Ramirez L (1977) Anatomical and functional account on the lateral nasal cartilages. Acta Anat 97(4):393–399

Gonzales-Ulloa M, Castillo A, Stevens E, Alverez Fuertes G, Leonelli F, Ubaldo F (1954) Preliminary study of the total restoration of the facial skin. Plast Reconstr Surg 13(3):151–161

Hur MS, Hu KS, Park JT, Youn KH, Kim HJ (2010) New anatomical insight of the levator labii superioris alaeque nasi and the transverse part of the nasalis. Surg Radiol Anat 32(8):753–756

Hur MS, Hu KS, Youn KH, Song WC, Abe S, Kim HJ (2011) New anatomical profile of the nasal musculature: dilator naris vestibularis, dilator naris anterior, and alar part of the nasalis. Clin Anat 24(2):162–167

Jackson JT (1985) Local flaps in head and neck reconstruction, 1st edn. Mosby, St Louis

Jackson JT (2007) Local flaps in head and neck reconstruction, 2nd edn. Quality Medical Pub, St Louis

Janeke JB, Wright WK (1971) Studies on the support of the nasal tip. Arch Otolaryngol 93(5):458–464

Jewett SB, Baker RS (2011) Anatomic considerations. In: Baker RS (ed) Principles of nasal reconstruction. Springer, New York/Heidelberg/London

Lang J (1989) Clinical anatomy of the nose, nasal cavity and paranasal sinuses. Thieme Medical Publishers Inc, New York

Lessard ML, Daniel RK (1985) Surgical anatomy of septorhinoplasty. Arch Otolaryngol 111(1):25–29

Letourneau A, Daniel RK (1988) The superficial musculoaponeurotic system of the nose. Plast Reconstr Surg 82(1):48–57

Marchac D (1970) Lambeau de rotation fronto-nasal. Ann Chir Plast Esthet 15(1):44–49

Marchac D, Toth B (1985) The axial frontonasal flap revisited. Plast Reconstr Surg 76(5):686–694

Masson JK, Mendelson BC (1977) The banner flap. Am J Surg 134(3):419–423

McGregor IA, McGregor FM (1986) Cancer of the face and mouth: pathology and management for surgeons. Churchill Livingstone, Edinburgh/London/Melbourne/New York

Millard DR Jr (1981) Aesthetic reconstructive rhinoplasty. Clin Plast Surg 8(2):169–175

Nakajima H, Imanishi N, Aiso S (2002) Facial artery in the upper lip and nose: anatomy and a clinical application. Plast Reconstr Surg 109(3):855–861

O'Hara D, Greenberg S, LaRossa D (1997) Superficial nasalis aponeurotic system (SNAS) flap reconstruction of nasal defects. Ann Plast Surg 38(4):379–384

Ofodile FA, Bokhari FJ (1992) Columella incision in open rhinoplasty in Blacks (Letter). Plast Reconstr Surg 89(5):991–992

Ofodile FA, James EA (1997) Anatomy of alar cartilages in blacks. Plast Reconstr Surg 100(3):699–703

Ofodile FA, Bokhari FJ, Ellis C (1993) The black American nose. Ann Plast Surg 31(3):209–218

Oneal RM, Beil RJ Jr, Schlesinger J (1996) Surgical anatomy of the nose. Clin Plast Surg 23(2):195–222

Oneal RM, Beil RJ Jr, Izenberg PH, Schlesinger J (2000) Surgical anatomy of the nose. Oper Tech Plast Reconstr Surg 7(4): 158–167

Potter JK, Rogers T, Finn R (2000) Macroscopic and microscopic details of the cartilaginous nasal pyramid. J Oral Maxillofac Surg 58(8):867–876

Rieger RA (1967) A local flap for repair of the nasal tip. Br J Plast Surg 40(2):147–149

Riml S, Wallner H, Larcher L, Kompatscher P (2011) The Superficial Nasalis Aponeurotic System (SNAS) flap for nasal tip reconstruction. Plast Reconstr Surg 128(1):19–22

Rintala AE, Asko-Seljavaara S (1969) Reconstruction of midline skin defects of the nose. Scand J Plast Reconstr Surg 3(2): 105–108

Rohrich RJ, Gunter JP, Friedman RM (1995) Nasal tip blood supply: an anatomic study validating the safety of the transcolumellar incision in rhinoplasty. Plast Reconstr Surg 95(5): 795–799

Rohrich RJ, Muzaffar AR, Gunter JP (2000) Nasal tip blood supply: confirming the safety of the transcolumellar incision in rhinoplasty. Plast Reconstr Surg 106(7):1640–1641

Rohrich RJ, Griffin JR, Ansari M, Beran SJ, Potter JK (2004) Nasal reconstruction-beyond aesthetic subunits: a 15-year review of 1334 cases. Plast Reconstr Surg 114(6):1405–1416

Saban Y, Amodeo AC, Hammou JC, Polselli R (2008) An anatomical study of the nasal superficial musculoaponeurotic system: surgical applications in rhinoplasty. Arch Facial Plast Surg 10(2): 109–115

Saban Y, Amodeo CA, Bouaziz D, Polselli R (2012) Nasal arterial vasculature: medical and surgical applications. Arch Facial Plast Surg 14(6):429–436

Song R, Ma H, Pan F (2002) The "levator septi nasi muscle" and its clinical significance. Plast Reconstr Surg 109(5):1707–1712

Standring S (2008) Gray's anatomy. The anatomical basis of clinical practice, 40th edn. Churchill Livingstone-Elsevier, Edinburg

Tardy ME (1990) Surgical anatomy of the nose. Raven, New York

Thomaidis VK et al (2006) The dorsal nasal flap (article in Greek). Hell Arch Oral Maxillofac Surg 7(1):19–26

Toriumi DM, Mueller RA, Grosch T, Bhattacharyya TK, Larrabee WF Jr (1996) Vascular anatomy of the nose and the external rhinoplasty approach. Arch Otolaryngol Head Neck Surg 122(1): 24–34

Watanabe K (1994) New ideas to improve the shape of the ala of the Oriental nose. Aesthetic Plast Surg 18(4):337–344

Yotsuvanagi T, Yamashita K, Urushidate S, Yokoi K, Sawada Y (2000) Nasal reconstruction based on aesthetic subunits in Orientals. Plast Reconstr Surg 106(1):36–44

Zitelli JA (1989) The bilobed flap for nasal reconstruction. Arch Dermatol 125(7):957–959

Cheek

5

The cheek is a convex area of either side of the face constituting the face's largest anatomic and aesthetic constituent. It is bounded superiorly by the zygomatic arch and the orbital-cheek crease, inferiorly by the lower border of the mandible, laterally by the preauricular crease, and medially, from up to down, by the nasofacial sulcus, the nasolabial crease, and the labiomandibular creases (Fig. 5.1).

According to the morphologic-anatomic differences of the bony foundation and the soft tissue covering it, the cheek can be further subdivided into infraorbital, zygomatic, nasolabial, buccal, and parotidomasseteric subunits (Fig. 5.2).

The above subunits of the cheek are primarily anatomic in orientation as opposed to their aesthetic value. In contrast with other areas of the face such as the nose that the subunit approach during reconstruction focused attention, the cheek demands less symmetry due to the fact that its counterpart is not comparable from the same point of view.

5.1 Layered Anatomy

The soft tissues and the fasciae of the cheek are arranged concentrically over the bony skeleton. From an anatomic and surgical point of view, these structures are layered as follows:

1. Skin
2. Subcutaneous tissue
3. Musculoaponeurotic layer (SMAS-mimic muscles)
4. Parotidomasseteric fascia
5. Buccal space and contents
6. Deep muscular layer
7. Retaining ligaments

Surgically important nerves and vessels travel through these layers often changing planes.

5.1.1 Skin

The skin of the cheek histologically consisted of the same components across genders and its subunits. Keratinized epithelium, hair follicles, and sebaceous and sweat glands are not homogenous throughout its entirety showing differences in thickness (ranging from 0.6 mm at the infraorbital subunit to 2.1 mm at the nasolabial subunit), quality, and laxity in each of the cheek's subunits and across genders.

Fig. 5.1 The boundaries of the cheek

V.K. Thomaidis, *Cutaneous Flaps in Head and Neck Reconstruction*,
DOI 10.1007/978-3-642-41254-7_5, © Springer-Verlag Berlin Heidelberg 2014

Fig. 5.2 Cheek subunits

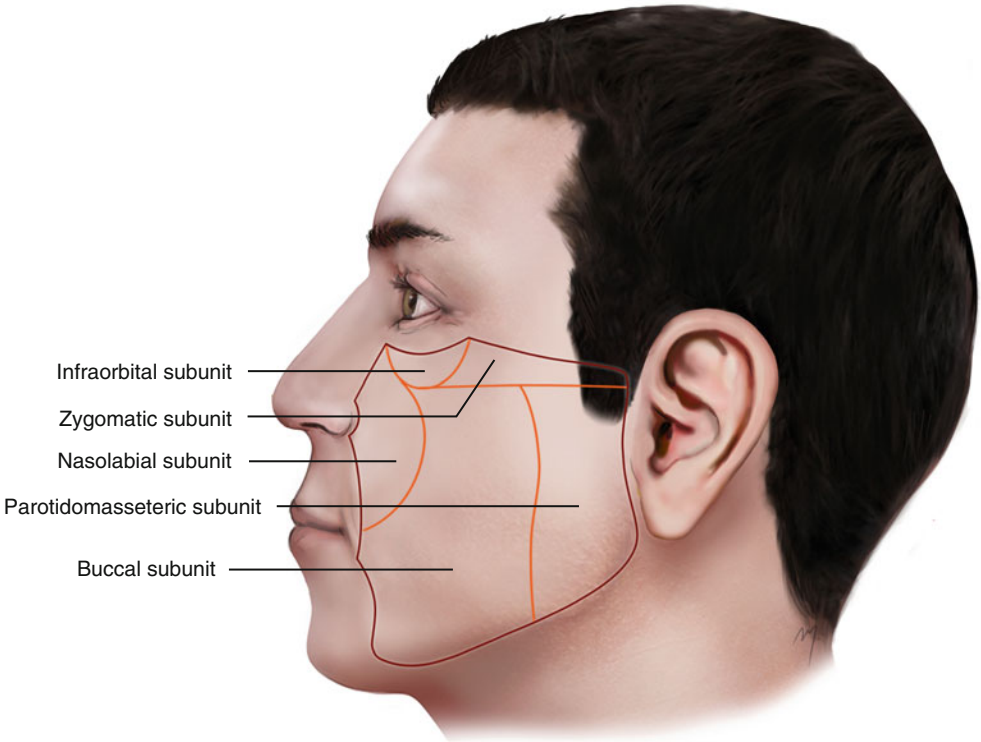

5.1.1.1 Skin and Cheek Subunits

5.1.1.1.1 Infraorbital Subunit

The skin of the infraorbital subunit is very thin with little laxity that becomes even thinner as it reaches the eyelids. Reconstructive options that involve this neighboring area to the lower lid may easily lead to ectropion. Skin incisions here must always run horizontally, parallel to the direction of the infraorbital RST lines. Every tension that is applied to the lower lid must be very carefully calculated with respect to the above factors. In addition, incisions can be camouflaged in the lower lid crease and almost become invisible after a short time.

5.1.1.1.2 Zygomatic Subunit

The zygomatic subunit is defined by the bony zygomatic complex. The skin of this subunit is attached to the underlying fascia due to fibrous retaining ligaments. The zygomatic subunit transitions from a convex area, the malar prominence, to a flatter one. Effort should be made to rebuild this protrusion by choosing an appropriate flap thickness.

5.1.1.1.3 Parotidomasseteric (Preauricular) Subunit

This subunit is bounded by the preauricular crease and a line that begins at the anterior center third of the zygomatic subunit and ends in front of the mandible's corner. This area corresponds to the underlying parotid gland. The skin of the parotidomasseteric subunit is moderately thin and to some degree fixed to the underlying fascia showing a relative absence of laxity, especially at its most lateral preauricular part. As the skin continues medially, the thickness, laxity, and tissue availability increase particularly in elders. Incisions at this area can be hidden in the preauricular crease.

5.1.1.1.4 Buccal Subunit

The buccal cheek subunit consists of skin thicker than the rest of the other subunits, which is freely mobile over the underlying fasciae and fat. Its most medial border is the labiomandibular crease. Just lateral to the crease, the labiomandibular fold is formed by an excess of subcutaneous fat (jowl fat pad). Flaps that include the buccal subunit of the cheek become very flexible with abundant excessive tissue movement.

5.1.1.1.5 Nasolabial Subunit

The skin of the nasolabial subunit resembles the characteristics of the skin of the buccal subunit, being thick and mobile, but encompasses an important facial complex, the nasolabial crease and the nasolabial fold.

Fig. 5.3 Relaxed skin tension lines (RSTLs) at the cheek

The nasolabial crease is the boundary between the cheek and the lips. Lateral to this, the nasolabial fold descends from the side of the nose to the angle of the mouth (Mallouris et al. 2013). The nasolabial crease is formed by direct (due to the absence of SMAS) dermal attachments from the underlying levator labii superioris alaeque nasi and orbicularis oris muscles (Gassner et al. 2008). The nasolabial fold is formed by the redundancy of subcutaneous fat (nasolabial fat pad) that is present lateral to the nasolabial crease in contrast to the almost absent fat medial to the nasolabial crease on the lips.

Close proximity of the nasolabial subunit with nasal ala, lip, and commissure must be considered for possible distortion, which must be prevented during flap reconstruction. The nasolabial crease does not only represent the medial boundaries of the cheek to the lips and the nose but also constitutes a line where a scar can easily be camouflaged. Furthermore, the nasolabial crease parallels the axis of the facial artery and serves as a landmark to its course.

The relaxed skin tension lines (RSTLs) on the cheek run horizontally at its upper-medial part and curve in a vertical direction as they descend to its mid- and lower third (Fig. 5.3).

5.1.2 Subcutaneous Layer

Just under the cheek skin lays the subcutaneous layer (Fig. 5.4). The subcutaneous layer of the cheek mainly consists of fat and connective tissue fibers running through it connecting the SMAS layer with the dermis. Vascular perforators run vertically into the subcutaneous layer as they come from the deep arteries and pass through the SMAS layer to the overlying skin. In the same manner, final neural rami are distributed to the skin undersurface. The subcutaneous layer does not show a homologous thickness like other regions of the head. It varies from being very thick in the nasolabial area and very thin (almost disappearing) close to the eyelids and the lips. The subcutaneous tissue of the cheek is characterized by the way that the fat of this layer is arranged. The subcutaneous fat is compartmentalized in multiple, distinct superficial fat pads or pockets. Retaining ligaments usually border these compartments. Within these compartments the adipose tissue is accumulated in different volumes forming the unique contour of the cheek. The fat pads that are found in the cheek have been described in detail (Owsley 1993; Pessa et al. 1998; Rohrich and Pessa 2007; Gierloff et al. 2012; Pilsl et al. 2012). The main superficial fat pads of the cheek are the malar fat pad, the nasolabial fat pad, and the jowl fat pad.

5.1.2.1 Superficial Fat Pads of the Cheek (Fig. 5.4)

The nasolabial fat pad extends lateral and parallel to the nasolabial crease and is responsible for the formation of the nasolabial fold.

The malar fat pad is located lateral to the nasolabial fat pad at the zygomatic region where it thickens to form the malar prominence. It extends superiorly toward the inferior and lateral orbital margins. Its lateral part may extend even up to the parotis. This fat pad plays an important role in facial rejuvenation procedures.

The jowl fat pad is the most inferiorly situated fat pad and lying lateral to the depressor anguli oris muscle.

The aging process in addition to the synchronous loss of ligament suspension results in fat pad ptosis. This leads to an increased prominence of the folds and the characteristic appearance of the elder face.

5.1.3 SMAS and Superficial Muscle Layer

The third layer of the cheek consisted of the SMAS and the superficial layer of the mimic muscles.

5.1.3.1 SMAS

The SMAS (superficial musculoaponeurotic system) is a single and continuous fibromuscular tissue layer of the face (Fig. 5.5). It consists of collagen, elastin and muscle fibers, fat cells, and interstitial fluid. The SMAS layer varies in its micro- and macrostructure among different areas and can

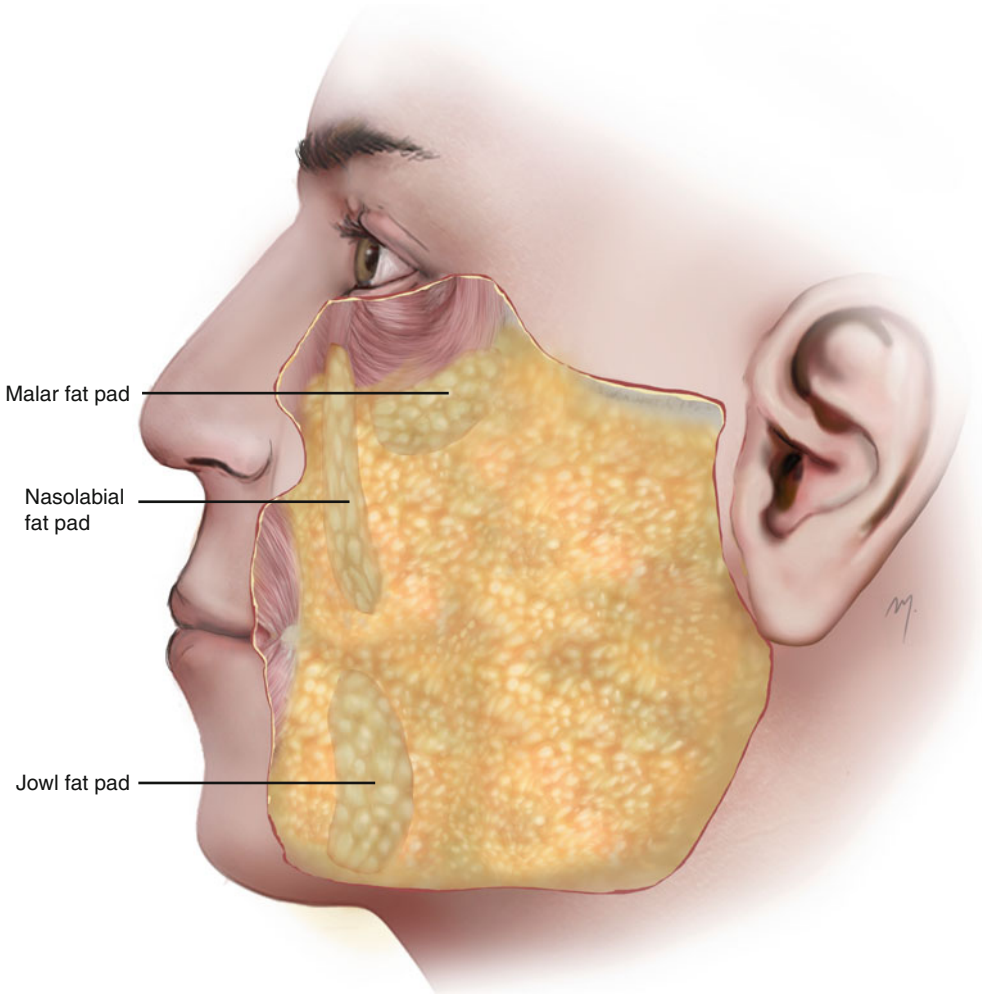

Fig. 5.4 Subcutaneous layer of the cheek and superficial fat pads

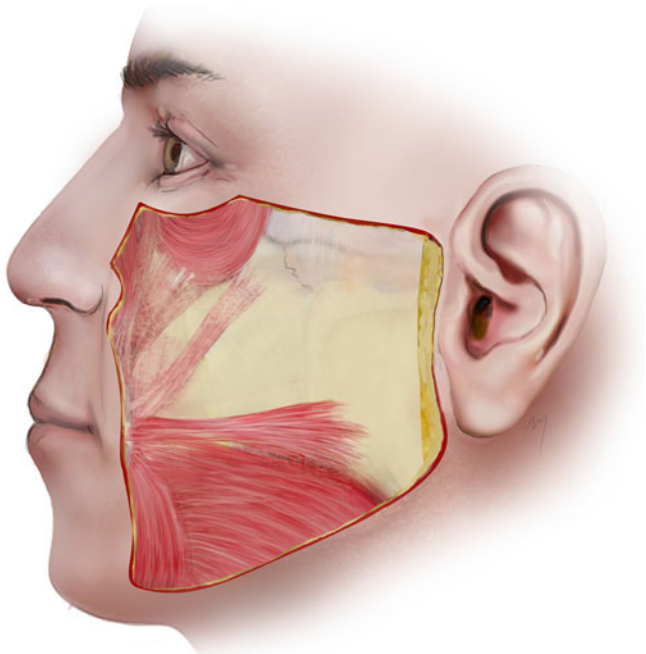

Fig. 5.5 The SMAS in lateral face

appear as more adipofascial or musculofascial in nature. It has no bony attachments and supports the overlying skin. This layer contains the tendon fibers of the mimic muscles that attach to the overlying skin and thus plays an important functional role in facial movement, as it distributes the forces of the muscles to the skin.

The SMAS, first described in detail as a single structure by the classic anatomic work of Mitz and Peyronie (1976), was originally defined as the fibromuscular layer in the parotid and cheek area that divides the subcutaneous fat in two discrete layers and that it is in continuity superior with the frontalis muscle and inferiorly with the platysma. Prior the definition of the SMAS by Mitz and Peyronie (1976), Skoog (1974) had already introduced dissection in a deep ("sub-SMAS") plane for face-lifts.

Ever since its introduction, much controversy was raised in important cadaveric and histologic studies that rose questions that have not yet been definitively answered. The main points of disagreement can be summarized as follows: a clear anatomic definition, extent of SMAS in the various regions of the face and the head, the form of relation to the mimic muscles (having been described as

enveloping, overlying, or merging), the number of facial muscles related to the SMAS, whether it is separate from the parotid fascia, or if it is a distinct layer from the head and neck superficial fascia (De Castro 1980; Jost and Levet 1984; Ruess and Owsley 1987; Thaller et al. 1990; Stuzin et al. 1992; Gosain et al. 1993; Yousif et al. 1994; Fuleihan 1994; Har-Shai et al. 1996, 1997; Gardetto et al. 2003; Levet 2004; Gassner et al. 2008). Parallel to the controversies regarding the SMAS, a variety of face-lifting techniques had been developed related to it (Skoog 1974; Owsley 1983; Hamra 1990; Mendelson 1992; Kamer 1996; Baker 1997).

In the posterior cheek, the SMAS lies over the parotid fascia as a clear, relatively dense layer and adheres firmly with it in a zone of 2–3 cm (Gardetto et al. 2003). Thus, the elevation of the SMAS in this area is difficult and can be achieved only by sharp dissection.

Inferiorly the SMAS passes the lower border of the mandible becoming continuous with the platysma muscle and lies over the investing layer of the deep cervical fascia. Superiorly it crosses over the zygomatic arch and becomes continuous with the temporoparietal fascia of the temple.

Extending over the masseter muscle, the SMAS covers in its upper half the zygomatic and the upper buccal branch of the facial nerve (that are running beneath the masseteric fascia) and the parotid duct. Over the lower half of the masseter, it becomes the roof of an avascular areolar tissue layer, the "premasseteric space" Mendelson et al. (2008). This layer lies immediately superficial to the masseteric fascia which constitutes its floor. It passes over the buccinator muscle, where Gassner et al. (2008) demonstrated the presence of a zone of fusion between SMAS and buccinator muscle.

In the upper cheek, the SMAS is continuous with the inferolateral portion of the orbicularis muscle. Anteriorly, medial to the zygomaticus major and to the nasolabial fold, the SMAS becomes a thin, fragile, and discontinuous fibrous network connected in variable extent and a lesser or greater degree with the mimic muscles. The SMAS in this region does not appear as a clear identifiable, dissectible layer. The histologic differences of SMAS in the various areas of the face (Gardetto et al. 2003; Ghassemi et al. 2003; Gassner et al. 2008), especially those posterior and lateral to the nasolabial fold, led some authors to deny the presence of a SMAS at the anterior region of the cheek (Jost and Levet 1984; Levet 2004; Gassner et al. 2008) or even at the whole cheek (Gardetto et al. 2003). At the modiolus the SMAS merges with the orbicularis oris, zygomaticus major, and buccinator muscles.

5.1.3.2 Superficial Mimic Muscle Layer

The superficial layers of the muscles that are associated with the cheek are the orbicularis oculi, levator labii superioris alaeque nasi, levator labii superioris, zygomaticus minor, zygomaticus major, risorius, platysma, and depressor anguli oris muscles. These muscles can be topographically distinguished in an upper and a lower group (Figs. 5.6 and 5.9).

5.1.3.2.1 Orbicularis Oculi Muscle

The inferior segment of the circularly running fibers of the orbital part of the orbicularis muscle (see Chap. 3) constitutes the superficial muscle layer of the infraorbital region of the cheek (Fig. 5.6). Often the lower border of the orbicularis oculi muscle lies over the upper lip levator muscle complex, and its lateral border may extend over the upper third of the zygomaticus major muscle.

5.1.3.2.2 Suborbicularis Oculi Fat (SOOF)

Immediately under the inferolateral portion of the orbicularis oculi muscle and over the periosteum, a fat pocket termed "suborbicularis oculi fat" or SOOF is found (Fig. 5.7). This fat pocket belongs to the deep fat pockets of the face. The SOOF was described as a submuscular and supraperiosteal fat excess that is situated over the zygoma and acts as a mechanism for the orbicularis oculi muscle to glide (Aiache and Ramirez 1995; Aiache 2001). It is analogous to the retroorbicularis oculi fat (ROOF) of the supraorbital area. It shows a horizontal medial part and a vertical lateral part (Hwang et al. 2008; Rohrich et al. 2009). Due to this it has been described having a "hockey stick head shape" with a horizontal length measuring 48 mm and a vertical height of 27 mm (Hwang et al. 2007c). The SOOF may slightly extend over the inferolateral orbital rim and protrude also slightly from the periphery of the orbicularis oculi muscle over the lip levator muscles.

5.1.3.2.3 Levator Labii Superioris Alaeque Nasi Muscle

The lateral slip of the levator labii superioris alaeque nasi (see Chap. 4) is the muscular border between cheek and nose (Fig. 5.6). It inserts to the upper lip and blends with fibers of the orbicularis oris and levator labii superioris muscles. It belongs to the upper lip levator muscles.

5.1.3.2.4 Levator Labii Superioris Muscle

The fibers of the levator labii superioris muscle (Fig. 5.6) originate from the infraorbital rim, just above the infraorbital foramen. The muscle runs inferiorly and slightly oblique to the upper lip. Before it inserts, its fibers blend with fibers of the zygomaticus minor muscle. It inserts to the upper lip between the insertions of the lateral slip of the levator labii superioris alaeque nasi and the zygomaticus minor muscles.

Branches of the facial and infraorbital arteries supply the muscle. Levator labii superioris is innervated by the zygomatic and buccal branches of the facial nerve.

Levator labii superioris muscle elevates the upper lip.

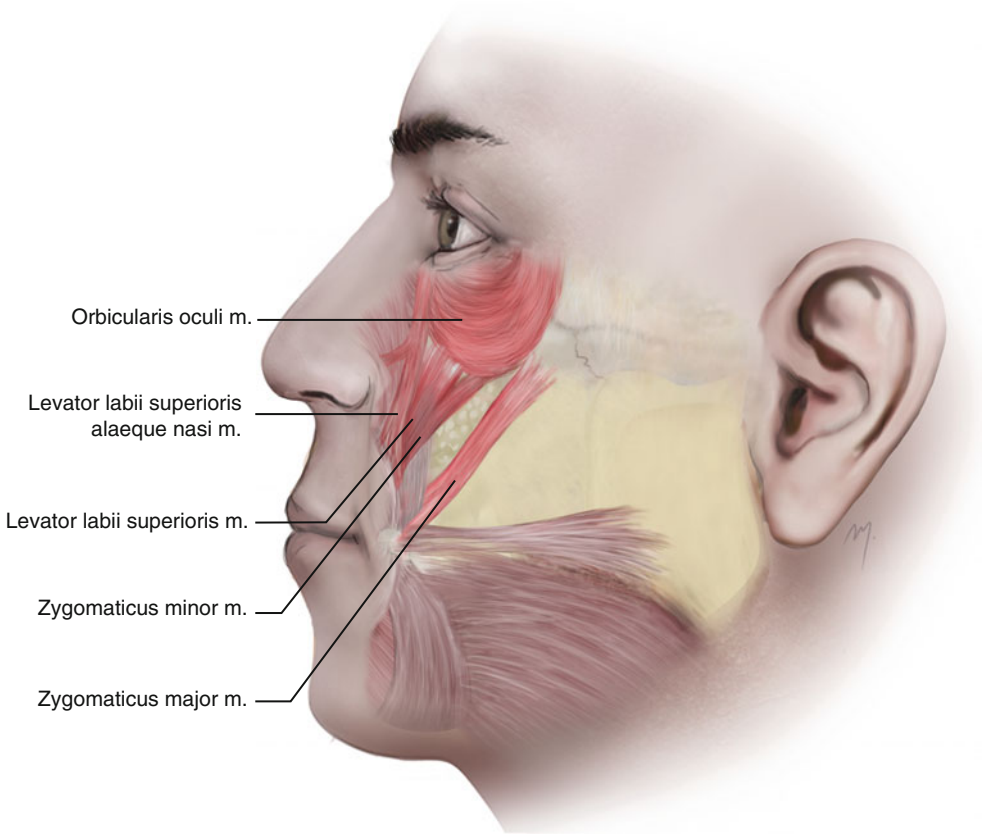

Fig. 5.6 The upper group of the superficial cheek muscles: orbicularis oculi, levator labii superioris alaeque nasi, levator labii superioris, zygomaticus minor, zygomaticus major

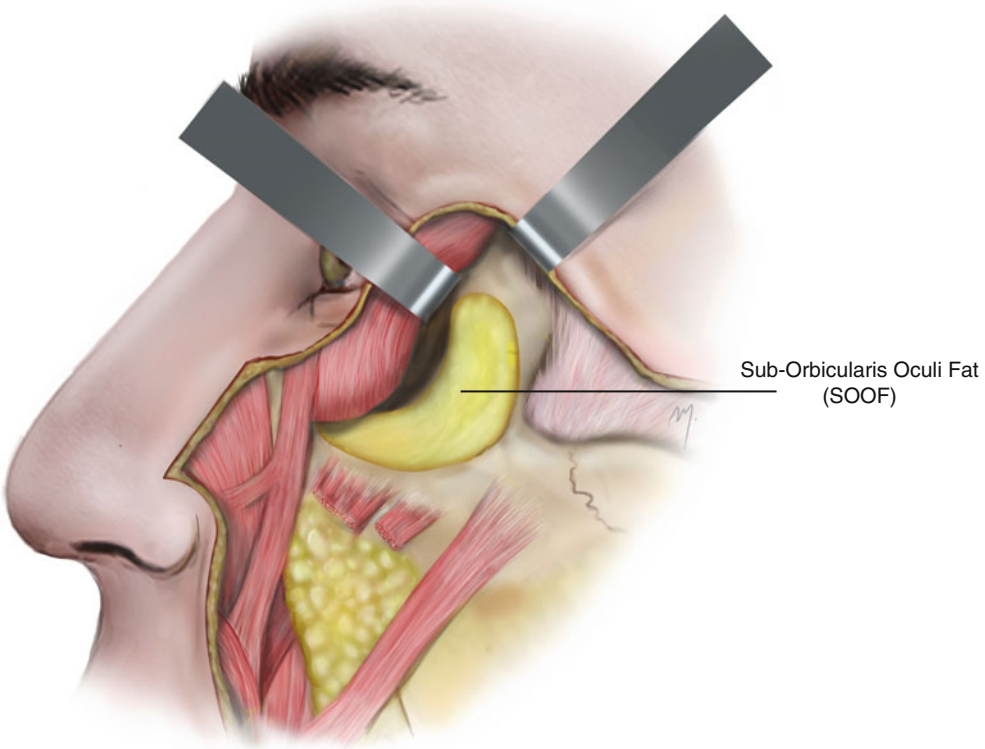

Fig. 5.7 The SOOF. The buccal extension of the buccal fat pad is seen below the lip levators

5.1.3.2.5 Zygomaticus Minor Muscle

The zygomaticus minor muscle has been found to be present in approximately 36–42 % of individuals (Pessa et al. 1998; Waller et al. 2008).

The zygomaticus minor muscle originates (Fig. 5.6) from the lateral aspect of the zygomatic bone just behind the zygomaticomaxillary suture. Some of its fibers originate from the orbicularis oculi muscle. It runs downward and medially into the upper lip. As it continues, its fibers blend with fibers of the orbicularis oculi muscle in various sites, which is the reason that the zygomaticus minor is in many cases difficult to distinguish (Youn et al. 2012). It inserts to the upper lip, but before its insertion, it blends with levator labii superioris muscle.

The superior labial branch of the facial artery supplies the muscle. Innervation is supplied by rami of the zygomatic and buccal branches of the facial nerve. It elevates the upper lip.

5.1.3.2.6 Zygomaticus Major Muscle

The zygomaticus major muscle (Fig. 5.6) originates from the zygomatic bone, anterior to the zygomaticotemporal suture and lateral to the origin of the zygomaticus minor muscle.

Because the zygomaticus major muscle serves as an important landmark to deep-plane (sub-SMAS) dissection, many attempts have been made to identify its upper part and origin by using several bony landmarks (Mowlavi and Wilhelmi 2004; Spiegel and DeRosa 2005; Miller et al. 2007).

A simple and accurate landmark depicting the origin of the zygomaticus major muscle was proposed by Tremolada et al. (1994). According to them, its origin is represented by the point where a line that connects the lateral canthus with the mandibular angle crosses the inferior edge of the zygomatic bone (Fig. 5.8). The origin of the zygomaticus major sometimes may be covered by the inferolateral part of the orbicularis oculi muscle.

The zygomaticus major runs in an oblique direction toward the angle of the mouth.

It may appear bifid, having two separate muscle bands, in the 35–40 % of individuals (Pessa et al. 1998; Hu et al. 2008). In these cases the muscle originates normally and at the infrazygomatic region divides in a superior and an inferior bundle. The superior bundle inserts at the oral commissure and the inferior below it. Its mean width is approximately 12 mm (Pessa et al. 1998).

The muscle fibers insert into the labial angle, where they blend with the fibers of the levator anguli oris, the depressor anguli oris, and orbicularis oris muscles, risorius, buccinator. The muscle fibers that converge at the oral commissure form a tendinous node that firmly attaches to the dermis at the labial angle that is termed modiolus (see Chap. 6). The zygomaticus major muscle short before its insertion at the commissure is bifurcated into one superficial and one deep insertion head where the levator anguli oris muscle passes between them (Nairn 1975; Frellinger et al. 1987). In a detailed study, Shim et al. (2008) found that the above pattern is present in 60 % of the cases while in about 24 % the muscle divides into three insertion heads and in the remainder no division occurs. Depending on the insertion pattern, the muscle fibers blend each time with different muscle fibers of the modiolar region.

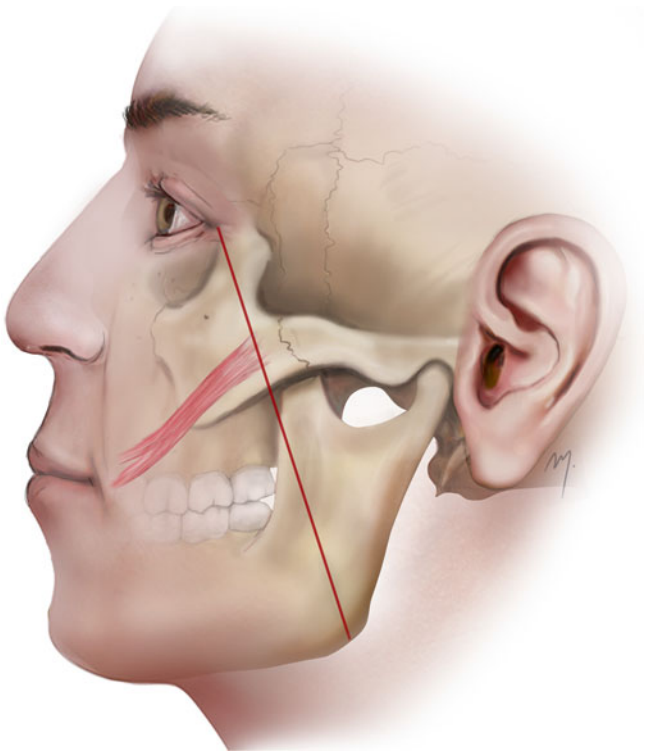

Fig. 5.8 Origin of zygomaticus major muscle (According to Tremolada et al. 1994)

Its vascular supply comes from the superior labial branch of the facial artery. The muscle is innervated by rami of the zygomatic and buccal branches of the facial nerve.

This muscle belongs to the levator muscles of the oral commissure as it draws the angle of the mouth upward and laterally.

5.1.3.2.7 Risorius Muscle

The risorius (Fig. 5.9) is an inconstant muscle that is present in only 6 % of the individuals (Pessa et al. 1998). When present, the risorius muscle is variable in shape and form and is located at the lateral aspect of the cheek.

Its fibers usually arise from the SMAS over the parotis and from the platysma muscle. It may also originate from the zygomatic arch. Depending on its origin, the muscle fibers run anteriorly in an oblique or horizontal axis. It inserts to the angle of the mouth.

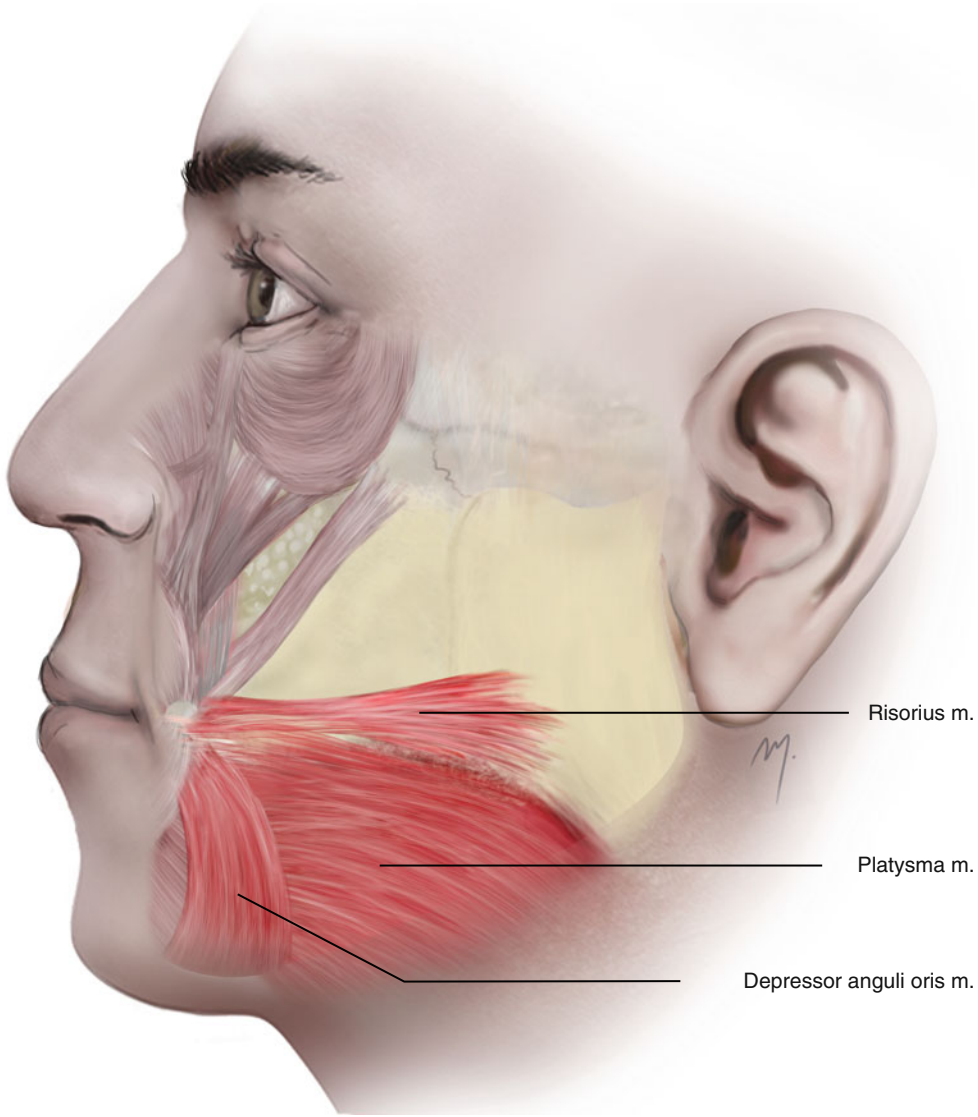

Fig. 5.9 The lower group of the superficial cheek muscles

The superior labial branch of the facial artery supplies the risorius. Buccal branches of the facial nerve innervate the muscle. Risorius retracts the angle of the mouth laterally.

5.1.3.2.8 Platysma Muscle

The platysma muscle (Fig. 5.9) is a neck muscle (see Chap. 8) but its lateral fibers cover a wide area of the inferior cheek. Superiorly the platysma becomes continuous with the SMAS, representing an anatomically homogenous unit that maintains its muscular consistency and direction of fibers as it crosses the mandible. The lateral fibers of the platysma muscle, coming from the neck, cross the mandible, pass over and cover the lower part of the parotid fascia and the masseteric fascia, and run superomedially. They continue deep to the risorius muscle, reaching the posterolateral border of the depressor anguli oris. They converge with the facial muscles at the lower lip. A portion of platysma muscle fibers also converges to the modiolus of the angle of the mouth and is referred to as platysma pars modiolaris.

The platysma muscle pulls the lower lip down and the corner of the mouth downward and laterally.

5.1.3.2.9 Depressor Anguli Oris Muscle

The depressor anguli oris muscle belongs to the depressor muscles of the oral commissure.

The depressor anguli oris muscle (Fig. 5.9) originates from the mandible inferior to the mental foramen and some fibers from the platysma. It has a linear origin that extends from the mental tubercle to a lateral distance of about 36 mm (Hur et al. 2008). Its muscle fibers run upward converging toward the angle of the mouth. It inserts to the angle of the mouth with its fibers blending with fibers of the orbicularis oris and risorius muscles. The inferior labial branch of the facial artery and the mental branch of the maxillary artery supply the muscle. The buccal and mandibular branches of

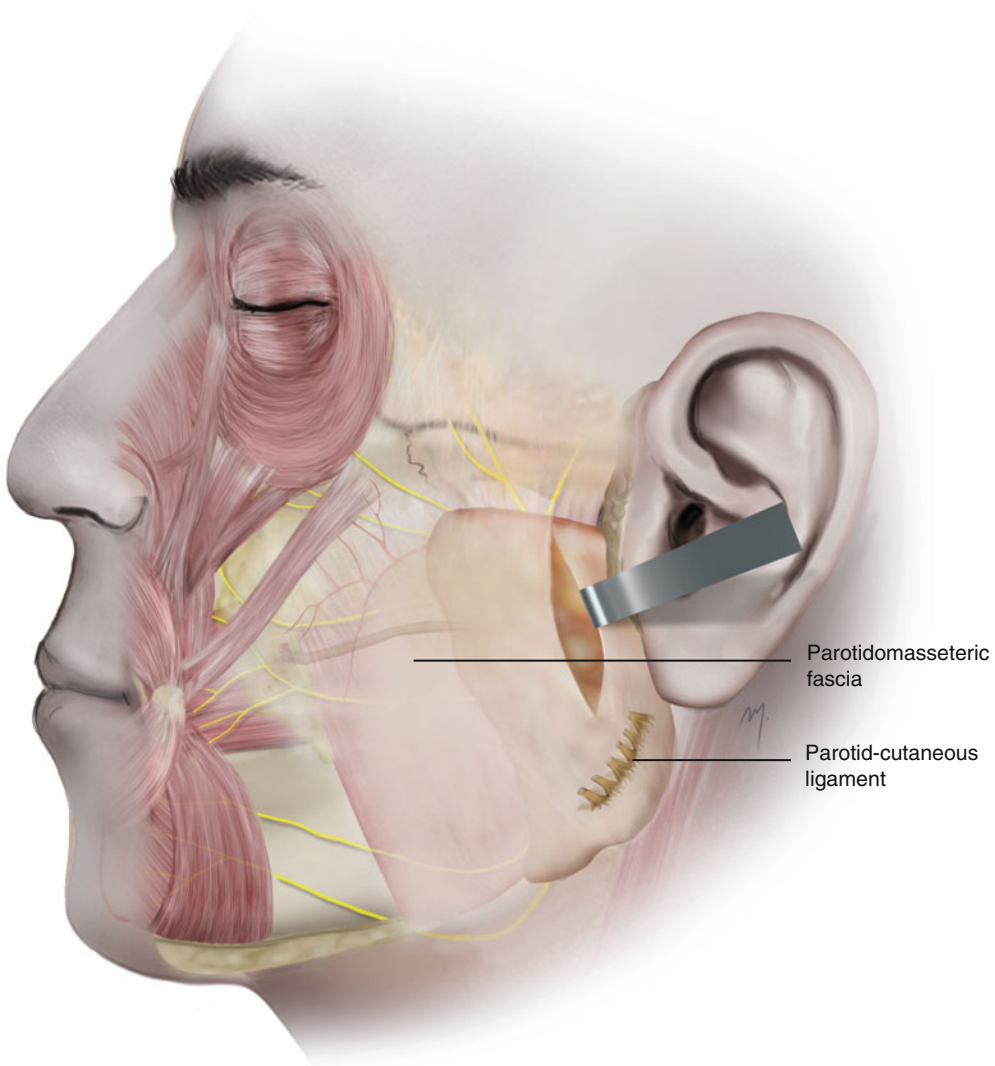

Fig. 5.10 The parotidomasseteric fascia and the parotid-cutaneous ligament

the facial nerve innervate the depressor anguli oris. The depressor anguli oris pulls the angle of the mouth downward and laterally.

5.1.4 Parotidomasseteric Fascia

Just below the SMAS is a thin and glazed fascia that lies over the parotis posteriorly and over the masseter muscle anteriorly, termed the parotidomasseteric fascia (Fig. 5.10). This fascia can be found having a variable thickness and transparency, making the underlying structures slightly distinguishable.

The parotidomasseteric fascia is formed from the continuation of the investing layer of the deep cervical fascia to the head. The investing layer of the deep cervical fascia at the mandible splits in a lateral and a medial layer to surround the outer and the inner surfaces of the mandible body, respectively. As it extends superiorly, the lateral layer covers the outer surfaces of the parotis and masseter muscle and is termed parotidomasseteric fascia. Above the zygomatic arch, the parotidomasseteric fascia corresponds to the loose areolar tissue layer of the temporal area but is quite different in nature. The parotidomasseteric fascia must not be confused with the masseter muscle fascia that invests directly the masseter muscle and lies in deeper layer.

The parotidomasseteric fascia covers the parotid duct, branches of the facial nerve, and the transverse facial artery that runs beneath it and may be felt as they protrude. It also lies over the buccal fat pad and extends anteriorly blending with the epimysium of the facial muscles.

Over the parotis the fascia may show a variable thickness and strength and is densely adherent to the overlying SMAS. A false retaining ligament found here, the parotid-cutaneous ligament, amplifies the restraint of the skin. The parotid-cutaneous ligament (Fig. 5.10) is situated as a fibrous band along the posteroinferior part of the parotid gland that originates from the parotid fascia and running to the dermis

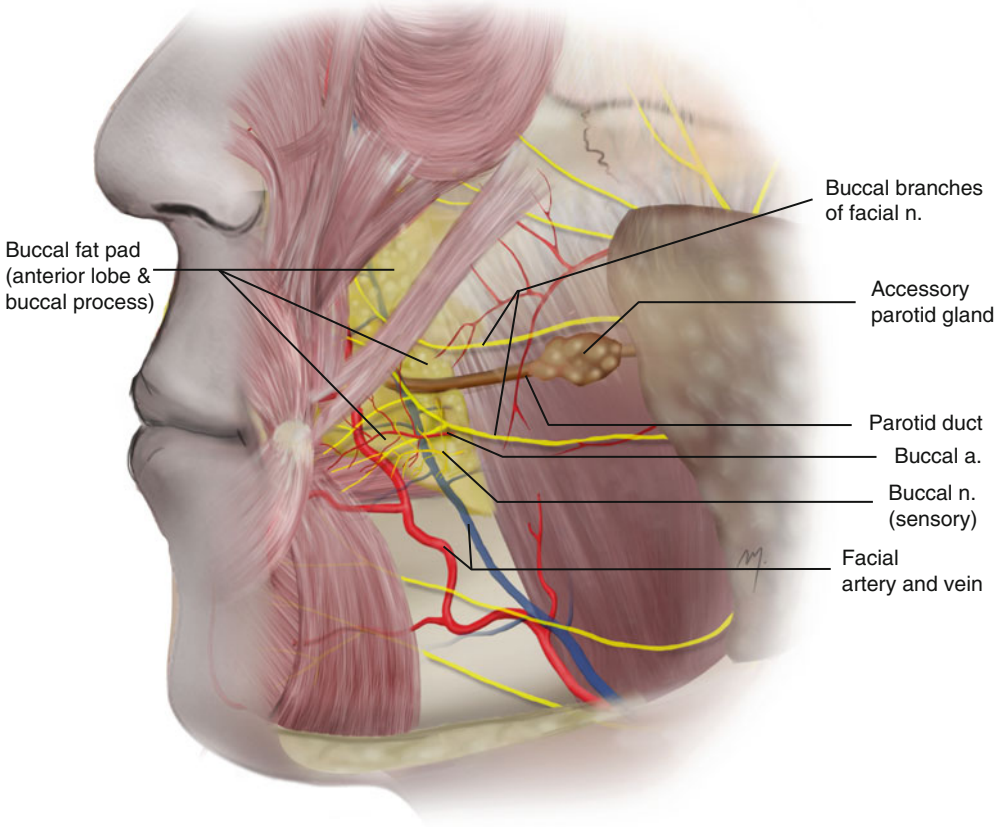

Fig. 5.11 Buccal space and its contents

anchors the skin. It is felt as resistance when elevating the skin over the parotis and has to be released. In contrast to the above area, over the lower half of the masseter muscle, Mendelson et al. (2008) described a loose areolar space, the "premasseter space", that exists between the parotidomasseteric fascia and the SMAS platysma. This space contains no vital structures and can serve as a safe avascular sub-SMAS dissection plane.

5.1.5 Buccal Space

The parotid masseteric fascia bounds the lateral border of the buccal space found beneath it. It is filled by the buccal fat pad and its extensions and important structures that are contained in this compartment. The contents of the buccal space are the buccal fat pad and its extensions that almost fill the space, the parotid duct and minor salivary glands, the inconstant accessory parotid gland, buccal nodes, and nerves and vessels (Fig. 5.11). The nerves found in this space are the motor buccal nerve (branch of the facial nerve) and the sensory buccal nerve (division of V3). The vessels found here are the facial artery and vein and the buccal artery, all of which are examined below.

The buccal fat pad (of Bichat) is one of the deep fat pads that provide fullness to the cheek. Bichat was the first to describe it in (1802) as an encapsulated (with a thin capsule), fatty mass that fills the buccal space and has the buccinator muscle medially and the masseter muscle laterally. It shows a body and multiple extensions. The buccal fat pad is well developed and evident in infants. In adults its mean volume ranges from 9 to 10 ml, being grater in males, and its mean thickness is 6 mm (Loukas et al. 2006b). It plays an important role in suckling, mastication, and aesthetics, as it is located in a protrusive position of the cheek. Zhang et al. (2002) described in details the body and the processes of the buccal fat pad. He mentioned that the body of the buccal fat pad consists of three lobes (an anterior, an intermediate, and a posterior), fixed by ligaments to the surrounding structures. According to this description that has been further accepted (Loukas et al. 2006b; Yousuf et al. 2010), the anterior lobe is triangular in shape, is located below the zygoma, and extends anterior to the buccinator, under the zygomatic major, filling the deep space below the labii superioris muscle. The intermediate lobe is developed in children and thin in the adults and is situated around the posterior and the anterior lobe. The posterior lobe is located in the masticatory space and the surrounding spaces. The buccal fat pad shows four extensions: the pterygoid process, the pterygopalatine process, the buccal process, and the temporal process. The pterygoid process fills the pterygoid space, while the pterygopalatine extends to the pterygopalatine fossa. The temporal process is the buccal fat pad's extension into the temporal region. This extension in

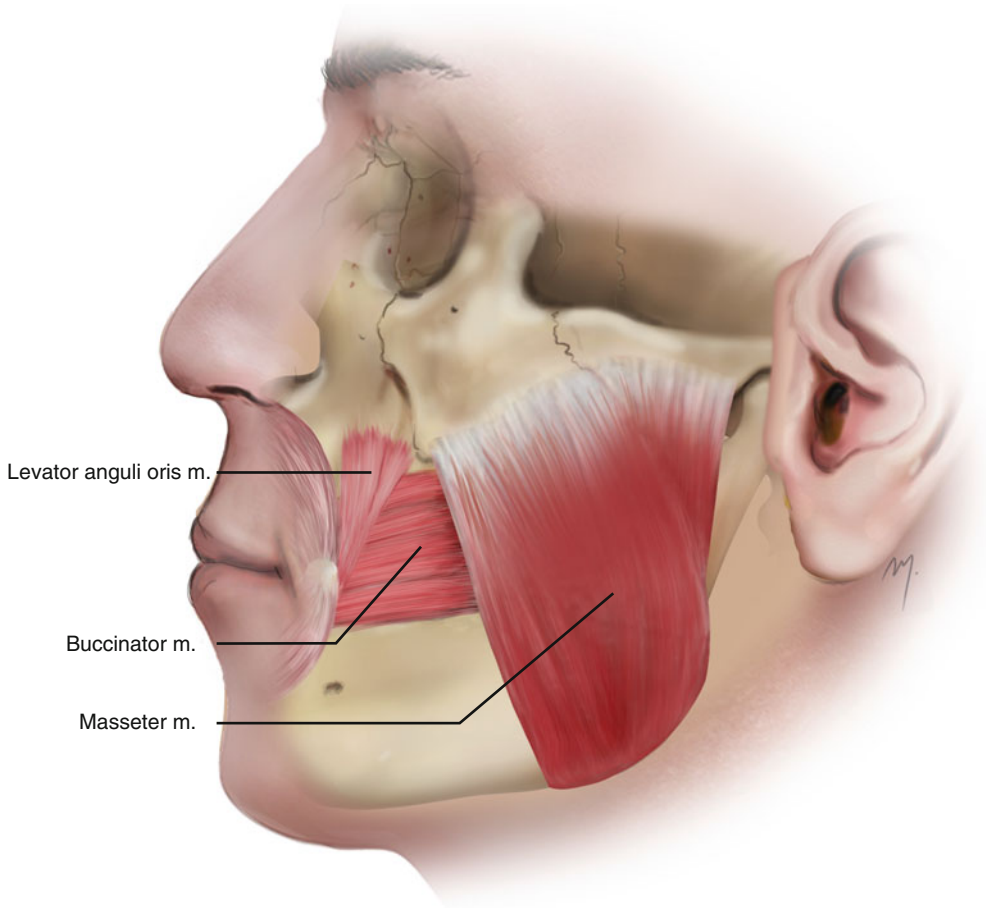

Fig. 5.12 Deep muscle layer of the cheek

the temporal area is termed as deep temporal fat pad that lies between the temporalis fascia and the outer surface of the temporalis muscle (the superficial temporal fat pad is not a part of this extension but a distinct entity) (Stuzin et al. 1989, 1990). Functionally this extension allows the temporalis muscle to glide easily under the zygomatic arch. The buccal process is the most superficial and is the extension of the buccal fat pad body below the parotid duct. The parotidomasseteric fascia covers the buccal fat pad in its lateral aspect, and the buccal branch of the facial nerve and the parotid duct are related to it. The buccal branch of the facial nerve crosses usually (74 %) superficial to the buccal fat pad but sometimes (26 %) small branches of the nerve pass through its buccal extension (Hwang et al. 2005). The arteries that supply the buccal fat pad are derived from the buccal and deep temporal branches of the maxillary artery, from the transverse facial branch of the superficial temporal artery, and from branches of the facial artery. The buccal fat pad has been widely used as a flap in the closing of oroantral fistulas. It is also a very useful tool in mucosa resurfacing in nearby to it through and through cheek defects.

The parotid duct (Stensen's duct), with a length of 6–7 cm, arises from the anterior border of the parotis and runs horizontally over the masseter muscle. At its anterior border, it turns sharply, passing through the buccal fat pad, pierces the buccinator, and opens to the oral cavity, opposite the upper second molar. Its trajectory can be represented by a line connecting the tragus with the commissure. The buccal branches of the facial nerve are related to the parotid duct as they are running parallel, above and below to it. The parotid duct passes along the lateral surface of the buccal fat pad and its buccal extension. It has been reported that in 26 % of the individuals the parotid duct can also be found deep to the buccal extension of the fat pad (Hwang et al. 2005).

The facial artery courses through the buccal space at its anterior part while the facial vein is found slightly posterior.

5.1.6 Deep Muscle Layer

The deep muscle layer of the cheek consists of the masseter, buccinator, and levator anguli oris muscles.

5.1.6.1 Masseter Muscle

The masseter muscle (Fig. 5.12), a quadrilateral in shape muscle, anatomically belongs to the masticatory muscles but topographically it occupies the frontal half of the parotidomasseteric region of the cheek. The parotid gland lies over

its posterior part, and the buccal, the lower zygomatic branches of the facial nerve, and the parotid duct run over its surface. The masseter muscle consists of three layers that blend anteriorly: the superficial layer being the largest, the intermediate layer, and the deep layer.

The superficial layer originates by a thick aponeurosis from the maxillary process of the zygomatic bone and the anterior two-thirds of the inferior border of the zygomatic arch. The intermediate layer originates from the deep surface of the anterior two-thirds of the zygomatic arch and from the lower border of its posterior third. The deep layer originates from the deep surface of the zygomatic arch.

The fibers of the superficial layer run inferiorly and posteriorly to the mandible in an oblique axis, while the fibers of the intermediate and deep layer run in the same direction slightly more vertical.

The superficial layer inserts into the angle and the lower posterior half of the lateral surface of the mandibular ramus, the intermediate layer into the central part of the ramus, and the deep layer into the upper part of the ramus and the coronoid process.

It has not been clarified whether fibers of the masseter muscle are attached to the auricular disk of the temporomandibular joint (Yung et al. 1990; Velasco et al. 1993; Loughner et al. 1996). It has been reported that in about the half of the individuals, muscle fibers of the deep layer of the masseter attach to the auricular disk and capsule (Matsunaga et al. 2009).

The masseter muscle is supplied by the masseteric branch of the maxillary artery and small branches, which arise from the facial and the transverse facial arteries. Additionally, the deep temporal artery contributes to the masseter supply by means of a small muscular branch (Won et al. 2012). The masseter receives its nerve supply from a branch of the anterior trunk of the mandibular nerve.

The masseter primarily elevates the mandible to occlude the teeth.

5.1.6.2 Buccinator Muscle

The buccinator muscle (Fig. 5.12) is a thin and quadrilateral muscle that forms the base of the bucal space, and fills the gap between the maxilla and the mandible.

It originates in the form of a horseshoe from the maxilla, the mandible, and the pterygomandibular raphe. Its superior border is attached to the outer surface of the alveolar process of the maxilla, its posterior border to the anterior margin of the pterygomandibular raphe, and its inferior border to the outer surface of the alveolar process of the mandible.

The fibers of the buccinators run almost parallel to the angle of the mouth. The posterior part of the muscle is situated initially deep to the ramus of the mandible and to the masseter muscle being separated from them by the buccal fat pad. Its anterior part runs under the zygomaticus major, risorius, levator, and depressor anguli oris muscles and under the facial artery, the facial vein, and branches of the facial and buccal nerves. The parotid duct, after curving the frontal border of the masseter muscle, pierces the buccinator at the level of the maxillary third molar and enters the mouth opposite the maxillary second molar tooth. Deep in the muscle lies the submucosal layer of the oral cavity.

The buccinator muscle has been described as consisting of four muscle fiber bands: the upper band originating from the maxilla, the second band originating from the pterygomandibular raphe, the third band extending from the mandible, and an inconstant most inferior band originating from the mandible under the previous one, running to the midline and merging with its contralateral (Mortellaro et al. 2001; D'Andrea and Barbaix 2006; Hur et al. 2011).

The buccinator inserts into the labial angle, the upper and the lower lip in the following manner: The upper fibers of the buccinator continue as fibers of the lower part of the orbicularis oris muscle while the lower fibers continue as fibers of the upper part of the orbicularis oris muscle, intersecting each other.

The uppermost fibers continue as fibers of the upper part of the orbicularis oris muscle and the lowermost fibers continue as fibers of the lower part of the orbicularis oris muscle.

Small muscle fibers of the buccinator muscle, lengthening from 3 to 10 mm, form a distinct bundle that extends to the terminal portion of the parotid duct, functioning in the saliva secretion (Kang et al. 2006).

The vascular supply of the buccinator muscle has been described in detail due to its use as a flap for intraoral covering (Bozola et al. 1989; Carstens et al. 1991; Zhenmin Zhao et al. 1999). It receives its blood supply from branches of the facial and the internal maxillary arteries. The facial artery provides posterior, inferior, and anterior branches to the buccinator, which supply the posterior, inferior, and anterior portions of the muscle, respectively. The internal maxillary artery contributes to the vascular supply of the buccinator mainly due to the buccal artery and a contribution of the posterior-superior alveolar artery.

The buccal artery after branching from the second part of the maxillary artery runs deep into the mandibular ramus, anterior and inferior to the lateral pterygoid muscle, and supplies the posterior part of the buccinator. It anastomoses with the posterior buccal branch of the facial artery.

The posterior-superior alveolar artery enters the posterior-superior part of the buccinator and supplies this part of the muscle. Small branches of the infraorbital artery also supply the anterior-superior part of the buccinator.

The buccal branch of the facial nerve provides the motor innervation to the buccinator muscle.

The buccinator compresses the cheek and also acts to propel food during mastication, sucking, and whistling. It also participates in the lateral retraction of the oral commissure.

5.1.6.3 Levator Anguli Oris Muscle

The levator anguli oris muscle (Fig. 5.12) belongs to the levators of the oral commissure muscles and is the deepest

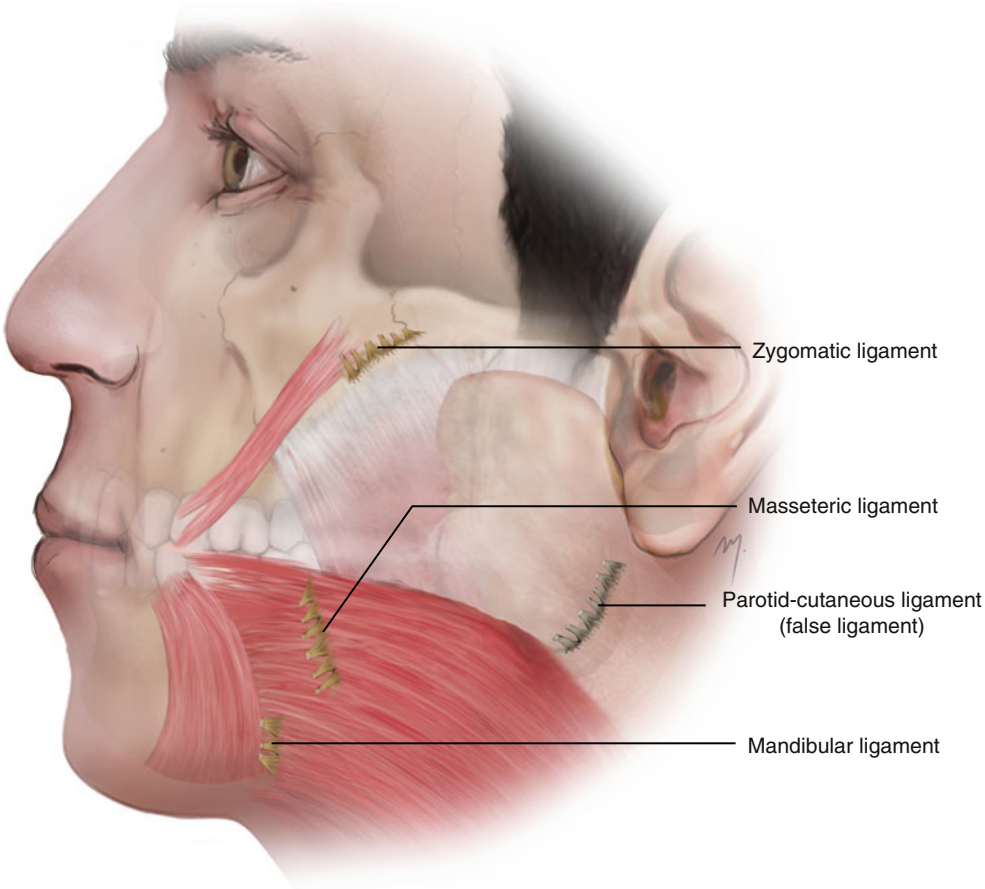

Fig. 5.13 True retaining ligaments at the cheek

muscle of the upper lip levator complex. It is rectangular in shape with a length of 4.8 cm and a width of 1.2 cm (Ewart et al. 2005).

Levator anguli oris muscle originates from the canine fossa of the maxilla, approximately 1 cm inferiorly to the infraorbital foramen. The muscle runs inferiorly, covered by the levator labii superioris and zygomaticus minor muscles. It inserts into the labial angle, converging with the fibers of the zygomaticus major, depressor anguli oris, and orbicularis oris and the fibers of the other muscles that form the modiolus.

The levator anguli oris muscle is supplied by the superior labial branch of the facial artery and the infraorbital branch of the maxillary artery. It receives its nerve supply from the rami of the zygomatic and buccal branches of the facial nerve. Levator anguli oris muscle raises the angle of the mouth.

5.1.7 Retaining Ligaments

Several ligaments support the facial skin in its normal anatomic position against gravitational forces. These ligaments, referred to as retaining ligaments, were first described by Furnas (1989). The retaining ligaments of the cheek draw attention due to their role in the aging process and in the rejuvenation procedures of the face (Stuzin et al. 1992; Pilsl and Anderhuber 2010; Furnas 1994; Mendelson 1995, 2009). The retaining ligaments run as fibrous bands from the deep facial structures to the overlying dermis. The retaining ligaments of the cheek are found in specific locations and can be felt as resistance to flap elevation and must be released as they cross through the dissection plane.

Several retaining ligaments have been described in the cheek (zygomatic ligament, masseteric ligament, mandibular ligament, platysma-auricular ligament, buccomaxillary ligament, platysma-mandibular ligament, subcutaneous parotid masseteric ligament) and are often the same ligaments with different nomenclature. The bands of the ligaments may originate from the periosteum and are termed as true retaining ligaments, or they may originate from the SMAS and insert as the previous into the dermis and are termed as false retaining ligaments.

The true ligaments of the cheek (Fig. 5.13) that arise from the osseous background of the cheek are the following.

The zygomatic ligament (McGregor's patch) originates as a series of fibrous septa from the periosteum at the junction of the zygomatic arch and zygomatic body just lateral to the zygomaticus major muscle.

The masseteric ligaments are found as they extend along the anterior border of the masseter muscle.

The mandibular ligament originates from the periosteum of the external surface of the mandibular body, 5 mm superiorly to the inferior edge and lateral to the depressor anguli oris muscle.

5.1.8 Arterial Supply

The cheek receives its blood supply mainly from branches of the external carotid artery, with a minor contribution of the internal carotid artery due to a small branch of the ophthalmic artery. The arteries of the external carotid that contribute to its arterial vasculature are the infraorbital, the transverse facial, and the facial arteries. The contribution of the internal carotid system happens by the small zygomaticofacial artery.

5.1.8.1 Infraorbital Artery

The infraorbital artery is one of the three branches of the maxillary artery, together with the mental and buccal arteries, that supply the face.

The infraorbital artery arises from the third part of the maxillary artery. It enters the orbit through the posterior part of the inferior orbital fissure. It runs on the floor of the orbit along the infraorbital groove and enters the infraorbital canal in company with the infraorbital nerve. On its course in the infraorbital groove and canal, it gives branches for the inferior rectus and inferior oblique muscles, the nasolacrimal sac and the anterior superior alveolar artery, and sometimes the middle superior alveolar artery.

The artery emerges onto the face through the infraorbital foramen (Fig. 5.14). The infraorbital artery is located in the middle and superficial of the infraorbital nerve bundle in about 74 % of the cases, lateral to it in 20 %, and in the remainder medial to it (Hu et al. 2006). As it exits to the face, through the infraorbital foramen, it lies under levator labii superioris muscle and very quickly divides into its lower lid, nasal, and superior labial and cheek branches.

The lower lid branches run upward under the cover of the orbicularis oculi muscle, and after piercing it they distribute to the skin of the lower eyelid. The nasal branches of the infraorbital artery distribute to the lateral side of the nose. The superior labial branches are larger and numerous. They run inferiorly between the levator labii superioris and the levator anguli oris and are distributed to the upper lip and the anterior part of the cheek. Multiple anastomosing branches connect the infraorbital artery with the angular, the dorsal nasal, the transverse facial, and the buccal arteries.

5.1.8.2 Zygomaticofacial Artery

The zygomaticofacial artery constitutes the contribution of the internal carotid artery to the cheek. It is a branch of the lacrimal artery, which in turn is branched from the ophthalmic artery of the internal carotid. The lacrimal artery runs forward at the junction of the orbital roof and the orbit lateral wall. Within the orbit, it gives off the zygomatic artery, which subdivides into the zygomaticotemporal and zygomaticofacial artery.

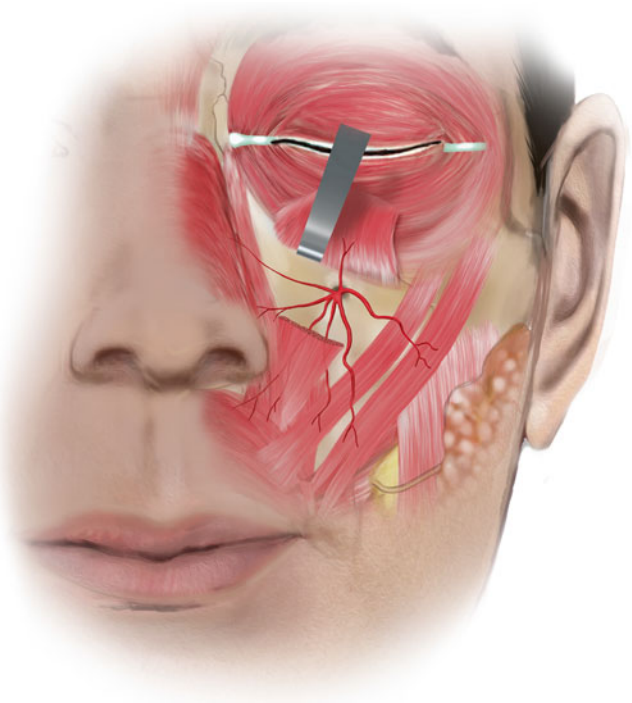

Fig. 5.14 The infraorbital artery at the face

The zygomaticofacial artery appears on the cheek (Fig. 5.15) through the zygomaticofacial foramen and supplies the skin of the malar region. The zygomaticofacial foramen varies in its position and is expected to be found in a mean distance of 1.1 cm from the inferolateral orbital margin (Loukas et al. 2008). When the zygomaticofacial artery exits, it immediately supplies the skin of the malar region. In cases where the inferolateral portion of the orbicularis oculi muscle extends over the zygomaticofacial foramen, the artery pierces the muscle to reach the subcutaneous tissue. The zygomaticofacial artery anastomoses with the transverse facial and zygomaticoorbital arteries.

5.1.8.3 Superficial Temporal Artery: Preauricular Course

The superficial temporal artery is the smaller of the two terminal branches of the external carotid artery (the other one being the maxillary artery). The bifurcation of the external carotid artery happens at the level of the neck of the mandibular condyle, deep or even within the parotis that identifies the origin of the superficial temporal artery. The artery runs upward as a continuation of the external carotid artery and passes over the zygomatic arch continuing along the side

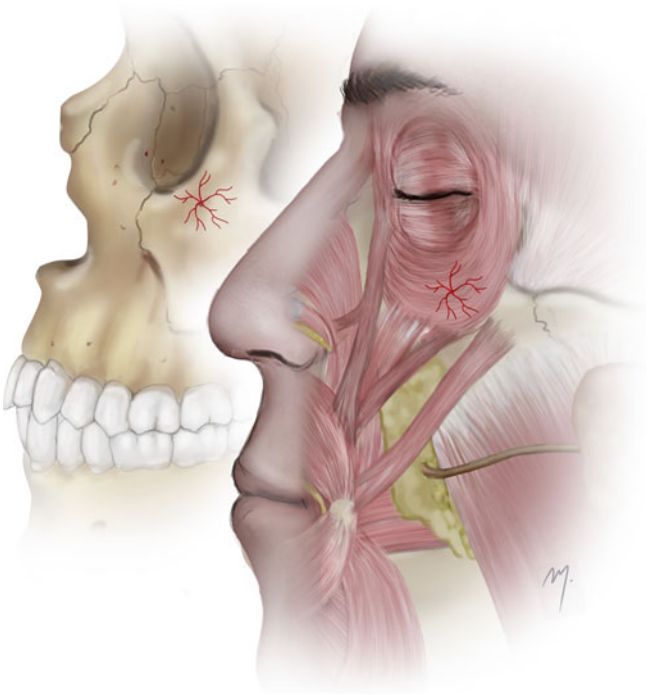

Fig. 5.15 Zygomaticofacial artery

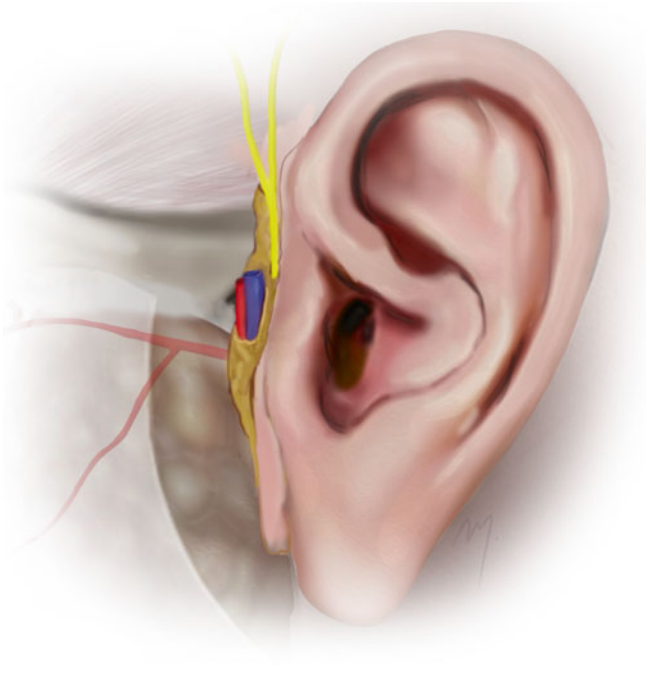

Fig. 5.16 Superficial temporal artery at the preauricular region and its relation to the superficial temporal vein and the auriculotemporal nerve

of the head where it bifurcates to the frontal and parietal branches.

Its long course can be distinguished in two parts: a first preauricular part at the cheek and a second temporal part above the zygomatic arch.

5.1.8.3.1 Preauricular Course

After its origin, the superficial temporal artery continues upward giving off the transverse facial artery after which it appears at the superior border of the parotid gland. It pierces the parotidomasseteric fascia and continues along within the SMAS temporoparietal fascia layer.

Ascending from the parotid gland, the superficial temporal (Fig. 5.16) artery passes at a distance ranging from 0.5 to 1.0 cm in front of the anterior edge of the tragus, in a depth of up to 1.0 cm. The mean diameter of the superficial temporal artery here ranges between 2 and 2.7 mm (Stock et al. 1980; Lang 1995; Chen et al. 1999; Pinar and Govsa 2006).

Even though many variations exist, the most usual in the pretragal area is that superficial temporal vein which accompanies the artery, runs laterally to it and in a more superficial level. The auriculotemporal nerve runs lateral or superficial to the artery and in a variable unpredictable relation to the vein. As many scalp and facial flaps involve a preauricular incision and a preauricular flap elevation, the above relation of the vessels and the distance from the tragus must be kept in mind so as to avoid injury.

The superficial temporal artery gives off two small branches, the middle and the lower auricular arteries (the

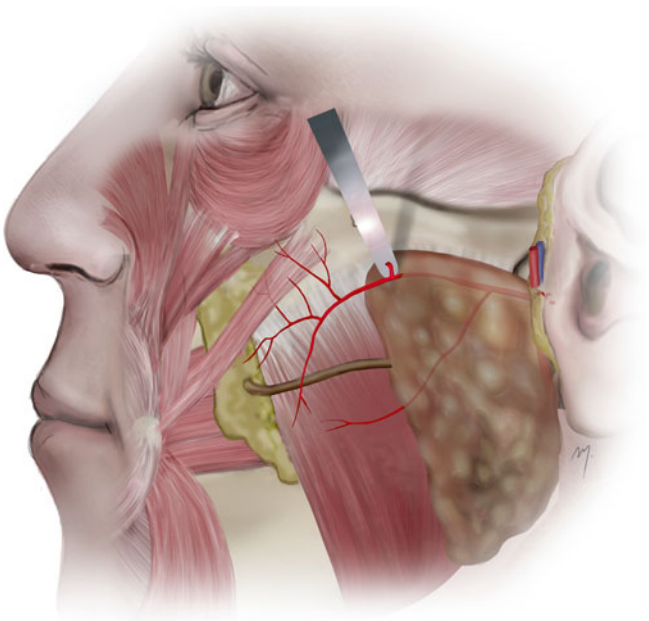

Fig. 5.17 The transverse facial artery

upper auricular artery is branched from a higher level at the temporal course of the superficial temporal artery) that contribute to the supply of the auricle (see Chap. 7).

5.1.8.4 Transverse Facial Artery

The transverse facial artery (Fig. 5.17) arises from the superficial temporal artery before it emerges from the gland.

In 70 % of cases, it arises as one branch and in the rest as two or three (Yang et al. 2010). It is situated in a plane deep to the facial nerve.

In their detailed study, Yang et al. (2010) found out that the transverse facial artery usually divides within in the parotid substance into two trunks that in most cases emerge from the anterior border of the gland, as superior and inferior branches, and described their course as follows.

The superior branch, the largest one, emerges from the upper part of the parotis and courses forward into the cheek, located between the zygomatic arch and the parotid duct in a distance of about 1.5 cm inferiorly to the zygomatic arch. It usually gives off a descending branch that crosses the parotid duct and supplies the area below the duct together with the inferior branch. The superior branch also gives branches to the superior part of the masseter, to the zygomaticus major, and multiple branches to the soft tissues of the malar area.

The inferior branch, smaller than the previous, emerges from the lower part of the parotis and runs superficial to the masseteric fascia, coursing inferior to the parotid duct. It distributes to the masseter muscle terminating as muscular or as cutaneous branch. The inferior branch in about 27 % terminates its course within the parotid gland as muscular branch.

Due to its numerous branches, the transverse facial artery supplies the parotid gland, the parotid duct, the facial nerve, the masseter muscle, and a large area of the cheek skin.

An important large cutaneous perforator of the transverse facial artery (Fig. 5.18), located approximately 3 cm lateral and 3.5 cm inferior to the lateral canthus, provides the main direct blood supply to the skin of the preauricular area and the lateral cheek, defining its vascular territory (Whetzel and Mathes 1992, 1997; Schaverien et al. 2009). The territory, perfused by this perforator, extends superiorly 1–2 cm above the zygomatic arch, inferiorly 2 cm above the border of the mandible, anteriorly over the malar eminence to the lateral canthus, and posteriorly 1–2 cm anterior to the ear (Whetzel and Mathes 1992; Whetzel and Stevenson 1997). This perforator branch is sectioned during elevation of flaps when dissecting in this area. However, the viability of the flaps is guaranteed due to collateral flow from the multiple anastomosing branches of the neighboring arteries.

The transverse facial artery anastomoses with the zygomaticoorbital, the lacrimal and the infraorbital arteries superiorly, the facial and the masseteric arteries anteriorly, and the buccal artery deeply.

The development of the transverse facial artery is anatomically and functionally related inversely to the development of the facial artery. The facial artery may be underdeveloped and end as superior or inferior labial artery (see Sect. 5.1.8.7). In these cases the missing territory of the facial artery is "taken over" to a variable extent, by the ipsilateral transverse artery (Cormack and Lamberty 1994).

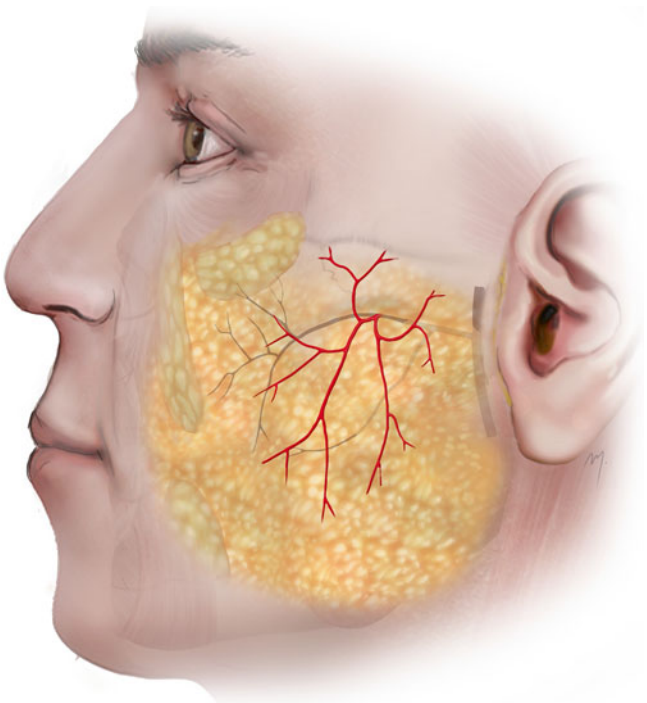

Fig. 5.18 Cutaneous perforator of the transverse facial artery

A giant and largely dilated transverse facial artery has also been reported to counterpoise the complete agenesis of a facial artery (Tubbs et al. 2005).

5.1.8.5 Buccal Artery

The buccal artery (Fig. 5.19) is a small branch that arises from the second part of the maxillary artery. It runs between the medial pterygoid and the attachment of the temporalis muscle, crosses the buccinator, and just anterior to the anterior edge of the masseter muscle pierces the buccal fat. It supplies the skin of an area over the buccinator muscle and anastomoses with branches of the infraorbital and facial artery.

The artery is located about 3 cm lateral to the oral commissure and at the same level 5 mm medial to the medial aspect of the masseter muscle.

5.1.8.6 Facial Artery (Facial Part)

The facial artery is a long, major facial vessel, with important branches, that starts from the carotid triangle and usually ends to the inner canthus. This long course can be distinguished into a cervical and facial part. The cervical part of the facial artery is the segment from its carotid artery origin to the point where it curves around the lower border of the mandible to enter the face (see Chap. 8).

The cervical part of the facial artery as it comes from the posterior aspect of the submandibular gland reaches the lower mandibular border, curves around it, passes just in front of the anterior edge of the masseter muscle, pierces the

Fig. 5.19 Buccal artery

deep fascia, and enters the face. At this point the facial artery, with its accompanying vein, lies immediately under the platysma and crosses with the mandibular branch of the facial nerve lying underneath it. When a dissection in this area is performed, it must be protected, as it lies very superficial at this point (where its pulsation is most palpable). In this region, its external diameter is about 2.6 mm (Pinar et al. 2005).

5.1.8.6.1 Facial Part

As the facial artery enters the face (Fig. 5.20), it courses tortuously up and forward toward the alar base, lying under the platysma and the fat of the cheek. It ascends passing lateral to the oral commissure in a distance that has been reported to range between 8 and 23 mm (Loukas et al. 2006a; Pinar et al. 2005; Park et al. 1994; Schulte 2001). Most of the time the facial artery is expected to be 1.5–2.0 cm lateral to the oral commissure and running up medial to the nasolabial fold (Fig. 5.21). The range of the distance from the oral commissure where the facial artery can be found is of great importance when designing a Gillies fan flap or a Karapandzic flap for lip reconstruction; the viability of these flaps requires an intact facial artery that must be identified and preserved.

Near the angle of the mouth, the facial artery is under the cover of the zygomaticus major (or it may pass through its insertion heads) and the risorius muscles. It is superficial to buccinator and levator anguli oris muscles. Here it gives off small branches to the anterior part of the buccinator and to the zygomaticus major muscles. Above the labial commissure level in the upper lip, the facial artery usually lies medially in relation to the nasolabial sulcus. Turning cephalad, it passes either over or through the levator labii superioris and runs along the side of the nose, usually through the levator labii superioris alaeque nasi, toward the inner canthus, where it anastomoses with the dorsal nasal artery. Partial myotomy of the above superficial muscles must be done to expose the facial artery in cases that it is needed in flap surgery. The buccal fat pad is situated under the artery at this point. The distal and terminal part of the facial artery, after giving off its last branch, the lateral nasal artery, is termed the angular artery.

The branches (Fig. 5.20) given off by the facial part are the premasseteric artery, the labiomental artery, the inferior and superior labial arteries (see Chap. 6), and the inferior alar and the lateral nasal arteries (see Chap. 4). As mentioned above the terminal part of the artery distal to its terminal branch is named angular artery.

The premasseteric artery is a small and not always present branch that arises at the lower border of the mandible and ascends along the anterior border of the masseter muscle. The labiomental artery is an inconstant branch running horizontally to the chin.

After giving off the lateral nasal artery, it ascends along the nasal side, immediately under the skin, giving off small branches and finally anastomoses with the dorsal nasal artery, which establishes the communication between the external and internal carotid arteries.

The mean distances of the points where the facial artery branches originate are shown in Fig. 5.21.

The facial part of the facial artery anastomoses with the mental artery, the transverse facial artery, the infraorbital artery, and the ophthalmic artery (due to the dorsal nasal artery).

The facial artery shows multiple (mean six) perforating branches that supply large areas of facial skin and are more densely located at the level of the commissure (Fig. 5.22).

5.1.8.7 Facial Artery Variations

The variations and the branching pattern of the facial artery have been investigated thoroughly (Mitz et al. 1973; Kozielec and Jozwa 1977; Midy et al. 1986; Niranjan 1988; Whetzel and Mathes 1992; Park et al. 1994; Crouzet et al. 1998; Nakajima et al. 2002; Pinar et al. 2005; Loukas et al. 2006a).

Surprisingly great differences exist, ranging from frequency of types of branching patterns, in their description and nomenclature (specifically regarding the arteries to the nose) among the investigators.

A variation of the facial arteries course is exhibited when the artery is underdeveloped, and thus, the artery does not reach its normal ending point.

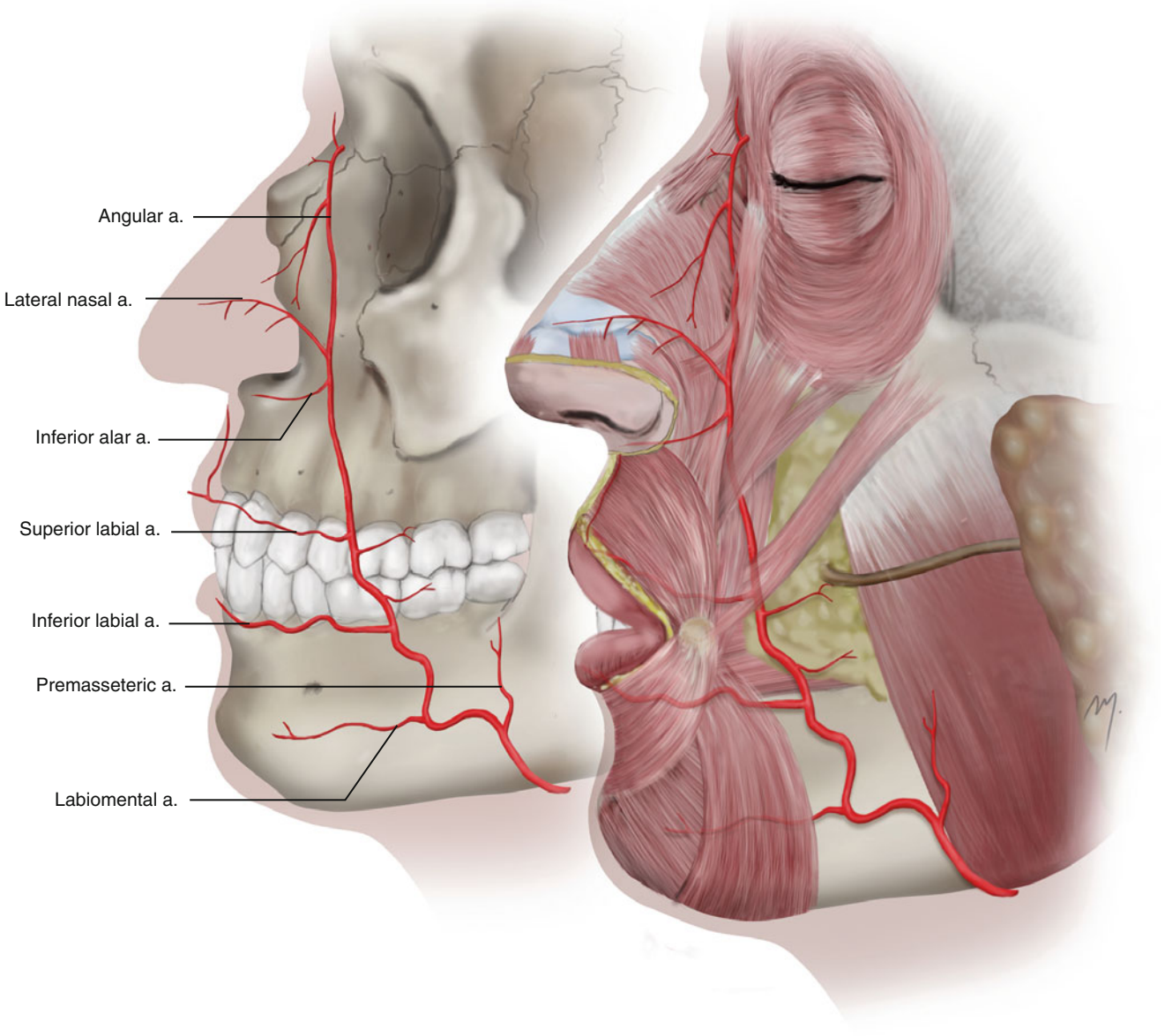

Fig. 5.20 The facial artery at the cheek

In general the result is that each type is missing a subsequent branch starting from the angular artery. Four major types of facial artery exist (Fig. 5.23). The first two types are the most common and represent about the 90 % of cases.

5.1.8.7.1 Typical

In the typical form, the facial artery is completely developed and ends with its final angular artery.

5.1.8.7.2 Ending as Lateral Nasal

In this form, the angular artery is absent and the facial artery ends to its lateral nasal branch. In this type, sometimes the angular artery is present as "ectopic." It arises individually at the level or from a slightly lower point of the commissure and ascends to the inner canthus.

5.1.8.7.3 Ending as Superior Labial

When both angular and lateral nasal arteries are not present, the facial artery ends to the superior labial artery. In these cases, often a "reverse" inferior alar artery is branched from the columellar artery and courses along the inferior margin of the nostril.

5.1.8.7.4 Ending as Inferior Labial

In very rare cases, the facial artery consists, in its facial part, only of the inferior labial artery.

In the various types where the facial artery is underdeveloped, other neighboring arteries of the face—infraorbital, ophthalmic, transverse facial, or even a hyperdeveloped contralateral—assume the role of supplying the area.

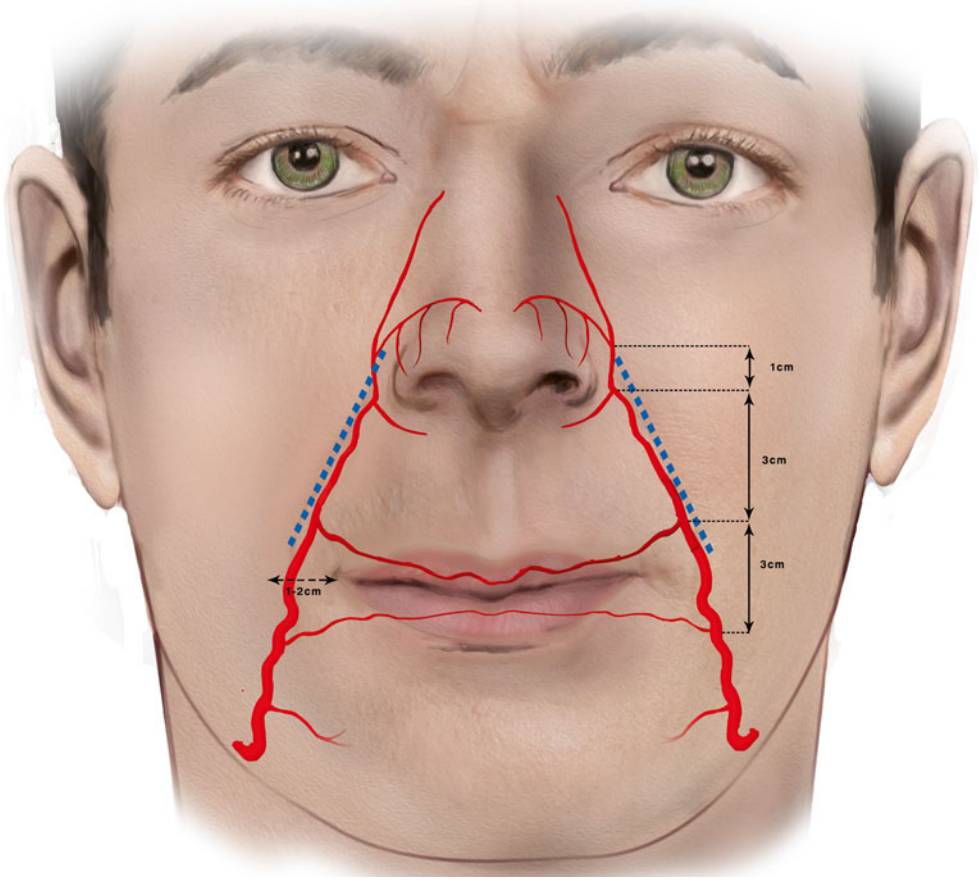

Fig. 5.21 The facial artery passes 1–2 cm lateral to the oral commissure and usually lies medial to the nasolabial fold (*blue dotted line*). The mean distances of the origin points of the facial artery branches are indicated

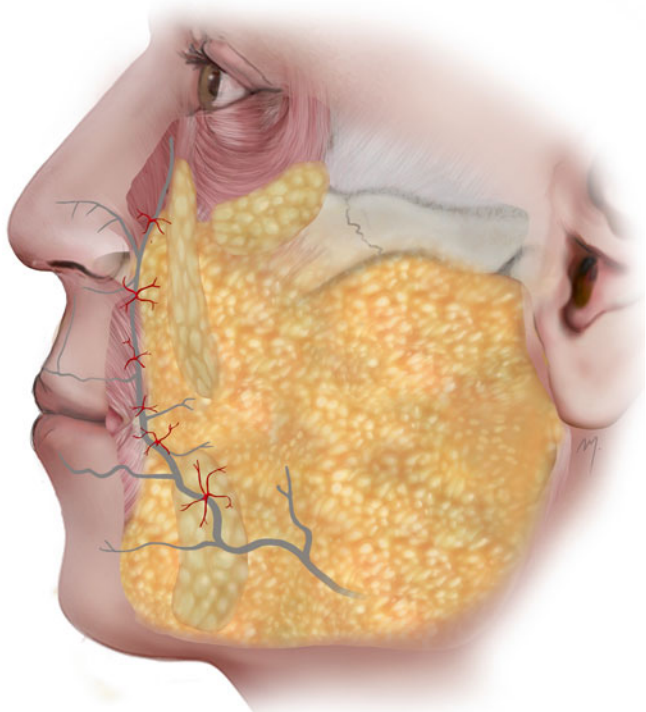

Fig. 5.22 Facial artery perforators to the skin

It has been clarified that contrary to what previously had been believed, no ethnic differences exist in the pattern of the facial artery branching (Koh et al. 2003; Loukas et al. 2006a).

5.1.9 Venous Drainage

The small veins of the cheek generally follow the associated arteries and converge to larger ones that drain to the named larger veins of the cheek. The facial vein provides the major venous drainage to the cheek. It appears to the cheek (Fig. 5.24) as continuation of the angular vein running at the side of the nose (see Chap. 4).

The facial vein continues running within the buccal space lying above the buccal extension of the buccal fat pad. Although the facial vein runs in a same direction as the facial artery it is situated posterior to the facial artery in a variable distance. At the level of the nasal ala the mean distance of the facial vein and artery has been measured to be 16.3 mm and at the oral commissure 13.6 mm (Zhao et al. 2000). As the facial vein proceeds to the lower border of the mandible it approximates the artery and the two vessels run in close prox-

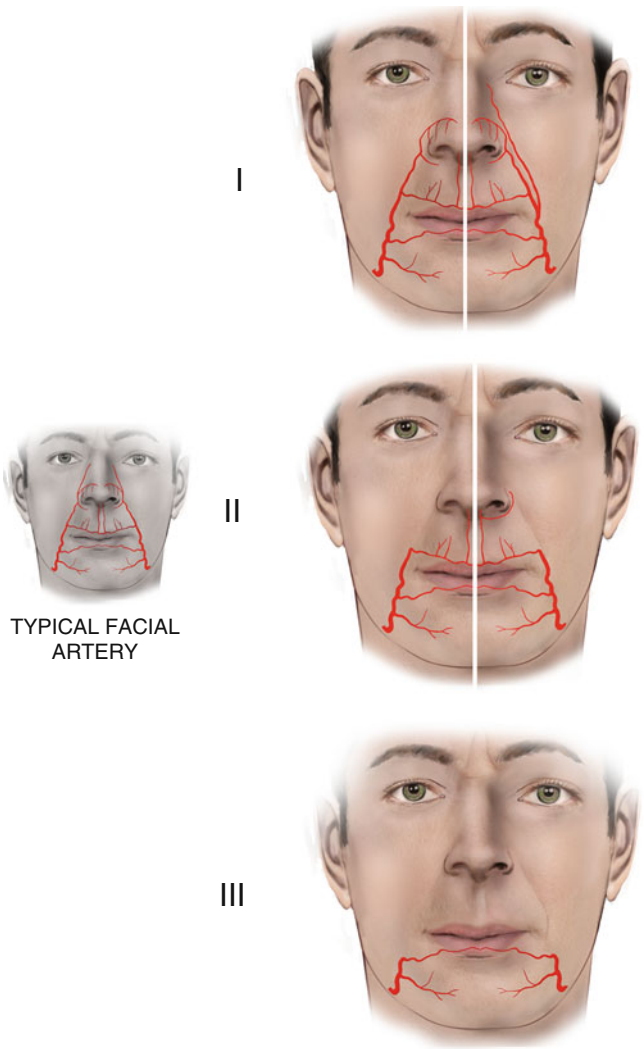

Fig. 5.23 Facial artery variations

imity. It crosses the lower mandibular border lying beneath the platysma and continues down in the neck where it drains into the common facial vein and the internal jugular vein.

The facial vein at the cheek receives the lateral nasal (superior alar) and the inferior alar veins of the nose, the venae commitante of the lips, and the buccinator and masseteric veins. It communicates also with the infraorbital vein.

The transverse facial, infraorbital, mental, and buccal veins contribute to the venal system of the cheek draining the first into the superficial temporal vein and the next three into the pterygoid venous plexus.

5.1.10 Sensory Innervation

Sensory innervation of the cheek comes from the infraorbital nerve and zygomaticofacial nerve, branches of the maxillary division of the trigeminal nerve, and the auriculotemporal, the mental, and the buccal nerves, branches of the mandibular division, the third and largest division, of the trigeminal nerve (Fig. 5.25). The anterior branch of the great auricular nerve (C2-C3) with its final filaments, contributes to the innervation of the skin of the parotidomasseteric region.

5.1.10.1 Infraorbital Nerve

The intraorbital continuation of the maxillary nerve just after it passes through the inferior orbital fissure is named the infraorbital nerve constituting actually the terminal branch of the maxillary nerve. It courses on the floor of the orbit along the infraorbital groove in common course with the infraorbital artery and enters the infraorbital canal.

The infraorbital nerve (Fig. 5.26) exits to the face through the infraorbital foramen. It lies under levator labii superioris and over levator anguli oris muscles and divides into its terminal palpebral, nasal, and superior labial branches. The terminal branches of the infraorbital nerve in about 40 % of the cases exit the infraorbital foramen as a completely separated bundle; in the remainder they may be fused and separate after a short course (Hu et al. 2006).

The palpebral branches of the infraorbital nerve run upward under the cover of the orbicularis oculi muscle, and after piercing it they distribute to the skin of the lower eyelid. Near the lateral canthus, they anastomose with branches of the facial and zygomaticofacial nerves. The nasal branches of the infraorbital nerve distribute to the skin of the lateral side of the nose and to the ala. They anastomose with the external nasal nerve. The multiple superior labial branches are the larger one. They run inferiorly under cover of the levator labii superioris muscle and are distributed to the skin and the mucosa of the anterior part of the cheek and the upper lip. They anastomose with filaments of the facial nerve.

The infraorbital foramen is located at a point usually 8–10 mm below the inferior orbital rim and approximately 25–30 mm from the midline (Fig. 5.27). This point may range between 3 and 15 mm from the inferior orbital rim and between 18 and 33 mm from the midline (Aziz et al. 2000; Chrcanovic et al. 2011).

5.1.10.1.1 Infraorbital Nerve Blockade

Excision of small or medium lesions and minor flap reconstruction can be achieved by local or better by regional anesthesia. The infraorbital block provides anesthesia to the half of the upper lip in its whole thickness and can be performed either extraorally or intraorally (Fig. 5.28).

For an extraoral nerve block, the infraorbital foramen is palpated inferior to the infraorbital rim. If this is unclear, then the point of injection is situated 2.5 cm lateral to the midline and 1 cm below the orbital rim. At this point about 1 ml of local anesthetic solution is injected just above the bone with the needle carried slightly cephalad. Entering the foramen should be avoided because direct injection within the foramen may result in nerve damage.

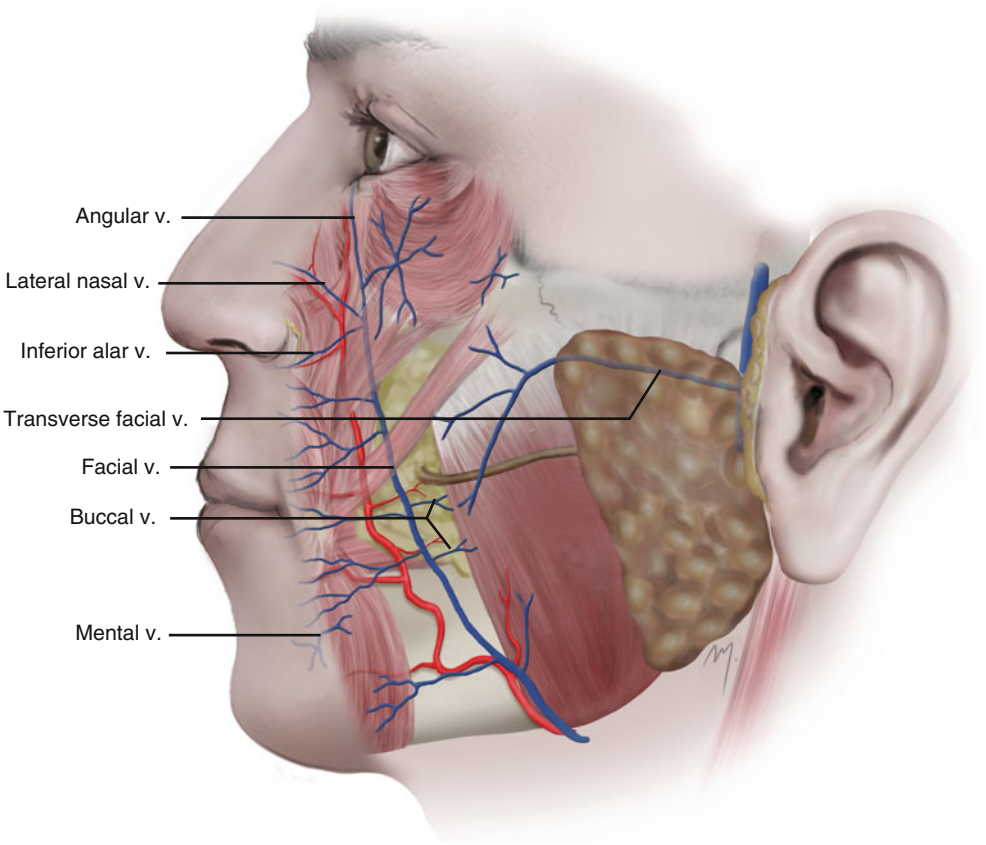

Fig. 5.24 The venous drainage of the cheek

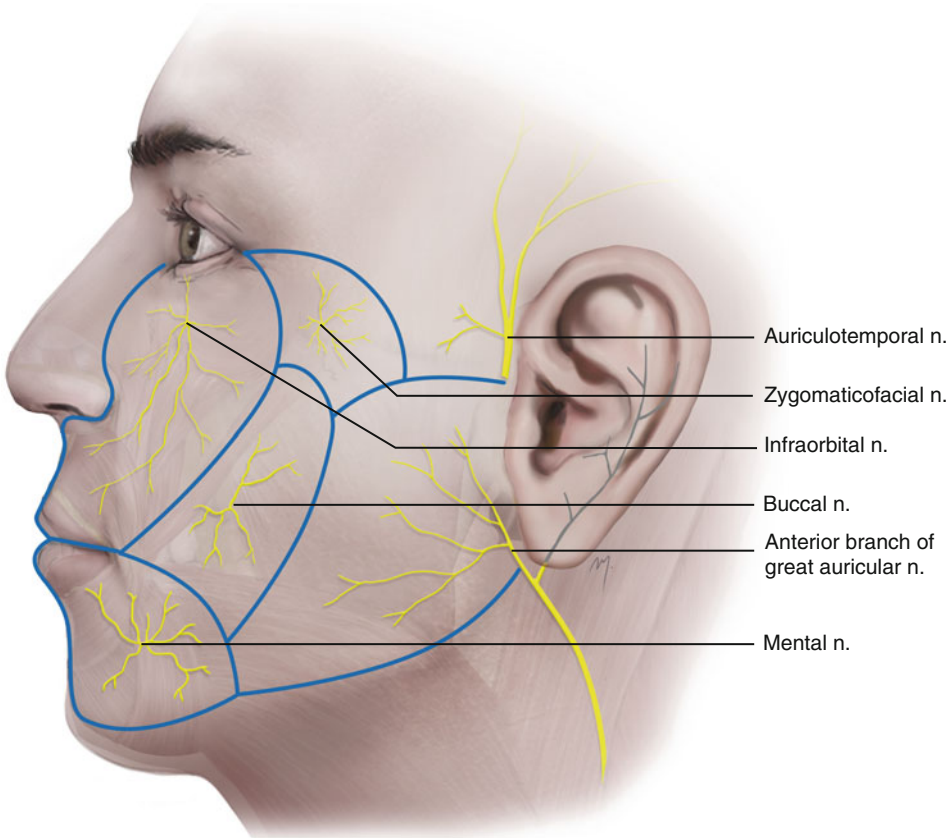

Fig. 5.25 Sensory innervation of the cheek

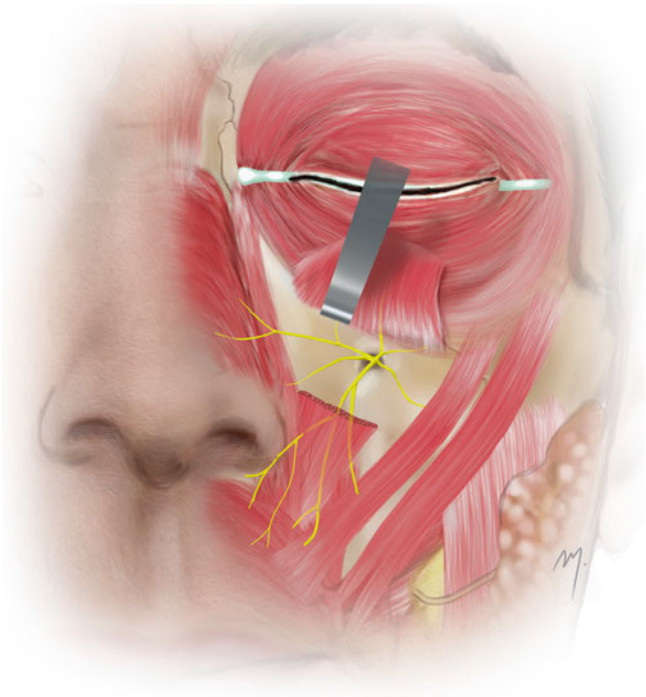

Fig. 5.26 The infraorbital nerve

At an intraoral block of the infraorbital nerve, the needle is inserted slightly lateral to the buccal sulcus above the first premolar teeth. It proceeds upward, parallel to the long axis of the first premolar and targeting the infraorbital foramen. When the tip of the needle is palpated near the foramen, the anesthetic solution is injected.

5.1.10.2 Zygomaticofacial Nerve

The zygomaticofacial nerve is the second of the two branches of the zygomatic nerve along with the zygomaticotemporal nerve (see Chap. 2) that is branched from the maxillary nerve and runs along the inferolateral border of the orbit.

The zygomaticofacial nerve exits the face (Fig. 5.29) through the zygomaticofacial foramen that is situated in the zygomatic bone 2 cm lateral and 2 cm inferior to the lateral canthus. It pierces the overlying orbicularis oculi muscle and distributes in an area to the skin over the prominence of the cheek up to the lateral canthal area. It anastomoses with the zygomatic branches of the facial nerve and the palpebral branches of the maxillary nerve.

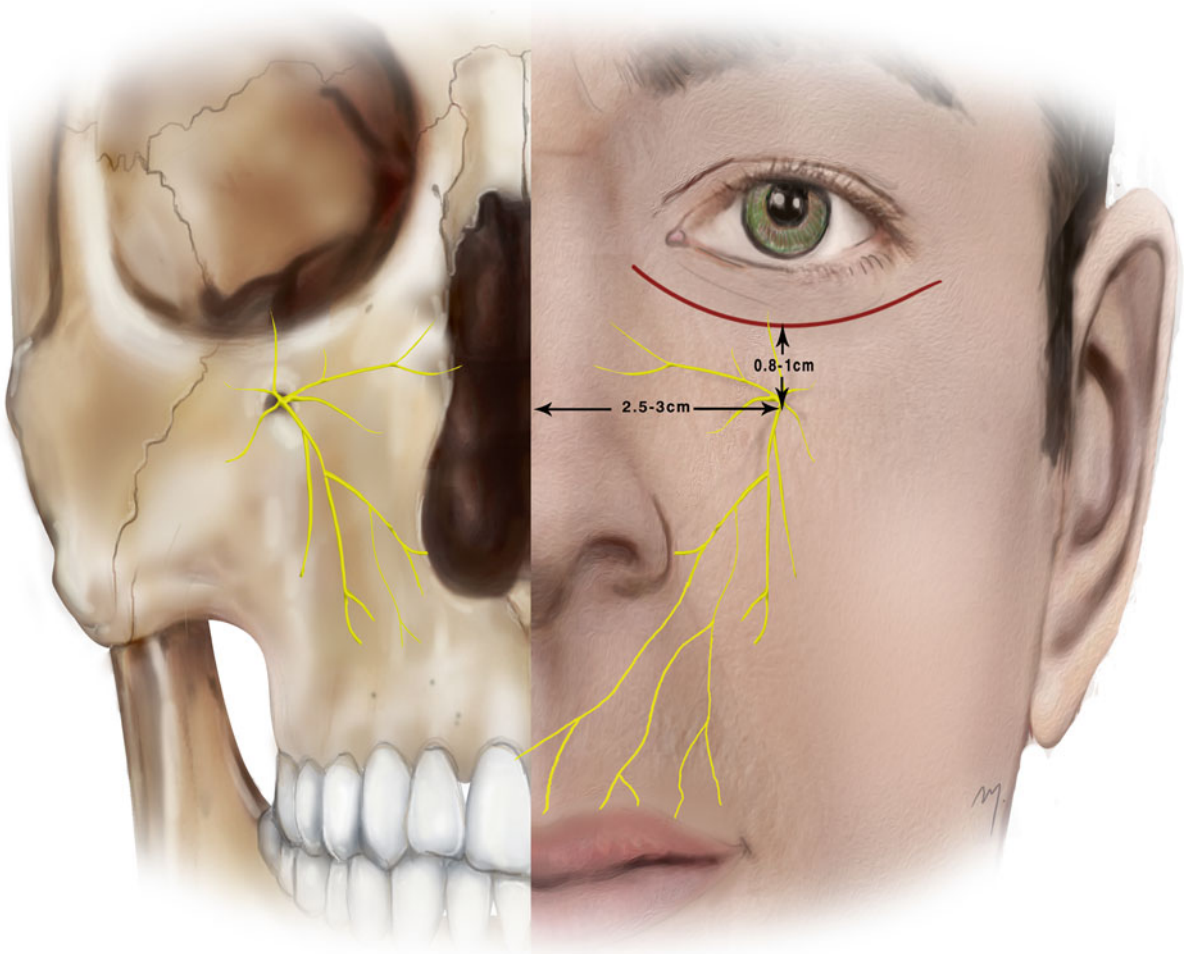

Fig. 5.27 Landmarks of infraorbital nerve

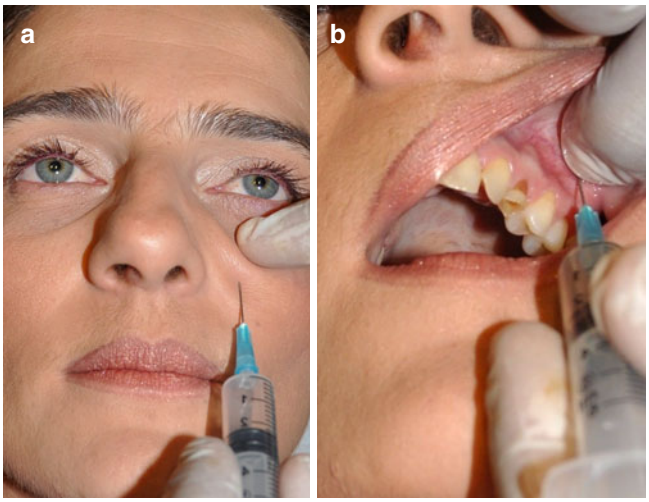

Fig. 5.28 Block of the infraorbital nerve. (**a**) Extraorally. (**b**) Intraorally

Fig. 5.29 Zygomaticofacial nerve

5.1.10.3 Auriculotemporal Nerve: Preauricular Course

Although the auriculotemporal nerve supplies only in a small part of the posterior zygomatic subunit, its first part runs at the cheek just in front of the auricle together with the superficial temporal artery and vein.

The auriculotemporal nerve is a branch of the posterior trunk of the mandibular nerve and is located at the posterior

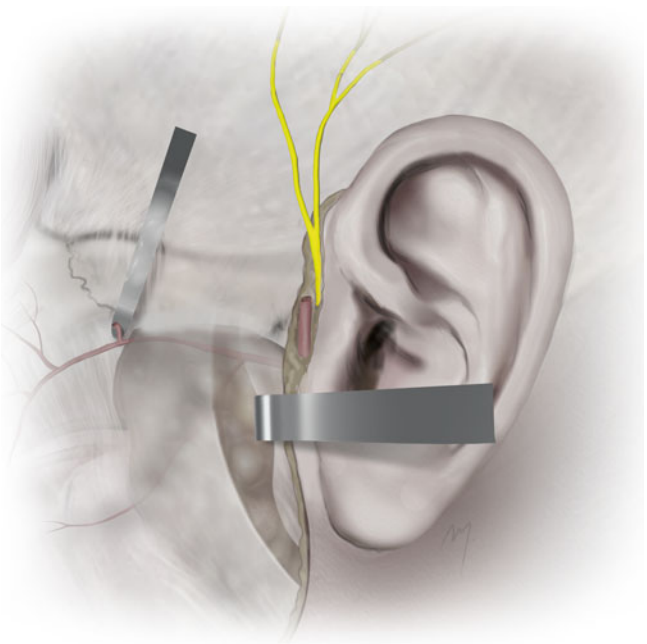

Fig. 5.30 Auriculotemporal nerve at the cheek

border of the cheek. As the mandibular nerve descends from the foramen ovale and after giving off the nervous spinosus (meningeal branch) and the nerve to the medial pterygoid, it divides into an anterior and a posterior trunk. The posterior trunk gives off the auriculotemporal nerve along with the lingual and inferior alveolar nerves.

The auriculotemporal nerve arises from the mandibular nerve mostly by one or two and seldom by three or four roots. In the cases where it arises by two roots, these usually encircle the middle meningeal artery. It then runs backward lying on the surface of tensor veli palatini and under the lateral pterygoid muscles and passes between the neck of the mandible and the sphenomandibular ligament.

The auriculotemporal nerve exits the cheek (Fig. 5.30) behind the temporomandibular joint within the superficial substance of parotis. It then runs upward, passing over the posterior root of the zygomatic arch to the temporal area.

The auriculotemporal nerve runs parallel to the superficial temporal artery located in 80 % superficial or posterior to it (Jeong et al. 2010). It is of clinical interest that the auriculotemporal nerve in about one-third (30 %) has a direct relationship with the temporal artery that could constitute a trigger for migraine headaches (Janis et al. 2010). In its course it gives off branches to the external acoustic meatus and the anterior portion of the auricle, the temporomandibular joint, the parotis, and over the zygomatic arch the final superficial temporal branches (see Chap. 2).

5.1.10.4 Buccal (Sensory) Nerve

The buccal nerve is branched from the anterior trunk of the mandibular nerve (V3) at the infratemporal fossa. It runs

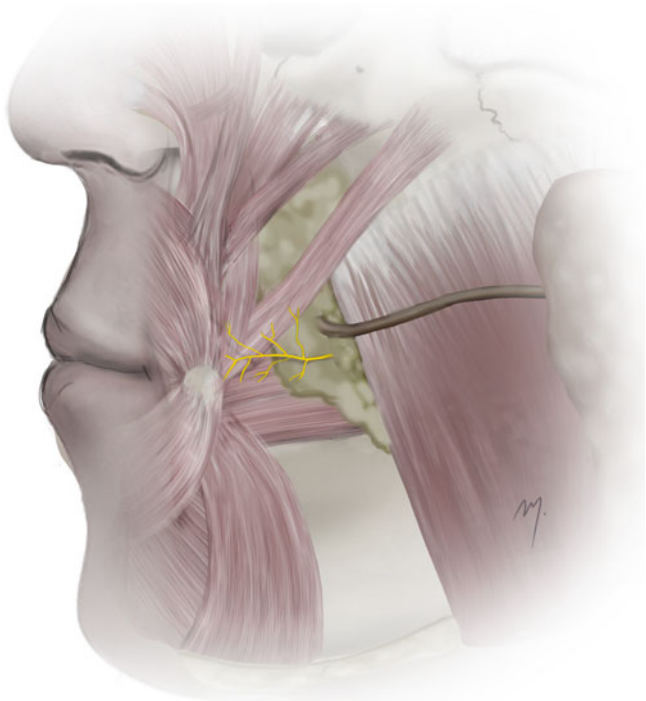

Fig. 5.31 Buccal nerve

anteriorly between the two heads of the lateral pterygoid and then inferiorly through the lower part of the temporalis muscle, continuing to the undersurface of the mandibular ramus.

The nerve appears in the cheek (Fig. 5.31) close to the anterior border of the masseter muscle, superficial to the buccinator muscle, and anastomoses with buccal branches of the facial nerve (Standring 2008). It supplies the skin and mucosa of the central part of the cheek.

5.1.10.5 Mental Nerve

The mental nerve, after its exit through the mental foramen, results in branches that mainly supply the chin and the lower lip (see Chap. 6) but it also contributes due to some short rami to the innervation of the nearby cheek skin.

5.1.10.6 Great Auricular Nerve

The anterior branch of the great auricular nerve (see Chap. 8) due to its final filaments innervates the skin of the parotidomasseteric area.

5.1.11 Motor Innervation

Motor innervation of the mimic muscles that are distributed to the cheek comes from the peripheral branches of the facial nerve. There is a highly variable anatomy in the branching pattern of the facial nerve and in the course of these branches to the cheek, temple, and neck, and what follows is an averaged description.

5.1.11.1 Facial Nerve

The facial nerve trunk exits the posterior cranial fossa entering the temporal bone via the internal acoustic meatus. After coursing through the facial (Fallopian) canal, it emerges from the base of the skull at the stylomastoid foramen.

5.1.11.1.1 Extratemporal Course

At this point, the main nerve trunk lies in a depth of approximately 2–2.5 cm, in front of the mid-earlobe. But the classical precise landmarks useful in parotid surgery are the cartilaginous tragal pointer of the external auditory canal with the nerve situated 1 cm deep and inferior to this, the tympanomastoid suture line where the trunk is identified 6–8 mm below it, and the posterior belly of digastric where the nerve lies 1 cm deep to this.

As the facial nerve emerges from the stylomastoid foramen, it gives off the digastric branch for the posterior belly of the digastric muscle, the stylohyoid branch for the stylohyoid muscle, and communicating branches with the transverse cervical nerve and the posterior auricular nerve (see Chap. 2).

It then runs anteroinferiorly over the styloid process for a distance approximately 12 mm and enters the parotis through its posteromedial surface.

5.1.11.1.2 Intraparotid Course

Within the parotid gland, the nerve soon divides into its two primary trunks, the temporofacial (superior) trunk and cervicofacial (inferior) trunk lying over the retromandibular vein and the external carotid artery. The two primary trunks branch further resembling the so-called "pes anserinus" (goose's foot) and form the parotid plexus. The presence of the facial nerve plexus within the parotid substance divides the gland into its surgically so-called superficial and deep "lobes."

From the two main temporofacial and cervicofacial trunks that form the parotid plexus, the facial nerve gives rise to five main terminal branches. These branches diverge within the parotid gland and exit the gland by its anterior margin. The five terminal branches supply the mimic muscles of the face and are named according to the region that they are distributed: temporal (or frontal), zygomatic, buccal, marginal mandibular, and cervical. The facial nerve, within the parotid substance, courses superficially to the retromandibular vein. The inferior branches of the facial nerve in 5–10 % of the cases have been reported to lie deep to the retromandibular vein (Wang et al. 1991; Kopuz et al. 1995).

The terminal branches of the facial nerve can be predicted to exit the anterior margin of the parotis, approximately 4 cm anterior to the tragus along the transverse axis of the zygomatic arch (Wilhelmi et al. 2003).

5.1.11.1.3 Frontal Branch

The frontal (temporal) branch of the facial nerve (Fig. 5.32) runs mostly at the temple to supply mainly the mimic

Fig. 5.32 The facial nerve

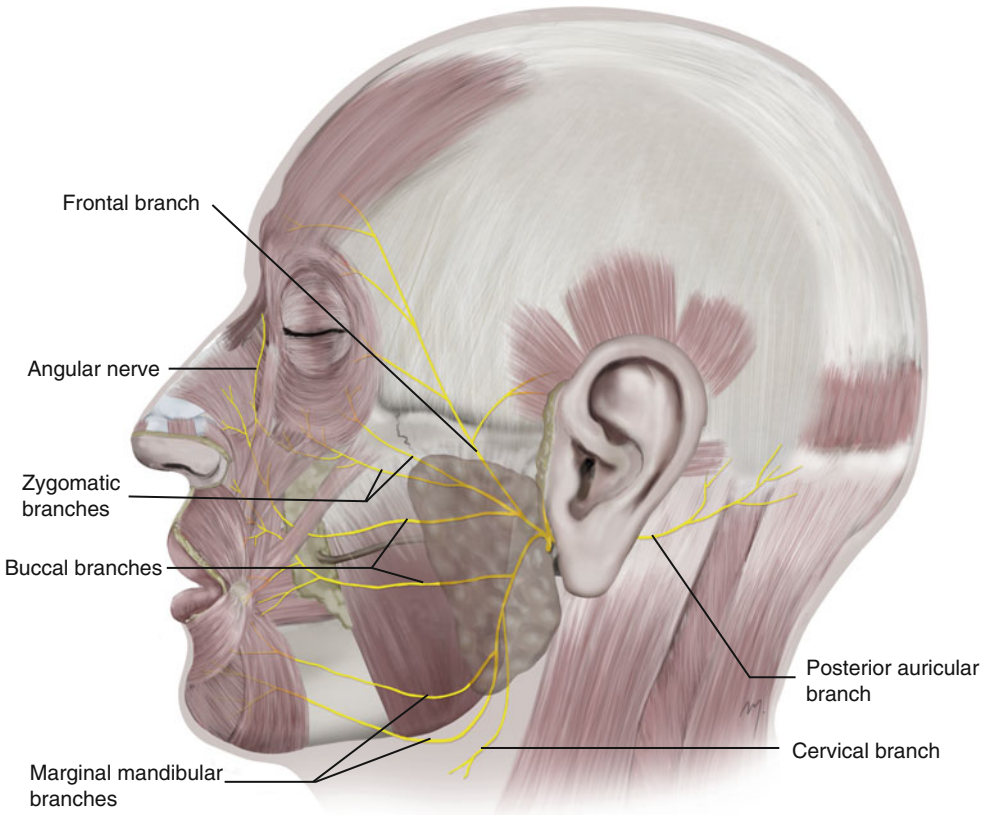

muscles that surround the upper and lateral orbit. At the cheek area, the nerve is involved due to its initial course at the zygomatic subunit: The frontal branch arises from the temporofacial trunk and leaves the upper border of the parotid gland. It travels deep to the parotidomasseteric fascia toward the middle third of the zygomatic arch. As it crosses the superficial surface of the zygomatic arch, it divides into two to four rami. Above the zygomatic arch, it travels along the undersurface of the temporoparietal fascia (Stuzin et al. 1989). The area of increased nerve jeopardy is the zone where the nerve crosses the zygomatic arch. At this area the nerve lies very superficial even within the temporoparietal fascia as stated by Stuzin et al. (1989) or in a deeper plane, over the periosteum, as stated by Owsley and Agarwal (2008) and Trussler et al. (2010) (see Chap. 2).

5.1.11.1.4 Zygomatic Branch

The zygomatic branch (Fig. 5.32) arises from the temporofacial trunk of the facial nerve division usually as two or three rami and very rare as a single ramus (70, 27, and 3 % respectively) (Saylam et al. 2006a).

Course

After emerging from the posterior border of the parotid gland, the zygomatic branches course initially below the lower border of the zygomatic arch under cover of the parotidomasseteric fascia. As they reach the orbicularis oculi muscle, they travel through the SOOF becoming more superficial and innervate the muscle from its undersurface. The superior ramus crosses the zygomatic bone in the same depth as the frontal branch of the facial nerve, ascends to the lateral orbital rim and innervates the lateral part of the orbicularis oculi muscle. Some tiny branches may be encountered traveling to the lower lateral border of the orbicularis oculi muscle over the zygomaticus major muscle.

The inferior ramus continues medially to the infraorbital region, passing below the origin of the zygomaticus major muscle, and innervates the lower part of the orbicularis oculi muscle from its undersurface. Precisely the orbicularis oculi muscle is supplied by means of neural plexuses. The superior ramus of the zygomatic nerve forms an anastomotic plexus with the temporal branches of the facial nerve that supplies the superolateral part of the orbicularis oculi, and the inferior ramus forms a same plexus with connections to the buccal branch that supplies the inferolateral part of the orbicularis oculi muscle (Ouattara et al. 2004). Small branches of the inferior ramus innervate the upper part of the upper lip levators. Typical neural interconnections between the zygomatic and the buccal branches exist, but furthermore they form also the angular nerve (see below).

The course of the zygomatic branch lies always under the oblique line that connects the tragus and the lateral palpebral

commissure, and from the midpoint of this line, its vertical distance varies from 6 to 29 mm (mean 19 mm) (Saylam et al. 2006a).

5.1.11.1.5 Buccal Branch

The buccal branch (Fig. 5.32) originates from either the temporofacial trunk or the cervicofacial trunk, or from both of them.

Course

The buccal branch emerges from the parotid gland usually (60 %) as a double branch (an upper and a lower) or as single (40 %). It runs horizontally forward, beneath the parotidomasseteric fascia in close relation to the parotid duct. When presented as one branch, it runs in most of the cases inferior to the duct, and when the buccal branch is presented as dual, the upper branch runs superior and the lower branch inferior to the duct. The mean vertical distance of the buccal branch either inferior or superior to the parotid duct is 5.5 mm (range between 1 and 14 mm) (Pogrel et al. 1996). The buccal branches (or a single branch), after emerging from the anterior border of the parotis, run over the masseter muscle fascia (which must not be confused with the overlying parotidomasseteric fascia). It crosses superficial to the buccal fat pad but sometimes (26 %) small branches of the nerve pass through the buccal extension of the buccal fat pad (Hwang et al. 2005). As it passes over the buccinator muscle, it sends rami to it and, finally, results in its final subbranches. The lower subbranches enter to the inferior segments of the orbicularis oris muscle and the upper portion of the depressor anguli oris muscle from their undersurface and innervate them. The upper subbranches continue under the cover of the zygomaticus major and the upper lip levator muscles but run above the levator anguli oris muscle and reach the upper segments of orbicularis oris muscle from its undersurface. They innervate the upper part of the orbicularis oris muscle and the lower part of the upper lip levators and lower part of the nasal muscles. In cases where a second (upper) branch is present, it runs also beneath the zygomaticus major and the upper lip levator muscles and supplies the same former muscle groups.

Caminer et al. (2006) found that the buccal branch, after receiving a contribution from the zygomatic branch, forms a branch and term it the angular nerve, which runs superiorly, crosses over the medial canthus, and supplies the medial part of orbicularis oculi, the procerus, and a part of the corrugator (oblique head) (Caminer et al. 2006).

The buccal branch of the facial nerve is connected to the sensory buccal nerve of the mandibular nerve (Rodel and Lang 1996) and to the external nasal nerve. Moreover, it anastomoses with the inferior ramus of the zygomatic nerve, forms a plexus, and participates in the innervation of the inferolateral part of the orbicularis oculi muscle (Ouattara et al. 2004). As mentioned above it participates along with the inferior ramus of the zygomatic nerve to the formation of the inferolateral orbital nerve plexus (Ouattara et al. 2004).

5.1.11.1.6 Marginal Mandibular Branch

The marginal mandibular branch (Fig. 5.32) originates from the cervicofacial trunk of the facial nerve.

Course

It emerges from the caudal border of the parotis usually as two branches (60–65 %) and less often as one branch (23 %). Three branches occur seldom (9 %). Rarely (3 %), the marginal mandibular branch may be present as four branches (Dingman and Grabb 1962; Ziarah and Atkinson 1981). The emergence point of the nerve from the parotis is usually on the mandibular angle level, or very close to it.

The marginal mandibular branch passes in a trajectory that runs to the lower border of the mandible and then curves up and forward to the lower lip and chin. In this course it has an importance to surgery in relation to the inferior border of the mandible. In a variable percentage of approximately 47–80 %, the nerve runs superior to the lower border of the mandible and in the remainder inferiorly to the lower border (Dingman and Grabb 1962; Ziarah and Atkinson 1981). In the later cases, the marginal mandibular branch, running down, crosses once across the inferior border of the mandible and, turning up, crosses it again for the second time in the vast majority of people, at the point where the facial artery crosses the mandible or posterior to it and, rarely, anterior to this point. When the marginal mandibular branch appears having more than one branches, these are distributed the same superiorly and inferiorly in relation to the lower border of the mandible. The marginal branch when coursing below the inferior border of the mandible runs in a variable distance from it, usually up to 1.5–2 cm. Incisions that are placed at least 3 cm below the inferior border always ensure the integrity of the nerve.

The classic descriptions of the anatomy of the marginal mandibular branch of the facial nerve refer that the nerve runs deep to the platysma. However, Owsley and Agarwal (2008) "put" the nerve in a deeper plane and described the detailed and accurate planar anatomy of its course. According to them, the marginal mandibular nerve emerges from the parotid and initially lies deep to the parotidomasseteric fascia or its neck continuation: the investing layer of the deep cervical fascia when a branch (or branches) extends below the lower mandibular border. Near the point where the facial artery curves around the mandibular border, the marginal mandibular nerve penetrates the parotidomasseteric fascia (investing layer of the deep cervical fascia) that continues immediately deep to the platysma, changing level and becoming more superficial. The nerve is at great risk in thin patients with a thin layer of subcutaneous tissue. Moreover

the variability in thickness and development of the platysma muscle that also in older patients might be very thin in this area make it difficult to determine clearly the anatomy of the fascial layers, jeopardizing even more the mandibular branch.

The nerve crosses the anterior facial vessels always lying superficially to them. Continuing forward becomes more superficial and penetrates the muscles of the lower lip and chin to their undersurface.

The marginal mandibular branch supplies the risorius, the inferior part of the orbicularis oris, the depressor anguli oris, the depressor labii inferioris, and the mentalis muscles. It shows interconnections with the buccal, the zygomatic, and the cervical branches of the facial nerve and the sensory mental nerve (Schwember and Rodrigez 1988; Rodel and Lang 1996; Hwang et al. 2007b).

5.1.11.1.7 Cervical Branch

The cervical branch originates from the cervicofacial trunk of the facial nerve, usually as one and seldom as two branches, and travels down to the neck to innervate the platysma muscle (see Chap. 8).

5.1.11.1.8 Branching and Anastomotic Patterns of the Facial Nerve

In an attempt to sort out the variability of the branching pattern and the existing anastomoses of the facial nerve, Davis et al. (1956), in their classic anatomic study of 350 facial nerves, grouped these in six types.

Type I

In type I (13 %), no anastomoses occur between the adjacent branches and the five terminal branches spread out to the face in a radial form.

Type II

In type II (20 %), anastomoses occur between the various branches of the temporofacial trunk, to a distal point beyond the anterior border of the parotis.

Type III

In type III (28 %), a single and large anastomotic branch, which runs beyond the anterior margin of the parotis and crosses the parotid duct, connects the temporofacial and the cervicofacial trunks.

Type IV

In type IV (24 %), anastomotic branches, forming loops, exist between the temporal, zygomatic, and buccal branches.

Type V

Type V (9 %) is characterized by two anastomotic branches that connect the cervicofacial with the temporofacial trunks.

Type VI

In type VI (6 %), a rich anastomotic network exists connecting all of the branches of the facial nerve except for the cervical one.

5.2 Flaps Derived from the Cheek

All types of local flaps can be derived from the cheeks providing a wide range of restoration options. Random pattern advancement, transposition, and rotation flaps work well in this region and are used to reconstruct primarily the cheek itself, but also the nearby nose, lips, and lower lid.

5.2.1 Flap Design Concerning Vascular Anatomy

The blood supply of the cheek skin is mainly originating from branches of the facial, transverse facial, and infraorbital arteries. The rest of the arteries encountered at the cheek supply smaller areas that often overlap to the major vascular territory of the facial, transverse facial, and infraorbital arteries (Fig. 5.33). Neighboring arteries also contribute to the cheek skin perfusion at its periphery. For instance, the zygomaticoorbital artery, an artery that runs at the temple, supplies the skin of the zygomatic subunit. Likewise the submental artery contributes to the supply of the inferior cheek.

The skin of the cheek receives its blood supply from cutaneous and myocutaneous perforators that diverge from the underlying arteries and form the arterial plexuses. As already mentioned important cutaneous perforators are derived from the transverse facial and facial arteries.

Due to the rich anastomotic network that exists at the cheek, extensive collateral flow is ensured even from adjacent vascular territories. This enables the cheek to provide safely all types of local flaps wherever they will be based. Hence the decision on choosing what type and where to base a cheek flap accounts more in the factors out of the strict vascular anatomy.

5.2.2 Danger Zones of the Facial Nerve at the Cheek

The facial nerve is fully protected, without any risk during flap surgery, as long as it remains within the parotis, forming its plexus. The terminal branches exit the anterior margin of the parotis, as already mentioned, approximately 4 cm anterior to the tragus along the transverse axis of the zygomatic arch (Wilhelmi et al. 2003). As the branches of the facial nerve travel through the fascial layers, they course to superficial planes in predicted areas which constitute zones where the nerve is in increased jeopardy during surgery (Fig. 5.34).

The danger zone where the temporal branch is in great risk is the zone where it crosses the zygomatic arch. This zone with high rate of accuracy corresponds to the middle third of the zygomatic arch.

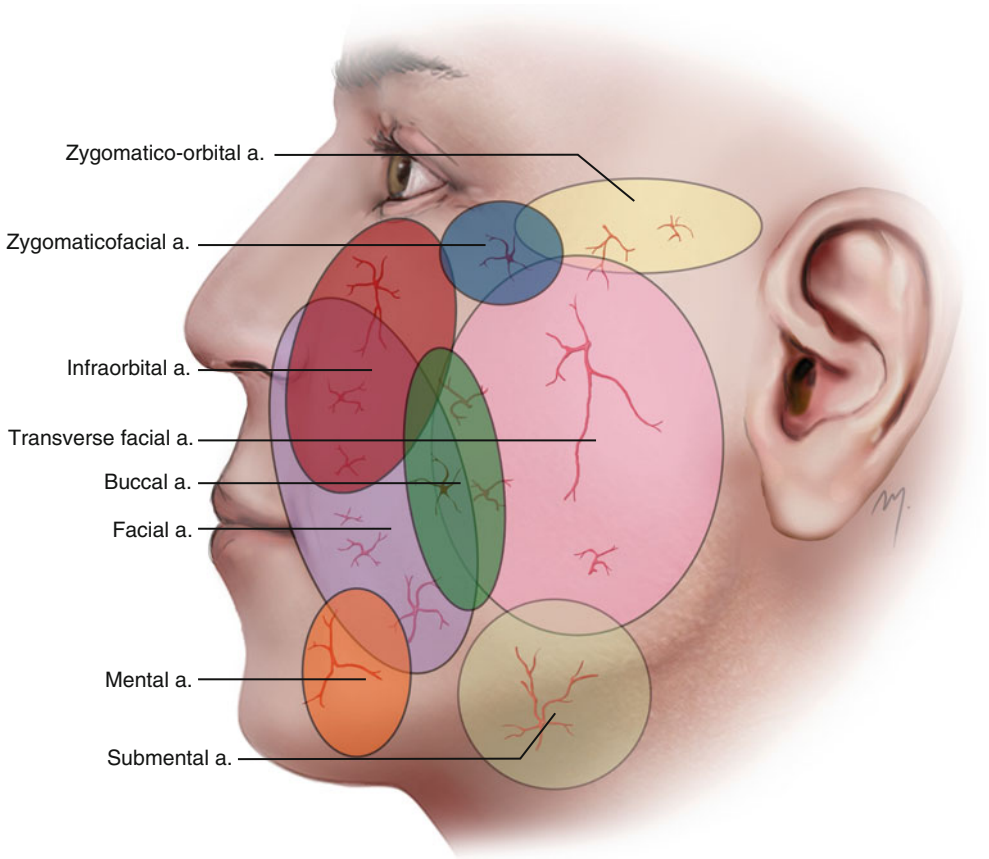

Fig. 5.33 Vascularization of the cheek skin

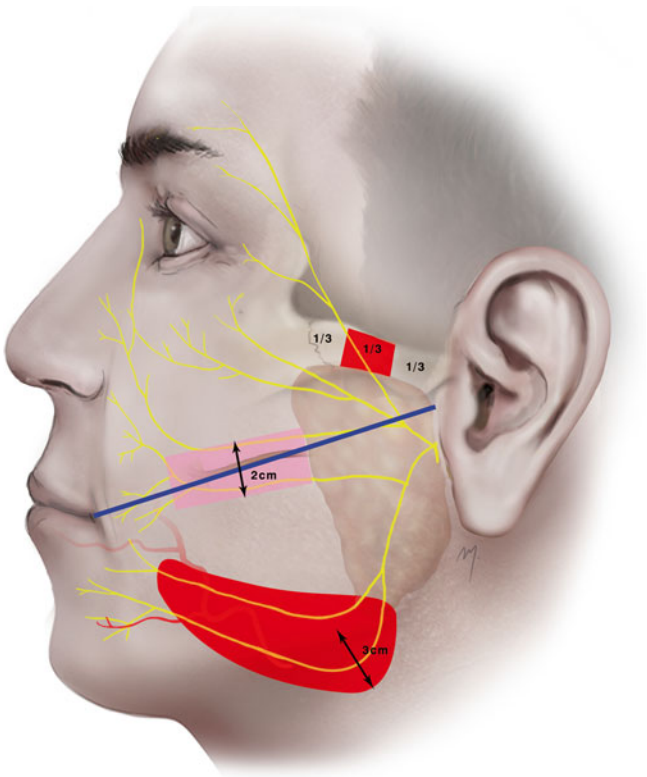

Fig. 5.34 Zones at risk of the facial nerve at the cheek. *Red* indicates the zones where the facial nerve is at great risk. *Purple* indicates the zone where the facial nerve is at a relative risk

The marginal mandibular branch(es) is in great risk within a zone 2 cm above and 3 cm below the inferior mandibular border extending at the buccal and submandibular areas, and its frontal tip curves above the inferior border of the mandible at the anterior border of the masseter muscle (location of facial artery).

The buccal branch is in a relative risk as long as it travels in a deep plane and is at risk of injury more frequently in flap elevation at the sub-SMAS plane (see below). The buccal branch, either one or two, is expected to be found at the buccal area usually in a zone of 1 cm above and 1 cm below the line that connects the oral commissure to the tragus.

5.2.3 Flap Elevation Concerning Anatomic Planes

A flap derived from the cheek can be raised in the subcutaneous level or in a deeper level below the SMAS layer.

5.2.3.1 Subcutaneous Dissection Plane

Most of the flaps that are derived from the cheek are elevated at the subcutaneous plane (Fig. 5.35). This is the safest plane of elevation, so far as all of the vital anatomic structures lie beneath the SMAS.

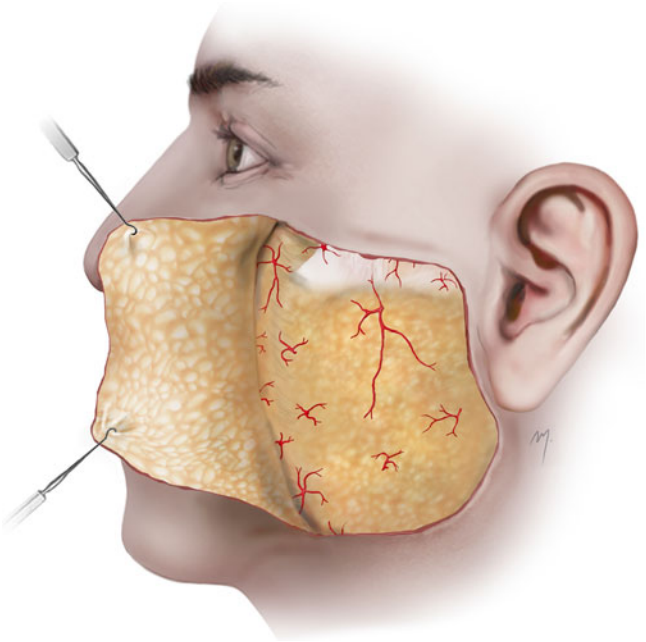

Fig. 5.35 Dissection in the subcutaneous plane

The flap consists of skin and subcutaneous tissue and is raised by sharp dissection. Several perforating vessels coming from deep to the skin are encountered and transected but bleeding is easily controlled by cauterization.

The thickness of the flap depends not only on the depth of the excised area, thus the needed volume that has to be restored, but also of the extent of the flap that has to be raised. Small flaps can be raised just dissecting between the subcutaneous fat, leaving a portion of fat below the skin and a portion above the SMAS. Given that almost most of the flaps that are derived from the cheek are of random pattern, those of great extent must be elevated in a deep subcutaneous level, thick enough to include enhanced vascular supply. Even though the subcutaneous plane is a safe plane, when dissecting deep one must be cautious not to change by mistake the dissection plane and to have in mind exactly what might run beneath the dissection area. SMAS is not clearly identifiable in every cheek unit; neither the subcutaneous layer is of same thickness in every cheek subunit and differs also among the individuals. The course and the depth of the facial nerve at every cheek subunit must be constantly considered even if the dissection is subcutaneous.

At the infraorbital the subcutaneous fat is very thin and the dissection plane lies at the level over the orbicularis oculi muscle with the final branches of the zygomatic and buccal branches of the facial nerve well protected as they run to its undersurface. At the zygomatic subunit, at its anterior third, the malar fat pad facilitates the subcutaneous dissection, but moving posterior the subcutaneous fat thins and the frontal branch of the facial nerve crosses the mid-third of the zygomatic arch. Although the encountered fasciae of that area cover the frontal nerve, the fusion of planes at this level risks inadvertent nerve injury. At the parotid subunit, no danger for the facial nerve exists as it is well protected by the parotid gland. At the buccal subunit, the buccal branches of the facial nerve are in relative danger when dissecting at a deep subcutaneous plane. Even though the buccal branches are protected by the overlying parotidomasseteric fascia and SMAS, the SMAS might become very thin at this area and dissection must proceed with care so as to avoid an accidental transition of the dissection plane to a deeper one. At the inferior border of the buccal subunit, the marginal nerve is protected by the platysma and the deep cervical fascia but the subcutaneous dissection must be always performed with great caution. As the buccal subunit transitions to the nasolabial subunit, the presence of the nasolabial fat pad makes the subcutaneous dissection very easy and safe. Having in mind the course of the facial nerve is of paramount importance even when dissecting through the subcutaneous fat, especially where it crosses very superficially (lower border of mandible, zygomatic arch) as it is easy to harm. The retaining ligaments that are encountered in the region where a cheek flap is raised are felt as resistance in flap elevation and must be released by sharp dissection.

5.2.3.2 Deep (Sub-SMAS) Dissection Plane

It has been proven that the SMAS is not an avascular layer as it was believed but contains arterial vascularity within its mass from branches of the perforators that pass through it on their perpendicular way to the subdermal plexus (in contrast the SMAS does not contain veins) (Schaverien et al. 2009).

In certain circumstances like in patients with microcirculation deficiency (smokers, diabetics, those with peripheral artery disease and radiation in head and neck) and where a large flap has to be elevated, deep dissection under the SMAS layer (Fig. 5.36), similar to the deep-plane face-lift, adds perfusion to the overlying skin and increases flap mobility. This dissection comes in question in large rotation flaps where large areas of cheek skin have to be elevated with or without a neck extension (cervicofacial flap, see Chap. 8) or a thoracic extension (facial cervicothoracic flap, see Chap. 9). The flap is then termed as composite or deep-plane flap. The deep-plane flap (composite) is actually an implementation of the deep-plane rhytidectomy as was described by Hamra (1990). The deep-plane flap was first described by Barton and Zilmer (1982), but was popularized by Kroll et al. (1994) and focused attention furthermore (Becker and Langford 1996; Longaker et al. 1997; Delay et al. 1999; Tan and MacKinnon 2006).

This plane enhances the flap viability and thickness but puts the facial nerve at risk of injury, needing meticulous and very careful dissection. Precisely, the deep-plane dissection is a real sub-SMAS dissection only where SMAS exists.

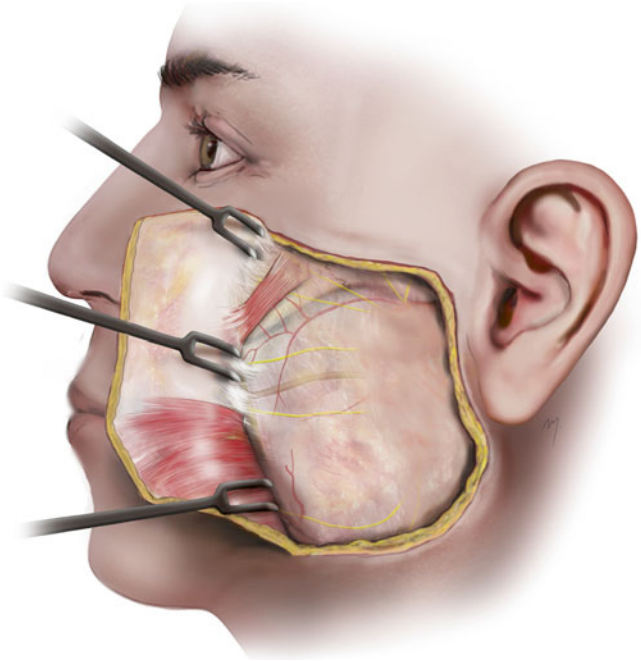

Fig. 5.36 Dissection in the deep plane

Elevation starts with sharp preauricular dissection; thus the SMAS is adherent to the underlying parotidomasseteric fascia. Usually the preauricular incision starts as subcutaneous for about 1–2 cm and then deepens to the sub-SMAS plane, avoiding this adherent zone. At this stage the facial nerve and its plexus are well protected deep to the parotid substance. The parotid-cutaneous ligament is felt as resistance and is released. Anterior to the border of the parotis, the dissection proceeds bluntly over the parotidomasseteric fascia. The underlying buccal and zygomatic branches of the facial nerve, the parotid duct, and the outer surface of the buccal fat may be found to be glistening. The fascia is thin and clear and protrudes beneath the parotidomasseteric fascia. At the lower half of the masseter muscle, the sub-SMAS dissection proceeds more easily and quickly by bluntly dissecting in the areolar tissue plane that overlies the parotidomasseteric fascia and was defined by Mendelson et al. (2008) as "the premasseter space." The platysma muscle, due to its variable extent and development, will not be found in a standard area during this step of dissection. The deep dissection proceeds deep to the platysma muscle, which constitutes the SMAS continuation. Due to the fact that this type of dissection concerns rotation flaps that extend also inferiorly to the neck, it is implied that the platysma muscle has been already found at the neck and raised with the neck part of the composite flap.

Fibrous septa of the masseteric ligament that are found are freed up and dissection continues. Reaching the lower anterior border of the masseter is the danger zone of the marginal mandibular branch of the facial nerve. As already mentioned near the point where the facial artery curves around the mandibular border, the marginal nerve penetrates the parotidomasseteric fascia or its neck continuation: The investing layer of the deep cervical fascia becomes more superficial and continues immediately deep to the platysma crossing the facial vessels (Owsley and Agarwal 2008). Here dissection is performed bluntly with extreme caution and the nerve must be protected. If dissection needs to continue further medially, the mandibular ligament has to be released.

At the upper part close to and specifically over the zygomatic arch, the dissection must transition to a subcutaneous plane. This protects the rami of the frontal branch from injury, as they cross its mid-third from deep to superficial fascial planes, ingrown within the temporoparietal fascia. Moving forward the origin and the lateral border of the zygomaticus major muscle is reached (identification helped by the line proposed by Tremolada, see above) and dissection proceeds above the muscle. Maintaining the dissection plane superficial or subcutaneous over the zygomaticus major muscle, the zygomatic branches of the facial nerve are avoided and protected as they travel on the deep muscle surface. Depending on the needed flap extent, the zygomatic retaining ligaments are released and dissection remains at the same level over the zygomatic muscles. At the periorbital zone, dissection can be performed over the orbicularis oculi muscle and not under it, as it is done in deep rhytidectomies. Thus the final branches of the zygomatic and buccal branches of the facial nerve are well protected as they run to its undersurface.

All types of local flaps can be derived from the cheeks providing a wide range of restoration options. Random pattern advancement, transposition, and rotation flaps work well in this region and are used to reconstruct primarily the cheek itself but also the nearby nose, lips, and lower lid.

5.2.4 Rhomboid Flaps

The rhomboid flaps can be used to close small- and moderate-sized defects located at every subunit of the cheek. Even though the rhomboid flap is a random pattern flap, vascularity is never a problem, and at any axis the flap is arranged, it always survives. When creating the rhomboid defect, the flap limb can be derived from four positions around it. The decision on which of the four alternatives will be used must be based upon the tissue availability and maximal laxity of the chosen donor site and positioning of scars as possible along the relaxed skin tension lines. For defects that lie at the periphery of the cheek, the options are restricted to the presence of facial features, like the eyelids, lips, nose, and auricle, and special care must be given not to distort their normal position.

5.2.4.1 Rhomboid Flap at Reconstruction of the Nasolabial Alar Base Area

The patient presented had a nevus at the upper nasolabial fold in close proximity to the alar lobule (Fig. 5.37a, b).

The rhomboid flap is outlined having its base superiorly (Fig. 5.37c, d). The lesion is excised in rhomboid manner creating a small defect (Fig. 5.37e). The flap is undermined in the subcutaneous plane (Fig. 5.37f) and is controlled if it reaches the defect without tension (Fig. 5.37g). A key suture is placed and the donor site is closed firstly (Fig. 5.37h). The flap is sutured in place without tension and the restoration is completed without any distortion. A great part of the suture

Fig. 5.37 (**a**, **b**) A nevus located at the upper nasolabial fold close to the alar lobule. (**c**, **d**) Rhomboid flap outlined. (**e**) Excision of the lesion. (**f**) Flap raised. (**g**) Flap transferred to the defect without tension. (**h**) Closure of the donor site. (**i**) Final closure

Fig. 5.37 (continued)

line is positioned parallel to the nasolabial fold and to the alar-facial sulcus (Fig. 5.37i).

5.2.4.2 Rhomboid Flap at Reconstruction of the Infraorbital Area

In the presented case (Fig. 5.38a, b), a basal cell carcinoma is located at the infraorbital subunit. The risk in this area involves the distortion of the lower eyelid from the positioning of the rhomboid flap. Having that in mind, the rhomboid flap is placed in an axis that no (or minimal) tension will act on the eyelid (Fig. 5.38a, b). The lesion is excised in the usual manner (Fig. 5.38c). The superiorly based flap is raised in the subcutaneous plane (Fig. 5.38d) and reaches the defect without any tension or pulling down of the eyelid (Fig. 5.38e). The donor site is sutured (Fig. 5.38f) and the restoration is completed achieving the goals (Fig. 5.38g). Although the rhomboid flap is not a round flap, sometimes pincushioning may occur but it resolves quickly (Fig. 5.38h, i). Care is taken when selecting the appropriate position of the rhomboid flap so that two limbs of the multininear scar are camouflaged within natural rhytids. This leads to a very good aesthetic result, especially in small defects.

5.2.4.3 Rhomboid Flap at Reconstruction of the Zygomatic Area

In the case presented (Fig. 5.39a), a rhomboid flap is used to cover a defect at the zygomatic subunit. The rhomboid flap is positioned so as to borrow preauricular tissue for the covering (Fig. 5.39b, c). The lesion is excised in the usual manner as a rhombus (Fig. 5.39d) and the flap is raised in the subcutaneous plane (Fig. 5.39e). This donor site may provide a slightly stiff flap that does not reach the recipient site immediately without tension (Fig. 5.39f). This problem resolves with ease by further undermining (the surrounding skin) (Fig. 5.39g). Donor site is closed at first (Fig. 5.39h) followed by suturing of the flap to the recipient site (Fig. 5.39i). The postoperative result shows a satisfactory restoration (Fig. 5.39j).

5.2.4.4 Rhomboid Flap at Reconstruction of the Lateral Canthal Area

Cheek skin can be transferred superiorly, by means of a rhomboid flap to reconstruct the lateral canthal area (Fig. 5.40a). The chosen rhomboid flap (Fig. 5.40b, c) takes advantage of the cheek skin laxity, produces minimal distortion, and does not put the frontal branch of the facial nerve at

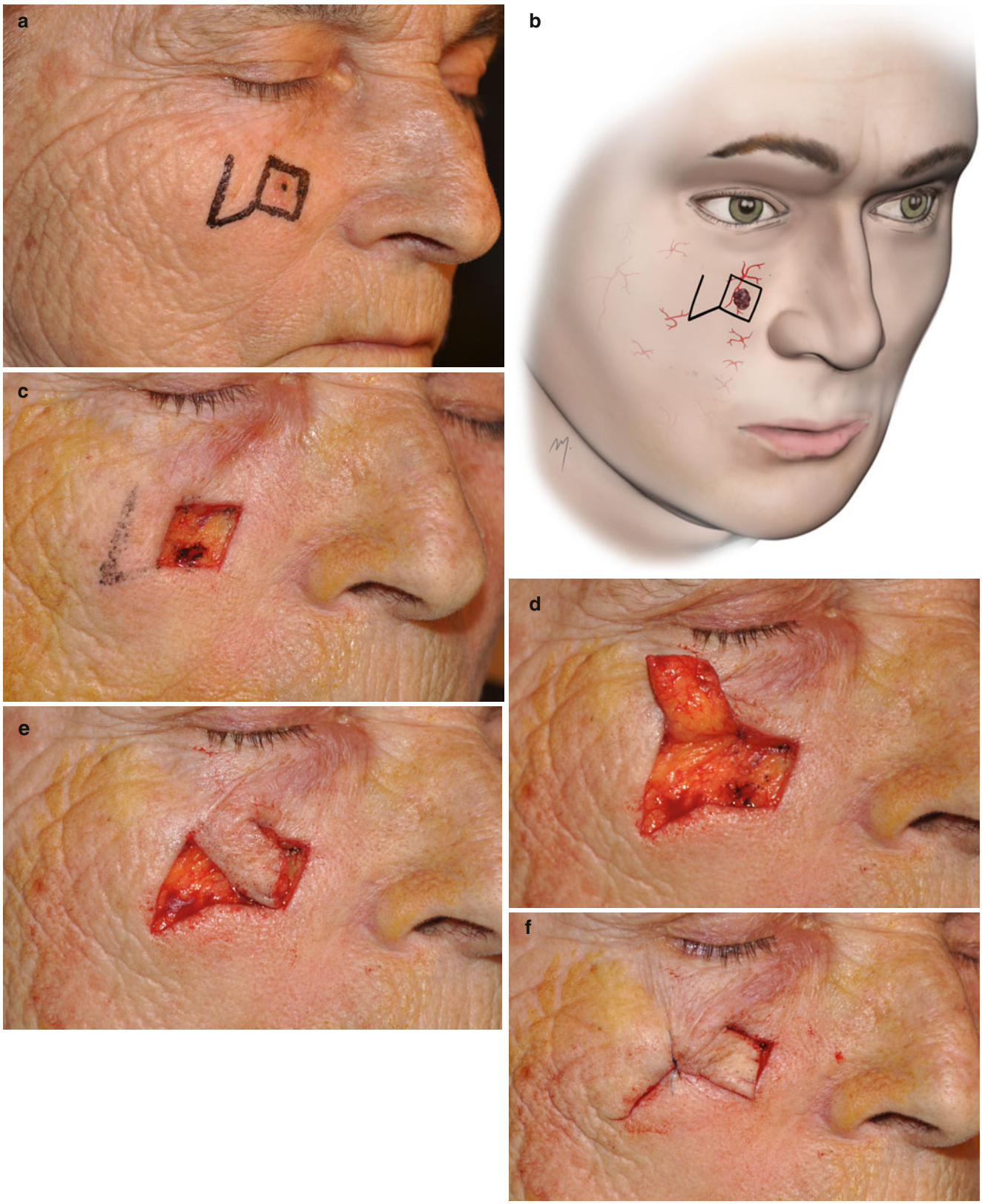

Fig. 5.38 (**a**, **b**) Lesion located at the infraorbital subunit and the rhomboid flap outlined. (**c**) Lesion excised. (**d**) The rhomboid flap raised. (**e**) Flap transferred to the defect. (**f**) Closure of the donor site. (**g**) Final restoration. (**h**) At 2 months postoperative, slight pincushioning is still present. (**i**) At 6 months postoperative, the pincushion has resolved and the result is excellent

Fig. 5.38 (continued)

Fig. 5.39 (**a**) A lesion located at the zygomatic subunit. (**b**, **c**) Rhomboid flap outlined. (**d**) Lesion excised. (**e**) Flap raised. (**f**) Flap does not reach the defect at once and further undermining is needed. (**g**) The defect now is reached without tension. (**h**) Closure of the donor site. (**i**) Final restoration. (**j**) Postoperative result at 6 months

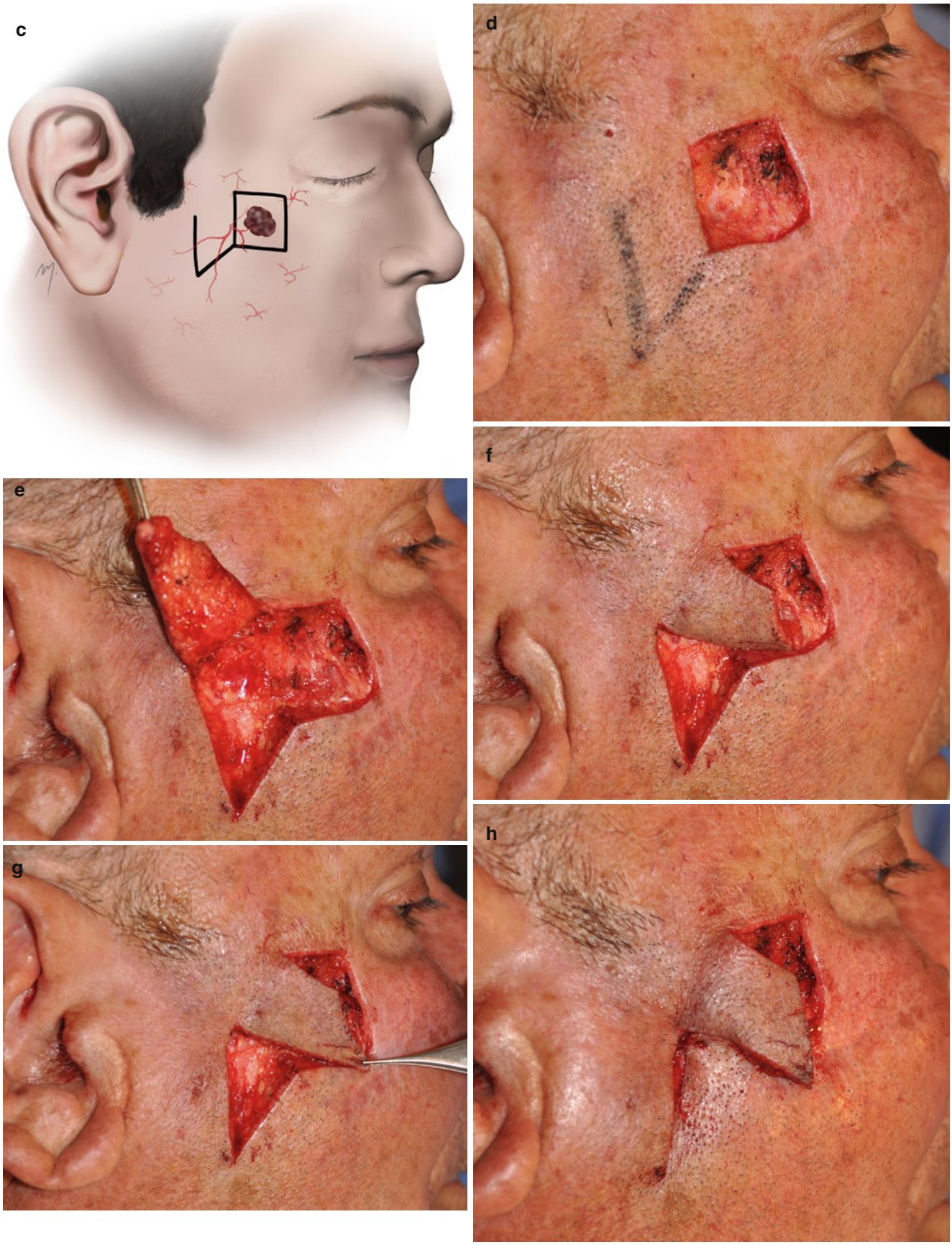

Fig. 5.39 (continued)

Fig. 5.39 (continued)

Fig. 5.40 (**a**) A basal cell carcinoma at the lateral canthal area. (**b**, **c**) Outline of the rhomboid flap. (**d**) Flap sutured in place

risk. The flap was raised in the subcutaneous plane and covered the defect (Fig. 5.40d).

5.2.4.5 Rhomboid Flap at Reconstruction of the Buccal Area

Medium and relatively large buccal defects can be reconstructed by transferring skin from the parotidomasseteric region by means of a rhomboid flap. Decision and careful planning is based upon the size of the defect and the availability of the needed skin from the parotidomasseteric region. If the defect is expected to be large, this approach is better to be considered in older patients with excessive skin laxity. Distortion of facial features is usually not the problem in small- and medium-sized defects that are located in a central position at the buccal area as long as they are not in close adjacency to the restoration.

Restriction in the orientation and the choice of the base when designing a rhomboid flap in this area is that vertical scars over the body of the mandible and the neck that may be produced must be avoided. A vertical incision on the neck may result in a scar that contracts causing a band and over the mandible may result in a scar that stretches becoming indrawn and difficult to correct (Jackson 2007). Thus, a rhomboid flap that transfers parotidomasseteric skin to the recipient site can be based either superiorly or inferiorly.

5.2.4.5.1 Superiorly Based Rhomboid Flap

A basal cell carcinoma is located at the lower buccal subunit in the patient presented (Fig. 5.41a). A superiorly based rhomboid flap is outlined so as to transfer skin from the parotidomasseteric subunit to close the defect, avoiding vertical scars over the mandibular body (Fig. 5.41b, c). Excision is performed and clear margins are revealed by frozen section biopsies (Fig. 5.41d). The flap is raised in a deep level, above the parotidomasseteric fascia (Fig. 5.41e). The flap was transferred to the defect (Fig. 5.41f) and the donor site closed primarily. In large defects, despite the skin laxity, some degree of tension is expected (Fig. 5.41g). The postoperative appearance at 3 months following surgery shows a satisfactory result (Fig. 5.41h, i).

5.2.4.5.2 Inferiorly Based Rhomboid Flap

In a lesion located at the same region as in the previous patient but in a slightly higher position (Fig. 5.42a), an inferiorly based rhomboid flap can be used for the reconstruction (Fig. 5.42b, c). Closure of the inferiorly based rhomboid flap would be easier than if the flap was based superiorly, and this can be done in this situation as long as no vertical line lies on the mandibular body. The reconstruction was performed in the usual manner (Fig. 5.42d) resulting in a satisfactory closure (Fig. 5.42e).

5.2.5 Bilobed Flaps

The bilobed flap, a double transposition flap that is mostly used in the nose, can also be included in the armamentarium of cheek reconstruction based in the same principles. The flap is a random pattern flap and can resurface moderate-sized defects at the anterior cheek.

5.2.5.1 Bilobed Flap at Reconstruction of the Buccal Subunit

The patient presented in Fig. 5.43a had an ulcerative basal cell carcinoma of the buccal subunit of the cheek. The site of surgical excision is marked and the outline of a laterally based

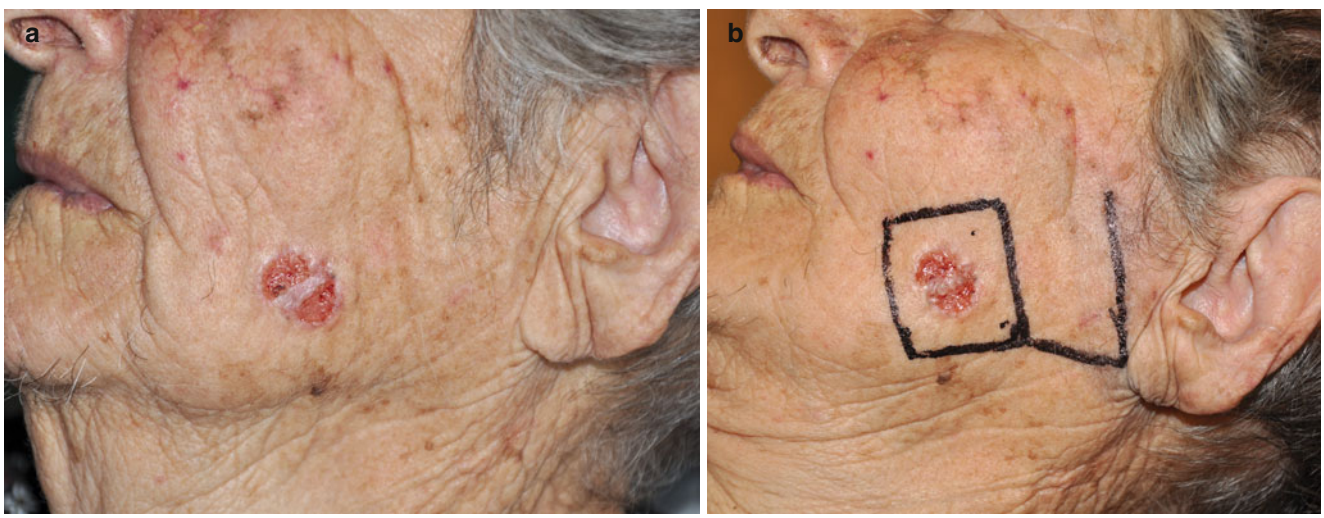

Fig. 5.41 (**a**) Basal cell carcinoma at the buccal subunit of the cheek. (**b**, **c**) Rhomboid flap is outlined. (**d**) Excision performed. Platysma fibers are left intact at the base of the defect. (**e**) Flap raised above the parotidomasseteric fascia. (**f**) Flap transferred to the defect. (**g**) Immediate postoperative view. Despite the fair skin laxity, some degree of tension occurred. (**h**) Result at 3 months. (**i**) Symmetry and contour undisturbed

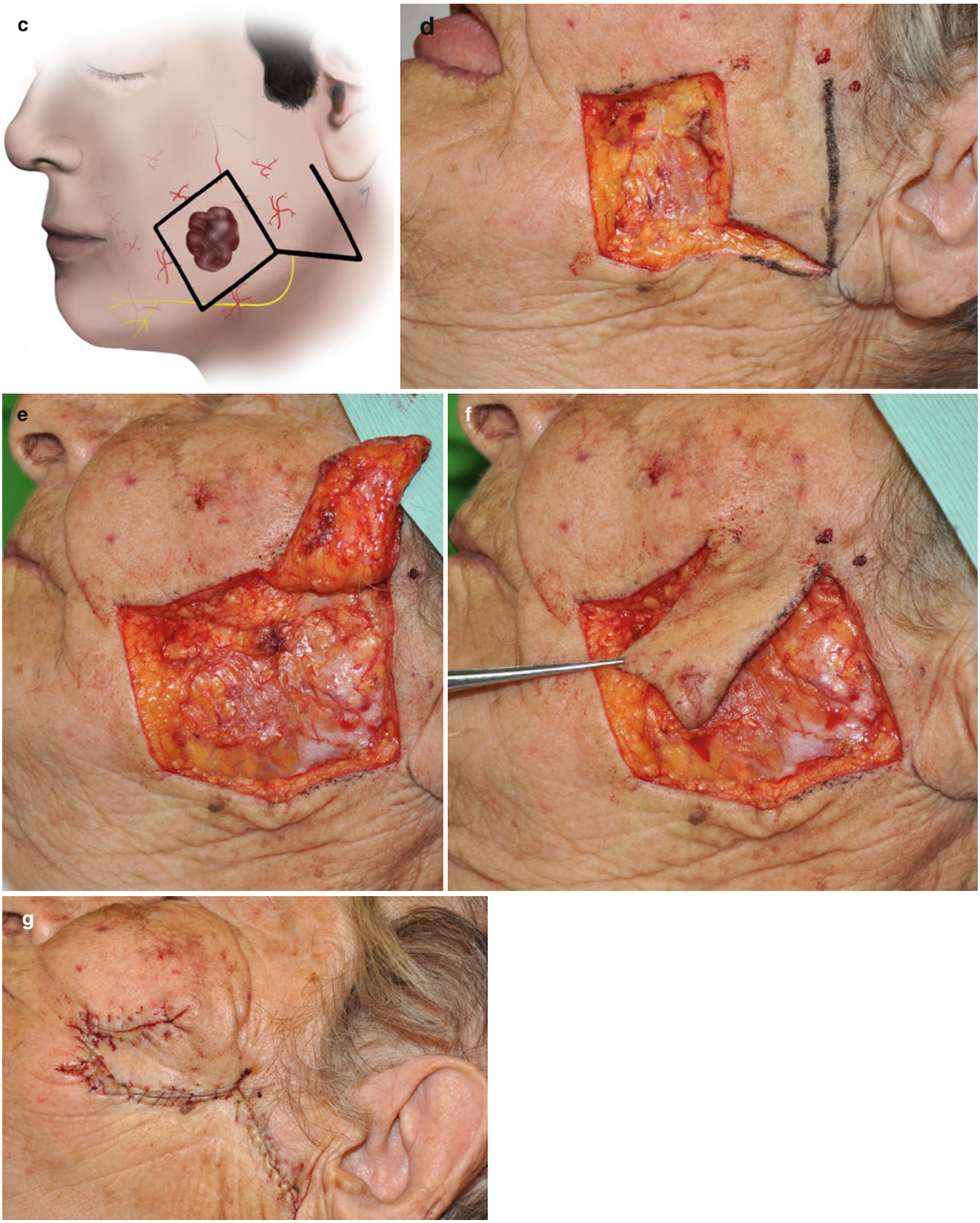

Fig. 5.41 (continued)

Fig. 5.41 (continued)

bilobed flap is created (Fig. 5.43b, c). The flap next to the defect will transfer skin of the lower cheek and is designed in an axis of 45° to the axis of the primary defect and at the same or slightly smaller size. The second flap is outlined at the upper part of the neck and is situated to an axis of approximately 45° to the axis of the first limb and smaller in size. Thus, the total angle of transposition of the bilobed flap is about 90°. The elasticity of the cheek skin allows a design of the bilobed flap of up to 90° for each flap and a total of 180°, easy rotation in cases where a so large rotation arc is needed. One Burow's triangle is excised at the base of the flap and a second one at the apex of the second lobe to allow easier rotation without the formation of dog-ears.

The flap is elevated in the subcutaneous plane and rotated into position (Fig. 5.43d, e). It is sutured into position with ease (Fig. 5.43f). Usually there is no need of wide undermining, especially in old patients with loose skin. The bilobed flap does not need as extensive undermining and mobilization as the corresponding rotation flap that would be used in the same area, but leads to extensive and obvious scaring (Jackson 2007). This is obvious in the postoperative result where the multicircular nature of the scars cannot be camouflaged in linear natural creases (Fig. 5.43g).

5.2.5.2 Bilobed Flap at Reconstruction of the Upper Lip

In certain circumstances the bilobed flap provides many advantages that must be taken under consideration and seems to be an appropriate reconstructive solution. In the case presented, a basal cell carcinoma is located at the most anterior border of the cheek. The defect that will be created involves the nasolabial area and extends to the skin of the lateral region of the upper lip. The oral commissure is intact but in very close proximity to the defect. Any restoration must not interrupt its normal position. A bilobed flap in this situation provides to the upper lip similar skin tissue from the lower lip (Fig. 5.44a, b). It does not need extensive mobilization and most importantly ensures an undisturbed commissure. The oral commissure is balanced between the two lobes of the flap maintaining its normal position under neutralized tension.

The lesion is excised and free tumor margins are revealed by frozen section biopsies. Deep excision was performed to the level of perioral muscles (Fig. 5.44c). The first lobe of the flap is elevated at the plane just superficial to the perioral muscles so as to provide the needed bulk, leaving intact the modiolus and the muscles attached to it (Fig. 5.44d).

The flap is transposed to the recipient side (Fig. 5.44e). There is no need to excise the Burow's triangle as long as a standing cone is not formed. The flap is raised as usual (Fig. 5.44f). Even though its base is relatively narrow, vascularization is ensured by the several perforators of the facial artery. The second lobe covers the secondary defect with ease (Fig. 5.44g). Final closure is achieved easily and without tension (Fig. 5.44h) and the final result is very satisfactory and there is no distortion of the oral commissure (Fig. 5.44i).

5.2.6 Subcutaneous Island Pedicle Flaps (V-Y Advancement Flaps)

The subcutaneous island pedicle flaps are a very useful tool in cheek reconstruction because they can be harvested from every

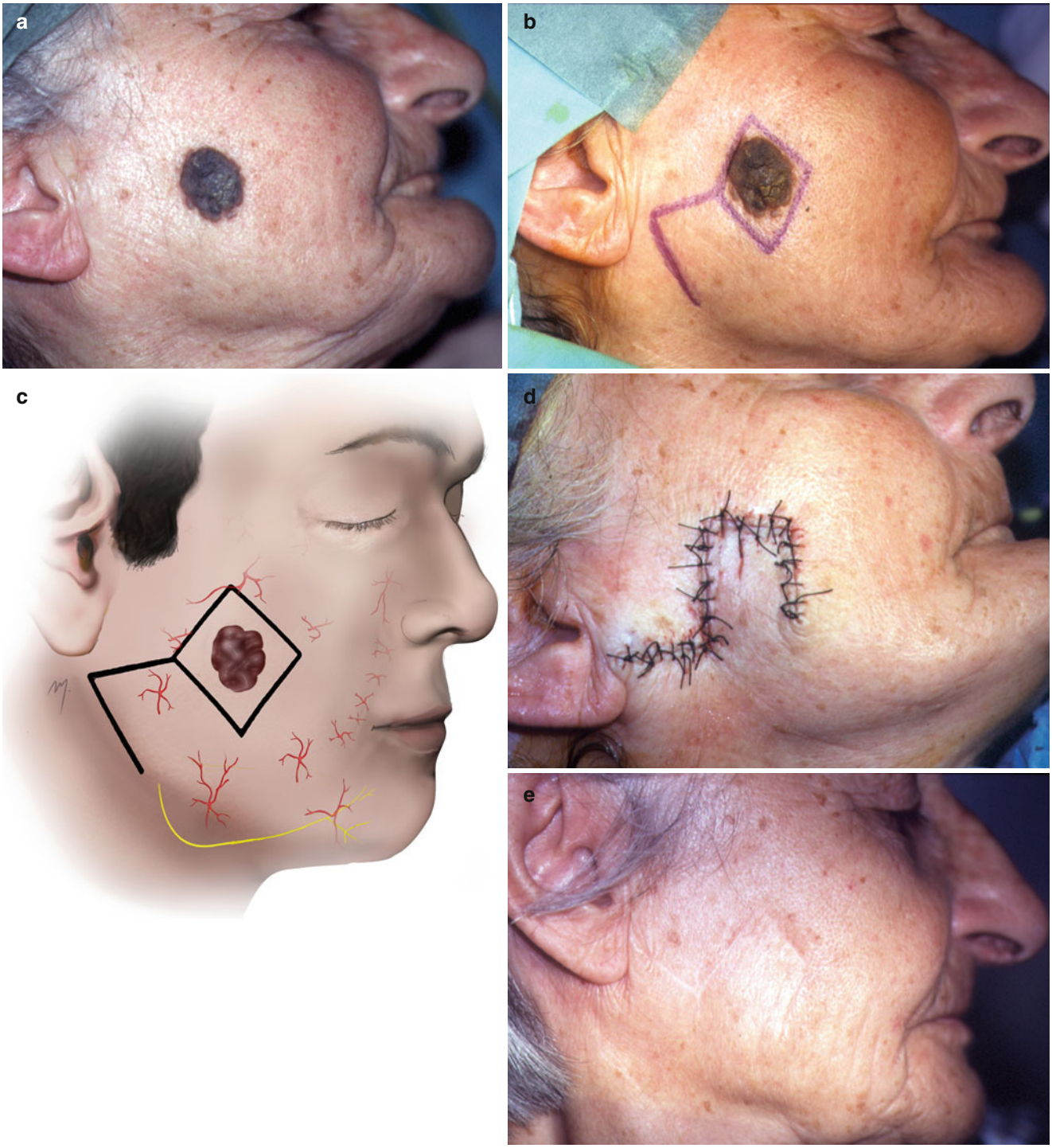

Fig. 5.42 (**a**) A lesion at the buccal subunit. (**b**, **c**) The inferiorly based rhomboid flap outlined. (**d**) Rhomboid flap closure. (**e**) Postoperative appearance

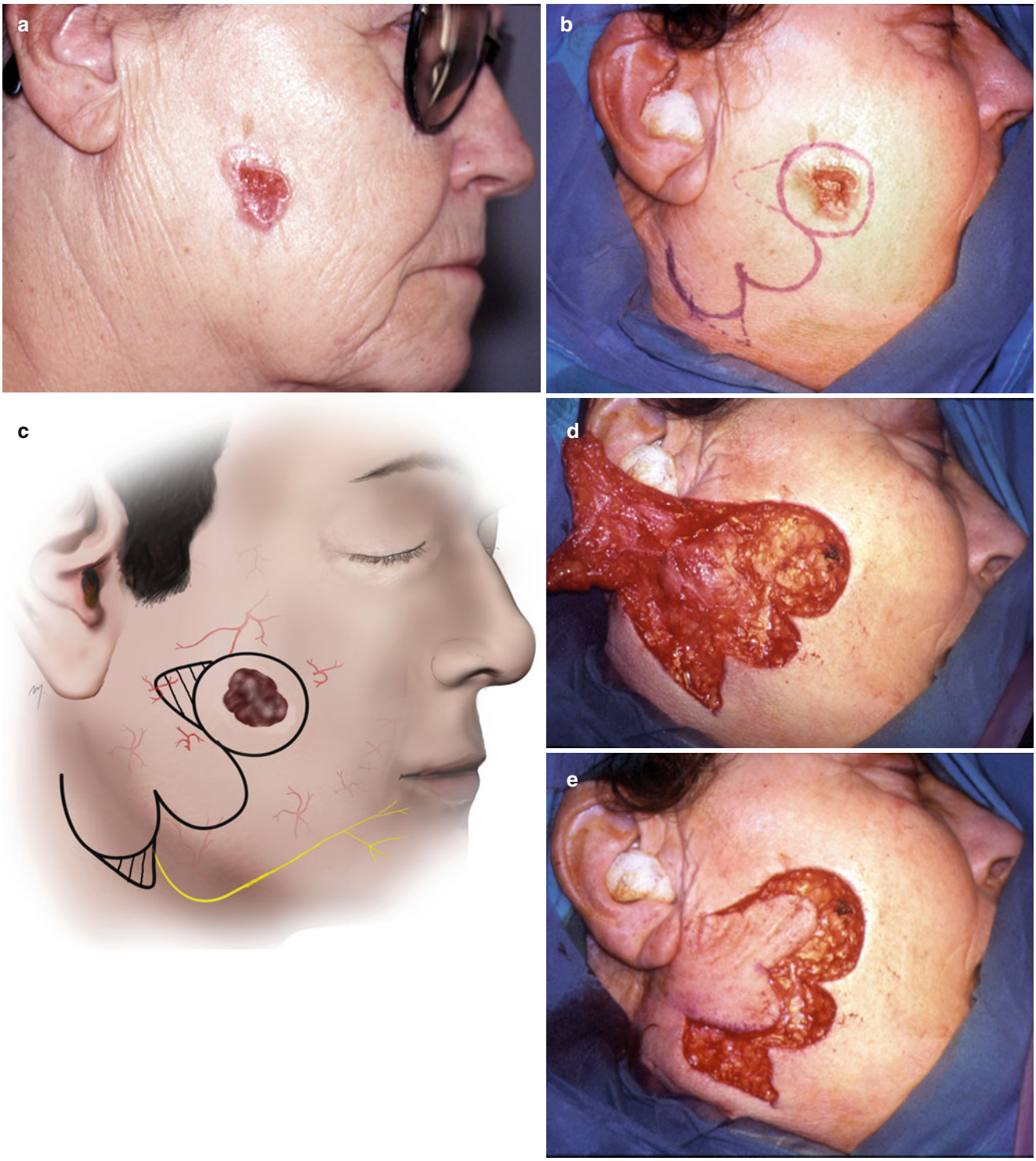

Fig. 5.43 (**a**) Basal cell carcinoma of the buccal subunit. (**b**, **c**) Plan of excision and outline of the bilobed flap. (**d**) Flap elevated. (**e**) Flap transferred to defect. (**f**) Final closure of the defect. (**g**) Postoperative result at 1 year

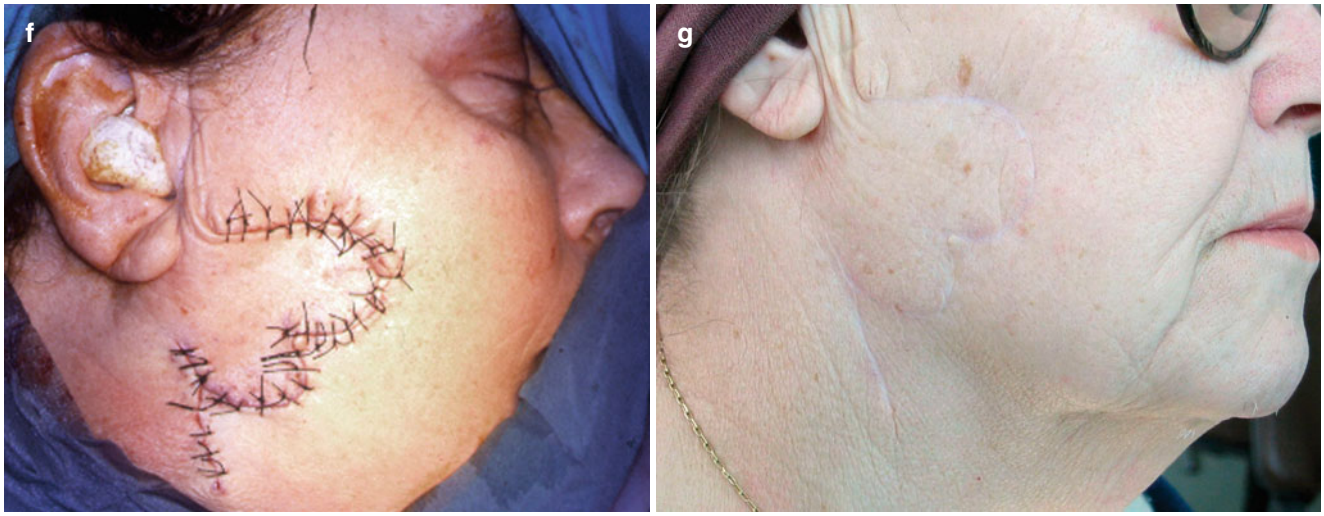

Fig. 5.43 (continued)

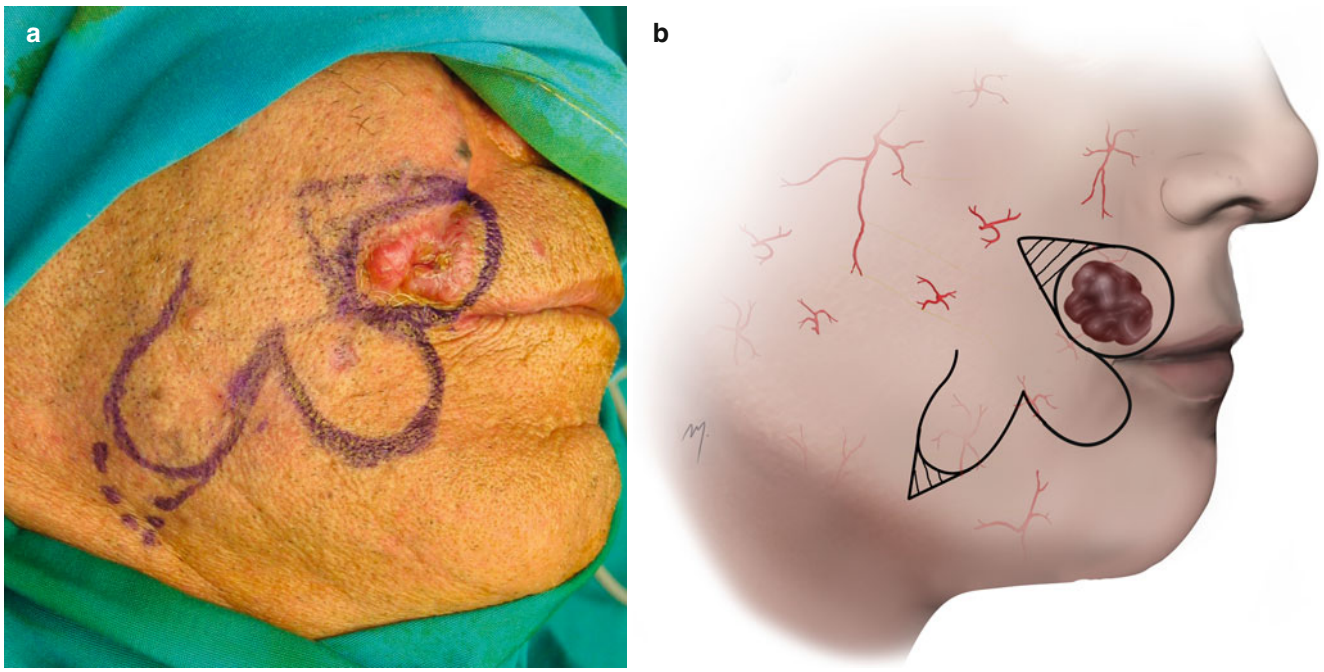

Fig. 5.44 (**a**, **b**) Outline of the excision and the bilobed flap. (**c**) Lesion needed to be excised deep to the perioral muscles. (**d**) The first lobe is elevated superficial to the muscle layer. (**e**) First flap fits to the defect. (**f**) The flap fully mobilized based in a narrow pedicle. (**g**) Second lobe into place. (**h**) Immediate postoperative view. (**i**) Result at 9 months. No distortion of the commissure

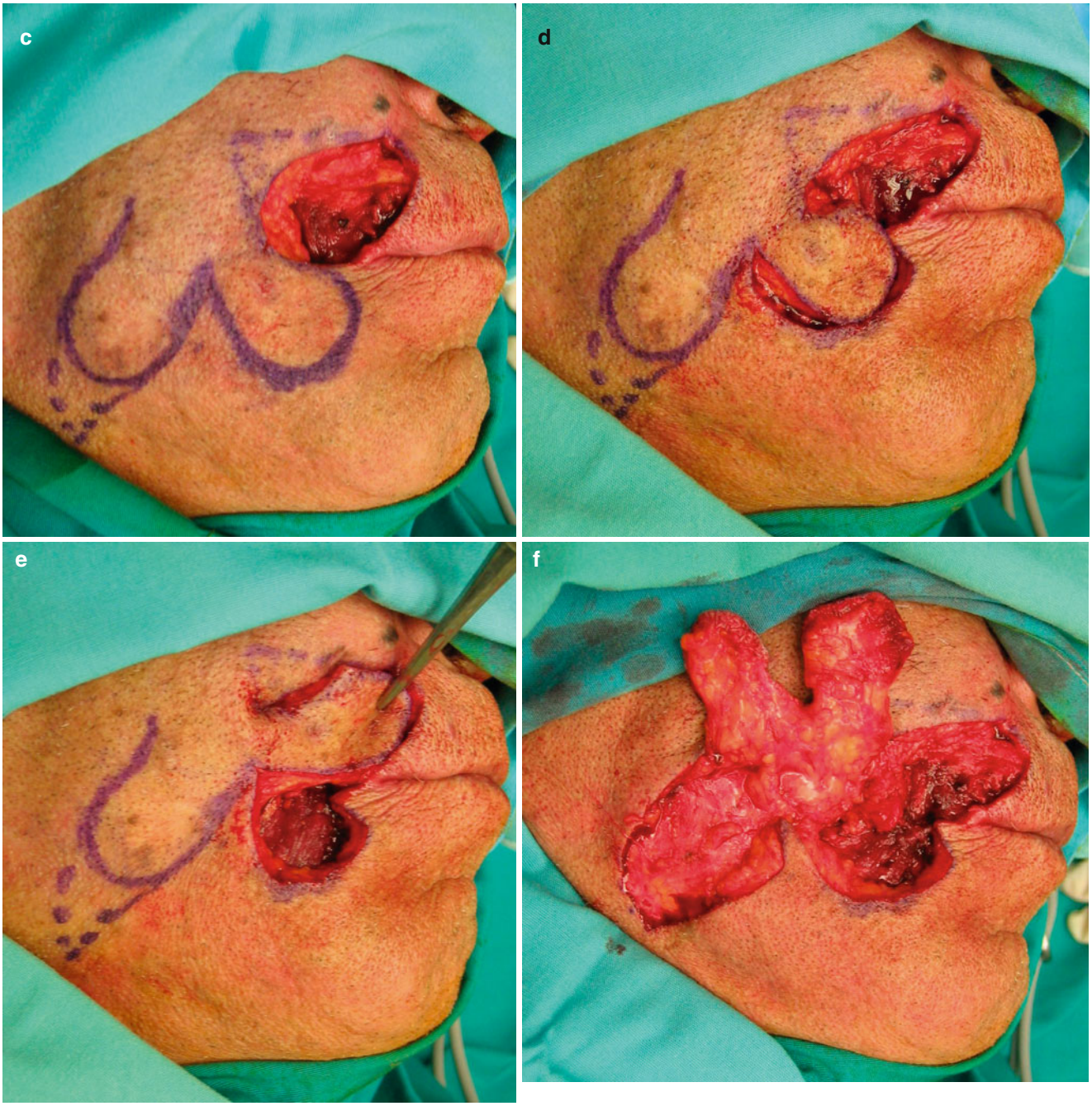

Fig. 5.44 (continued)

Fig. 5.44 (continued)

cheek subunit that provides adequate mobility (usually from the nasolabial and malar area) and advanced to a variety of recipient sites of the cheek. The island pedicle flaps are advancement flaps that provide immediately adjacent to the defect skin excellent in texture and color match. These flaps are random pattern flaps and receive their blood supply from perforators that arise from deeper regional axial vessels and ascend to its subcutaneous pedicle. The concept of a detached from its surrounding tissues "skin island" as a flap that is based only to its underlying subcutaneous tissue was first introduced by Esser (1917) and popularized by Barron and Emmett (1965).

The placement of the flap base and the direction of the axis of movement depend on the area to be reconstructed and ideally must be determined by the direction of the RST lines.

5.2.6.1 Subcutaneous Island Pedicle Flap Horizontally Advanced at Reconstruction of the Infraorbital Area

This flap uses the looser cheek skin from the area lateral to the lesion and advances it medially to the infraorbital defect.

The outline of the island pedicle flap is presented in a patient with a small lesion located at the median part of the infraorbital area (Fig. 5.45a, b). The excision is outlined in rectangular form and the island flap is designed as a triangle in a length two times the dimension of the rectangle side. The flap borrows skin from the malar region, which provides excess and mobile tissue to transfer. The flap will be positioned on a horizontal axis and its trailing edges are placed along the RSTLs (Fig. 5.45c).

The lesion is excised in healthy margins (Fig. 5.45d) and the skin island detached from the surrounding tissues (Fig. 5.45e). Mobilization of the flap is performed by blunt dissection through the subcutaneous plane in each of the flap sites and its apex for a distance of about 1.5 cm beveling slightly away from the pedicle (Fig. 5.45f, g). Performing dissection in this way, widens the flap base increasing the vascularization. During this stage fibrous bands that are encountered must be detached from the flap periphery providing thus additional mobility. During the deep subcutaneous dissection stage, special attention is given in the course

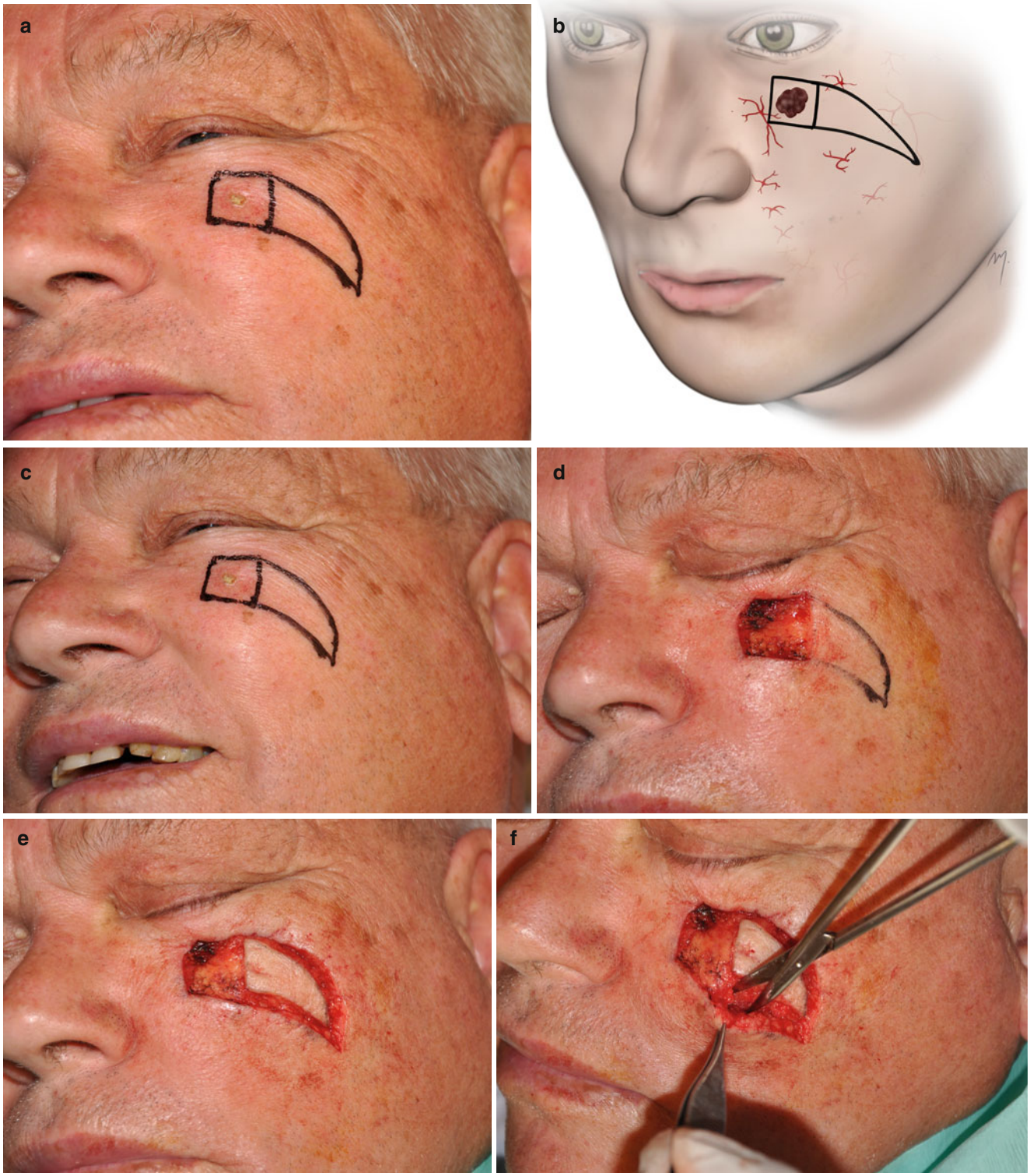

Fig. 5.45 (**a**, **b**) A lesion of the median suborbital region and the design of an island pedicle flap. (**c**) Incisions placed along RST lines. (**d**) The defect after excision of the lesion. (**e**) The skin island fully freed from the surrounding skin. (**f**, **g**) Undermining is performed in the subcutaneous plane (in a centrifugal dissection) in the whole perimeter of the flap, beveling slightly away from the pedicle. (**h**) Flap control. (**i**) Back-cutting of the leading edge of the flap in subcutaneous plane maximizes mobility and decreases tension to the lower eyelid. (**j**) Final closure in a V-Y fashion. The flap has been positioned horizontally (in a horizontal axis). (**k**) Result at 1 month after surgery. (**l**) No traction to the lower eyelid

Fig. 5.45 (continued)

of nerves and large vessels so as to protect and not damage them.

The flap is controlled continuously (Fig. 5.45h) if it sets without any tension, especially in this area where a downward tension to the lower eyelid may result to ectropion. If additional mobility is needed, a portion of the skin of the leading edge of the flap can be detached from the base by back-cut in a subcutaneous plane (Fig. 5.45i). This maneuver decreases tension and does not compromise the flap when at least the 60 % of the skin island, at this area, remains attached to the pedicle. The flap is advanced and sutured in a V-Y closure and its final position lies horizontally (Fig. 5.45j). The reconstruction resurfaced the defect successfully without any distortion of the eyelid (Fig. 5.45k, l).

5.2.6.2 Subcutaneous Island Pedicle Flap Obliquely Advanced at Reconstruction of the Malar Region

In the case presented in Fig. 5.46a, a lentigo maligna is located at the malar region. The island pedicle that is outlined has its movement axis in an oblique position as this is determined by the direction of the RST lines and its base located inferolaterally (Fig. 5.46b, c). The length of the triangle is twice the length of the rectangle side. The lesion was excised in clear margins (Fig. 5.46d) and the flap was undermined in the usual manner (Fig. 5.46e). The flap is sutured in place in a V-Y fashion (Fig. 5.46f).

5.2.6.3 Subcutaneous Island Pedicle Flap Vertically Advanced at Reconstruction of the Superomedial Cheek Area

In defects that are located at the superomedial cheek aspect (even immediately below the lower eyelid) or even higher at the medial canthal area, a vertical, inferiorly based island flap can be used successfully. In a basal cell carcinoma located at the superomedial part of the cheek (Fig. 5.47a), a vertical island pedicle flap was planned to close the defect (Fig. 5.47b, c). The trailing edges of the flap were positioned parallel to the nasal sidewall and the nasolabial groove defining its vertical orientation. Again the flap length is 2 times the length of the rectangle side. The flap was undermined as usual, advanced superiorly, and covered the defect (Fig. 5.47d). Gravity is not a problem and a risk of ectropion is minimal. The way that the donor site is closed supports the elevated flap, and withstands gravitational forces with its vertical orientation.

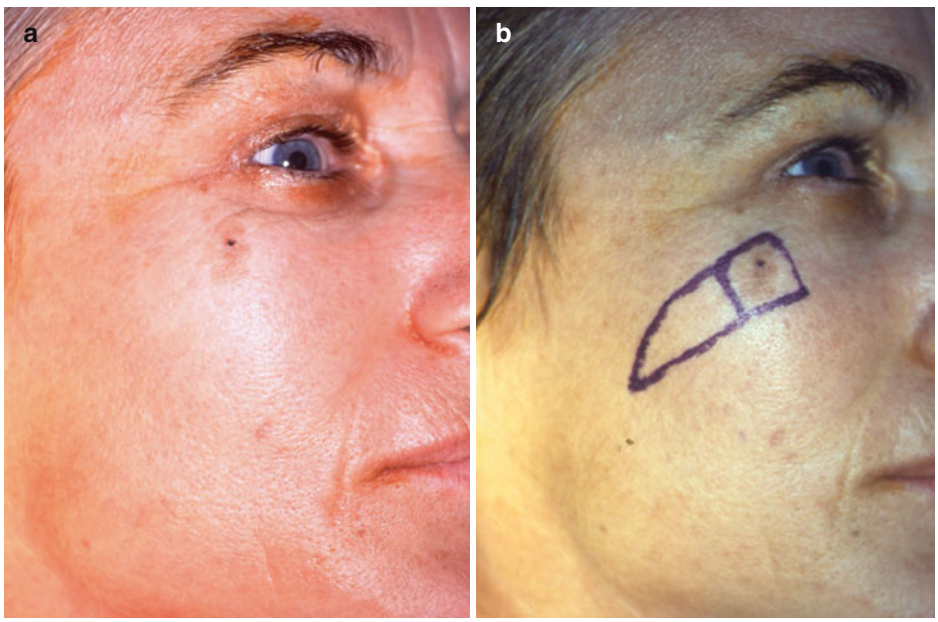

Fig. 5.46 (**a**) Lesion at the malar region. (**b**, **c**) Outline of the island pedicle flap. (**d**) Lesion excised. (**e**). The flap undermined. (**f**) Final closure in a V-Y fashion. The flap has been positioned obliquely (in an oblique axis)

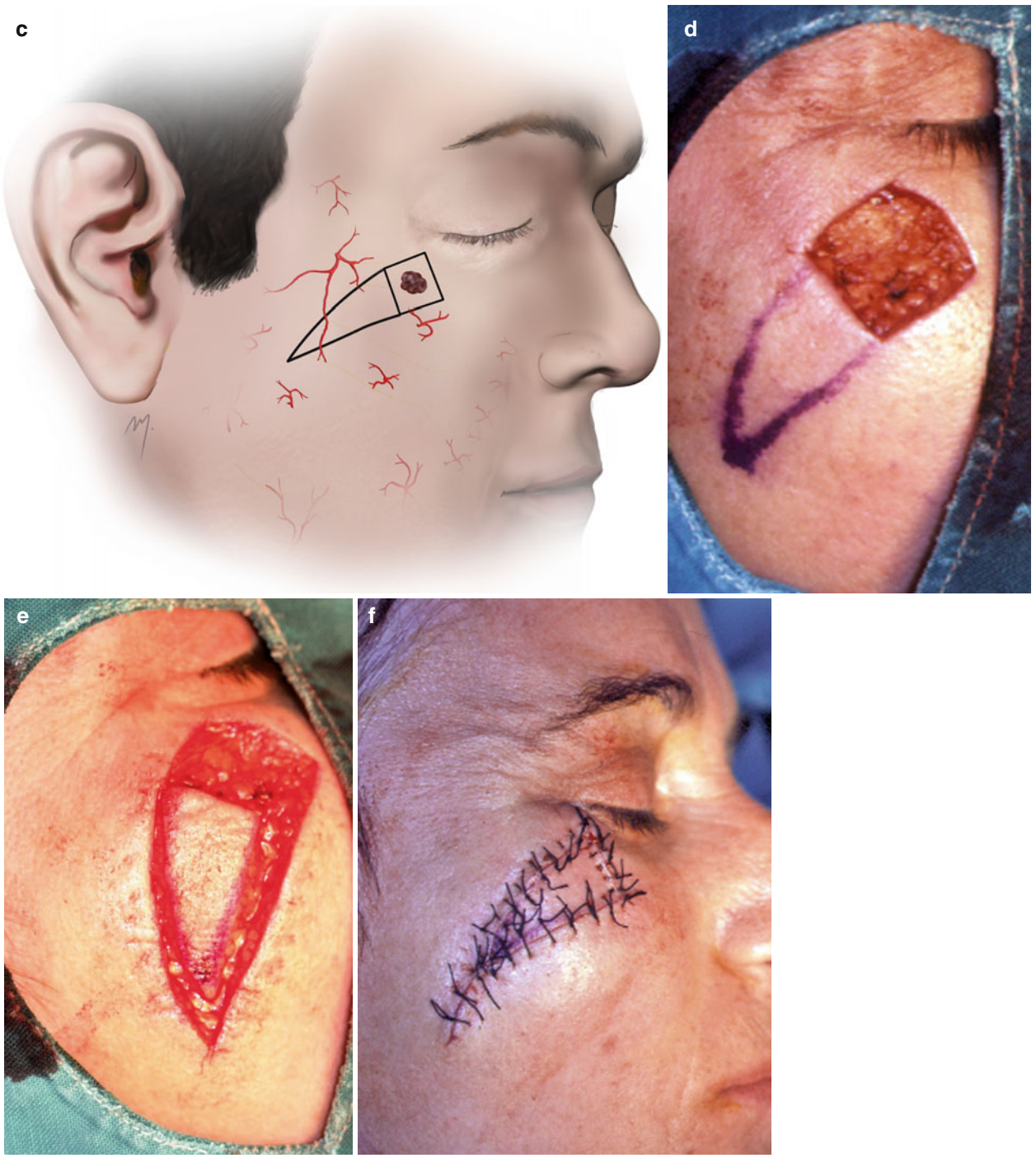

Fig. 5.46 (continued)

Fig. 5.47 (**a**) Pigmented basal cell carcinoma. (**b**, **c**) Vertical island pedicle flap outlined. (**d**) Final closure in a V-Y fashion. The flap has been positioned in a vertical axis

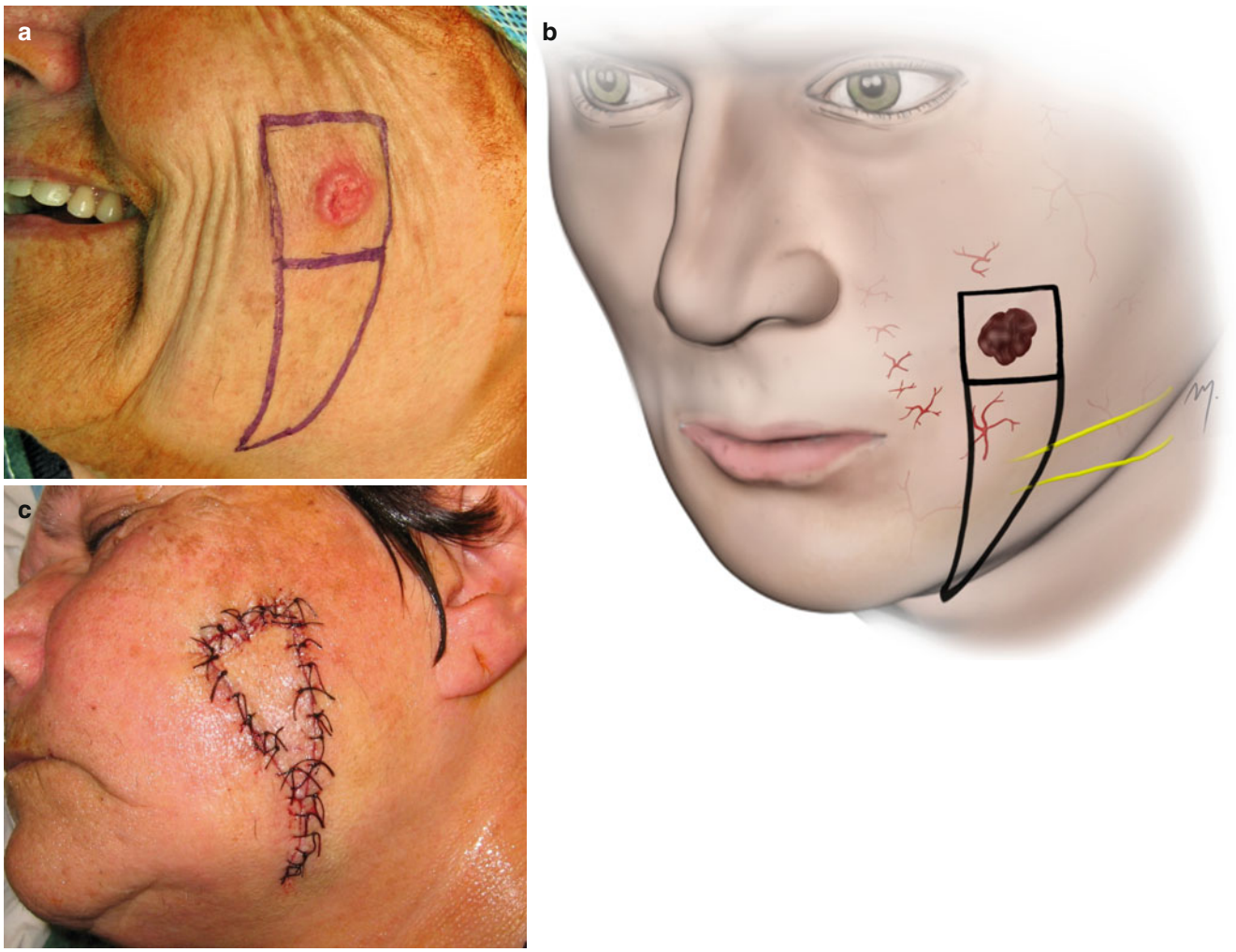

Fig. 5.48 (**a**–**c**). Large subcutaneous island pedicle flaps can be derived from the buccal subunit of the cheek. The direction of the RSTLs determines the axis of movement

5.2.6.4 Subcutaneous Island Pedicle Flap Vertically Advanced at Reconstruction of the Buccal Subunit

The characteristics of the buccal subunit allow the design and advancement of large subcutaneous island pedicle flaps (Fig. 5.48). The advancement axis of flap here is almost vertical as it is imposed by the direction of the RSTLs at the buccal subunit.

5.2.6.5 Double Island Pedicle Flap at Reconstruction of the Zygomatic Area

Two island pedicle flaps, evenly opposed or angled as in the case presented, can be created so as to share a defect. Two adjacent nevi located at the zygomatic and temporal subunit were excised, and the total defect was reconstructed by a double island pedicle flap (Fig. 5.49a, b). Dissection of the flaps was done with extreme care preserving the branches of the facial nerve. One flap advanced skin from the preauricular area while the other from the temporal area. The two flaps were sutured in place sharing the produced defect (Fig. 5.49c). The final result is functionally and aesthetically satisfactory (Fig. 5.49d, e).

5.2.7 Nasolabial Subcutaneous Island Pedicle Flaps

When an island pedicle flap has its subcutaneous base at the nasolabial area (along the course of the facial artery) and its axis along to it, it is then termed as nasolabial island flap. An island flap situated at this position reclaims all of the advantages of this area: availability of elastic and mobile skin and subcutaneous tissue, generous blood supply through perforators of the facial artery, and scar camouflage. Moreover, due

Fig. 5.49 (**a**, **b**) Two angled island pedicle flaps. (**c**) The two flaps shared the defect. (**d**, **e**) Result at 2 months and at 1 year. No impairment of the facial nerve occurred

to the fact that the closure of the produced donor defect of an island flap needs minor secondary tissue movement, important nearby facial features (upper and lower lip, ala, commissure) remain undistorted even when large flaps are raised.

5.2.7.1 Nasolabial Subcutaneous Island Pedicle Flap at Reconstruction of the Medial Cheek-Upper Lip-Alar Junction Area

In the patient presented in Fig. 5.50a, a recurrent basal cell carcinoma is located at the junction of the cheek-upper lip-alar base, presenting in cystic form and a deeply invasive nodule. The patient had a nasal restoration of the alar lobule and rim 1 year ago with an unclear, superiorly based nasolabial flap.

Despite the fact that a nasolabial flap had already been used at the first operation, a new one is outlined (Fig. 5.50b, c) but longer than in the usual manner so as to widen the vascular plexus beyond the former, thereby catching as many as possible of the several perforators of the facial artery that are encountered densely near the mouth angle and enhance its robustness. This description concerns to the conventional nasolabial flap and not to the flaps that are based in only one single facial perforator as facial artery perforator flaps (Hofer et al. 2005) and is beyond the purpose of the present book.

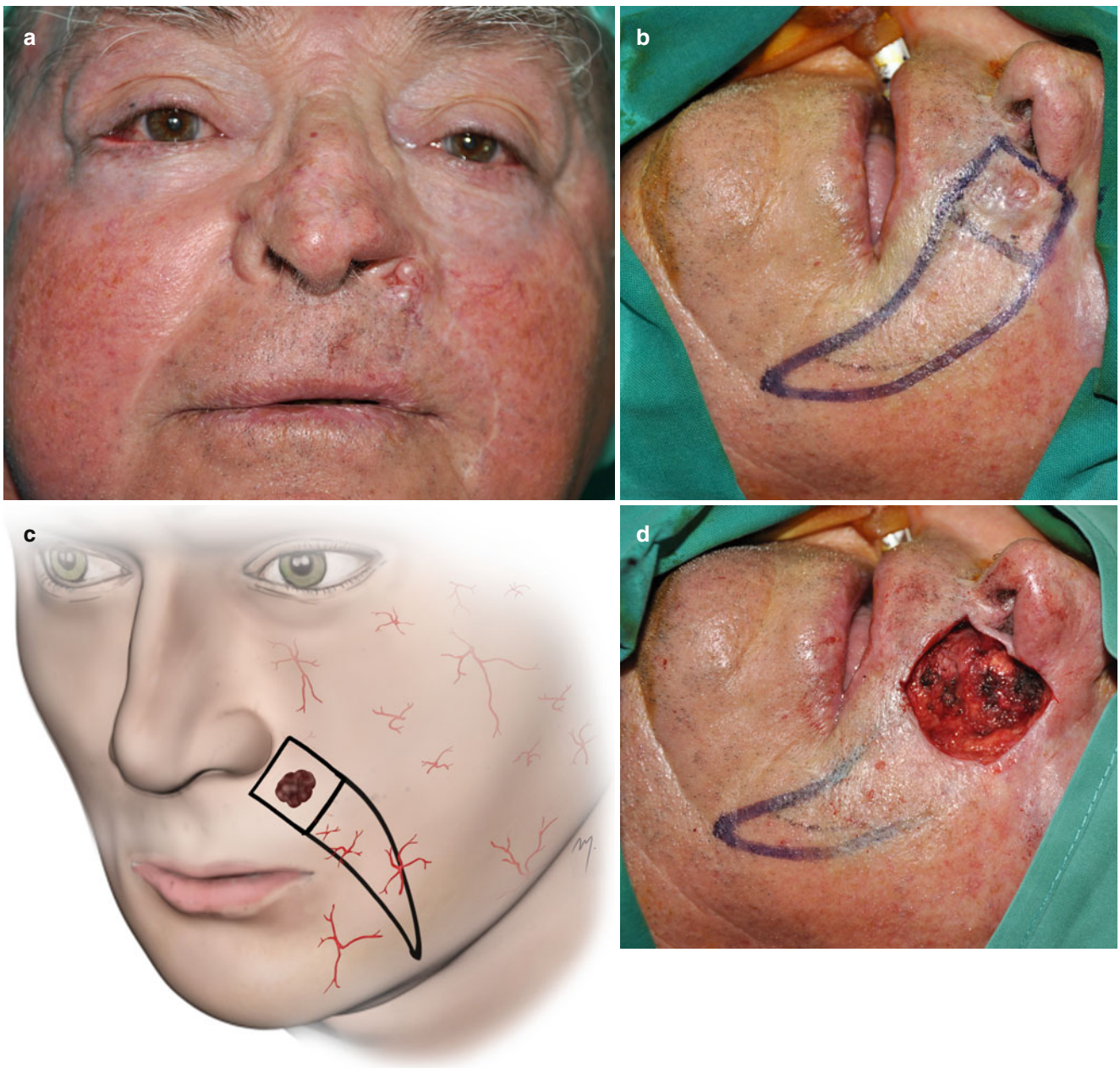

Fig. 5.50 (**a**) A recurrent basal cell carcinoma. (**b**, **c**) Excision lines and a nasolabial island flap outlined. (**d**) Excision performed leaving a deep defect. (**e**) Mobilization of the flap. (**f**) Bulky tissue is advanced to the defect. (**g**) Immediate postoperative view. (**h**, **i**) Satisfactory result at 2 months postoperative. Lip retains its position and function. (**j**) Contour is fully imputed. No attempt to restore the previously restored nasal ala was made at this stage. Scars are hidden within the RST lines

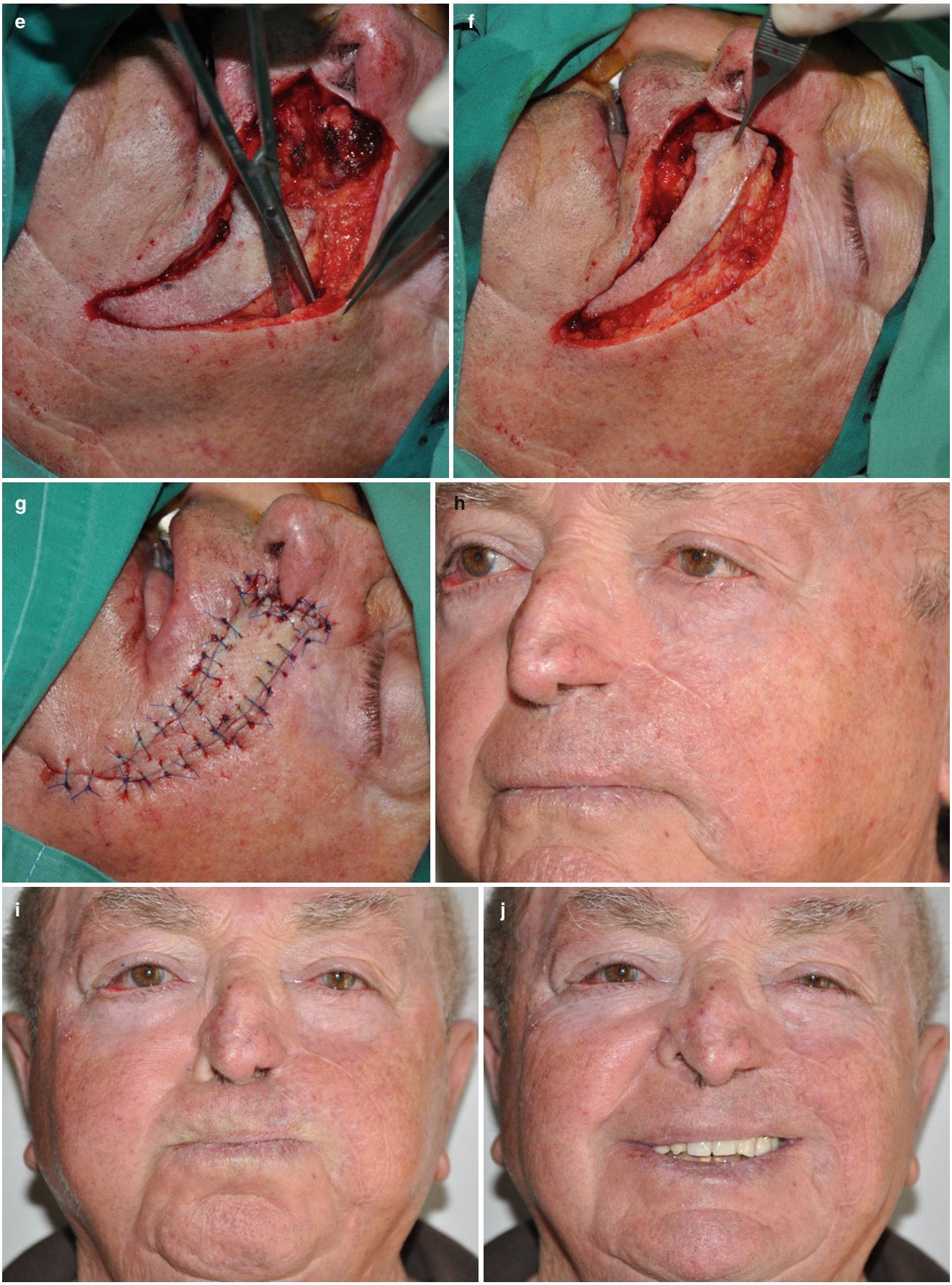

Fig. 5.50 (continued)

Tumor excision was performed in a deep tissue plane (Fig. 5.50d), and tumor margins were revealed by frozen section biopsies. Thus, this reconstruction requires not only resurface of the skin but also restoration of the bulk. The thickness of the subcutaneous layer at the nasolabial area can provide this needed amount of tissue.

The flap was undermined, slightly beveling, around its subcutaneous pedicle for about a 2–2.5 cm distance (Fig. 5.50e). Dissection is carried out bluntly and sharply down to the level of the cheek muscles. Fibrous bands (from the pedicle) to the surrounding fat are encountered and released.

Additional mobility is gained if a portion of the skin of the periphery of the flap is detached from the pedicle by back-cut in the subcutaneous plane. This maneuver decreases tension and does not compromise the flap when at least the central third of the skin island remains attached to the pedicle. The subcutaneous pedicle of an island flap can be narrowed at this degree and still perfuse the skin island only in the nasolabial area, where the facial artery encounters as already mentioned numerous perforators. The nasolabial island flap was advanced to the defect (Fig. 5.50f) and sutured in place without tension (Fig. 5.50g). The postoperative appearance at 2 months following surgery shows a satisfactory functional and aesthetic result (Fig. 5.50h–j).

5.2.7.2 Nasolabial Island Flap at Reconstruction of the Medial Canthal-Nasal Side Area

The nasolabial flap can reach even more superiorly located midsized defects of the medial canthal region and the nasal side. The patient seen in this case had an ulcerative basal cell carcinoma of the medial canthal-nasal area. The proposed excision and the nasolabial flap were outlined (Fig. 5.51a, b). The lesion was excised and clear margins were revealed by frozen section biopsies (Fig. 5.51c). A part of the underlying periosteum had to be sacrificed, but the remainder provided a sufficiently vascularized bony bed. The medial canthal tendon was preserved. After undermining, the flap was advanced superiorly, covered the defect, and was sutured in place (Fig. 5.51d).

5.2.8 Cheek Rotation Flaps

The wide surface of the cheek and its tissue laxity constitutes an ideal donor site for rotation flaps of various extents. Cheek rotation flaps are very reliable random pattern flaps as long as a strong vascular plexus and a wide base support them. The arc length of the rotation flap at the cheek adheres to the general rules of the rotation flap design but it is determined by the variable skin laxity of the different cheek subunits and must be individualized after thorough examination of the skin properties.

5.2.8.1 Deep-Plane Cheek Rotation Flap Inferiorly Based

The patient seen at this case had a recurrent basal cell carcinoma previously treated by surgery and radiotherapy (Fig. 5.52a). The rotation flap was designed having its base inferiorly (Fig. 5.52b). The lesion was excised as a triangle and clear margins were revealed by frozen section biopsies (Fig. 5.52c). The lesion was excised at the deep subcutaneous level but the flap elevation transitions in a deep, sub-SMAS, level (Fig. 5.52d). Previous radiation had impaired the microcirculation, and the deep dissection plane increases the vascularity of the flap. The flap was rotated and sutured in place with ease (Fig. 5.52e). The postoperative result at 4 months following surgery is shown in Fig. 5.52f.

5.2.8.2 Cheek Rotation Flap Medially Based at Reconstruction of the Upper Buccal Subunit

The buccal subunit provides rotation flaps that usually can be designed with an arc shorter than usual due to the laxity of this region. Such a case is seen in Fig. 5.53a–c. The lesion was excised in clear margins (Fig. 5.53d) and the flap was elevated in the subcutaneous plane. There is no risk of damage for the buccal branches of the facial nerve. The flap fills the surgical defect without tension (Fig. 5.53e) accomplishing an excellent result (Fig. 5.53f).

5.2.8.3 Cheek Rotation Flap Medially Based at Reconstruction of the Lower Buccal Subunit

The same flap as in the previous case, also with a short arc, can be placed in a more inferior position to reconstruct a defect at the lower buccal subunit (Fig. 5.54a, b). Even though the flap is raised at the subcutaneous plane, meticulous dissection must be performed as long as the flap here is situated at the danger zone of the marginal mandibular branch of the facial nerve (Fig. 5.54c). The rotation flap was dissected, was mobilized, and reached the defect (Fig. 5.54d). Final suturing was performed without tension (Fig. 5.54f), and the early postoperative result was satisfactory without any facial nerve damage (Fig. 5.54g).

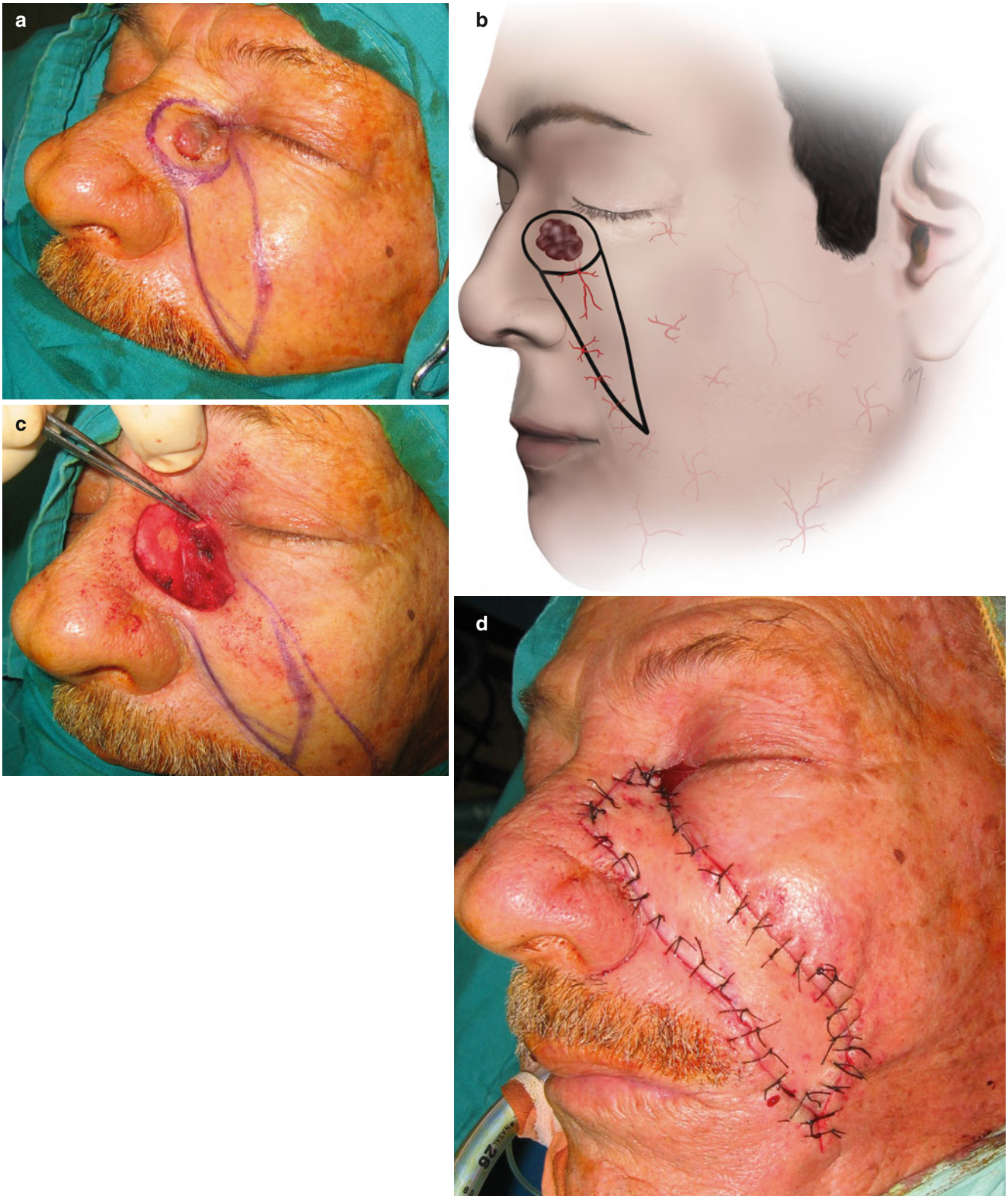

Fig. 5.51 (**a**, **b**) Outline of the nasolabial flap. (**c**) The defect after excision. The lower edge of the anterior limb of the medial canthal tendon is pointed. (**d**) Flap sutured in place

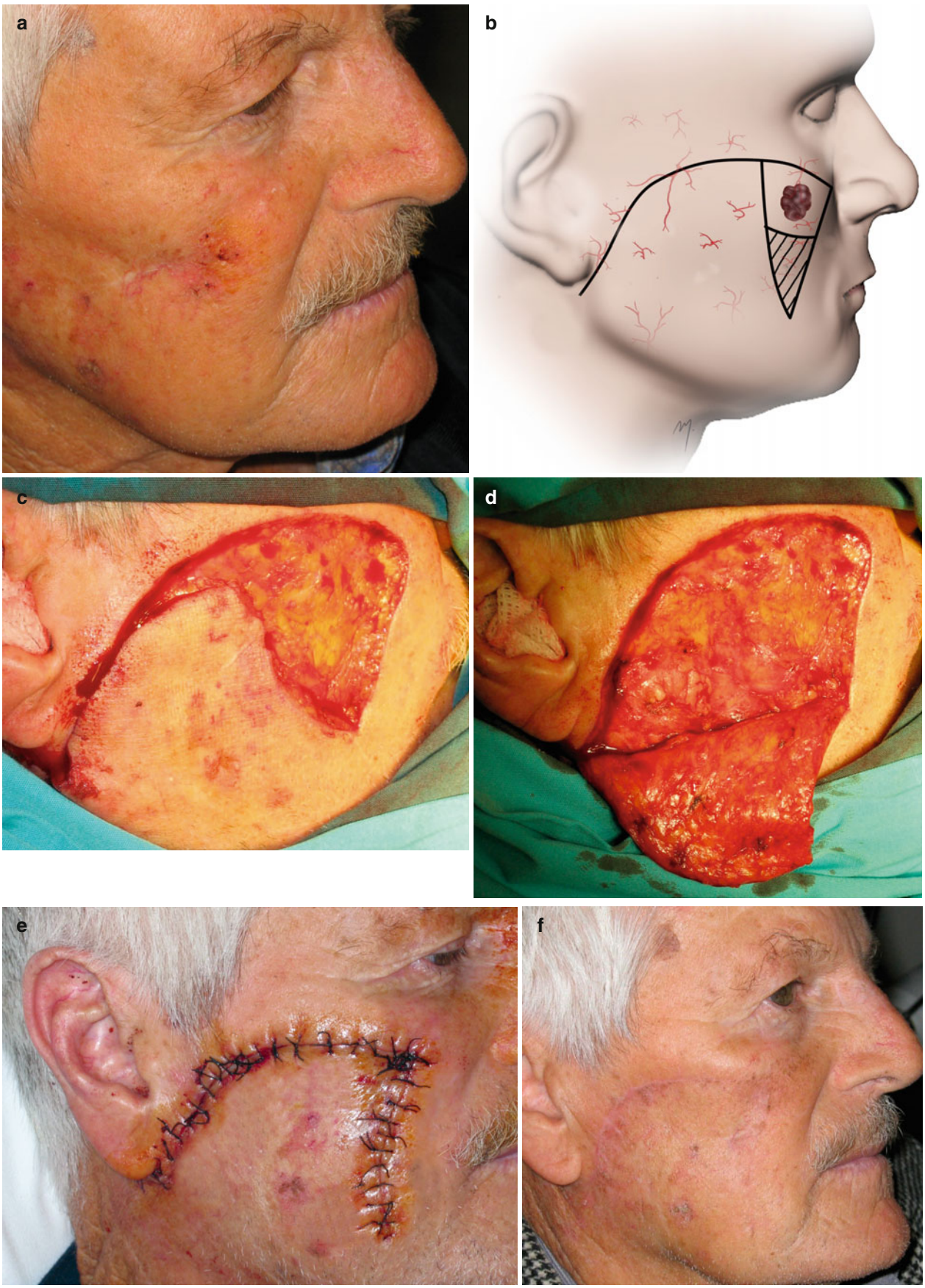

Fig. 5.52 (**a**) A recurrent basal cell carcinoma located at the cheek. (**b**) The flap outlined. (**c**) The defect is triangulated and restoration is performed with an inferiorly based cheek rotation flap. (**d**) Flap is raised in the deep plane. (**e**). Rotation flap sutured in place. (**f**) Postoperative result at 4 months

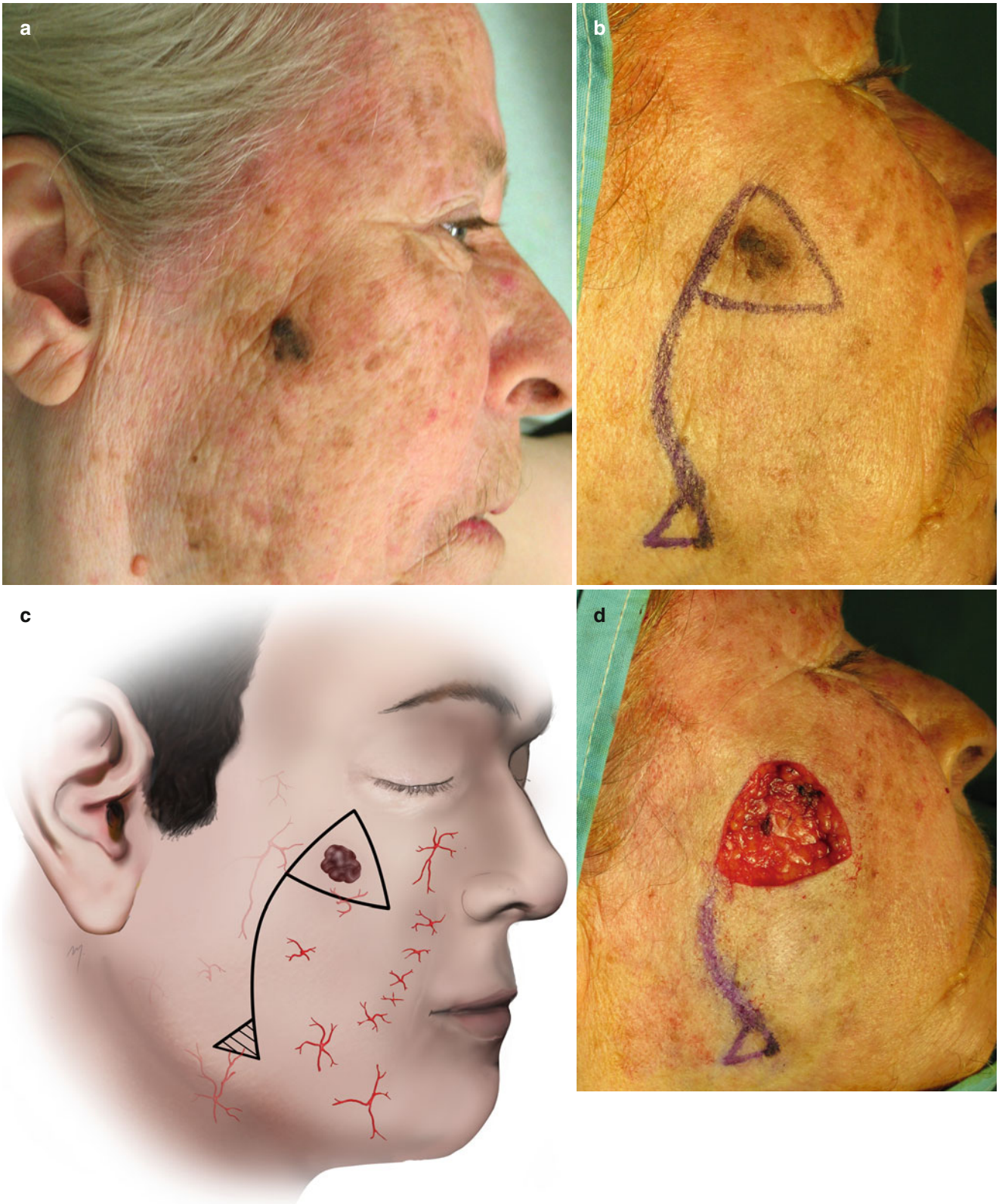

Fig. 5.53 (**a**) A lesion at the upper buccal subunit. (**b**, **c**) A rotation flap with a relative short arc is able to reach the defect. (**d**) The lesion is excised as a triangle. (**e**) The rotation flap sutured in place. (**f**) Result at 12 months

Fig. 5.53 (continued)

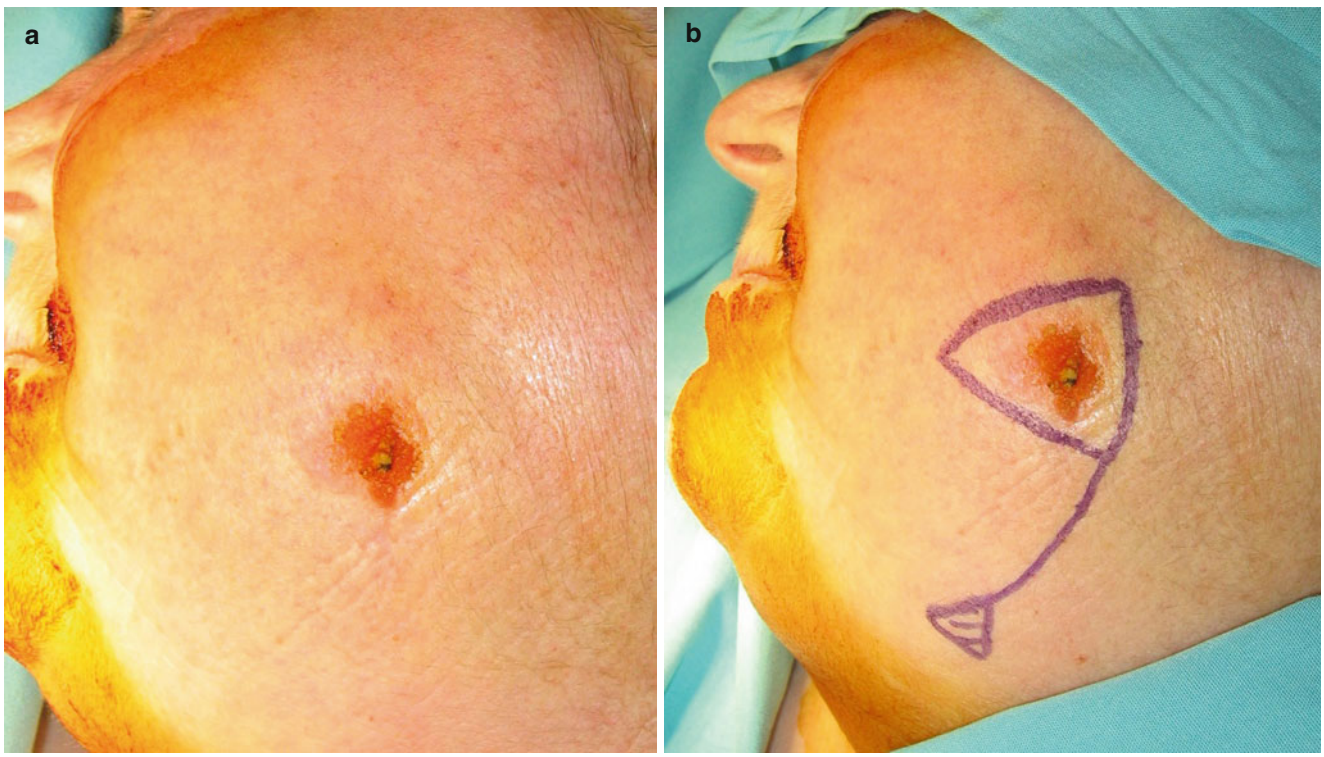

Fig. 5.54 (**a**) A basal cell carcinoma located at the lower buccal subunit. (**b**) The rotation flap outlined. (**c**) The flap is situated at the danger zone of the marginal mandibular branch of the facial nerve. (**d**) Flap raised at the subcutaneous level. (**e**) The flap fully mobilized to reach the defect without tension. (**f**) Immediate postoperative view. (**g**) Result at 2 months

Fig. 5.54 (continued)

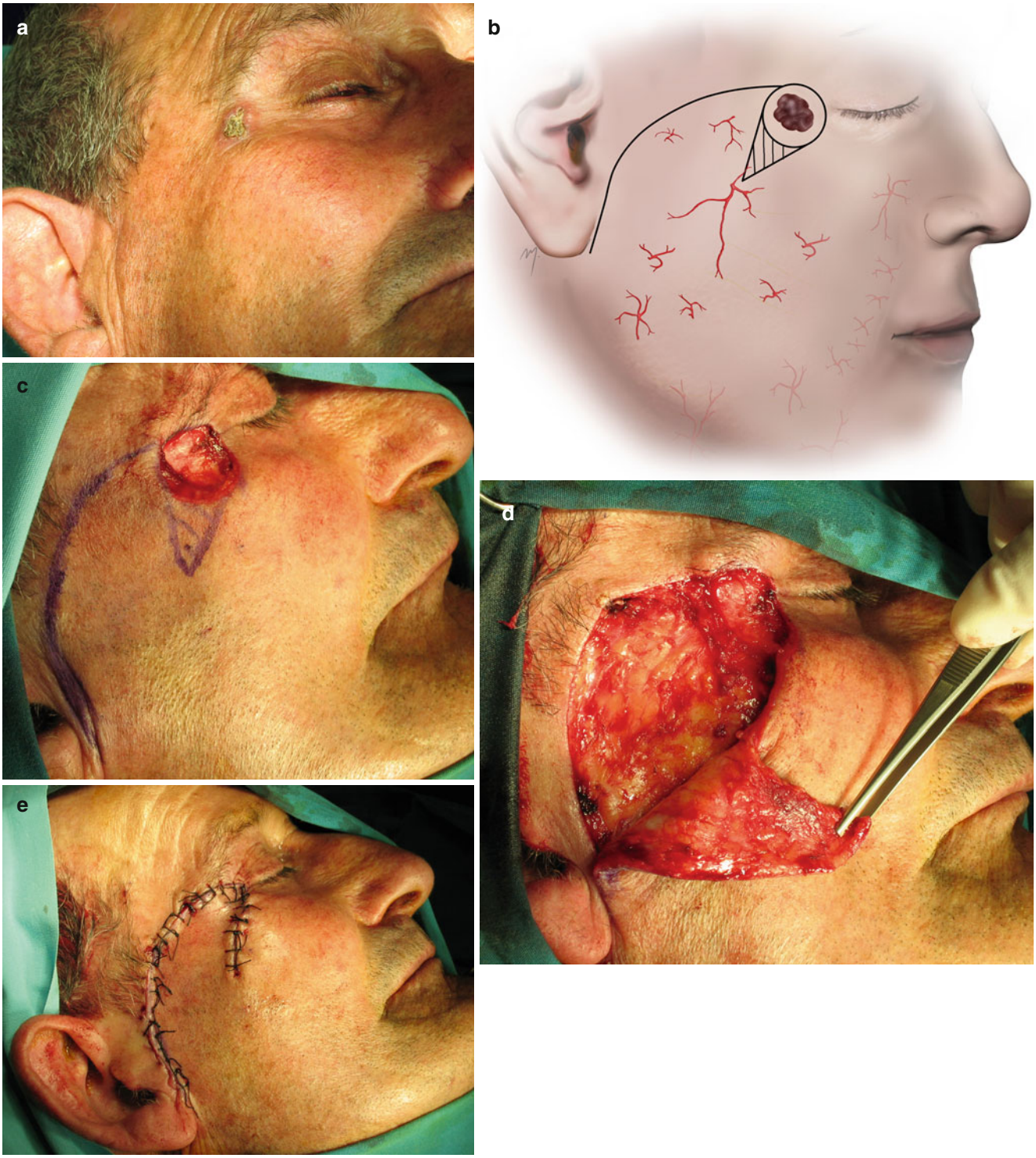

Fig. 5.55 (**a**) A basal cell carcinoma located at the lateral canthal region. (**b**, **c**) Outline of an inferiorly based rotation flap with a relative long arc. (**d**) Elevation of the flap at the superficial subcutaneous plane. (**e**) The flap is sutured in place without any tension

5.2.8.4 Cheek Rotation Flap Inferiorly Based at Reconstruction of the Lateral Canthal Area

The patient presented in Fig. 5.55a had a basal cell carcinoma located at the lateral canthal region. The rotation flap that was used in this case was designed with a relative long arc (Fig. 5.55b, c). This was determined by the laxity of the donor site aiming in a flap without tension that could distort the recipient area. The flap was dissected in a superficial subcutaneous plane (Fig. 5.55d), with extreme care over the

zygomatic arch, so as to avoid damage of the frontal branch of the facial nerve. The rotation flap reached the defect tensionless without causing any distortion (Fig. 5.55e).

5.2.8.5 Cheek Rotation Flap Laterally Based at Reconstruction of the Infraorbital Subunit (Imre Flap)

Defects of the infraorbital subunit of the cheek can be closed by a laterally based rotation according to the initial description of Imre (1928) that transfers tissue from the nasolabial subunit (Fig. 5.56a, b). The flap is raised in the subcutaneous plane. It is undermined in that extent where it reaches the defect without tension and is sutured in place (Fig. 5.56c). As with any incision that is made in the infraorbital crease, edema of the eyelid may occur as a complication in the early postoperative period, which resolves within the first year (Fig. 5.56d, e).

5.2.9 Cheek Rotation-Advancement Flaps

5.2.9.1 Mustardé Flap

Mustardé originally described this flap for the reconstruction of wide lower eyelid defects (Mustardé 1991). However, it is a very useful rotation-advancement flap that can be used to transfer skin from the lateral cheek-resurfacing medium to large defects that are located at the infraorbital region.

The patient presented in Fig. 5.57a had a large cystic basal cell carcinoma of the infraorbital subunit of the cheek. The defect is triangulated and the Mustardé flap is outlined (Fig. 5.57b, c). The incision line of the flap starts from the base of the triangle running laterally and curves upward and outward from the lateral canthus. This is done to anchor the flap in a level superior to the eyelid reducing the pull of the flap to it and avoiding thus ectropion formation. The incision line then descends into the preauricular skin crease and typically ends to the earlobe. If additional mobilization will be needed, the incision can be extended around the ear lobule into the retroauricular region and ending at the neck. The tumor is excised above the level of orbicularis oculi muscle and clear margins are revealed by frozen section (Fig. 5.57d).

The undermining of the flap is performed in the subcutaneous plane (Fig. 5.57e), and elevation starts from its superior and medial part. Even though elevation of the flap is performed above the SMAS layer, great attention must be given not to lose that plane when dissecting over the zygomatic arch so far as the frontal branch of the facial nerve crosses the zygomatic arch and lies very superficially. Elevation continues over the parotidomasseteric area at the base of the flap usually up to the mandibular angle in the same face-lift plane, and almost the whole cheek is undermined and raised. The flap is checked if it rotates reaching the recipient site without any tension. This is of great importance because even a small degree of tension will act on the lid drawing it down and leading to severe ectropion. If despite the wide undermining the flap fits under tension, additional mobilization is gained from its retroauricular and neck extension.

After adequate mobilization has been achieved, the flap is sutured in place (Fig. 5.57f). The flap is anchored with absorbable subcutaneous sutures to the periosteum of the frontal process of the maxilla and to the periosteum of the supraorbital rim and the zygomatic bone. Mobilization of the skin of the temple may be also needed to facilitate donor site closure. The postoperative result at 6 months shows a satisfactory reconstruction (Fig. 5.57g). Of the abovementioned preventive measures taken, minimal pulling down of the lower lid often occurs but seldom needs secondary correction.

5.2.9.2 Mustardé Flap for Malar Reconstruction

The patient presented in Fig. 5.58a had a basal cell carcinoma of the lateral infraorbital region. According to the principles of the original Mustardé flap, with a same design, a laterally positioned flap can be used to reconstruct the defect located just lateral to the infraorbital subunit. The defect is triangulated and the flap is outlined (Fig. 5.58b, c). The flap is elevated in the usual manner, deep to the subcutaneous plane, and resurfaces the defect with ease (Fig. 5.58d, e). The use of this flap results in a very satisfactory postoperative appearance (Fig. 5.58f).

5.2.9.3 Cheek Rotation-Advancement Flap Inferiorly Based

Preauricular skin can be transferred medially to close defects by means of inferiorly based cheek rotation-advancement flaps. At the patient presented in Fig. 5.59a–c, an inferiorly based cheek rotation-advancement flap was used to reconstruct a small defect of the zygomatic subunit.

5.2.9.4 Deep-Plane Cheek Rotation-Advancement Flap Anteriorly Based

A patient with microvascular disease exhibits a large basal cell carcinoma located at the zygomatic subunit of the cheek (Fig. 5.60a). Excision of the lesion and reconstruction of a cheek rotation-advancement anteriorly based flap and raised in the deep plane was planned. The flap was outlined (Fig. 5.60b, c). It slightly extends to the upper neck in a quite similar to the cervicofacial flap (see Chap. 8) manner. The lesion was excised in a circular manner in tumor free margins (Fig. 5.60d). The frontal branch of the facial nerve lies deeper of the excision plane. A triangle was excised triangulating the defect (Fig. 5.60e).

The lesion was excised at the deep subcutaneous level but the flap elevation transitioned from cephalad to caudal in a

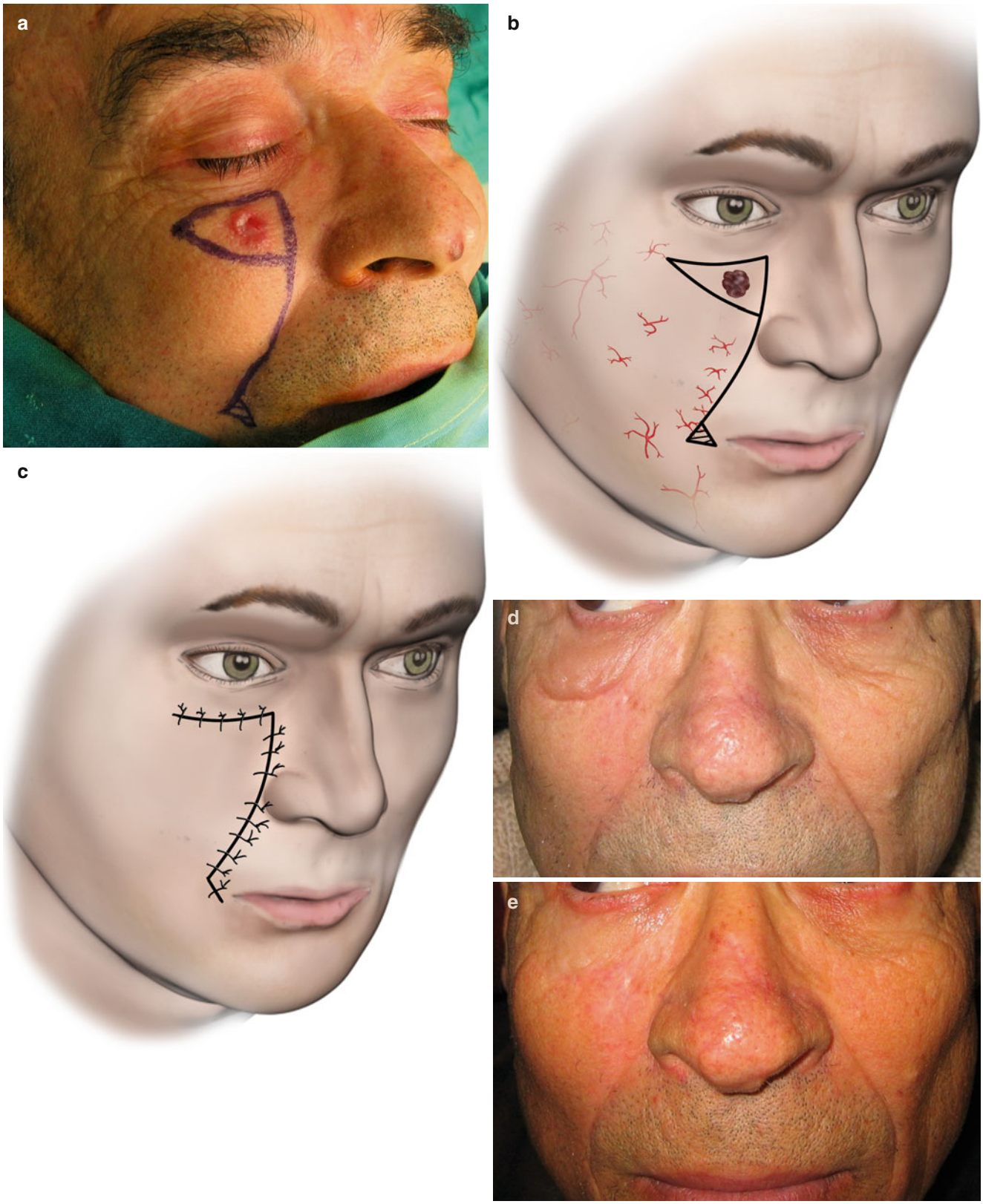

Fig. 5.56 (**a**, **b**) The defect is triangulated and from its base a curved incision is outlined along the nasolabial crease. A small Burow's triangle is excised at the inferior distal end. (**c**) Flap sutured in place. (**d**) Result at 1 month. Edema of the lower lid is present. (**e**) Result at 1 year. Lower lid edema is completely resolved

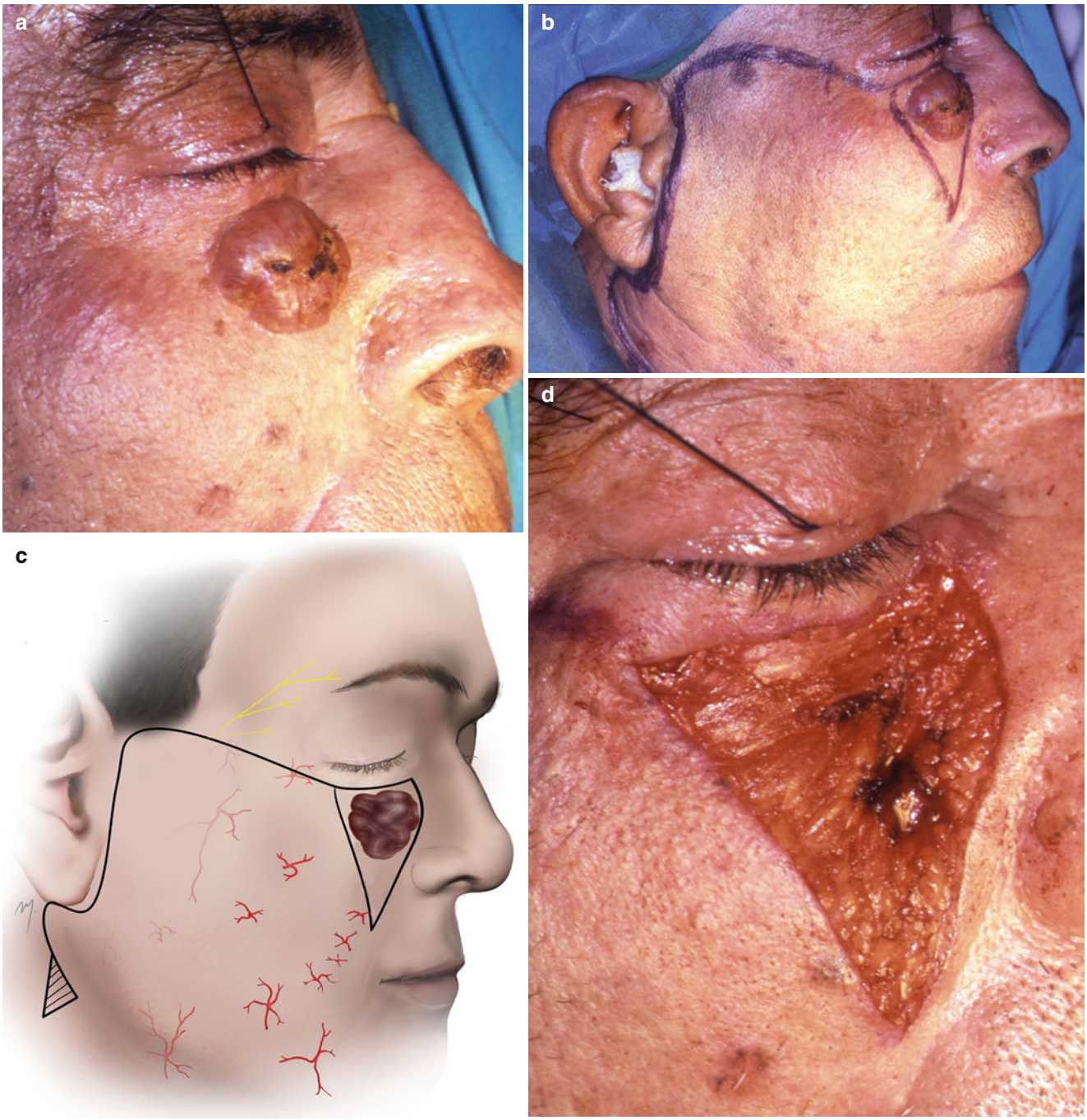

Fig. 5.57 (**a**) Cystic basal carcinoma of the infraorbital region. (**b**, **c**) Excision of the lesion in a triangular form and the outline of the Mustardé flap. (**d**) Tumor excised. The orbicularis oculi muscle is intact. (**e**) The flap is elevated in the subcutaneous (face-lift) plane. (**f**) Flap sutured in place. Deep sutures anchor the flap to periosteum. (**g**) Postoperative result at 6 months

deep, sub-SMAS, level and a thick and robust flap was raised (Fig. 5.60f, g). The flap was sutured in place without tension resurfacing the defect (Fig. 5.60h). The final result is satisfactory, as long as symmetry and contour are maintained and the scars remain quite hidden (Fig. 5.60i, j).

5.2.10 Cheek Flaps for Nose and Lip Reconstruction

The cheek can also be a donor site and transfer tissue in nasal reconstruction. This includes usually the reconstruction of

Fig. 5.57 (continued)

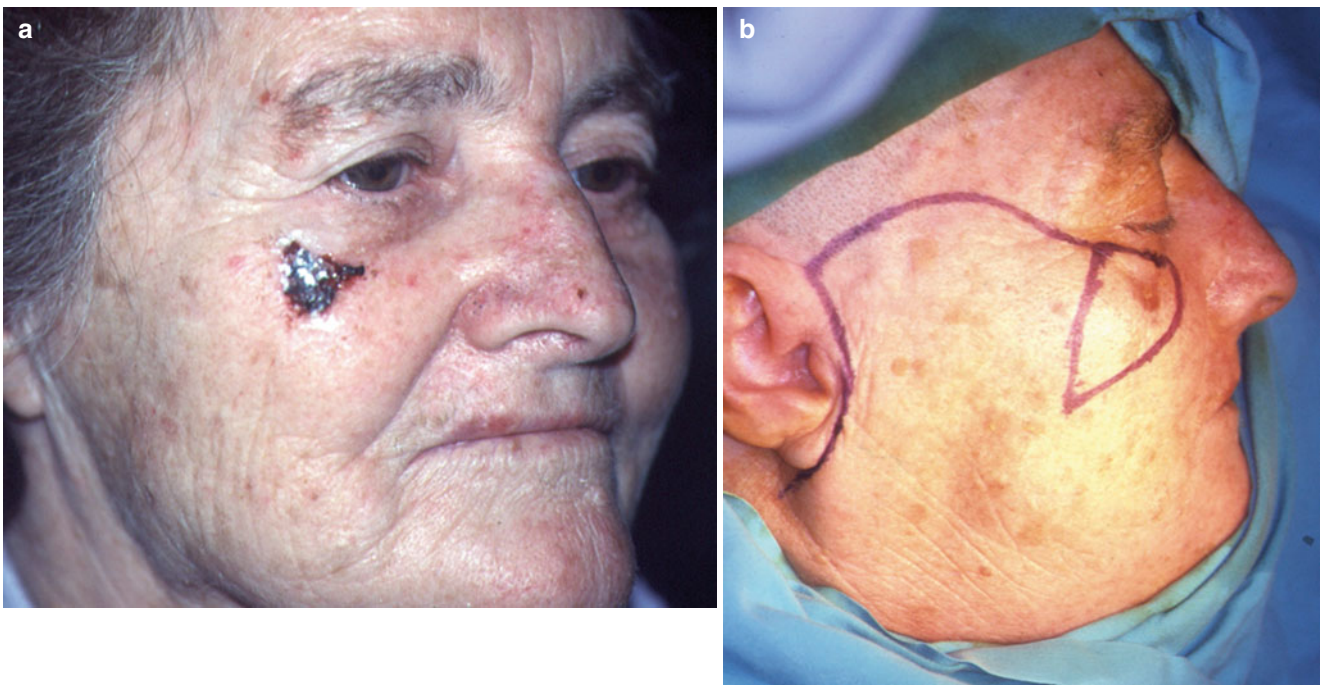

Fig. 5.58 (**a**) A basal cell carcinoma located just lateral to the infraorbital subunit of the cheek. (**b**, **c**) The flap outlined. (**d**) Flap elevated. (**e**) Flap in place. (**f**) Result at 9 months postoperatively

Fig. 5.58 (continued)

the nasal lobule, the nasal lining, the medial canthal region as presented above, and in selected cases the nasal side.

5.2.10.1 Island Pedicle Flap at Reconstruction of the Upper Nasal Sidewall

An island pedicle flap donated from the cheek can reconstruct midsized defects of the nasal sidewall. Although this is not the ideal reconstructive option (shallowing of nose-cheek junction will occur), the island pedicle flap provides an extremely viable, quick, and one-flap solution in selected patients.

The patient seen in Fig. 5.61 had an ulcerative basal cell carcinoma of the nose that led to a through and through nasal defect. The medical status of the patient imposed a short lasting operation and reconstruction with a well-vascularized flap. Moreover at this area there is no need to reconstruct any

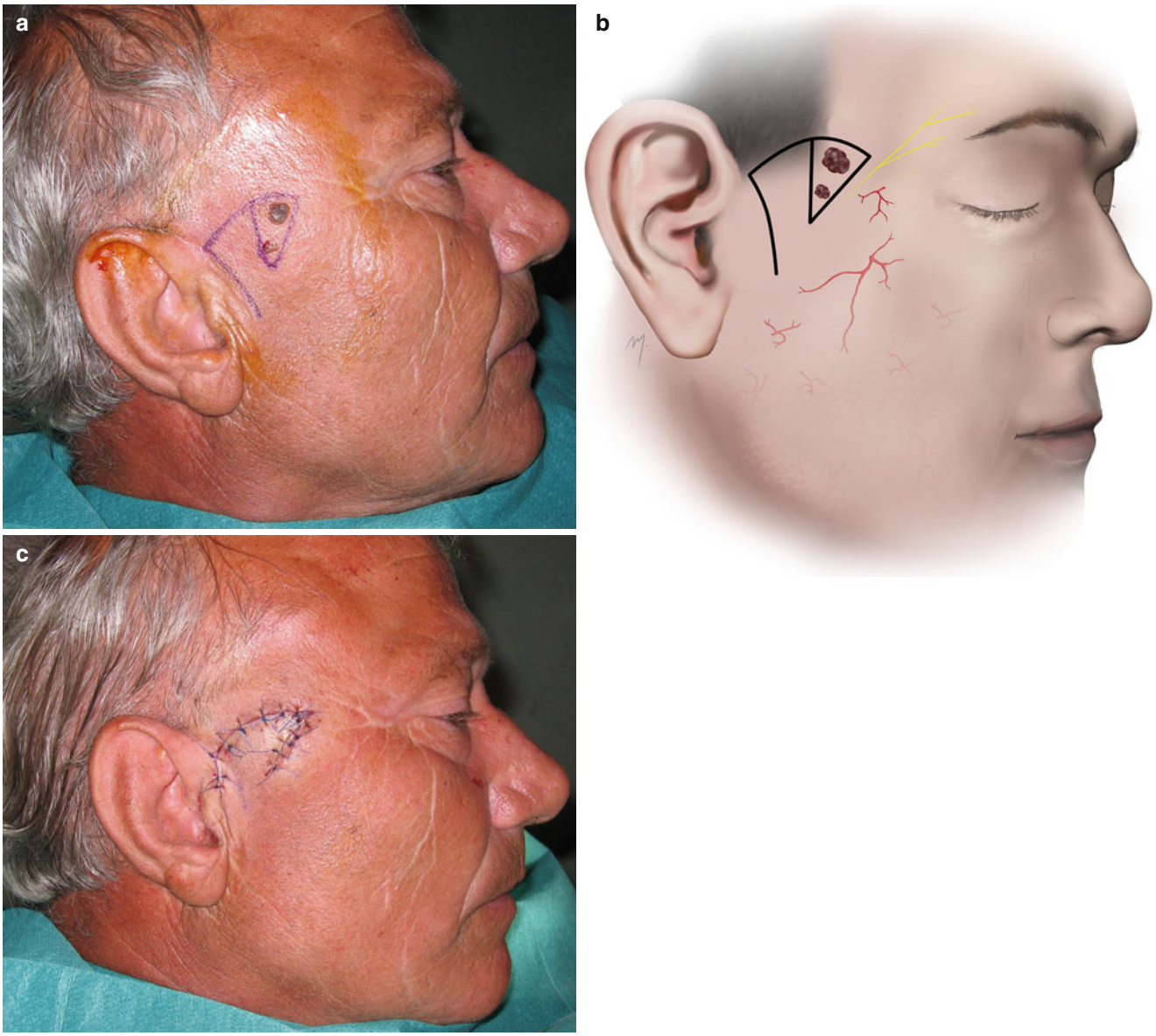

Fig. 5.59 (**a**, **b**) A small inferiorly based cheek rotation-advancement flap is used to reconstruct a defect of the zygomatic subunit. (**c**) Flap sutured in place

deep (mucosal or bony) structure. A flap needs only to cover the defect overlapping and anchored to a zone of healthy bone margin. Thus, it must survive over this narrow (weak vascular) bed, and with time the bare undersurface reepithelializes without any contraction. The designed island flap fulfills these demands and is perfused by a rich anastomotic network from the several arteries that are distributed to its base and was chosen for the restoration (Fig. 5.61a, b). After undermining in the way already described, the flap was advanced superiorly, covered the through and through defect, and was sutured in place (Fig. 5.61c). The restoration results in a flattening in some degree of the nasal-facial line (Fig. 5.61d).

5.2.10.2 Island Pedicle Flap at Reconstruction of the Lower Nasal Side

In small nasal side defects that are located just next to a shallow nose-cheek junction, an island pedicle flap from the nearby nasolabial cheek can give a satisfactory result.

The patient demonstrated in Fig. 5.62 had a small nevus located at the nasal side. The proposed defect was too small and did not involve the lobule and the nose-cheek junction appeared to be shallow. An island pedicle flap was designed from the vicinity of the nasolabial fold with a length twice the length of the side of the defect (Fig. 5.62a, b). The flap was advanced and closure was achieved in a V-Y fashion

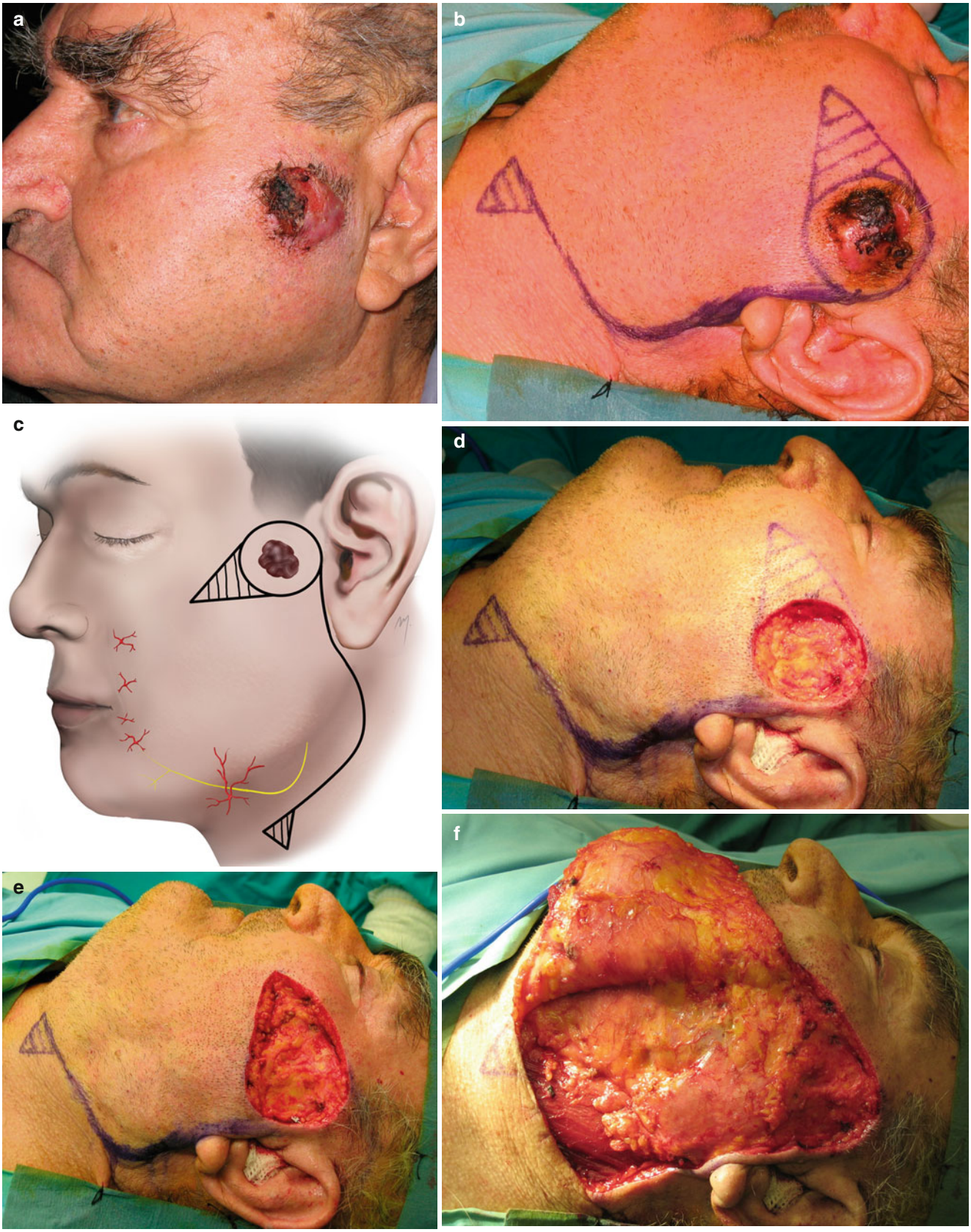

Fig. 5.60 (**a**) A large basal cell carcinoma located at the zygomatic subunit of the cheek. (**b**, **c**) Flap design. The flap is extended to the upper neck. (**d**) Excision of the lesion. (**e**) Defect triangulated. (**f**) Sub-SMAS elevation of the flap. The platysma muscle is incorporated on the undersurface of the flap and the parotidomasseteric fascia, left in place, very thin and shiny. (**g**) A thick and robust flap was raised. (**h**) Flap sutured in place. (**i**, **j**) Result at 6 months

Fig. 5.60 (continued)

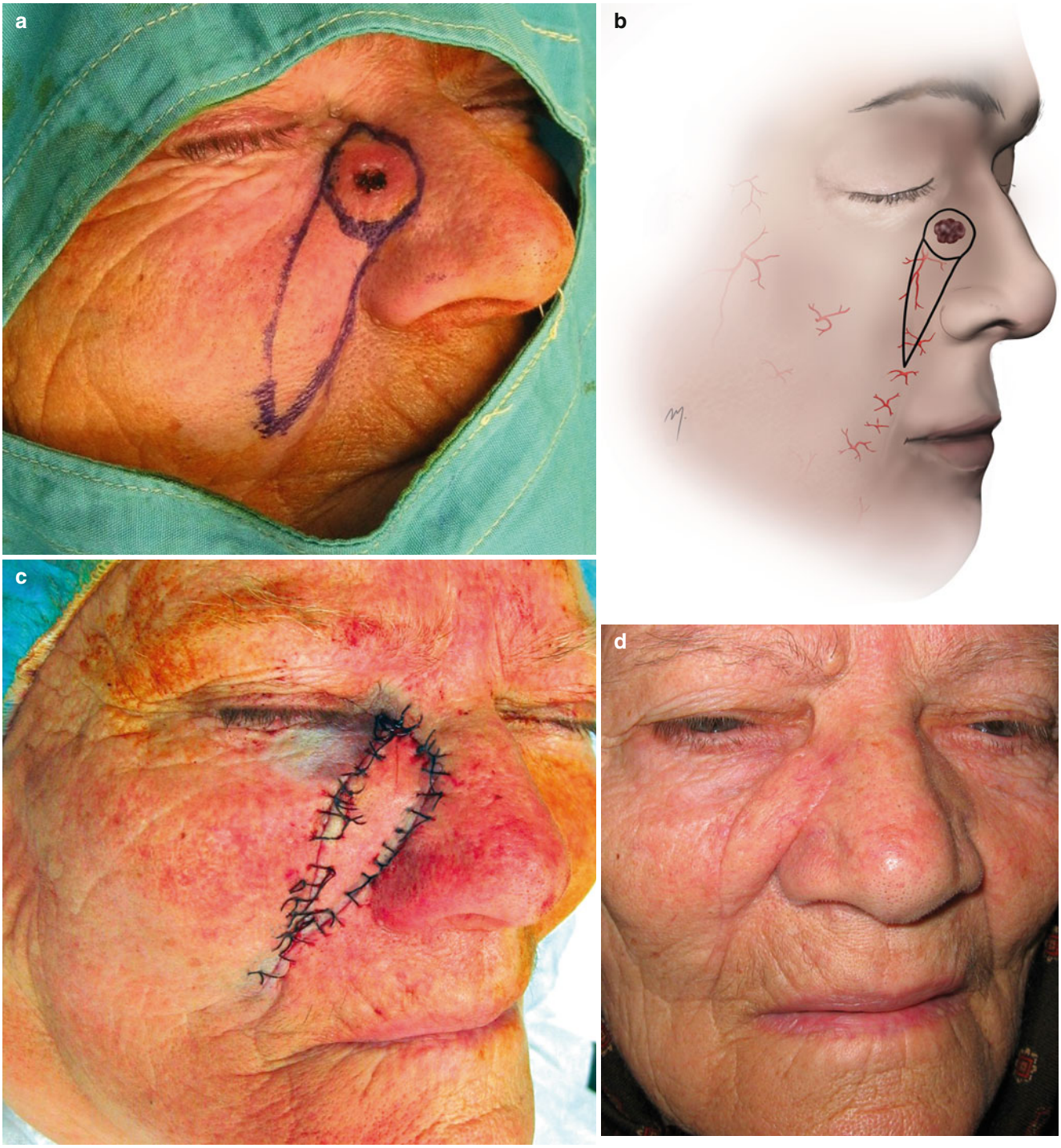

Fig. 5.61 (**a**, **b**) Outline of the flap. (**c**) Flap in position. (**d**) Final result

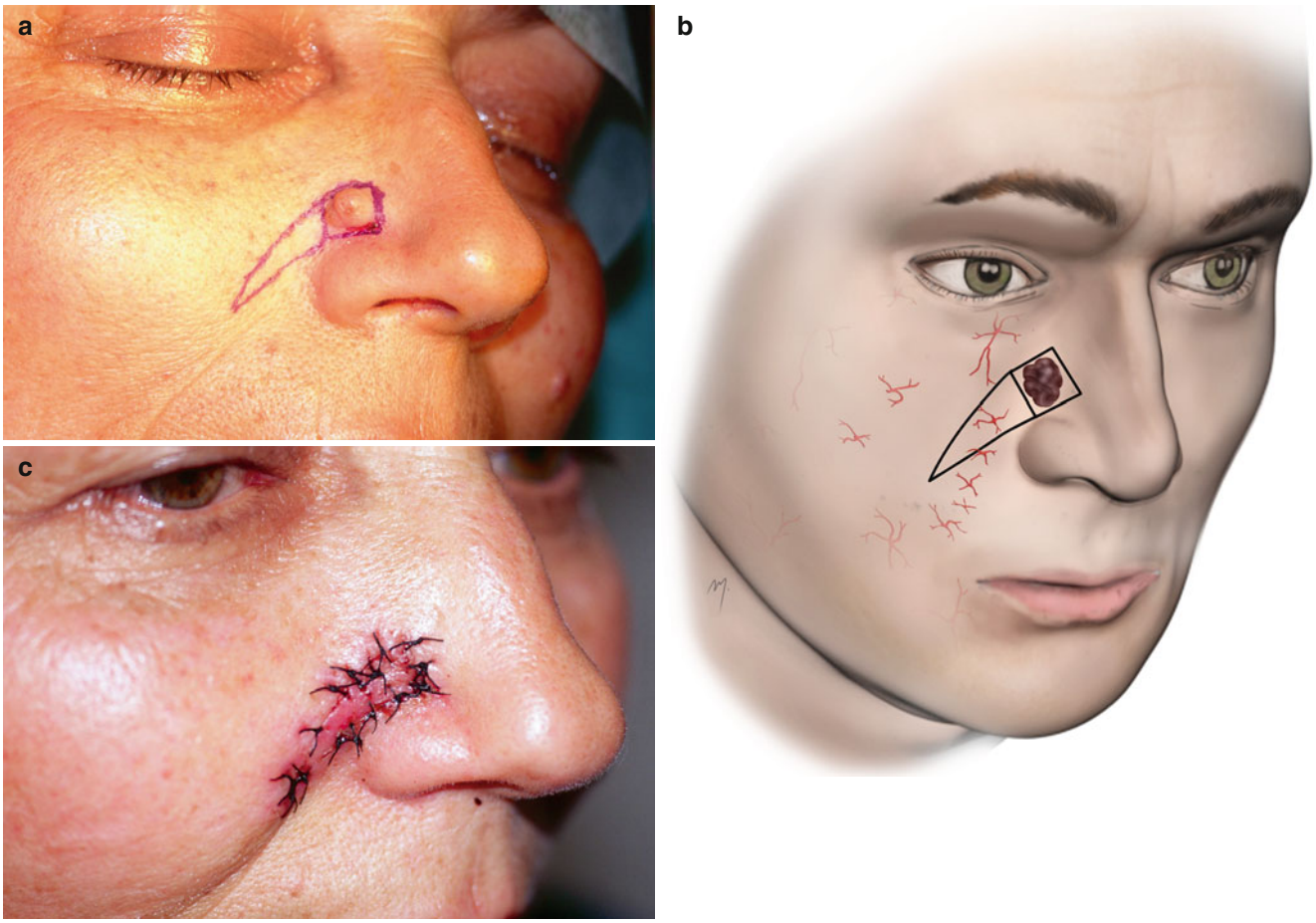

Fig. 5.62 (**a**, **b**) A small nevus at the nose-cheek junction. (**c**) Flap sutured in place

without any distortion (Fig. 5.62c). The flap is almost fully camouflaged as being the upper part of the nasolabial fold. This reconstruction must be avoided in larger defects.

5.2.10.3 Cheek Advancement Flap at Reconstruction of the Nasal Side

Cheek advancement flaps horizontal to the dorsal sidewall of the nose have been used in the past. After the introduction of the nasal subunit principle, the maintenance of the nasofacial sulcus that is distorted by this method gained interest. The excision is outlined as a square and the flap is outlined with the incision lines running laterally to the cheek and parallel to natural creases. The base of the flap is slightly wider than its leading edge and its length twice the length of the defect (Fig. 5.63a, b). Two small triangles at its base are excised to prevent dog-ear formation.

The flap is advanced to the defect and sutured in place. The upper limb of the flap does not exercise any tension to the lower lid, and the lower limb is placed at the nasolabial line (Fig. 5.63c). The postoperative result shows a satisfactory result with minimal distortion of the nasal-facial sulcus (Fig. 5.63d).

From the perspective of a subunit approach, this flap is ideal to resurface the cheek in a combined nose-cheek defect up to the nose-cheek junction and to resurface the rest of the nose defect with a second flap or a skin graft (Jackson 2007).

5.2.10.4 Nasolabial Flaps in Nasal Reconstruction

A nasolabial flap can be used in nasal reconstruction for its lateral wall and ala but also for the columella usually as a two-stage pedicled flap.

The nasolabial flap, even widespread in nasal reconstruction, never gives an excellent result at once because it almost always leads to pincushioning and flattening of the nasofacial sulcus. However, it is easy to design and to perform, is very reliable, and seldom gets lost. Thus, it has been characterized as a favorite flap of inexperienced surgeons (Jackson 1985). Despite its disadvantages, it remains a very useful and extremely safe tool especially in old patients with comorbidities and reduced healing reserves. As mentioned this type of reconstruction is very quick to perform, needing reduced operating time, is ideal for patients with a poor medical history, and can resurface quite large nasal defects with minimal risk. If the flap can be thinned safely, this will

Fig. 5.63 (**a**, **b**) Cheek advancement flap outlined. (**c**) Flap advanced and sutured in place. (**d**) Result at 5 months

reduce the possibility of pincushioning. Otherwise, the produced pincushion can be corrected by a debulking procedure in a second time but this often is denied by the old patients that do not have special aesthetic demands. If aesthetics comes in first priority, a rather different reconstructive solution must be considered. In an attempt to reduce the possibility of the pincushioning and the shallowing of the nasofacial groove, wide undermining of the donor and defect sites, significant thinning of the flap, excision of large Burow's triangle that improves the transposition movement, and the application of periosteal sutures to maintain the nasofacial sulcus have been proposed (Zitelli 1990).

A nasolabial flap that reconstructs the nose is based most of the time superiorly but can also be based inferiorly. Despite the fact that the nasolabial flap is not the optimal solution in external nasal coverage, in contrary it provides a big amount of tissue for successful internal nasal lining in the fashion of a turn-over flap.

5.2.10.4.1 Superiorly Based Nasolabial Flap for Reconstruction of Medial Alar Defects

In the case presented, a patient has a basal cell carcinoma at the medial third of the ala that involves also the junction of three nasal subunits (Fig. 5.64a).

Fig. 5.64 (**a**) A basal cell carcinoma at the junction of the alar tip sidewall subunits of the nose. (**b**, **c**) The area of the proposed excision and the superiorly based nasolabial flap is outlined. (**d**) The surgical defect. The underlying lateral crus of the alar cartilage is intact. (**e**) The flap raised in a deep level. The levator labii superioris alaeque nasi muscle is clearly seen. (**f**) Flap transpositioned to the defect. (**g**) The flap is sutured in place

Fig. 5.64 (continued)

The nasolabial flap is outlined having its base superiorly and two Burow's triangles are outlined to be excised if needed (Fig. 5.64b, c). The needed length of the flap is determined by measuring with a gauze. The flap is of random pattern and receives its blood supply due to its subcutaneous and subdermal plexus that is perfused from branches of vessels (nasal branches of infraorbital, angular, dorsal nasal) round its base. The lesion was excised in clear margins revealed by frozen section biopsies. The defect involved full-thickness skin and nasalis muscle and not the underlying lateral crus of the alar cartilage and its perichondrium (Fig. 5.64d). The flap is raised in a deep level to gain enhanced vascularity due to the medical status of the patient (significant peripheral vascular disease) (Fig. 5.64e). The flap is transferred almost horizontally to reach the defect (Fig. 5.64f).

The flap was sutured in place covering the defect and the donor site was closed easily placing the closure line into the natural nasolabial line (Fig. 5.64g). No thinning of the flap was done at this stage so as not to compromise its vascularity.

5.2.10.4.2 Superiorly Based Nasolabial Flap for Reconstruction of Lateral Alar Defects

If the alar defect lies very close to the alar-facial sulcus and even a small skin portion of the junction has to be reconstructed, it becomes more difficult to restore the normal anatomy.

In the case presented, a basal cell carcinoma located at the lateral portion of the alar lobule just adjacent to the alar-cheek groove (Fig. 5.65a) is planned to be excised and the defect reconstructed with a nasolabial flap superiorly based (Fig. 5.65b, c). The arc of "rotation" in these situations is the minimum possible. The flap was undermined in the usual way, transferred to the recipient site, and sutured in place (Fig. 5.65d). The postoperative result shows that even the flap has not been pincushioned in a great degree; however, the alar-facial sulcus has been moderately flattened (Fig. 5.65e).

5.2.10.4.3 Superiorly Based Nasolabial Flap for Nasal Sidewall Reconstruction

Based on the same principles, the nasolabial can reconstruct sidewall defects of the nose. A basal cell carcinoma is located at the nasal sidewall in the patient seen in Fig. 5.66a. A superiorly based nasolabial flap is outlined in the usual manner but situated in a higher position than in the previous cases (Fig. 5.66b). The closure needs more undermining than in the lower positioned nasolabial flaps with the aim also to avoid extensive traction to the lower lid. After this has been done, the flap is sutured in place (Fig. 5.66c).

5.2.10.5 Nasolabial Flaps as Turn-In Flaps in Nasal Lining

The nasolabial flap provides a big amount of tissue for successful internal nasal lining in lateral large through and through nasal defects in the fashion of a turn-over flap. In the case of Fig. 5.67, a large amount of tissue was needed to line the nose internally. A nasolabial turn-in flap was chosen as the best solution (Fig. 5.67a). The flap was incised to its whole perimeter in a manner of a skin island and then raised in the subcutaneous plane, leaving a subcutaneous pedicle at its base (Fig. 5.67b).

A strip of 4–5 mm of skin at its base adjacent to the defect was deepithelialized prior the final setting. This maneuver does not trap skin tissue that could lead to cyst formation. The flap was turned into place and sutured with the remained nasal mucosa (Fig. 5.67c).

5.2.10.6 Two-Stage Nasolabial Flap for Lip Skin Reconstruction

The nasolabial flap provides a great amount of tissue that can be used for the reconstruction of large lip skin defects. A basal cell carcinoma located at the lateral subunit of the upper lip is shown in the patient demonstrated in Fig. 5.68a. A superiorly based nasolabial flap is planned to reconstruct the defect (Fig. 5.68b, c). After excision in clear margins has completed, the flap is raised at the subcutaneous tissue level (Fig. 5.68d) and transposed medially to close the defect (Fig. 5.68e). The flap is sutured in place and the nasolabial defect is closed directly. The flap pedicle remains for a period of 2–3 weeks and at the second surgical stage is divided and the final restoration takes place (Fig. 5.68f).

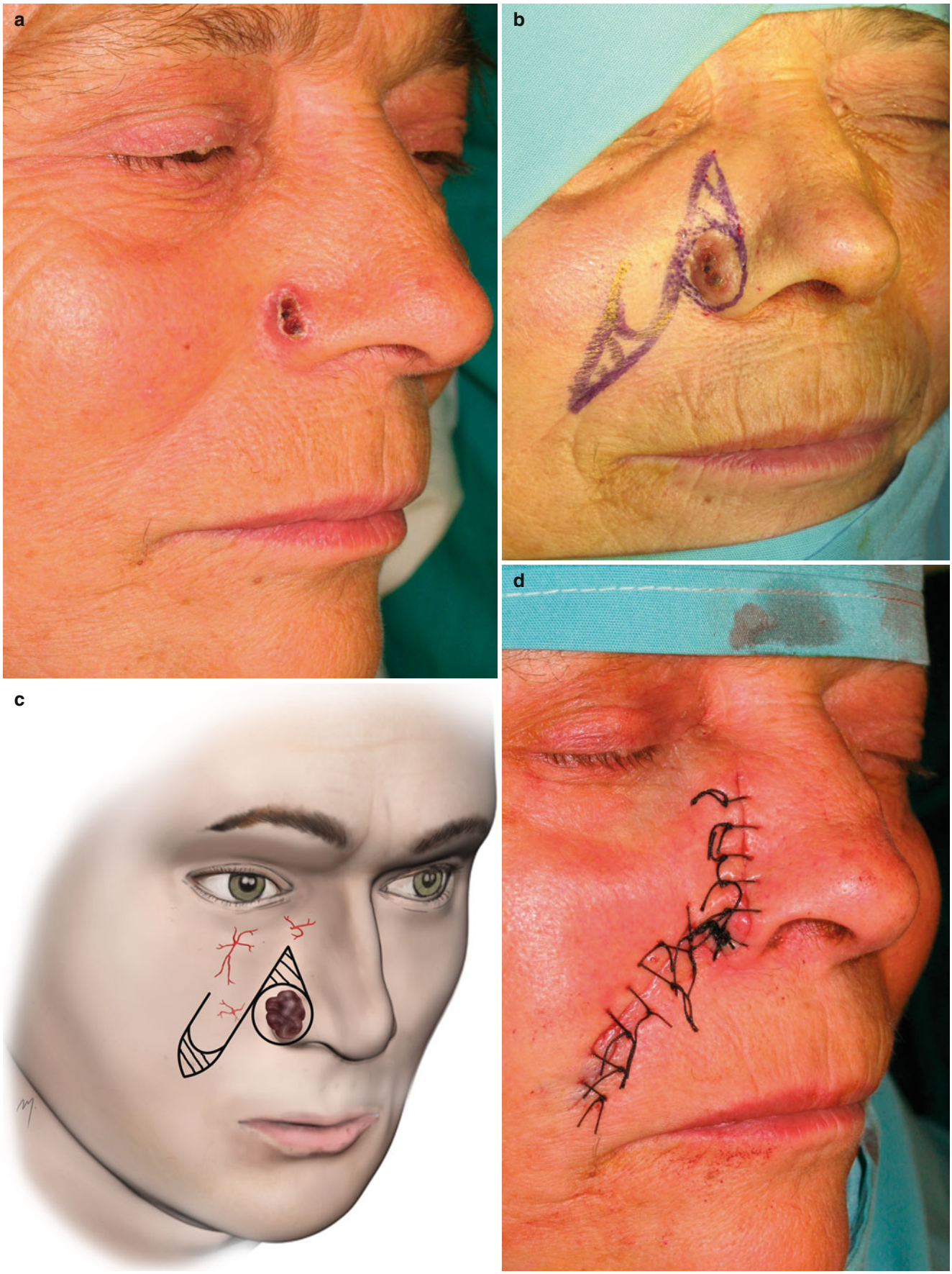

Fig. 5.65 (**a**) Lesion located at the alar lobule just adjacent to the alar-cheek sulcus. (**b**, **c**) A superiorly based nasolabial flap is outlined. (**d**) The flap sutured in place. (**e**) Result at 6 months

Fig. 5.65 (continued)

Fig. 5.66 (**a**) Basal cell carcinoma of the nasal sidewall. (**b**) Nasolabial flap outlined. (**c**) Flap sutured into position

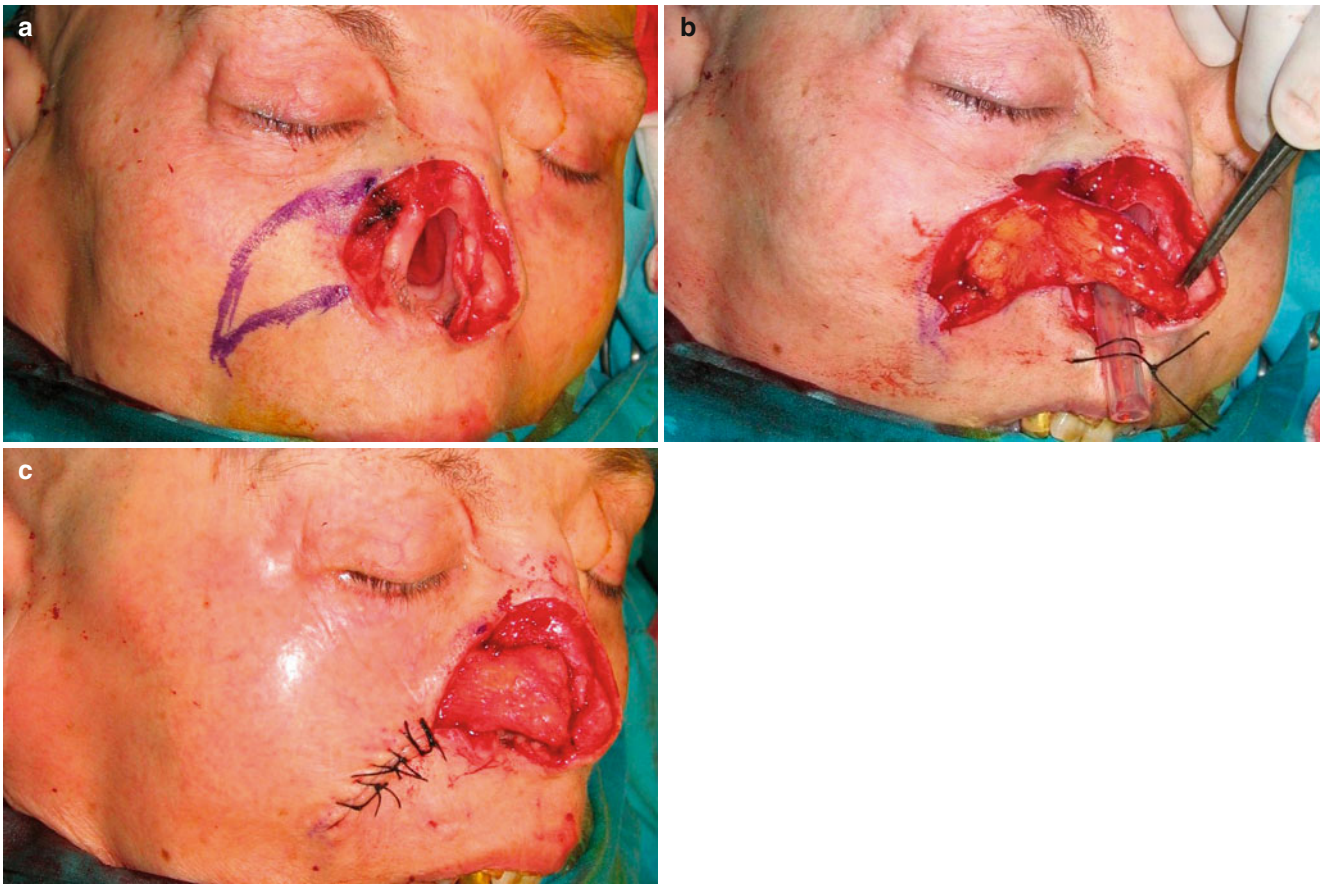

Fig. 5.67 (**a**) A one-stage nasolabial flap is outlined for internal nasal lining. (**b**) Flap raised and turned to the defect. (**c**) Internal nasal lining reconstruction completed

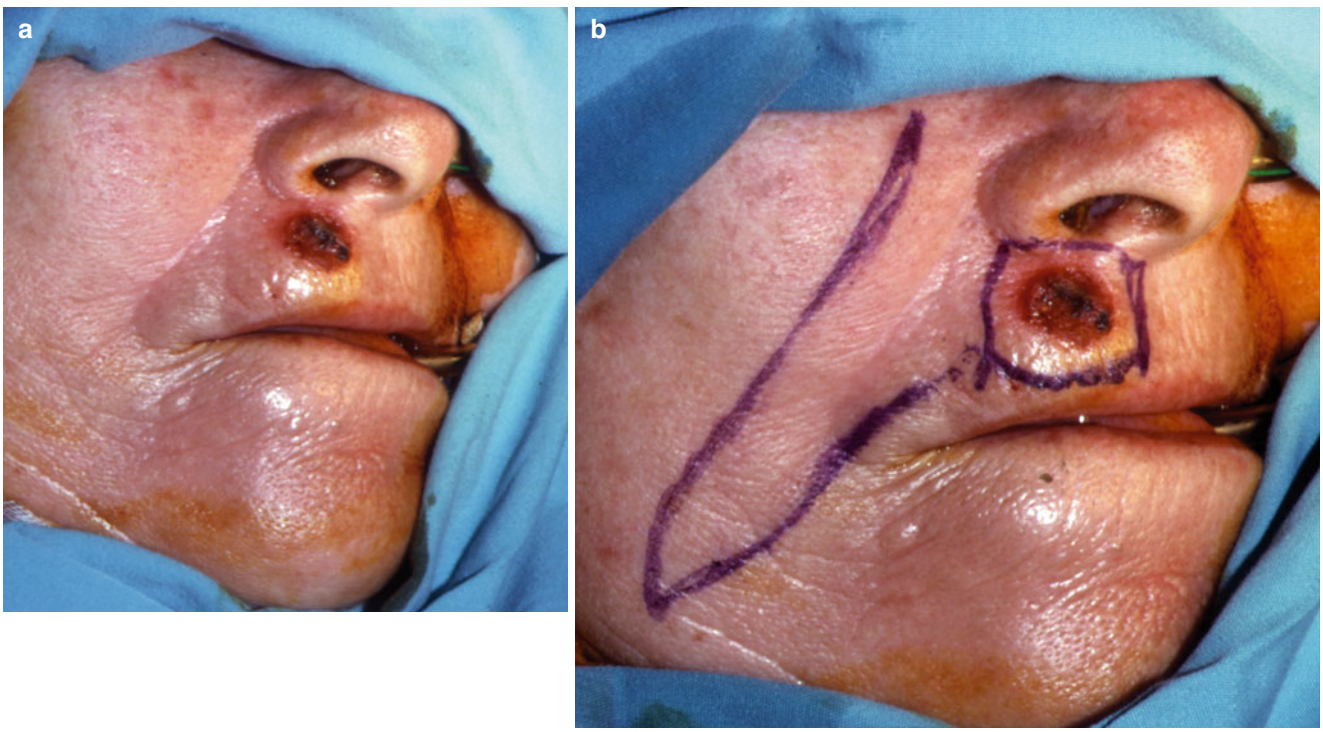

Fig. 5.68 (**a**) Basal cell carcinoma of the upper lip. (**b**, **c**) The proposed excision and a superiorly based nasolabial flap are outlined. (**d**) The flap is elevated. (**e**) Transposition to the defect with ease final suturing. Pedicle remains for 2–3 weeks. (**f**) Pedicle divided

Fig. 5.68 (continued)

References

Aiache A (2001) The suborbicularis oculi fat pad: an anatomic and clinical study. Plast Reconstr Surg 107(6):1602–1604

Aiache AE, Ramirez OH (1995) The suborbicularis oculi fat pads: an anatomic and clinical study. Plast Reconstr Surg 95(1):37–42

Aziz SR, Marchena JM, Puran A (2000) Anatomic characteristics of the infraorbital foramen: a cadaver study. J Oral Maxillofac Surg 58(9):992–996

Baker SR (1997) Triplane rhytidectomy: combining the best of all worlds. Arch Otolaryngol Head Neck Surg 123(11):1167–1172

Barron JN, Emmett AJJ (1965) Subcutaneous pedicle flaps. Br J Plast Surg 18:51–78

Barton FE, Zilmer ME (1982) The cervicofacial flap in cheek reconstruction: anatomic and clinical observations. Presented at the annual scientific meeting of the American Society of Plastic and Reconstructive Surgeons, Honolulu Hawaii

Becker FF, Langford FP (1996) Deep-plane cervicofacial flap for reconstruction of large cheek defects. Arch Otolaryngol Head Neck Surg 122(9):997–999

Bichat F (1802) Anatomie Generale, Applique a la Physiologie et a la Medecine. Brosson Gabon and Cie, Paris
Bozola AR, Gasques JA, Carriquiry CE, Cardoso de Oliveira M (1989) The buccinator musculomucosal flap: anatomic study and clinical application. Plast Reconstr Surg 84(2):250–257
Caminer DM, Newman MI, Boyd JB (2006) Angular nerve: new insights on innervation of the corrugator supercilii and procerus muscles. J Plast Reconstr Aesthet Surg 59(4):366–372
Carstens MH, Stofman GM, Hurwitz DJ, Futrll JW, Patterson GT, Sotereanos GC (1991) The buccinator myomucosal island pedicle flap: anatomic study and case report. Plast Reconstr Surg 88(1):39–50
Chen TH, Chen CH, Shyu JF, Wu CW, Lui WY, Liu JC (1999) Distribution of the superficial temporal artery in the Chinese adult. Plast Reconstr Surg 104(5):1276–1279
Chrcanovic BR, Abreu MH, Custódio AL (2011) A morphometric analysis of supraorbital and infraorbital foramina relative to surgical landmarks. Surg Radiol Anat 33(4):329–335
Cormack GC, Lamberty BGH (1994) The arterial anatomy of skin flaps, 2nd edn. Churchill Livingstone, Edinburgh
Crouzet C, Fournier H, Papon X, Hentati N, Cronier P, Mercier P (1998) Anatomy of the arterial vascularization of the lips. Surg Radiol Anat 20(4):273–278
D'Andrea E, Barbaix E (2006) Anatomic research on the perioral muscles, functional matrix of the maxillary and mandibular bones. Surg Radiol Anat 28(3):261–266
Davis RA, Anson BJ, Budinger JM, Kurth IE (1956) Surgical anatomy of the facial nerve and parotid gland based upon a study of 350 cervicofacial halves. Surg Gynecol Obstet 102(4):385–412
De Castro CC (1980) The anatomy of the platysma muscle. Plast Reconstr Surg 66(5):680–683
Delay E, Lucas R, Jorquera F, Payement G, Foyatier JL (1999) Composite cervicofacial flap for reconstruction of complex cheek defects. Ann Plast Surg 43(4):347–353
Dingman RO, Grabb WC (1962) Surgical anatomy of the mandibular ramus of the facial nerve based on the dissection of 100 facial halves. Plast Reconstr Surg 29:266–272
Esser JFS (1917) Island flaps. NY Med J 106:264–265
Ewart CJ, Jaworski NB, Rekito AJ, Gamboa MG (2005) Levator anguli oris: a cadaver study implicating its role in perioral rejuvenation. Ann Plast Surg 54(3):260–263
Frellinger G, Gruber H, Happak W, Penchmann U (1987) Surgical anatomy of the mimic muscle system and the facial nerve: importance for reconstructive and aesthetic surgery. Plast Reconstr Surg 80(5):686–690
Fuleihan NS (1994) The nasolabial fold and the SMAS. Plast Reconstr Surg 94(7):1091–1093
Furnas DW (1989) The retaining ligaments of the cheek. Plast Reconstr Surg 83(1):11–16
Furnas DW (1994) The superficial musculoaponeurotic plane and the retaining ligaments of the face. In: Psillakis JM (ed) Deep face-lifting techniques. Thieme Medical Publishers Inc, New York
Gardetto A, Dabering J, Raimer C, Piegger J, Piza-Katzer H, Fritsch H (2003) Does a superficial musculoaponeurotic system exist in the face and neck? An anatomical study by the tissue plastination technique. Plast Reconstr Surg 111(2):664–672
Gassner HG, Rafii A, Young A, Murakami C, Moe KS, Larrabee WF Jr (2008) Surgical anatomy of the face: implications for modern face-lift techniques. Arch Facial Plast Surg 10(1):9–19
Ghassemi A, Prescher A, Riediger D, Axer H (2003) Anatomy of the SMAS revisited. Aesthetic Plast Surg 27(4):258–264
Gierloff M, Stöhring C, Buder T, Wiltfang J (2012) The subcutaneous fat compartments in relation to aesthetically important facial folds and rhytides. J Plast Reconstr Aesthet Surg 65(10):1292–1297
Gosain AK, Yousif NJ, Madiedo G, Larson DL, Matloub HS, Sanger JR (1993) Surgical anatomy of the SMAS: a reinvestigation. Plast Reconstr Surg 92(7):1254–1263
Hamra ST (1990) The deep-plane rhytidectomy. Plast Reconstr Surg 86(1):53–61
Har-Shai Y, Bodner SR, Egozy-Golan D, Lindenbaum ES, Ben-Izhak O, Mitz V, Hirshowitz B (1996) Mechanical properties and microstructure of the superficial musculoaponeurotic system. Plast Reconstr Surg 98(1):59–70
Har-Shai Y, Bodner SR, Egozy-Golan D, Lindenbaum ES, Ben-Izhak O, Mitz V, Hirshowitz B (1997) Viscoelastic properties of the superficial musculoaponeurotic system (SMAS): a microscopic and mechanical study. Aesthetic Plast Surg 21(4):219–224
Hofer SO, Posch NA, Smit X (2005) The facial artery perforator flap for reconstruction of perioral defects. Plast Reconstr Surg 115(4):996–1003
Hu KS, Kwak HH, Song WC, Kang HJ, Kim HC, Fontaine C, Kim HJ (2006) Branching patterns of the infraorbital nerve and topography within the infraorbital space. J Craniofac Surg 17(6):1111–1115
Hu KS, Jin GC, Youn KH, Kwak HH, Koh KS, Fontaine C, Kim HJ (2008) An anatomic study of the bifid zygomaticus major muscle. J Craniofac Surg 19(2):534–536
Hur MS, Hu KS, Cho JY, Kwak HH, Song WC, Koh KS, Lorente M, Kim HJ (2008) Topography and location of the depressor anguli oris muscle with a reference to the mental foramen. Surg Radiol Anat 30(5):403–407
Hur MS, Hu KS, Kwak HH, Lee KS, Kim HJ (2011) Inferior bundle (fourth band) of the buccinator and the incisivus labii inferioris muscle. J Craniofac Surg 22(1):289–292
Hwang K, Cho HJ, Battuvshin D, Chung IH, Hwang SH (2005) Interrelated buccal fat pad with facial buccal branches and parotid duct. J Craniofac Surg 16(4):658–660
Hwang K, Jin S, Park JH, Chung IH (2007a) Cutaneous distribution of zygomaticofacial nerve. J Craniofac Surg 18(3):575–577
Hwang K, Jin S, Park JH, Kim DJ, Chung IH (2007b) Relation of mental nerve with mandibular branch of the facial nerve. J Craniofac Surg 18(1):165–168
Hwang SH, Hwang K, Jin S, Kim DJ (2007c) Location and nature of retro-orbicularis oculus fat and suborbicularis oculi fat. J Craniofac Surg 18(2):387–390
Hwang K, Nam YS, Choi HG, Han SH, Hwang SH (2008) Cutaneous innervation of lower eyelid. J Craniofac Surg 19(6):1675–1677
Imre J Jr (1928) Szehmejplasztikak (Lidplastik). Studium Kiadasa, Budapest
Jackson JT (1985) Local flaps in head and neck reconstruction, 1st edn. Mosby, St Louis
Jackson JT (2007) Local flaps in head and neck reconstruction, 2nd edn. Quality Medical Pub, St Louis
Janis JE, Hatef DA, Ducic I, Ahmad J, Wong C, Hoxworth RE, Osborn T (2010) Anatomy of the auriculotemporal nerve: variations in its relationship to the superior temporal artery and implications for the treatment of migraine headaches. Plast Reconstr Surg 125(5):1422–1428
Jeong SM, Park KJ, Kang SH, Shin HW, Kim H, Lee HK, Chung YG (2010) Anatomical consideration of the anterior and lateral cutaneous nerves in the scalp. J Korean Med Sci 25(4):517–522
Jost G, Levet Y (1984) Parotid fascia and face lifting: a critical evaluation of the SMAS concept. Plast Reconstr Surg 74(1):42–51
Kamer FM (1996) One hundred consecutive deep plane face lifts. Arch Otolaryngol Head Neck Surg 122(1):17–22
Kang HC, Kwak HH, Hu KS, Youn KH, Jin GC, Fontaine C, Kim HJ (2006) An anatomical study of the buccinator muscle fibers that extend to the terminal portion of the parotid duct, and their functional roles in salivary secretion. J Anat 208(5):601–607
Koh KS, Kim HJ, Oh CS, Chung IH (2003) Branching patterns and symmetry of the course of the facial artery in Koreans. Int J Oral Maxillofac Surg 32(4):414–418
Kopuz C, Ilgi S, Yavuz S, Onderoglu S (1995) Morphology of the retromandibular vein in relation to the facial nerve in the parotid gland. Acta Anat (Basel) 152(1):66–68

Kozielec T, Jozwa H (1977) Variation of the course of the facial artery in the prenatal period in man. Folia Morphol (Warsz) 36(1):55–61

Kroll SS, Reece GP, Robb G, Black J (1994) Deep-plane cervicofacial rotation-advancement flap for reconstruction of large cheek defects. Plast Reconstr Surg 94(1):88–93

Lang J (1995) Skull base and related structures, atlas of clinical anatomy. Schattauer Stuttgart, New York

Levet Y (2004) A discussion of the article "anatomy of the SMAS revisited" by Drs Ghassemi et al. Aesthetic Plast Surg 28(2):123–124

Longaker MT, Glat PM, Zide BM (1997) Deep-plane cervicofacial "hike": anatomic basis with dog-ear blepharoplasty. Plast Reconstr Surg 99(1):16–21

Loughner BA, Gremillion HA, Larkin IH, Mahan PE, Watson RE (1996) Muscle attachment to the lateral aspect of the articular disk of the human temporomandibular joint. Oral Surg Oral Med Oral Pathol 82(2):139–144

Loukas M, Hullett J, Louis RG Jr, Kapos T, Knight J, Nagy R, Marycz D (2006a) A detailed observation of variations of the facial artery, with emphasis on the superior labial artery. Surg Radiol Anat 28(3):316–324

Loukas M, Kapos T, Louis RG Jr, Wartman C, Jones A, Hallner B (2006b) Gross anatomical, CT and MRI analyses of the buccal fat pad with special emphasis on volumetric variations. Surg Radiol Anat 28(3):254–260

Loukas M, Owens DG, Tubbs RS, Spentzouris G, Elochukwu A, Jordan R (2008) Zygomaticofacial, zygomaticoorbital and zygomaticotemporal foramina: anatomical study. Anat Sci Int 83(2):77–82

Mallouris A, Yiacoumettis A, Thomaidis V, Karayiannakis A, Simopoulos C, Kakagia D, Tsaroucha A (2013) A record of skin creases and folds. Eur J Plast Surg 35:847–854

Matsunaga K, Usui A, Yamaguchi K, Akita K (2009) An anatomical study of the muscles that attach to the articular disc of the temporomandibular joint. Clin Anat 22(8):932–940

Mendelson BC (1992) Correction of the nasolabial fold: extended SMAS dissection with periosteal fixation. Plast Reconstr Surg 89(5):822–833

Mendelson BC (1995) Extended sub-SMAS dissection and cheek elevation. Clin Plast Surg 22(2):325–339

Mendelson B (2009) Chapter 6: Facelift anatomy, SMAS, retaining ligaments and facial spaces. In: Aston SJ, Steinbrech DS, Walden J (eds) Advances in aesthetic surgery. Elsevier Limited, London

Mendelson BC, Freeman ME, Woffles W, Huggins RJ (2008) Surgical anatomy of the lower face; the premasseter space, the jowl and the labiomandibular fold. Aesthetic Plast Surg 32(2):185–195

Midy D, Mauruce B, Vergnes P, Caliot P (1986) A contribution to the study of the facial artery, its branches and anastomoses; application to the anatomic vascular bases of facial flaps. Surg Radiol Anat 8(2):99–107

Miller PJ, Smith S, Shah A (2007) The subzygomatic fossa: a practical landmark in identifying the zygomaticus major muscle. Arch Facial Plast Surg 9(4):271–274

Mitz V, Peyronie M (1976) The superficial musculoaponeurotic system (SMAS) in the parotid and cheek area. Plast Reconstr Surg 58(1):80–88

Mitz V, Ricbourg B, Lasau JP (1973) Les branches faciales de l'artere faciale chez l'adulte: Typologie, variation et territoires cutanes respectifs. Ann Chir Plast 18(4):339–350

Mortellaro C, Manuzzi W, Caligiuri F, Vota A, Pavese M, Di Vincenzo S, Margolo N (2001) Surgical buccinator muscle myotomy in dentoskeletal class II alterations. J Craniofac Surg 12(5):409–425

Mowlavi A, Wilhelmi BJ (2004) The extended SMAS facelift: identifying the lateral zygomaticus major muscle border using bony anatomic landmarks. Ann Plast Surg 52(4):353–357

Mustardé JC (1991) Reconstruction of the lower eyelid. In: Mustardé JC (ed) Repair and reconstruction in the orbital region, 3rd edn. Churchill Livingstone, London

Nairn RI (1975) The circumoral musculature structure and function. Br Dent J 138(2):49–56

Nakajima H, Imanishi N, Aiso S (2002) Facial artery in the upper lip and nose: anatomy and a clinical implication. Plast Reconstr Surg 109(3):855–861

Niranjan NS (1988) An anatomical study of the facial artery. Ann Plast Surg 21(1):14–22

Ouattara D, Vacher C, de Vasconcellos JJ, Kassanyou S, Gnanazan G, N'Guessan B (2004) Anatomical study of the variations in innervation of the orbicularis oculi by the facial nerve. Surg Radiol Anat 26(1):51–53

Owsley JQ (1983) SMAS-platysma face lift. Plast Reconstr Surg 71(4):573–576

Owsley JQ (1993) Lifting the malar fat pad for correction of prominent nasolabial folds. Plast Reconstr Surg 91(3):463–474

Owsley JQ, Agarwal CA (2008) Safely navigating around the facial nerve in three dimensions. Clin Plast Surg 35(4):469–477

Park C, Lineaweaver WC, Buncke HJ (1994) New perioral arterial flaps: anatomic study and clinical application. Plast Reconstr Surg 94(2):268–276

Pessa JE, Zadoo VP, Adrian EK Jr, Yuan CH, Aydelotte J, Garza JR (1998) Variability of the midfacial muscles: analysis of 50 hemifacial cadaver dissections. Plast Reconstr Surg 102(6):1888–1893

Pilsl U, Anderhuber F (2010) The septum subcutaneum parotideomassetericum. Dermatol Surg 36(12):2005–2008

Pilsl U, Anderhuber F, Rzany B (2012) Anatomy of the cheek: implications for soft tissue augmentation. Dermatol Surg 38(7Pt2):1254–1262

Pinar YA, Govsa F (2006) Anatomy of the superficial temporal artery and its branches: its importance for surgery. Surg Radiol Anat 28(3):248–253

Pinar YA, Bilge O, Govsa F (2005) Anatomic study of the blood supply of perioral region. Clin Anat 18(5):330–339

Pogrel MA, Schmidt B, Ammar A (1996) The relationship of the buccal branch of the facial nerve to the parotid duct. J Oral Maxillofac Surg 54(1):71–73

Rodel R, Lang J (1996) Peripheral branches of the facial nerve in the cheek and chin area. Anatomy and clinical consequences. HNO 44(10):572–576

Rohrich RJ, Pessa JE (2007) The fat compartments of the face. Anatomy and clinical implications for cosmetic surgery. Plast Reconstr Surg 119(7):2219–2227

Rohrich RJ, Arbique GM, Wong C, Brown S, Pessa JE (2009) The anatomy of suborbicularis fat: implications for periorbital rejuvenation. Plast Reconstr Surg 124(3):946–951

Ruess W, Owsley JQ (1987) The anatomy of the skin and fascial layers of the face in aesthetic surgery. Clin Plast Surg 14(4):677–682

Saylam C, Ucerler H, Orhan M, Ozek C (2006a) Anatomic guides to precisely localize the zygomatic branches of the facial nerve. J Craniofac Surg 17(1):50–53

Saylam C, Ucerler H, Orhan M, Ozek C (2006b) Anatomic landmarks of the buccal branches of the facial nerve. Surg Radiol Anat 28(5):462–467

Schaverien MV, Pessa JE, Saint-Cyr M, Rohrich RJ (2009) The arterial and venous anatomies of the lateral face lift flap and the SMAS. Plast Reconstr Surg 123(5):1581–1587

Schulte DL, Sherris DA, Kasperbauer JL (2001) The anatomical basis of the Abbé flap. Laryngoscope 111(3):382–386

Schwember G, Rodrigez A (1988) Anatomic surgical dissection of the extraparotid portion of the facial nerve. Plast Reconstr Surg 81(2):183–188

Shim KS, Hu KS, Kwak HH, Youn KH, Koh KS, Fontaine C, Kim HJ (2008) An anatomical study of the insertion of the zygomaticus major muscle in humans focused on the muscle arrangement at the corner of the mouth. Plast Reconstr Surg 121(2):466–473

Skoog T (1974) Plastic surgery: new methods. Saunders, Philadelphia

Spiegel JH, DeRosa J (2005) The anatomical relationship between the orbicularis oculi muscle and the levator labii superioris and

zygomaticus muscle complexes. Plast Reconstr Surg 116(7):1937–1942
Standring S (2008) Gray's anatomy. The anatomical basis of clinical practice, 40th edn. Churchill Livingstone-Elsevier, Edinburg
Stock AL, Collins HP, Davidson TM (1980) Anatomy of the superficial temporal artery. Head Neck Surg 2(6):466–469
Stuzin JM, Wagstrom L, Kawamoto HK, Wolfe SA (1989) Anatomy of the frontal branch of the facial nerve: the significance of the temporal fat pad. Plast Reconstr Surg 83(2):265–271
Stuzin JM, Wagstrom L, Kawamoto HK, Baker TJ, Wolfe SA (1990) The anatomy and clinical applications of the buccal fat pad. Plast Reconstr Surg 85(1):29–37
Stuzin JM, Baker TJ, Gordon HL (1992) The relationship of the superficial and deep facial fascias: relevance to rhytidectomy and aging. Plast Reconstr Surg 89(3):441–449
Tan ST, MacKinnon CA (2006) Deep plane cervicofacial flap: a useful and versatile technique in head and neck surgery. Head Neck 28(1):46–55
Thaller SR, Kim S, Patterson H, Wildman M, Daniller A (1990) The submuscular aponeurotic system (SMAS): a histologic and comparative anatomy evaluation. Plast Reconstr Surg 86(4):690–696
Tremolada C, Fissette J, Candiani P (1994) Anatomical basis for a safe and easier approach to composite rhytidectomy. Aesthetic Plast Surg 18(4):387–391
Trussler AP, Stephan P, Hatef D, Schaverien M, Meade R, Barton FE (2010) The frontal branch of the facial nerve across the zygomatic arch: anatomical relevance of the high-SMAS technique. Plast Reconstr Surg 125(4):1221–1229
Tubbs RS, Salter EG, Oakes WJ (2005) Unilateral agenesis of the facial artery with compensation by a giant transverse facial artery. Folia Morphol (Warsz) 64(3):226–228
Velasco MJR, Vezquez RJF, Collado JJ (1993) The relationships between temporomandibular joint disc and related masticatory muscles in humans. J Oral Maxillofac Surg 51(4):390–395
Waller BM, Cray JJ, Burrows AM (2008) Selection for universal facial emotion. Emotion 8(3):435–439
Wang TM, Lin CL, Kuo KJ, Shih C (1991) Surgical anatomy of the mandibular ramus of the facial nerve in Chinese adults. Acta Anat (Basel) 142(2):126–131
Whetzel TP, Mathes SJ (1992) Arterial anatomy of the face: an analysis of vascular territories and perforating cutaneous vessels. Plast Reconstr Surg 89(4):591–603
Whetzel TP, Mathes SJ (1997) The arterial supply of the face lift flap. Plast Reconstr Surg 100(2):480–486
Whetzel TP, Stevenson TR (1997) The contribution of the SMAS to the blood supply in the lateral face lift flap. Plast Reconstr Surg 100(4):1011–1018
Wilhelmi B, Mowlavi A, Neumeister M (2003) The safe face lift with bony anatomic landmarks to elevate the SMAS. Plast Reconstr Surg 111(5):1723–1726
Won SY, Choi DY, Kwak HH, Kim ST, Kim HJ, Hu KS (2012) Topography of the arteries supplying the masseter muscle: using dissection and Sihler's method. Clin Anat 25(3):308–313
Yang HJ, Gil YC, Lee HY (2010) Topographical anatomy of the transverse facial artery. Clin Anat 23(2):168–178
Youn KH, Park JT, Park DS, Koh KS, Kim HJ, Paik DJ (2012) Morphology of the zygomaticus minor and its relationship with the orbicularis oculi muscle. J Craniofac Surg 23(2):546–548
Yousif NJ, Gosain A, Matloub HS, Sanger JR, Madiedo G, Larson DL (1994) The nasolabial fold: an anatomic and histologic reappraisal. Plast Reconstr Surg 93(1):60–69
Yousuf S, Tubbs RS, Wartmann CT, Kapos T, Cohen-Gadol AA, Loukas M (2010) A review of the gross anatomy, functions, pathology, and clinical uses of the buccal fat pad. Surg Radiol Anat 32(5):427–436
Yung JP, Carpentier P, Marguelles-Bonnet R, Meunissier M (1990) Anatomy of the temporomandibular joint and related structures in the frontal plane. Cranio 8(2):101–107
Zhang HM, Yan YP, Qi KM, Wang JQ, Liu ZF (2002) Anatomical structure of the buccal fat pad and its clinical adaptations. Plast Reconstr Surg 109(7):2509–2518
Zhao Z, Li S, Xu J, Li Y, Huang W, Yang M, Mu L, Liu Y, Zhai H, Jin J, Li J, Li J, Fu X (2000) Color Doppler flow imaging of the facial artery and vein. Plast Reconstr Surg 106(6):1249–1253
Zhenmin Zhao Z, Li S, Yan Y, Li Y, Yang M, Mu L, Huang W, Liu Y, Zhai H, Jin J, Ma X (1999) New buccinator myomucosal island flap: anatomic study and clinical application. Plast Reconstr Surg 104(1):55–64
Ziarah HA, Atkinson ME (1981) The surgical anatomy of the mandibular distribution of the facial nerve. Br J Oral Surg 159(3)
Zitelli JA (1990) The nasolabial flap as a single-stage procedure. Arch Dermatol 126(11):1445–1448

Lips and Chin

6

The area surrounding the mouth is constituted by two subunits: the lips and the chin. These are examined together because anatomically they share almost the same structures and from a surgical point of view the excision of lower lip lesions and the reconstructive flaps that are designed very often involve both areas.

The lips are not only an important structure that dominates in facial aesthetics but also a valuable in function, motile organ that plays a major role in food intake, speech, and facial expression. Its shape and thickness differs between the upper and lower lip and varies significantly from individual to individual and among the ethnic groups. The chin is the round-shaped area just inferior to the lower lip and corresponds to the osseous chin (mental protuberance and mental tubercles of the mandible).

6.1 Subunits-Topographic Landmarks

The lips and the chin are bounded (Fig. 6.1) from the cheek superiorly by the nasolabial crease and inferiorly by the labiomandibular crease. Both creases correspond to the line where the cheek muscles attach to the orbicularis oris. In young persons, they are shallow and they deepen during aging process becoming more obvious. Superiorly the upper lip is separated from the nose by the alar facial sulcus and the nasal base. Inferiorly the inverted U-shaped mentolabial crease separates the lower lip from the chin. All of the perioral creases are ideal sites for placing and hiding the incisions of many flaps designed for lip reconstruction.

Both lips are divided into the upper and lower vermilion subunit (mucosal lips) and the upper and lower cutaneous lip (skin lips) subunits. The upper lip is further divided into a central subunit: the philtrum and two lateral subunits.

The chin constitutes a single unit and is bounded superiorly by the mentolabial crease, inferiorly by the inferior border of the osseous chin, and laterally by the rounded and shallow lateral extensions of the mentolabial crease.

The philtrum of the upper lip (Fig. 6.2) constitutes an aesthetically important anatomic area in the upper lip. This shallow groove exhibits a width that is about one-fifth of the total width of the upper lip and is bounded in both of its lateral sites by two columns, the philtrum columns. The columns are formed by a thickening of the orbicularis muscle and an increase of connective tissue (Latham and Deaton 1976; Briedis and Jackson 1980). Garcia de Mitchell et al. (2008) implied that the columns coincide with ascending arterial branches that originate from the superior labial arteries and a membrane extending from the underlying muscle to the dermis. Superiorly the philtrum attaches to the columella and inferiorly at the free lip edge forms the tubercle. Corresponding to the tubercle, a shallow dimple is presented in the lower lip, where the tubercle rests in lip closure. The junction between the skin and the red part (vermilion) in the upper lip forms in its middle a double curved line, the Cupid's bow (Cupid: Roman God of love). The two peaks of the bow concur with the lower end of the philtrum columns. The normal cutaneous-vermilion junction is a result from the anterior projection of the pars marginalis of the orbicularis oris muscle (Mulliken et al. 1993). The vermilion of the upper and the lower lips join at the corner of the mouth and form the oral commissure (labial commissure).

The above aesthetic subunits and anatomic landmarks should be taken into account when planning and performing reconstruction of the lips to achieve optimal functional and cosmetic results as far as at the lips any distortion of them is very obvious.

6.2 Anatomy

Structurally each lip (Fig. 6.3) is composed of a muscle, the orbicularis muscle that is invested extraorally by the skin and subcutaneous tissue, intraorally by mucosa and submucosa,

V.K. Thomaidis, *Cutaneous Flaps in Head and Neck Reconstruction*,
DOI 10.1007/978-3-642-41254-7_6, © Springer-Verlag Berlin Heidelberg 2014

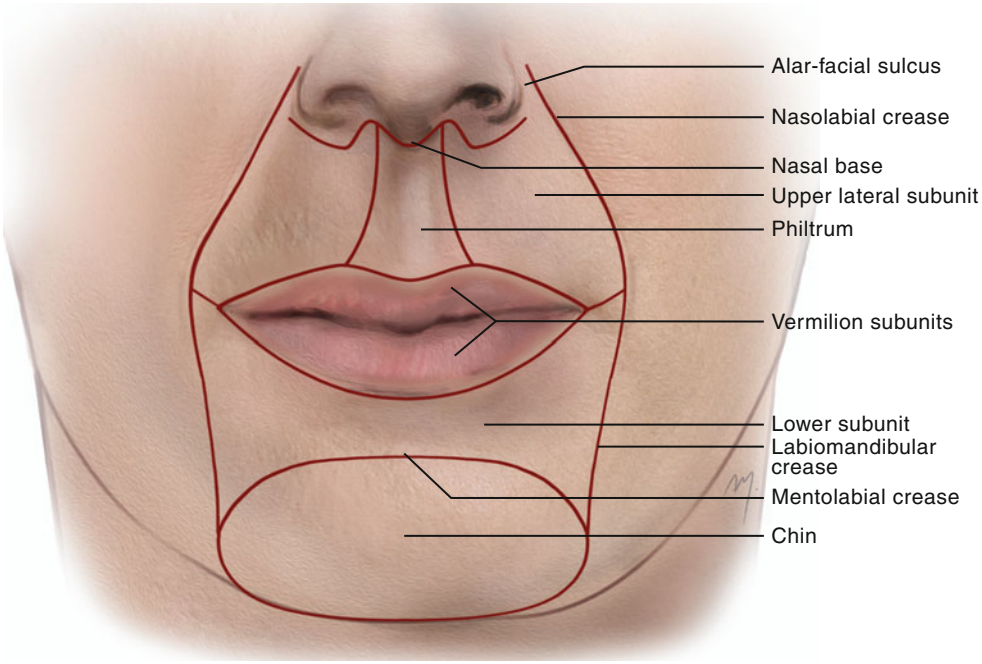

Fig. 6.1 Boundaries and subunits of the lips and chin

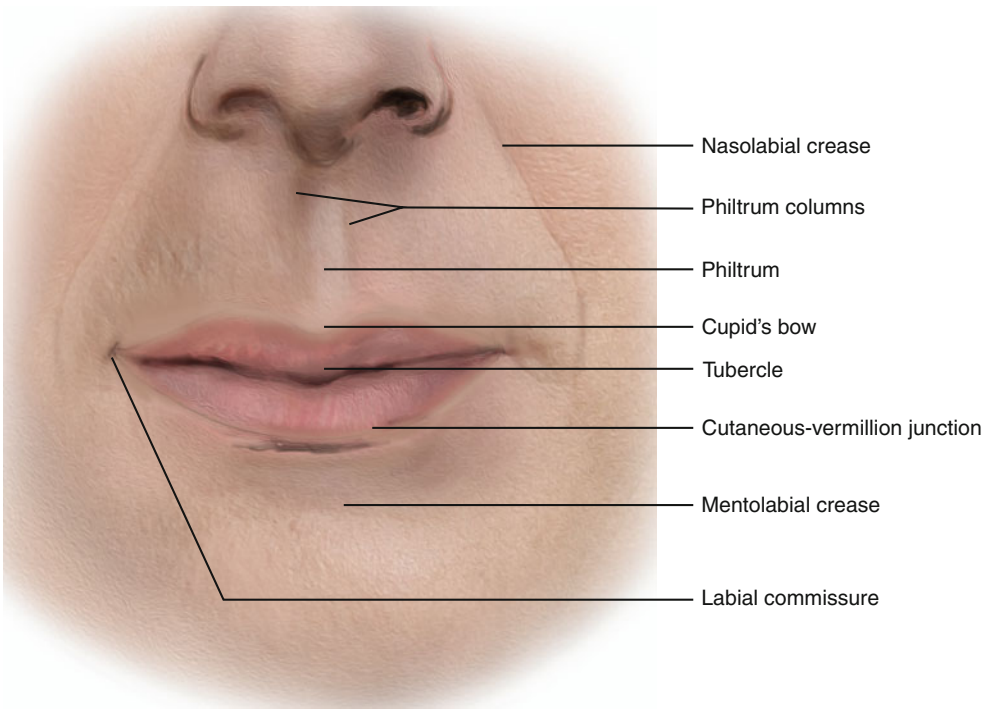

Fig. 6.2 Topographic landmarks of the lips

and over its free edge by the vermilion. The orbicularis muscle is the muscular component of the lip that occupies great amount of the structure creating its bulk. This component provides the lips with a great elasticity allowing them to be stretched in a considerable degree that facilitates in the closure of lip defects. The chin (Fig. 6.3) is structured by its skin, the subcutaneous tissue, and the chin muscles.

6.2.1 Skin and Subcutaneous Tissue-Mucosa-Vermilion

The skin surrounds the outer surface of the lip whereas the mucosa its inner surface. A transition area that differs in the keratinization pattern surrounds the free external lip surface and is named the vermilion (or the vermilion border).

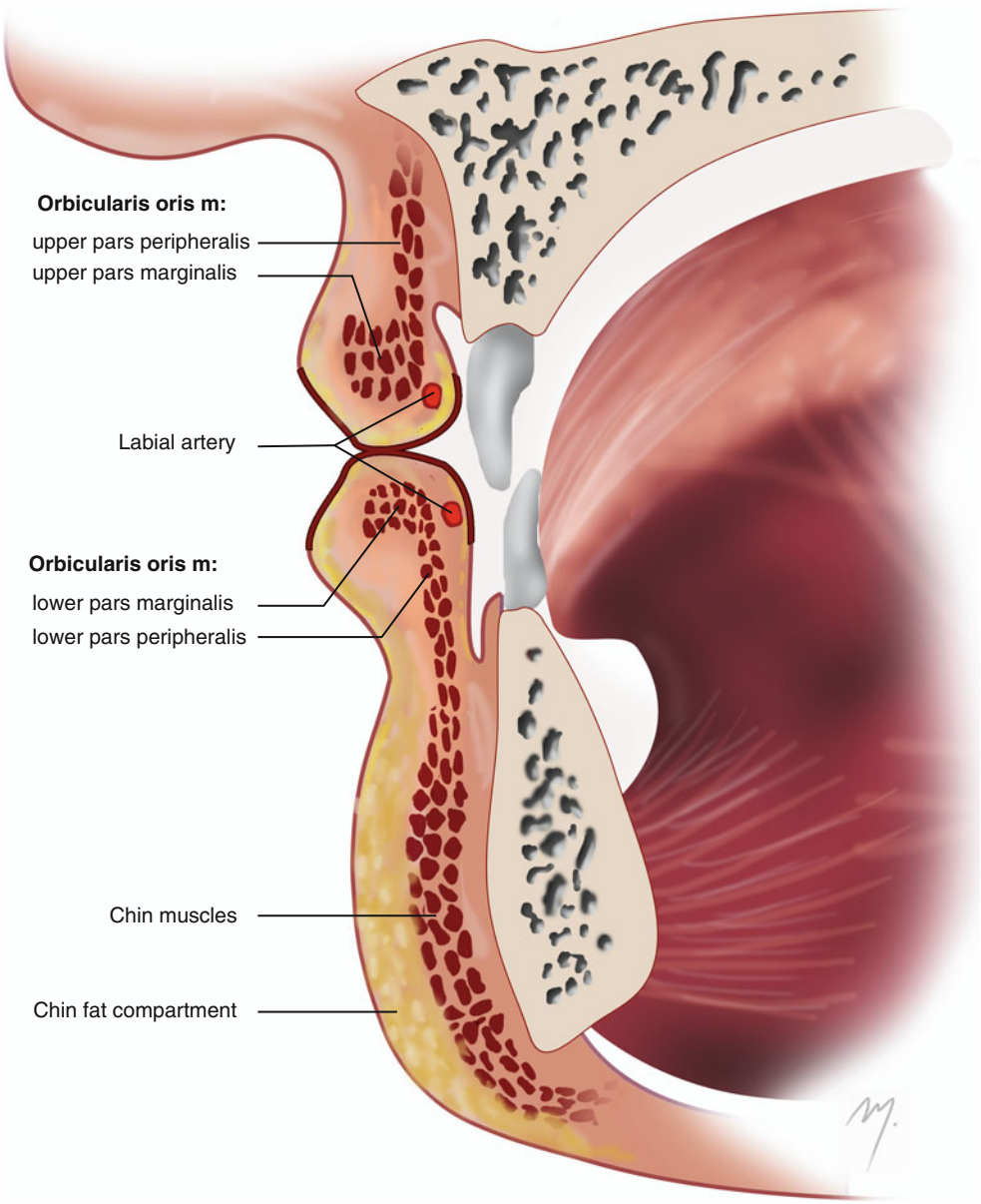

Fig. 6.3 Cross section of lips and chin

The skin of the lips is similar but slightly thinner (mean 1.9 mm) to that of the adjoining cheek, containing hair follicles, predominantly in the male, and sebaceous and sweat glands. The subcutaneous tissue consists of connective tissue and muscular fibers. Subcutaneous adipose tissue is almost absent in the lips. The subcutaneous tissue is firmly attached to the underlying orbicularis oris muscle. The skin of the chin constitutes the continuation of the lip skin containing also hair follicles predominantly in the male and sebaceous and sweat glands but becomes much thicker. It is the thickest skin of the face, with an average thickness of 2.6 mm. Although subcutaneous fat is almost absent at the lips, at the chin area, it fills a distinct subcutaneous compartment, the chin fat compartment (Fig. 6.3). The relaxed skin tension lines (RSTLs) on the perioral area run in a curved vertical direction as they descend to the mandibular border (Fig. 6.4).

The lip mucosa is similar to the neighboring buccal mucosa. The submucosa layer contains numerous minor salivary glands and is loosely connected to the underlying muscle. This provides an easy surgical plane that separates the mucosa from the muscle and can be used as an advancement mucosal flap.

The vermilion consists of very thin mucosa, with no or only few glands beneath it. The numerous underlying blood capillaries impart its red color. It is of various breadth and narrows to the commissures. The transition from vermilion to mucosa usually occurs just posterior to the line of lip closure. Vermilion

continuity must be ensured in every lip reconstruction; especially in the vermilion-skin junction, as well as every asymmetry above 1mm of this line is very obvious.

6.2.2 Muscles

6.2.2.1 Orbicularis Oris Muscle

The orbicularis oris muscle (Fig. 6.5) is a round-shaped, circumferential muscle constituting the muscular substance of the lips and being the primary mediator of oral competence. This multilayered muscle is divided in two parts, the large pars peripheralis located posteriorly and the small pars marginalis located anteriorly. The muscle fibers that constitute each part differ not only in their anatomic location but also in their immunohistochemical characteristics (Hwang et al 2007a). The small pars marginalis is limited to the vermilion, although it has been reported that in the upper lip, it extends for a few millimeters above the vermilion border (Hwang et al. 2007a, b).

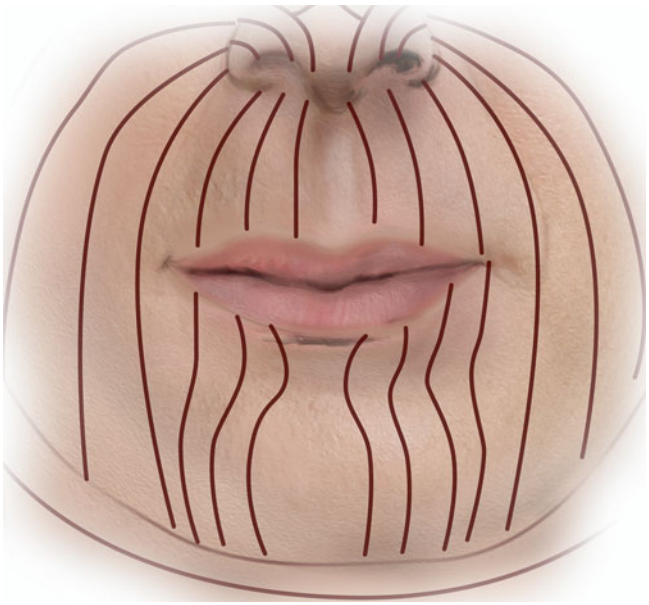

Fig. 6.4 Relaxed skin tension lines (RSTLs) at the lips and chin

Strictly anatomic the orbicularis muscle differs from a "real" sphincter (e.g., the orbicularis oculi muscle) with the manner of undisrupted running fibers that surround an opening. The pattern of its complicated micro-architecture has been controversial over the years (Lightoller 1925; Nairn 1975; Latham and Deaton 1976; Briedis and Jackson 1980; Williams and Warwick 1980; Mooney et al. 1988; Namnoum et al. 1997; Hwang et al. 2007b). However, the old detailed description of Lightoller (1925) is still accepted (Standring 2008). According to this description, the orbicularis oris muscle consists of a left and a right upper pars peripheralis segment, a left and right lower pars peripheralis segment, and the corresponding pars marginalis segments. Each of the parts is fan-shaped with their stem attached to the modiolus (see below), where these constituents are open in the pars peripheralis and closed in the pars marginalis.

The fibers of the pars peripheralis originate within the modiolus and are reinforced by fibers of buccinator, zygomaticus major, and levator anguli oris muscles in the upper lip and by the fibers of buccinator and depressor anguli oris

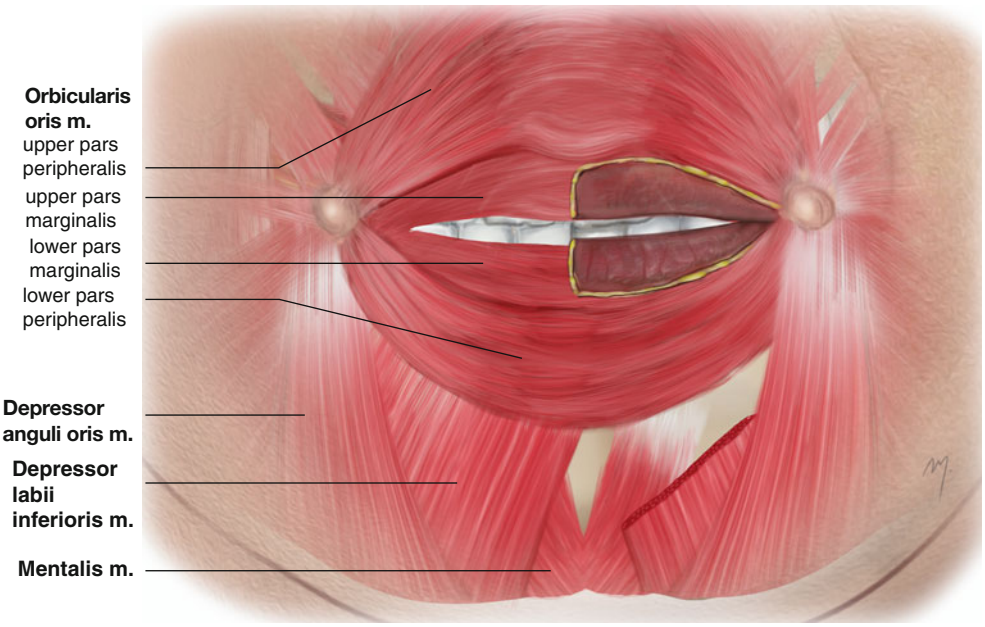

Fig. 6.5 Muscles of the lips and chin. The orbicularis oris muscles are divided in the pars marginalis and the pars peripheralis

muscles in the lower lip. The fibers of the pars peripheralis travel in various directions (transversally, longitudinally, and obliquely) (Rogers et al. 2009). They enter the free lip and aggregate toward the medial plane for a few millimeters, where they intermingle with their corresponding opposites, and continue to their dermal insertions. Upper fibers of the upper lip traverse near the nasolabial sulcus and proceed to adhere to the sulcus, the nasal ala, and the septum, whereas the lower fibers of the lower lip attach to the mentolabial sulcus. Fibers of the pars marginalis also originate from the modiolus and they traverse anteriorly to the fibers of the pars peripheralis. They integrate with their contralateral pairs and extend a few millimeters past the midline and attach to the vermilion zone (Latham and Deaton 1976; Standring 2008).

6.2.2.1.1 Incisivus Labii Superioris and Incisivus Labii Inferioris Muscles

Two muscular slips are associated as accessory muscles of the orbicularis oris: the incisivus labii superioris and the incisivus labii inferioris muscles. These muscles actually connect the orbicularis oris to the maxilla and the mandible.

The incisivus labii superioris muscle is attached to the incisive fossa of the maxilla, deep to the orbicularis oris. Its fibers run lateral, parallel to the fibers of the orbicularis oris muscle blending with them. They attach at the modiolus and blend with fibers of the levator anguli oris muscle (Standring 2008).

The incisivus labii inferioris muscle is attached to the incisive fossa of the mandible, lateral to the mentalis and initially deep to the orbicularis oris. Its fibers curve laterally and superiorly to the angle of the mouth and attach to the modiolus (Standring 2008). The muscle is present in approximately 98 % and merges with fibers of the orbicularis oris and buccinator muscles (Hur et al. 2011).

Deep to the orbicularis muscle, both in the upper and lower lips, the presence of a submuscular fat layer has been described that its volume seems to play an important role to the appearance of the youthful lip and its atrophy results in the aging lip (Rohrich and Pessa 2009).

The orbicularis oris muscle receives its blood supply from the superior and inferior labial arteries, the mental artery, the infraorbital artery, and the transverse facial artery. The buccal and the mandibular branches of the facial nerve supply the motor innervation to the orbicularis oris.

The main function of the orbicularis oris is to close the lips sealing the mouth. The orbicularis oris muscle in association with other muscles is used for the production of labial elevation and depression. These abilities enable the production of speech, the pressing of the labia against the teeth, and the ability to hold food within the mouth during mastication.

6.2.2.2 Depressor Anguli Oris Muscle

The depressor anguli oris muscle has been described at the cheek (see Chap. 5), but a portion of its medial part is encountered also to the lateral aspect of the chin (Fig. 6.5).

6.2.2.3 Depressor Labii Inferioris Muscle

The depressor labii inferioris muscle is a muscle quadrilateral in shape that lies beneath the depressor anguli oris (Fig. 6.5). The muscle originates from the oblique line of the mandible, in an area between the symphysis and the mental foramen, where its fibers blend with fibers of the platysma muscle. The muscle fibers run superomedially and insert into the skin of the lower lip. They blend with fibers of the orbicularis oris muscle. Its action pulls the lower lip downward and laterally. The muscle is supplied by the inferior labial and the mental artery. The marginal mandibular branch of the facial nerve innervates the muscle.

6.2.2.4 Mentalis Muscle

The small mentalis muscle (Fig. 6.5) is located close to the midline. It lies beneath the depressor labii inferioris muscle being the deepest muscle in that area. Immediately deep to each of the mentalis muscle, a layer of fat has been noted that might influence the depth of the mentolabial sulcus (Rohrich and Pessa 2009).

The muscle arises from the mandibular incisive fossa. Its muscle fibers run inferiorly and medially to the midline and insert to the skin of the chin. The muscle directly elevates the chin and wrinkles the skin of the chin. Indirectly it protrudes the lower lip. The muscle is supplied by the inferior labial and the mental artery. The marginal mandibular branch of the facial nerve innervates the muscle.

6.2.2.5 The Modiolus

The modiolus (Fig. 6.6) is a nodular, palpable, and mobile anatomic structure located slightly lateral to each oral commissure. It is formed by several different muscles that are derived from a common embryological origin and converge to the oral commissure (Pélissier et al. 2000).

The modiolus actually appears as a dense, fibromuscular mass formed by the multiple converging fibers of the levator anguli oris, the depressor anguli oris, the pars marginalis of orbicularis oris, the risorius, the buccinator, and the zygomaticus major muscles. Lateral fibers of the depressor labii muscle and medial fibers of the platysma muscle (platysma pars modiolaris) also converge to the modiolus. Not only muscle fibers but also fasciae, like SMAS and parotidomasseteric fascia, contribute to the formation of the modiolus (Al-Hoqail and Abdel Meguid 2009).

The modiolus has a cone-like configuration, with its base adjacent to the buccal mucosa extending to the dermis of the skin (Demiryurek et al. 2003). Its base extends vertically about 20 mm above and 20 mm below a horizontal line through the oral commissure, while its apex is centered about 12 mm lateral to the oral commissure (Standring 2008). Being attached firmly at the dermis, it functions as scaffold that transmits the multiple muscle actions to the oral commissure.

The modiolus plays a very important role not only in function but also in aesthetics, a fact that was portrayed even from the classic ancient Greek era, as Zufferey (2002) has emphasized: "The modiolus has been a well-known morphologic structure since antiquity. No other school of sculpture has better portrayed the modiolus of young adults than the sculptors of classic Hellenic beauty, who recognized the importance of the modiolus." This small structure should be taken into account in reconstruction in this area so as not to imperil its functional and aesthetical integrity (Fig. 6.6).

6.2.2.5.1 Muscles that Act on the Lips

All of the cheek and chin muscles, the platysma, and one nasal muscle, the levator labii superioris alaeque nasi, act on the lips. These muscles integrate with the orbicularis oris and work synergistically to allow the full range of lip movement. According to the basic action they induce to the lips, they are distinct in elevators, depressors, protruders, and retractors (Figs. 6.7 and 6.8). Their action can be detected either on the entire lip or on the mouth corner. The upper lip elevators are the levator labii superioris alaeque nasi, the levator labii superioris, and the zygomaticus minor. In the lower lip depressors, the depressor labii inferioris and the platysma are included. The lower lip protruder is only the mentalis muscle. The levator anguli oris and zygomaticus major muscles achieve elevation of the labial angle. The angle of the mouth is depressed by the depressor anguli oris and by fibers of platysma muscle. Lateral retraction of the labial angle is accomplished by the buccinator and risorius. These basic muscle actions to the lips are summarized in Tables 6.1 and 6.2.

Fig. 6.6 The modiolus

6.2.3 Arterial Supply

The arterial distribution of the lips and chin is not constant, showing a great degree of variability in the location, course, and dimensions of these arteries. The lips are supplied mainly by the superior and inferior labial arteries with the contribution of the infraorbital, the mental, the labiomental, and the submental arteries. The chin is supplied mainly by the mental artery, the labiomental artery, and the terminal part of the submental artery, while small branches of the inferior labial artery contribute to the vascularization of its upper part.

6.2.3.1 Superior Labial Artery

The superior labial artery (Fig. 6.9) originates from the facial artery at most times superior or at the level of the labial commissure and occasionally inferior to it. The diameter of the superior labial artery at its origin ranges from 1 to 1.8 mm (Park et al. 1994; Crouzet et al. 1998; Magden et al. 2004; Pinar et al. 2005; Al-Hoqail and Meguid 2008).

The point at which the superior labial artery branches from the facial artery and the distance between its origin and the labial commissure is highly variable (Fig. 6.10) ranging from 0.4 to 2.5 cm, with a mean distance between 1.0 and 1.8 cm (Schulte et al. 2001; Loukas et al. 2006; Magden et al. 2004; Al-Hoqail and Meguid 2008). This point depends on the branching pattern of the facial artery and on the distance that the facial artery passes from the labial commissure. Thus, accurate landmarks cannot be determined.

The superior labial artery travels forward in a tortuous course to the upper lip, passing deep to the zygomaticus major muscle. The superior labial artery is usually larger and more tortuous in its course than the inferior one. Into the upper lip, it enters the orbicularis oris muscle and travels between the muscle and the mucosa, along the edge of the upper lip. In about 15–20 %, the artery runs partially invested by the muscle (Schulte et al. 2001; Loukas et al. 2006).

Several small branches ascend contributing to the vascularization of the nostril base. A larger artery that branches at the philtrum and ascends to the columella of the nose is named the columellar artery (see Chap. 4). Finally the superior labial artery anastomoses with its contralateral forming the upper lip arterial arc.

6.2.3.2 Inferior Labial Artery

The inferior labial artery (Fig. 6.9) is branched from the facial artery generally below or at the level of the labial commissure and seldom above it. Its mean diameter in its origin ranges from 1.2 to 1.4 mm (Edizer et al. 2003; Pinar et al. 2005; Al-Hoqail and Meguid 2008). As with the superior labial artery, the point at which the inferior labial artery branches from the facial artery and the distance

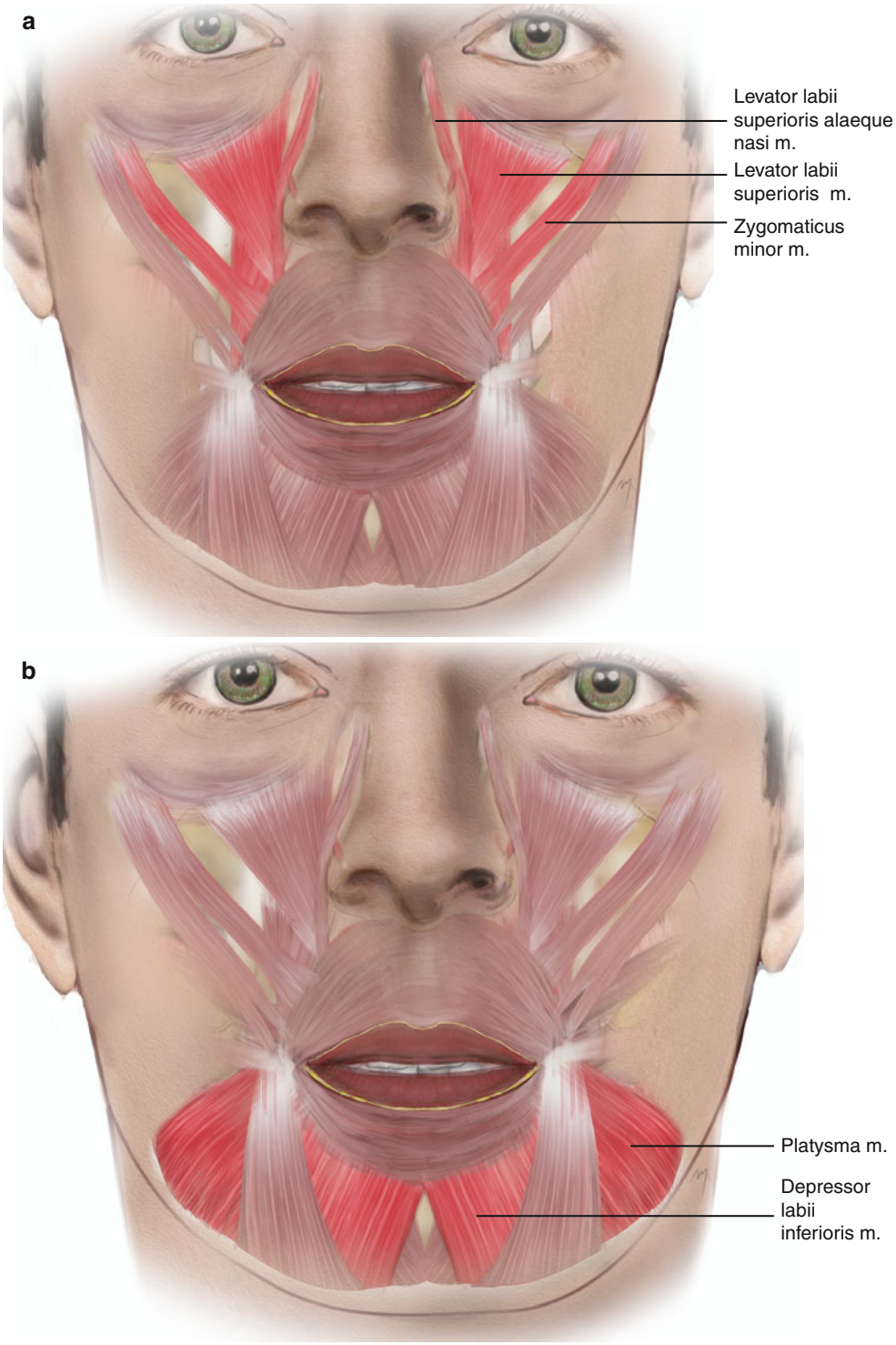

Fig. 6.7 Muscles that act on the lips. (**a**) Upper lip elevators. (**b**) Lower lip depressors. (**c**) Lower lip protruders

Fig. 6.7 (continued)

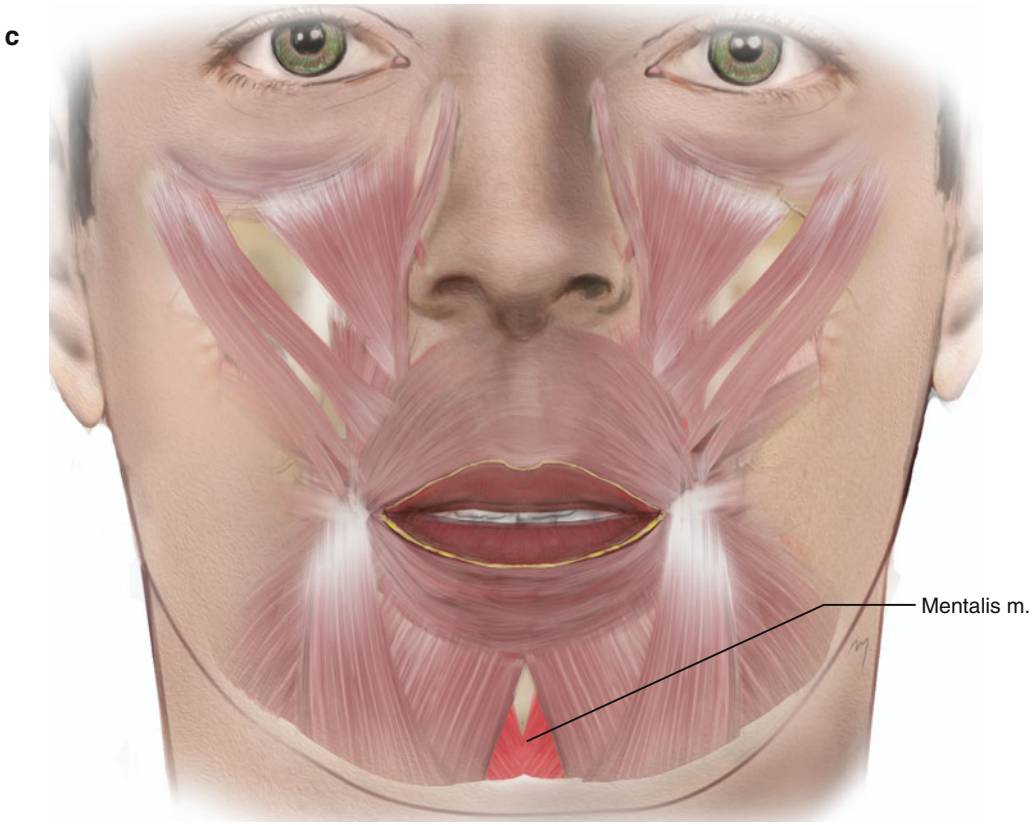

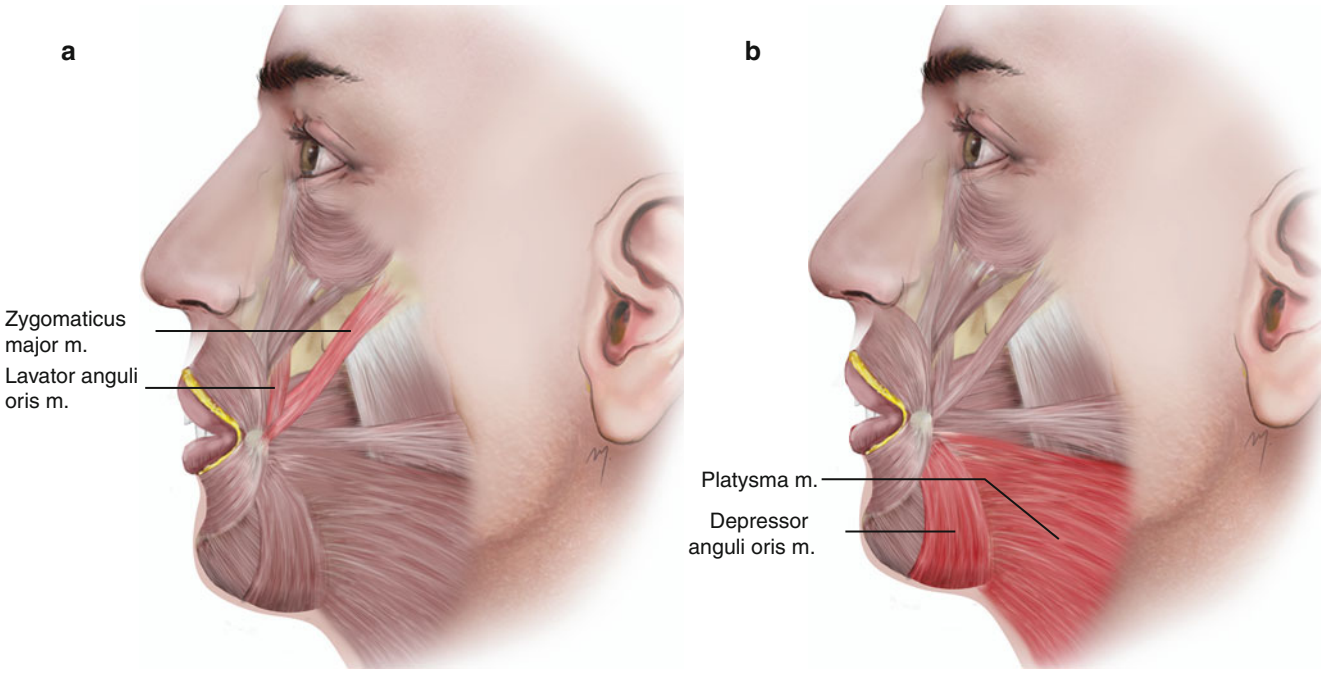

Fig. 6.8 Muscles that act at the labial angle. (**a**) Labial angle elevators. (**b**) Labial angle depressors. (**c**) Labial angle retractors

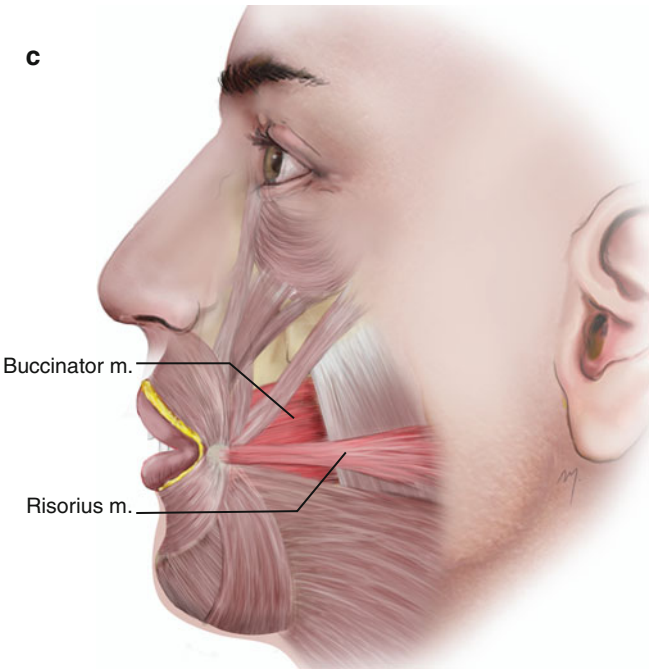

Fig. 6.8 (continued)

Table 6.1 Muscles that act on the lips

Upper lip elevators (Fig. 6.7a)	Lower lip depressors (Fig. 6.7b)	Lower lip protruders (Fig. 6.7c)
Levator labii superioris alaeque nasi	Depressor labii inferioris	Mentalis
Levator labii superioris	Platysma	–
Zygomaticus minor	–	–

Table 6.2 Muscles that act at the labial angle

Elevators (Fig. 6.8a)	Depressors (Fig. 6.8b)	Lateral retractors (Fig. 6.8c)
Levator anguli oris	Depressor anguli oris	Buccinator
Zygomaticus major	Platysma	Risorius

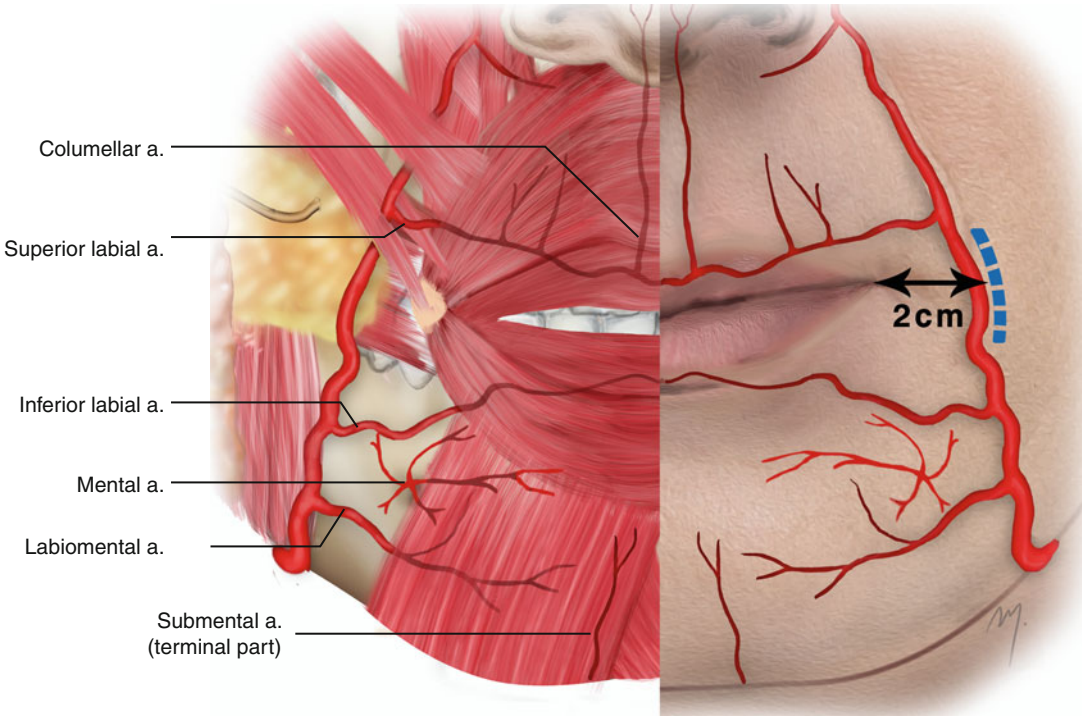

Fig. 6.9 Arterial supply to the lips and chin (the depressor anguli oris muscle has been removed)

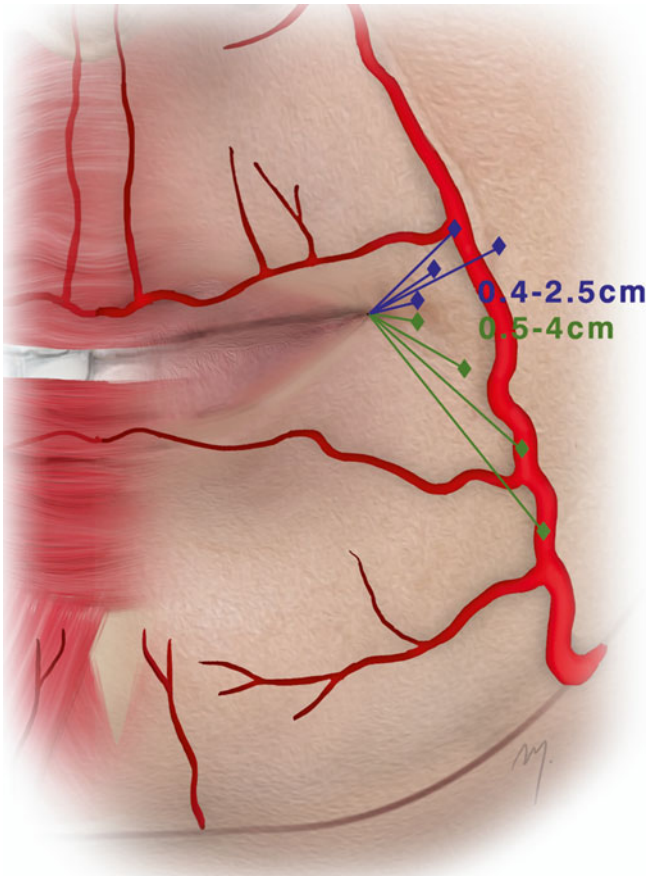

Fig. 6.10 Range of the distances of emerging points of the superior labial artery (*blue lines*) and the inferior labial artery (*green lines*) from the oral commissure

between its origin and the labial commissure exhibit a high variability (Fig. 6.10) ranging from 0.5 to 4 cm with a mean distance between 2 and 2.5 cm, whereas there are cases where it originates even at the lower margin of the mandible (Edizer et al. 2003; Pinar et al. 2005; Al-Hoqail and Meguid 2008).

After branching from the facial artery, it runs tortuously upward and forward deep to the depressor anguli oris muscle in its course to the lower lip. The artery penetrates the orbicularis oris muscle and runs tortuously along the edge of the lower lip lying between the muscle and the mucous membrane. In about 13 %, the artery can be found traveling within the orbicularis oris muscle (Schulte et al. 2001).

6.2.3.3 Mental Artery

The mental artery (Fig. 6.9) is a terminal branch of the inferior alveolar artery (which in turn is a branch of the maxillary artery). As the inferior alveolar artery runs within the mandibular canal, together with the inferior alveolar nerve, at the premolar teeth root level, it divides into the incisive and the mental arteries. The mental artery emerges onto the chin area through the mental foramen, while the incisive artery continues to the midline, below the lower incisors. Its branches supply the chin muscles and the overlying skin and anastomose with the terminal part of the submental artery and the inferior labial arteries.

6.2.3.4 Labiomental Artery

The labiomental artery (Fig. 6.9) is an inconstant branch of either the facial or the inferior labial arteries. It contributes to the vascular supply of the mental area and the lower lip. After emerging it runs horizontally between the depressor anguli oris and the depressor labii inferioris muscles to the midline. It anastomoses with branches of the mental artery and the terminal part of the submental artery.

6.2.3.5 Terminal Part of Submental Artery

The central part of the chin is mainly vascularized by the terminal part of the submental artery (Fig. 6.9). The submental artery is a cervical branch of the facial artery that initially courses below the mandible and as it reaches the midline turns and ascends vertically to the chin (see Chap. 8). It anastomoses with the mental, the labiomental, and the inferior labial arteries. It mainly supplies the skin of the chin and contributes to the supply of the lower lip.

6.2.4 Venous Drainage

Although in the classic anatomic textbooks a superior and an inferior labial veins are mentioned, from a surgical point of view, the lip venous system does not exhibit any sizable and distinguish vessel. A diffuse network of small venae comitantes coalesces into the facial vein draining the lips (Carty and Pribaz 2010) (Fig. 6.11). In a similar manner, the chin is drained by a network of unnamed small veins. The mental vein contributes to the venous system of the chin draining into the pterygoid venous plexus.

6.2.5 Innervation

6.2.5.1 Motor Innervation of Lips and Chin

The motor innervation to the lips and chin (Fig. 6.12) is provided by the zygomatic, the buccal, and the marginal branches of the facial nerve that innervate all of the perioral muscles.

The lip elevators are supplied by the zygomatic and buccal branches, the lip depressors by the marginal mandibular branches, and the lateral retractors by the buccal branches. The fibers of the facial nerve branches enter the perioral muscles usually in a radial form from their undersurface.

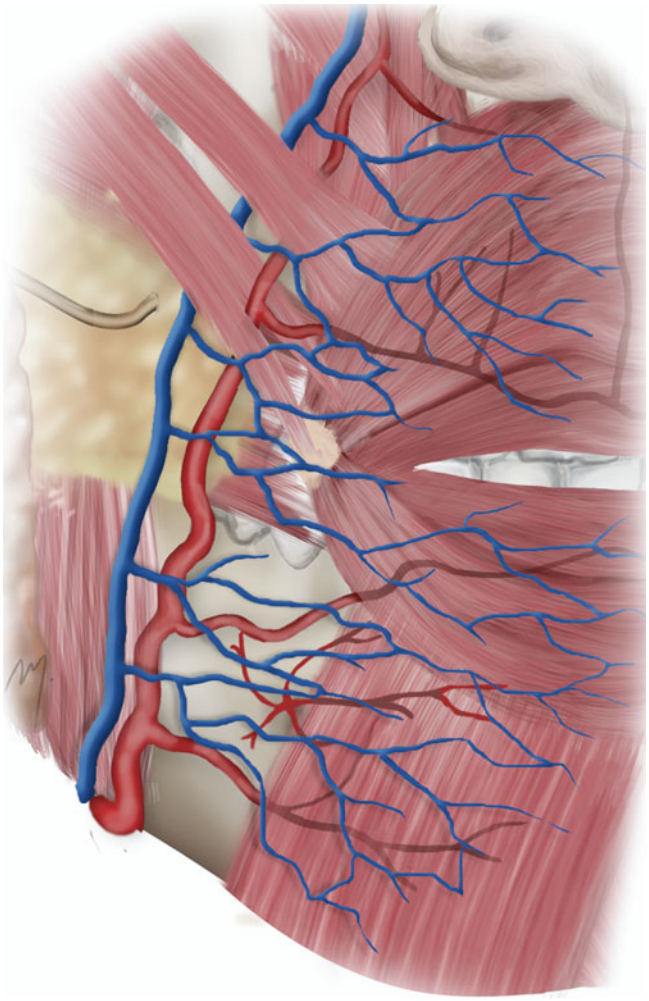

Fig. 6.11 Venous drainage of the perioral area

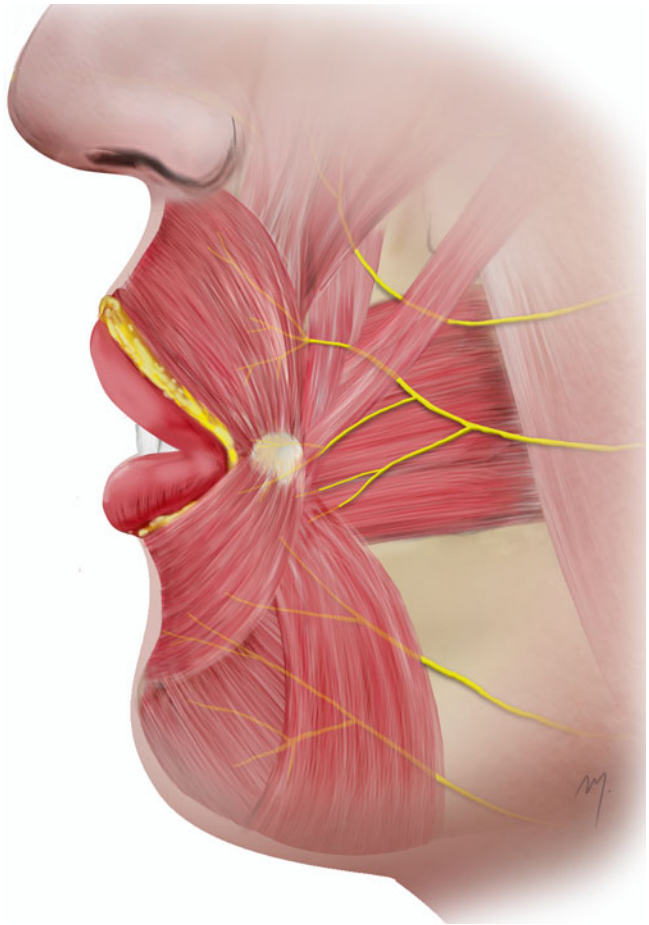

Fig. 6.12 Motor innervation to the lips and chin

6.2.5.2 Sensory Innervation of the Lips and Chin

Sensation to the upper lip is mediated by the superior labial branches of the infraorbital nerve (V2). The lower lip and the chin derive sensibility from branches of the mental nerve (V3).

6.2.5.2.1 Superior Labial Branches of the Infraorbital Nerve

The superior labial branches of the infraorbital nerve (Fig. 6.13) (see also Chap. 5) originate from the infraorbital nerve immediately after it exits through the infraorbital foramen to the face. They run inferiorly beneath the levator labii superioris muscle and distribute to the skin and the mucosa of the upper lip.

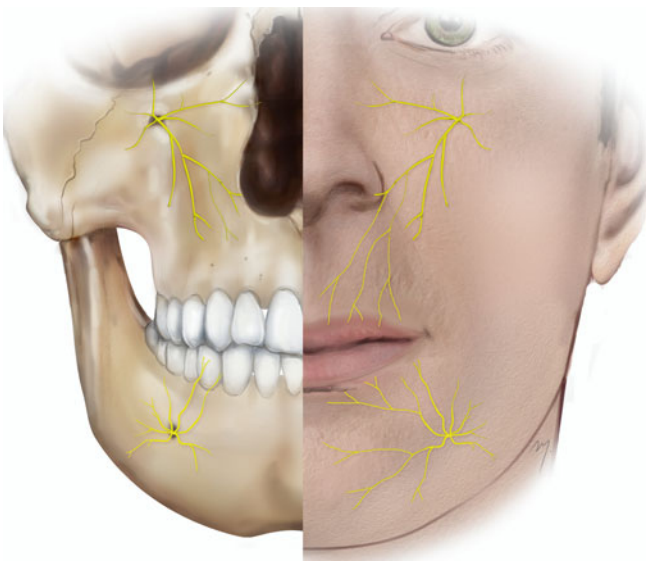

Fig. 6.13 Sensory innervation to the lips and chin

6.2.5.2.2 Mental Nerve

The mental nerve (Fig. 6.13) is the terminal part of the inferior alveolar nerve. The inferior alveolar nerves run through the mandibular canal, in company with the mandibular vessels. They exit in the chin through the mental foramen and upon exiting are termed mental.

Mental Foramen

The mental foramen shows a great variability in its position. It shows differences among ethnic groups and between genders (Greenstein and Tarnow 2006; Santini and Alayan 2012). Thus, highly accurate osseous landmarks cannot be provided as far as they change also with the dental status and the alveolar atrophic process. As a general rule in the dentate mandible, the mental foramen is located usually below the apex of the second mandibular premolar or between the apices of the first and second premolars. Palpation of the foramen may be difficult because of the overlying muscles and only radiologic examination could determine its position with accuracy.

As the mental nerve exits the mental foramen, it is located in the submucosa and can be extraorally or intraorally blocked by anesthetic. Some branches run anterior and slightly inferior to supply the skin of the chin, and others ascend to the skin and the mucous membrane of the lower lip. Short posterior branches innervate also the nearby cheek skin.

Mental Nerve Block

Regional block of each mental nerve anesthetizes the ipsilateral lower lip and chin, and as the infraorbital nerve blockade, it can be performed either extraorally or intraorally. The mental foramen if difficult to palpate is supposed to lie between the apices of the 1st and 2nd premolar teeth and slightly below that level. In the extraoral technique (Fig. 6.14), the needle is inserted 1 cm lateral to the foramen and proceeds directly to it. At the intraoral technique (Fig. 6.15), the needle is inserted at the buccal sulcus targeting directly to the area between the apices of the 1st and 2nd premolar teeth and slightly below. Injection of 1 ml local anesthetic is sufficient to result in anesthesia of the mental nerve.

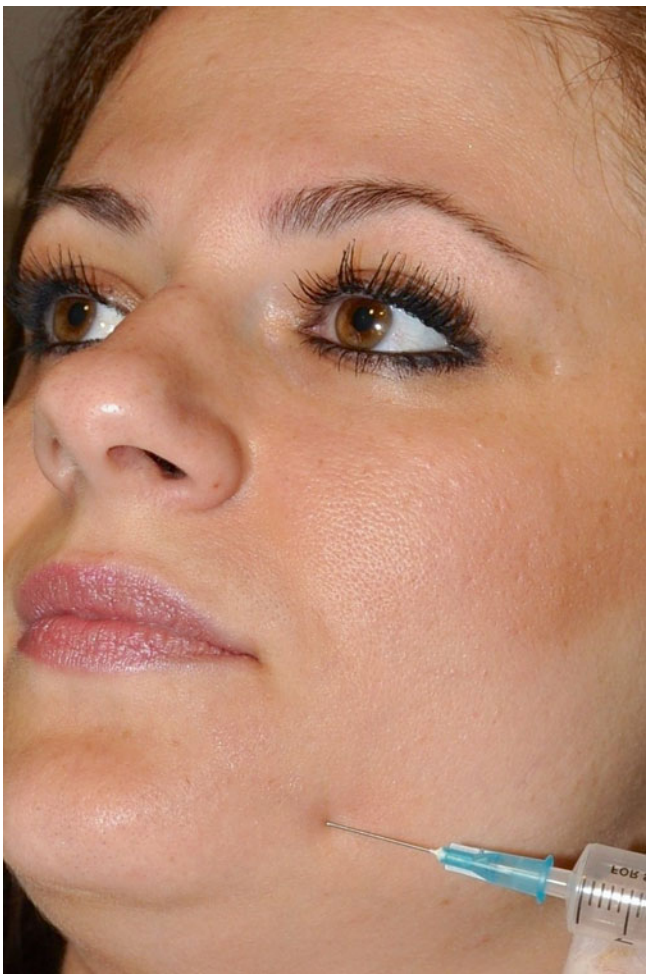

Fig. 6.14 Extraoral block of the mental nerve

6.3 Flaps Derived from the Perioral Area

The perioral area provides flaps that mainly can reconstruct only the lips and the chin that sometimes are based also at the nearby cheek. Often a defect involves both the chin and the lower lip, and both must be reconstructed.

In reconstructing the lip, the goals are the aesthetic outcome and the lip function. A reconstructed lip, which breeds the anatomic proportions, is bulky as needed to seal the oral opening, gains adequate oral opening and mobility to function, and is at the same time also an aesthetically ideal lip.

6.3.1 Flap Design Concerning Vascular Anatomy

The arteries of the perioral area form an arterial network as follows. At the lips, the superior and inferior labial arteries anastomose with its contralateral and form with the intermediate part of the facial artery the perioral arterial circle. Many types of full-thickness lip flaps can be safely based on this perioral circle. At the chin, a robust anastomotic network is formed by branches of the mental artery, the labiomental artery, and the terminal part of the submental artery, which perfuse the whole area and contribute to the supply of the lower lip.

The superior labial artery after originating from the facial artery travels to the midline becoming more and more close to the free lip margin. It is situated at about 5–15 mm from the lip margin at the labial commissure and 3–6 mm from it at the midline (Fig. 6.16).

Similar to its corresponding superior labial, the inferior labial artery as it approaches the midline courses closer to the free lip margin. It is located usually at about 10–15 mm from the lip margin at the labial commissure and 2–5 mm from it at the midline (Fig. 6.16).

The facial artery passes usually in a distance of 1.5–2 cm lateral to the oral commissure and runs upward usually situated medial to the nasolabial sulcus. This is of great importance when designing some axial perioral flaps

Fig. 6.15 Intraoral block of the mental nerve

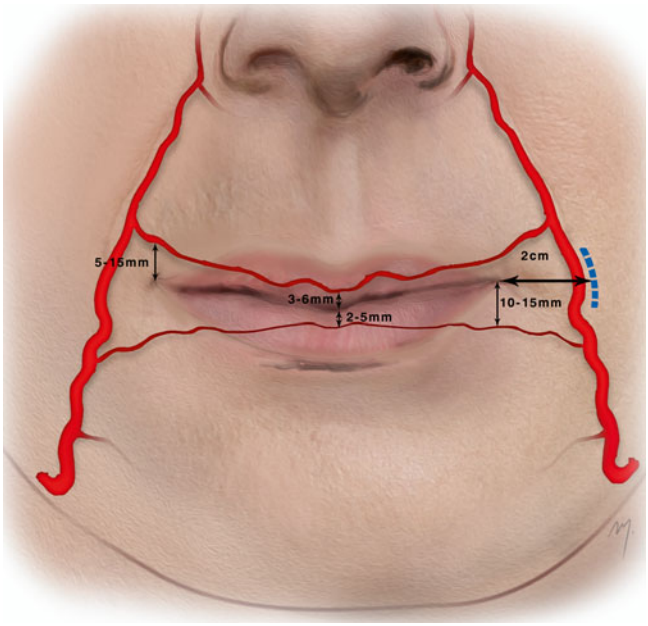

Fig. 6.16 Common distances of the perioral arterial circle from the oral commissure and the free lip margins

(e.g., Gillies fan flap, Karapandzic flap). The viability of these flaps requires intact facial and labial arteries that must be preserved. Considering this distance as the minimum in the flap design, the integrity of the feeding vessels is ensured.

The arterial anatomy of the lips has been extensively studied but still remains a modern issue of research, with controversial results showing of great differences and a multiform vascular branching and distributing pattern of the involved arteries (Schulte et al. 2001; Nakajima et al. 2002; Edizer et al. 2003; Kawai et al. 2004; Magden et al. 2004; Pinar et al. 2005; Loukas et al. 2006; Al-Hoqail and Meguid 2008). The landmarks already mentioned lie within a great range that must be kept in mind during flap design. However, only the meticulous and blunt dissection at the flap pedicle during surgery enables the identification and ensures the protection of the feeding vessels. Even though the standard, classic flaps that are derived from lips are extremely safe, it is wise in more sophisticated flap types or microsurgical reconstructions to evaluate preoperatively by Doppler ultrasonography the existence and the course of these arteries due to their (inconstant vascular anatomy) vascular variations.

6.3.2 Lip Mucosal Advancement Flap

This flap is used to reconstruct the vermilion defect after a lip-shave procedure. Lip-shave is the procedure of vermilionectomy and is performed in premalignant lesions (actinic cheilitis or leukoplakia) of the vermilion.

The patient seen in Fig. 6.17a had a well-defined leukoplakia of the lower lip. The removal of not the whole but only of the affected vermilion was decided (Fig. 6.17b). The usual rule is to excise the whole of the vermilion in a lip-shave procedure as it is demonstrated in the next case, but the reconstruction by a mucosal advancement flap in both cases is based upon the same principles. The vermilion is excised at the submucosal layer by sharp dissection (Fig. 6.17c) just above the muscle fibers of the pars marginalis of orbicularis oris (Fig. 6.17d).

After resection is completed, the buccal mucosa lining the lip is elevated in a plane deep to the minor salivary glands and superficial to orbicularis oris muscle (Fig. 6.17e). The mucosal flap is raised up to the labial sulcus and advances without tension to the bare lip (Fig. 6.17f). The flap is then sutured to the skin of the lip covering the defect (Fig. 6.17g). The procedure results in a normal lip (Fig. 6.17h).

6.3.2.1 Entire Vermilion Reconstruction by Lip Mucosal Advancement Flap

The pathologic changes of the vermilion are usually diffuse and multifocal so in the majority of cases total

vermilionectomy has to be performed as well as reconstruction of the whole vermilion by the lip mucosal advancement flap.

In the case demonstrated in Fig. 6.18a–e, the entire vermilion is excised as an ellipse and is reconstructed by the usual way with lip mucosa that is advanced to cover the whole defect.

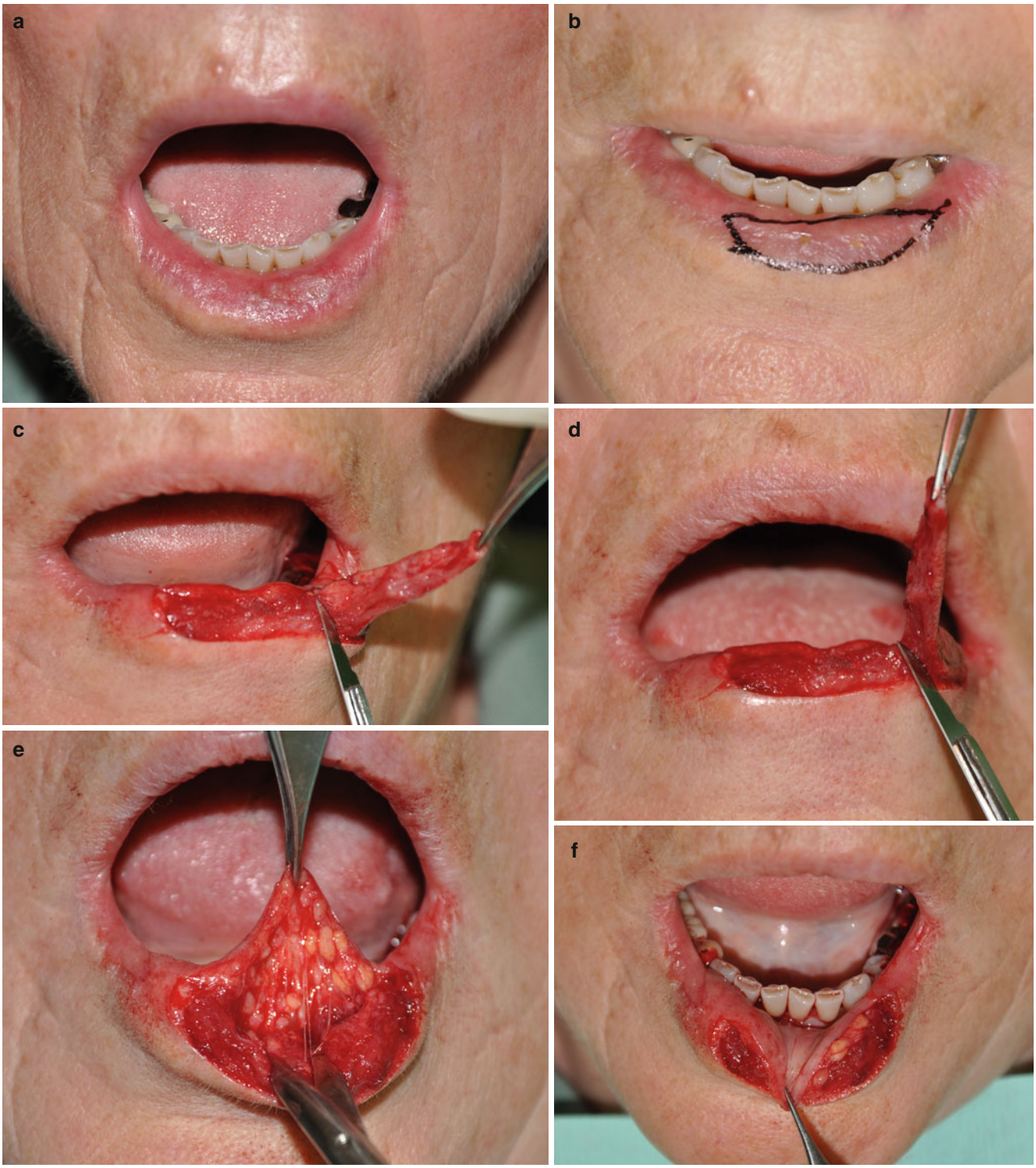

Fig. 6.17 (**a**) Well-defined leukoplakia of the lower lip. (**b**) Excision outlined. (**c**) The vermilion is striped in the submucosal layer. (**d**) The pars marginalis of orbicularis oris is left intact. (**e**) Mucosa is raised leaving the minor salivary glands on its undersurface. (**f**) The mucosal flap is advanced to the defect. (**g**) Final suturing. (**h**) The skin-vermilion line of the lip rendered in normal position

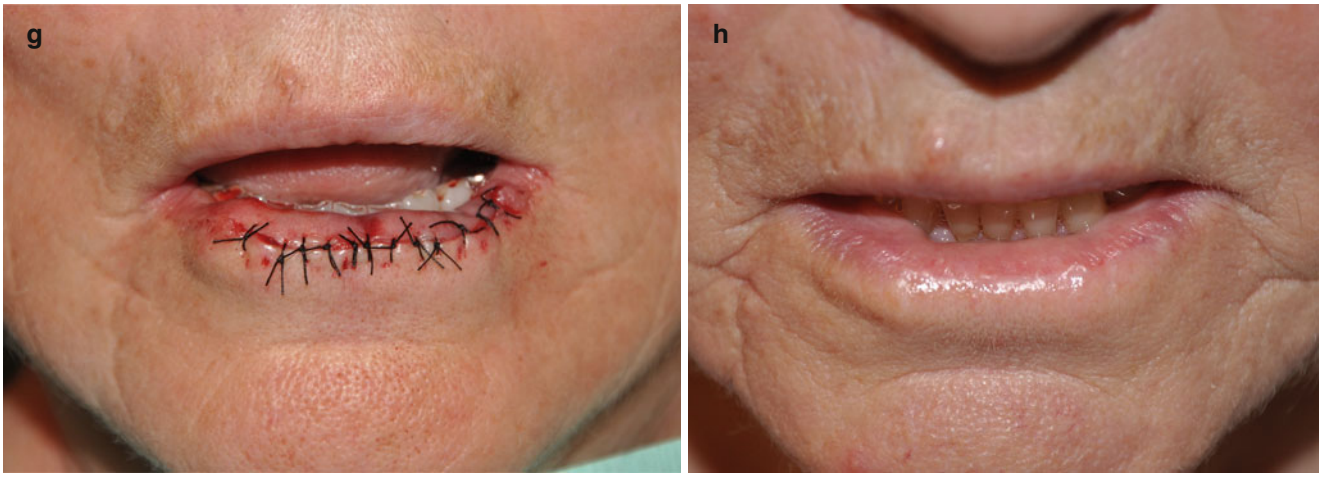

Fig. 6.17 (continued)

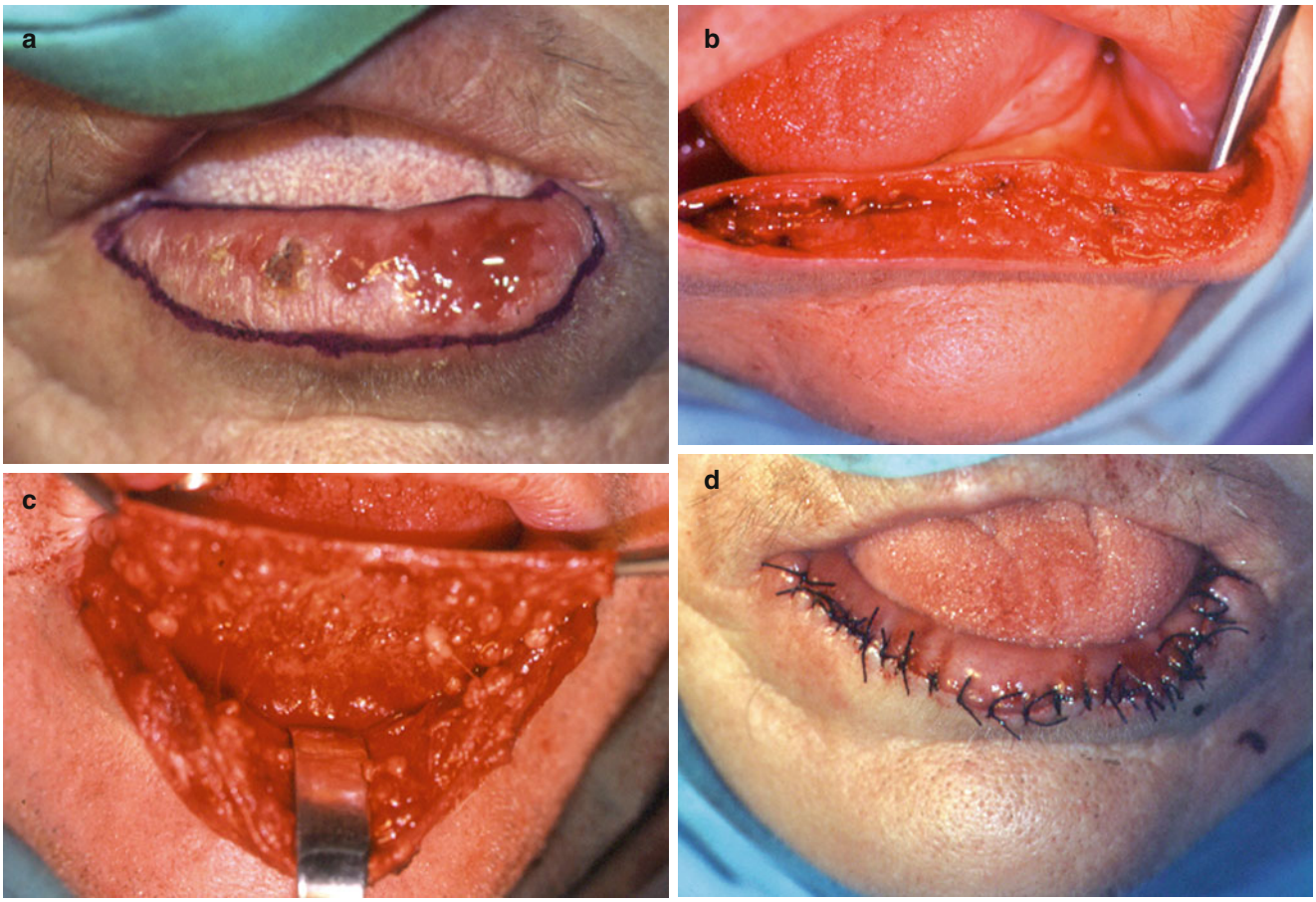

Fig. 6.18 (**a**) Elliptical excision of the entire vermilion is outlined. (**b**) The vermilion is striped above the orbicularis oris muscle. (**c**) Lip mucosal flap is raised. (**d**) Flap sutured in position

6.3.3 Vermilion Myocutaneous Advancement Flap

For deep vermilion defects that include also the pars marginalis of orbicularis oris muscle, a mucomuscular flap of the remaining vermilion can be advanced and restore the defect (Goldstein 1984). This flap includes the vermilion along with the underlying pars marginalis muscle as a single unit and is based on axial labial artery. The elasticity of the lips allows advantage of the flap of up to 30 % of the vermilion length.

In the patient seen in Fig. 6.19a, the vermilion of the lower lip at the right commissure had to be excised deep to the pars marginalis muscle due to a combined buccal-lip verrucous carcinoma. The outline of the flap is just an incision line along the mucocutaneous border of the lip from the defect to a point near the commissure of the opposite site up to the lateral quadrant of the lip so as to avoid damage to the inferior labial artery. If further mobilization is needed, flap preparation should be carried out using extreme caution so as to ensure that the inferior labial artery is included into the flap base.

The incision is made horizontally through the entire thickness thus completely cutting and separating the pars marginalis muscle with the supernatant vermilion from the underlying pars peripheralis muscle (Fig. 6.19b, c). During this phase special attention is given to the course of the labial artery in its various distances from the free lip margin, so that the vessel must always lie within the flap. The laterally based axial flap that is raised in this very simple manner is then advanced to the defect, sutured in place completing the reconstruction (Fig. 6.19d, e).

6.3.4 Mucosa Island Pedicle Flap (V-Y Advancement)

Exactly like the skin island flaps that are based subcutaneously, a mucosal island flap is based in the submucosa and can be designed to resurface vermilion defects.

In the presented case of a patient with a pyogenic granuloma of the upper lip, excision and reconstruction with an island flap is planned. The excision is outlined in rectangular form and the island flap is designed as a triangle (Fig. 6.20a, b). The general rule of 2:1 of length to base is not mandatory since the submucosal tissue layer is extremely lax. The lesion was excised in a superficial plane and the defect concerned only the vermilion (Fig. 6.20c). The flap was raised based on a submucosal pedicle (Fig. 6.20d). The flap advanced to resurface the defect and the donor site was closed in a V-Y fashion (Fig. 6.20e, f). The postoperative result is very satisfactory (Fig. 6.20g, h).

6.3.5 Barrel Technique

6.3.5.1 Double-Barrel Technique (Bilateral Advancement Flaps)

Strictly speaking, this technique is an improvement of the W-resection of the lip but resembles a bilateral advancement flap. This method can be used to close lip defects of 30–40 %. The remaining lip can effectively reconstruct the defect by means of simple advancement.

The lesion is excised in a rectangular form, and from its base, two crescent-like incisions are outlined around the labiomental sulcus (Fig. 6.21a, b). The rectangle is excised in the full thickness of the lip, and the crescent excision includes skin and subcutaneous tissue only (Fig. 6.21c).

The remaining lip is advanced and the defect is closed in layers (Fig. 6.21d). The final result is very satisfactory (Fig. 6.21e).

6.3.5.2 Single-Barrel Technique (Unilateral Advancement Flap)

For defects up to 30 % of the lip, the same method can be used as a single advancement flap. At the case demonstrated, a squamous cell carcinoma of the lip required excision of the 30 % of its total. The defect was reconstructed by the single-barrel technique (Fig. 6.22a–d).

6.3.6 Karapandzic Flap

The Karapandzic flap (Karapandzic 1974) constitutes one of the best methods in lip reconstruction. It is a double sliding-rotation neurovascular myocutaneous flap that can be used in closing defects of up to three-fourths of the length of the lower lip. It is easy and quick to perform, uses similar tissue in its full thickness from the adjacent donor site, and restores lip aesthetics and most of all lip function (Fig. 6.23).

The patient presented in Fig. 6.24a, b had a squamous cell carcinoma of the lower lip, and excision and a Karapandzic flap reconstruction were planned. The defect was excised in a rectangular form, and from its base two incisions, one on each side, are outlined parallel to the lip and prolonged along the mentolabial and nasolabial creases around the commissure into the upper lip. The flaps provided are equal to the height of the lip.

After the resection of the lip is completed, the initial incisions of the flaps are made through the skin and subcutaneous tissue. By blunt dissection in a radial fashion, the orbicularis muscle both in the lower and upper lip is freed from its attachments. In most cases when dissecting at the nasolabial crease, the facial artery and the vein are encountered and preserved. It is very important to dissect parallel to the directions of the incoming nerves and vessels and preserve them so as to gain the vascularity of the flap and the mobility and sensibility of the new lip (Fig. 6.24c, d). The lip mucosa at the medial part of the flaps up to the level of the commissures is incised now, thus, fully mobilizing the flaps. After the required mobility has been obtained, the two flaps are sliding medially and sutured without tension in layers (Fig. 6.24e, f).

The cosmetic and functional postoperative result of the Karapandzic flap is always almost excellent (Fig. 6.24g, h).

Fig. 6.19 (**a**) The mucomascular vermilion flap with its base laterally is outlined. (**b**, **c**) Flap raised with its base laterally to the opposite site. (**d**) The flap is advanced to the defect. (**e**) Early postoperative result at 2 months

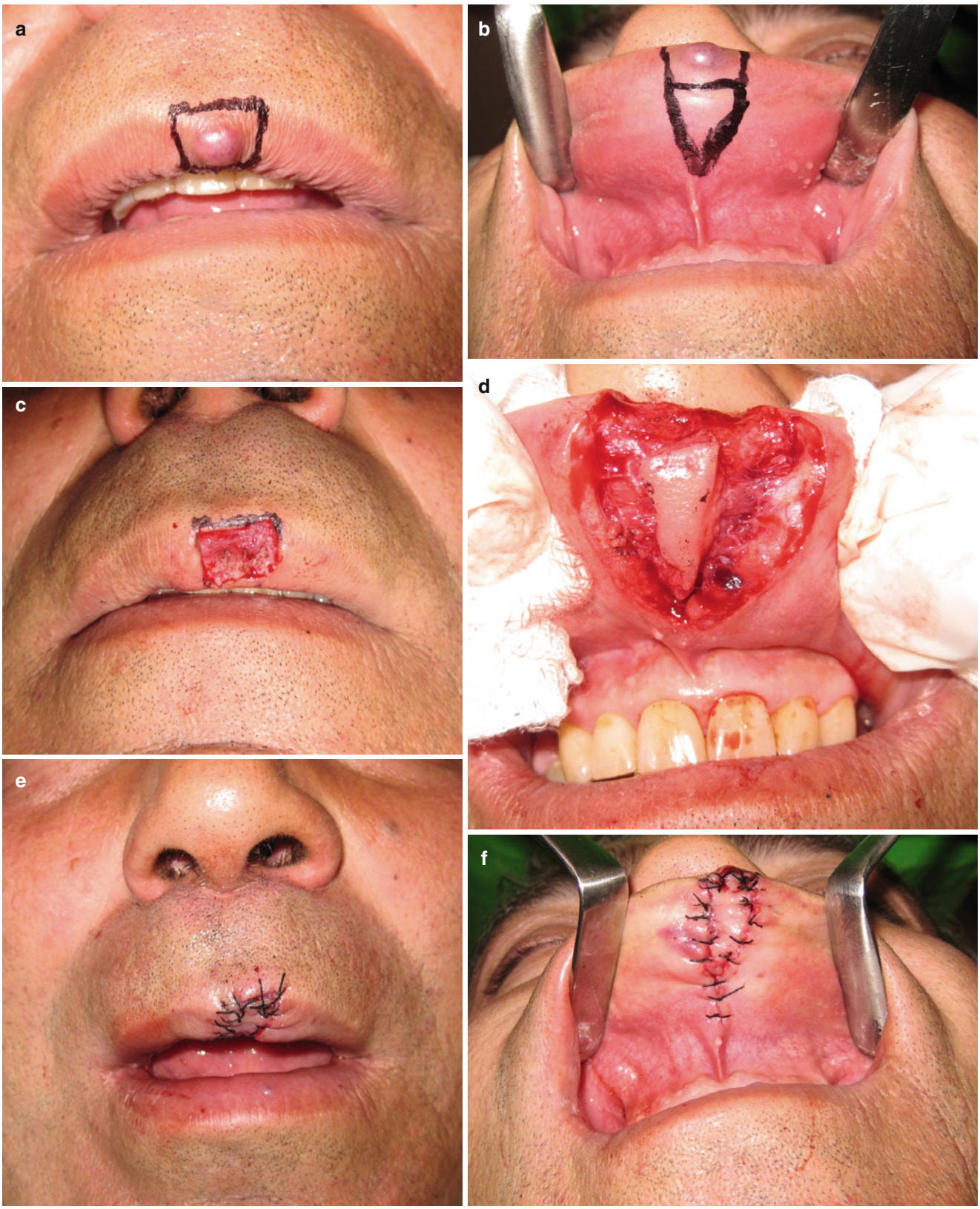

Fig. 6.20 (**a**) Pyogenic granuloma of the upper lip vermilion. (**b**) Flap outlined. (**c**) The lesion is excised. (**d**) Flap is based on a submucosal pedicle. (**e**) Flap sutured in place. (**f**) V-Y closure of the donor site. (**g**, **h**) Result at 2 weeks

Fig. 6.20 (continued)

The suture lines follow the natural creases hiding the scars, and the new lip is sensible and mobile. The flap brought the muscle fibers with the proper direction and restored the orbicularis oris in a normal continuity gaining thus its mobility and its "sphincter" function.

The Karapandzic flap when used at its defect-size borderline (defect of 75 % of the total lip) always causes a slight to moderate microstomy that may need secondary correction as is demonstrated in the following case.

In this case a lower lip carcinoma is planned to be excised with simultaneous bilateral neck dissection (Fig. 6.25a, b). Almost 80 % of the lip has to be excised and reconstruction was performed with a Karapandzic flap resulting in microstomy (Fig. 6.25c). Although the microstomy improves in some degree with time, a corrective plastic procedure of the commissures was needed (Fig. 6.25d, e).

6.3.6.1 Karapandzic Flap Combined with Lip Mucosal Advancement Flap

A squamous cell carcinoma of the lip is not uncommonly involved with areas of leukoplakia of the vermilion. Then the excision of the primary tumor has to be combined with a lip-shave operation. Such a case with a Karapandzic flap combined with a simultaneously lip mucosal advancement flap is demonstrated in the patient in Fig. 6.26. The incision lines of the resection and the Karapandzic flap are outlined (Fig. 6.26a). The operation starts with the lip-shave part and continues with the resection of the tumor en bloc (Fig. 6.26b, c). In the usual way, the Karapandzic flap closes the lip defect, and the advancement mucosal flap covers the vermilion surface. The postoperative result is satisfactory; the lower lip and the vermilion have been completely restored (Fig. 6.26d, e).

The Karapandzic flap is a double sliding flap and must never be used as single. If it is used only from one side without its corresponding, another flap must be used from the other side in combination (see below).

6.3.7 Bernard-Webster Flap

This technique is a double cheek advancement flap that reconstructs near-total or total lip defects. It was originally described by Bernard (1852) and was modified by Webster et al. (1960).

In the patient presented in Fig. 6.27a, a squamous cell carcinoma has affected the whole lower lip. Total lip reconstruction is planned to be done with the Webster technique (Fig. 6.27b, c). The total lower lip is outlined to be excised as a quadrilateral segment from commissure to commissure. Horizontal incisions, one on each side, extend laterally from the commissure slightly curving upward and from the base of the lower lip defect to the medial cheek slightly curving downward. Four triangles situated above and below the lateral end of the flaps are also outlined. By this, two advancement cheek flaps have been determined that bring new tissue from the cheek. As "new lip tissue" is provided, microstomia (a disadvantage of other reconstructive procedures) is avoided. Moreover the commissure is reconstructed in a better way.

The whole lower lip is excised and clear margins are revealed by frozen section biopsies (Fig. 6.27d).

The horizontal incisions are carried so as to divide the orbicularis muscle. If the flap base needs to be situated more laterally, the dissection is carried out above the buccinator

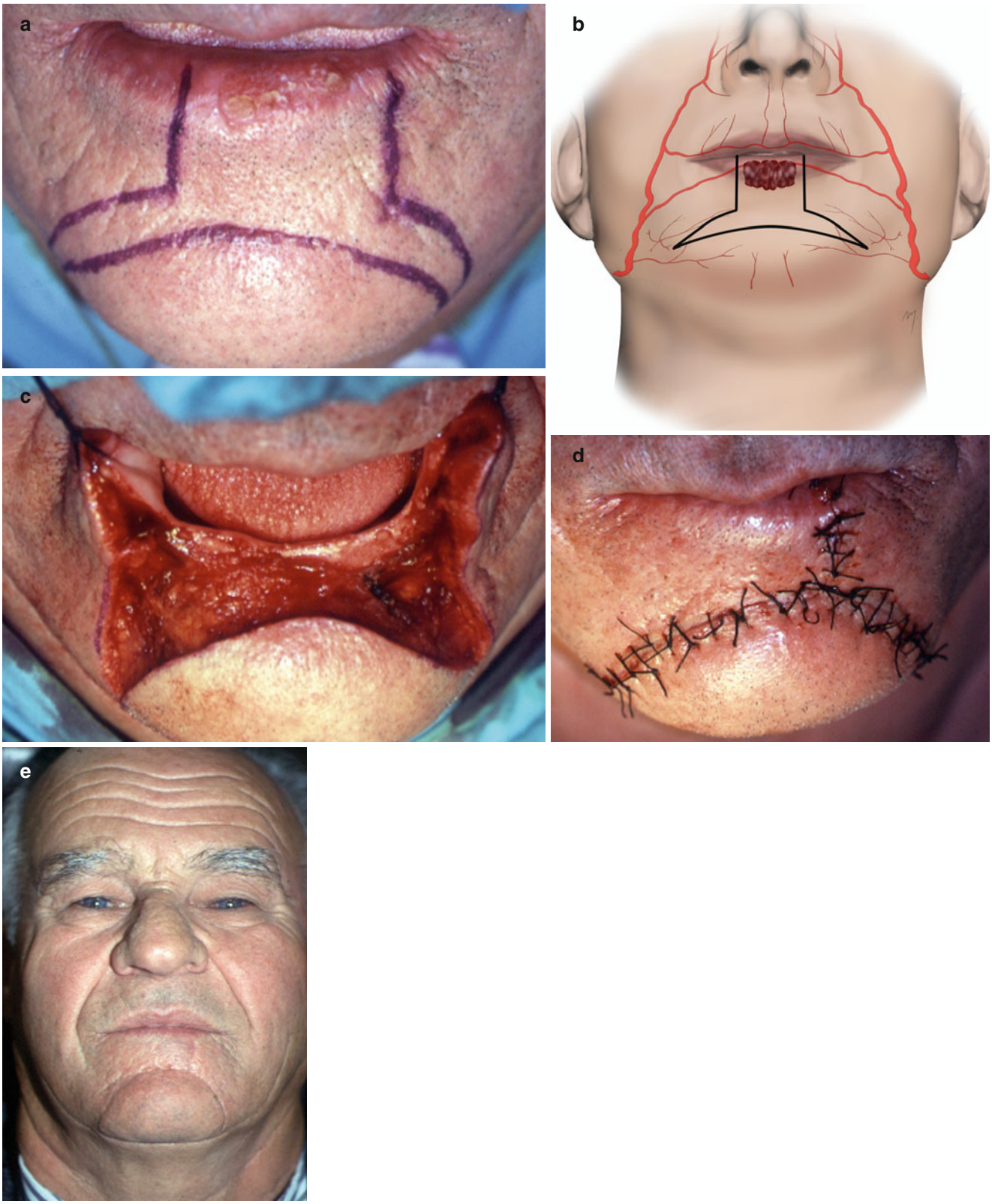

Fig. 6.21 (**a**, **b**) Double barrel outlined. (**c**) Excision completed. (**d**) Closure of the defect. (**e**) Result at 4 months

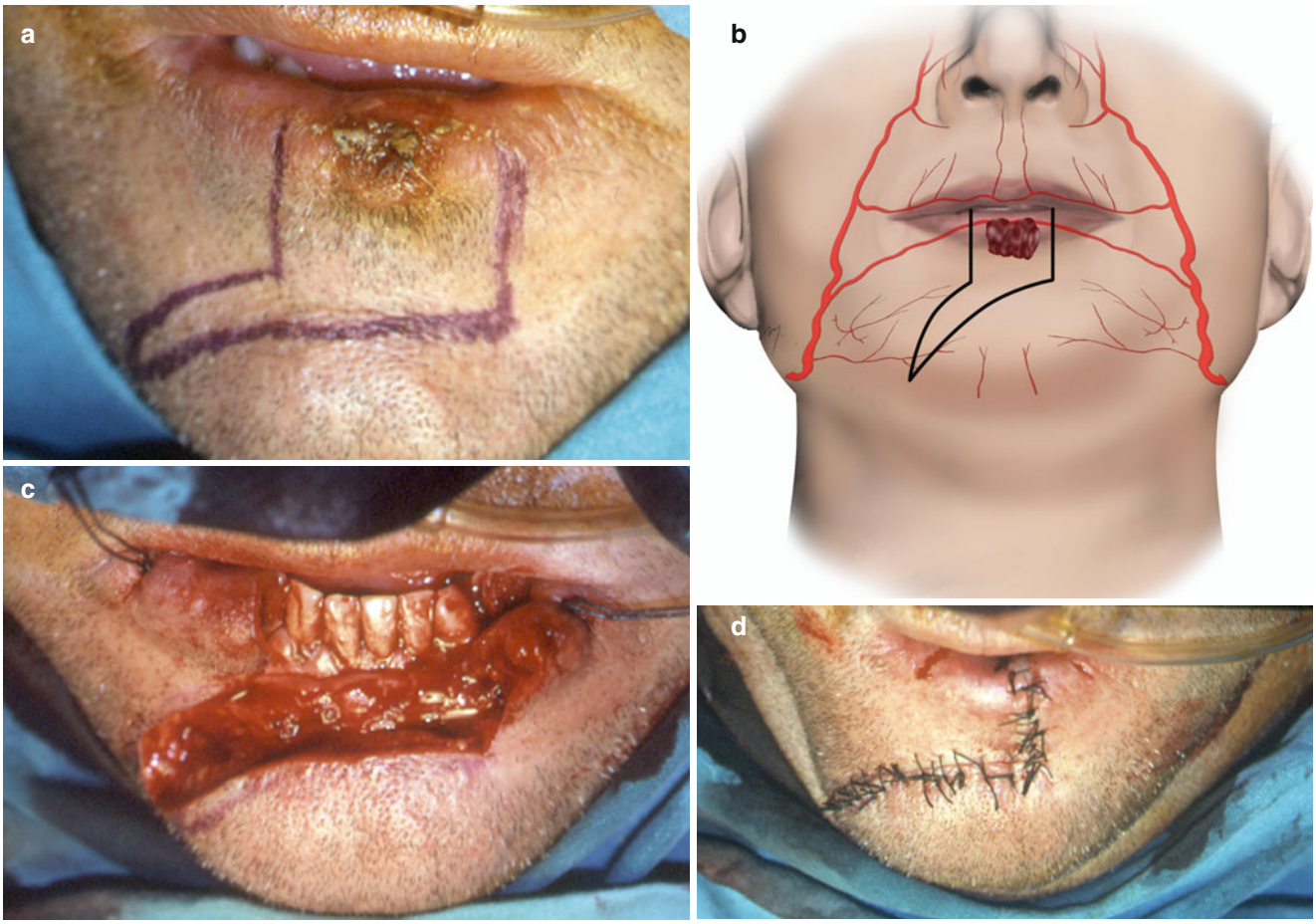

Fig. 6.22 (**a**, **b**) Single barrel. (**c**) Excision completed. (**d**) The defect has been restored by simple advancement

muscle. No mucosal cuts are performed at this stage. Next, the triangles are excised including only skin and subcutaneous tissue. The mucous membrane of the upper triangles is now incised in their medial and lateral sides leaving the bases intact. They turn over and with some trimming are rolled and sutured over the bare superior border of the advancement flap, forming thus the new vermilion (Fig. 6.27e). The two flaps are then advanced to the midline and sutured in layers (Fig. 6.27f).

The postoperative result is almost typical and expected in these reconstructions, to show a tight lip combined with an apparent fullness of the upper lip, especially in edentulous patients (Fig. 6.27g). Appropriate prosthodontic treatment improves these disadvantages.

6.3.7.1 Unilateral Bernard-Webster Technique Combined with Karapandzic Flap

The Bernard-Webster technique can be used unilateral and combined with other lip flaps. A useful combination is the one with a Karapandzic flap. This can be used in near-total lip defects where a portion of healthy lip remains to the one site. In these cases the Karapandzic flap is designed at the site of the remaining lip and the Bernard-Webster flap at the opposite.

In the patient presented in Fig. 6.28 with a squamous cell carcinoma of the lower lip, about 75 % of the lip must be resected. The left commissure is also included in the resection. A Karapandzic flap is used to the right side and a Webster flap to the left (Fig. 6.28a, b). The use of a Webster flap gains more length and forms a more sharp lip angle. The lip was excised and the Karapandzic flap was raised in the typical fashion. At the right side, the Bernard-Webster flap is prepared and new vermilion is formed in the usual manner (Fig. 6.28c). The flaps reached the defect without any tension and were sutured in place (Fig. 6.28d, e). The result is satisfactory and the advantages provided by both of the flaps have been reclaimed (Fig. 6.28f).

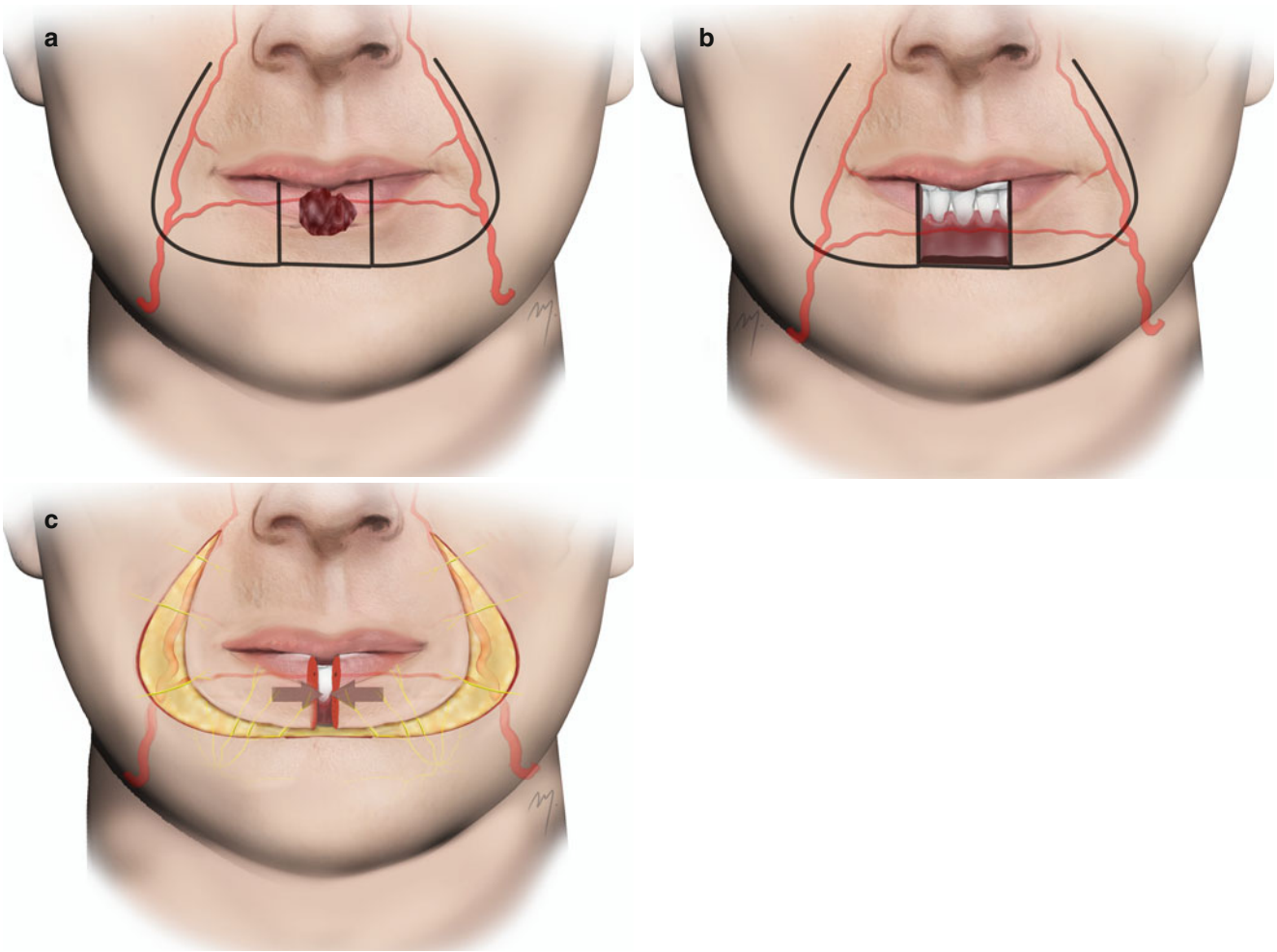

Fig. 6.23 (**a**–**c**) The Karapandzic flap is a double sliding-rotation neurovascular flap. The flap incisions are deepened by dividing muscles and subcutaneous tissue but sparing the neurovascular structures rebuilding thus a fully functional lip that preserves its mobility and its sensibility

6.3.7.2 Bernard-Webster Technique Combined with Neck Management Procedures

In cases of a lip carcinoma where a simultaneous neck dissection has to be performed, the incision lines of the lip reconstruction flap can be incorporated to the incisions for the neck dissection flap (Lentrodt and Luhr 1971; Lentrodt 1975).

In the patient shown, an extensive lower lip carcinoma is planned to be excised in combination with a supraomohyoid neck dissection (Fig. 6.29a, b).

A Webster flap has been outlined at the left side, while a Karapandzic flap will be used from the right side to reconstruct the lip. The inferior incision of the Webster flap method has been extended around the chin to the neck and joined to an apron flap for a supraomohyoid lymph node dissection (Fig. 6.29c, d).

The supraomohyoid neck dissection was performed and nearly the entire lip had been excised (Fig. 6.29e). The Webster flap was raised from the left side and the Karapandzic flap raised from the right side. The flaps were advanced closing the lip defect, and the lip and neck incisions sutured in place (Fig. 6.29f). The postoperative result shows a wide mouth opening, but the typical overhanging upper lip, as in every Webster technique, is present (Fig. 6.29g, h).

6.3.8 Bernard-Fries Technique

In cases where not only the lip but also the chin has to be resected, the principles of the Fries (1973) modification of Bernard operation can be a useful option. According to this, the lip is not excised as a rectangle but in the form of a V (or W) that extends from commissure to commissure. As the flaps are extended inferiorly, simultaneous reconstruction of the whole lip and a big portion of the chin can be achieved by advancement on each side of the defect. In the following case, a classic Bernard-Fries technique was planned initially for the reconstruction of a very wide lip and chin defect that finally was slightly modified.

The patient demonstrated in Fig. 6.30a had an extensive lower lip carcinoma expanded to the chin requiring total

lower lip and chin resection. The lip resection was outlined in a wide W-shape that included the whole chin (Fig. 6.30b, c). The tumor was resected and clear margins were revealed by frozen section biopsies (Fig. 6.30d).

New vermilion was formed as already described in the Bernard-Webster technique (Fig. 6.30e). Suturing the initially designed as a W without any other maneuver resulted in approximation of the flaps, to close the large chin defect,

Fig. 6.24 (**a**) Squamous cell carcinoma of the lower lip. (**b**) Resection lines and the Karapandzic flap outlined. (**c**, **d**) Preservation of the neurovascular structures at the lateral and inferior limb of the flap. Motor and sensory supply to the lip is ensured. (**e**) The Karapandzic flaps fully mobilized. (**f**) The flaps rotated and sutured in place. (**g**, **h**) Result at 6 months show satisfactory cosmetic and functional result

Fig. 6.24 (continued)

under tension. This was improved through a horizontal incision to the neck that allowed final closure with significantly reduced tension (Fig. 6.30f). The final result led to a tight lower lip and an overhanging upper lip that is always expected in these procedures (Fig. 6.30g, h).

6.3.9 McGregor's Fan Flaps

The fan flap is a method of transposing nasolabial tissue into the lower lip and was first described by Gillies (1957). McGregor (1983) improved the design of the classic Gillies fan flap, focusing in the flap movement, into a modification that provides a better outcome, especially in cases where the resection extends to the angle of the mouth and involves the half of the lip. According to McGregor's design, the lip is excised as a square, and a rectangular in shape, vertical full-thickness cheek flap is outlined lateral to the defect. The width of the rectangle is equal to the hight of the defect and its length two times its width. The flap is based in a narrow pedicle at the ipsilateral oral commissure. This extremely narrow pedicle contains the superior labial vessels. The flap is then elevated in full thickness and rotated 90° around its base, taking up a horizontal position and fills the defect. By McGregor's modification the pivot point at the commissure remains static, maintaining thus the initial, normal position of the mouth angle in the new lip.

Bilateral fan flaps can reconstruct the whole lower lip while a tongue flap reconstructs the vermilion. Such a case is demonstrated (Fig. 6.31a–f).

6.3.10 Bilateral Perialar Crescenting Advancement Flaps

The bilateral perialar crescenting advancement flaps (modified Burow's technique) are a very satisfactory technique suitable to reconstruct defects involving up to one-third of the width of the upper lip.

The patient presented had an infiltrative lesion situated at the mid-part of the upper lip (Fig. 6.32a). The proposed

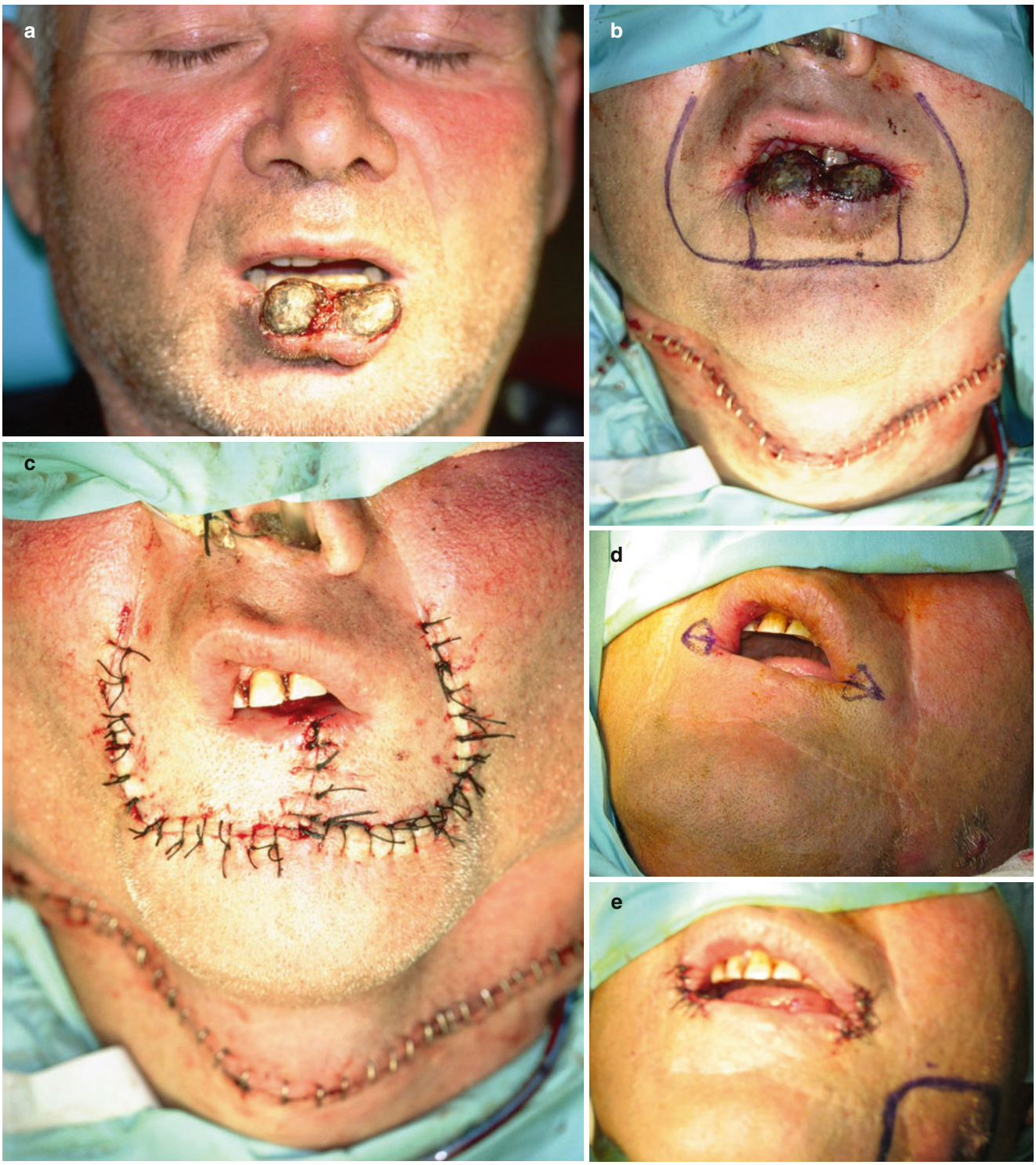

Fig. 6.25 (**a**) Squamous cell carcinoma of the lower lip. (**b**) Outline of the Karapandzic flap. (**c**) Immediate postoperative view. (**d**, **e**) Commissure correction in the same patient 9 months later

Fig. 6.26 (**a**) Incision lines outlined. (**b**, **c**) The vermilion is excised in conjunction with the primary tumor. (**d**, **e**) Result at 3 and 12 months

rectangular excision of the tumor and the perialar crescenting incisions are outlined (Fig. 6.32b, c).

The lesion is resected through and through, and at the perialar crescents, the skin and subcutaneous tissue only are excised. The mucosa is freed in the buccolabial sulcus, and two laterally based flaps are developed (Fig. 6.32d). After adequate undermining and mobilization, the residual lateral parts of the upper lip are advanced medially, sutured in layers, and reconstructed the upper lip (Fig. 6.32e).

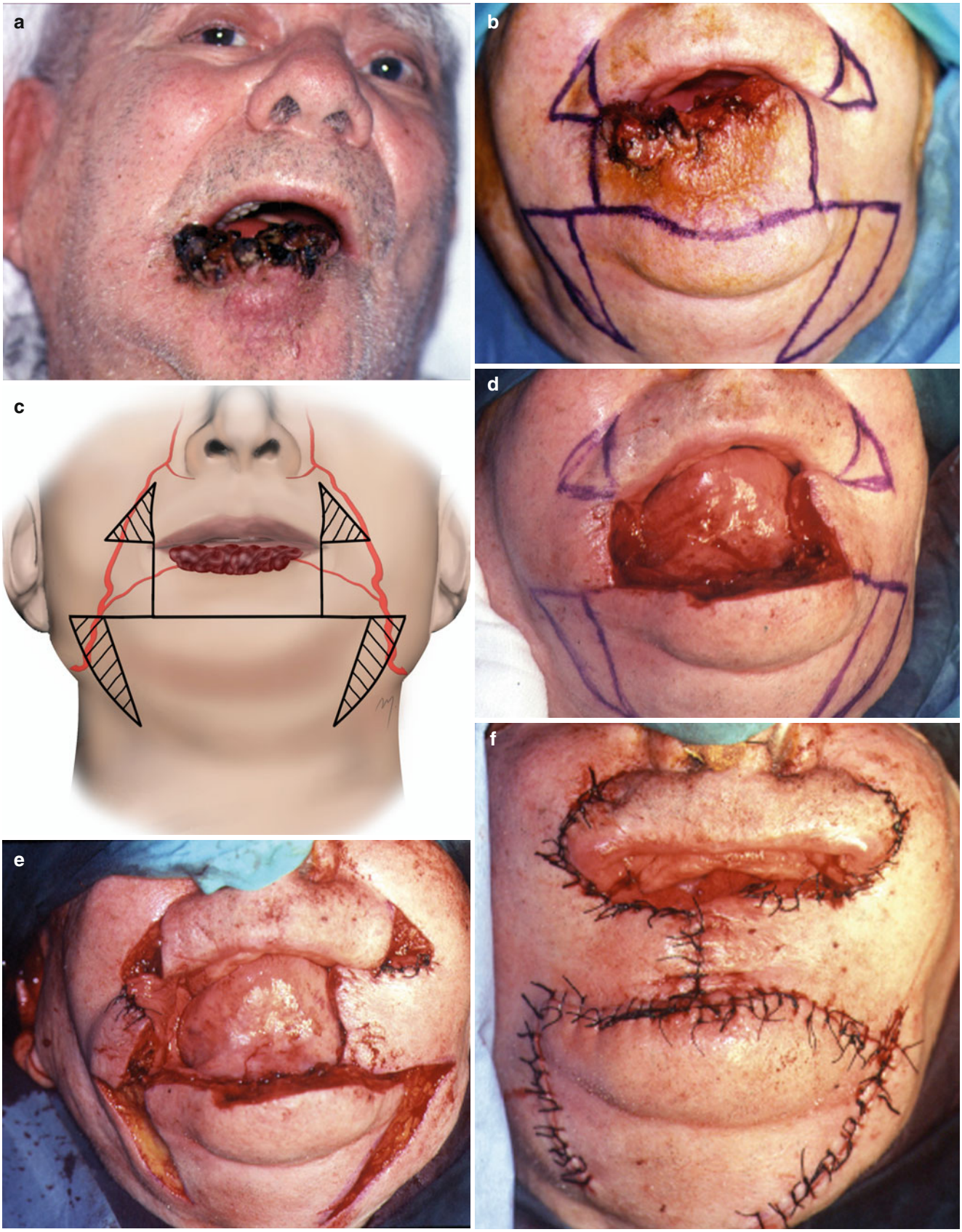

Fig. 6.27 (**a**) Squamous cell carcinoma involving the whole lower lip. (**b**, **c**) Flap design. (**d**) Total lower lip defect. (**e**) Incisions carried out through the orbicularis muscle. New vermilion is formed by turning over the mucosa of the upper triangles. (**f**) Immediate postoperative view. (**g**) Postoperative view at 1 year

Fig. 6.27 (continued)

Postoperatively even the fact that the Cupid's bow has lost its harmony, the overall result is satisfactory (Fig. 6.32f).

6.3.11 Reverse Karapandzic Flap

The simple and genius method of the Karapandzic flap, as described for lower lip reconstruction, can also be used for full-thickness upper lip defects in a reverse form. Again two double sliding-rotation neurovascular myocutaneous flaps according to the same technical principles are able to close defects of up to 75 % of the length of the upper lip.

The patient seen in Fig. 6.33a, b presented with a squamous cell carcinoma of the lateral subunit of the upper lip, spreading to its midsection. Excision of almost the entire lateral subunit and the philtrum is needed. A reverse Karapandzic flap reconstruction is outlined (Fig. 6.33c, d). The defect is excised in a rectangular form, and from its base, two incisions one on each side are outlined parallel to the upper lip, run parallel to the nasolabial crease, and curve around the commissure into the lower lip. The flaps that are provided must correspond to the height of the lip.

After the resection of the lip and philtrum is completed, the incisions of the flap are made through the skin and subcutaneous tissue (Fig. 6.33e). The orbicularis muscle is detached from its attachments by blunt dissection, leaving the incoming nerves and vessels intact tension. Dissecting at the nasolabial crease, the facial artery and vein are encountered and preserved.

Adequate mobility is needed to allow sliding and approximation of the flaps without tension (Fig. 6.33f) and suturing in place (Fig. 6.33g). Even the fact that the delicate anatomy of the normal philtrum cannot be rendered, the final result as in the lower lip is good in terms of aesthetics and function (Fig. 6.33h).

6.3.12 Abbe-Estlander Flap

The transfer of a triangular-shaped full-thickness segment of lip tissue from the lower lip to a full-thickness upper lip defect was popularized by Abbe in 1898, and this flap become classic, also described until today. Even though the concept seems to be very logical as "lip reconstructs lip," the upper and the lower lip are not adjacent in direct contact tissues but exhibit a completely different shape, thickness, and often texture especially at the vermilion. This results always in a patch appearance of the reconstruction. Consequently, if remaining tissue from the same lip is available, its use can cover the defect providing a reliable reconstruction and enhancing the long-term aesthetic result. On the contrary, the same principle gives much better results when used to reconstruct a partial commissure defect and is known as the Abbe-Estlander flap.

An Abbe-Estlander flap is described in the case demonstrated. The patient in this case had a previous lip reconstruction of an undistinguished technique that resulted in a short and tight upper lip with disturbance of the oral commissure. Reconstruction was decided to be done by bringing "new lip tissue" from the lower lip by means of an Abbe-Estlander flap (Fig. 6.34a–d).

6.3.13 Skin Island Pedicle Flap (V-Y Advancement)

The perioral area can provide skin island subcutaneous pedicle flaps to resurface medium-sized skin defects of the lips. Given that the skin of the upper lip is affected more often than the skin of the lower lip by basal cell carcinomas, which most of the time does not need a full-thickness excision (the latter being affected more often to its red margin by squamous cell carcinomas), this flap finds its ideal position to the upper lip. Such a typical position of the skin island pedicle flap is the one presented.

The patient presented in Fig. 6.35a had a benign tumor located at the lateral subunit of the upper lip. An inferolaterally based island pedicle flap was chosen to reconstruct the defect. The length of the triangular flap was twice the length of the defect, and its upper side was positioned in the nasolabial crease (Fig. 6.35b, c). After adequate mobilization was gained, the flap was advanced and sutured in place leading to a satisfactory postoperative result (Fig. 6.35d, e).

6.3.14 Zisser Technique for Commissure Reconstruction

Zisser (1975) proposed a technique to remold the commissure after tumor excision. This technique is best suited for small defects up to 2 cm. A squamous cell carcinoma of the

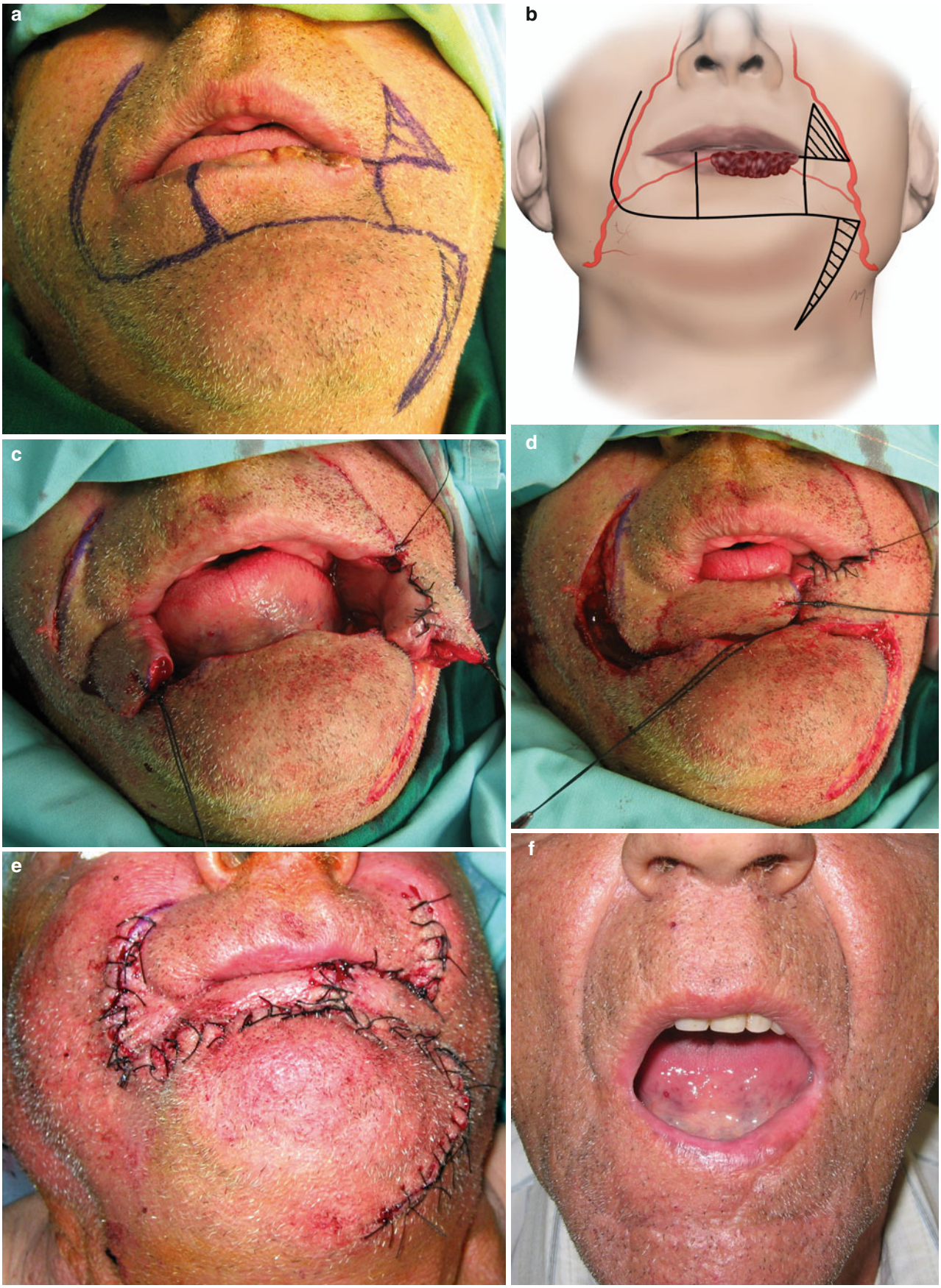

Fig. 6.28 (**a**, **b**) A unilateral Bernard-Webster flap in combination with a Karapandzic flap is outlined. (**c**) Flaps raised and new vermilion is formed. (**d**) The Karapandzic flap is rotated and Bernard-Webster flap advanced to the defect. (**e**) Immediate postoperative view. (**f**) Result at 4 months

oral commissure is presented in Fig. 6.36a, b. Tumor resection and commissure reconstruction is planned by the Zisser method (Fig. 6.36c, d).

According to the Zisser method, the tumor is excised in a crescent-shaped manner. From the upper and the lower periphery of the resection line, two Burow's triangles are drawn: the superior one parallel to the nasolabial crease and the inferior one parallel to the labiomandibular crease. A small triangle divided by a horizontal incision along the lip line is outlined at the lateral periphery into two smaller equal in length to the portion of the commissure to be resected. The philosophy of the technique is that the small peripheral triangle that represents the new commissure will be advanced to the new normal position.

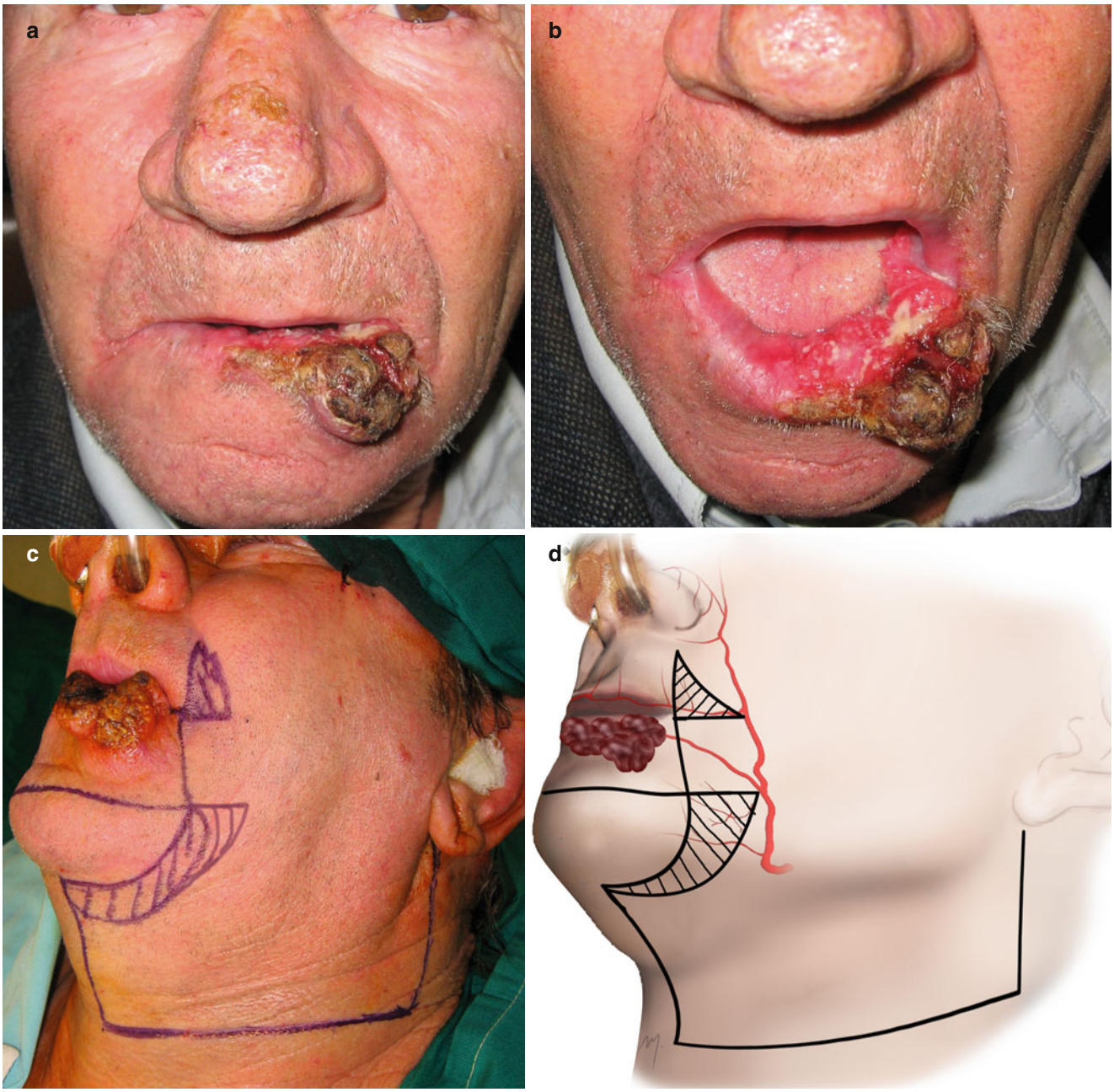

Fig. 6.29 (**a**, **b**) Extensive squamous cell carcinoma of the lower lip. (**c**, **d**) The Webster flap has been incorporated to the apron flap. (**e**) Tumor resection and supraomohyoid neck dissection completed. (**f**) Suturing completed. (**g**, **h**) Result at 6 months

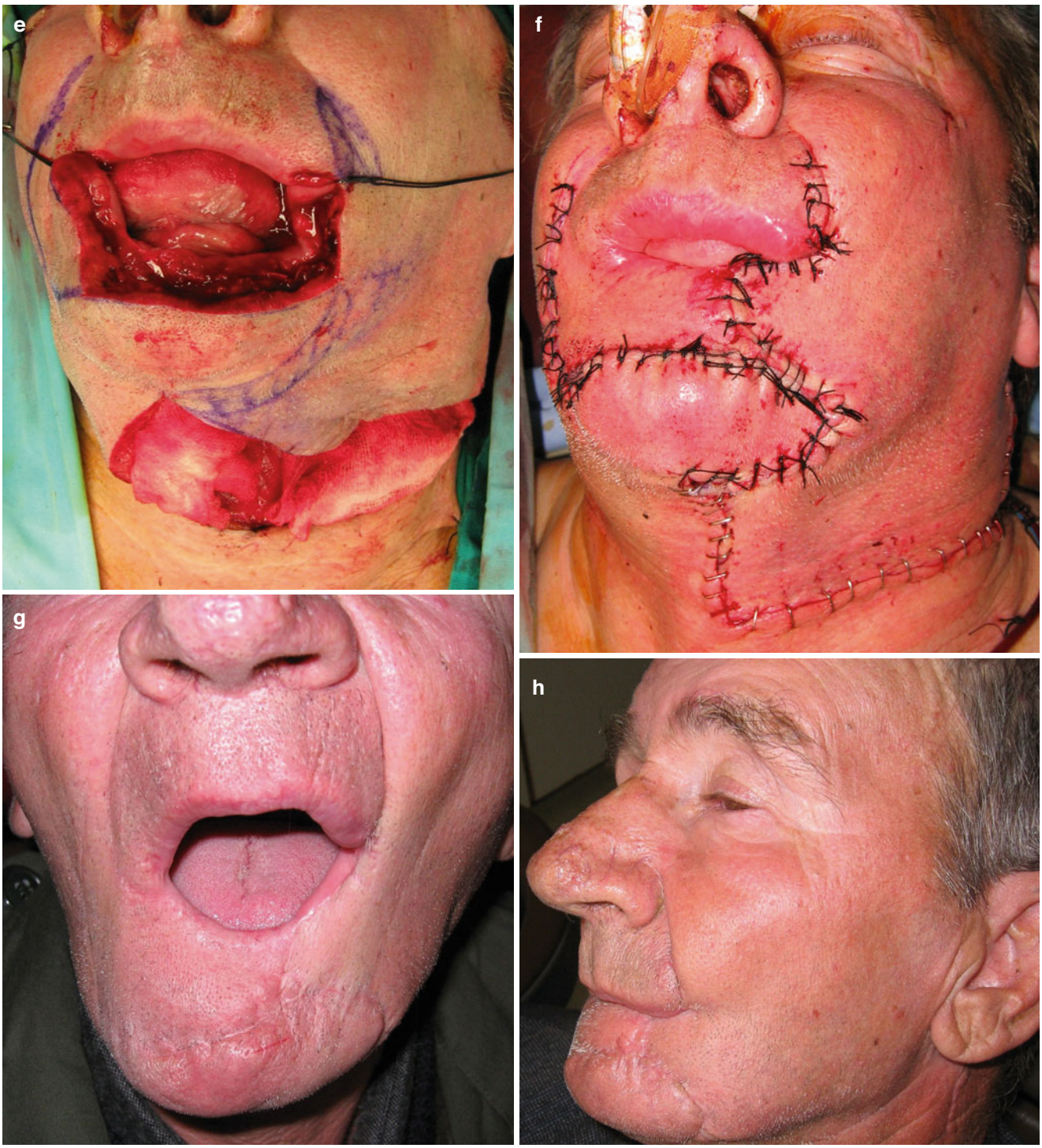

Fig. 6.29 (continued)

The tumor is resected in a crescent as was planned, and the Burow's triangles are excised removing only the skin and subcutaneous tissue (Fig. 6.36e, f). By suturing the excised Burow's triangles, the "new" commissure is advanced to its new position. The two small triangles are separated by a cutting through all layers at the horizontal

incision. Each of them is deepithelialized and covered by turning over the undermined buccal mucosa so as the red margin is reconstructed (Fig. 6.36g).

The reconstruction of commissure rarely leads to a perfect result, and secondary refinement procedures most often are needed (Fig. 6.36h).

6.3.15 Jackson Technique for Commissure Reconstruction

The Jackson technique uses two skin and mucosal rhomboid flaps to reconstruct the commissure (Jackson 1985).

According to the Jackson technique, the defect is excised in a rhomboid fashion. From the 120° angles of the defect, rhomboid flaps are outlined. The rhomboid flaps are raised consisting of skin or alternatively skin and mucosa. The 120° angles of the rhomboid flaps are approximated and sutured to form the commissure in the correct place. To achieve this, adjustment of the flaps is necessary by removing the appropriate portion of the distal part of the flaps. Raw areas of the reconstructed lips are resurfaced with mucosal advancement. The Jackson technique is demonstrated in the patient in Fig. 6.37a–g.

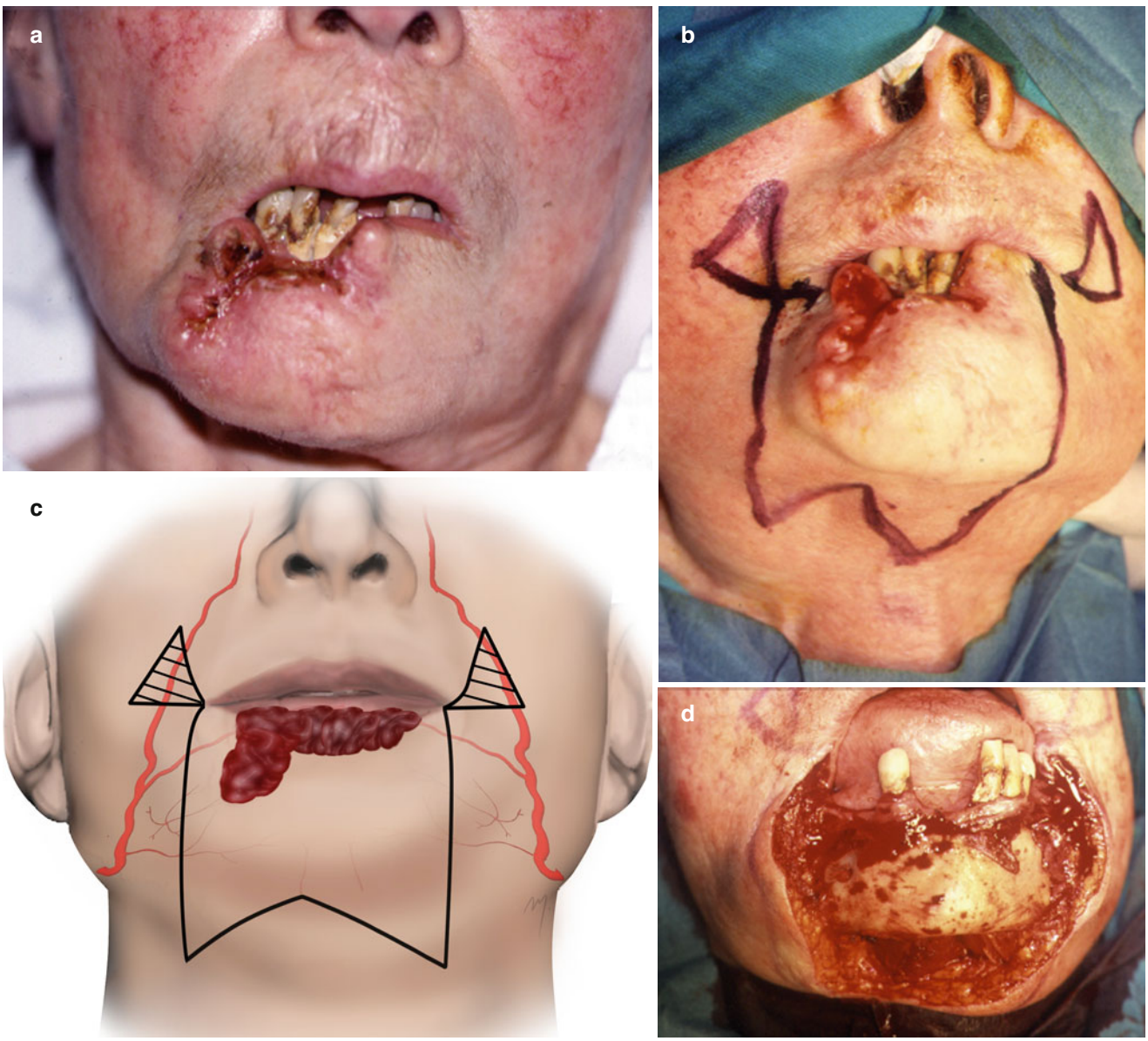

Fig. 6.30 (**a**) A squamous cell carcinoma of the lip and chin. (**b**, **c**) Based on the Bernard-Fries technique, the tumor is excised in the form of a W. (**d**) The tumor resected. (**e**) Vermilion reconstructed. (**f**) A horizontal incision extended to the neck reduced tension at closure. (**g**, **h**) The result leads to the expected tight lower lip and overhanging upper lip

Fig. 6.30 (continued)

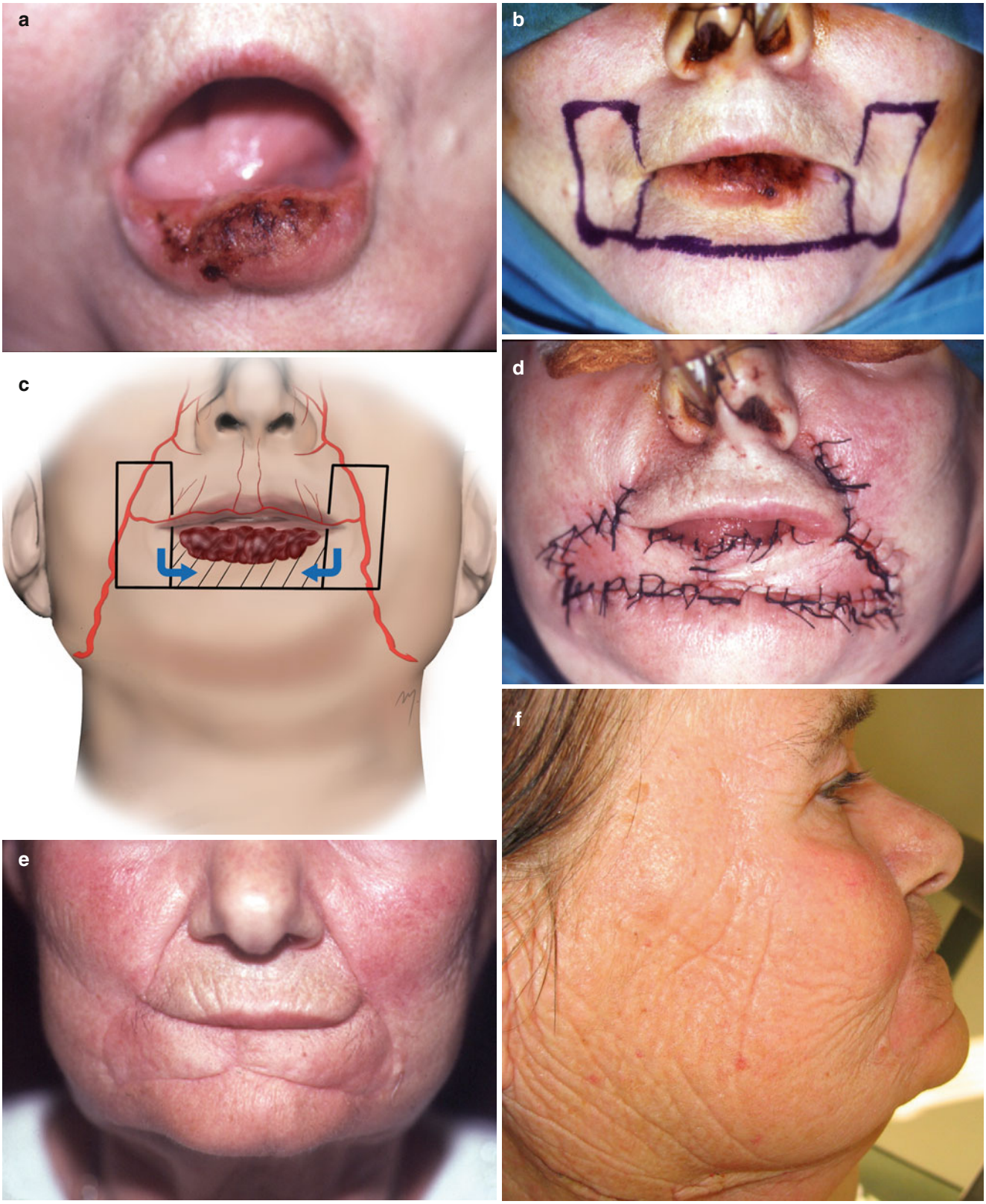

Fig. 6.31 (**a**) A squamous cell carcinoma involving the whole lower lip. (**b**, **c**) Bilateral McGregor's fan flaps outlined. The flaps are pedicled on the superior labial vessels. (**d**) The flaps rotated and sutured into position. The vermilion was reconstructed with a tongue flap. (**e**, **f**) Result at 4 months after operation (With kind permission from Dr. Ioannis Tsamis)

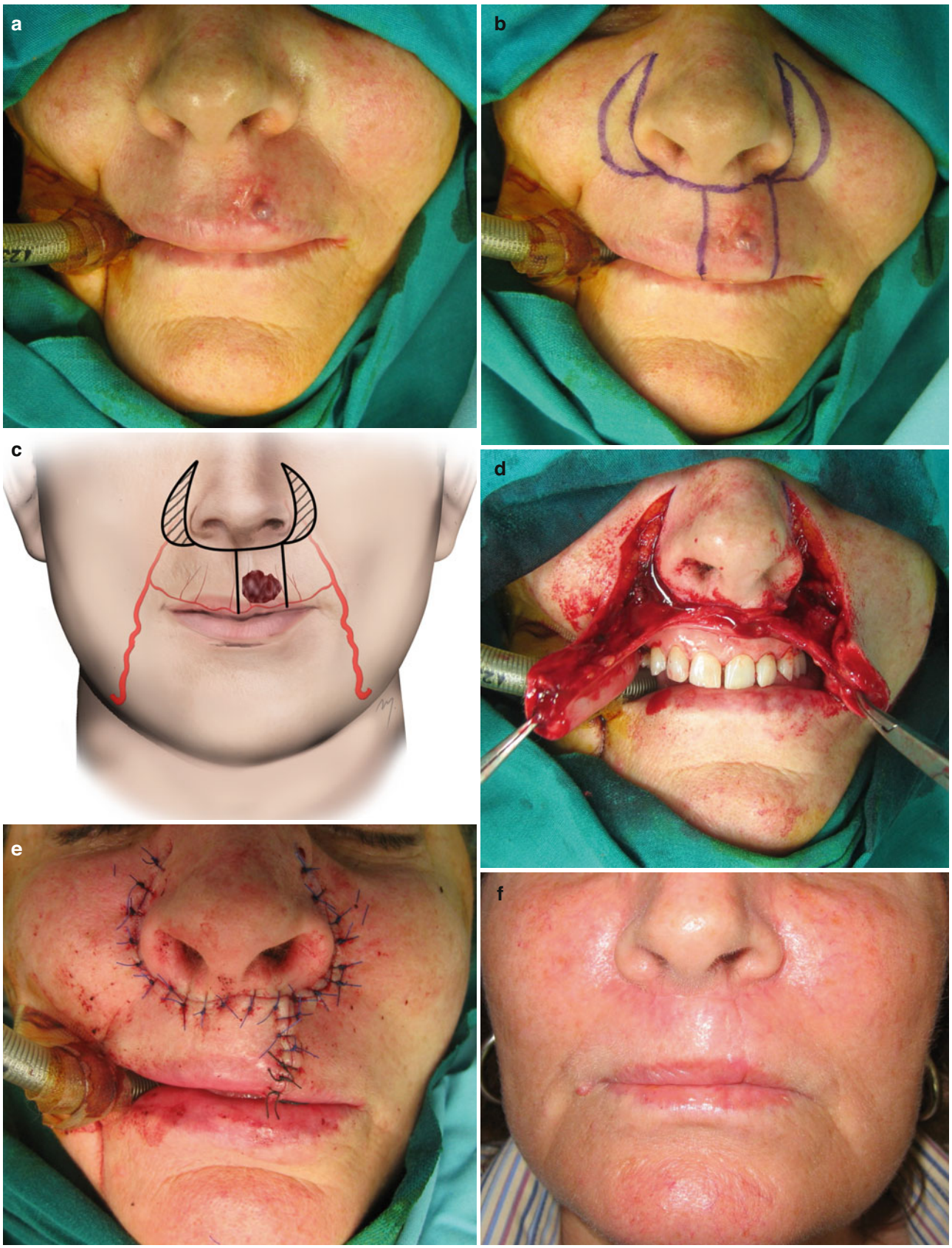

Fig. 6.32 (**a**) Lesion of the upper lip. (**b**, **c**) The plan of excision and reconstruction is outlined. (**d**) Bilateral upper lip advancement flaps are mobilized. (**e**) Final suturing. (**f**) Postoperative appearance 3 months later

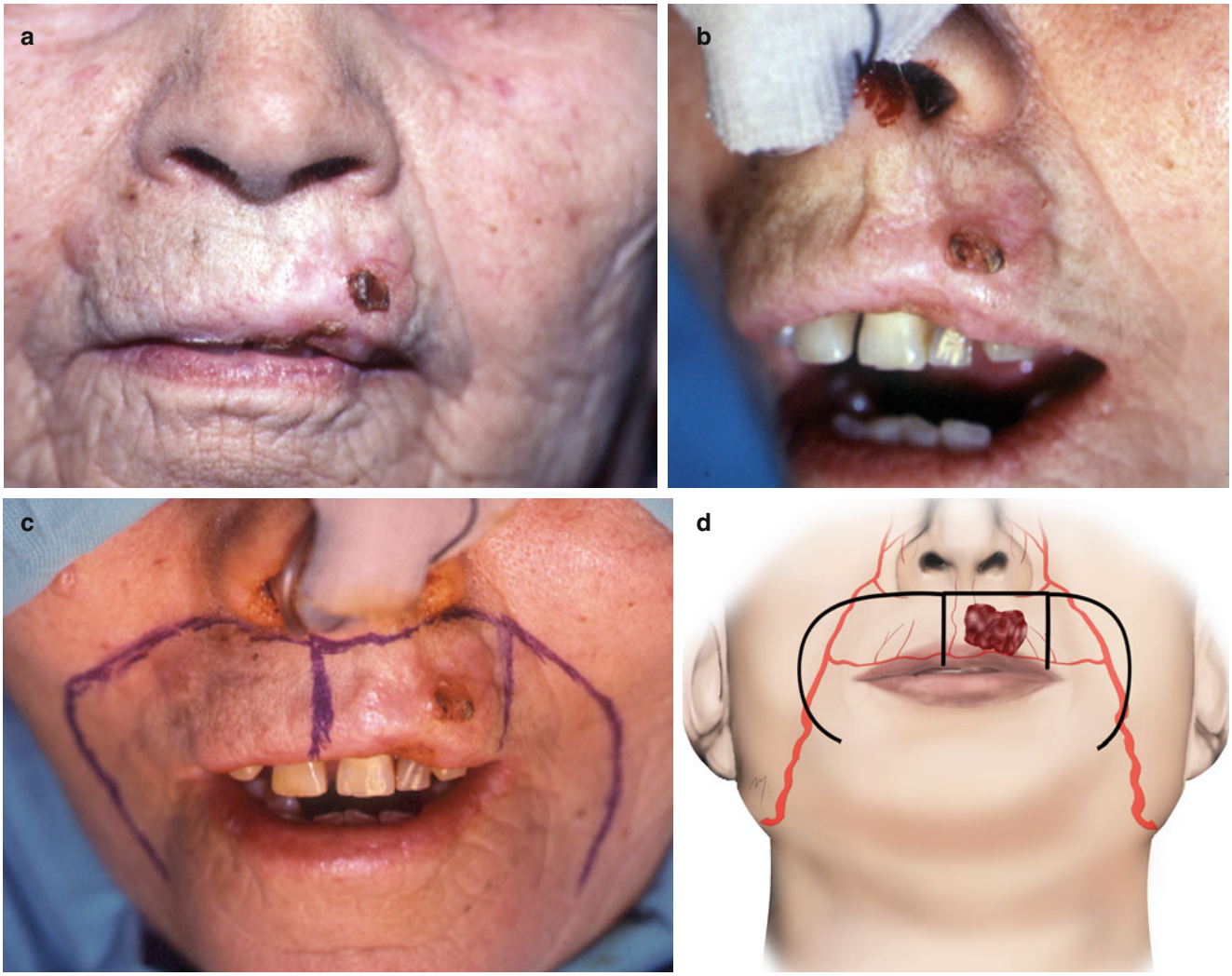

Fig. 6.33 (**a**, **b**) Squamous cell carcinoma of the lateral aspect of the upper lip spreading to the philtrum. (**c**, **d**) Reverse Karapandzic flap is outlined. (**e**) Almost the entire lateral subunit and the philtrum of the upper lip have been excised. (**f**) Flaps reach the defect with fluent. (**g**) Final suturing. (**h**) Result at 6 months

Fig. 6.33 (continued)

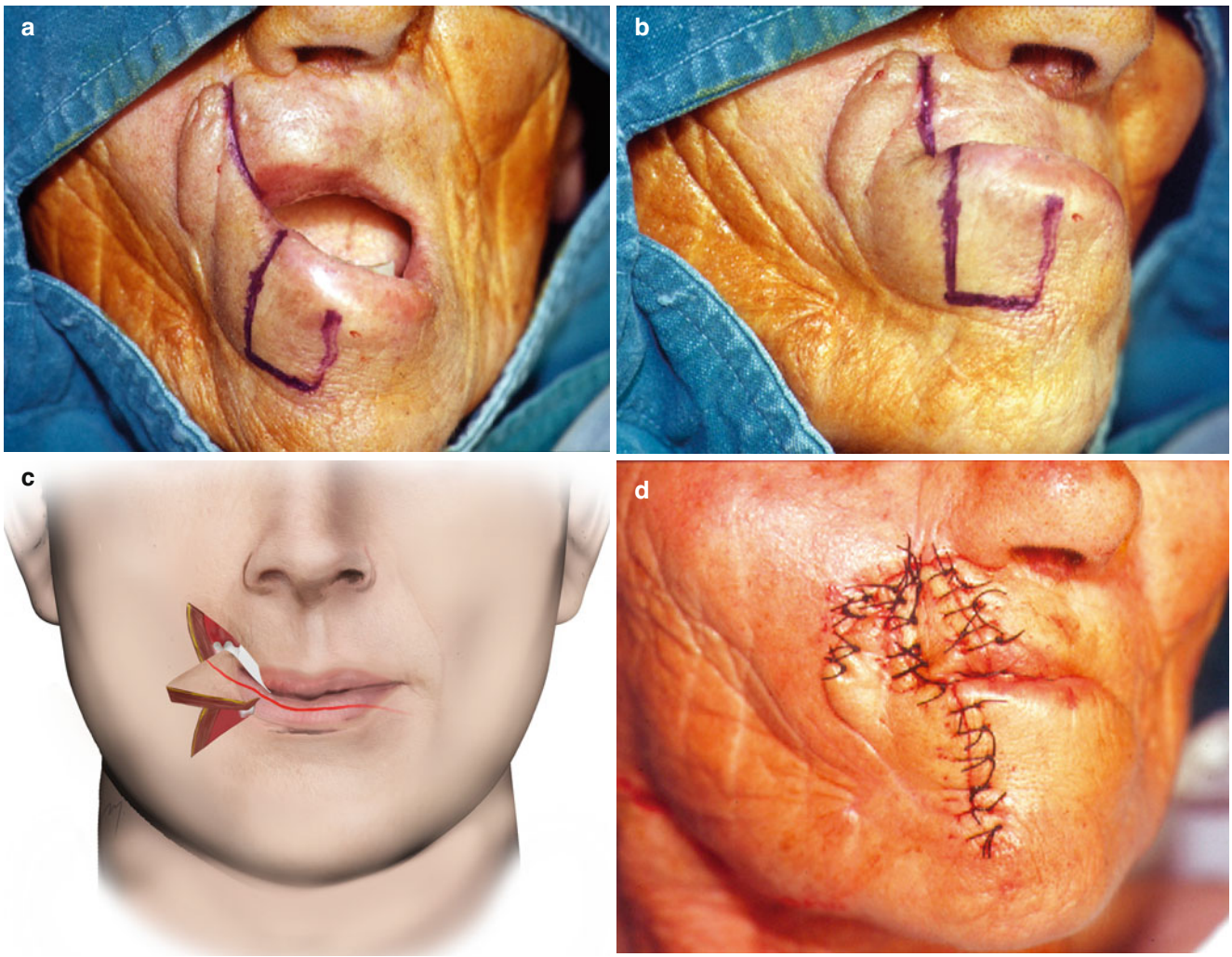

Fig. 6.34 (**a**–**d**) Abbe-Estlander flap (With kind permission from Dr. Ioannis Tsamis)

Fig. 6.35 (**a**) A benign tumor located at the upper lip. (**b**, **c**) Subcutaneous island pedicle flap is outlined. (**d**) Immediate postoperative view. (**e**) Result at 4 months

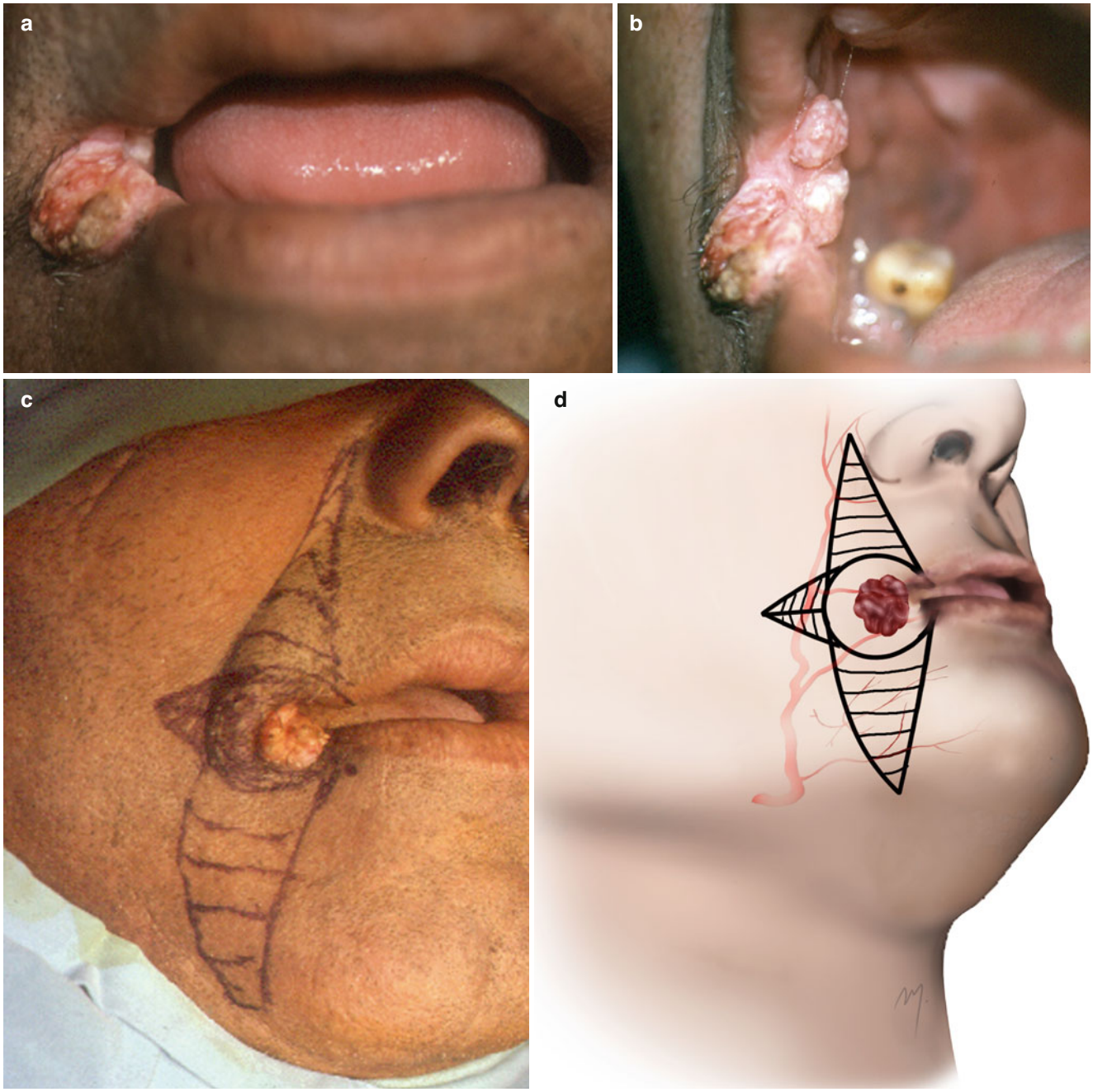

Fig. 6.36 (**a**, **b**) A squamous cell carcinoma located at the commissure (**c**, **d**) Area of excision and flaps outlined. (**e**) Defect after tumor removal. (**f**) Burow's triangles are excised. (**g**) New commissure is formed. (**h**) Result at secondary refinement

Fig. 6.36 (continued)

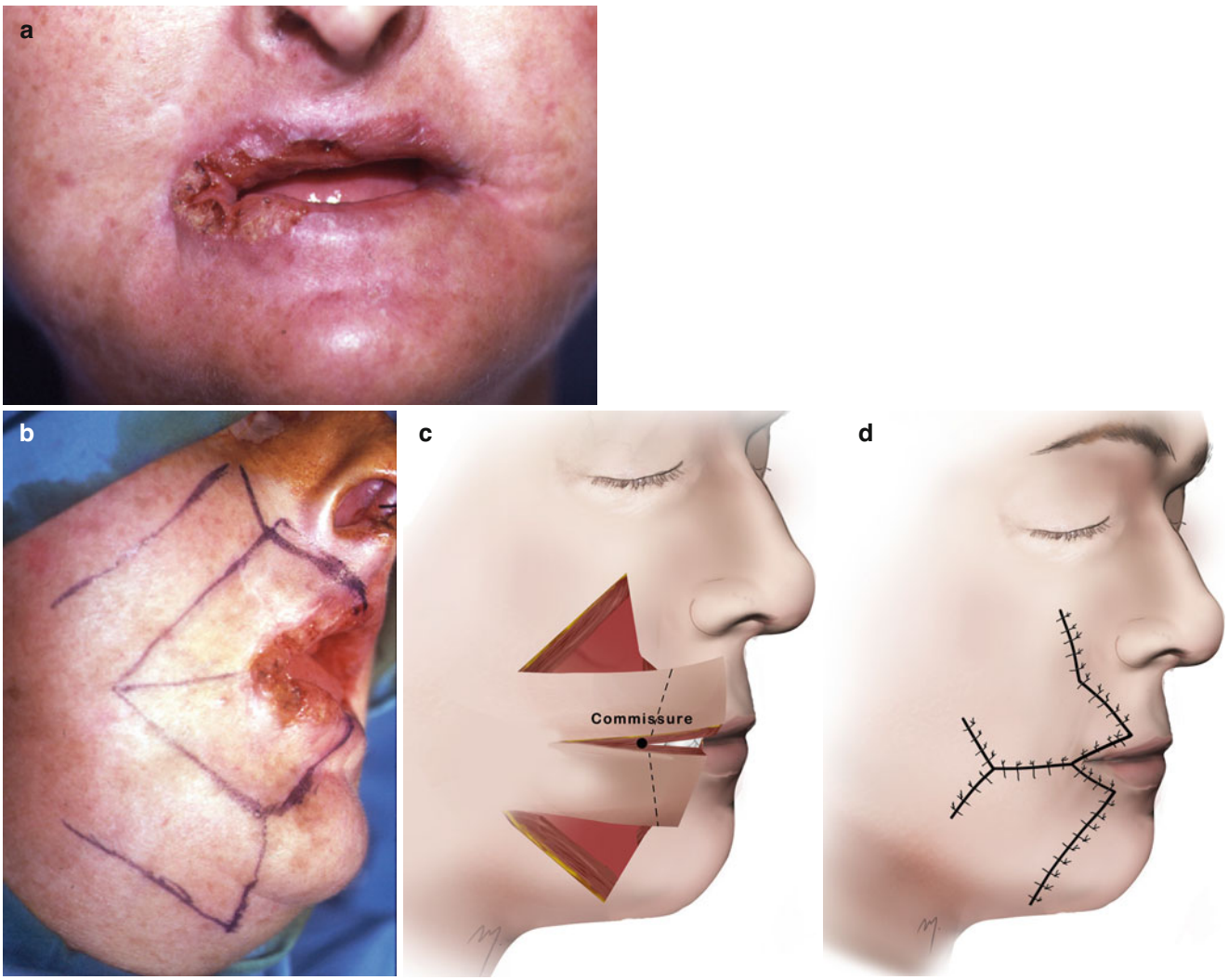

Fig. 6.37 Jackson technique for commissure reconstruction. (**a**) Squamous cell carcinoma of the commissure. (**b**) Flaps according to the Jackson method are outlined. (**c**) Adjustment of the flaps and "new" commissure placed in position. (**d**) Final suturing. (**e**–**g**) Result at 4 months (With kind permission from Dr. Ioannis Tsamis)

Fig. 6.37 (continued)

References

Al-Hoqail RA, Abdel Meguid EM (2009) An anatomical and analytical study of the modiolus: enlightening its relevance to plastic surgery. Aesthetic Plast Surg 33(2):147–152

Al-Hoqail RA, Meguid EM (2008) Anatomic dissection of the arterial supply of the lips: an anatomical and analytical approach. J Craniofac Surg 19(3):785–794

Bernard C (1852) Cancer de la levre inferieure: restauratio a l'aide de lembeaux quadrilataires-lateraux querison. Scalpel 5:162–164

Briedis J, Jackson IT (1980) The anatomy of the philtrum: observations made on dissections in the normal lip. Br J Plast Surg 34(2):128–132

Carty JM, Pribaz JJ (2010) Lip and cheek reconstruction. In: Siemionow MZ, Eisenmann-Klein M (eds) Plastic and reconstructive surgery. Springer, Heidelberg/London/New York

Crouzet C, Fournier H, Papon X, Hentati N, Cronier P, Mercier P (1998) Anatomy of the arterial vascularization of the lips. Surg Radiol Anat 20(4):273–278

Demiryurek D, Bayramoglu A, Erbil KM, Onderoglu S, Sargon MF, Aldur MM, Korkusuz P, Nazikoglu A (2003) Three-dimensional structure of the modiolus. A computerized reconstruction study. Saudi Med J 24(8):846–849

Edizer M, Mağden O, Tayfur V, Kiray A, Ergür I, Atabey A (2003) Arterial anatomy of the lower lip: a cadaveric study. Plast Reconstr Surg 111(7):2176–2181

Fries R (1973) Advantages of a basic concept in lip reconstruction after tumour resection. J Maxillofac Surg 1(1):13–18

Garcia de Mitchell CA, Pessa JE, Schaverien MV, Rohrich RJ (2008) The philtrum: anatomical observations from a new perspective. Plast Reconstr Surg 122(6):1756–1760

Gillies HM (1957) Principles and art of plastic surgery. Little Brown, Boston

Goldstein MH (1984) A tissue-expanding vermilion myocutaneous flap for lip repair. Plast Reconstr Surg 73(5):768–770

Greenstein G, Tarnow D (2006) The mental foramen and nerve: clinical and anatomical factors related to dental implant placement: a literature review. J Periodontol 77(12):1933–1943

Hur MS, Hu KS, Kwak HH, Lee KS, Kim HJ (2011) Inferior bundle (fourth band) of the buccinator and the incisivus labii inferioris muscle. J Craniofac Surg 22(1):289–292

Hwang K, Kim DJ, Hwang SH (2007a) Immunohistochemical study of differences between the muscle fiber types in the pars peripheralis and marginalis. J Craniofac Surg 18(3): 591–593

Hwang K, Kim DJ, Hwang SH (2007b) Musculature of the pars marginalis of the upper orbicularis oris muscle. J Craniofac Surg 18(1):151–154

Jackson JT (1985) Local flaps in head and neck reconstruction, 1st edn. Mosby, St Louis

Karapandzic M (1974) Reconstruction of lip defects by local arterial flaps. Br J Plast Surg 27(1):93–97

Kawai K, Imanishi N, Nakajima H, Aiso S, Kakibuchi M, Hosokawa K (2004) Arterial anatomy of the lower lip. Scand J Plast Reconstr Surg Hand Surg 38(3):135–139

Latham RA, Deaton TG (1976) The structural basis of the philtrum and the contour of the vermilion border: a study of the musculature of the upper lip. J Anat 121(1):151–160

Lentrodt J (1975) Contribution to the reconstruction of the lower lip after tumor resection combined with neck dissection. J Maxillofac Surg 3(3):139–145

Lentrodt J, Luhr HG (1971) Reconstruction of the lower lip after tumor resection combined with radical neck dissection. Plast Reconstr Surg 48(6):579–583

Lightoller GH (1925) Facial muscles: the modiolus and muscles surrounding the rima oris with some remarks about the panniculus adiposus. J Anat 60(1):1–85

Loukas M, Hullett J, Louis RG Jr, Kapos T, Knight J, Nagy R, Marycz D (2006) A detailed observation of variations of the facial artery, with emphasis on the superior labial artery. Surg Radiol Anat 28(3):316–324

Magden O, Edizer M, Atabey A, Tayfur V, Ergür I (2004) Cadaveric study of the arterial anatomy of the upper lip. Plast Reconstr Surg 114(2):355–359

McGregor IA (1983) Reconstruction of the lower lip. Br J Plast Surg 36(1):40–47

Mooney MP, Siegel MI, Kimes KR, Todhunter J (1988) Development of the orbicularis oris muscle in normal and cleft lip and palate human fetuses using three-dimensional computer reconstruction. Plast Reconstr Surg 81(3):336–345

Mulliken JB, Pensler JM, Kozakewich HP (1993) The anatomy of Cupid's bow in normal and cleft lip. Plast Reconstr Surg 92(3):395–403

Nairn RI (1975) The circumoral musculature: structure and function. Br Dent J 138(2):49–56

Nakajima H, Imanishi N, Aiso S (2002) Facial artery in the upper lip and nose: anatomy and a clinical application. Plast Reconstr Surg 109(3):855–861

Namnoum JD, Hisley KC, Graepel S, Hutchins GN, Vander Kolk CA (1997) Three-dimensional reconstruction of the human fetal philtrum. Ann Plast Surg 38(3):202–208

Park C, Lineaweaver WC, Buncke HJ (1994) New perioral arterial flaps: anatomic study and clinical application. Plast Reconstr Surg 94(2):268–276

Pélissier P, Pistre V, Bustamante K, Martin D, Baudet J (2000) The modiolus. Comparative anatomy, embryological and physiological review, surgical importance. Ann Chir Plast Esthet 45(1): 41–47

Pinar YA, Bilge O, Govsa F (2005) Anatomic study of the blood supply of perioral region. Clin Anat 18(5):330–339

Rogers CR, Mooney MP, Smith TD, Weinberg SM, Waller BM, Parr LA, Docherty BA, Bonar CJ, Reinholt LE, Deleyiannis FW, Siegel MI, Marazita ML, Burrows AM (2009) Comparative microanatomy of the orbicularis oris muscle between chimpanzees and humans: evolutionary divergence of lip function. J Anat 214(1):36–44

Rohrich RJ, Pessa JE (2009) The anatomy and clinical implications of perioral submuscular fat. Plast Reconstr Surg 124(1):266–271

Santini A, Alayan I (2012) A comparative anthropometric study of the position of the mental foramen in three populations. Br Dent J 212(4):E7

Schulte DL, Sherris DA, Kasperbauer JL (2001) The anatomical basis of the Abbé flap. Laryngoscope 111(3):382–386

Standring S (2008) Gray's anatomy. The anatomical basis of clinical practice, 40th edn. Churchill Livingstone-Elsevier, Edinburgh

Webster RC, Coffey RJ, Kelleher RE (1960) Total and partial reconstruction of the lower lip with innervated muscle-bearing flaps. Plast Reconstr Surg Transplant Bull 25:360–371

Williams PL, Warwick R (1980) Gray's anatomy, 36th edn. Churchill Livingstone, Edinburgh

Zisser G (1975) A contribution to the primary reconstruction of the upper lip and labial commissure following tumour excision. J Maxillofac Surg 3(4):211–217

Zufferey JA (2002) Importance of the modiolus in plastic surgery. Plast Reconstr Surg 110(1):331–334

Auricle

7

The auricle (pinna) together with the external acoustic meatus constitutes the external ear. It is a morphologically unique, highly variable in size and shape structure and a predominant feature of the face.

7.1 Anatomy of the Auricle

The auricle consisted of an elaborate cartilaginous skeletal structure that is covered by a cutaneous investor, which conforms to its shape.

The convex and concave elements of the cartilaginous framework are responsible for the configuration of the auricle and correspond to the landmarks of the auricle (Fig. 7.1).

7.1.1 Skin and Subcutaneous Tissue

The skin that covers the auricle is very thin with minimal subcutaneous tissue. It attaches to the underlying cartilage and exhibits surgically important differences between the lateral and cranial (medial) surfaces of the auricle. The skin of the lateral surface firmly adheres to the perichondrium with reduced mobility, and the subcutaneous tissue is scant (Fig. 7.2). The attachment of the skin to the cartilage increases as it passes across the concha to continue into the external auditory meatus.

At the cranial surface of the auricle, the skin is thicker and less adherent to the perichondrium, with greater mobility, and more subcutaneous tissue is present (Fig. 7.3). The lobule contains no cartilaginous structure and consisted solely of skin and subcutaneous fatty tissue.

7.1.2 Muscles

The musculature of the external ear includes extrinsic and intrinsic muscles. The extrinsic muscles are three very thin fans of muscle fibers that form the auricularis anterior, auricularis superior, and auricularis posterior muscles (Fig. 7.4). They are encompassed by the temporoparietal fascia and connect the auricle to the scalp and the skull (see Chap. 2). The anterior and posterior ligaments reinforce the attachment of the external ear to the skull.

The intrinsic muscle group includes the helicis major, helicis minor, tragicus, antitragicus, transversus auriculae, and obliquus auricular muscles. These muscles are highly variable and often underdeveloped. Seldomly, they can be seen grossly as very thin and scattered muscle fibers. All of these muscles are innervated by the temporal and the posterior auricular branches of the facial nerve.

7.1.3 Vascular Anatomy

The arterial supply of the auricle is provided by a rich anastomotic network that is formed by branches of the posterior auricular and the superficial temporal arteries (Fig. 7.5). The posterior auricular artery has been found to be the dominant blood supply for the auricle (Park et al. 1992; Imanishi et al. 1997; Pinar et al. 2003).

The superficial temporal artery gives rise to three small branches that travel to the anterior part of the lateral auricular surface. These branches are the superior, middle, and inferior auricular arteries and are distributed to the anterior and lateral aspects of the auricle. The superior auricular artery enters the helical root and continues along the margin of helix ("helical artery") and communicates with the posterior auricular artery forming an arterial arcade ("helical arcade") (Song et al. 1996; Moschella et al. 2003; Erdmann et al. 2009).

The posterior auricular artery after branching from the external carotid artery ascends and divides into the occipital and auricular branches. The auricular branch courses along the retroauricular sulcus passing beneath the posterior auricular muscle and gives off three branches to the cranial surface of the auricle. These branches further

V.K. Thomaidis, *Cutaneous Flaps in Head and Neck Reconstruction*,
DOI 10.1007/978-3-642-41254-7_7, © Springer-Verlag Berlin Heidelberg 2014

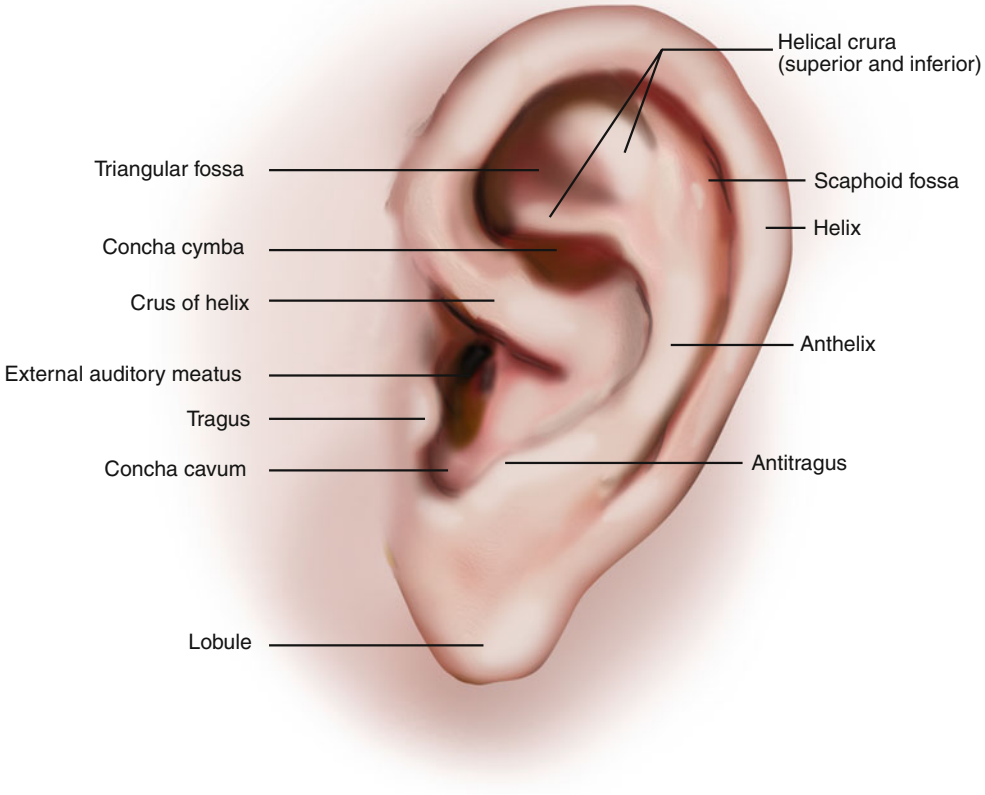

Fig. 7.1 Topographic landmarks of lateral surface of auricle

subdivide giving off twigs that run to the free margin of the helical rim and pass round it to the lateral surface and others that penetrate the cartilage reaching also the lateral surface. Through these perforators the posterior auricular artery participates in a great degree in the vascularization of the lateral surface of the auricle. Park et al. (1992) found out that major perforators of the posterior auricular artery appear at the anteroauricular surface at the triangular fossa, the cymba cocha, the helical root, the cavum cocha, and the earlobe.

Venous drainage of the auricle accompanies the arterial supply. The posterior auricular veins drain into the external jugular vein, while the anterior auricular veins drain into the superficial temporal and posterior facial veins.

7.1.4 Sensory Innervation

The auricle is innervated from the great auricular nerve, the lesser occipital nerve, and the auriculotemporal nerve (Fig. 7.6).

The great auricular nerve (C2, C3) after emerging from Erb's point ascends toward the lobule and at a level approximately to the lower pole of the parotis divides into an anterior and a posterior part (see Chap. 8). The posterior branch travels behind the ear lobule and innervates the postauricular skin and most of the helix, antihelix, and lobule.

The lesser occipital nerve (C2, C3) also emerges at Erb's point and ascends along the posterior margin of the sternocleidomastoid muscle (see Chap. 8). At the postauricular region, it gives off branches that supply the skin of the superior and medial posterior auricle and helix.

The auriculotemporal nerve (from the mandibular division of the trigeminal nerve), after it exits to the cheek, ascends in front of the auricle together with the superficial temporal artery and vein (see Chap. 5). It gives off branches to the external acoustic meatus and the anterior portion of the auricle (tragus, crus of the helix, and the anterior part of the helix).

Small areas on both aspects of the auricle and the concha probably are innervated by the facial nerve and the auricular branch of the vagus nerve (Standring 2008).

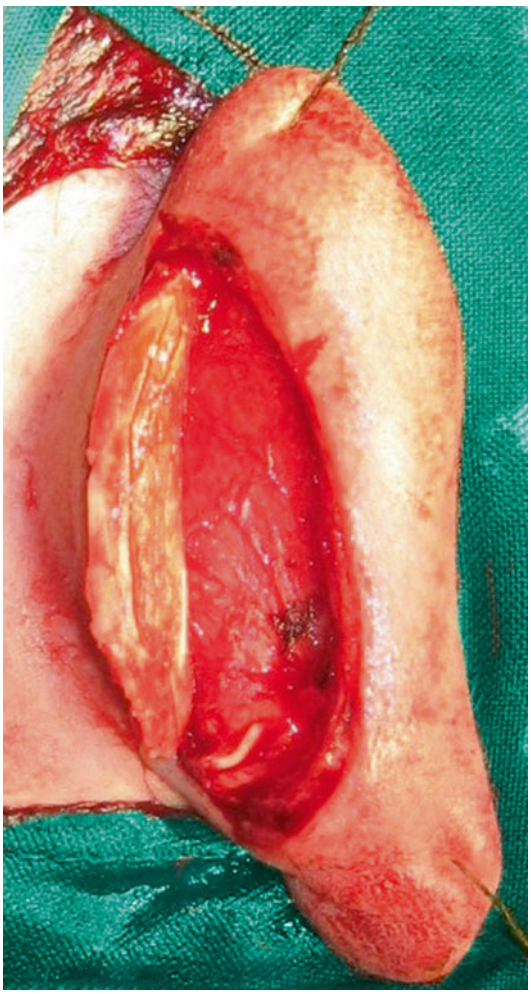

Fig. 7.2 The skin of the lateral surface of the auricle is almost devoid of subcutaneous tissue

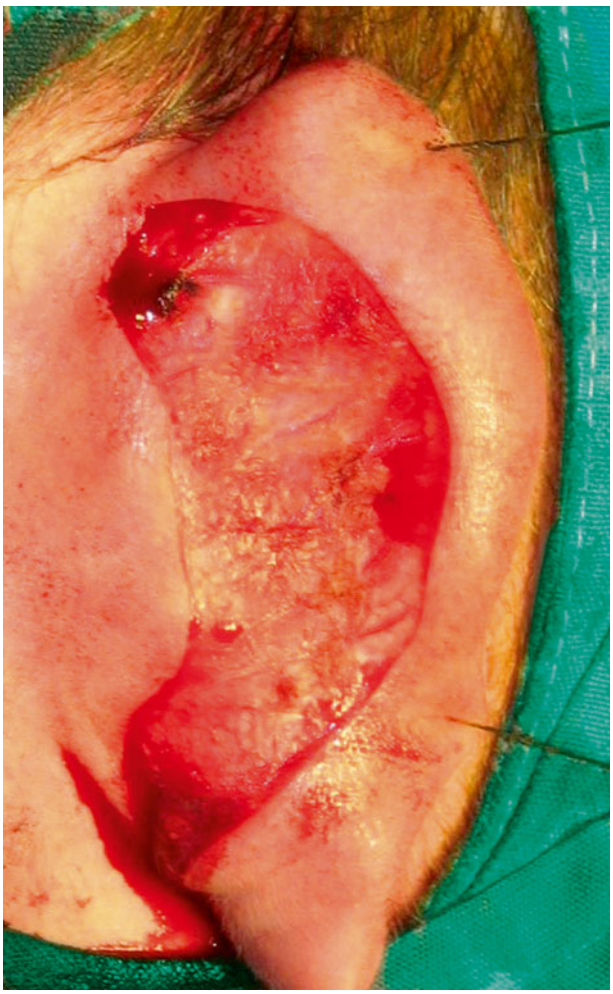

Fig. 7.3 At the medial surface of the auricle, the skin is thicker and more subcutaneous tissue is present

7.2 Flaps Derived from the Auricle

Only a few simply designed flaps can be derived from the auricle, and these are provided to reconstruct small defects of the auricle itself.

7.2.1 Auricular Skin Flaps

The auricular skin can provide under certain circumstances small flaps, based on the general flap principles, to reconstruct small defects of the auricle. The most useful one is the rotation auricular skin flap. Bilobed flaps derived from the posterior auricular surface have been also described (Vergilis-Kalner and Goldberg 2010).

A small auricular rotation skin flap is presented in the following case. The patient had a pyogenic granuloma at the skin of the external surface of the auricle (Fig. 7.7a). The excision of the lesion resulted in a small skin defect (Fig. 7.7b). Given that the skin of the auricle, especially in its lateral surface, is firmly adherent to the perichondrium with almost no mobility; even for a small defect, a flap is needed for reconstruction. In this case the only rotation flap that can be used is the one that is based inferomedially (Fig. 7.7c–e).

7.2.2 Chondrocutaneous Helical Rim Advancement Flap

The method of advancing the helical rim as a chondrocutaneous flap was first described by Antia and Buch (1967) as a single-stage method to close helical rim defects. In its initial design, the helix is freed from the antihelix by an incision in the helical sulcus through the anterior skin and cartilage. The

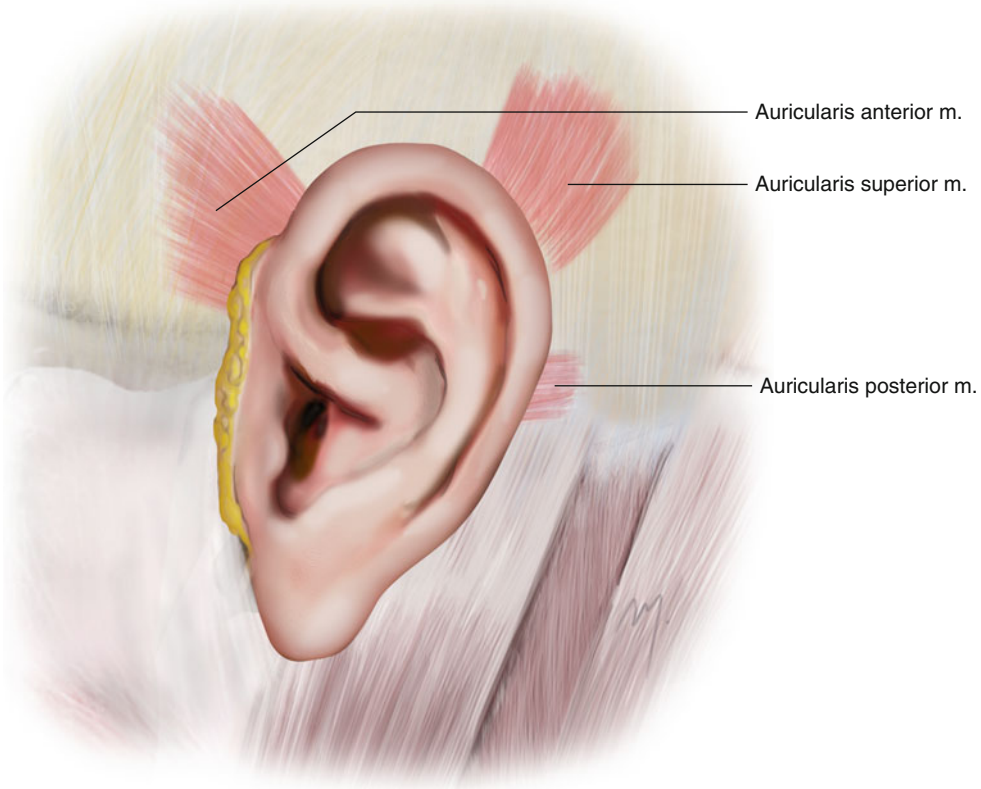

Fig. 7.4 Extrinsic auricular muscles

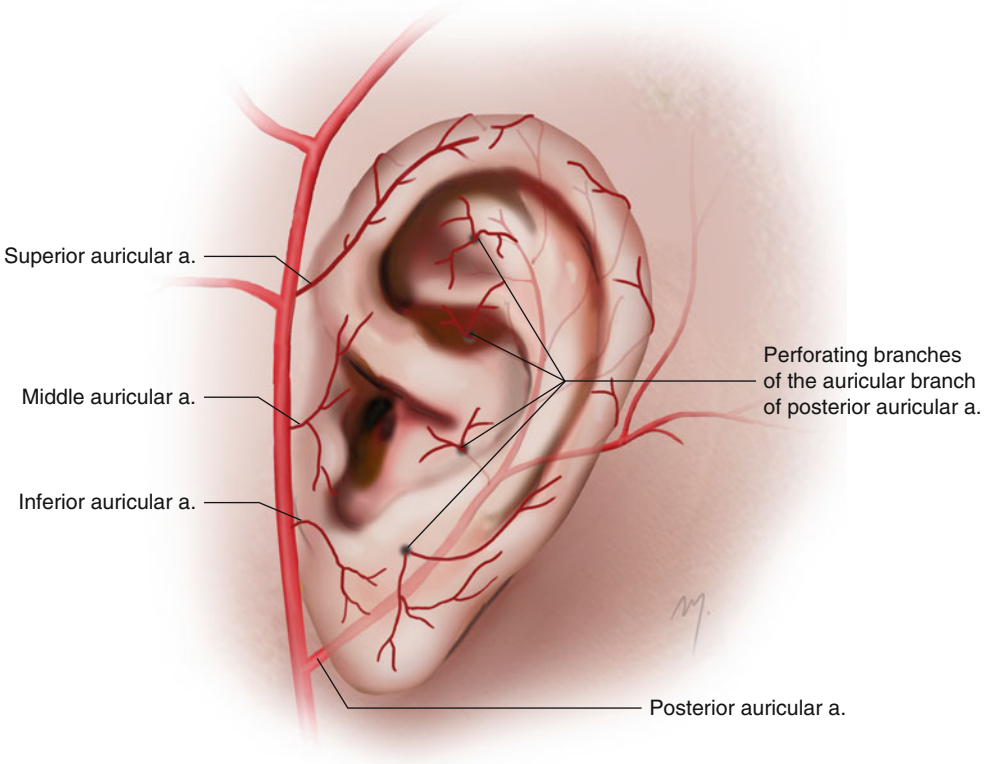

Fig. 7.5 Arterial vascularization of the auricle

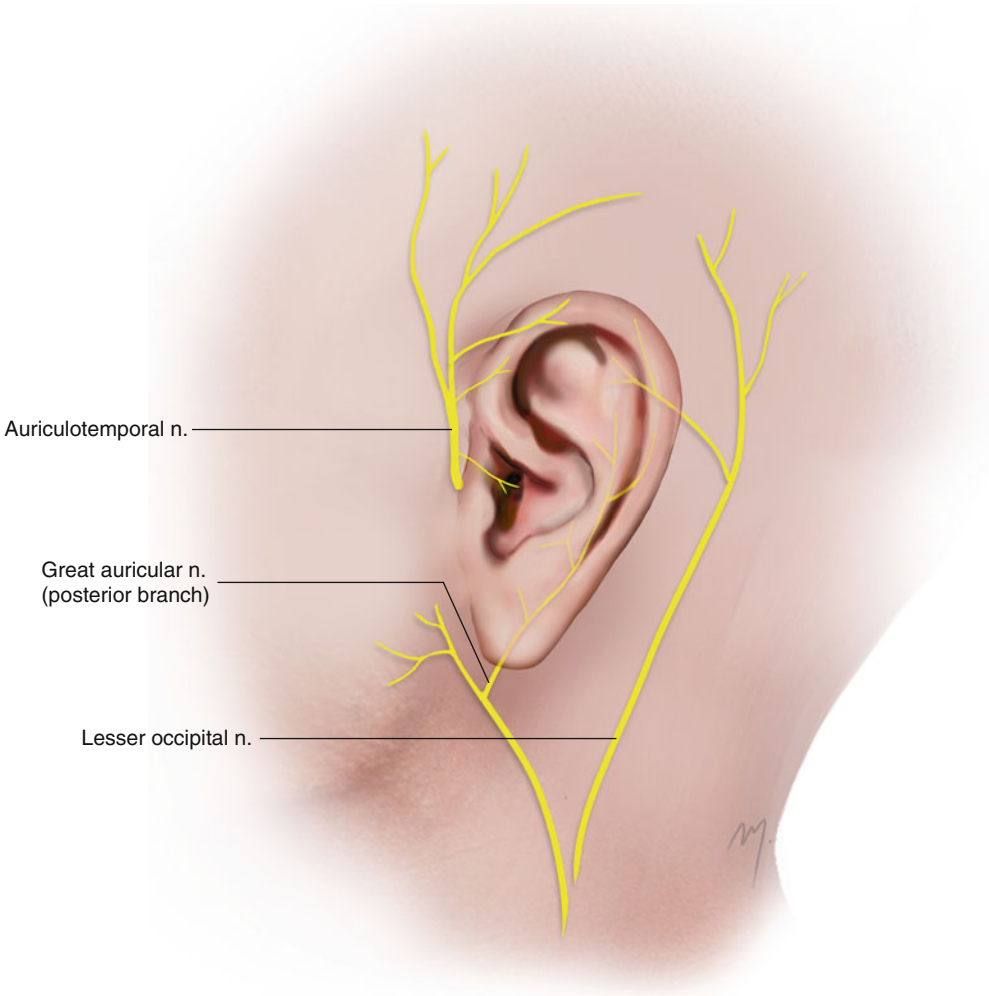

Fig. 7.6 Sensory innervation of the auricle

flap is then advanced to the rim defect, maintaining its continuity with the posterior skin. As the posterior skin is left intact, the flap is mainly and widely pedicled on the posterior skin.

Given that almost 70 % of the auricle defects are located at the rim, the chondrocutaneous helical rim advancement flap is a widely used flap both with its original design and with various modifications (Majumdar and Townend 2000; Butler 2003; Krunic et al. 2006; Skaria 2008; Medeiros et al. 2009). Jackson (1985) has simplified the original design by freeing the helix completely from the antihelix performing the helix rim incision through the full thickness of the pinna as a through and through incision. This places the flap based solely on its attachment at the ear lobule. Such a case is presented in the following.

The patient in Fig. 7.8a exhibits a basal cell carcinoma of the helical rim located at the transition from the mid to the upper third. Excision lines and a chondrocutaneous helical rim advancement flap, based on the artery of the lobe, were outlined (Fig. 7.8b, c). Even though the helix is completely freed from the antihelix, setting the flap on a narrow pedicle seems risky despite that the flap is reliable. It is perfused through the earlobe arterial network that is formed from the inferior auricular branch of the superficial temporal artery and the lobular perforator of the posterior auricular artery. It cannot be considered an axial flap so it must not be very long. If this flap is designed very long to reach defects of the upper helical third, distal necrosis may occur.

The lesion was excised in rectangular shape, in safe margins, including skin and cartilage (Fig. 7.8d). A full-thickness incision, through the anterior skin, cartilage, and postauricular skin, was made along the anterior helical sulcus. The flap was raised including all the cartilage and skin thickness of the helix (Fig. 7.8e).

The flap was prepared up to the level of antitragus, and a small Burow's triangle was excised at its base (Fig. 7.8f).

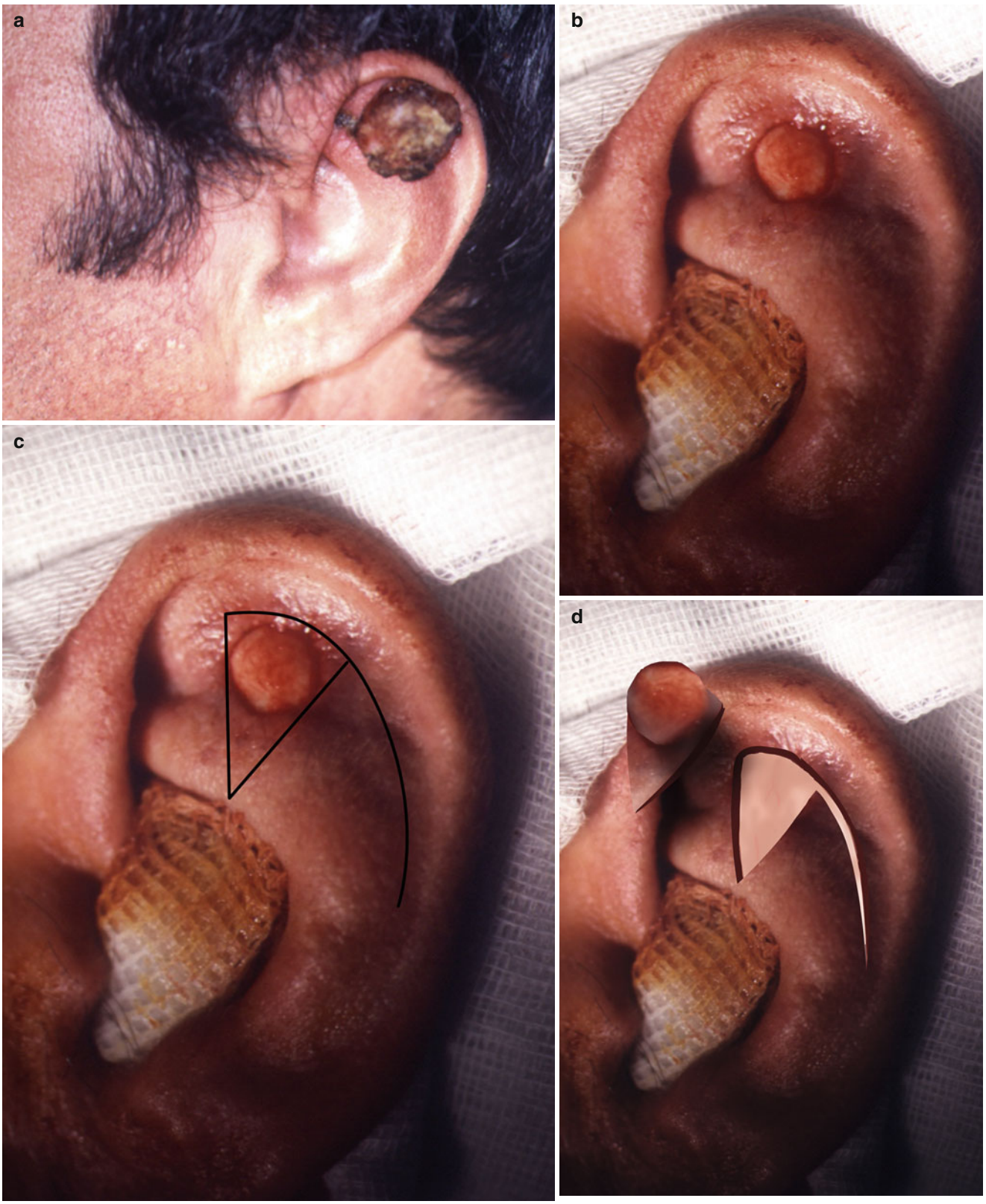

Fig. 7.7 (**a**–**e**) Auricular rotation skin flap

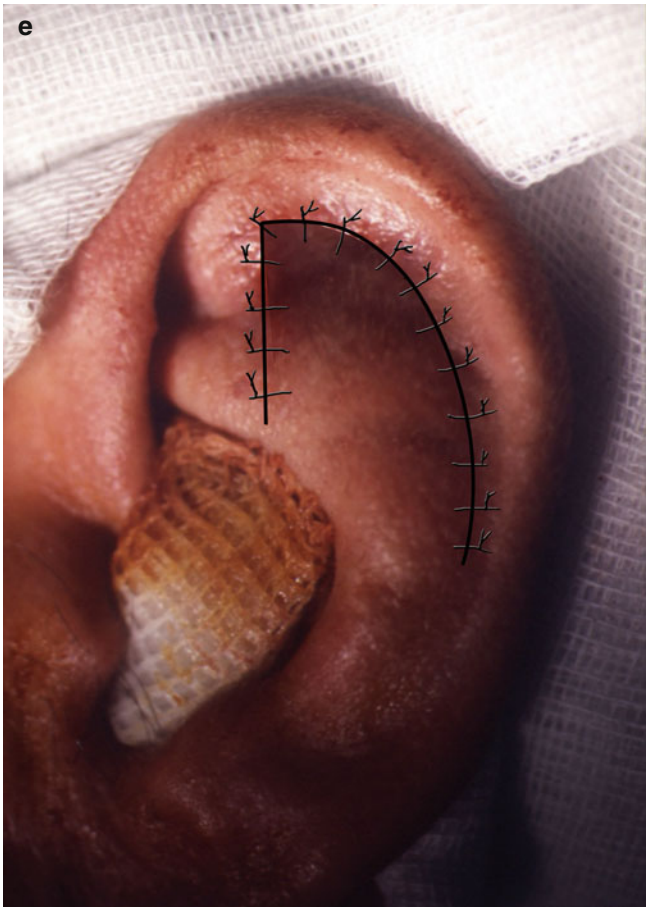

Fig. 7.7 (continued)

The flap was advanced to the recipient site without tension (Fig. 7.8g). The cartilage and skin of both the anterior and posterior surfaces of the auricle were sutured (Fig. 7.8h, i). The flap healed well without any sign of tip necrosis and reconstructed fully the helix (Fig. 7.8j, k).

7.2.3 Postauricular Subcutaneous Pedicle Island Flap

Postauricular skin can be transferred to the anterior auricle as an island subcutaneous pedicle flap. The skin is derived partly from the back of the auricle and partly from posterior to the sulcus. The skin is fully detached except the zone at the cephalic-auricular sulcus where it remains attached to the subcutaneous tissue, which becomes its pedicle. The skin island is turned around, as the subcutaneous pedicle becomes its hinge resembling a "revolving door" and is brought to the defect. The donor site is closed primarily.

Although it is much easier to transfer skin by this flap to the concha resurfacing conchal defects, with meticulous dissection and mobilization of the pedicle, the skin island can reach even slightly more anterior defects as in the case demonstrated (Fig. 7.9a–e).

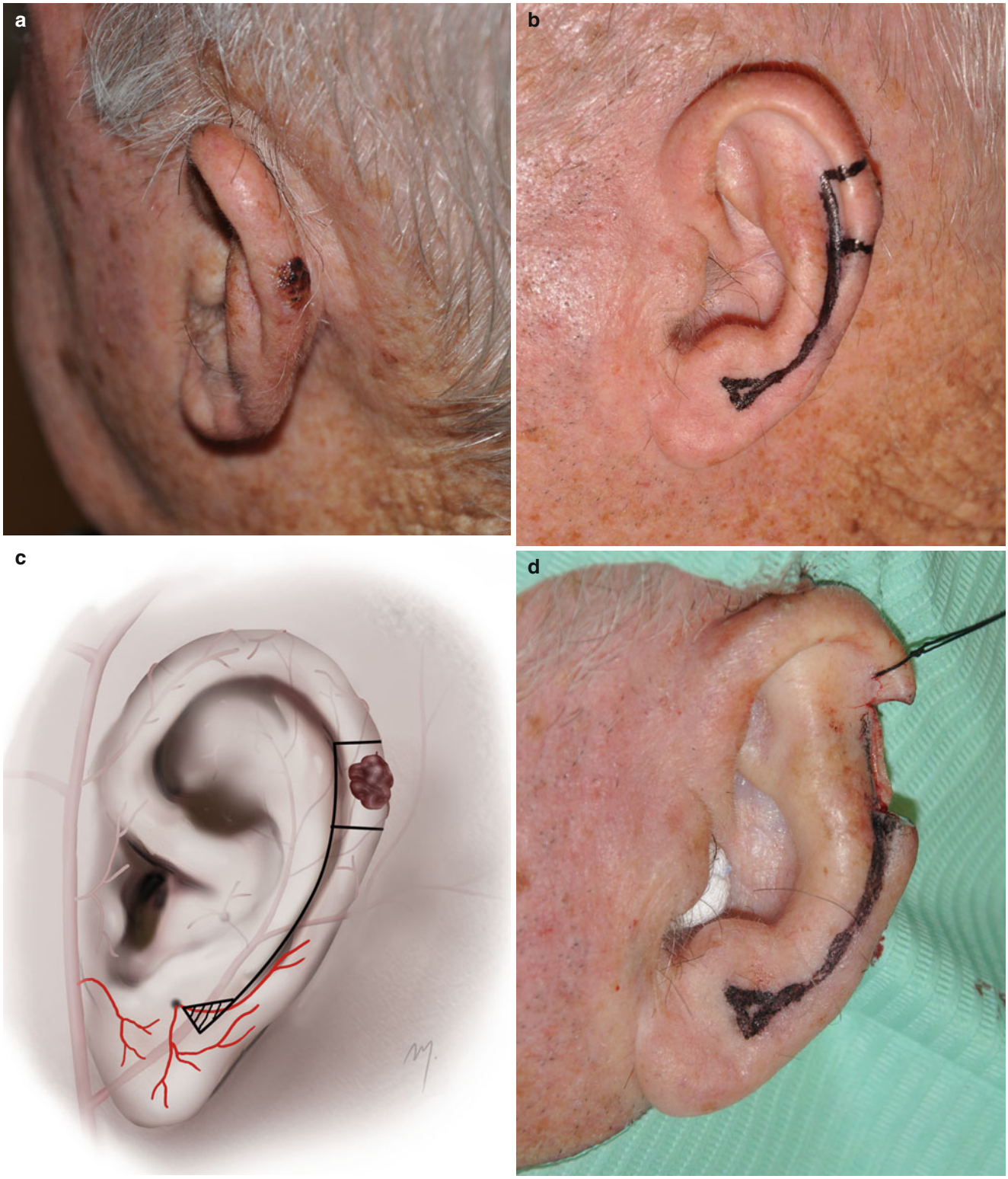

Fig. 7.8 (**a**) Basal cell carcinoma located at the helical rim. (**b**, **c**) A chondrocutaneous helical rim advancement flap is outlined. (**d**) The lesion excised. (**e**) The flap was raised as a chondrocutaneous unit that includes both skin and cartilage of the helix. (**f**) Flap fully mobilized. (**g**) Advancing to recipient site. (**h**, **i**) Flap sutured in position. Skin is sutured in both outer and inner surfaces of the auricle. (**j**) Early postoperative result (10 days). No necrosis occurred. (**k**) Late postoperative result

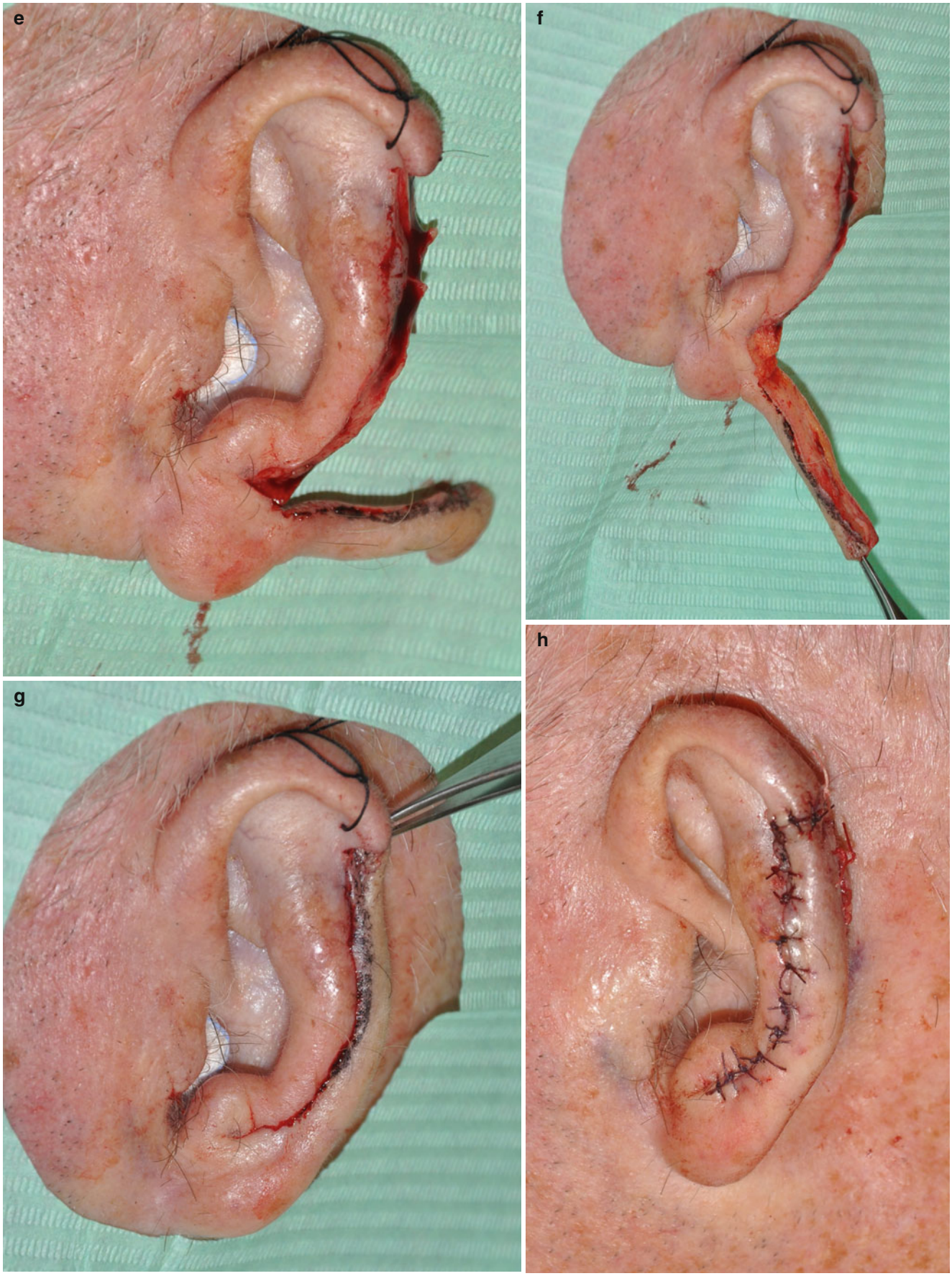

Fig. 7.8 (continued)

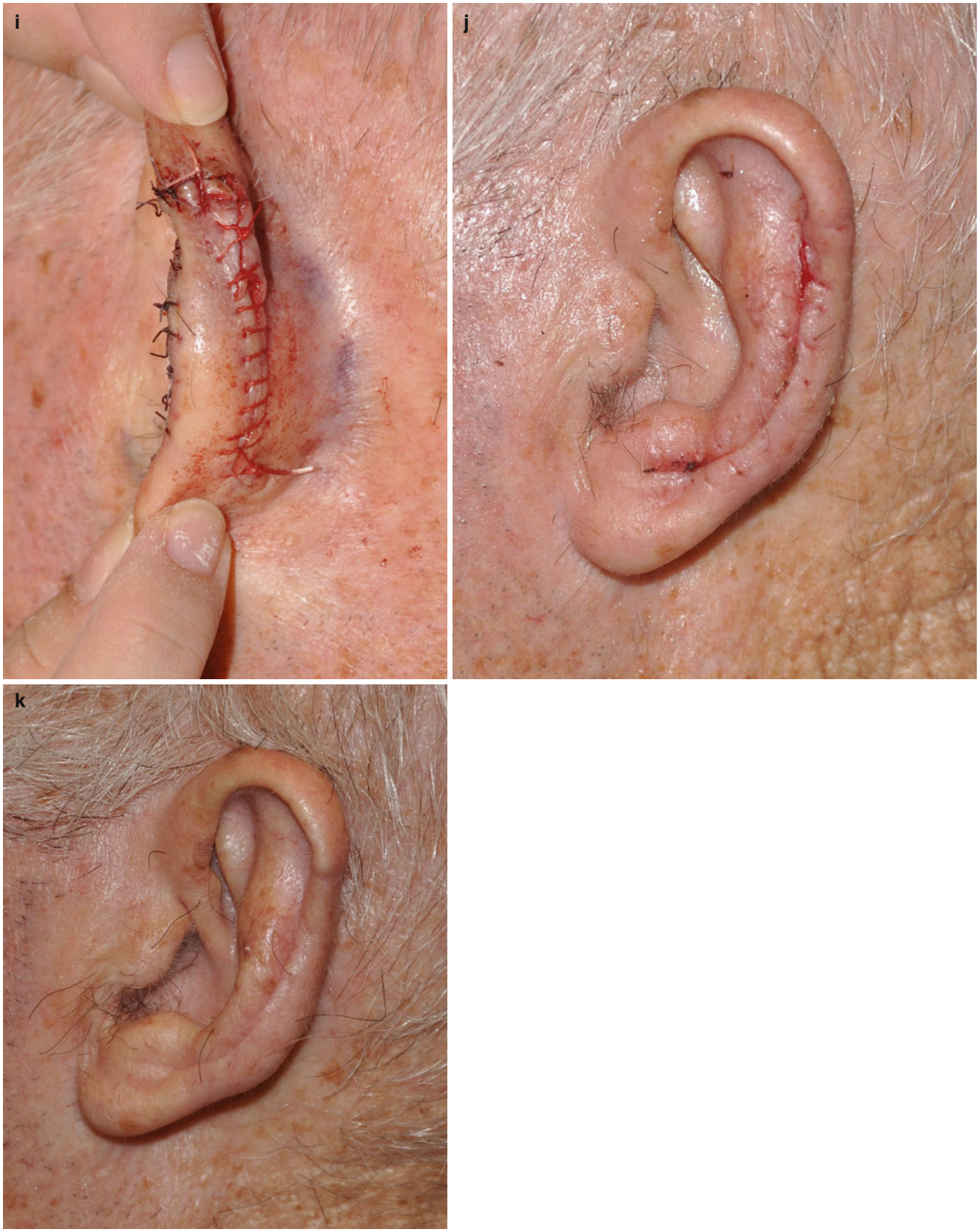

Fig. 7.8 (continued)

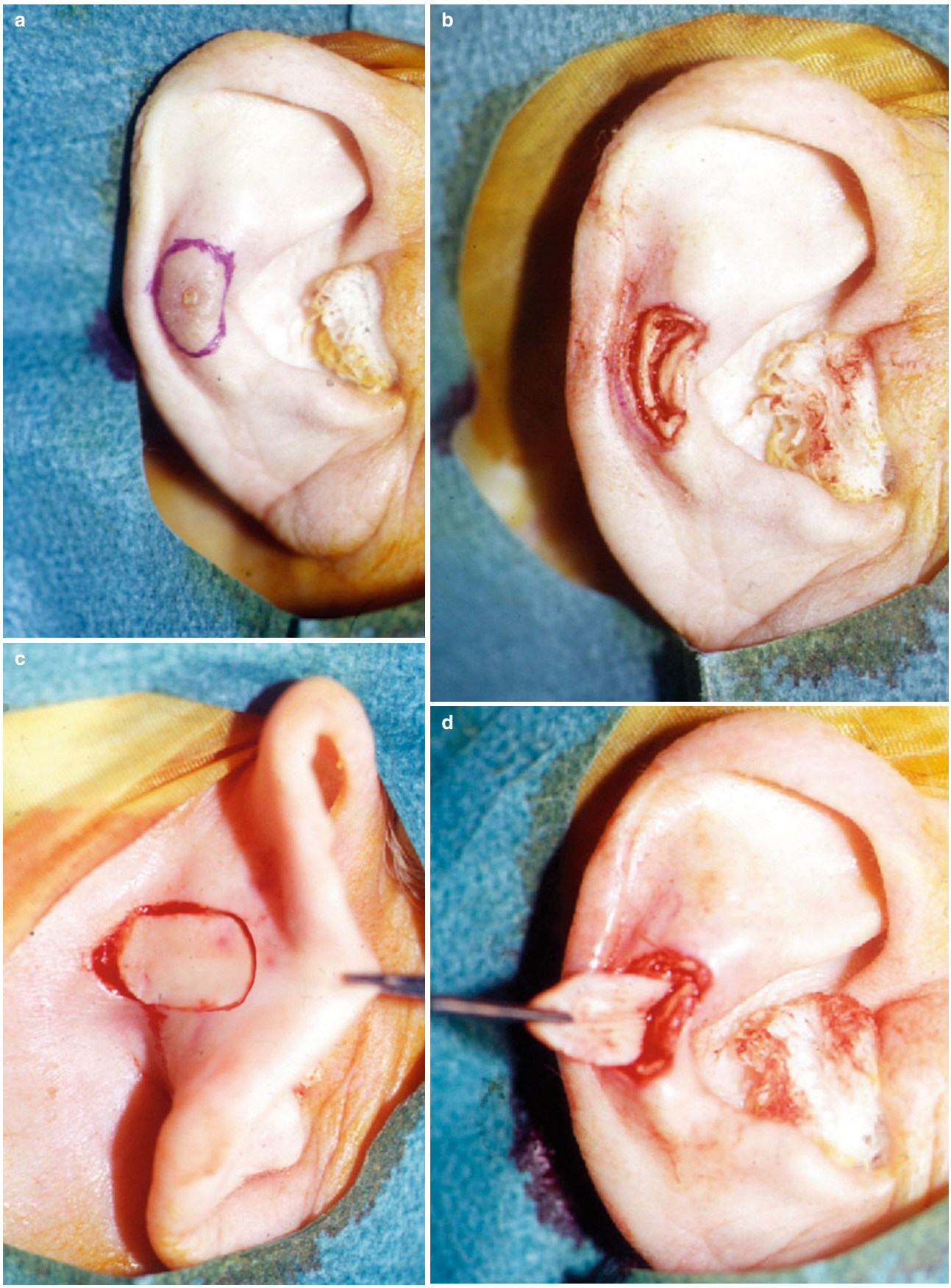

Fig. 7.9 Postauricular subcutaneous pedicle island flap (With kind permission from Dr. Ioannis Tsamis). (**a**) Resection margins of the lesion outlined. (**b**) The defect after resection. (**c**) Postauricular subcutaneous pedicle island flap outlined. (**d**) Flap tunneled. (**e**) Flap sutured in place

Fig. 7.9 (continued)

References

Antia NH, Buch VI (1967) Chondrocutaneous advancement flap for the marginal defects of the ear. Plast Reconstr Surg 39(5):472–477

Butler CE (2003) Reconstruction of marginal ear defects with modified chondrocutaneous helical rim advancement flaps. Plast Reconstr Surg 111(6):2009–2013

Erdmann D, Bruno AD, Follmar KE, Stokes TH, Gonyon DL, Marcus JR (2009) The helical arcade: anatomic basis for survival in near-total ear avulsion. J Craniofac Surg 20(1):245–248

Imanishi N, Nakajima H, Aiso S (1997) Arterial anatomy of the ear. Okajimas Folia Anat Jpn 73(6):313–323

Jackson JT (1985) Local flaps in head and neck reconstruction, 1st edn. Mosby, St Louis

Krunic AL, Weitzul S, Taylor RS (2006) Chondrocutaneous advancement flap for reconstruction of helical rim defects in dermatologic surgery. Australas J Dermatol 47(4):296–299

Majumdar A, Townend J (2000) Helix rim advancement for reconstruction of marginal defects of the pinna. Br J Oral Maxillofac Surg 38(1):3–7

Medeiros J, Belerique M, Antunes E, Franco D, Franco T (2009) Chondrocutaneous marginal ear flap. J Craniofac Surg 20(3): 862–863

Moschella F, Cordova A, Pirrello R, De Leo A (2003) The supra-auricular arterial network: anatomical bases for the use of superior pedicle retro-auricular skin flaps. Surg Radiol Anat 24(6): 343–347

Park C, Lineaweaver WC, Rumly TO, Buncke HJ (1992) Arterial supply of the anterior ear. Plast Reconstr Surg 90(1):38–44

Pinar YA, Ikiz ZA, Bilge O (2003) Arterial anatomy of the auricle: its importance for reconstructive surgery. Surg Radiol Anat 25(3–4): 175–179

Skaria AM (2008) The modified chondrocutaneous advancement flap for the reconstruction of helical defects of the ear. Dermatol Surg 34(6):806–810

Song R, Song Y, Qi K, Jiang H, Pan F (1996) The superior auricular artery and retroauricular arterial island flaps. Plast Reconstr Surg 98(4):657–667

Standring S (2008) Gray's anatomy. The anatomical basis of clinical practice, 40th edn. Churchill Livingstone-Elsevier, Edinburg

Vergilis-Kalner IJ, Goldberg LH (2010) Bilobed flap for reconstruction of defects of the helical rim and posterior ear. Dermatol Online J 16(10):9

Neck

8

The neck is the part of the body that joins the head and the trunk. It is bounded superiorly by the base of the cranium and the inferior border of the mandible and inferiorly by the thoracic inlet (Fig. 8.1).

More precisely, the superior limits run along the external occipital protuberance, the superior nuchal line, the mastoid apophyses, the anteroinferior borders of the external auditory canals, and the posterior and inferior mandibular borders. The lower limits lie along the superior border of the sternum and the clavicles, the acromioclavicular joints, and a line that joins the acromioclavicular joints to the spinous process of the seventh vertebra. A plane extending from the transverse vertebral processes to the anterior edges of the trapezius muscles divides the neck into a posterior and an anterior part.

8.1 Superficial Anatomy of the Anterior Neck

8.1.1 Skin and Subcutaneous Tissue

The skin that covers the neck although pliable is under tension due to the presence of the underlying platysma muscle. Its thickness is approximately 0.6 mm but becomes thicker at the submental area. It contains hair follicles, predominantly in the male, and sebaceous and sweat glands. During aging process, it becomes loose exhibiting a saggy appearance. Due to its pliability and mobility, greatly enhanced in the elderly, the skin of the neck constitutes an important tissue reservoir and is a first choice donor site for harvesting regional flaps nearly similar skin quality in the reconstruction of large facial defects.

The relaxed skin tension lines (RSTLs) at the neck run horizontally parallel one to each other (Fig. 8.2). Placing incisions transversely into wrinkles whenever possible, this hides the scars and enhances the cosmetic result. The layer of subcutaneous tissue lies between the dermis of the skin and the deep cervical fascia. It contains various amounts of adipose tissue, cutaneous nerve filaments, and small blood and lymphatic vessels. The subcutaneous fat at the neck seems to form fat compartments in specific areas in a manner analogous to the superficial fat pads of the face. A fat compartment that is located at the submental region has been described in detail in recent studies (Hatef et al. 2009; Pilsl and Anderhuber 2010).

The platysma muscle (one of the superficial neck muscles; see below) is running within the subcutaneous tissue separating it into a thin superficial adipofascial layer that fixes the platysma tightly to the skin and a deep adipofascial layer consisting of loose fascial and poor fat tissue that enables the platysma to move over the underlying muscles (Imanishi et al. 2005). The subcutaneous dissection, when elevating a flap in the neck area that is covered by platysma muscle, has a dual form and is either subdermal or subplatysmal being demarcated by this muscle sheet.

All the anatomic structures are under the cover of the platysma. The subcutaneous tissue along with the platysma composes the superficial cervical fascia.

8.1.2 Platysma Muscle

The platysma is a superficial neck muscle located in its lateral aspect (Fig. 8.3); phylogenetically, it is accepted to be remnants of the panniculus carnosus. More precisely, it is a thin, broad, and quadrilateral muscle sheet and constitutes a major component of the SMAS layer. It is situated within the subcutaneous tissue and over the investing layer of the deep cervical fascia. Its length is usually about 20 cm and its width 10 cm. The platysma shows a great variability in size and thickness, may be absent or hypoplastic, and during aging process becomes thinner and difficult to determine.

The platysma originates from the superficial fascia over the upper part of the pectoralis major muscle in a plane corresponding even up to the 2nd and 3rd ribs and from the

V.K. Thomaidis, *Cutaneous Flaps in Head and Neck Reconstruction*,
DOI 10.1007/978-3-642-41254-7_8, © Springer-Verlag Berlin Heidelberg 2014

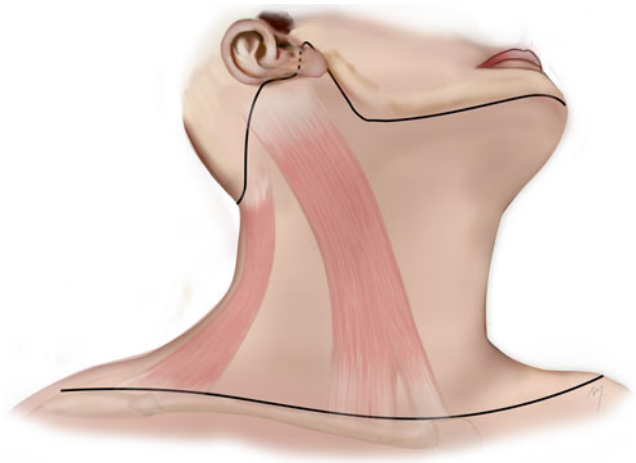

Fig. 8.1 Boundaries of the neck

Fig. 8.3 The platysma muscle

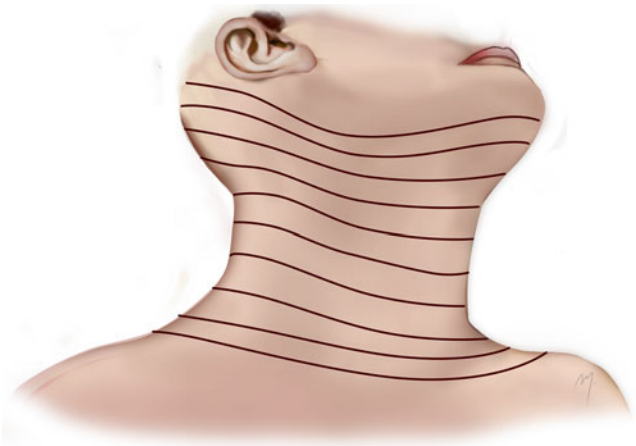

Fig. 8.2 Relaxed skin tension lines (RSTLs) at the neck

superficial fascia over the upper part of the deltoid muscle. The muscle fibers run parallel each other, upward, and medially crossing the clavicle toward the cheek. The medial border of the platysma ends at the submental region forming with its contralateral an inverted V, with the apex located in a variable level between the chin and the thyroid cartilage, either covering thus the submental area totally with muscle fibers or leaving it devoid of muscles fibers (de Castro 1980).

The lateral border of the platysma in the neck extends in a variable width beyond and over the external jugular vein. Entering the face, it continues in a curved fashion in a variable extent and ends at the labial commissure. After the fibers cross the mandible, they insert into the skin of the lower cheek and the oral commissure and blend with muscle fibers of the perioral muscles. It has been reported that the facial extent of the platysma may occupy more than 50 % of the face (Shah and Rosenberg 2009). At the mental area, some muscle fibers cross the midline and interlace with corresponding fibers of the contralateral muscle, and at the anterior part of the mandible, some others insert into the bone.

The platysma muscle receives its blood supply from a wide anastomotic network formed by arteries that distribute on each different part of the muscle. The upper part is supplied mainly by the submental artery and with contribution of direct perforators from the facial artery. The lower part is supplied by branches of the transverse cervical and the suprascapular artery, while the middle part by the superior thyroid artery. According to the posterior extent of the muscle, the occipital and the posterior auricular arteries may supplementary contribute to the vascularization of its lateral part. These arteries are described in detail below. According to its arterial supply, the platysma can be harvested as myocutaneous flap in three different types: having its pedicle superiorly, inferiorly, or laterally. The dominant arterial supply of the platysma comes from the submental artery and due to that fact a superiorly based platysma flap appears with enhanced vascularity and safety. The venous drainage of the platysma muscle is through the external jugular vein, the anterior jugular vein, the superior thyroid vein, the submental vein, and the facial vein (Uehara et al. 2001; Agarwal et al. 2004).

The platysma muscle is innervated by the cervical branch of the facial nerve which enters the muscle from its deep

surface in the space between the mandibular angle and the sternocleidomastoid muscle. The marginal mandibular branches of the facial nerve run also deep to the platysma but do not take part in its innervation. The muscle is a lower lip and oral commissure depressor. When all of the muscle fibers contract, the skin of the neck wrinkles.

8.1.3 Investing Layer of the Deep Cervical Fascia

Beneath the platysma muscle lies the investing layer of the deep cervical fascia (Fig. 8.4). The investing layer of the deep cervical fascia is the outermost fascia of the three neck layers of the deep cervical fascia: the other two being the intermediate pretracheal layer and the deep prevertebral layer. It is a continuous sheet of fibrous tissue, encircling completely the neck. It attaches posteriorly to the spines of the cervical vertebrae and to the nuchal ligament. Passing anteriorly around the neck, it splits and envelopes first the trapezius muscle and then the sternocleidomastoid muscle and the submandibular gland. The investing layer forms the roof of the posterior triangle of the neck and the floor of the submandibular triangle. In the midline it is attached to the chin, the body of the hyoid bone and the manubrium of the sternum. Inferiorly, the investing layer is attached to the sternum, the clavicle, and the acromion. Superiorly, it is attached to the external occipital protuberance, the superior nuchal lines, the tip of the mastoid process, the tympanic plate, and the styloid process. It splits at the lower border of the mandible into a medial and a lateral layer which continue up to the cheek.

The pretracheal layer is found below the hyoid bone; surrounds the trachea, the esophagus, the larynx, and the thyroid gland; and envelopes the infrahyoid strap muscles.

The prevertebral layer is the innermost cervical fascia and invests the prevertebral muscles and encloses the scalene and the levator scapulae muscles. The investing layer of the deep cervical fascia is the fascia commonly associated with flap surgery. Likewise, the fascial layers of the head are the source of considerable controversy with respect to the organization and nomenclature of the investing layer of the neck, while some authors even challenge its existence (Zhang and Lee 2002; Nash et al. 2005).

8.1.4 Sternocleidomastoid Muscle

Apart from the platysma muscle, the sternocleidomastoid and the anterior borders of the trapezius muscles are encountered in a superficial level just beneath the platysma level (Fig. 8.5).

The sternocleidomastoid muscle is originated by two heads, a medial termed the sternal head and a lateral one termed the clavicular head. The sternal head originates from the upper part of the anterior surface of the manubrium sterni and runs superolateral and posterior in a slightly oblique direction. The clavicular head originates from the upper surface of the medial third of the clavicle and runs upward in a more vertical direction than the sternal head. There are cases where the clavicular head exhibits variability in its origin breadth, being as narrow as the sternal head or widening to the origin of the trapezius.

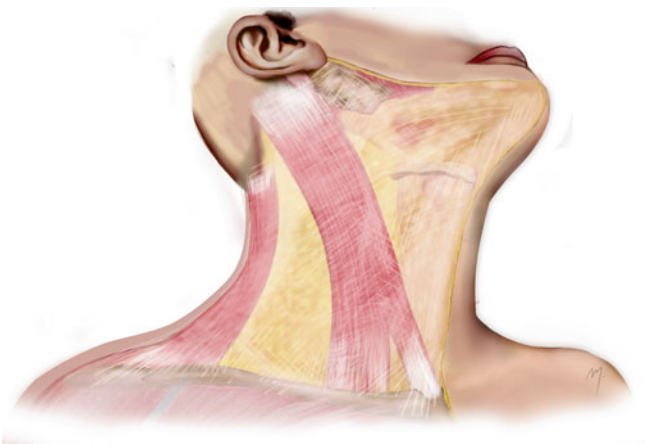

Fig. 8.4 The investing layer of the deep cervical fascia

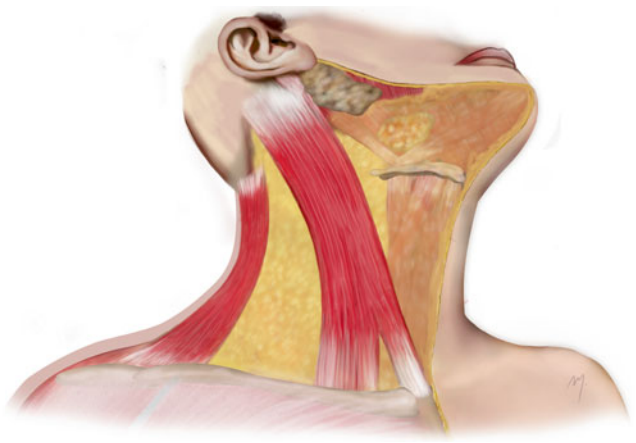

Fig. 8.5 The sternocleidomastoid muscle and the trapezoid muscle at the neck

The sternal and the clavicular heads as they run upward merge together in a level between the middle and the lower third of the neck and form a thick and round muscle belly. The muscle continues to the mastoid region passing obliquely to the side of the neck. It inserts by a tendon into the lateral surface of the mastoid process and, by an aponeurosis, into the lateral half of the superior nuchal line.

The upper part of the muscle is supplied from branches of the occipital and small contribution of branches of the posterior auricular arteries in its most upper part. Despite this, the sternocleidomastoid branch of the occipital artery has also been reported to supply lower levels of the sternocleidomastoid muscle (Fróes et al. 1999). Its middle part is supplied by the sternocleidomastoid branch of the superior thyroid artery. The lower part of the muscle is supplied in more than 80 % by a branch arising from the suprascapular artery, and in the cases where this branch does not exist, a longer sternocleidomastoid branch of the superior thyroid artery or branches from the transverse or superficial cervical arteries undertake the blood supply (Kierner et al. 1999).

The sternocleidomastoid muscle is innervated by the accessory nerve.

When the muscle acts unilateral, it tilts the head to its own side and simultaneously rotates it so as turning the face toward the opposite side. When acting bilateral, it draws the head forward.

8.1.5 Trapezius Muscle

The trapezius muscle (see Chap. 2) is also a muscle of the upper limb. Its upper part and especially its anterior margin constitute the most posteriorly located superficial muscle of the lateral neck (Fig. 8.5). The anterior margin of the trapezius makes up also the posterior border of the posterior neck triangle and is a landmark in the design of flaps (e.g., cervicopectoral flap). Even though the anterior muscle margin is easily palpated, this becomes somewhat difficult in the anesthetized patient where the muscle is under relaxation.

8.1.6 Triangles of the Neck

The side of the neck is divided by the sternocleidomastoid muscle, which crosses the neck in an oblique direction, into an anterior and a posterior triangle (Fig. 8.6).

8.1.6.1 Anterior Triangle

The base of the anterior triangle lies superiorly and is formed by the border of the mandible and a line that extends from the mandibular angle to the mastoid process, while its apex is situated inferior at the sternum. Anteriorly, it is bounded by the midline of the neck and posteriorly by the anterior margin of the sternocleidomastoid.

The anterior triangle is further subdivided into the following:

8.1.6.1.1 Submental Triangle

The submental triangle has its base at the body of the hyoid bone and its apex at the chin. The anterior bellies of both digastric muscles form the side pleura of the triangle. The mylohyoid muscles form its floor. The contents of the triangle are the submental lymph nodes, some small veins

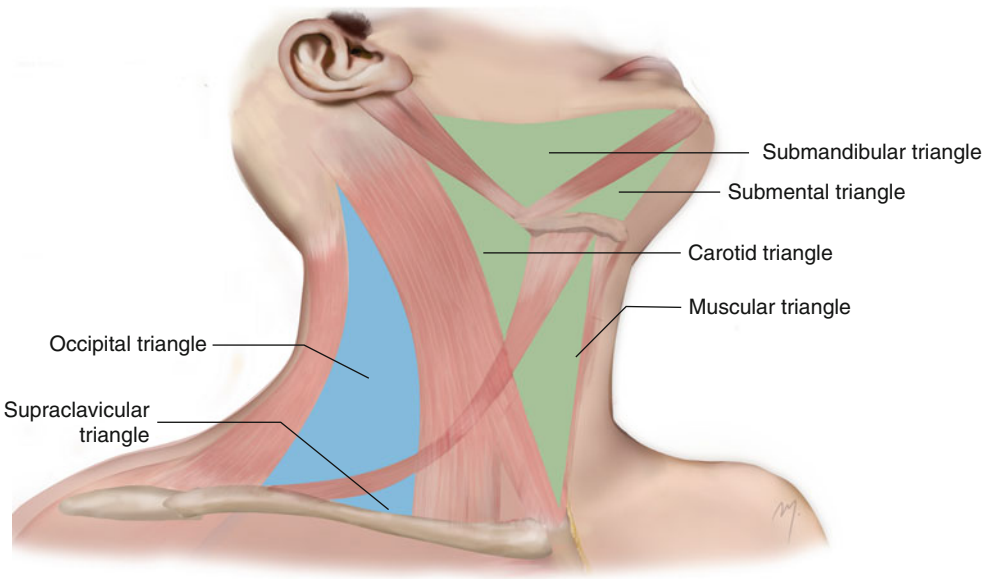

Fig. 8.6 The triangles of the neck. *Blue color* indicates the posterior triangle and the *green color* the anterior triangle

that unite to form the anterior jugular vein, and the terminal part of the submental artery as it turns to ascend to the chin.

8.1.6.1.2 Submandibular Triangle

The submandibular triangle (digastric triangle) is bounded superiorly by the border of the mandible and the line extending from its angle to the mastoid process, posteriorly by the posterior belly of the digastric and the stylohyoid muscle, and anteriorly by the anterior belly of the digastric muscle. The mylohyoid, hyoglossus, and constrictor pharyngis muscles form the floor of the submandibular triangle.

The structures that are of interest in flap surgery when dissecting in a subplatysmal plane in the area of the submandibular triangle are the facial vein, the facial artery as it curves around the mandibular border to enter the face, the submental artery, and the cervical and marginal branches of the facial nerve.

8.1.6.1.3 Carotid Triangle

The boundaries of the carotid triangle are superiorly the posterior belly of the digastric and the stylohyoid muscles, anteriorly the superior belly of the omohyoid muscle, and posteriorly the anterior border of the sternocleidomastoid muscle. The inferior and middle pharyngeal muscles form the floor of the triangle. When removing the platysma, a part of the external and the anterior jugular veins and cutaneous cervical branches appear in the superficial level of the triangle.

8.1.6.1.4 Muscular Triangle

The borders of the muscular or visceral triangle of the neck are the midline of the neck anteriorly, the superior belly of omohyoid muscle superiorly, and the anterior margin of the sternocleidomastoid inferiorly. It contains the muscles of the neck: sternohyoid, superior belly of omohyoid, sternothyroid, and thyrohyoid. The first two form the superficial layer of these muscles.

8.1.6.2 Posterior Triangle

The base of the posterior triangle corresponds to the superior surface of the middle third of the clavicle and its apex at the superior nuchal line at the point where the sternocleidomastoid and trapezius muscles approximate to each other. Anteriorly, the posterior triangle is bordered by the posterior border of sternocleidomastoid and posteriorly by the anterior margin of the trapezius. The posterior triangle is subdivided into the occipital and the supraclavicular triangles by the inferior belly of the omohyoid muscle, which runs crossing the space about 2–2.5 cm above the clavicle.

8.1.6.2.1 Occipital Triangle

The occipital triangle is the upper and larger part of the posterior triangle. Its floor is formed from the top down by the semispinalis capitis at the apex, the splenius capitis, the lavatory scapulae, the scalenus posterior, and the scalenus medius muscles.

The platysma covers the lower part of the triangle in a various degree.

The important surface structures found at this triangle are the branches of the cervical plexus as they radiate emerging from the posterior border of the sternocleidomastoid muscle and the spinal accessory nerve as it emerges slightly superiorly and runs obliquely, crossing the triangle in its middle to reach the trapezius. All of these neural branches emerge from the posterior border of the sternocleidomastoid within 2 cm above or below a point termed Erb's point. Erb's point is located at the posterior border of the sternocleidomastoid muscle approximately in the mid of its mastoid and sternoclavicular attachments and serves as an important landmark. Identifying this point is useful not only in locating the emerging point of the mentioned nerves so as to protect them during surgery but also in blocking the cutaneous nerves of the cervical plexus by gaining anesthesia of almost the bigger part of the neck skin.

8.1.6.2.2 Supraclavicular Triangle

The supraclavicular triangle (omoclavicular triangle) is the lower and smaller part of the posterior triangle with a variable size that depends on the outspread of the clavicular attachments of the sternocleidomastoid and trapezius muscles. The first rib, the scalenus medius, and a part of the scalenus anterior and the first slip of the serratus anterior muscle form its floor. The triangle is covered almost fully by the platysma and in the superficial level is crossed by the supraclavicular nerves and the external jugular vein as it descends across the posterior edge of the sternocleidomastoid.

8.1.7 Arteries That Supply the Skin of the Neck

The skin of the neck is supplied by musculocutaneous and direct cutaneous perforators of branches of the external carotid artery and of the thyrocervical trunk of the subclavian artery.

8.1.7.1 Branches of the External Carotid Artery That Contribute to the Neck Skin Supply

8.1.7.1.1 Facial Artery (Cervical Part)

The facial artery arises from the external carotid artery, as one of its anterior branches, at the carotid triangle (Fig. 8.7). It

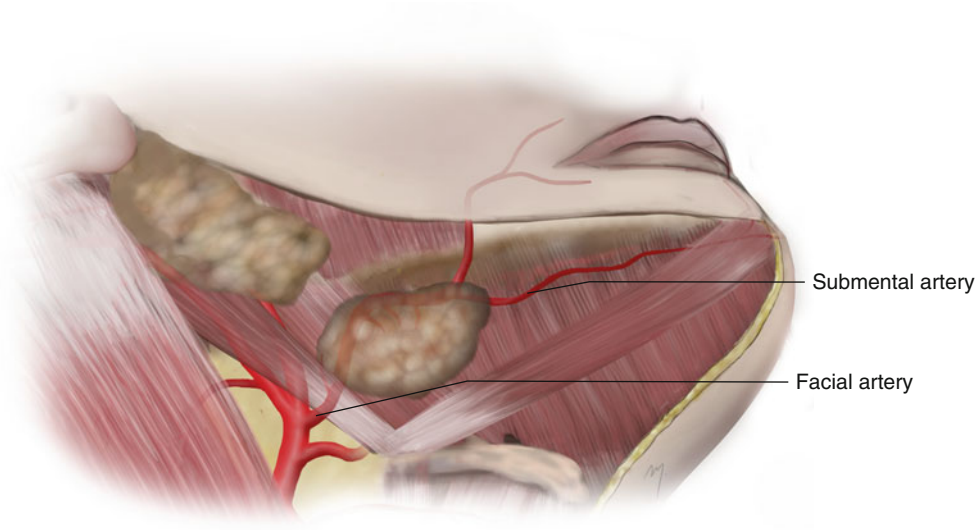

Fig. 8.7 The cervical part of the facial artery

usually ends at the inner canthus as angular artery and anastomoses with the dorsal nasal artery (see Chap. 4). For descriptive purposes, this long course is divided in a cervical and a facial part according to the area where the vessels run.

The facial artery arises as an anterior branch of the carotid artery immediately above the greater horn of the hyoid bone and above the lingual artery (Fig. 8.7). It lies beneath the platysma and the hypoglossal nerve often runs above it. Its diameter ranges from 1.7 to 3.6 mm (mean 2.6 mm) (Zhao et al. 2000). In about 20 % of the cases, the facial and the lingual arteries arise with a common trunk from the external carotid artery (Shima et al. 1998).

The facial artery after its origin runs upward and forward, deep to the stylohyoid and the posterior belly of the digastric. Above the stylohyoid, it turns down and forward between the medial pterygoid muscle and the posterior aspect of the submandibular gland. As it reaches the lower border of the mandible, it curves around it, just in front of the anterior edge of the masseter muscle; pierces the deep fascia, lying immediately deep to platysma; and enters the face, continuing as the facial part, running toward the alar base, and giving off its branches to the face (see Chap. 5). At the point where the artery crosses the mandible, it lies very superficial, and its pulsation is most palpable. The facial artery, with its accompanying vein, crosses deep the mandibular branch of the facial nerve.

In the neck, the facial artery gives off the ascending palatine, the tonsillar, the glandular, and the submental arteries. The ascending palatine artery arises close to the origin of the facial artery, runs up between styloglossus and stylopharyngeus to the side of the pharynx, and ascends along it, between the superior constrictor of the pharynx and the medial pterygoid toward the skull base. Its branches supply the soft palate, the tonsils, and the auditory tube and anastomose with its opposite fellow, the greater palatine branch of the maxillary artery and the tonsillar and the ascending pharyngeal arteries.

The tonsillar artery ascends between medial pterygoid and styloglossus and after penetrating the superior constrictor of the pharynx enters the tonsil. It supplies the tonsil and the root of the tongue. The glandular branches are 3–4 and supply the submandibular salivary gland, lymph nodes, and a small area of overlying skin as cutaneous perforators.

8.1.7.1.2 Submental Artery

The submental artery constitutes the largest cervical branch of the facial artery. It branches off at a point deep to the submandibular gland or at its superior edge as the facial artery separates from the submandibular gland. The artery originates in a point of 5–7 mm from the border of the mandible (Martin et al. 1993; Magden et al. 2004). At its origin, the mean diameter of the artery has been reported ranging between 1 and 2 mm (Martin et al. 1993; Faltaous and Yetman 1996; Pinar et al. 2005a, b).

It runs forward on the surface of the mylohyoid below the border of the mandibular body. As it reaches the anterior belly of the digastric muscle, it continues running either deep to it in 70 % or superficial to it in 30 % of the cases (Faltaous and Yetman 1996). At the symphysis of the mandible, it turns around the lower border of the mandible body, enters the chin, and divides into a superficial branch and deep branch, which anastomose with the inferior labial and mental arteries, supplying the chin and the lower lip (see Chap. 6).

During its course in the submandibular triangle, the artery gives off numerous small branches to the submandibular and sublingual glands and to the adjacent muscles and platysma. It also gives off perforating cutaneous branches in a number of 1–4 (Curran et al. 1997; Kim et al. 2002a, b) (Fig. 8.8). These branches pierce the platysma, supply the skin over the submental triangle, and anastomose with their contralaterals,

providing a strong arterial pedicle for designing flaps in the submental region. Moreover, the submental artery anastomoses with the mental, the inferior labial, and the sublingual arteries, a network that is of great importance to the blood supply of platysma muscle and the superiorly based platysma flap (Lasjaunias et al. 1979).

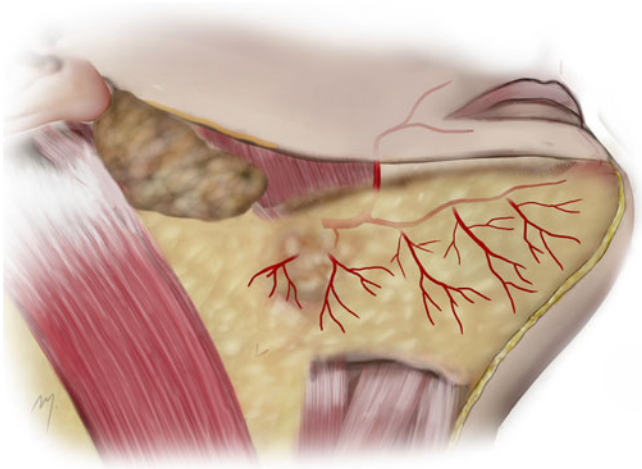

Fig. 8.8 Submental artery cutaneous perforators

8.1.7.1.3 Superior Thyroid Artery

The superior thyroid artery is described as the first branch of the external carotid artery. It arises beneath the anterior border of the sternocleidomastoid muscle just below the level of the greater horn of the hyoid bone (Fig. 8.9). In relation to the carotid bifurcation, it arises in 65 % of the cases at the same level or above it. In 35 % of the cases, it arises below the level of bifurcation from the common carotid artery (Ozgur et al. 2009).

It courses inferiorly and medially, to the apex of the lobe of the thyroid gland. In its course in the carotid triangle, the superior thyroid artery lies only beneath the skin and the platysma. As it descends, it then passes beneath the omohyoid and sternothyroid muscles with the external laryngeal nerve usually lying medially to it. The superior thyroid artery ends at the thyroid gland where it divides into the anterior, isthmal, posterior, and lateral thyroid final branches.

Through its course, the superior thyroid artery gives off the following branches: the infrahyoid artery, the superior laryngeal artery, the sternocleidomastoid artery, the cricothyroid artery, and the final thyroid branches. The branches of the superior thyroid artery that contribute to the neck skin supply are the infrahyoid and the sternocleidomastoid arteries.

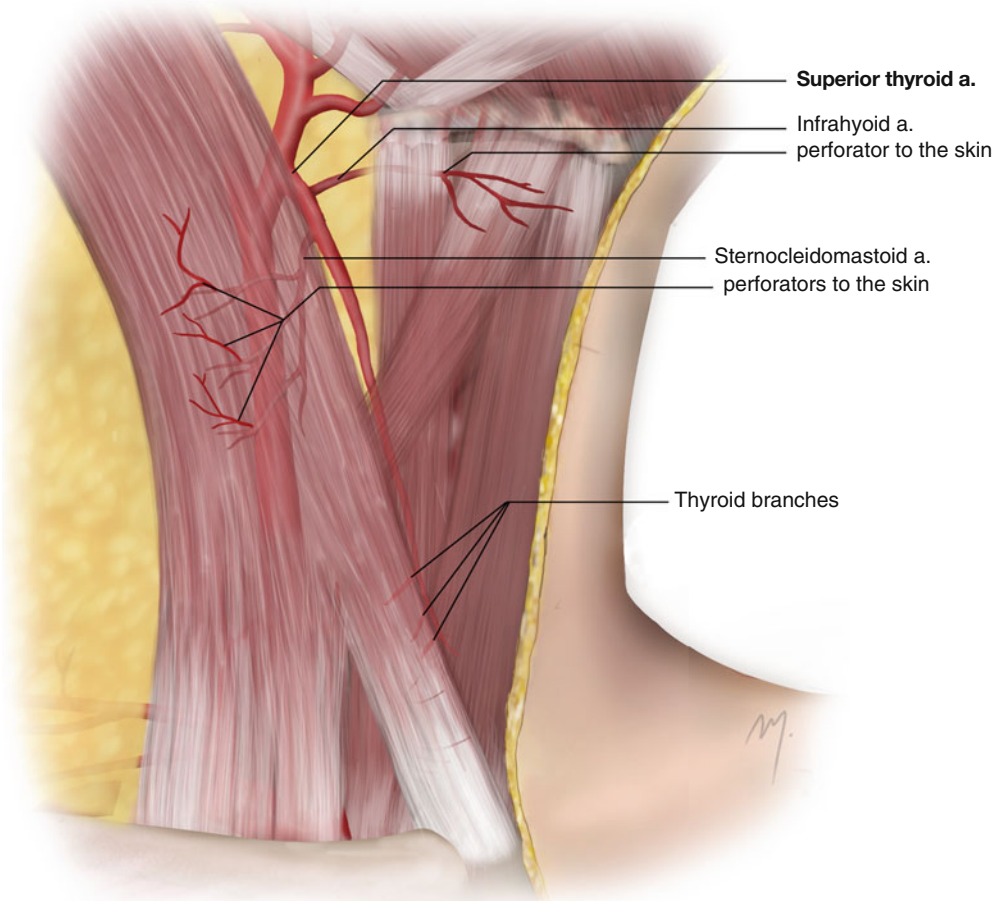

Fig. 8.9 Superior thyroid artery

8.1.7.1.4 Infrahyoid Artery

This is a small branch running along the lower border of the hyoid bone and supplies the superior portion of the infrahyoid strap muscles and the overlying part of the skin.

8.1.7.1.5 Sternocleidomastoid Artery

The sternocleidomastoid branch arises from the superior thyroid artery in about 80–85 % of the cases, while in the remainder it originates directly from the external carotid artery (Hu et al. 2006; Ozgur et al. 2009). When it originates from the superior thyroid artery, this occurs approximately 0.5–1 cm from the origin of the superior thyroid artery (Hurwitz et al. 1983). It courses downward and laterally across the carotid sheath and at the medial margin of the middle portion of the sternocleidomastoid muscle enters the muscle on its deep surface. The precise point where the sternocleidomastoid artery enters the muscle is situated in a distance of 3 cm away from the origin of the superior thyroid artery (Hu et al. 2006). Small perforators perforate the mid-third of the sternocleidomastoid muscle and supply the overlying platysma and skin. In the same area, a mostly constant direct cutaneous perforator has been found to emerge at the anterior border of the sternocleidomastoid muscle in its mid-portion (Fig. 8.10). This branch travels initially below the platysma, and after piercing it courses subcutaneously to the midline adjoining its contralateral supplying a large area of the anterior neck skin (Hurwitz et al. 1983; Wilson et al. 2012). Recently, Wilson et al. (2012) raised long perforator flaps that extended even beyond the midline, pedicled on just one of these cutaneous perforators.

The infrahyoid artery anastomoses with its contralateral in the midline. Anastomoses between the muscular branches of the superior thyroid artery and the muscular branches of the inferior thyroid artery (which supplies the inferior portion of these muscles) are formed passing through the entire musculature (Eliachar et al. 1984).

8.1.7.1.6 Occipital Artery: Sternocleidomastoid Branches

The occipital artery (see Chap. 2) contributes to the vascular supply of the upper part of the neck by two small branches, the lower and the upper sternocleidomastoid branches (Fig. 8.11).

The occipital artery branches from the posterior aspect of the external carotid artery about 2 cm from its origin and opposite to the origin of the facial artery. It courses up and back deep to the posterior belly of the digastric muscle and in front of the internal carotid artery, the internal jugular vein, and the vagus, the hypoglossal, and the accessory nerves. Running to the occipital area, it passes in the occipital groove and the medial

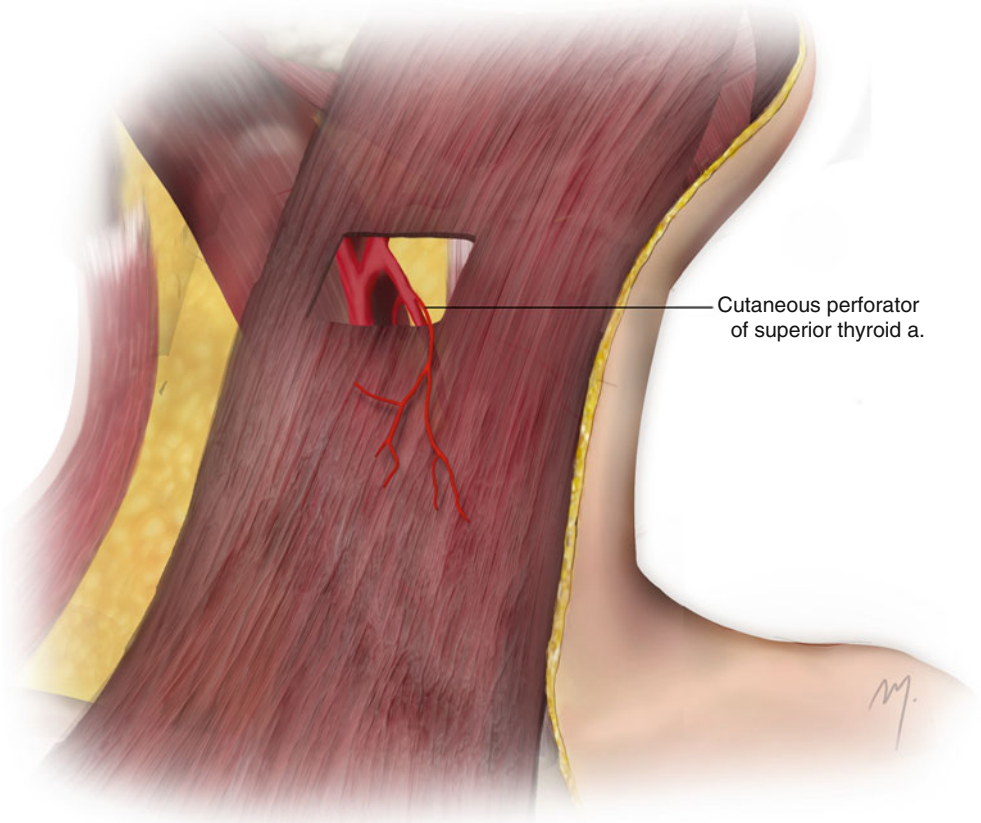

Fig. 8.10 Cutaneous perforator of the superior thyroid artery

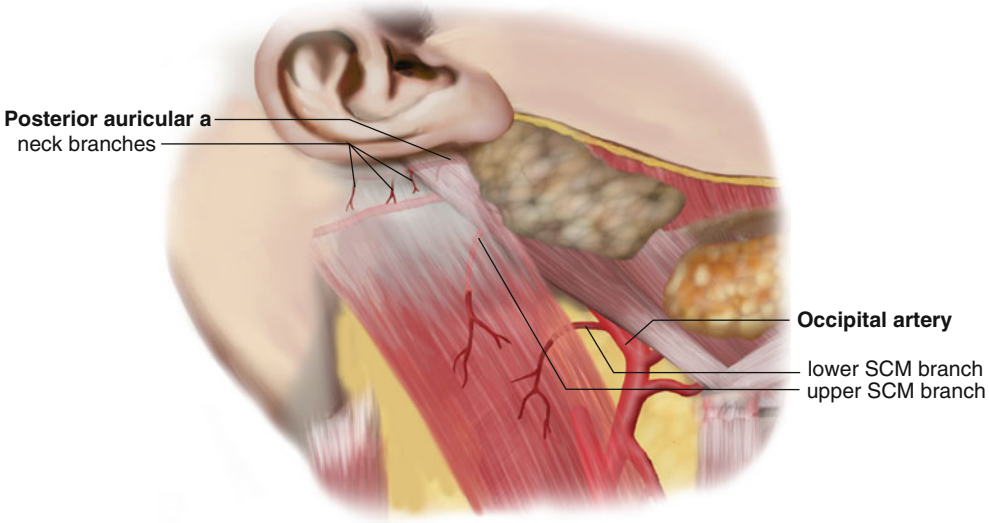

Fig. 8.11 Musculocutaneous perforators of the lower and upper sternocleidomastoid branches of the occipital artery and musculocutaneous perforators of the posterior auricular artery

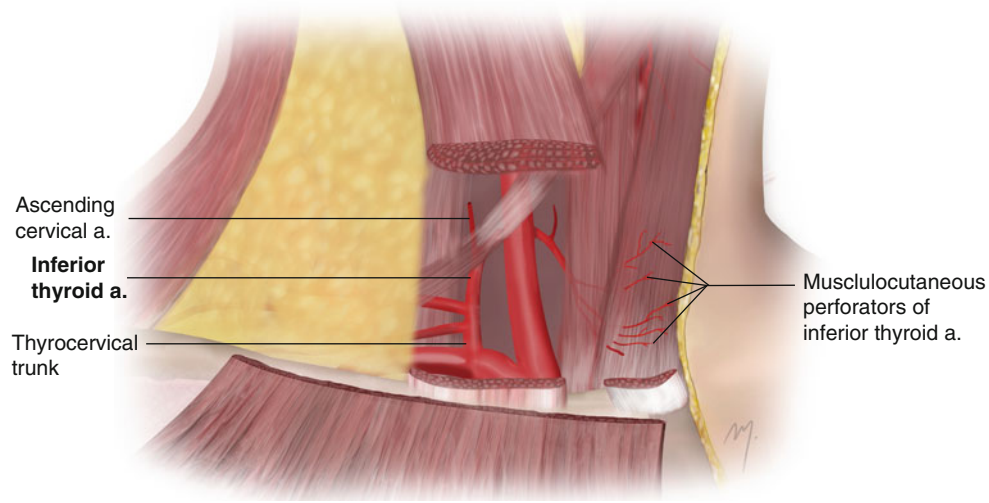

Fig. 8.12 The inferior thyroid artery and its branches. Perforators through the muscular branches supply the skin

aspect of the mastoid process deep to the attachments of the sternocleidomastoid muscle. At this part, it gives off the lower and the upper sternocleidomastoid branches.

The lower sternocleidomastoid branch arises from the starting point of the occipital artery, courses posteroinferiorly over the hypoglossal nerve, and enters the sternocleidomastoid muscle. The upper sternocleidomastoid branch arises from the occipital artery, after a short distance from the previous one, immediately after it crosses the accessory nerve. This branch runs in a same posteroinferiorly course in company with the accessory nerve entering the deep surface of the sternocleidomastoid muscle. Musculocutaneous perforators of both of the branches supply the upper third of the sternocleidomastoid muscle and a quite large area of the upper neck skin.

8.1.7.1.7 Posterior Auricular Artery: Neck Branches

The posterior auricular artery supplies the digastric and the stylohyoid muscles as well as the parotid gland. The artery gives off small branches to the neck that contribute to the vascularization of the uppermost part of the sternocleidomastoid and the overlying skin (Fig. 8.11).

8.1.7.2 Branches of the Thyrocervical Trunk Contributing to the Neck Skin Supply

8.1.7.2.1 Inferior Thyroid Artery

The inferior thyroid artery is usually branched from the thyrocervical trunk of the subclavian artery (Fig. 8.12). It ascends anterior to the medial border of the scalenus anterior muscle. At the level below the sixth cervical transverse process, it turns medially situated between the vertebral vessels and the carotid sheath. Finally, it descends to the lower border of the thyroid gland, lying on the longus colli muscle and coming in a variable relation to the recurrent laryngeal nerve (Tang et al. 2012).

The inferior thyroid artery gives off the inferior laryngeal artery, the ascending cervical artery, and pharyngeal,

tracheal, esophageal, thyroid, and muscular branches. The inferior laryngeal artery runs upward on the trachea accompanied by the recurrent laryngeal nerve and enters the larynx supplying the laryngeal muscles and its mucous membrane. The ascending cervical artery arises at the point where the inferior thyroid artery turns medially to run behind the carotid sheath. It runs upward on the anterior tubercles of the transverse processes of the cervical vertebrae situated between the scalenus anterior and longus capitis muscles. It supplies the neighboring neck muscles and gives off spinal branches into the vertebral canal. The artery anastomoses with the deep cervical, occipital, and ascending pharyngeal arteries.

The pharyngeal, tracheal, and esophageal branches supply the lower part of the pharynx, the trachea, and the esophagus. The thyroid branches supply the thyroid and parathyroid glands and anastomose with the superior thyroid artery glandular branches.

8.1.7.2.2 Muscular Branches

These branches supply the longus colli and the scalenus anterior and inferior pharyngeal constrictor. Muscular branches also supply the inferior parts of the sternohyoid and the sternothyroid muscles (Görmüs et al. 2004). Perforators through these muscular branches supply also the overlying skin in the lower part of the muscular triangle of the neck and anastomose with the contralaterals (Fig. 8.12).

8.1.7.2.3 Superficial Cervical Artery/Transverse Cervical Artery

The superficial cervical artery arises usually as an independent vessel from the thyrocervical trunk or in common with the dorsal scapular artery in about 30 % of cases. The common arterial trunk of the superficial cervical artery and the dorsal scapular artery is termed transverse cervical artery.

When a transverse cervical artery is present, it arises from the thyrocervical trunk and runs laterally on the base of the posterior triangle of the neck (Fig. 8.13). It is situated over the scalenus anterior muscle and the trunks of the brachial plexus and beneath the inferior belly of the omohyoid muscle. In the middle part of its course, it gives off myocutaneous platysma branches that supply the lower third of the overlying platysma muscle and the skin of the base of the posterior triangle of the neck. It reaches the anterior border of the levator scapulae and divides into its two branches: an ascending superficial one named from now on the superficial cervical artery and a descending deep one named the dorsal scapular artery.

The ascending superficial cervical artery courses upward, lying beneath the anterior margin of the trapezius muscle, and gives off an ascending and a descending branch. Muscular branches supply the middle and lateral parts of the trapezius muscle (Haas et al. 2004). Through musculocutaneous perforators, the overlying skin is also fused. It anastomoses with the superficial ramus of the descending branch of the occipital artery. The ascending cervical artery, a branch of the inferior thyroid artery, must not be confused with the ascending superficial cervical artery.

The descending dorsal scapular artery runs beneath the levator scapulae to the superior medial angle of the scapula and descends under the cover of the rhomboid muscle up to the inferior angle. In the cases where the superficial cervical and the dorsal scapular arteries arise independently, the superficial cervical artery replaces and substitutes the transverse cervical artery until its course to the anterior border of the levator scapulae muscle.

A small artery is branched from the superficial cervical/transverse cervical artery named the supraclavicular artery. The supraclavicular artery arises at the medial portion of the omoclavicular (supraclavicular) triangle and courses laterally. At the angle between the anterior border of the trapezius

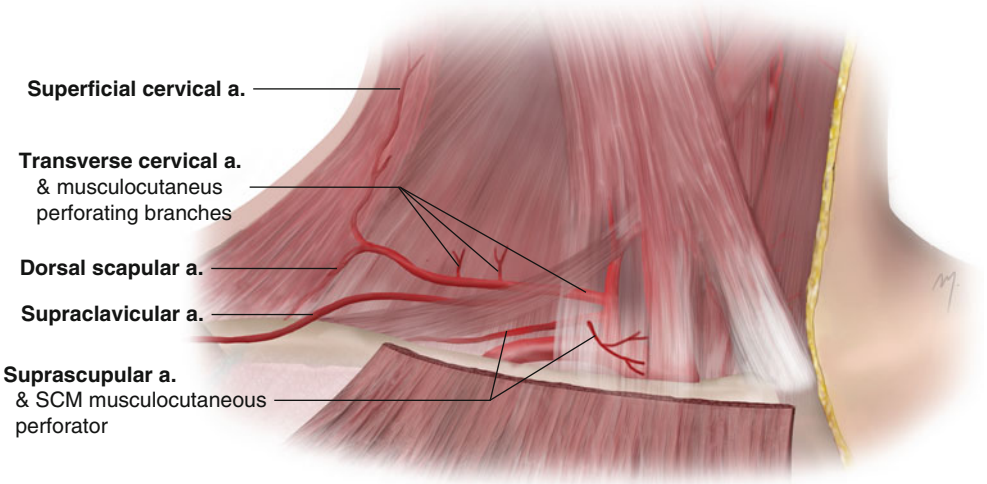

Fig. 8.13 The transverse cervical and the suprascapular arteries

and the superior border of the clavicle, it pierces the deep cervical fascia, crosses the clavicle, and travels subcutaneously to the deltoid region supplying the skin of the lateral and upper part of the deltoid region.

8.1.7.2.4 Suprascapular Artery (Sternocleidomastoid Branch-Platysma Branches)

The suprascapular artery (or transverse scapular artery) (Fig. 8.13) is branched from the thyrocervical trunk and lies at a lower level than the transverse cervical artery. It runs initially inferolaterally across the scalenus anterior and the phrenic nerve under the cover of the sternocleidomastoid muscle. It continues parallel to the clavicle behind it and runs toward the superior border of the scapula. In its course, it crosses in front of the subclavian artery and the brachial plexus. It passes over the superior transverse scapular ligament and supplies the supraspinatus and infraspinatus muscles.

Short after its origin, as it runs behind the clavicular head of the sternocleidomastoid, it gives off a branch that enters the muscle from its undersurface and supplies the most inferior part of it and a small area of the overlying skin. In the cases where this branch does not exist, a longer sternocleidomastoid branch of the superior thyroid artery or branches from the transverse or superficial cervical arteries undertake its blood supply (Kierner et al. 1999). The suprascapular artery gives off small branches that supply the inferior part of the platysma muscle and through these muscular perforators the overlying neck skin.

8.1.8 Superficial Veins of the Neck

A rich venal network is encountered at the neck, which as anywhere else in the human body is determined by great variability. The veins that are superficially located and involved in skin surgery are described below according to a classic anatomic approach (Fig. 8.14).

The facial vein after it crosses the lower mandibular border, situated below the mandibular branch of the facial nerve, enters the neck. After receiving the submental vein, it runs obliquely backward lying under the platysma and superficial to the external surface of the submandibular gland. The complex of the facial and submental veins at this area is of great importance in the survival of the submental island flap. Close to the angle of the mandible at a point anterior and inferior to it, the facial artery joins the anterior branch of the retromandibular (posterior facial) vein forming the common facial vein, which descends and near the greater cornu of the hyoid bone enters the internal jugular vein.

The posterior auricular vein coming from behind the auricle, near the angle of the mandible at a point below or sometimes within the parotis, joins the posterior branch of the retromandibular (posterior facial) vein forming the external jugular vein.

The external jugular vein descends crossing obliquely the sternocleidomastoid muscle. The vein is covered by the lateral border of the platysma in a variable degree.

Its axis corresponds to the line connecting the mandibular angle with the middle of the clavicle. At the root of the neck, close to scalenus anterior, it perforates the deep fascia and drains into the subclavian vein. The external jugular vein at its mid-third receives the posterior external jugular vein, a vessel that descends from the occipital region.

The anterior jugular vein arises at the lower part of the submental triangle and runs downward between the anterior border of the sternocleidomastoid and the median line. At the lower part of the neck, it turns laterally passing deep to the sternocleidomastoid muscle and joins the termination of the external jugular vein or opens directly into the subclavian vein.

8.1.9 Nerves

The superficially located motor nerves at the neck are the marginal and cervical branches of the facial nerve, and the accessory nerve. The sensory nerves are the greater auricular nerve, lesser occipital nerve, transverse cervical nerve, and supraclavicular nerves, all of which are the cutaneous nerves of the cervical plexus.

8.1.9.1 Motor Nerves

8.1.9.1.1 Facial Nerve

Marginal Mandibular Branch

The marginal mandibular branch of the facial nerve after it exits the parotid may be found below the inferior border of the mandible in a distance usually within 2 cm from it (Fig. 8.15). It lies beneath the platysma muscle, and its exact course through the neck fasciae is described in detail in Chap. 5. The facial nerve crosses the anterior facial vessels lying always superficially to them. Effort must be made to place incisions at least 3 cm below the inferior border so as to ensure the integrity of the marginal mandibular nerve.

Cervical Branch

The cervical branch originates from the cervicofacial trunk of the facial nerve.

It emerges from the lower pole of the parotid gland usually as a single branch (80 %) or as two branches (20 %) (Ziarah and Atkinson 1981). It continues running down and forward to the neck (Fig. 8.15). In contrast to the marginal mandibular branch that initially runs under the cover of the deep cervical fascia, the cervical branch pierces the fascia immediately after it exits the parotis (Owsley and Agarwal 2008).

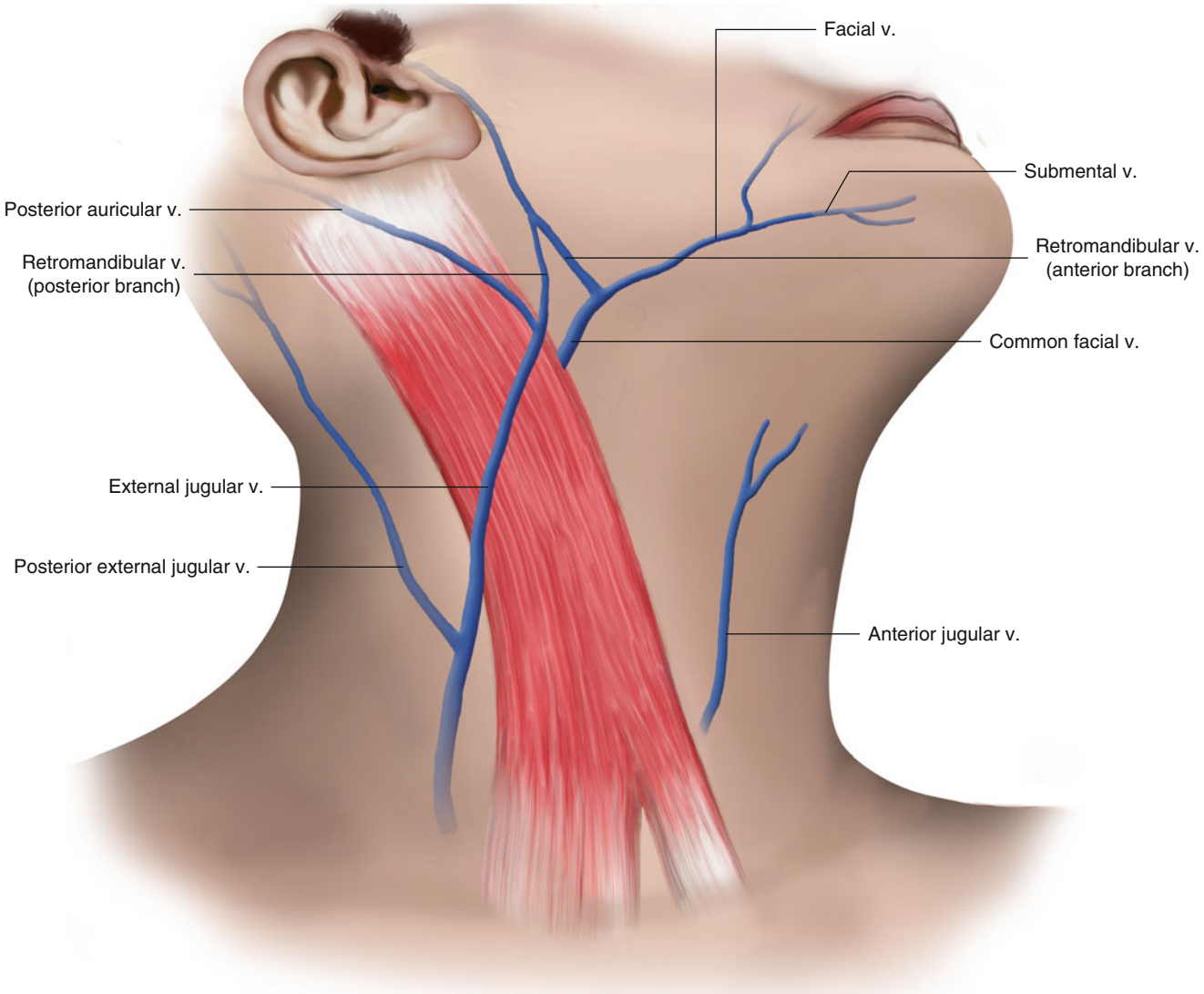

Fig. 8.14 The superficial veins of the neck

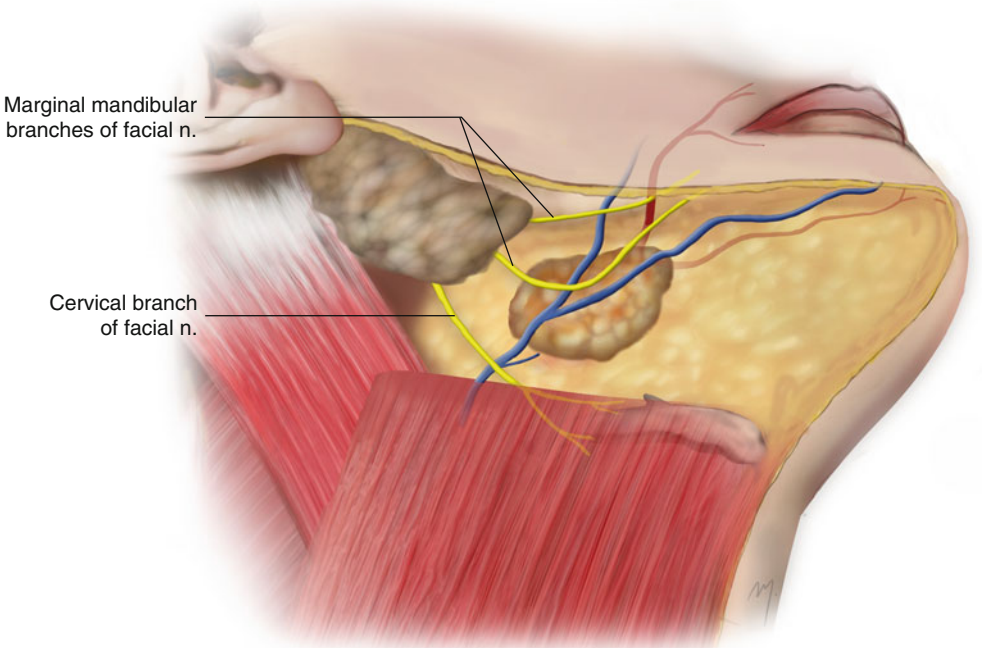

Fig. 8.15 The marginal mandibular and the cervical branch of the facial nerve at the neck

It runs under the cover of the platysma muscle, and at the level of the hyoid bone it usually divides into two to three subbranches that supply the platysma muscle. The cervical branch lies in its initial course approximately 8 mm posterior to the angle of the mandible, and as it runs at the submandibular area, it becomes situated at a distance of 15–45 mm from the inferior border of the mandible (Salinas et al. 2009). The cervical branch of the facial nerve communicates with the transverse cutaneous cervical nerve.

8.1.9.1.2 Accessory Nerve

The accessory nerve is considered as the XI cranial nerve. It originates in the cranium from the union of a cranial and a spinal root that unite for a short part of its course. The accessory nerve exits the skull from the jugular foramen and divides once again. The medial branch that corresponds to the cranial root is shorter and thinner and joins the vagus nerve superior to the inferior vagal ganglion. It participates in the innervation of the larynx and the soft palate.

The lateral branch that corresponds to the spinal root consists of motor fibers and is the largest and thicker branch. It runs inferiorly and posteriorly and passes anteriorly (in 75 %) or posteriorly (in 25 %) to the internal jugular vein. It crosses the transverse process of the atlas and descends medial to the styloid process. It enters the sternocleidomastoid muscle at the upper quadrant of its anterior border. It runs within the sternocleidomastoid substance and exits the muscle at the midpoint of its posterior border, which usually coincides with the area under the exit of the lesser occipital and above the exit of the great auricular. It continues at the posterior neck triangle from top to bottom and from front to rear and enters the trapezius muscle at its anterior border.

The accessory nerve usually is not in danger when raising a subcutaneous flap in the region of the posterior neck triangle. However, a subplatysmal dissection in inexperienced surgeons could risk inadvertent nerve injury. Useful landmarks to identify its peripheral portion and to protect it are (Fig. 8.16):

1. The accessory nerve emerges from the posterior margin of the sternocleidomastoid within 1.5–2.0 cm superiorly to Erb's point (see below).
2. The accessory nerve enters the trapezius muscle to the junction of the inferior one-third and the mid-third of the anterior border of the trapezius. This point corresponds to a distance of about 4 cm above the clavicle.

These two landmark points determine the zone within the nerve that travels in the posterior neck triangle.

8.1.9.2 Cutaneous Nerves (Cervical Plexus)

The ventral rami of the upper four cervical nerves (C1–C4) form the cervical plexus, which gives rise to deep muscular and communicating branches and superficial cutaneous branches. The cutaneous branches of the cervical plexus, the greater auricular nerve, the lesser occipital nerve, the transverse cervical nerve, and the supraclavicular nerves, arise in the neck radiating within 2 cm above or below Erb's point (Fig. 8.17). Each of the four cutaneous branches emerges separately in 50 % of the cases, whereas in the remaining, two or more neighboring branches may arise together at the same point before they separate (Kim et al. 2002a, b).

8.1.9.2.1 Lesser Occipital Nerve

The lesser occipital nerve receives fibers from the second cervical nerve (C2) and in a lesser degree from the third

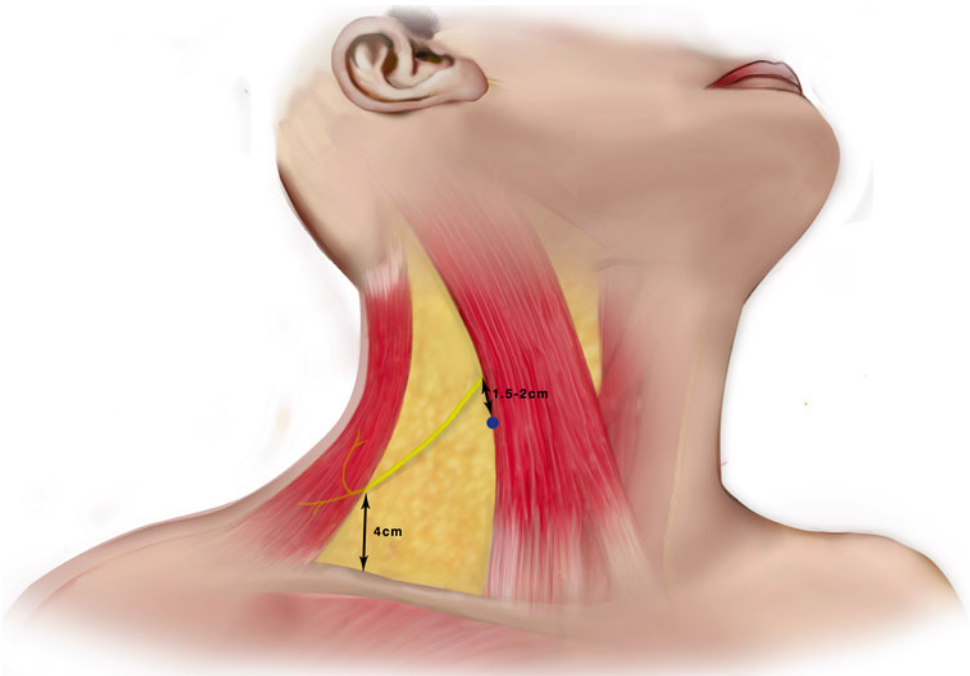

Fig. 8.16 Landmarks of the accessory nerve at the posterior neck triangle

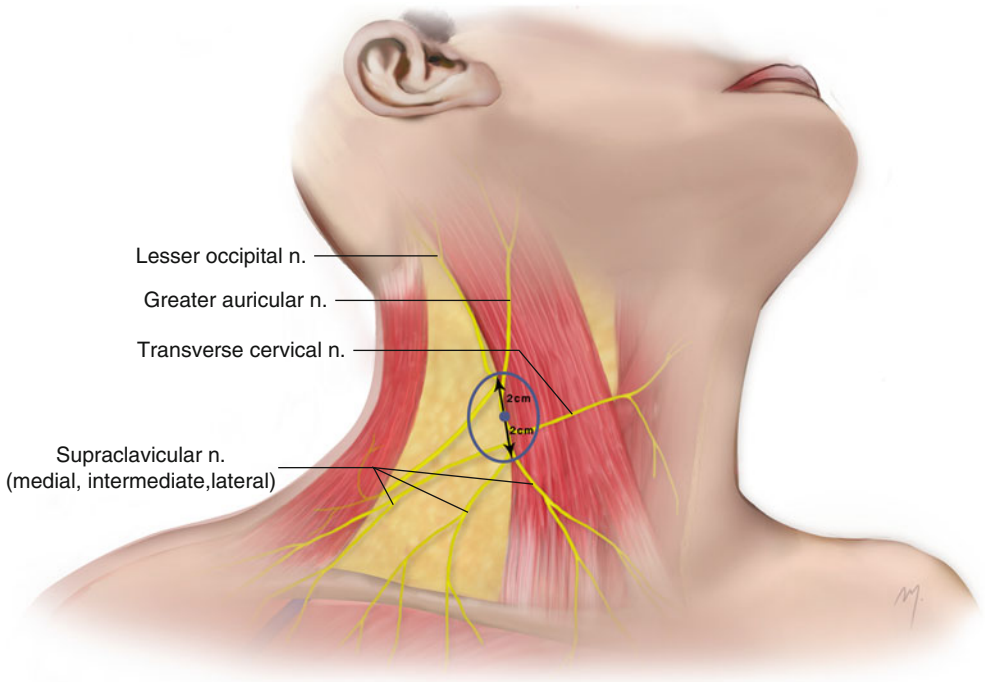

Fig. 8.17 The cutaneous branches of the cervical plexus radiating within 2 cm above and below to Erb's point

cervical nerve (C3). After emerging from the posterior border of the sternocleidomastoid muscle, it often winds around the accessory nerve and exits at a point above the exit point of the accessory nerve. It then runs ascending along the posterior margin of the sternocleidomastoid muscle. Traveling to the occipital area, near the cranium, it emerges from the deep fascia into the subcutaneous tissue to supply the skin of the lateral posterior part of the scalp. It anastomoses with the greater occipital, the great auricular, and the posterior auricular (facial nerve branch) nerves.

8.1.9.2.2 Greater Auricular Nerve

The greater auricular nerve receives fibers from the second (C2) and the third (C3) cervical nerves. It emerges as the rest of the cutaneous nerves from the posterior border of the sternocleidomastoid muscle. It pierces the deep fascia, forms a circle around the posterior muscle border, and ascends traveling on its lateral aspect and crossing to its mid. In this initial part of its course, it usually lies beneath the platysma and in proximity to the external jugular vein. As it reaches the lower pole of the parotis, it divides into an anterior and a posterior branch. The anterior branch innervates the skin over the parotid region and anastomoses in the gland with the facial nerve (Standring 2008). The posterior branch travels behind the ear lobule to supply the skin of the mastoid process and the posterior aspect of the auricle (see Chap. 2). Cutaneous filaments supply, with a variable extent, the skin over the upper third of the sternocleidomastoid muscle and over the posterior part of the submandibular triangle.

8.1.9.2.3 Transverse Cervical Nerve

The transverse cervical nerve receives, as the great auricular nerve, fibers from the second (C2) and the third (C3) cervical nerves. After it emerges from the sternocleidomastoid, in the level of its midpoint, it curves around its posterior border, perforates the deep fascia, and runs transversely over the surface of the sternocleidomastoid to its anterior border. It is situated deep to platysma muscle and deep to the external jugular vein. Near the anterior border of the sternocleidomastoid, it divides into ascending and descending branches.

The ascending branches perforate the platysma and distribute to the skin of the submandibular, the submental, the carotid, and the upper half of the muscular triangles. Some filaments communicate with the cervical branch of the facial nerve and form a plexus under the platysma (Standring 2008). The descending branches, after they perforate the platysma, distribute to the skin of the lower half of the muscular triangle and the anterolateral part of the neck.

8.1.9.2.4 Supraclavicular Nerves

The supraclavicular nerves arise as a common trunk that is formed of fibers from the third (C3) and fourth (C4) cervical nerves. The common trunk of the supraclavicular nerves short after it emerges from the posterior border of the muscle divides into three branches: medial, intermediate, and lateral. These three branches descend, diverging, in the posterior neck triangle, and short before the clavicle, they pierce the deep cervical fascia and the platysma, become subcutaneous, and distribute to the upper part of the deltopectoral region.

The medial supraclavicular nerves descend medially and cross over the external jugular vein and the clavicular and sternal heads of sternocleidomastoid. They supply the skin of the medial part of the upper thoracic region. The intermediate supraclavicular nerves descend, cross the clavicle, and supply the skin of the middle and lateral part of the upper thoracic region. The lateral supraclavicular nerves descend laterally, across the outer surface of the trapezius muscle and the acromion, and distribute to the skin of the upper and posterior part of the shoulder. There is always an overlapping of all of the terminal rami of the supraclavicular branches.

8.2 Flaps Derived from the Neck

The cervical skin serves as an abundant source of flap material that can be transferred to cover large facial defects. The regional neck flaps provide skin quite similar in color, texture, and thickness regarding the skin of the lateral face and must be the first choice when a local flap is not sufficient to reconstruct a sizeable defect.

8.2.1 Flap Design Concerning Vascular Anatomy

Summarizing the previous detailed anatomic description, the skin of the neck is vascularized from top to bottom as follows (Fig. 8.18). The neck branches of the posterior auricular artery supply the skin of the uppermost sternocleidomastoid area. Musculocutaneous perforators of the upper and lower sternocleidomastoid branches of the occipital artery supply the skin of the upper third of the sternocleidomastoid area. Direct cutaneous branches of the facial and submental arteries supply the skin over the submandibular and the submental triangle. A large area of skin of the anterior and lateral part of the mid-third of the neck is supplied by musculocutaneous perforators of the infrahyoid and sternocleidomastoid branches and mainly by the direct cutaneous perforator of the superior thyroid artery. The posterior part of the skin of the mid-third of the neck is mainly supplied by musculocutaneous branches of the superficial cervical/transverse cervical artery. The skin of the most anteriorly lower part of the neck is supplied by perforators of the muscular branches of the inferior thyroid artery. The

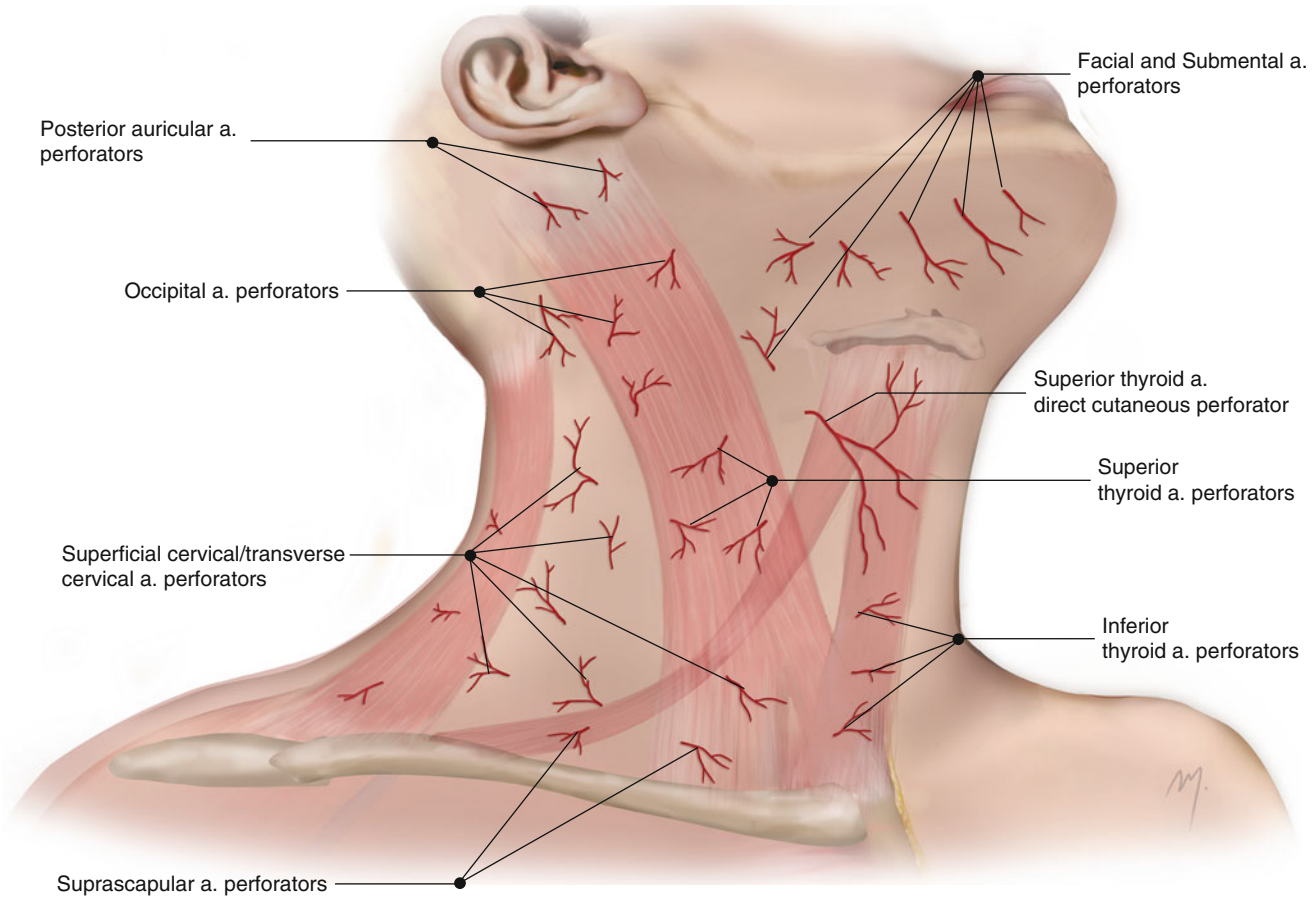

Fig. 8.18 Arteries that supply the skin of the neck through direct cutaneous or musculocutaneous perforators

middle and lateral part of the lower neck is mainly supplied by musculocutaneous perforators of the superficial cervical/transverse cervical artery, while the suprascapular artery contributes to the supply of a small area of the midportion of the lower part of the neck through its sternocleidomastoid and the platysmal branches.

All of these branches form a large anastomotic network that communicates with the contralateral at the midline ensuring also retrograde flow. Almost all of the cervical cutaneous flaps are random pattern flaps and must be designed with a wide base that ensures adequate perfusion from as more as possible of perforators.

8.2.2 Cervicofacial Flap

The cervicofacial flap is a rotation advancement flap, which is used for reconstruction of large lateral or medial cheek defects. It consists of a facial and a cervical part. Depending on the location and the size of the defect, the proportion of the facial to the neck part is changing. The higher a defect lies, the grater the facial part is and vice versa.

In the patient presented in Fig. 8.19a, a preauricular basal cell carcinoma is planned to be excised and the defect reconstructed by a cervicofacial flap. The excision lines are outlined and the defect is triangulated. Flap line starts as an extension of the inferior excision line, curving around the lobule to the postauricular area. It then runs inferomedially ending into a neck crease (Fig. 8.19b). The level of the inferior flap line into the neck determines the portion of the neck skin of the flap and is defined by the size and location of the defect as already mentioned but also by the laxity of the neck skin. A small Burow's triangle is outlined at the point where a standing cone usually is formed.

The lesion was excised in clear margins revealed by frozen section biopsies (Fig. 8.19c). A portion of the ear lobule had to be sacrificed. After wide and adequate undermining, the flap can reach and close the defect without tension (Fig. 8.19d, e). The result is excellent as long as most of the scar lines lie within natural creases (Fig. 8.19f).

8.2.3 Deep-Plane Cervicofacial Flap

In patients with microcirculation deficiency, smokers, diabetics, or those who had a prior radiation therapy, there is always a great risk of flap necrosis especially in large random pattern flaps. In such cases, flap vascularity enhances when it is raised in a deep (sub-SMAS plane). The facial part of the deep plane cervicofacial flap is raised (as already described at Chap. 5), and the cervical part is elevated beneath the platysma muscle, as the platysma constitutes the SMAS component at the neck. Moreover, when a deep surgical defect is produced, the deep-plane dissection provides a thicker flap that reconstructs more efficiently the facial contour.

Such a patient is presented, in whom the defect that is produced by the excision of a lesion was reconstructed by a deep-plane cervicofacial flap (Fig. 8.20a–h).

8.2.4 Cervical Rotation Flap Anteriorly Based

In the patient presented, an ulcerative basal cell carcinoma was located at the parotidomasseteric area. A cervical rotation flap anteriorly based was planned to reconstruct the defect (Fig. 8.21a, b). In a posteriorly located defect, the cervical rotation flap is based anteriorly and vice versa. The laxity of the neck tissues determines the length of the arc of the flap. Usually (especially in elderly patients with relaxed skin), an arc of a length three times the width of the defect is sufficient.

The tumor was excised in clear margins, and the flap was raised incorporating the investing layer of the deep cervical fascia to enhance its vascularity (Fig. 8.21c, d). The flap was rotated covering the defect without tension, and a satisfactory postoperative result was gained (Fig. 8.21e, f).

8.2.5 Cervical Rotation Flap Posteriorly Based

Unlike the previous case when a defect of the lower face is anteriorly located and an adjacent cervical rotation flap is chosen for reconstruction, this must be based posteriorly.

The patient presented in Fig. 8.22a had a large basal cell carcinoma of the lower buccal region extended to the chin. A rotation flap from the adjacent neck was designed with its base posteriorly (Fig. 8.22b, c). The length of the arc of the flap was slightly more than three times of the width of the defect. Its inferior limb was turned to a more horizontal direction placed within a natural neck crease. The lesion was excised, and the flap was elevated in a deep plane, brought without tension to the defect and sutured in place (Fig. 8.22d–g). The postoperative result is excellent (Fig. 8.22h).

8.2.6 Submental Transposition Flap

The submental flap is a transposition laterally based flap that transfers adjacent matching submental neck skin to cover defects of the entire chin.

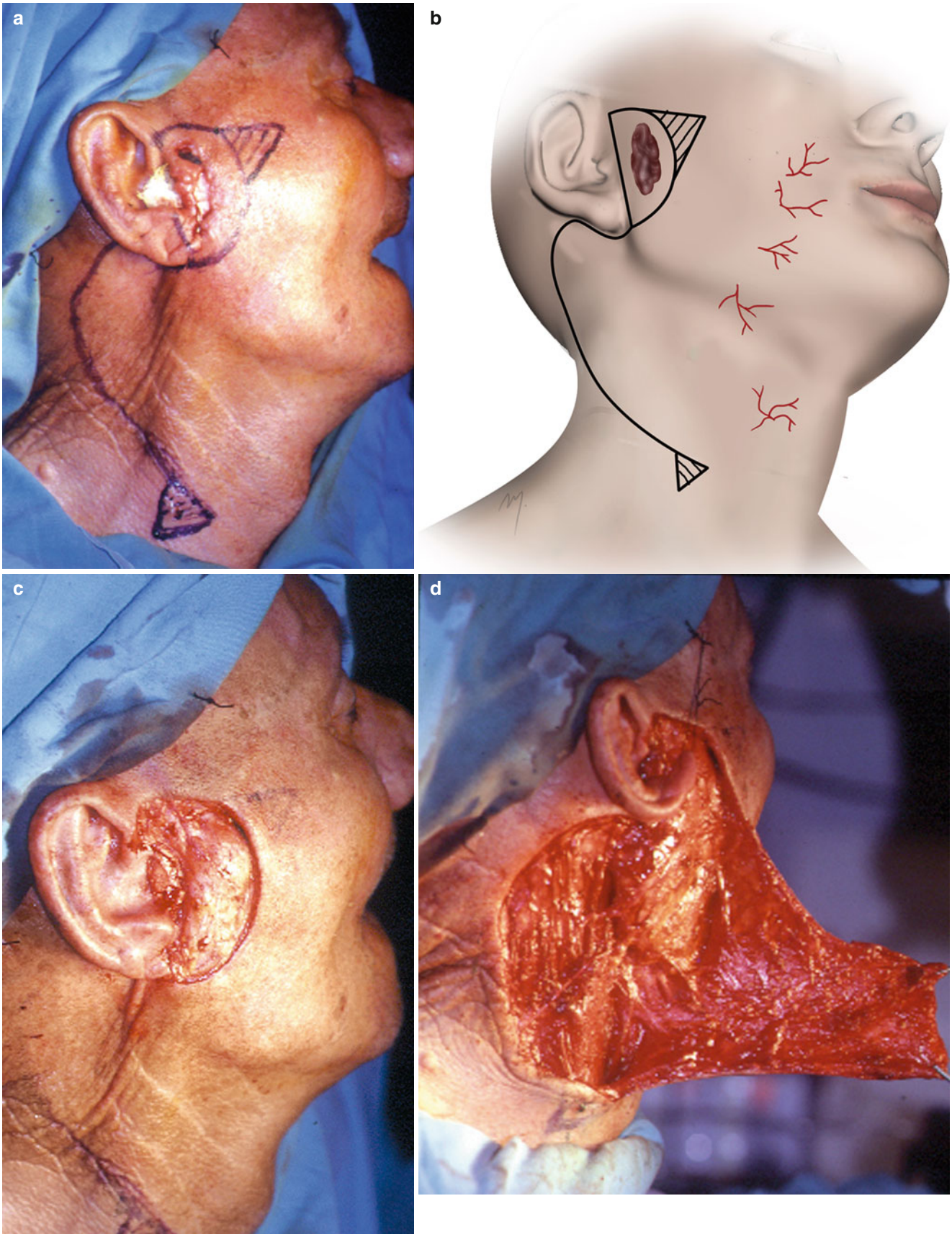

Fig. 8.19 (**a**, **b**) Excision line and cervicofacial flap outlined. (**c**) The cheek defect after excision of the lesion. (**d**) Cervicofacial flap elevated. (**e**) Immediate postoperative view. (**f**) Postoperative result at 6 months

Fig. 8.19 (continued)

The patient presented in this case had a recurrent basal cell carcinoma of the mental region. Almost the entire chin skin needs to be excised, and the defect resurfaced by adjacent cervical skin of the submental area (Fig. 8.23a, b). A transverse submental flap is outlined extending beyond the midline. It can be based laterally either to the left or to the right side. The flap is a random pattern flap and must be designed with a maximal 3:1 ratio of length to width, and as well its width must permit direct closure of the donor site. A large Burow's triangle is outlined and is to be excised at the lateral defect margin to the side of the flap base, so as to prevent a standing cone formation when the flap will be transposed. After tumor excision, the flap was raised below the platysma muscle (Fig. 8.23c). The submental flap reached the defect without tension and is sutured in place, and the donor site was closed with ease by motivating the mid-neck skin (Fig. 8.23d, e).

The reconstruction maintains the color, texture, and hair growth but slightly flattens the convex contour of the chin (Fig. 8.23f).

8.2.7 Submental Artery Island Flap

The submental artery island flap is a relatively new axial flap based in the submental artery and was first described by Martin et al. in 1993. The flap provides skin from the submental region that matches in color and texture to the facial skin and is supple enough, with a large arc of rotation and donor site that can be closed primarily.

The patient seen in Fig. 8.24a had a recurrent basal cell carcinoma of the cheek. The tumor was nodular in nature and deeply invasive. This would create not only a wide but also a deep surgical defect. The appropriate flap had to be supple and provide not only cover but also enough bulk to restore the contour of the cheek.

A submental artery island flap was chosen for the reconstruction (Fig. 8.24b, c). Initially, the angle and the lower border of the mandible are marked, and the courses of the facial and submental arteries are outlined. The flap is then designed in the submental area in an elliptical fashion long enough to reach the defect (the flap can cross the midline up to the opposite mandibular angle). The superior limit is drawn just below the mandibular border. The position of the inferior limit depends on the needed flap width but must be assessed that it is within a range that permits direct closure of the donor site. The tumor was excised in clear margins revealed by frozen section biopsies leaving a wide and deep surgical defect (Fig. 8.24d, e). The flap provides the necessary tissue bulk to reconstruct the cheek contour. Dissection starts from the distal part and is carried down through the

platysma muscle until the anterior belly of the opposite digastric muscle is reached. It then proceeds over its outer surface (Fig. 8.24f). When the anterior belly of the ipsilateral digastric muscle is found, it is detached and included to the flap dissecting in the plane deep to it. By this maneuver, the submental artery running either deep or superficial to the

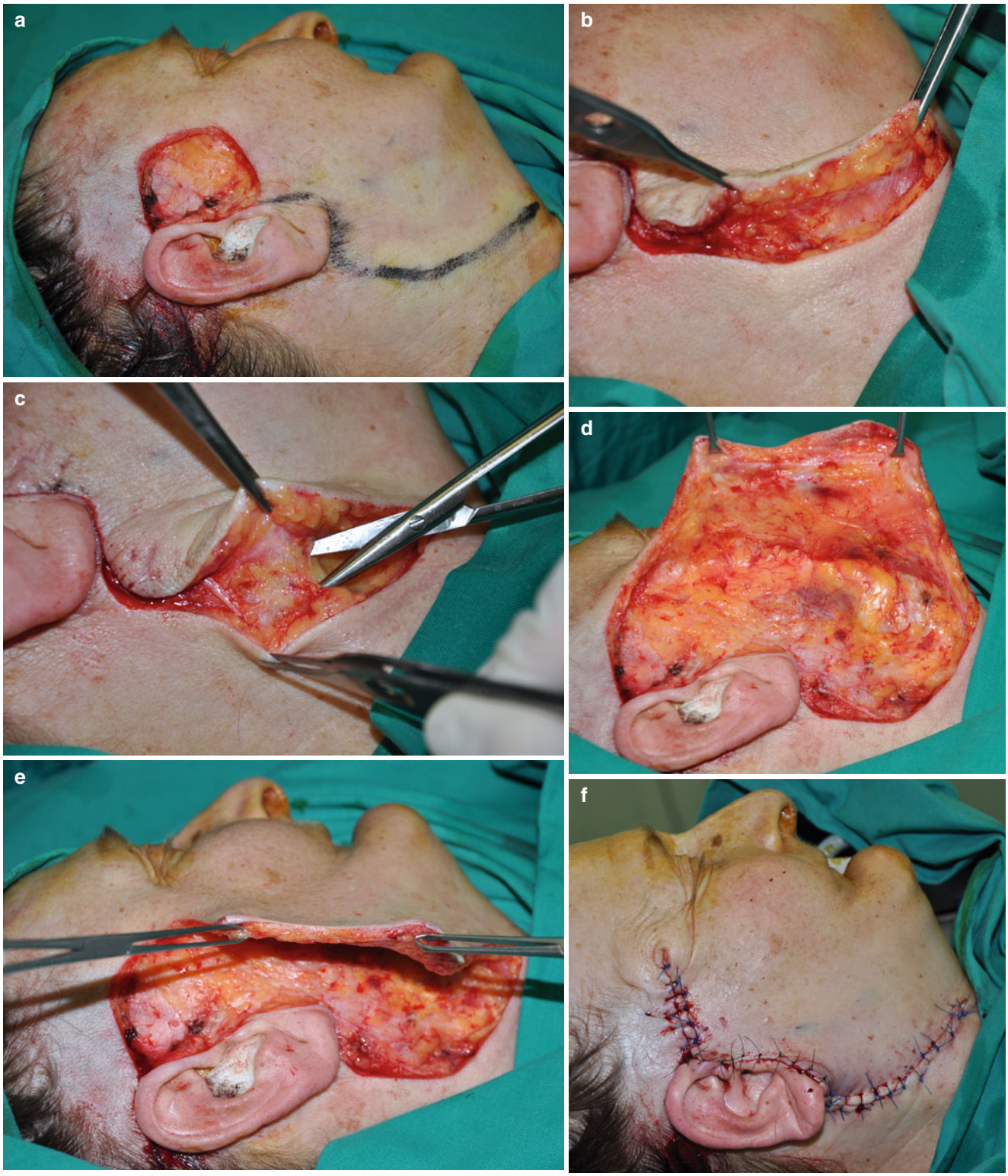

Fig. 8.20 (**a**) A deep-plane cervicofacial flap planned. (**b**) Exposure of platysma. (**c**) Transected platysma muscle. (**d**) Sub-SMAS elevation of the flap. (**e**) A thick flap is raised. (**f**) Immediate postoperative view. (**g**, **h**) Result at 3 months

Fig. 8.20 (continued)

anterior belly is caught within the flap. Special care is taken in the preservation of the mandibular branch of the facial nerve. Afterward, the flap is separated from the outer surface of the submandibular gland. Dissection proceeds to the origin of the submental vessels (Fig. 8.24g). The narrow pedicle includes the submental artery and vein at the point where they branch from the corresponding facials. A cuff of tissue must be maintained so as to protect them (Fig. 8.24h). The skin over the narrow bridge that comes in between the flap and the defect was striped, and the flap is sutured in place (Fig. 8.24i, j). The donor site was closed primarily by advancing neck skin (Fig. 8.24k). The postoperative result at 3 months is very satisfactory, and the contour of the cheek is completely restored (Fig. 8.24l, m).

8.2.8 Platysma Myocutaneous Flap (PMF)

The principle of transferring neck skin with the underlying platysma was first described by Robert Gersuny, an Austrian surgeon in 1887. Gersuny (1887) rotated a skin-platysma flap to reconstruct a full-thickness defect of the cheek. This initial idea reappears much later, when Futrell et al. (1978) describe the platysma island flap in cases of intraoral reconstruction, which did not gain widespread acceptance as at the same time Ariyan (1979) introduced the pectoralis major musculocutaneous flap that became the "first choice" flap in head and neck reconstruction. A platysma-based clavicular island flap, according to the same principles, had, since 1970, already started to be performed by Tessier but remained unpublished. He was inspired by the former experience of Barron and Emmett with island flaps, and the flap was termed as the Barron-Tessier flap (Tessier et al. 2011).

Three potential designs of the PMF based on the source of the platysma blood supply are available (Coleman et al. 1982, 1983; Ariyan 1997, 2003; Baur and Helman 2002): (a) the superiorly based flap with arterial blood supply from the submental branch of the facial artery, (b) the inferiorly based flap with arterial blood supply from the transverse cervical artery, and (c) the posteriorly based flap with arterial blood supply from occipital and posterior auricular arteries.

The superiorly based version and the posteriorly based flap have been used mainly in oropharyngeal defects, while inferiorly based flap obviously has no application in head and neck reconstruction. The matter concerning the survival of the superiorly based platysma muscle flap when ligating the facial artery, a standard procedure of the neck dissection in level 1, has been controversial. There are reports which state that it is not possible to use the platysma muscle in combination with neck dissection due to the increased flap lost when the facial artery has been transected (Coleman et al. 1982, 1983; Conley et al. 1986). On the contrary, based on the anatomic observation that the most significant vascular supply to the superiorly based platysma flap comes

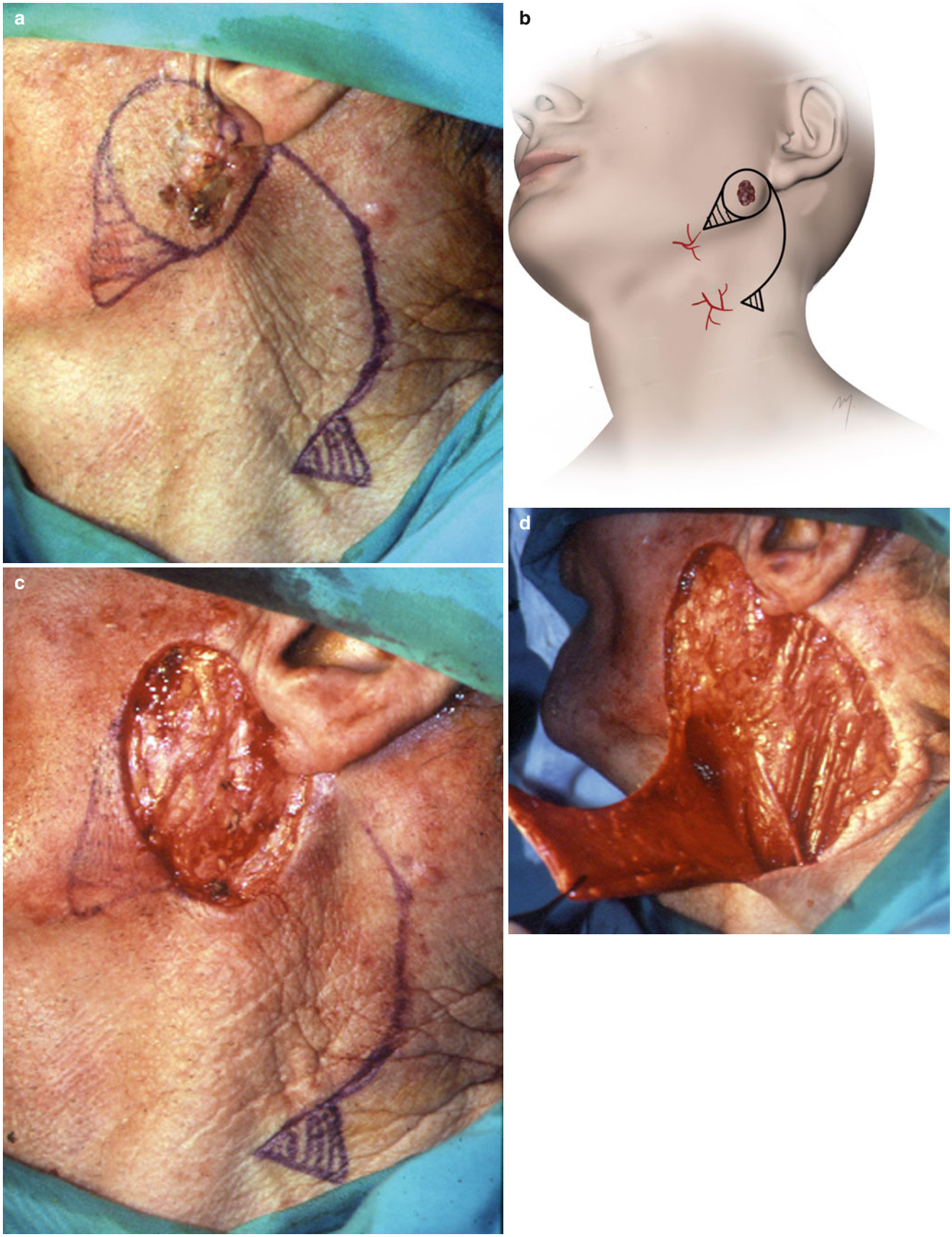

Fig. 8.21 (**a**, **b**) Outline of the area to be resected and of the anteriorly based cervical rotation flap. Two Burow's triangles will be excised. (**c**) Tumor excised. (**d**) Flap incorporates the investing layer of the deep cervical fascia. (**e**) Flap sutured in place. (**f**) Postoperative result at 1 year

Fig. 8.21 (continued)

through the submental artery, so as an intact facial artery is not crucial to its vascularization (Hurwitz 1983), it has been stated that ligation of the facial artery (leaving the submental artery intact) does not enhance the incidence of flap necrosis, due to the retrograde flow that occurs from the distal submental arterial anastomosis either to the ipsilateral and contralateral lingual artery, mental artery, inferior labial artery, or contralateral or submental artery (Lasjaunias et al. 1979; Rabson et al. 1985; McGuirt et al. 1991; Ruark et al. 1993; Uehara et al. 2001; Koch et al. 2012).

The patient shown in Fig. 8.25a had a (malignant tongue ulcer) squamous cell carcinoma of the tongue, probably developed by the chronic traumatic injury of the upper canine and N_0 neck. A glossectomy via a paramedian mandibulotomy approach, supraomohyoid neck dissection, and reconstruction with a superiorly based island platysma flap is planned (Fig. 8.25b).

The proposed skin island is outlined, usually in elliptical form, at the base of the lateral neck, inferior to the apron approach outline. Its size is designed according to the anticipated defect that will result from the excision of the primary lesion. The exact position lies at a level that provides adequate length of the pedicle to be folded around the inferior border of the mandible bringing the skin paddle intraorally. In male patients, the skin paddle may be located even lower where the skin is bare of hair. The island incision line is incorporated to the apron flap outline via a small vertical incision (Fig. 8.25c). It is very important for the survival of the skin island not to be smaller than 4×2 cm in diameter so as to include enough perforating vessels from the platysma muscle to the skin surface (Coleman et al. 1982; Uehara et al. 2001).

Skin incision starts from the horizontal limb of the apron flap, at the level just superficial to platysma muscle (Fig. 8.25d).

Dissection is carried out sharply with a scalpel continuing cephalad, and the apron flap is elevated at the subdermal (or supraplatysmal) level (Fig. 8.25e). At the lateral border of the platysma muscle, the external jugular vein is found and preserved. If platysma muscle extends over and beyond the external jugular vein, this should be ligated distally and raised with the flap being incorporated to it. At the medial border, the anterior jugular vein may also be found and whenever possible included to the flap.

Cephalic dissection ends just below the inferior border of the mandible. Skin incision is then made around the skin paddle with additional exposure of the platysma of at least 1 cm around the skin island (Fig. 8.25f).

The platysma muscle is then transected 1 cm inferior to the edge of the skin paddle, and the free edges of platysma and skin are sutured together. Dissection proceeds now cephalad in the subplatysmal plane, including the investing layer of the deep cervical fascia and the fat lying deep to the platysma (deep adipofascial tissue) up to the inferior border of the mandible. The width of the flap pedicle corresponds to the full width of the platysma muscle. Special care is given at this point to the marginal mandibular branch of the facial nerve as it crosses deep to the platysma muscle. After the dissection is completed, the flap is fully mobilized transferring the skin paddle at its caudal part (Fig. 8.25g).

The flap is raised and supraomohyoid neck dissection performed. During neck dissection, the facial vessels are ligated. The primary lesion is approached through a paramedian mandibulotomy, and en bloc resection of the primary tumor along with the neck dissection specimen is performed (Fig. 8.25h). The platysma flap is rotated 180°, folded around the inferior border of the mandible, and transferred intraorally to reconstruct the tongue defect (Fig. 8.25i).

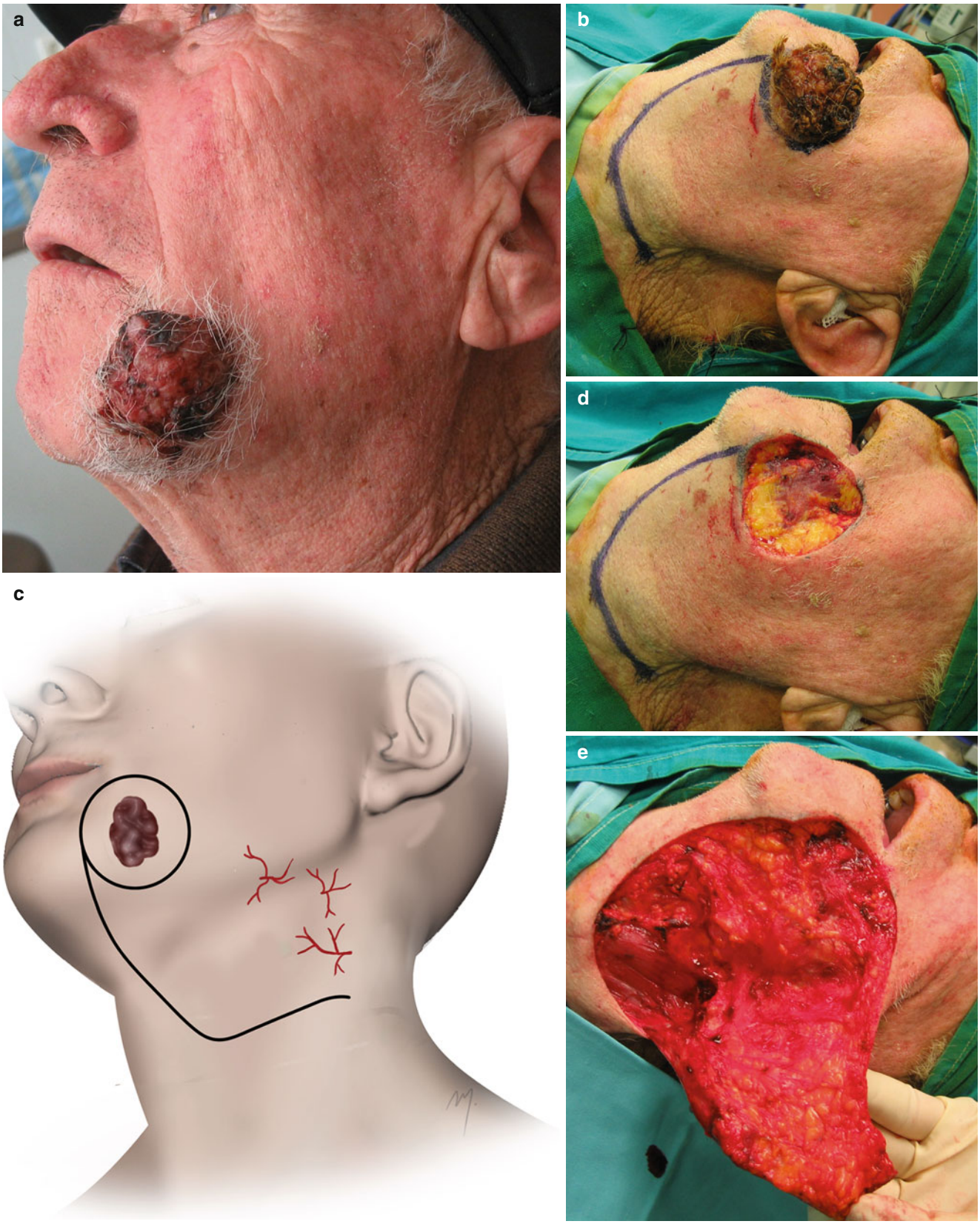

Fig. 8.22 (**a**) A lesion of the lower buccal region extended to the chin. (**b**, **c**) Flap outlined. (**d**) The lesion excised. (**e**) The flap elevated. (**f**) The flap reaches the defect without tension. (**g**) Positioning sutures. (**h**) Postoperative result

Fig. 8.22 (continued)

The paramedian mandibulotomy site is reconstructed with titanium mini plates and screws (Fig. 8.25j). The adequate flap pedicle length allows the skin island to reach the recipient site without stretching the flap and be sutured without tension (Fig. 8.25k, l). The surgical wounds are sutured, and the donor site is closed primarily with minor supraclavicular skin advancement. The postoperative result at 6 months shows a functional reconstruction (Fig. 8.25m, n) and satisfactory healing of the donor site (Fig. 8.25o, p).

The platysma flap has been "accused" of having increased complication rates, but these are similar compared to those of the pectoralis myocutaneous flap (Szudek and Taylor 2007). The most common complication is the partial necrosis of the skin island. The main reason for this is usually obstruction of venous drainage. So far as elevation and rotation of the superiorly based platysma flap abolish most of the anterior venal draining system, the main venous drainage of the flap is through the submental veins and with contribution of the external and anterior jugular vein, which whenever possible must be preserved and included to the flap in order to optimize the venous outflow. Venous obstruction is also prevented when the flap passes through a wide tunnel that does not compress the pedicle and is sutured to the recipient site without stretching and tension. Even if partial epidermolysis of the skin paddle occurs, the underlying platysma muscle remains viable, and, with bedside debridement, the flap re-epithelializes very quickly by secondary intention.

The platysma myocutaneous flap is an alternative regional reconstruction solution for relatively small- and midsized defects (up to 70 cm^2) in the head and neck area. It is a thin, pliable flap, and a second donor site is not required when it is combined with neck dissection, because it is easily obtained from the same operative field.

Apart from covering mucosal defects as the previous examples, it can be used in a variety of facial skin defects also based in the same operative principles.

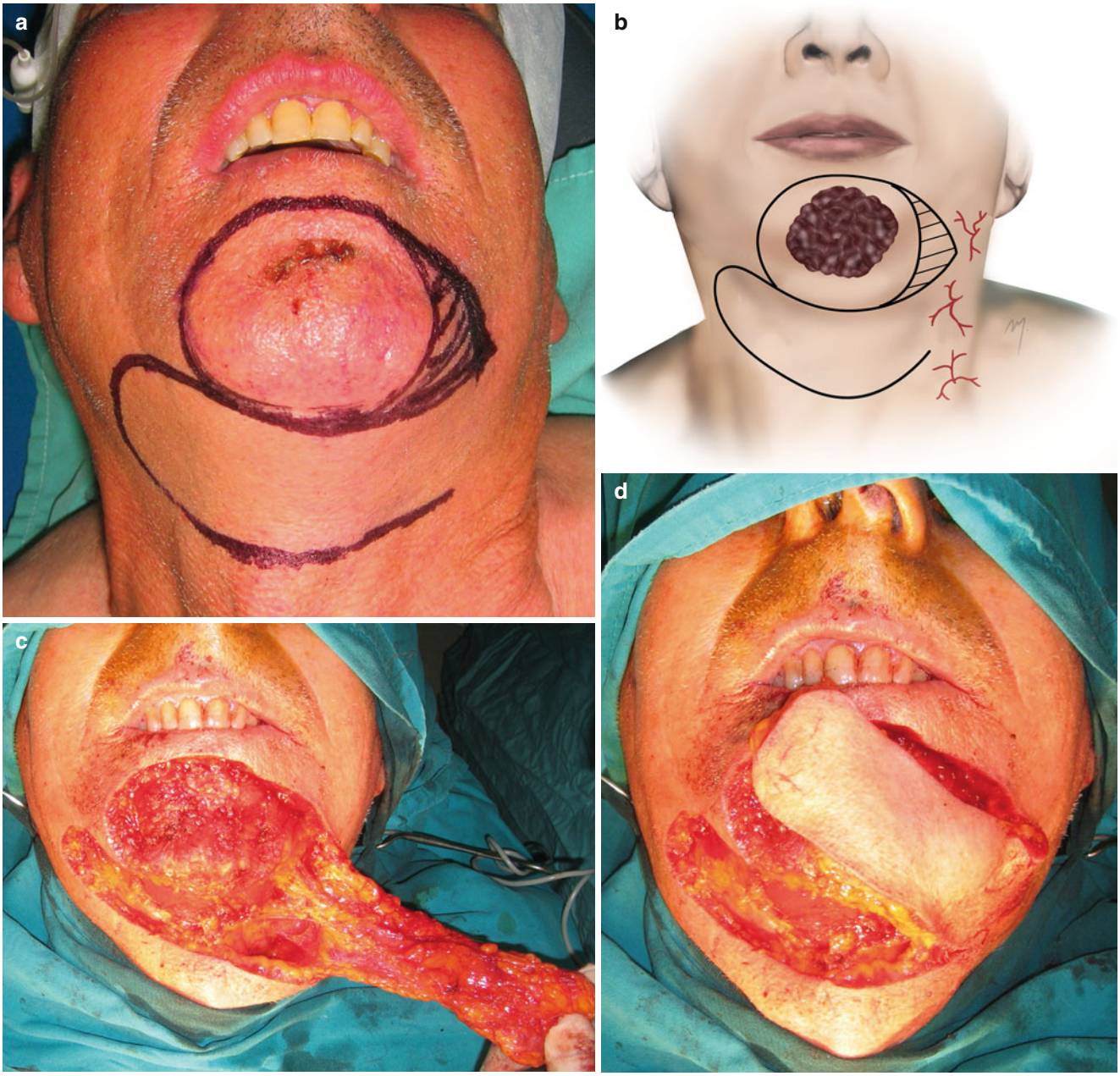

Fig. 8.23 (**a**, **b**) Flap outlined. (**c**) Flap raised in a subplatysmal plane. (**d**) Transferred to the recipient site. (**e**) The flap sutured in place. (**f**) Appearance at 3 months postoperatively

Fig. 8.23 (continued)

Fig. 8.24 (**a**) Deep invasive recurrent basal cell carcinoma of the cheek. (**b**, **c**) The angle and the lower border of the mandible are marked. The area of proposed excision and the submental artery flap are outlined with dotted lines. The submental artery as it branches from the facial artery is included in the flap. (**d**) The defect after excision of tumor. The tumor was excised to the level of the peripheral branches of the facial nerve. (**e**) The buccal branch of the facial nerve is pointed. (**f**) Incisions are made through skin and platysma down to the anterior bellies of the digastric muscles. (**g**) Flap elevation completed. The anterior belly of the ipsilateral digastric muscle is included in the flap. (**h**) The narrow pedicle of the flap. (**i**) Flap inserted into position after the skin over the narrow bridge was stripped. (**j**) Closure of the defect. (**k**) Closure of the donor site. (**l**, **m**) Result at 3 months. Cheek contour fully restored

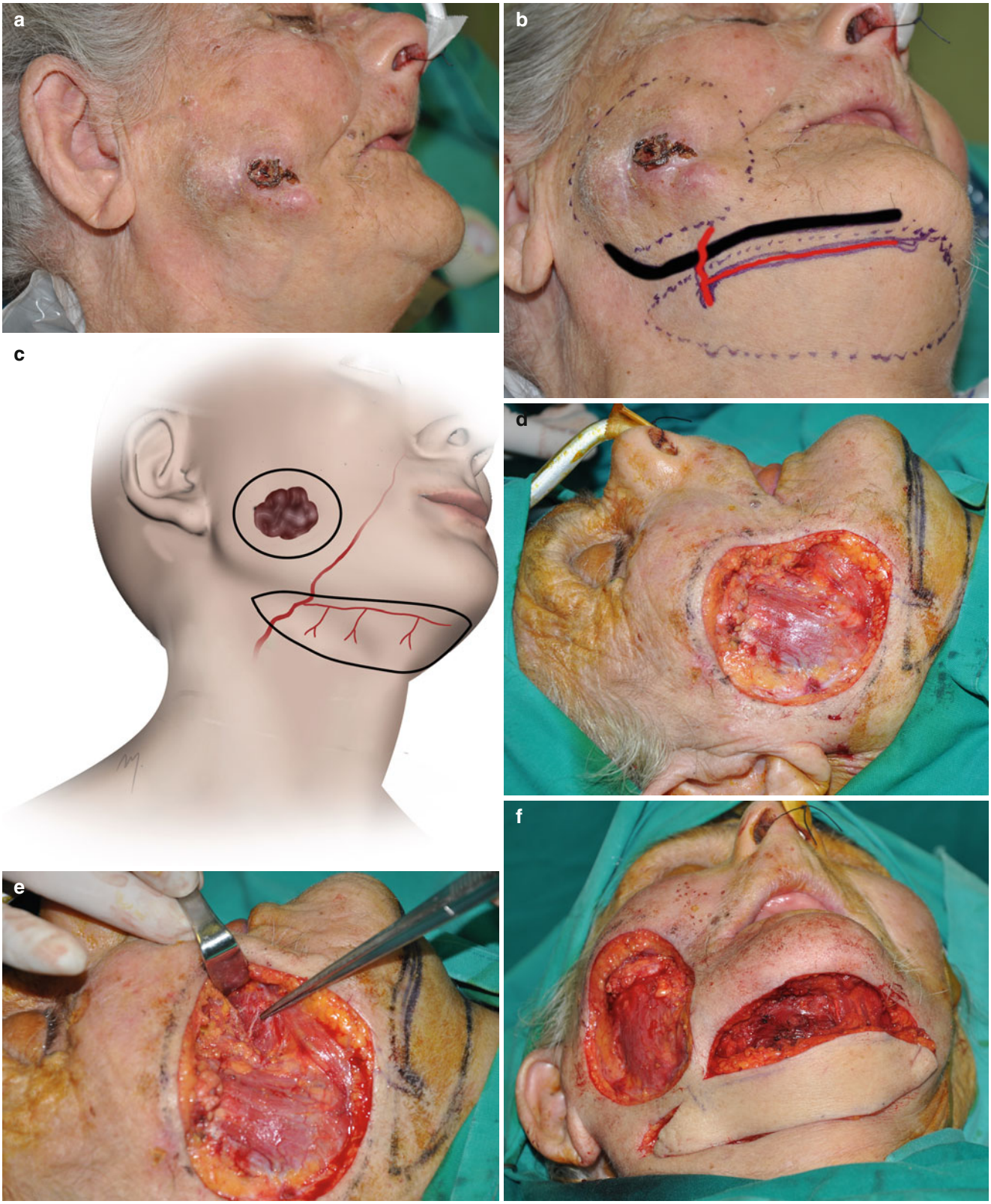
a
b
c
d
e
f

Fig. 8.24 (continued)

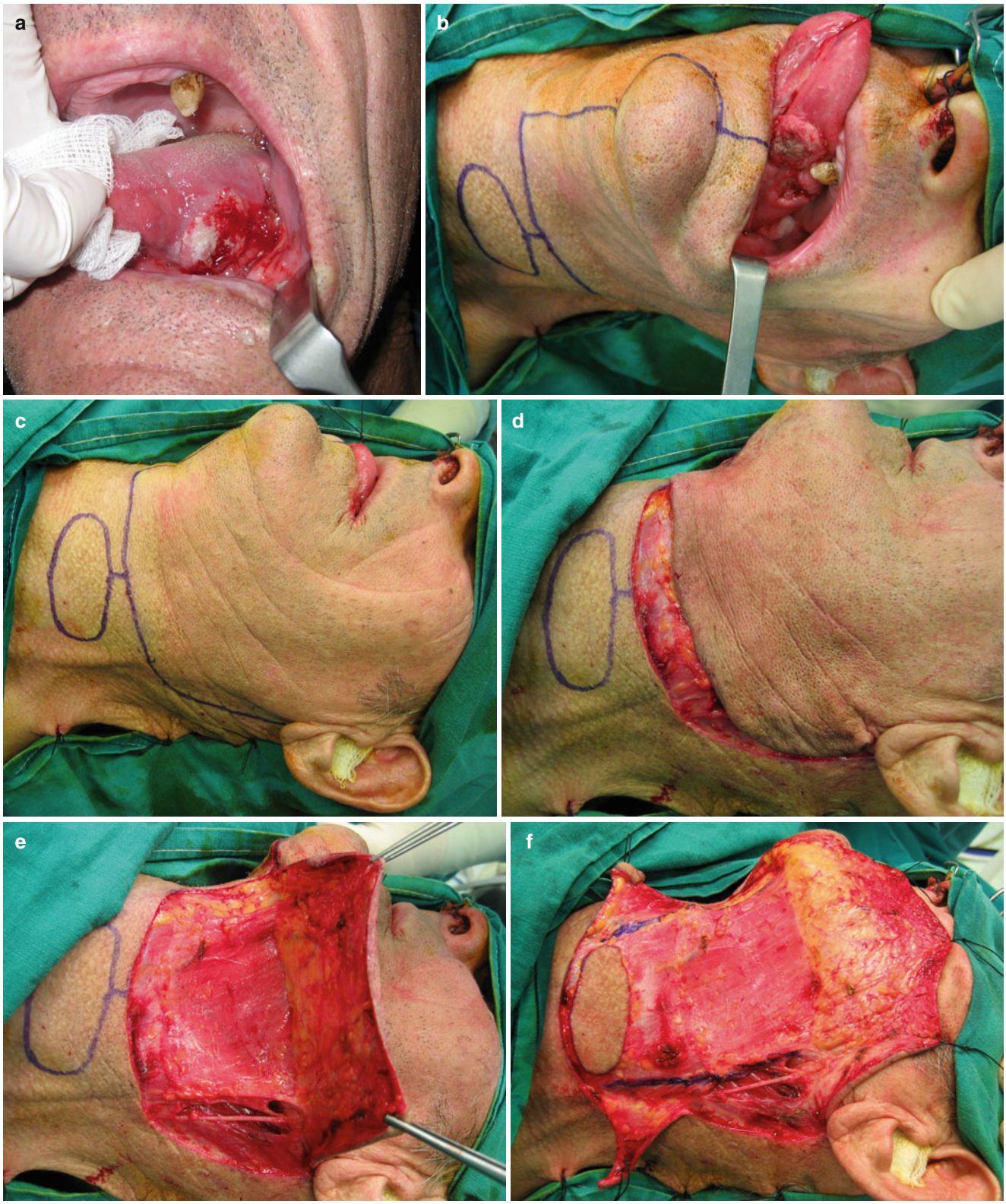

Fig. 8.25 (**a**) Squamous cell carcinoma of the lateral aspect of the tongue in its middle third. (**b**) The incision for mandibulotomy, the apron flap incision for the neck dissection, and the skin paddle are outlined. (**c**) Skin paddle incision is outlined and incorporated to the overall incision design. (**d**) Skin incision is made just superficial to the platysma muscle. (**e**) Elevation proceeds at the supraplatysmal level. The external jugular vein is found at the lateral platysma border and preserved. (**f**) Platysma muscle is fully exposed and also beyond the skin paddle. (**g**) The superiorly based island platysma flap is fully mobilized. (**h**) Access to the primary lesion via a paramedian mandibulotomy allows for a glossectomy in continuity with a supraomohyoid neck dissection in a monobloc fashion. (**i**) The platysma flap is folded around the inferior border of the mandible, and the transferred skin paddle is sutured in place. (**j**) Mandibular fixation is completed. (**k, l**) Immediate postoperative view of the reconstructed glossectomy defect. (**m–p**) Postoperative result at 6 months (From: Thomaidis et al. (2006), with permission)

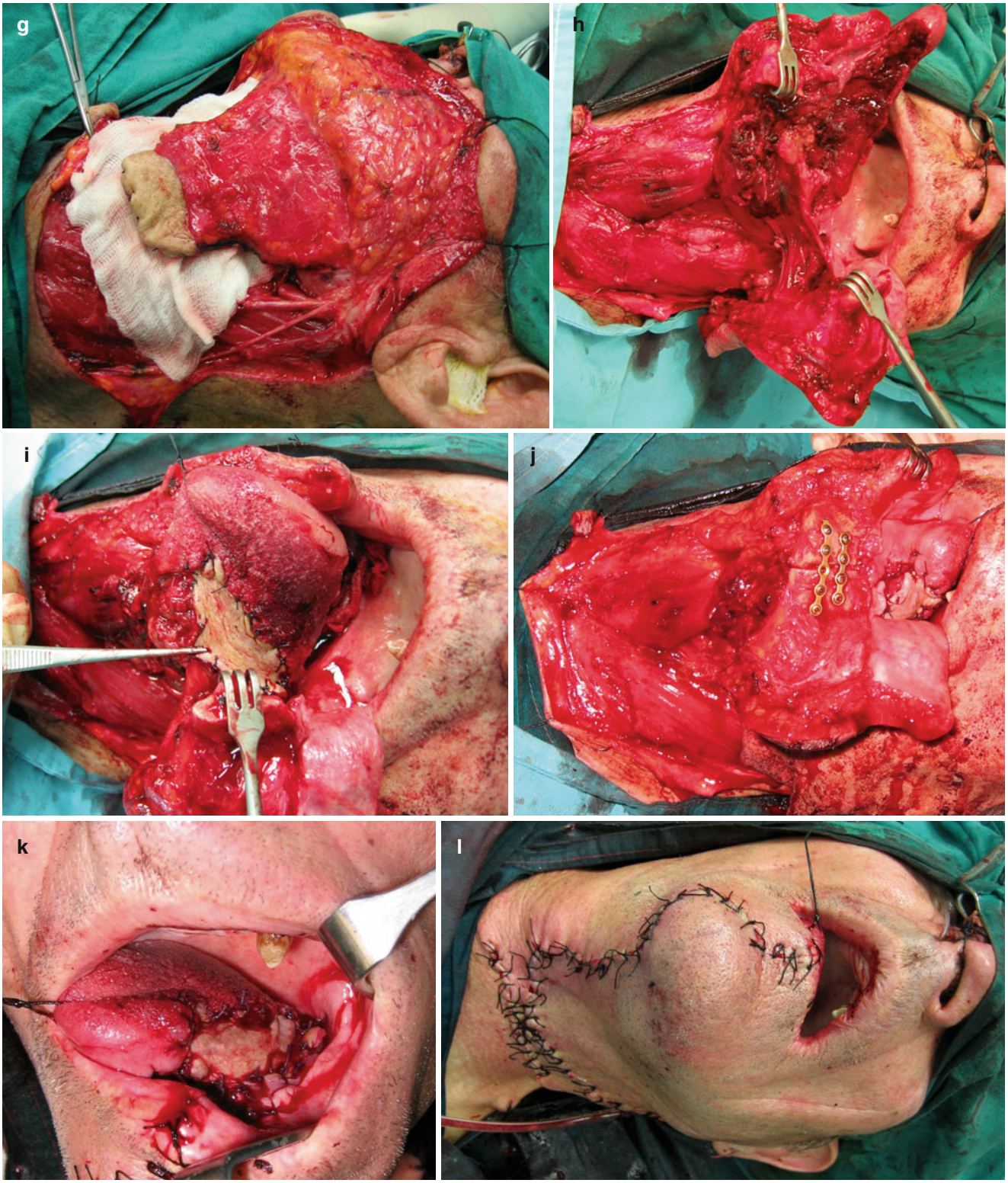

Fig. 8.25 (continued)

Fig. 8.25 (continued)

References

Agarwal A, Schneck CD, Kelley DJ (2004) Venous drainage of the platysma myocutaneous flap. Otolaryngol Head Neck Surg 130(3):357–359

Ariyan S (1979) The pectoralis major myocutaneous flap. A versatile flap for reconstruction in the head and neck. Plast Reconstr Surg 63(1):73–81

Ariyan S (1997) The transverse platysma myocutaneous flap for head and neck reconstruction. Plast Reconstr Surg 99(2):340–347

Ariyan S (2003) The transverse platysma myocutaneous flap for head and neck reconstruction: an update. Plast Reconstr Surg 111(1):378–380

Baur DA, Helman JI (2002) The posteriorly based platysma flap in oral and facial reconstruction: A case series. J Oral Maxillofac Surg 60(10):1147–1150

Coleman JJ 3rd, Nahai F, Mathes SJ (1982) Platysma musculocutaneous flap: clinical and anatomic considerations in head and neck reconstruction. Am J Surg 144(4):477–481

Coleman JJ 3rd, Jurkiewicz MJ, Nahai F, Mathes SJ (1983) The platysma musculocutaneous flap: experience with 24 cases. Plast Reconstr Surg 72(3):315–323

Conley JJ, Lanier DM, Tinsley P Jr (1986) Platysma myocutaneous flap revisited. Arch Otolaryngol Head Neck Surg 112(7):711–713

Curran AJ, Neligan P, Gullane PJ (1997) Submental artery island flap. Laryngoscope 107(11Pt1):1545–1549

De Castro CC (1980) The anatomy of the platysma muscle. Plast Reconstr Surg 66(5):680–683

Eliachar I, Marcovich A, Har Shai Y, Lindenbaum E (1984) Arterial blood supply to the infrahyoid muscles: an anatomical study. Head Neck Surg 7(1):8–14

Faltaous AA, Yetman RJ (1996) The submental artery flap: an anatomic study. Plast Reconstr Surg 97(1):56–60

Fróes LB, Castro De Tolosa EM, Camargo RD, Pompeu E, Liberti EA (1999) Blood supply to the human sternocleidomastoid muscle by the sternocleidomastoid branch of the occipital artery. Clin Anat 12(6):412–416

Futrell JW, Johns ME, Edgerton MT, Cantrell RW, Fitz-Hugh GS (1978) Platysma myocutaneous flap for intraoral reconstruction. Am J Surg 136(4):504–507

Gersuny R (1887) Plasticher Ersatz der Wangenscheimhaut. Zentralbl Chir 14:706–708

Görmüs G, Bayramoğlu A, Aldur MM, Celik HH, Maral T, Sargon MF, Demiryürek D, Aksit MD (2004) Vascular pedicles of infrahyoid muscles: an anatomical study. Clin Anat 17(3):214–217

Haas F, Weiglein A, Schwarzl F, Scharnagl E (2004) The lower trapezius musculocutaneous flap from pedicled to free flap: anatomical basis and clinical applications based on the dorsal scapular artery. Plast Reconstr Surg 113(6):1580–1590

Hatef DA, Koshy JC, Sandoval SE, Echo AP, Izaddoost SA, Hollier LH (2009) The submental fat compartment of the neck. Semin Plast Surg 23(4):288–291

Hu KS, Song WC, Kim SH, Choi SW, Han SH, Paik DJ, Kim HJ, Koh KS (2006) Branching patterns of the arterial branches supplying the middle vascular pedicle of the sternocleidomastoid muscle: a topographic anatomical study with surgical applications for the use of pedicles osteomuscular flaps. Surg Radiol Anat 28(1):7–12

Hurwitz DJ, Rabson JA, Futrell JW (1983) The anatomic basis for the platysma skin flap. Plast Reconstr Surg 72(3):302–314

Imanishi N, Nakajima H, Kishi K, Chang H, Aiso S (2005) Is the platysma flap musculocutaneous? Angiographic study of the platysma. Plast Reconstr Surg 115(4):1018–1024

Kierner AC, Aigner M, Zelenka I, Riedl G, Burian M (1999) The blood supply of the sternocleidomastoid muscle and its clinical implications. Arch Surg 134(2):144–147

Kim JT, Kim SK, Koshima I, Moriguchi T (2002a) An anatomic study and clinical applications of the reversed submental perforator-based island flap. Plast Reconstr Surg 109(7):2204–2210

Kim HJ, Koh KS, Oh CS, Hu KS, Kang JW, Chung IH (2002b) Emerging patterns of the cervical cutaneous nerves in Asians. Int J Oral Maxillofac Surg 31(1):53–56

Koch M, Künzel J, Mantsopoulos K, Zenk J, Iro H (2012) Defect closure after oral and pharyngeal tumor resection with the superiorly pedicled myocutaneous platysma flap: indications, technique, and complications. Eur Arch Otorhinolaryngol 269(9): 2111–2119

Lasjaunias P, Berenstein A, Doyon D (1979) Normal functional anatomy of the facial artery. Radiology 133(3Pt1):631–638

Magden O, Edizer M, Tayfur V, Atabey A (2004) Anatomic study of the vasculature of the submental artery flap. Plast Reconstr Surg 114(7):1719–1723

Martin D, Pascal JF, Baudet J, Mondie JM, Farhat JB, Athoum A, Le Gaillard P, Peri G (1993) The submental island flap: a new donor site. Anatomy and clinical applications as a free or pedicled flap. Plast Reconstr Surg 92(5):867–873

McGuirt WF, Matthews BL, Brody JA, May JS (1991) Platysma myocutaneous flap: caveats reexamined. Laryngoscope 101(11): 1238–1244

Nash L, Nicholson HD, Zhang M (2005) Does the investing layer of the deep cervical fascia exist? Anesthesiology 103(5):962–968

Owsley JQ, Agarwal CA (2008) Safely navigating around the facial nerve in three dimensions. Clin Plast Surg 35(4):469–477

Ozgur Z, Govsa F, Celik S, Ozgur T (2009) Clinically relevant variations of the superior thyroid artery: an anatomic guide for surgical neck dissection. Surg Radiol Anat 31(3):151–159

Pilsl U, Anderhuber F (2010) The chin and adjacent fat compartments. Dermatol Surg 36(2):214–218

Pinar YA, Bilge O, Govsa F (2005a) Anatomic study of the blood supply of perioral region. Clin Anat 18(5):330–339

Pinar YA, Govsa F, Bilge O (2005b) The anatomical features and surgical usage of the submental artery. Surg Radiol Anat 27(3):201–205

Rabson JA, Hurwitz DJ, Futrell JW (1985) The cutaneous blood supply of the neck: relevance to incision planning and surgical reconstruction. Br J Plast Surg 38(2):208–219

Ruark DS, McClairen WC Jr, Schlehaider UK, Abdel-Misih RZ (1993) Head and neck reconstruction using the platysma myocutaneous flap. Am J Surg 165(6):713–718

Salinas NL, Jackson O, Dunham B, Bartlett SP (2009) Anatomical dissection and modified Sihler stain of the lower branches of the facial nerve. Plast Reconstr Surg 124(6):1905–1915

Shah AR, Rosenberg D (2009) Defining the facial extent of the platysma muscle: a review of 71 consecutive face-lifts. Arch Facial Plast Surg 11(6):405–408

Shima H, von Luedinghausen M, Ohno K, Michi K (1998) Anatomy of microvascular anastomosis in the neck. Plast Reconstr Surg 101(1):33–41

Standring S (2008) Gray's anatomy. The anatomical basis of clinical practice, 40th edn. Churchill Livingstone-Elsevier, Edinburg

Szudek J, Taylor SM (2007) Systematic review of the platysma myocutaneous flap for head and neck reconstruction. Arch Otolaryngol Head Neck Surg 133(7):655–661

Tang WJ, Sun SQ, Wang XL, Sun YX, Huang HX (2012) An applied anatomical study on the recurrent laryngeal nerve and inferior thyroid artery. Surg Radiol Anat 34(4):325–332

Tessier P, Matthews DC, Kamerer D Jr, Ciminello FS, Gargano F, Wolfe SA (2011) Platysma-based myocutaneous clavicular island flap for intraoral reconstruction. Ann Plast Surg 67(6):S55–S69

Thomaidis VK et al (2006) The use of myocutaneous platysmal flap in the reconstruction of intraoral defects after tumor resection

combined with supraomohyoid neck dissection (article in Greek). Hell Arch Oral Maxillofac Surg 7(3):143–154
Uehara M, Helman JI, Lillie JH, Brooks SL (2001) Blood supply to the platysma muscle flap: an anatomic study with clinical correlation. J Oral Maxillofac Surg 59(6):642–646
Wilson JL, Rozen WM, Ross R, Findlay MW, Ashton MW, Behan FC (2012) The superior thyroid artery perforator flap: anatomical study and clinical series. Plast Reconstr Surg 129(3):641–646
Zhang M, Lee AS (2002) The investing layer of the deep cervical fascia does not exist between the sternocleidomastoid and trapezius muscles. Otolaryngol Head Neck Surg 127(5):452–454
Zhao Z, Li S, Xu J, Li Y, Huang W, Yang M, Mu L, Liu Y, Zhai H, Jin J, Li J, Li J, Fu X (2000) Color Doppler flow imaging of the facial artery and vein. Plast Reconstr Surg 106(6):1249–1253
Ziarah HA, Atkinson ME (1981) The surgical anatomy of the cervical branch of the facial nerve. Br J Oral Surg 19(3):171–179

Deltopectoral Region

9

9.1 Layered Anatomy

The pectoral and the deltoid regions constitute the donor sites of mainly two very popular regional fasciocutaneous flaps that are used in head-neck reconstruction: the cervicopectoral and the deltopectoral flaps. The anatomy relevant in the surgery of these flaps includes in layered arrangement the superficial fascia, the pectoral-deltoid fascia, and the pectoralis major and deltoid muscles.

9.1.1 Superficial Fascia in the Anterior Chest Wall

The superficial fascia in the anterior chest wall consists of loose areolar connective and adipose tissue and is loosely connected to the skin. Depending on gender and ethnicity, the superficial fascia may consist of more than one membranous sheet of varying thickness and variable amount of fat (Abu-Hijleh et al. 2006). The superficial fascia is perforated by small blood vessels and nerves that supply the skin. It is continuous with the SMAS layer at the neck and with the corresponding layer of the upper limb (and hence the deltoid region) superiorly and with that of the abdomen inferiorly. In the chest, it encompasses the mammary gland, giving off septa that pass between its lobes.

9.1.2 Pectoral and Deltoid Fascia

The pectoral fascia (Fig. 9.1) is a fibroelastic sheath that covers the pectoralis major muscle and corresponds to the deep cervical fascia. It is thin (mean thickness of 297 μm) and is thicker in the inferior thorax and thinner in the subclavicular region (Stecco et al. 2009a, b). It is connected to the pectoralis muscle through multiple intramuscular septa that are detached from its inner surface. The pectoral fascia superiorly is fused with the clavicle and the coracoid process and inferiorly is continuous with the ipsilateral and contralateral rectus abdominis sheaths. It consists of two layers: a superficial layer and a deep one. The superficial layer is thin and covers the outer surface of the pectoralis major muscle also separating the muscle from the mammary gland. The superficial layer crosses over the sternum and continues with the superficial layer of the contralateral pectoral fascia, whereas the deep layer covers the inner surface of the pectoralis major muscle and fuses with the sternal periosteum. The deep layer of the pectoral fascia forms the clavipectoral and the axillary fasciae.

The deltoid fascia is a fibrous membrane that overlies the deltoid muscle. Like the pectoral fascia, it sends intramuscular septa into the deltoid muscle. Superiorly it is attached to the clavicle, the acromion, and the spinal crest of the scapula; inferiorly it is continuous with the brachial fascia, medially with the pectoral fascia, and posteriorly with the infraspinous fascia (Standring 2008).

9.1.3 Pectoralis Major Muscle

The pectoralis major muscle (Fig. 9.2) is a triangular-shaped muscle that occupies the major part of the chest. It is separated from the deltoid muscle by a groove termed the deltopectoral groove. The deltopectoral groove transitions upward to the infraclavicular fossa (deltopectoral triangle) that can be seen as a small depression inferior to the clavicle. The cephalic vein runs in the deltopectoral groove and ascends deeply in the infraclavicular fossa where it pierces the clavipectoral fascia to join the axillary vein. The infraclavicular fossa contains furthermore the deltoid branch of the acromiothoracic artery.

The pectoralis major muscle arises from the anterior surface of the medial half of the clavicle; from the half of

V.K. Thomaidis, *Cutaneous Flaps in Head and Neck Reconstruction*,
DOI 10.1007/978-3-642-41254-7_9, © Springer-Verlag Berlin Heidelberg 2014

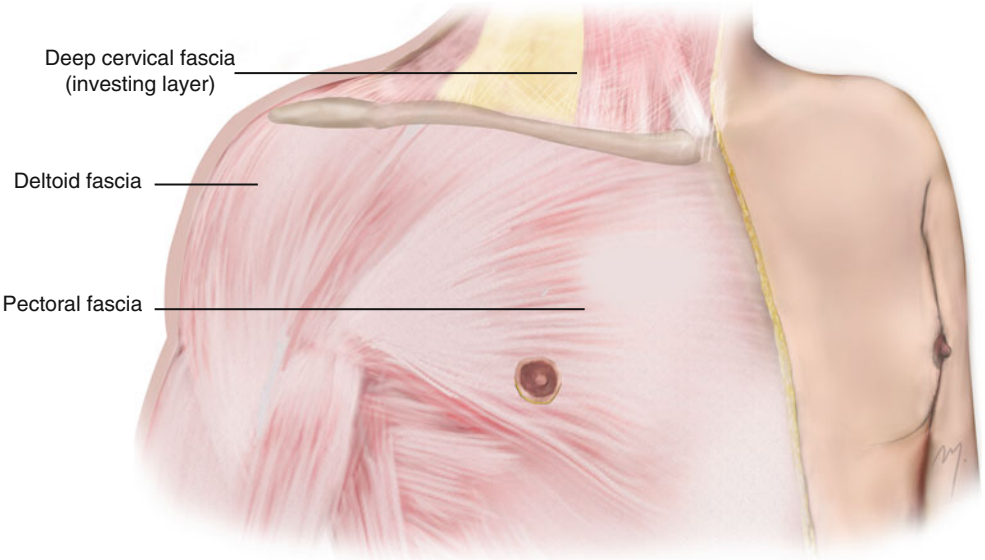

Fig. 9.1 Pectoral and deltoid fascia

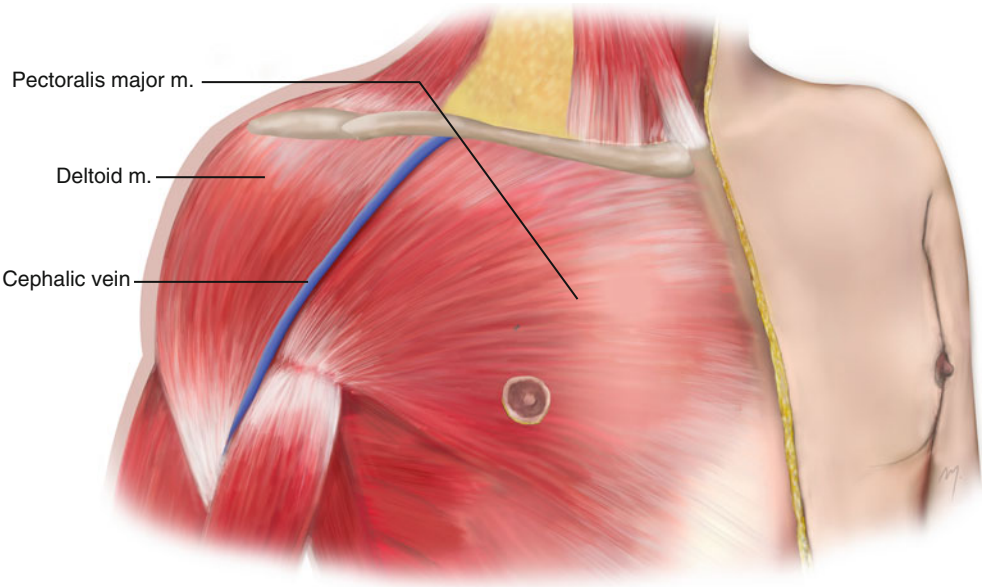

Fig. 9.2 Pectoralis major and deltoid muscles

the breadth of the anterior surface of the sternum, down to the level of the attachments of the sixth or seventh costal cartilage; from the cartilages of the first to seventh ribs; from the sternal end of the sixth rib; and from the aponeurosis of the external oblique muscle. According to the muscle fibers' origin, the pectoralis major exhibits a clavicular and a sternocostal part that are separated by a slight cleft. All of its muscle fibers run horizontally to converge to a tendon approximately 5 cm across. The upper muscle fibers descend obliquely and laterally, the middle fibers run horizontally and laterally, and the lower fibers ascend obliquely and laterally. The tendon that is formed from the converging muscle fibers of the pectoralis major is bilaminar in form (with an anterior and a posterior lamina) and is attached to the lateral lip of the intertubercular sulcus of the humerus.

The pectoralis major is supplied by a primary arterial pedicle from the pectoral branch of the thoracoacromial artery. The pectoralis major musculocutaneous flap is based on this primary arterial pedicle from the thoracoacromial

artery. The perforating branches of the internal thoracic artery and the lateral thoracic artery complete the vascular pedicles of the muscle.

Multiple smaller muscular vessels arising from the deltoid and clavicular branches of the thoracoacromial artery and the superior thoracic artery contribute to the supply of the most upper and lateral clavicular portion of the pectoralis major. It has been reported (Yang et al. 2003) that the pectoralis major muscle and the overlying skin are supplied in approximately 50.7 % by the pectoral branch, in 43 % by the perforating branches of the internal thoracic artery, and in the 6.6 % by the lateral thoracic artery. The pectoralis major musculocutaneous flap traditionally is based only to the pectoral branch of the thoracoacromial artery. Newly improved techniques of harvesting the pectoralis major myocutaneous flap preserve the lateral thoracic artery enhancing thus the vascularity of the distal skin island (Po-Wing Yuen 2006). The muscle is innervated from the medial and lateral pectoral nerves that are branches of the brachial plexus.

The pectoralis major muscle when both of its parts act adducts the humerus at the shoulder and rotates the humerus medially. It also draws the scapula anteriorly and inferiorly. Acting alone its clavicular part flexes the humerus at the shoulder and its sternocostal part extends it.

9.1.4 Deltoid Muscle

The deltoid muscle (Fig. 9.2) is one of the scapular muscles that surround the shoulder joint. It is a thick muscle, having a shape of an inverted Greek letter "delta."

The deltoid muscle originates from the anterior border and the superior surface of the lateral third of the clavicle, the lateral margin and the superior surface of the acromion, and the lower edge of the crest of the spine of the scapula. The muscle fibers descend forming the smooth contour of the shoulder and converge to form a short tendon. The tendon formed by the converging muscle fibers inserts to the deltoid tuberosity on the lateral aspect of the humerus. The deltoid muscle receives its blood supply from the acromial and deltoid branches of the thoracoacromial artery, the anterior and the posterior circumflex humeral arteries, the subscapular artery, and the deltoid branch of the profunda brachii. The muscle is innervated by the axillary nerve (C5, C6). When acting, the anterior muscle fibers flex and rotate the arm medially, the middle fibers abduct the arm, and the posterior fibers extend and rotate the arm laterally.

9.2 Arteries Supplying the Skin of the Deltopectoral Region

The skin of the deltopectoral region is supplied by branches of the acromiothoracic, internal thoracic, and lateral thoracic arteries and by the supraclavicular artery (Fig. 9.3).

9.2.1 Acromiothoracic Artery

The acromiothoracic (thoracoacromial) artery is a short arterial trunk (1–1.5 cm) that arises from the anterior aspect of the second part (sometimes it arises from the first part) of the axillary artery usually 3 cm from its starting point. Its mean diameter is 2–2.5 mm. It curves around the superior margin of the tendon of the pectoralis minor muscle, pierces the clavipectoral fascia, and after its origin gives off four branches: the pectoral, the acromial, the clavicular, and the deltoid branch.

The point related to the midclavicular line where the acromiothoracic artery originates from the axillary artery differs in the left and right sides probably due to the different embryologic origins of the right and left subclavian systems (the right originated from the brachiocephalic trunk and the left from the aortic arch). In the right side, the acromiothoracic artery originates from the axillary artery in a point 2–3 cm below the clavicle and laterally to the midclavicular line, and in the left side, 2–3 cm below the clavicle and usually medial to the midclavicular line (Nakajima et al. 1997; Park et al. 2004).

9.2.1.1 Branches

9.2.1.1.1 Pectoral Branch

The pectoral branch is the largest branch of the acromiothoracic artery and the main feeding vessel of the myocutaneous pectoralis major flap. It runs inferiorly on the deep surface of the pectoralis major muscle, after giving a branch to the pectoralis minor muscle. It penetrates the pectoralis major muscle and anastomoses within the muscle mass with the branches of the perforators of the internal thoracic and the lateral thoracic arteries. The course of the pectoral branch corresponds to a line that runs from the middle of the clavicle vertically downward and then turns medially at the point where it meets a line that connects the acromion and the xiphoid process, running along this line (Ariyan 1979; Freeman et al. 1981). The pectoral branch of the acromiothoracic artery supplies more of the half of the muscle parenchyma of the pectoralis major (Yang et al. 2003). Through the musculocutaneous perforators, it also supplies the over-

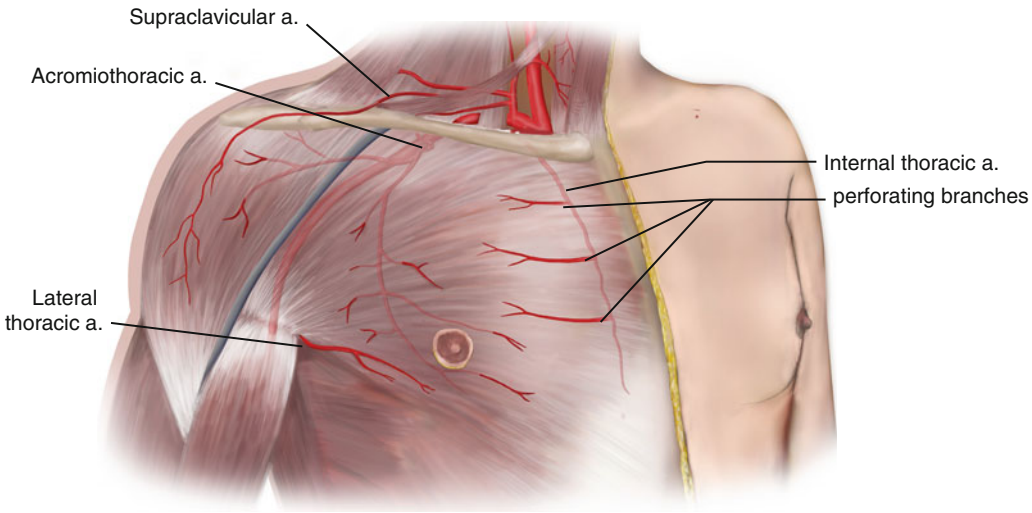

Fig. 9.3 Main arteries that supply the skin of the anterior chest and deltoid region

lying chest skin. The skin area that is supplied by the pectoral branch can range from 7×12 cm to 24×30 cm in the region between the 3rd and 6th rib from the parasternal line to the anterior axillary line (Kovacević et al. 2008).

9.2.1.1.2 Clavicular Branch

The clavicular branch runs superomedially, between the clavicular part of the pectoralis major muscle and the clavipectoral fascia, and supplies the subclavius muscle.

9.2.1.1.3 Deltoid Branch

The deltoid branch crosses pectoralis minor muscle and travels within the infraclavicular fossa in company with the cephalic vein. It supplies the pectoralis major and deltoid muscles.

9.2.1.1.4 Acromial Branch

This branch crosses the coracoid process and runs initially beneath the deltoid muscle, penetrates the muscle, runs over its surface, and reaches the acromion. The deltoid and the acromial branches of the acromiothoracic artery anastomose each other, and via musculocutaneous perforators and direct cutaneous branches, they supply the skin of the anterior part of the deltoid region.

9.2.2 Internal Thoracic Artery

The internal thoracic artery (internal mammary artery) arises from the inferior surface of the first part of the subclavian artery exactly opposite to the origin of the thyrocervical trunk. Its average diameter is approximately 3 mm. It runs inferiorly inside the chest in a parasternal plane, 1–1.5 cm lateral to the border of the sternum. It ends in the sixth intercostal space, where it divides into its terminal branches: the superior epigastric artery and the musculophrenic artery. It is accompanied by 1 or 2 veins, the internal thoracic veins, which ascend and drain into the brachiocephalic vein.

The internal thoracic artery gives off thymic branches that supply the thymus; sternal branches that supply the sternum and the medial part of the transversus thoracic muscle; the mediastinal arteries, which supply the structures of the anterior mediastinum; and the pericardiophrenic artery which travels in company with the phrenic nerve and supplies the pericardium and the perforating branches.

9.2.2.1 Perforating Branches

These are direct perforating branches that pierce through the internal intercostal muscles of the upper five or six intercostal spaces in company with the anterior cutaneous branches of the corresponding intercostal nerves and one perforating vein. They next penetrate the pectoralis major muscle comprising part of its blood supply. After penetrating the muscle, they become cutaneous, curve laterally, and supply the overlying skin. The perforator in the second intercostal space is usually the largest followed by the perforator in the third intercostal space and is termed as the "principal perforator" (Palmer and Taylor 1986). The average diameter of the second perforator has been found to measure 1.6 mm while the third perforator 1.4 mm and their lengths 9.6 and 8.7 cm, respectively (Schmidt et al. 2010).

These perforating branches of the internal thoracic artery constitute the dominant blood supply of the deltopectoral flap and of the pectoral portion of the cervicopectoral flap.

9.2.3 Lateral Thoracic Artery

The lateral thoracic artery (external mammary artery) arises from the second part of the axillary artery, being its second branch. The artery descends to the side of the chest initially along the lateral (axillary) border of the pectoralis minor muscle, afterward proceeds to the undersurface of the pectoralis major, and ends at the fifth intercostals space distributed to the lateral thoracic wall, the pectoral muscles, and the breast. It gives off branches that supply the serratus anterior and pectoral muscles and branches across the axilla to supply the subscapularis muscle and the axillary lymph nodes. It anastomoses with the subscapular, intercostal, acromiothoracic (pectoral branch), and internal thoracic arteries.

The lateral thoracic artery gives off cutaneous branches that course around the lateral border of the pectoralis major muscle and supply a portion of the skin of the lateral thoracic wall and the lateral part of the breast (Standring 2008).

A vessel that often has been confusingly described in this area is the superficial thoracic artery. The superficial thoracic artery constitutes either the direct continuation or a branch of the lateral thoracic artery (Standring et al. 2008; Loukas et al. 2006).

9.2.4 Supraclavicular Artery

An important cutaneous artery that contributes to skin supply of the deltoid region is the supraclavicular artery, a vessel that is branched from the superficial cervical/transverse cervical artery. The supraclavicular artery after arising at the medial portion of the omoclavicular (supraclavicular) triangle courses laterally. At the angle between the anterior border of the trapezius and the superior border of the clavicle, it pierces the deep cervical fascia, crosses the clavicle, and travels subcutaneously to the deltoid region. It supplies the skin of the lateral and upper part of the deltoid region, giving off branches to the pectoralis major muscle, which, after piercing the muscle, contribute also to the supply of the upper thoracic skin.

This vessel is the main feeding vessel in the design of an axial flap that uses the skin of the deltoid region (Pallua et al. 1997; Pallua and Magnus Noah 2000; Vinh et al. 2009; Hormozi and Shafii 2010; Pallua and Wolter 2013).

9.3 Superficial Veins

Small veins that coalesce into larger ones and drain into the anterior intercostal veins drain the anterior thoracic wall. The anterior intercostal veins which accompany the intercostal arteries are tributaries of the internal thoracic and musculophrenic veins. The veins that accompany the perforating branches of the internal thoracic artery drain directly into the internal thoracic vein. The internal thoracic vein, sometimes double, travels along the border of the sternum just medial to the internal thoracic artery and drains in turn into the brachiocephalic vein.

The lateral thoracic vein contributes to the venous drainage of the lateral chest wall and the breast. The lateral thoracic vein runs with the corresponding artery and drains into the axillary vein. The lateral thoracic vein normally is connected inferiorly with the superficial epigastric vein through the thoracoepigastric vein that runs superficially on the anterolateral aspect of the trunk (Fig. 9.4).

9.4 Cutaneous Nerves

The skin of the thorax receives its sensory innervation by cutaneous branches of the cervical and the thoracic nerves. The supraclavicular nerves of the cervical plexus (see Chap. 8) through their branches supply the skin of the upper thoracic region.

Particularly the medial supraclavicular branches supply the skin of the medial part of the upper thoracic region. The intermediate supraclavicular branches supply the skin of the middle and lateral part of the upper thoracic region. And the lateral supraclavicular branches distribute to the skin of the lateral part of the upper thoracic region and to the skin of the upper part of the deltoid region.

The thoracic nerves supply the skin of the anterior part of the anterior chest through their anterior cutaneous branches and the anterolateral part through the lateral cutaneous branches, respectively (Fig. 9.5).

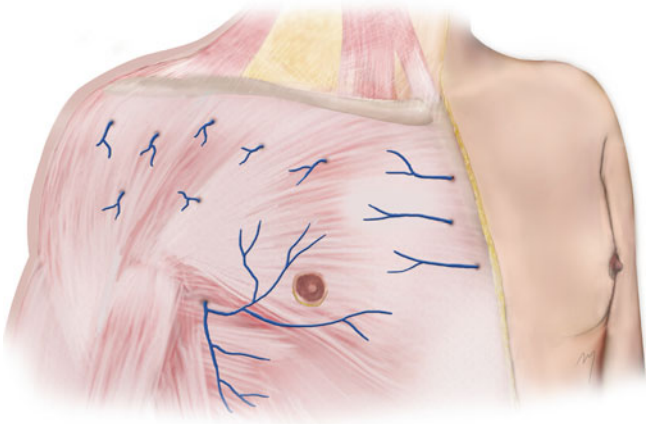

Fig. 9.4 Superficial veins of the anterior thorax

Fig. 9.5 Cutaneous nerves of the anterior thorax

9.5 Deltopectoral Flap

The deltopectoral flap is one of the two most widely used fasciocutaneous flaps in head and neck reconstruction that are derived from the deltopectoral region, the other one being the cervicopectoral flap.

The deltopectoral flap is a transposition flap that has first been designed by Aymard in 1917 for nose reconstruction. It received increased attention since 1965, when Bakamjian began using the flap for pharyngoesophageal reconstruction. The deltopectoral flap transfers the skin from the deltoid and thoracic region and shows similarities to the thoracic part of the cervicopectoral flap in terms of anatomy, vascularity, and surgical technique. The flap is of axial pattern, based on the internal thoracic artery perforators, in its medial part and of random pattern in its lateral part.

The deltopectoral flap had lost its popularity and was deported by the free vascularized flaps but recently has been reappearing in the international literature (Feng et al. 2006; Sharma and Panda 2006; Bey et al. 2009; Rebelo et al. 2009; Krijgh and Mureau 2012; Nayak and Nilamani 2012).

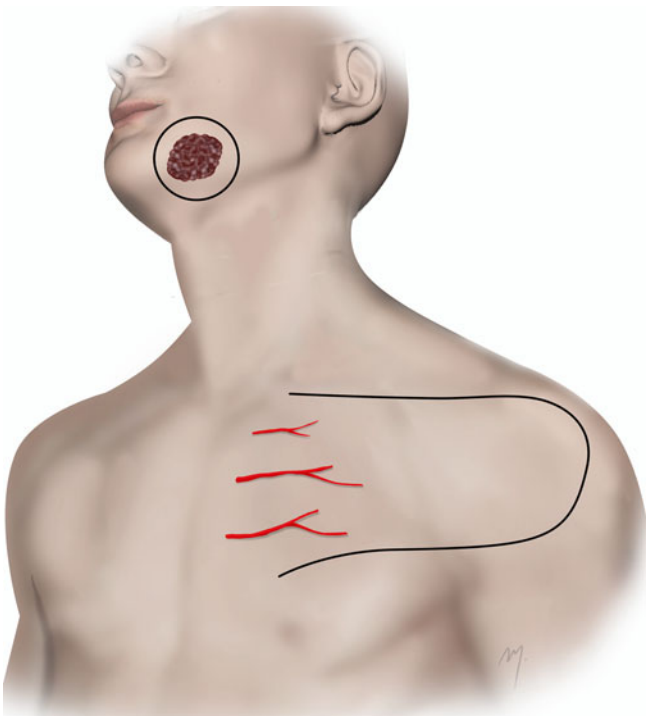

Fig. 9.6 Outline of the deltopectoral flap. The flap is of axial pattern in its medial part and of random pattern in its lateral part

9.5.1 Flap Design

The deltopectoral flap is designed in rectangular shape, in the upper thorax extending from the sternum in a variable degree to the anterior deltoid region. The base of the flap is situated parasternally 2 cm from the sternal edge. The superior boundary follows the clavicle, and the inferior boundary is parallel to the previous line over the 3rd or 4th intercostal space. The flap extends horizontally beyond the deltopectoral groove onto the deltoid region, in an extent depending on the needed length to reach the defect, and ends in a curvilinear distal margin (Figs. 9.6 and 9.7).

There are cases where to reach the defect the needed length of the flap compels it to extend to the lateral deltoid region and a flap delay is required at least 1 week prior to the flap harvest.

9.5.2 Flap Vascularity

The deltopectoral receives its blood supply from the perforating vessels of the internal mammary artery with the main contribution of the 2nd and 3rd perforators in its medial part

Fig. 9.7 Tumor resection margins and flap are outlined

Fig. 9.8 Incision is made through the deltopectoral fascia

having an axial blood supply at this part (Fig. 9.6). The distal part is of random pattern, so far as the musculocutaneous perforators of the deltoid and acromial branches of the acromiothoracic artery are cut during flap elevation.

9.5.3 Flap Elevation

The incision is made deep to the deltoid fascia at the deltoid region and deep to the pectoral fascia at the chest (Fig. 9.8). The flap is raised from distal to the base. The plane of dissection lies between the deltoid muscle and the deltoid fascia including the latter in the flap. As the dissection

Fig. 9.9 Flap raised. Internal thoracic perforator is seen at the lower part as it enters the subcutis

advances, the deltopectoral groove is reached. The cephalic vein passes deep to this area and in most of the cases can be avoided.

The lateral border of the pectoralis major is easily identified and dissection over the muscle continuous in the same plane beneath the pectoralis fascia. Sharp dissection is needed to release the flap from the clavicle as long as the pectoralis fascia fuses with the bone. Mild bleeding from musculocutaneous perforators can be encountered. Dissection stops 1.5–2 cm lateral to the lateral sternal border. The perforating branches of the internal thoracic artery may be seen if dissection extends toward them, as they perforate the pectoral muscle entering the subcutaneous tissue (Fig. 9.9).

The flap length is controlled so as to reach the defect without tension, sutured in place, and the pedicle tubed (Fig. 9.10a, b). The flap pedicle remains for a period of 2–3 weeks until neovascularization of the recipient site occurred (Fig. 9.11). At the second stage, the flap pedicle is divided and returned into place (Figs. 9.12, 9.13, and 9.14). The donor site defect can be covered with a split-thickness skin graft left to heal by secondary intention. The deltopectoral flap achieves usually a very good postoperative result providing tissue with a reasonable color match (Fig. 9.15).

9.5.4 Deltopectoral Flap Combined with Lining Flaps

The deltopectoral flap is a reliable flap that can be safely used in conjunction with other local or regional flaps in

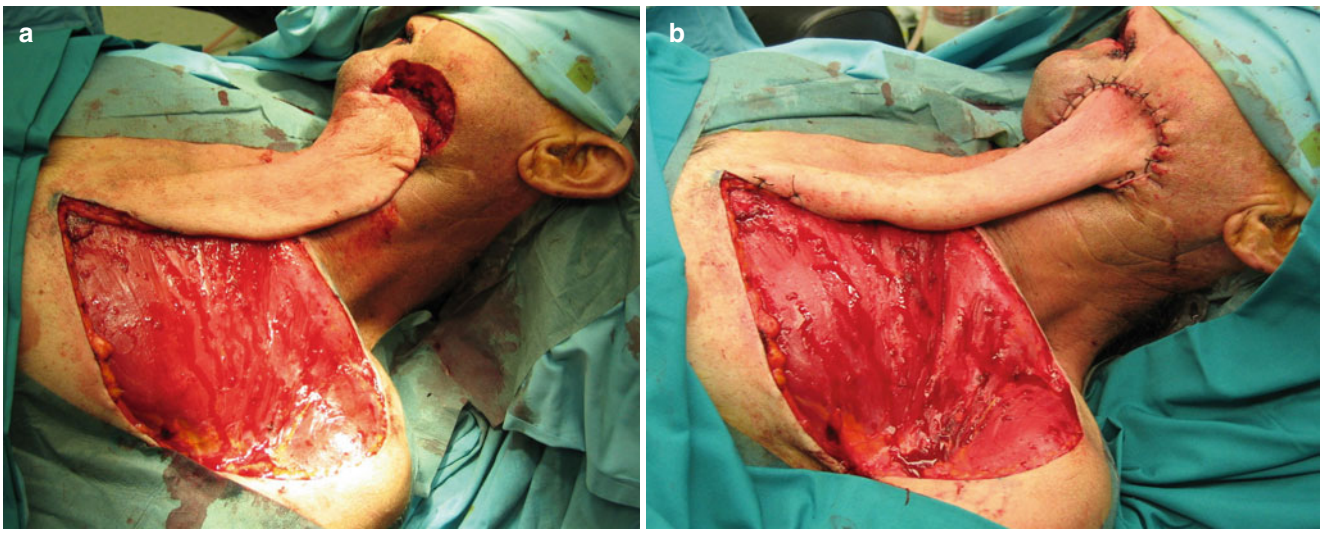

Fig. 9.10 (**a**) Flap is transpositioned to the recipient site. (**b**) The flap is sutured into the recipient site and its pedicle is tubed

Fig. 9.11 The flap pedicle remains for 2–3 weeks

Fig. 9.12 Second-stage operation

Fig. 9.13 Flap pedicle divided

through and through cheek defects. An example is given in the following case.

A large squamous cell carcinoma of the oral commissure is spread into the adjacent cheek skin and buccal mucosa in the patient presented in Fig. 9.16a, b. Tumor excision lead to a through and through cheek defect (Fig. 9.17) that must be reconstructed by internal and external lining. The neighboring buccal fat pad was intact and was unprepared as a buccal fat pad to resurface the defect intraorally (Fig. 9.18a, b). After a supraomohyoid neck dissection was performed, a deltopectoral flap was outlined and raised in the usual manner to provide external coverage (Figs. 9.19, 9.20, and 9.21). The buccal fat pad was sutured in place (Fig. 9.22) and the deltopectoral flap settled in a bed of reduced vascularity and sutured in the periphery (Fig. 9.23). The flap pedicle of the tubed deltopectoral flap remained for 3 weeks (Fig. 9.24a, b). After that period it was divided at the second surgical stage and final restoration took place (Fig. 9.25a, b). The deltopectoral flap had set well in place, and the postoperative appearance of the patient shows a satisfactory restoration (Fig. 9.26a, b).

Fig. 9.14 Flap pedicle returned and sutured in place

9.5.5 Deltopectoral Flap for Intraoral Lining

The deltopectoral flap is a useful tool for resurfacing also large intraoral defects. In the large oral cavity tumor shown in Fig. 9.27, a reconstruction was planned to be performed by a deltopectoral flap. Access to the tumor was gained through a lip-split approach and the elevation of a lower cheek flap (Fig. 9.28). After the lower cheek flap was elevated, the lesion was exposed and the resection margins outlined (Fig. 9.29). The tumor was excised in clear margins revealed by frozen biopsies, leaving a wide defect (Fig. 9.30a). Posterior marginal mandibulectomy was required (Fig. 9.30b). The deltopectoral flap was raised in the usual manner (Figs. 9.31 and 9.32).

The submandibular incision is not sutured in its central part leaving a sufficiently wide tunnel through which the

Fig. 9.15 (**a**, **b**) The postoperative result at 1 year

Fig. 9.16 (**a**, **b**) Oral commissure carcinoma

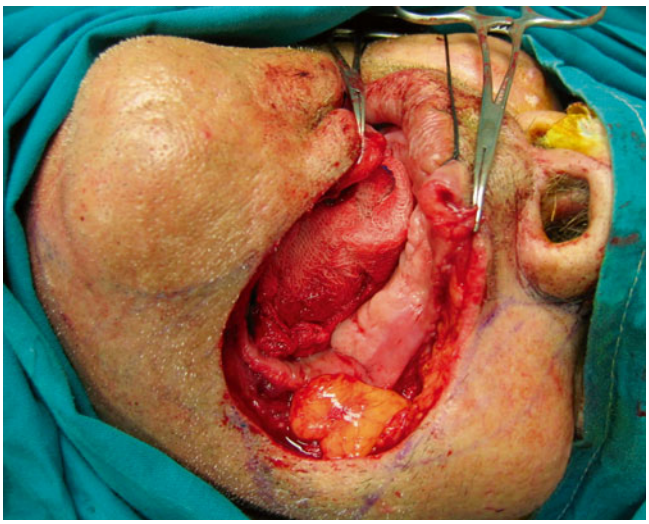

Fig. 9.17 Through and through defect after tumor excision. The buccal fat pad remains intact

deltopectoral flap passes intraorally reaching the defect (Figs. 9.33 and 9.34). The lower cheek flap returns to its normal position and is sutured. Care is taken not to tighten the submandibular tunnel, which can lead in struggling of the arterial supply and the venal outflow (Fig. 9.35).

After two weeks the pedicle is divided and final restoration takes place. The postoperative appearance of the patient 5 months following surgery shows a satisfactory functional and cosmetic result (Fig. 9.36a–c).

The deltopectoral flap is a reliable, safe, easy to perform, and quick to raise flap. It provides a thin, pliable, and large soft tissue with a reasonable color match. It can reach all regions of the lower and midface providing coverage in wide defects. Its main disadvantage is the second surgical procedure needed for the flap division.

9.6 Cervicopectoral Flap

The cervicopectoral flap is a large rotation flap that is best used in the reconstruction of large lateral facial defects. The cervicopectoral flap was first described by Becker (1978) and actually constitutes the thoracic extension of the cervicofacial flap.

It is consisted of a facial, a cervical, and a thoracic part. The cervical and the thoracic parts are of standard extent due to their standard design. The extent of its facial part depends on the remaining healthy facial skin after the excision of the facial lesion and the produced defect.

The flap is of axial pattern, based on the internal thoracic artery perforators, in its thoracic part and of random pattern

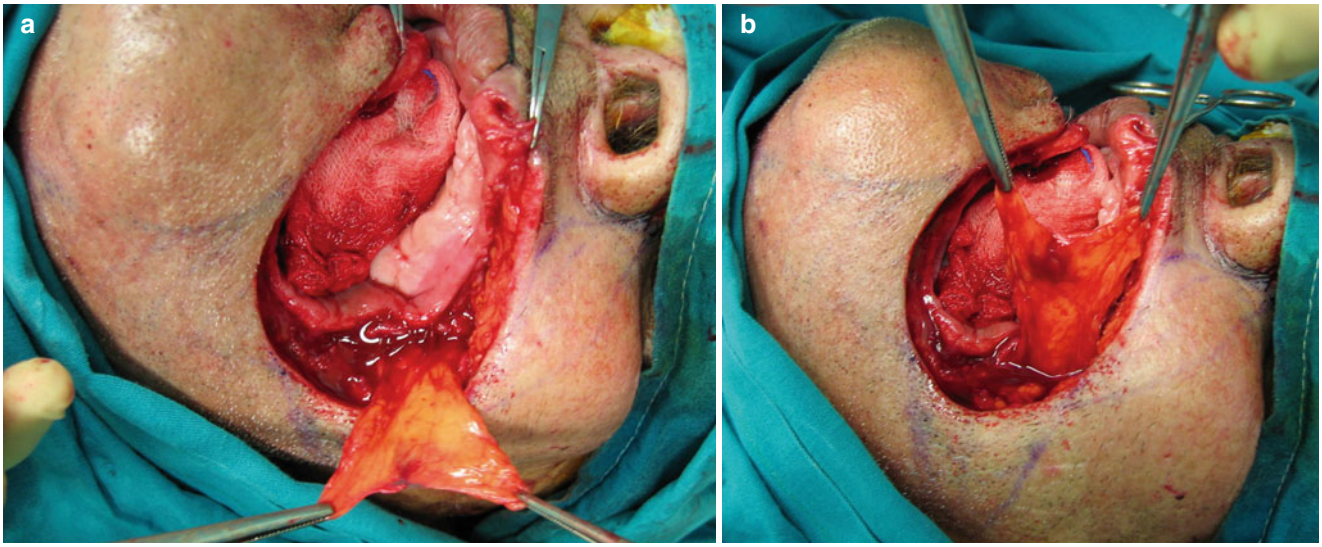

Fig. 9.18 (**a**) The buccal fat pad is dissected and prepared as a flap. (**b**) The buccal fat pad flap is of adequate length and width to provide intraoral lining

Fig. 9.19 Deltopectoral flap outlined

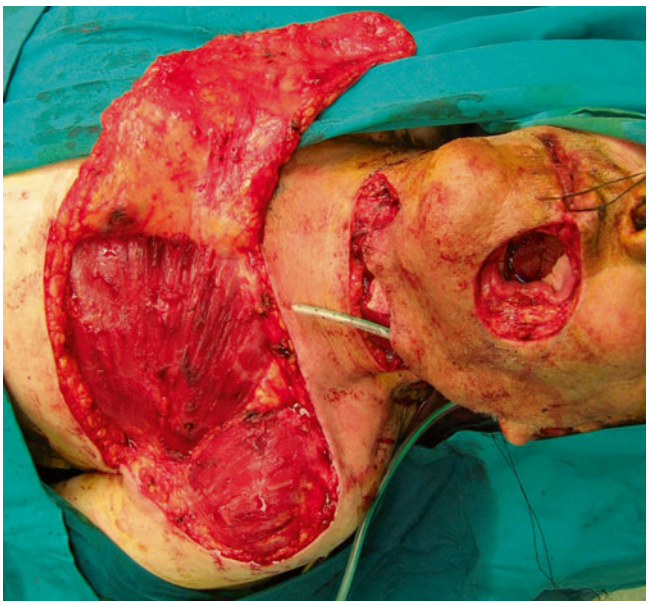

Fig. 9.20 Flap raised

in the rest of it. In a large basal cell carcinoma (Fig. 9.37) located at the lateral face, excision and reconstruction of the defect with a cervicopectoral flap is planned.

9.6.1 Flap Design

The proposed area of the cheek excision and the cervicopectoral flap are marked (Fig. 9.38). The inferior border of the resection is the upper border of the flap. The outline curves posteriorly around the earlobe and then runs inferiorly, in a distance of up to 2 cm, behind and parallel to the anterior border of the trapezius muscle. It then traverses the acromioclavicular part of the shoulder and the deltopectoral groove and continues along the lateral border of the pectoralis major muscle. The inferior limb of the flap turns to the anterior chest running parallel to the clavicle approximately 2–3 cm above the nipple. Due to the fact that the nipple is not a stable landmark especially in female patients, more precisely the level of the inferior limb must correspond to the third intercostal space. The horizontal inferior limb ends

Fig. 9.21 Flap length control

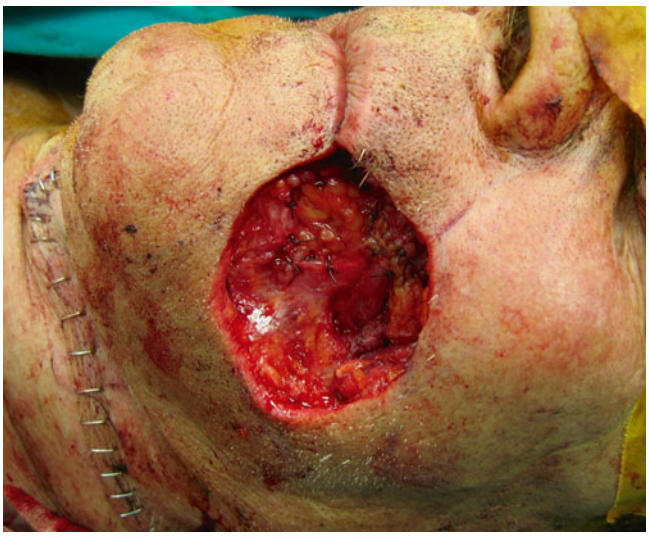

Fig. 9.22 Internal coverage completed

2 cm lateral to the sternal border. A back-cut at the flap's base might be needed to increase rotation.

9.6.2 Flap Vascularity

As the flap is raised from its periphery to its base, at the neck the vessels that supply the skin of the neck are cut. Starting from lateral to medial by row, these are lateral from top to bottom: the neck branches of the posterior auricular artery, the sternocleidomastoid branches of the occipital artery, the cutaneous branches of the transverse cervical artery and as dissection proceeds to the midline, the cutaneous branches of

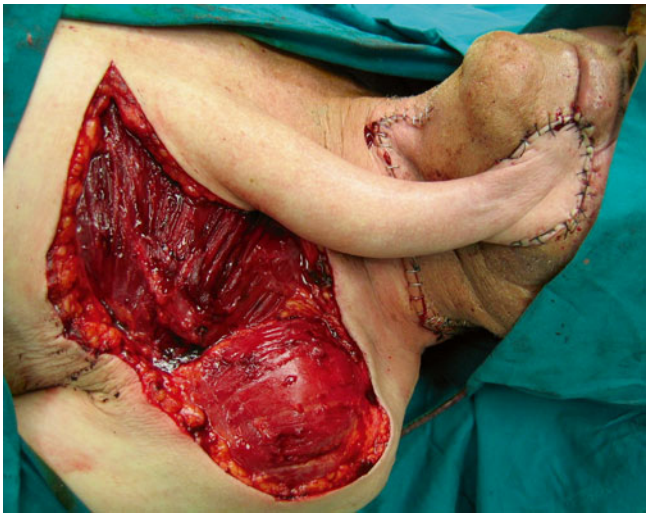

Fig. 9.23 The deltopectoral flap provides the external coverage of the defect

the facial artery, the cutaneous branches of the submental artery, and the cutaneous branches of the superior thyroid and suprascapular artery. At the thoracic part from lateral to medial, the vessels that are divided are the musculocutaneous perforators of the acromial, the deltoid, and the pectoral branches of the acromiothoracic artery. Despite this, the flap shows an excellent viability that is ensured in its wide base that is perfused by the rich anastomosis of the cutaneous vessels across the midline in the cervical skin and the maintenance of the perforating vessels from the internal mammary artery. The flap is essentially a mixed axial-patterned and random-patterned flap (Fig. 9.39). It is axial in the thoracic part where it catches the first four internal thoracic perforators. Random pattern is in its cervical part where at its base receives reverse flow from the anastomoses with the contralaterals: submental, superior thyroid, and inferior thyroid arteries.

The lesion was excised in clear margins revealed by frozen biopsies. The deep plane of excision was mostly above the parotidomasseteric fascia (Figs. 9.40 and 9.41).

9.6.3 Flap Elevation

9.6.3.1 Thoracic Part

At the thoracic part (Fig. 9.42), the incision is made through the superficial fascia of the chest deep to the deltoid and pectoral fascia. Elevation of the flap starts at the deltoid region in a plane deep to the deltoid fascia and over the deltoid muscle fibers. Preceding at the deltopectoral groove, the cephalic

Fig. 9.24 (**a**, **b**) Pedicle remains for 3 weeks

Fig. 9.25 (**a**, **b**) Pedicle division and final restoration

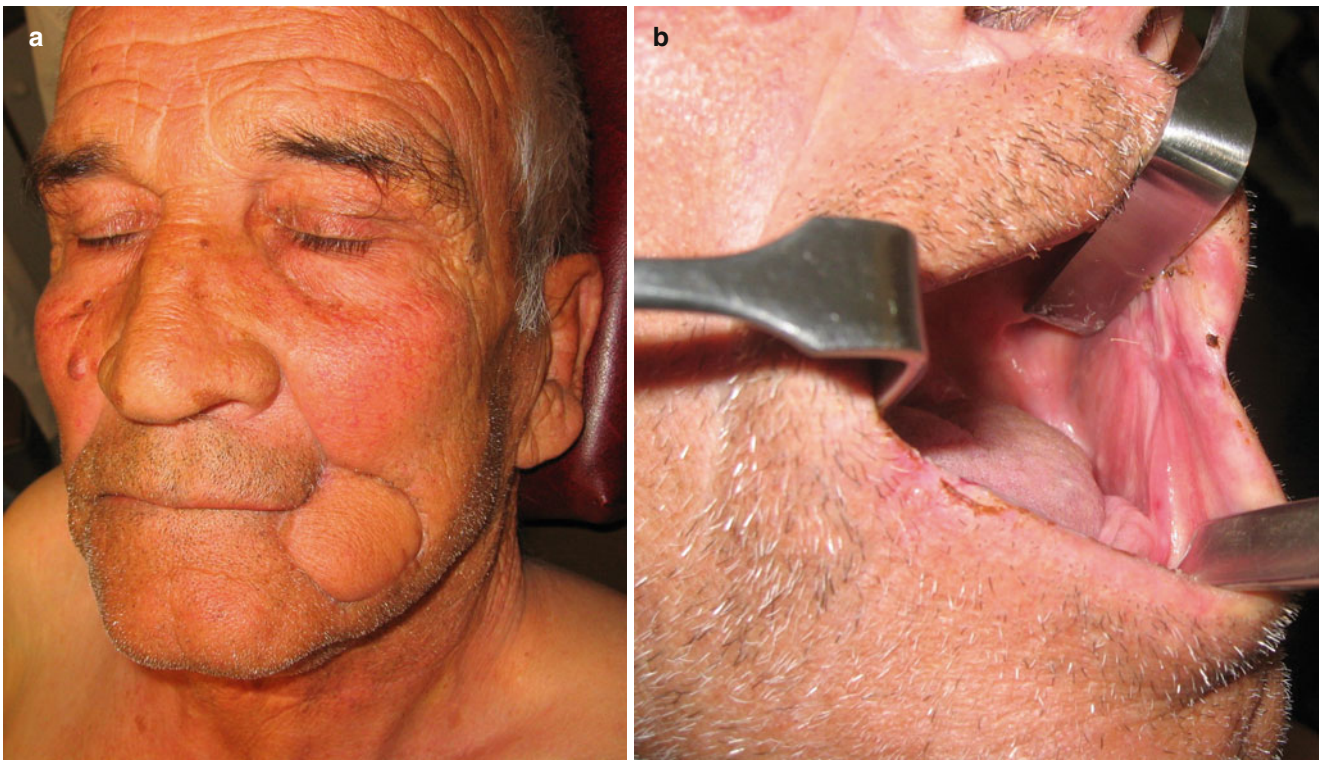

Fig. 9.26 (**a**) Result at 6 months. (**b**) Intraoral view

Fig. 9.27 Squamous cell carcinoma of the buccal mucosa

Fig. 9.28 Deltopectoral flap and lip-split approach outlined

vein passing deeply to it most of the time can be avoided and left intact. At the anterior chest, the plane of dissection continues deep to the pectoral fascia just above the fibers of the pectoralis major muscle. The fascia is fused with the clavicle, and sharp dissection by using a scalpel is needed to release it from the bone. Incorporation of the deltopectoral fascia in the flap strengthens its vascularity. Proceeding medially elevation is quick and easy without encountering any anatomical structure except small perforating vessels that are cauterized.

As the lateral border of the sternum is reached, the perforating branches of the internal thoracic artery may be located and preserved, each of them in its intercostal space. Alternatively the dissection can stop approximately 1.5–2 cm lateral to the lateral border of the sternum, protecting thus the perforating branches without locating them.

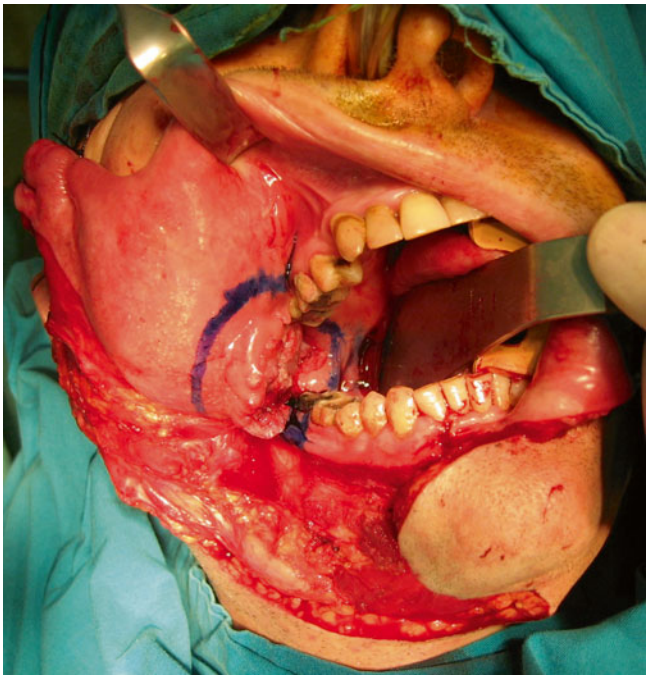

Fig. 9.29 Tumor exposed and the area of proposed excision outlined

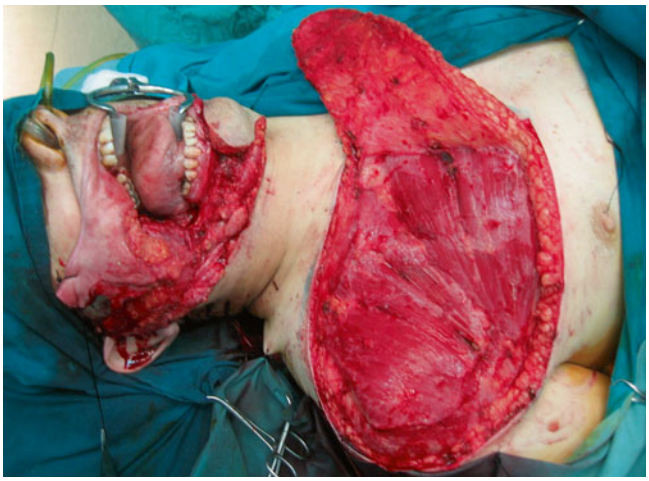

Fig. 9.31 The deltopectoral flap raised

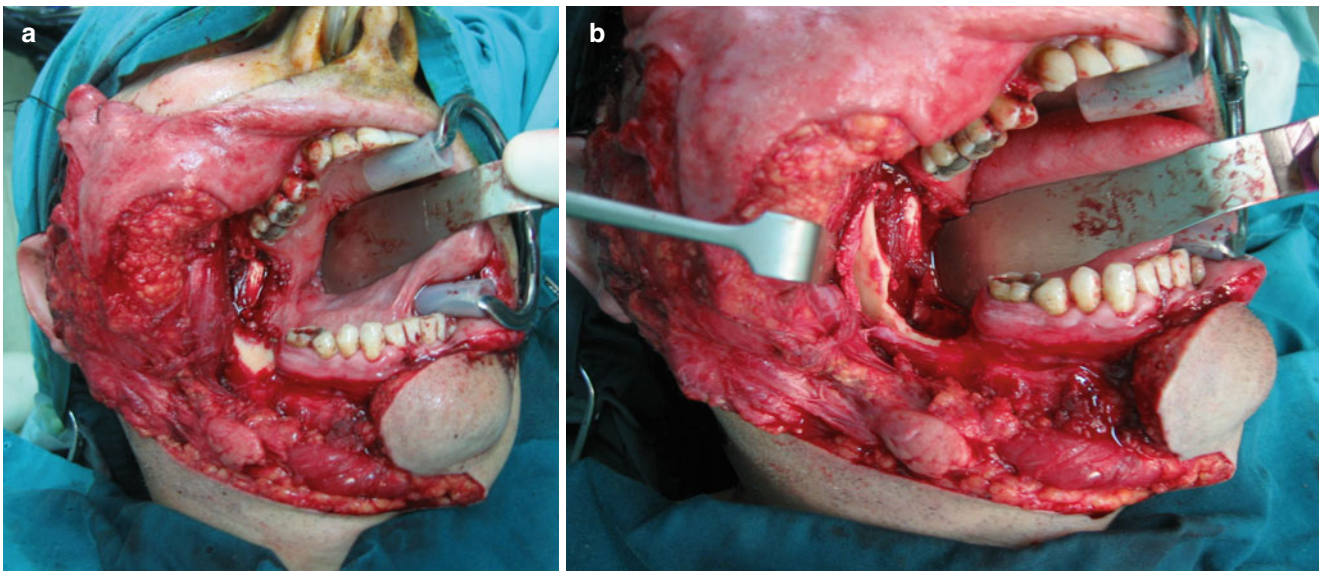

Fig. 9.30 (**a**) The defect after tumor excision. (**b**) Posterior marginal mandibulectomy was performed

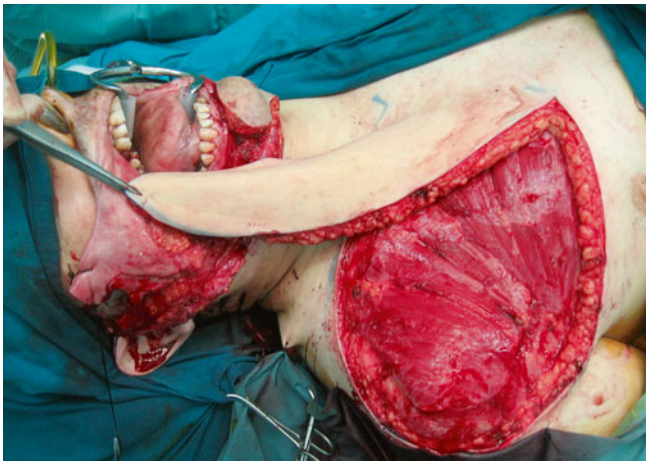

Fig. 9.32 Flap reaches the defect easily and without tension

Fig. 9.33 Deltopectoral flap passes through a submandibular tunnel intraorally

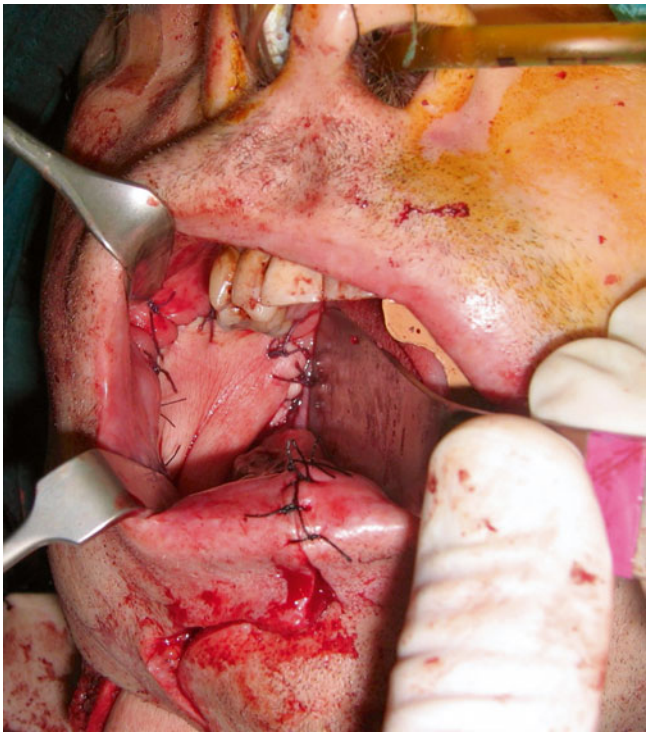

Fig. 9.34 Flap sutured in place resurfacing the intraoral defect

Fig. 9.35 Immediate postoperative view. The tubed pedicle passes freely through the tunnel without constriction

9.6.3.2 Cervical Part

The cervical part of the flap is elevated in the sub-SMAS layer, below the platysma muscle and above the investing layer of the deep cervical fascia. After incising deep to the trapezius muscle, the plane of dissection is easily created above it, until its anterior border. Moving on anteriorly, the elevation proceeds at the roof of the posterior neck triangle where the platysma might be very hypoplastic or even absent at this area especially in its posterior part, and from the other hand the investing layer of the deep cervical fascia might be indistinguishable. Therefore, the plane of dissection is slightly more difficult to determine taking care to avoid or to identify and protect the terminal part of the accessory nerve (Fig. 9.43).

Dissecting further anteriorly, the elevation proceeds with ease just under the platysma muscle. Reaching the sternocleidomastoid prominence, the muscles posterior border is easily identified. Care is taken to locate Erb's point, where the cutaneous branches of the cervical plexus and the accessory nerve emerge. Cutaneous filaments of the plexus that prevent mobilization of the flap can be sacrificed (Fig. 9.44). Elevation proceeds over the outer surface of the

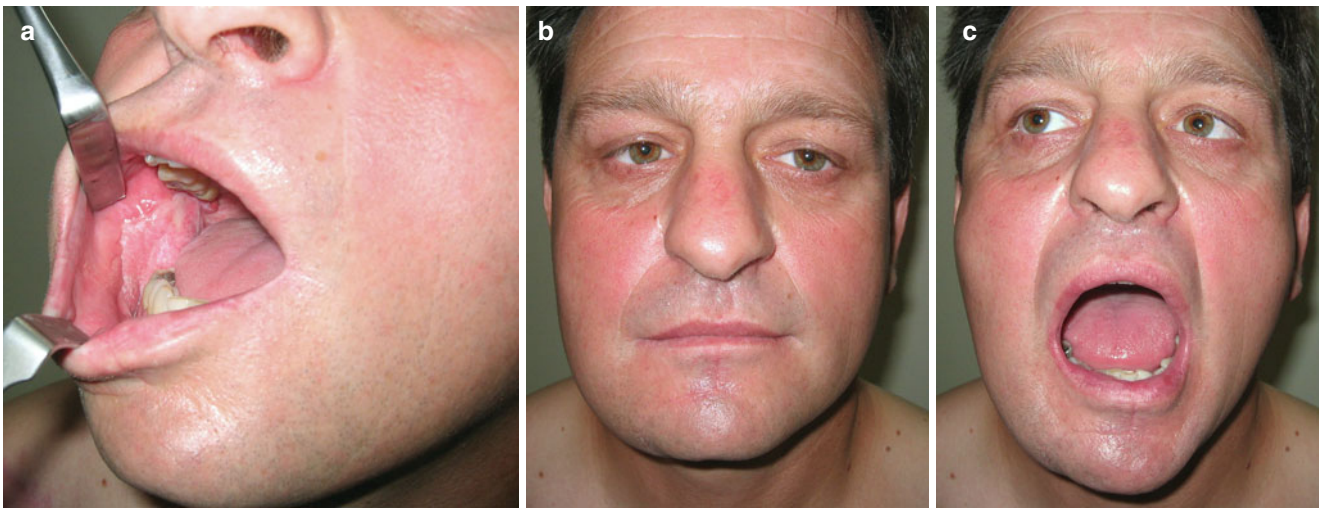

Fig. 9.36 Result at 5 months. (**a**) The defect fully restored. (**b**) The cheek lump produced from the bulk of the deltopectoral flap reduces with time. (**c**) Function is accomplished

Fig. 9.37 Preoperative view of a large basal cell carcinoma of the cheek

Fig. 9.38 Outline of the cervicopectoral flap

sternocleidomastoid continuing medially and stops near the midline of the neck were the anterior jugular vein might be found.

At the upper part of the cervical dissection of the flap, special care is taken to avoid or to identify and prevent the marginal branch of the facial nerve (Fig. 9.45a, b). The elevation continues on the subplatysmal plane to the midline of the neck exposing the lateral surface of the submandibular gland invested by the investing layer of the deep cervical fascia.

When following the subplatysmal plane, the superficial veins (e.g., external jugular vein, anterior jugular vein) are exposed and whenever possible are protected (Fig. 9.46).

As long as the vertical limb of the flap in the neck is in the same position as the incision in the Lazaridis modification of the Conley incision for neck dissection and the elevation of the flap sufficient enough to expose the neck, a simultaneous neck dissection can be performed with ease and with no need for further incisions (Lazaridis et al. 1994, 1997).

9.6.3.3 Facial Part

The extent of its facial part depends on the remaining healthy facial skin after the excision of the facial lesion and the produced defect. The flap can be elevated in its facial part either superficial to the superficial musculoaponeurotic system (SMAS) layer or in a deep sub-SMAS plane (Fig. 9.47). The superficial dissection plane provides protection of the branches of the facial nerve, but the sub-SMAS dissection

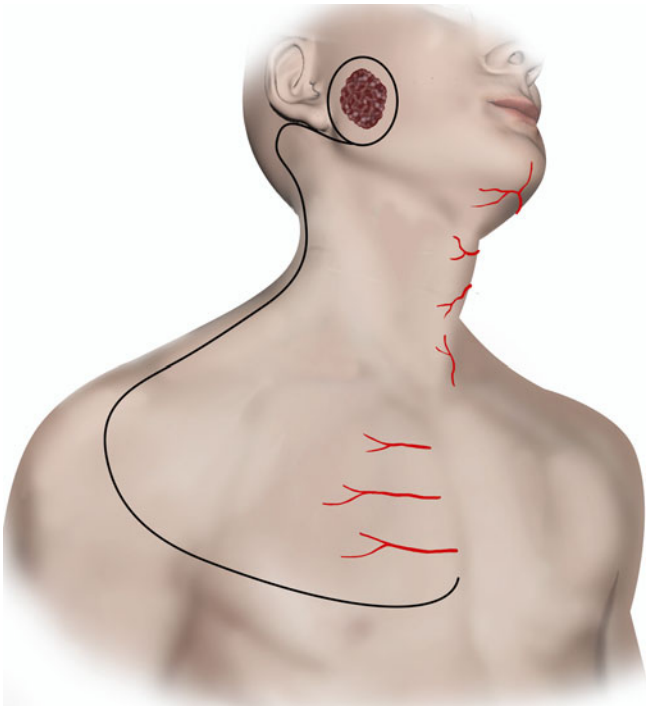

Fig. 9.39 The cervicopectoral flap is a mixed axial-patterned and random-patterned flap

Fig. 9.40 The cheek defect after the lesion has been excised

enhances vascularity of the facial part of the flap. The decision is made depending on the depth of the defect and the appropriate bulk of the transferred tissue that is needed to provide an improved contour and the patient's sufficiency in blood microcirculation, especially if the patient is prone to microangiopathy from diabetes mellitus, smoking, etc.

The above partitioned description in flap elevation is only for descriptive reasons as long as the flap is not raised by parts but as a whole from lateral to medial with the separate parts connected in the transition zones.

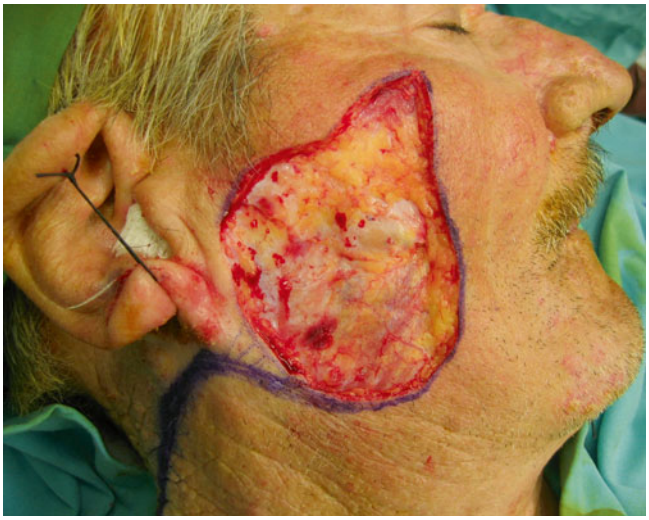

Fig. 9.41 The lesion had to be excised in its greater extent in the sub-SMAS layer. Parotidomasseteric fascia is clearly visible

Fig. 9.42 Elevation of the thoracic part deep to the deltopectoral fascia

After the flap has been fully mobilized (Fig. 9.48), parotidectomy and/or any type of neck dissection can be performed as already mentioned at this stage. The flap is then rotated (Fig. 9.49) to the recipient site and is controlled to reach and

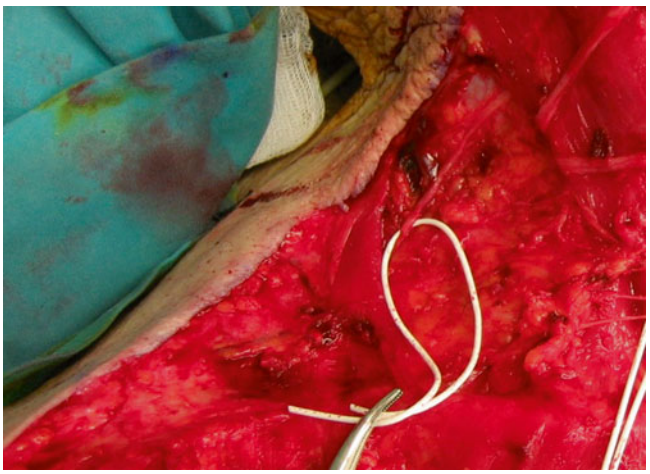

Fig. 9.43 Deep plane dissection at the posterior neck triangle may risk inadvertent injury of the accessory nerve

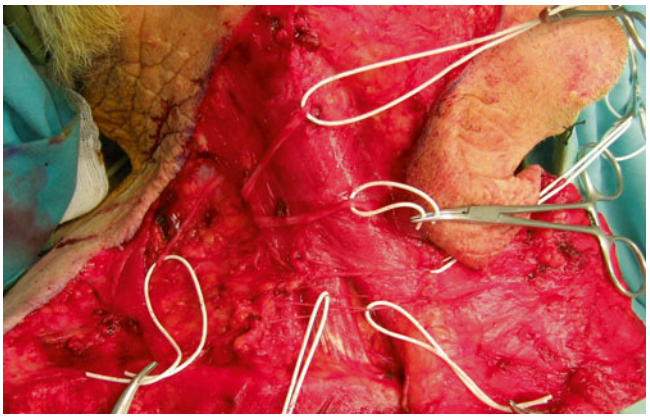

Fig. 9.44 Accessory nerve (*left*). Greater auricular nerve (*top*). Transverse cervical nerve (*middle*). Branches of the supraclavicular nerves (*bottom*). Filaments of the supraclavicular branches were sacrificed to allow further mobilization of the flap. The lesser occipital can just be seen above the exiting point of the accessory nerve

resurface the defect without tension. A back-cut at the sternal border of the inferior flap limb might help gaining more rotation if needed. Possible "dog-ear" may be formed medially at the upper border of the flap and at the axillary fold, which are trimmed as necessary. The flap is then sutured in position without tension. The donor site is closed primarily while

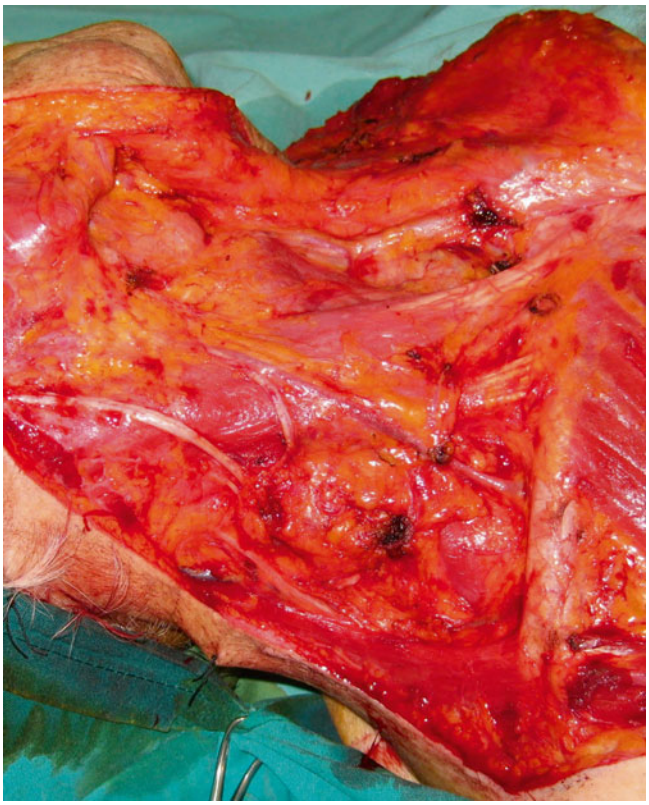

Fig. 9.46 Complete elevation of the cervical part of the flap. The trapezius muscle; the accessory, the greater auricular, and the transverse cervical nerves; and the external and anterior jugular veins are exposed

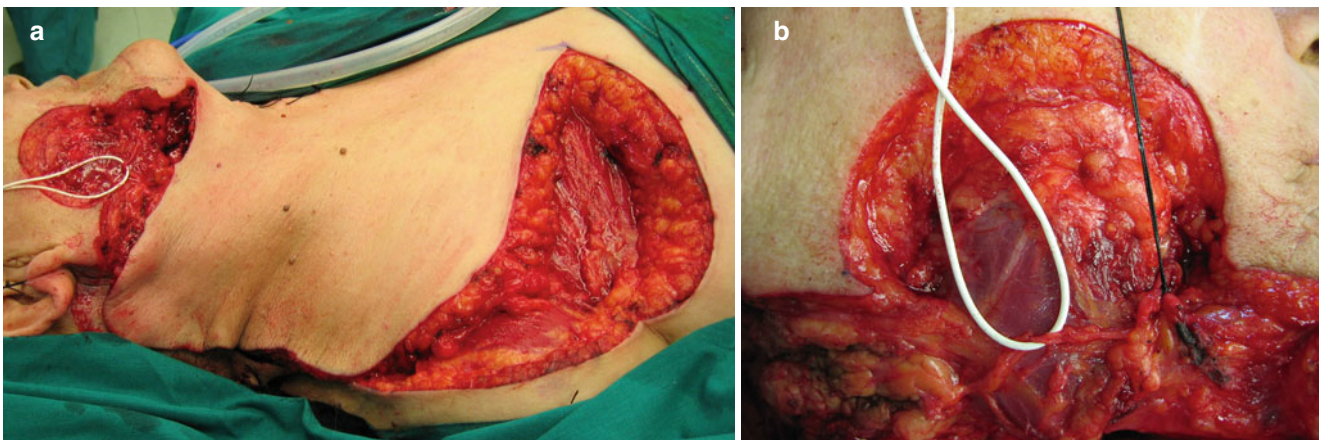

Fig. 9.45 (**a**) During the upper cervical part elevation, the marginal branch of the facial nerve must be protected. (**b**) The marginal branch of the facial nerve as it emerges from the parotis and runs superior to the lower border of the mandible superficial to the facial artery and vein. In this patient the lower pole of the parotis is cut and the facial pedicle ligated and cut, due to a simultaneous neck dissection (closeup view of Fig. 9.45a)

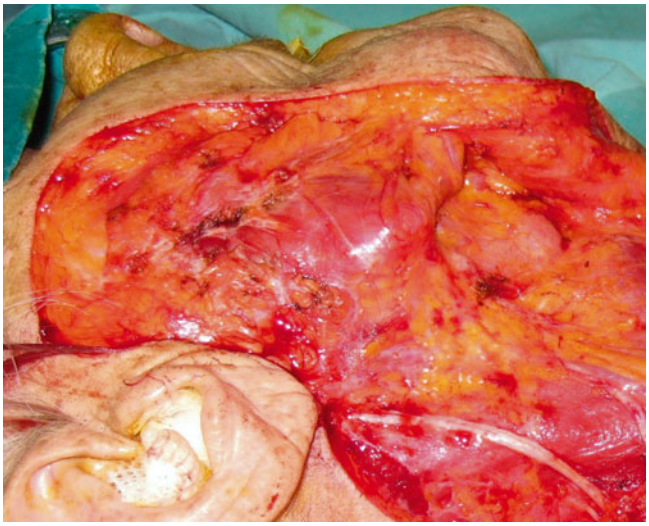

Fig. 9.47 Elevation of the facial part of the flap in this case is done in the sub-SMAS plane

Fig. 9.49 Flap is rotated to the recipient site

Fig. 9.48 The cervicopectoral flap fully mobilized

Fig. 9.50 Immediate postoperative view after wound closure and placement of suction drains

immobilization of the chest and deltoid skin may be needed to achieve suturing without tension (Fig. 9.50). The postoperative result is excellent as long as the flap provides tissues similar in color, thickness, and texture to the facial defect (Fig. 9.51a, b).

9.6.3.3.1 Flap Maximal Outward Extent

It is often referred that the cervicopectoral flap only reaches defects of the lower cheek, below the line that connects the tragus to the oral commissure. This is not true. In fact, the cervicopectoral flap can reach and resurface lateral defects beyond that line up to the midface. Such a case is seen in Fig. 9.52a–c, where the cervicopectoral flap reached and covered an orbital defect after a wide resection combined with an orbital exenteration.

The cervicopectoral flap is a reliable regional flap that provides adequate coverage to large lateral defects of the lower and middle face (cheek, orbit, periauricular region). It can also be used in cases where a big portion of the neck skin has been excised, leading to the reduction of the flap's cervical portion, the resulting neck defect can be resurfaced using the same design, if the flap is extended to the costal margin, with the inferior limb lying quite below the level of areola (Moore et al. 2005).

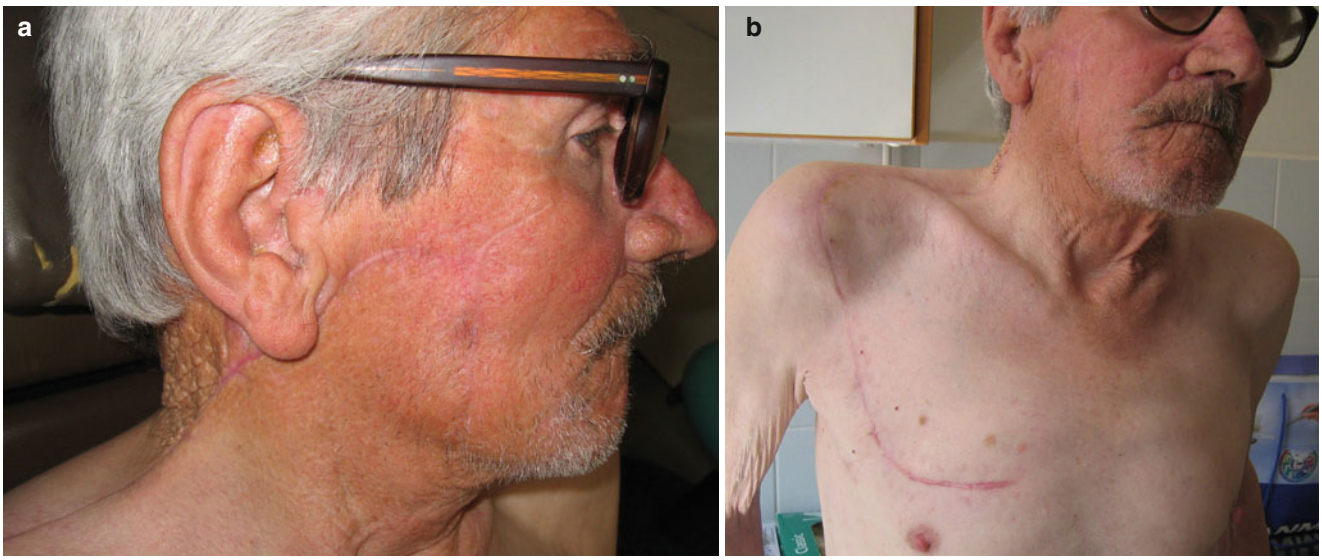

Fig. 9.51 (**a**, **b**) Postoperative result at 4 months

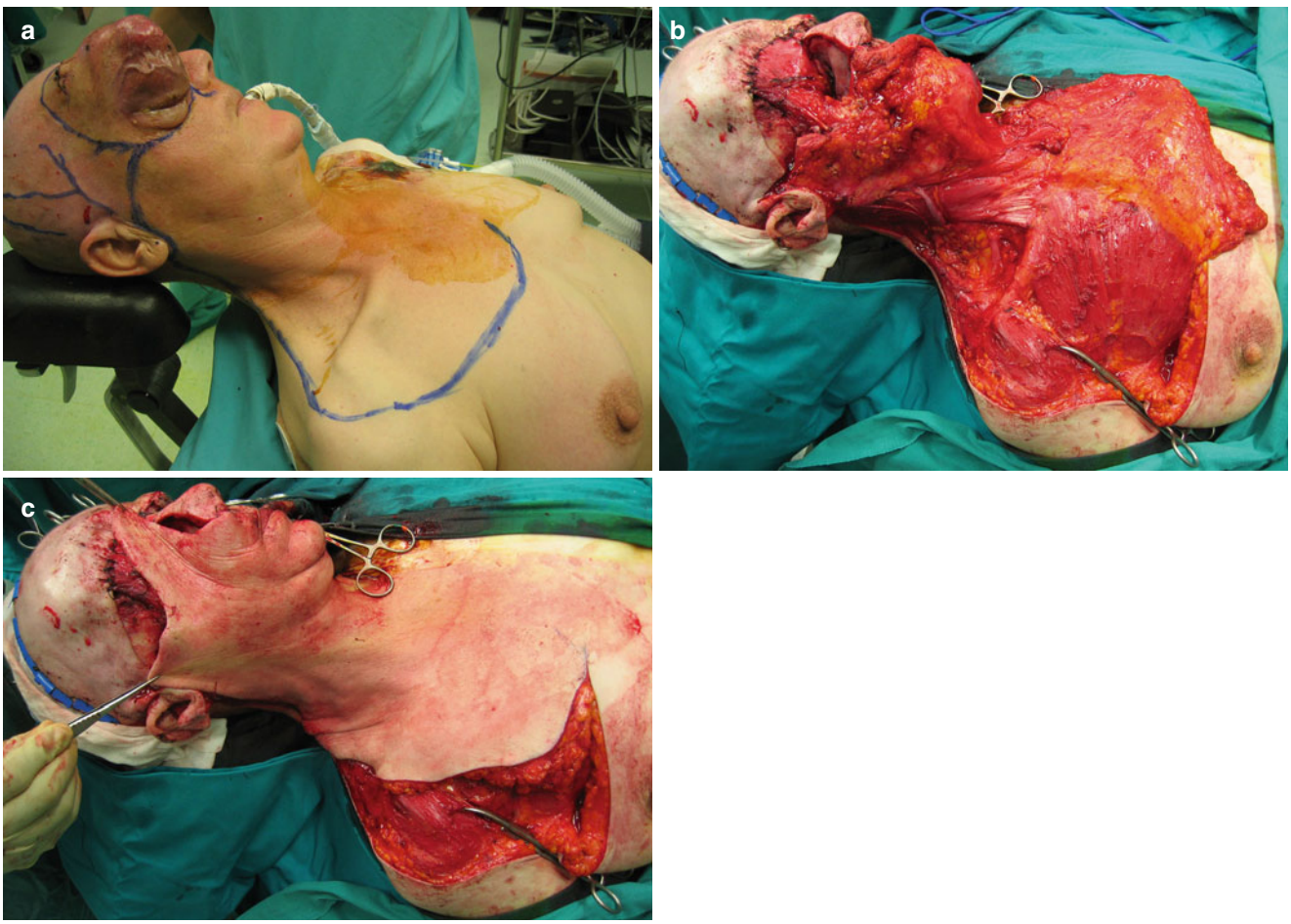

Fig. 9.52 (**a**) A large orbital tumor. Dissection lines are outlined and the cervicopectoral flap is one of the flaps, of the combined restoration, that will provide the external coverage. (**b**) The cervicothoracic flap is elevated. (**c**) The flap easily and without tension reaches the orbit

The cervicopectoral flap provides tissue similar in color, texture, and thickness and fulfills the criteria of functional and aesthetic results. It achieves adequate exposure of the neck and the parotid region; thus, if a neck dissection or a parotidectomy is needed, it can be performed simultaneously. It also can be combined with pectoralis major myocutaneous flap that provides the intraoral coverage, in full-thickness cheek defects in a single-stage reconstruction.

References

Abu-Hijleh MF, Roshier AL, Al-Shboul Q, Dharap AS, Harris PF (2006) The membranous layer of superficial fascia: evidence for its widespread distribution in the body. Surg Radiol Anat 28(6):606–619

Ariyan S (1979) The pectoralis major myocutaneous flap. A versatile flap for reconstruction in the head and neck. Plast Reconstr Surg 63(1):73–81

Aymard JL (1917) Nasal reconstruction. Lancet 2:888–892

Bakamjian VY (1965) A two-stage method for pharyngoesophageal reconstruction with a primary pectoral skin flap. Plast Reconstr Surg 36:173–184

Bey E, Hautier A, Pradier JP, Duhamel P (2009) Is the deltopectoral flap born again? Role in postburn head and neck reconstruction. Burns 35(1):123–129

Becker DW Jr (1978) A cervicopectoral rotation flap for cheek coverage. Plast Reconstr Surg 61(6):868–870

Feng GM, Cigna E, Lai HK, Chen HC, Gedebou TM, Ozkan O, Chana J (2006) Deltopectoral flap revisited: role of the extended flap in reconstruction of the head and neck. Scand J Plast Reconstr Surg Hand Surg 40(5):275–280

Freeman JL, Walker EP, Wilson JS, Shaw HJ (1981) The vascular anatomy of the pectoralis major myocutaneous flap. Br J Plast Surg 34(1):3–10

Hormozi AK, Shafii MR (2010) Bilateral tunneled supraclavicular island flaps for simultaneous reconstruction of massive facial defect and intraoral lining. J Craniofac Surg 21(6):1876–1879

Kovacević P, Ugrenović S, Kovacević T (2008) Vascularisation of pectoralis major myocutaneous flap: anatomical study in human fetuses and cadavers. Bosn J Basic Med Sci 8(2):183–187

Krijgh DD, Mureau MA (2012) Reconstructive options in patients with late complications after surgery and radiotherapy for head and neck cancer: remember the deltopectoral flap. Ann Plast Surg 71(2):181–185

Lazaridis N, Dalabiras S, Karakassis D (1994) Modification of the Conley incision for neck dissection. J Oral Maxillofac Surg 52(10):1046–1049

Lazaridis N, Tilaveridis I, Dalambiras S, Iordanidis S (1997) The fasciocutaneous cervicopectoral rotation flap for lower cheek reconstruction: report of three cases. J Oral Maxillofac Surg 55(10):1166–1171

Loukas M, Louis RG Jr, Wartmann CT (2006) Superficial lateral thoracic artery. Ann Plast Surg 57(4):475–476

Moore BA, Wine T, Netterville JL (2005) Cervicofacial and cervicothoracic rotation flaps in head and neck reconstruction. Head Neck 27(12):1092–1101

Nakajima K, Ide Y, Abe S, Okada M, Kikuchi A, Ide Y (1997) Anatomical study of the pectoral branch of thoracoacromial artery. Bull Tokyo Dent Coll 38(3):207–215

Nayak BB, Nilamani M (2012) Single stage reconstructions in head and neck surgery using deltopectoral and pectoralis major myocutaneous flaps. Indian J Plast Surg 45(1):151–153

Pallua N, Machens HG, Rennekampff O, Becker M, Berger A (1997) The fasciocutaneous supraclavicular artery island flap for releasing postburn mentosternal contractures. Plast Reconstr Surg 99(7):1878–1884

Pallua N, Magnus Noah E (2000) The tunneled supraclavicular island flap: an optimized technique for head and neck reconstruction. Plast Reconstr Surg 105(3):842–851

Pallua N, Wolter TP (2013) Moving forwards: the anterior supraclavicular artery perforator (a-SAP) flap: a new pedicled or free perforator flap based on the anterior supraclavicular vessels. J Plast Reconstr Aesthet Surg 66(4):489–496

Park HD, Min YS, Kwak HH, Youn KH, Lee EW, Kim HJ (2004) Anatomical study concerning the origin and course of the pectoral branch of the thoracoacromial trunk for the pectoralis major flap. Surg Radiol Anat 26(6):428–432

Po-Wing Yuen A (2006) Preservation of lateral thoracic artery to improve vascular supply of distal skin without compromising pedicle length in harvesting pectoralis major myocutaneous flap. J Plast Reconstr Aesthet Surg 59(12):1433–1435

Palmer JH, Taylor GI (1986) The vascular territories of the anterior chest wall. Br J Plast Surg 39(3):287–299

Rebelo M, Ferreira A, Barbosa R, Horta R, Reis J, Amarante J (2009) Deltopectoral flap: an old but contemporaneous solution for neck reconstruction. J Plast Reconstr Aesthet Surg 62(1):137–138

Schmidt M, Aszmann OC, Beck H, Frey M (2010) The anatomic basis of the internal mammary artery perforator flap: a cadaver study. J Plast Reconstr Aesthet Surg 63(2):191–196

Sharma RK, Panda N (2006) Old is still gold: use of deltopectoral flap for single-stage pharyngeal reconstruction. Plast Reconstr Surg 117(2):691–692

Standring S (2008) Gray's anatomy. The anatomical basis of clinical practice, 40th edn. Churchill Livingstone-Elsevier, Edinburgh

Stecco A, Macchi V, Masiero S, Porzionato A, Tiengo C, Stecco C, Delmas V, De Caro R (2009a) Pectoral and femoral fasciae: common aspects and regional specializations. Surg Radiol Anat 31(1):35–42

Stecco A, Masiero S, Macchi V, Stecco C, Porzionato A, De Caro R (2009b) The pectoral fascia: anatomical and histological study. J Bodyw Mov Ther 13(3):255–261

Vinh VQ, Van Anh T, Ogawa R, Hyakusoku H (2009) Anatomical and clinical studies of the supraclavicular flap: analysis of 103 flaps used to reconstruct neck scar contractures. Plast Reconstr Surg 123(5):1471–1480

Yang D, Marshall G, Morris SF (2003) Variability in the vascularity of the pectoralis major muscle. J Otolaryngol 32(1):12–15

Index

V.K. Thomaidis, *Cutaneous Flaps in Head and Neck Reconstruction*,
DOI 10.1007/978-3-642-41254-7, © Springer-Verlag Berlin Heidelberg 2014